# SEISMIC ANALYSIS AND RETROFITTING OF HISTORICAL BUILDINGS

EDITED BY: Antonio Formisano and Michele D'amato

**frontiers** Research Topics

## About Frontiers

Frontiers is more than just an open-access publisher of scholarly articles: it is a pioneering approach to the world of academia, radically improving the way scholarly research is managed. The grand vision of Frontiers is a world where all people have an equal opportunity to seek, share and generate knowledge. Frontiers provides immediate and permanent online open access to all its publications, but this alone is not enough to realize our grand goals.

## Frontiers Journal Series

The Frontiers Journal Series is a multi-tier and interdisciplinary set of open-access, online journals, promising a paradigm shift from the current review, selection and dissemination processes in academic publishing. All Frontiers journals are driven by researchers for researchers; therefore, they constitute a service to the scholarly community. At the same time, the Frontiers Journal Series operates on a revolutionary invention, the tiered publishing system, initially addressing specific communities of scholars, and gradually climbing up to broader public understanding, thus serving the interests of the lay society, too.

## Dedication to Quality

Each Frontiers article is a landmark of the highest quality, thanks to genuinely collaborative interactions between authors and review editors, who include some of the world's best academicians. Research must be certified by peers before entering a stream of knowledge that may eventually reach the public - and shape society; therefore, Frontiers only applies the most rigorous and unbiased reviews.
Frontiers revolutionizes research publishing by freely delivering the most outstanding research, evaluated with no bias from both the academic and social point of view. By applying the most advanced information technologies, Frontiers is catapulting scholarly publishing into a new generation.

## What are Frontiers Research Topics?

Frontiers Research Topics are very popular trademarks of the Frontiers Journals Series: they are collections of at least ten articles, all centered on a particular subject. With their unique mix of varied contributions from Original Research to Review Articles, Frontiers Research Topics unify the most influential researchers, the latest key findings and historical advances in a hot research area! Find out more on how to host your own Frontiers Research Topic or contribute to one as an author by contacting the Frontiers Editorial Office: researchtopics@frontiersin.org

# SEISMIC ANALYSIS AND RETROFITTING OF HISTORICAL BUILDINGS

Topic Editors:
**Antonio Formisano,** University of Naples Federico II, Italy
**Michele D'amato,** University of Basilicata, Italy

# Table of Contents

frontiers
in Built Environment

# Editorial: Seismic Analysis and Retrofitting of Historical Buildings

Antonio Formisano[1] and Michele D'Amato[2]*

[1] Department of Structures for Engineering and Architecture, University of Naples Federico II, Naples, Italy, [2] Department of European and Mediterranean Cultures, University of Basilicata, Matera, Italy

**Editorial on the Research Topic**

**Seismic Analysis and Retrofitting of Historical Buildings**

The proposed Special Issue has been addressed to conservation and protection of historical buildings with respect to the seismic action. It provides an overview of recent advances aimed for territorial and local evaluations of seismic performance of existing constructions having also historical value, either in masonry or in concrete. As for the methods applied at a territorial scale, essentially consisting of fast appraisal methods providing a score (or index) which are only based on qualitative evaluations, it is clearly pointed out that they may not substitute more refined and specific numerical models. They are only capable of quickly screening constructions in a certain area, and of individuating the priorities to be investigated in depth with more appropriate numerical investigations. As far as the application of these numerical models is concerned, different approaches may be followed in order to design adequate interventions capable of upgrading a construction up to a safety level of a newly constructed building. As highlighted within the manuscripts submitted, the knowledge requires acquisition of construction and geometrical details, including existing crack patterns, even before of materials properties. Moreover, the data acquisition should be done in an incremental and adaptive way with updated numerical models, for permitting of highlighting those parameters that considerably influence the seismic response. In this way, the invasiveness of the *in-situ* experimental tests is minimized, also from an economical point of view.

In the manuscript proposed by Chieffo and Formisano three different methods, coherent with a multi-level approach, are applied for seismic assessment of masonry buildings aggregates. The authors remark the importance of using appropriate numerical models, since territorial methods are not able in specifically predicting the seismic performance of a construction.

In Chiumento and Formisano, a preliminary seismic vulnerability assessment through a fast appraisal method is applied. The plan distribution influence of structural units belonging to the same masonry cluster is investigated. To this scope the lateral response of some independent structural units is compared with the global one, evaluated with non-linear pushover analyses. The comparisons reported show that isolated structural units have lower stiffness and strength than the ones calculated by referring to the entire compound.

In Cocco et al. at first an empirical method is used for assessing 140 buildings of the historic center of Campotosto. Afterwards, a methodology developed at the Padua University is applied to a building compound, representative of the entire buildings stock. Damage probability matrixes and fragility curves are shown and commented, and derived from the damage distribution of the sample considered. The authors confirm that, in the cases analyzed, the damage distribution may be well-predicted with a binomial probability function.

Particular attention to masonry churches is paid in Fabbrocino et al. The results of a preliminary seismic risk assessment of two territorial cases, affected by recent earthquakes occurred in Italy, are

shown in detail obtained with a new simplified method. This method provides a global resulting score to be used for numerical comparisons at a territorial scale. It may be easily implemented in the multi-level approach proposed within the current Italian Directive for evaluating and mitigating the seismic risk of cultural heritage.

In D'Amato et al. (a) this multi-level approach is applied to five masonry churches, belonging to the historical center "Sassi of Matera," a site protected by UNESCO having a moderate seismic hazard. The obtained results are also compared with the new simplified fast appraisal method suitable for territorial evaluations developed at the Basilicata University (Italy). Also, the second level of evaluation implying a macro-element approach is used. The authors point out that simpler methods may overestimate the actual seismic performance of a church.

Particular emphasis to the construction knowledge for a realistic seismic assessment is given in the paper submitted by Caprili and Puncello, where a multidisciplinary and multilevel knowledge procedure is proposed for providing a geometrical-structural model of a building for further numerical investigations. In the paper, four historical masonry cases study are considered and all are located in the Tuscany region.

A retrofitting design of an existing masonry building is conducted in Maraveas, where two different interventions are discussed to seismically retrofit a case study: by considering rigid diaphragms, or external bonding of timber walls with infilled masonry. Linear models are implemented with static and time history analyses, demonstrating the effectiveness of the interventions considered.

In two works, particular attention is paid to ancient masonry towers. Precisely, in Formisano and Milani, a series of non-linear static pushover analyses are performed by considering a tower independent on the adjacent ecclesiastic aggregate. Then, it is also investigated the entire compound including both the ecclesiastic complex and the tower. The authors conclude that the interaction reduces the seismic vulnerability of more than 20%. Benefits of some interventions are evaluated with pushover analyses, such as: the application of G-FRP sheets or reinforced plaster, both with the confinement of existing openings with steel frames. Whereas, in Ferrante et al. a tower is modeled with the Discrete Element Method, assuming rigid blocks and frictional joints. The dynamic behavior and influence of the inclined configuration is investigated with non-linear analyses, considering recorded seismic excitations. The investigations performed highlights that the tower inclination considerably increases its seismic vulnerability, demonstrated by greater values of displacements and energy dissipation in the inclined shape.

As for R.C. structures, in the paper of Miano et al. the seismic vulnerability of a case study is examined, resulting unsafe under both vertical and seismic loads. In the paper a rational approach to design the interventions is followed, with both on linear and non-linear dynamic analyses. The structural interventions effectiveness is measured coherently with the new Italian guidelines for seismic risk classification of constructions. A different interventions design strategy is followed in D'Amato et al., (b) where the seismic isolation is applied to a building, falling within a high seismic hazard area. The building, designed only for vertical loads without any specific regulation for lateral loads and reinforced with smooth bars, is retrofitted with a seismic isolation system composed by elastomeric and sliding isolators. A new methodology is also proposed for quickly evaluating the seismic capacity of the building by using the GMs recorded in the surrounding area during the 1980 Irpinia earthquake together with attenuation laws.

Pushover analyses are performed in Milosevic et al. to estimate the behavior factor of a particular type of mixed masonry-reinforced concrete buildings. The seismic response is evaluated with non-linear pushover analyses, considering both aleatory and epistemic uncertainties. From numerical investigations the behavior factor values result low due to the connection with the structural walls, and in accordance with the ones proposed in most recent seismic codes. Anyway, the authors recommend of carefully assessing the correct value to be assigned, since it highly depends on the specific typology of mixed buildings considered.

Finally, in Casamassima and D'Amato, the fatigue assessment is treated with particular attention to the existing masonry arches bridge. In this way their remaining service life, with possible traffic load limitations, may be estimated. In the manuscript a review of the state-of-the art about recent published fatigue models, also accounting for deterioration effects under cyclic loads is presented. Then, the results related to fatigue performance of a bridge are discussed. A comparison among different existing fatigue models demonstrate that, to date, their application may lead to opposite results. Therefore, appropriate stress-life curves for ancient masonry elements should be determined and implemented in order to evaluate the remaining service life with respect to the cyclic loads.

In conclusion, the studies presented show that it is impossible to generalize the investigations and interventions procedures. This is due to the fact that particular attention must be paid not only to the building typology investigated but also to its evolution through time with construction details. Finally, guidelines agree on applying reversible interventions that may be substituted in the future guaranteeing seismic protection for frequent earthquakes.

## AUTHOR CONTRIBUTIONS

All authors listed have made a substantial, direct and intellectual contribution to the work, and approved it for publication.

# Seismic Behavior of Lisbon Mixed Masonry-RC Buildings With Historical Value: A Contribution for the Practical Assessment

Jelena Milosevic[1], Rita Bento[1]* and Serena Cattari[2]

[1] Department of Civil Engineering, Architecture and Georesources, CERIS, Instituto Superior Técnico, Universidade de Lisboa, Lisbon, Portugal, [2] Department of Civil, Chemical and Environmental Engineering, University of Genoa, Genoa, Italy

The fact that linear analysis is still the most used procedure in the design engineering offices, studies which addresses issues associated to the estimation of the structural behavior factor values are relevant. In this study, the behavior factor of a particular type of mixed masonry-reinforced concrete buildings in Lisbon is estimated. The typology chosen in this study represents 30% of building stock in Lisbon; these buildings were built between 1930 and 1960 and thus were designed without considering the seismic-design requirements proposed in current codes. The evaluation of the behavior factors was based on the use of nonlinear static analyses, performed in the form of the sensitivity analysis and following the criteria proposed in the current seismic codes and literature. In the scope of the sensitivity analysis, aleatory and epistemic uncertainties have been considered in terms of the mechanical parameters and structural details, respectively with the aim to take into account different characteristics of the structures. In order to derive the most reliable values of the behavior factor for this typology, extensive research in terms of the historical information, structural characterization and definition of the mechanical parameters has been performed. The study indicates that the final values of behavior factor are low and depend most on the type of connections between structural walls. Although the obtained values of the behavior factor for this typology match well with the ones proposed in most recent seismic codes, it is recommended that the assessment of such factor of a specific class for a particular structural type building should always be careful evaluated.

Keywords: seismic behavior, mixed masonry-RC buildings, practical assessment, uncertainties, nonlinear static analyses, behavior factor

## INTRODUCTION

The proliferation in Lisbon of the use of reinforced concrete (RC) in the construction, particularly in apartment buildings, was developed throughout the first half of the twentieth century (approximately between 1930 and 1960). In this period, the mixed masonry-RC buildings firstly appeared as transition from masonry/timber to proper design RC buildings: they are commonly known by contractors and real estate dealers as "placa" buildings. Whole structures of RC were only widely adopted in apartment buildings from 1950s onwards. Until this decade, the partial use

of RC structural elements within specific areas and periods of time was mainly influenced by the following two issues: (i) the codes which introduced the requirement of the use of RC elements in specific parts in residential buildings and (ii) the construction of new neighborhoods to fill gaps in already urbanized or in expansion areas of the city.

In this study focus is given to the "Alvalade" area, an exceptional case study for both Architects and Engineers, as it was designed as a global project from city scale to construction detail. As Lisbon is in high seismic hazard area, and these buildings were typically designed without strictly considering the current seismic-design requirements, the seismic evaluation of these existing buildings is crucial for safety reasons and to preserve our built heritage. For an adequate seismic evaluation, it is relevant to: (i) compile and analysis the important historical data for generic characterization of the construction, as it is also referred in ISO 13822 (2010) and ICOMOS/ISCARSAH Committee (2003); (ii) characterize the main structural elements; (iii) model numerically the buildings, being aware of the aleatory and epistemic uncertainties, as they crucial role in performance-based earthquake engineering; and (iv) perform reliable global seismic analyses. For the global analysis of the structural system, attention will be given, in this work, to nonlinear static and to linear procedures, which are the ones most used in common practice. Despite the significant progress in nonlinear methods of analyses of old building structures in the last decades, there is still considerable resistance to use nonlinear procedures in practical engineering offices. Thus, it would be important to define values for the behavior factor (q for European practice and R for US practice) to be used in the seismic assessment of mixed masonry-RC buildings typology existent in Lisbon.

In this study, q-factor values are defined based on the nonlinear static sensitivity analysis (Cattari et al., 2015a), following the different methods proposed in CEN Eurocode 8 (2004) and in the related research (Tomaževič et al., 2004; Thomos and Trezos, 2005; Magenes and Menon, 2009; Senaldi et al., 2014). For the sensitivity analysis, both types of uncertainties are considered, epistemic and aleatory. In this way, q-factor is defined in a more adequately way, because it is counted for certain number of uncertainties; this is always quite important, due to the huge variety of the materials and structural elements in old masonry-RC buildings. After obtaining the values of the q-factor for each direction (X and Y), for two load patterns (uniform and triangular) and for all considered models (see section Modeling and Definition of Uncertainties), values are compiled and the final ones for the q-factor for the typology under study are proposed. Even the obtained values are matching well with the values proposed in CEN Eurocode 8 (2004) and NTC Italian Code for Structural Design (2008), it is recommended to evaluate the q-factor for each construction typology according to the specific characteristic of certain typology. In this way, seismic analysis will be more reliable and accurate. In fact, the numerical definition of the behavior factor of existent buildings is certainly a subject of research in order to make their seismic structural performance more predictable from the engineering point of view.

# THE MIXED MASONRY-RC BUILDINGS

## Historical Background

The growing importance of RC in Lisbon's construction of the twentieth century is directly proportional to the decline of timber construction. The construction of buildings using only timber structures is no longer possible after 1930, followed by appearance of the Regulation for the Urban Construction for the City of Lisbon (GRUC, 1930). In fact, after 1930, the use of RC became more common, particularly in kitchens and bathrooms. Throughout the decade of 1930s this material was increasingly being used in more elements of the construction: on the separation of commercial/ground floors and the floors above, on balconies and terraces and finally on most of the floors.

Meanwhile, in 1935, a new RC Regulation (RRCS, 1935) is approved, and the popularization of this "new" material was certainly enhanced by the national production which, since 1894, took place near Lisbon with a consequent drop in prices. The major architectonic advantage of the new technology was used by modernist Architects and Engineers in the design of the main façades. The full potential of RC was used to build cantilevers which usually constitute the balance of concrete floors, creating suspended, horizontal volumetric balconies or bow-windows (in a process similar to that of the overhanging stories in medieval buildings) and that states the image of buildings from the second half of the 1930s. From a conceptual point of view, in this decade the RC floors progressively replace the old timber floors. Nevertheless, until 1938, from a morphologic point of view, buildings remain identical, regardless the adopted solution– timber or concrete floors.

In 1938, began a much stricter control from the municipal services over the image but also the structure of the buildings. On new expanding areas of Lisbon city, and especially on the main streets and squares, the licensing services of Lisbon's city hall imposed a "stylized nationalist" (Fernandez, 1943) language which did not consent the concrete balconies and consoles used in the previous years. The municipal services required specific deployment perimeter which will originate the so-called "cod-tail" ("rabo de bacalhau") buildings. These buildings with an inverted "T" plan, which consists in general of two rectangles where the smallest one characterizes the open space in the rear wing (**Figures 1C,D**), appeared yet in the end of the 1930s, but their spread throughout Lisbon occurred in the following 10 years. In (**Figure 1**), the evolution of the buildings in terms of plan configuration is presented, as well as the layout of the rooms inside the buildings.

Thus, the mixed masonry-RC buildings are characterized by two main types in the plan: rectangular and "Rabo de Bacalhau" plan.

The use of RC slabs for buildings' floors, which seemed an irreversible trend by the end of the 1930s, has been detained in the early 1940s due to the Second World War and the consequent lack of iron.

One can say RC was used in a casuistic manner, following a cost-benefit balance differing from building to building. In fact, the slow and irregular introduction of RC in the structural elements in the average/common residential buildings in Lisbon,

**FIGURE 1** | An evolution of the shape of the buildings plan through the years. **(A)** Building plan with masonry/timber structure (1907). **(B)** Building with similar plan but with masonry RC structure (1937). **(C)** Building plan "rabo de bacalhau" with masonry/timber RC concrete (1944). **(D)** Building with similar plan "rabo de bacalhau" but with masonry RC (1944).
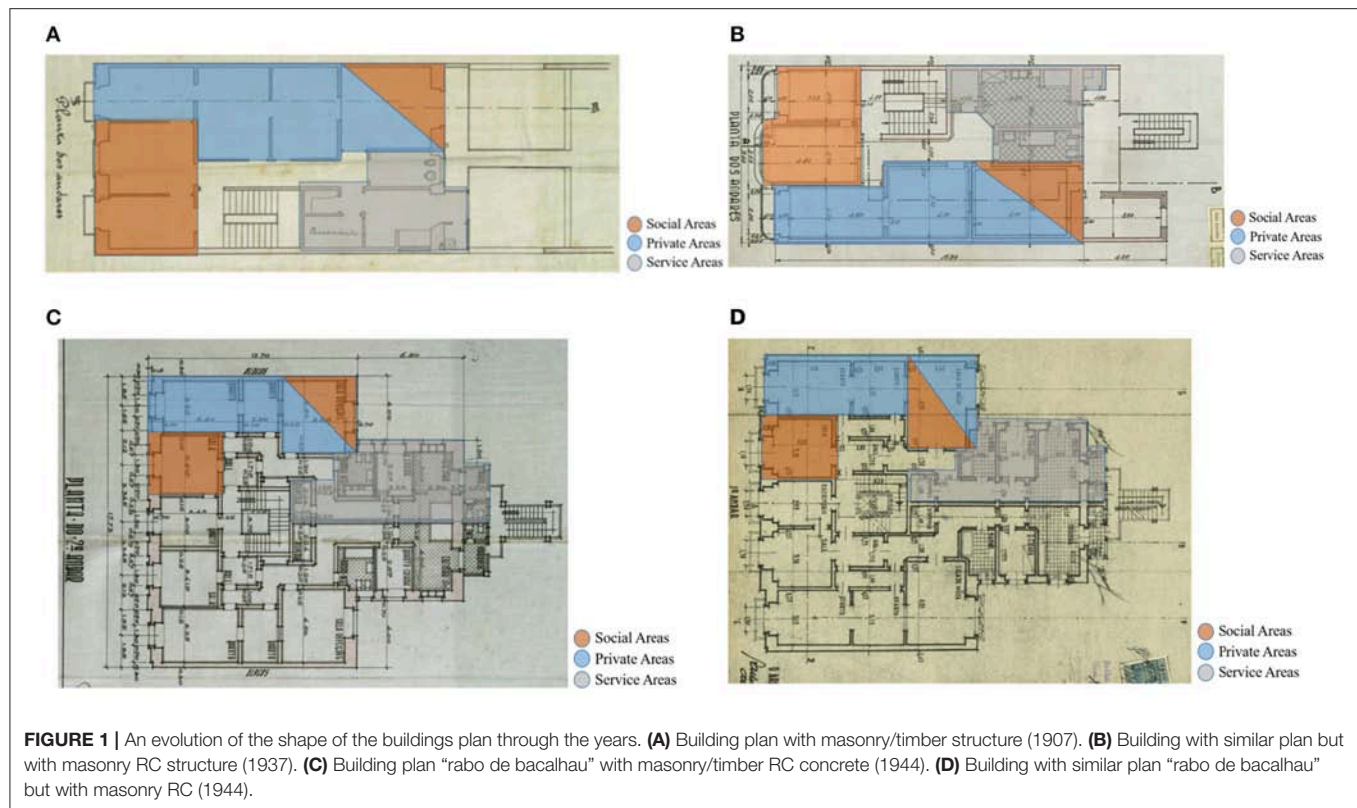
namely in the so-called "income buildings," that has been generically summarized in the mixed system of bearing masonry walls and RC slabs, has after all, a more complex and diverse history of which the most common solutions are:

a) Until 1930, buildings with an occasional use of concrete or RC in foundations, terraces, interior floors or rooftops;

b) From 1930 buildings use RC on floors of wet areas and in peripheral belts, remaining the floors in timber structure;

c) From 1935 onwards buildings with all interior and exterior floors, peripheral belts (eventually balconies and consoles on the main façade) in RC;

d) From the late 1930s on, buildings with every interior and exterior floor and some vertical and horizontal structures (walls or frames) in RC;

e) During the 40 s there is a set of buildings, which become relevant during World War II due to the iron scarcity, where both timber and RC floors coexist. During this period, it is common to find buildings in which only the wet areas, or the service stairs, or all the floors in the rear volumes, or the floors of the first floor or terrace are built with RC, the remaining being of wood.

## Geographic Distribution of the Mixed Masonry-RC Buildings in Lisbon and Plan Urbanization of "Bairro de Alvalade"

Apartment buildings with mixed structure of masonry and RC exist all over the city of Lisbon, although they are predominant in streets or areas urbanized during the 30 and 40 s. Particularly, two types can be distinguished: (i) the one urbanized by private promoters or following partial plans and (ii) the one with a greater official intervention by the state or the City Hall and already partially following the "De Groër Plan," that represents the first major urban plan for the whole Lisbon, developed from 1938 to 1948 (França, 1997).

In **Figure 2A** the areas of Lisbon are identified, with the apartment mixed buildings from the two types of groups. In the areas matching the first group (private promotion areas), there is many "deco" or "modernist" buildings (**Figure 2B**) whereas in the areas matching the second group (public promotion areas) prevail the buildings with a "nationalist" or "soft" modernist image (**Figure 2C**).

It should be mentioned that the area of "Alvalade" represents a major diversity of these types of buildings. Thus, in the following the focus will be given on this area.

Namely, the "Alvalade" neighborhood is a substantial central urban area in Lisbon, with relevant modern/neoclassic/art deco set of buildings, which deserve to be preserved. Moreover, this area corresponds to the first large-scale urban operation planned to expand Lisbon by public initiative prepared at the beginning of the 1940s (Alegre and Heitor, 2004).

The Urbanization Plan of "Alvalade" approved by the Portuguese government in 1945, was initiated in 1938. With an area of 230ha, "Alvalade" was designed as a "total" project– from city scale to construction detail. In that way, it is the only twentieth century Lisbon neighborhood where urban
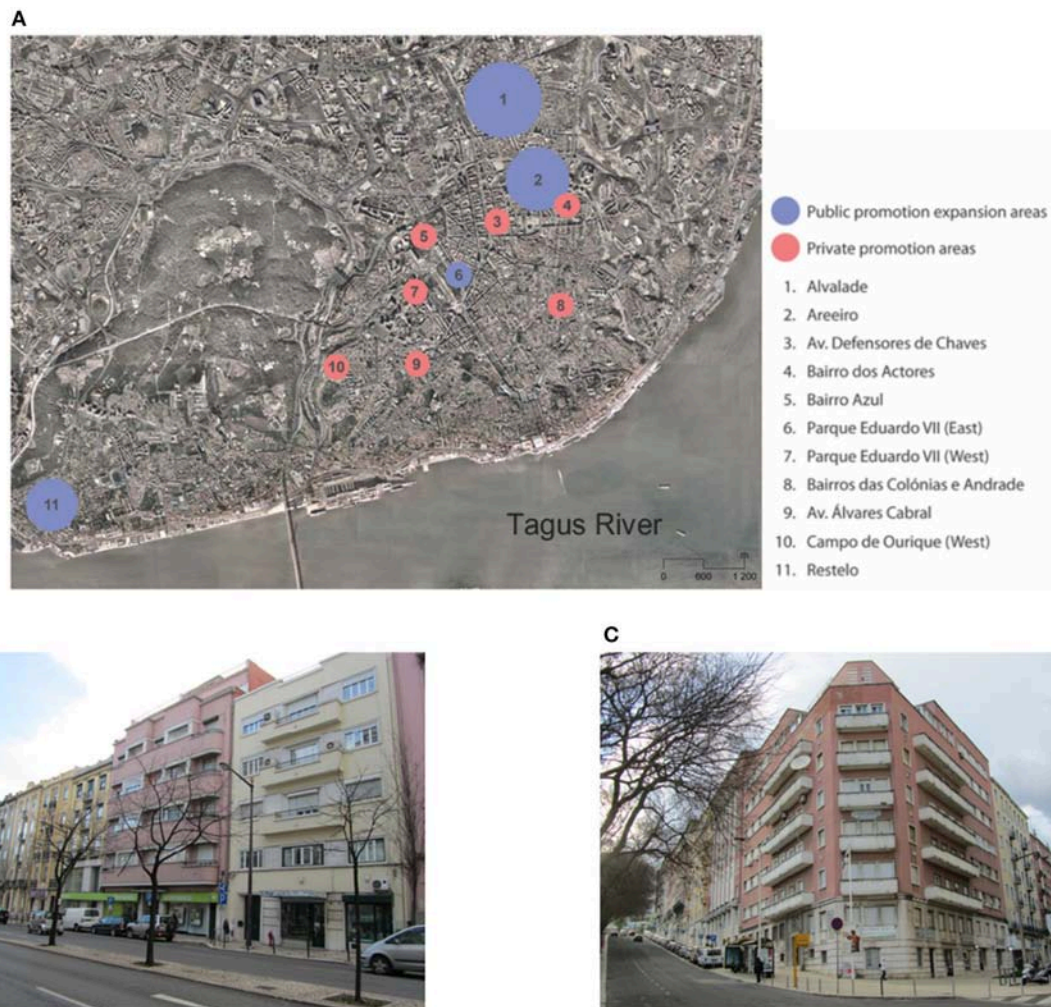
**FIGURE 2** | Some of the mixed masonry RC apartment buildings and their insertion areas. **(A)** Location of the buildings. **(B)** "Déco" and modernist buildings and **(C)** "Nationalist" or "soft" modern image buildings.

and building design was thought as one, totally coherent. Its significant extension within the city fabric and its social, design and construction concerns turn this Lisbon area an exceptional case study for both Architects and Engineers. It was only possible because the City Hall totally changed its current methodology for city planning.

This area was programed to integrate social and low rental housing, supported in equipment: school, market, civic center and small industry. In "Alvalade," opposite to major parts of the city, a high percentage of apartment buildings were not meant to be "income" buildings (which were private promoted as a financial product) as they belonged to public entities for social purposes.

The project of "Alvalade" is based on a rectangular hierarchical grid, divided by a net of main axes defining eight cells - cell I to VIII (**Figure 3A**). This approach allows the creation of "neighborhood units" with a strong concern in applying the principles of zoning, and assigning each cell to specific

functions (Alegre and Heitor, 2004). The "neighborhood units" were designed around a central element, the primary school, not exceeding the distance of 500 m from house to schools (**Figure 3E**). Pedestrian circulation is enabled by paths that cross the backyards of housing blocks. Other public facilities, particularly the market and the civic center, are distributed to be easily accessible by the dwellers of each cell. Public parks and gardens were designed as large common outdoor spaces for the enjoyment of residents (Alegre and Heitor, 2004).

The organization of "Bairro de Alvalade" (**Figure 3C**) resembles some Amsterdam areas (**Figure 3B**) and some proposals developed in Berlin (**Figure 3D**) for economic construction in the 1920–1930 decades (Costa, 2005). This is surely related with the international academic education of the Portuguese urban planner but also with research that was made by the city hall technicians, as presented in contemporary papers and reports edited by LNEC (the Civil Engineer National Laboratory).

**FIGURE 3 |** Comparison between "Bairro de Alvalade" in Lisbon and other cities. Areas in **(A)** "Bairro de Alvalade" and **(B)** Amsterdam (Costa, 2005). Buildings in **(C)** "Bairro de Alvalade" and **(D)** Berlin (Costa, 2005). **(E)** Primary school as a central element (City Hall)[1].

Firstly, the main characteristics of the buildings that belong to the area of "Alvalade" are analyzed in this work, whereas the detailed information regarding the constructive details and material used in these buildings is presented in Milosevic et al. (2018a). Initially, a database was prepared in a Geographic Information System (GIS) with the ArcGIS® program (ESRI, 2014; **Figure 3A**).

"Alvalade" area consists of a total of 1975 buildings and most of this stock, about 72%, represent the mixed masonry-RC cases, while "just" RC constitute 17%, and the remaining 11% belong to stone masonry buildings.

The urbanization of "Alvalade" began with the construction of houses which belong to the program of low rental housing located in cells I and II (between 1947 and 1950, **Figure 4A**) including the construction of 302 buildings (2,066 apartments) with three or four floors (two apartments per floor) without elevator. The construction of those two cells was divided in four constructed groups. The buildings in the first three groups were built with rubble stone masonry with hydraulic mortar for the exterior walls and brick masonry for the interior walls. In the last group, walls were built with hollow or massive concrete blocks masonry because of effective cost control. Floor and roof structures were made by timber beams, excepting for kitchen, bathrooms and stairs, where RC slabs were used.

Cell III from "Alvalade," was planned to be the commercial area of the neighborhood (**Figure 4B**). Cell IV is a predominantly area of single family houses in "Bairro de Alvalade," and their planning was conducted between 1948 and 1950, according to the indications of the urban plan (**Figure 4C**).

The construction of economic rent houses on cells V and VI was developed between 1949 and 1956. Cell V (**Figure 4D**) comprises about 108 buildings and the urbanization of this housing project was finalized in 1954. Furthermore, in the same year, the construction of 62 more buildings was planned for the cell VI (**Figure 4D**). It should be mentioned that, by then, the construction of Economic rent houses in "Bairro de Alvalade" started to decline, and only 42 buildings were built, representing about the 2/3 of the planned program. This period marks the end of the Economic rent houses in "Bairro de Alvalade."

Cell VII was developed between 1949 and 1951 and corresponding to a very fine quality architecture developed in "Alvalade" (**Figure 4E**). The design of the buildings is like the design of the Economic Rent Houses; however, these buildings are slightly larger, allowing for more spacious rooms, and have larger balconies. In cell VIII the project for mixed masonry RC apartment buildings was developed between 1949 and 1952 (**Figure 4F**). This project starts to integrate the architecture developed in "Alvalade" with an image closer to Modern European architecture. In those buildings, RC columns and slabs have important visual impact on the façades.

## STRUCTURAL CHARACTERIZATION OF BUILDINGS

The detailed structural characterization as well as the data need for the study of their structural seismic behavior of these buildings, from the "Bairro de Alvalade," are available in Milosevic et al. (2018a). The information given in this section would provide only the principal structural characteristics of the typology under examination.

---

[1] Available online at: http://cm-lisboa.pt/en (Consulted in 2015).

**FIGURE 4 |** Buildings from different cells. **(A)** Buildings in Cells I and II. **(B)** Buildings in Cell III. **(C)** Buildings in Cell IV. **(D)** Buildings in Cell V and VI. **(E)** Buildings in Cell VII. **(F)** Buildings in Cell VIII.

## Foundations

The typical foundation system was made with very stiff stone masonry and with hydraulic mortar. The foundation works as a thick continuous wall, which was enlarged in its base with a minimum depth which varies from 0.3 to 0.5 m, for the hard rock or for other type of terrain, respectively.

Further, in this period, the first RC foundations appear in some buildings, where the reinforced concrete was used: (i) isolated foundation; (ii) foundation below the side walls; or (iii) foundation slab.

## Masonry Walls

Existing exterior, interior and partition walls are constituted by a diversity of materials: rubble stone masonry (**Figure 5A**), solid or hollow brick (**Figure 5B**) and concrete block (**Figure 5C**) with hydraulic or cement mortar.

Typically, façade walls are rubble stone or brick masonry, as well as mixed rubble stone and brick with two types of mortar: hydraulic or cement. In some rare cases, concrete block masonry can also be found as a material for the façade walls. In general, these walls are characterized with reduction of the thickness in height of the buildings.

As concern the side walls, the same materials and analogous changes of the thickness in height as for the façade walls were used. The use of concrete blocks with cement mortar (cement:sand = 1:2) in the side walls started likewise to be used in this type of buildings.

For the buildings under study, together with the variation of the thickness of the walls, the type of materials may also vary in height. Namely, in case of the interior structural walls, solid brick was used for the lower floors, particularly for the first floor and basement, together with the staircases; on the other side, hollow brick was implemented in the upper floors. Still, exception appears in area of "Alvalade," mainly in Cell I and II, where the solid brick was used only for the walls around services stairs in the ground floor, which give the access from the back façade.

In the transition period, the wood as a material for the partition walls practically was eliminated, except in the case of attics or mansard or in the case of the certain conditions which do not permit the use of more durable material.

It should be mentioned that material used in the case of the basement' walls, when in the contact with the soil, was rubble stone and hydraulic mortar; in the parts which were placed below the ground level impermeable and resistant coating was used as covering on one side.

It should be mentioned that only in exceptional cases these buildings are not placed into the blocks. Thus, aggregate condition should be considered for the seismic assessment of an individual building that compose the block. Moreover, cases when the buildings share the side walls or not, should be also analyzed in detail, since that both situations can appear in these structures.

Finally, the connections between walls (interior/exterior; exterior/exterior) are probably one of the main weakness of these buildings when subjected to seismic actions. Namely, connection

**FIGURE 5 |** Masonry walls with different type of materials. **(A)** Rubble stone, **(B)** Brick, **(C)** Concrete block, **(D)** Connection between walls.

between the exterior and interior walls cannot be considered as appropriate, since that such walls were built with different materials; thus, vulnerability of this connection is increasing due to the difficulties of interlocking the different masonry units (e.g., rubble stone and brick). Moreover, even if the materials between exterior walls were the same, the connection cannot be considered completely reliable due to the bad quality of masonry at corners (**Figure 5D**), that can be associated to construction of connected walls at different times. In any case, additional *in-situ* inspections and experimental tests are recommended to confirm this issue.

## RC Beams and Columns

The characteristics of RC structural elements, as well as their location, depends on the number of floors in the building. For example, in case of the buildings from Cell I and II (Economic Income Houses, with a rectangular plan configuration), in general, only RC beams at the height of the window, i.e., lintels, are used. These elements avoid, for this typology, the out-plane behavior of the masonry walls, i.e., the activation of local mechanisms.

In the buildings from 3 to 5 floors, slender RC frame structures started to appear at the ground floor when larger spans and open spaces were needed to be used for commercial occupation. Then the concrete frame structure was extended to the exterior structure: on the corners of the building making the connection between the perimetral walls; only on the façade walls structure (front and back); or only on the back façade walls. For example, on "Rabo de Bacalhau" typology the prominent shape of the

building was made with a RC frame structure and concrete slabs.

The reinforcement of the RC structural elements was used in a casuistic manner. There is an evident absence of specific design features in terms of the amount and detailing of the reinforcement to ensure the structural safety and ductility of the system. The concrete used has a low to moderate resistance (varying between C16/20 and C20/25) and was slightly compact, whereas the steel corresponds to the class A235.

## Floors, Roof, and Stairs

There are mainly two types of floors: timber floors and RC slabs. The timber floors (**Figure 6**) are commonly constituted by parallel timber beams, made of Pinus pinaster Ait, spaced about 40 to 60 cm and with sections of $0.08 \times 0.16$ m$^2$ or $0.08 \times 0.18$ m$^2$. The floorboards are placed perpendicular to the timber beams and both elements are traditionally connected by wire nails. The timber floors are presented mainly at the front, in the social and private areas. These constructions represent the last examples of the use of timber floors and they started to be strengthened by peripheral RC beams supported on the exterior masonry walls.

The RC slabs started to be introduced in services areas located on the back of the buildings (kitchens, bathrooms, and balconies). These RC slabs were barely reinforced by steel rods and generally, with only one layer of reinforcement for positive moments; there is no guarantee on the continuity of the reinforcement between spans, thus, the slabs do not work as a continuous floor. RC slabs reinforced in two directions with the 0.10 m thickness were found *in situ*, too. As referred, the type of concrete used varies between
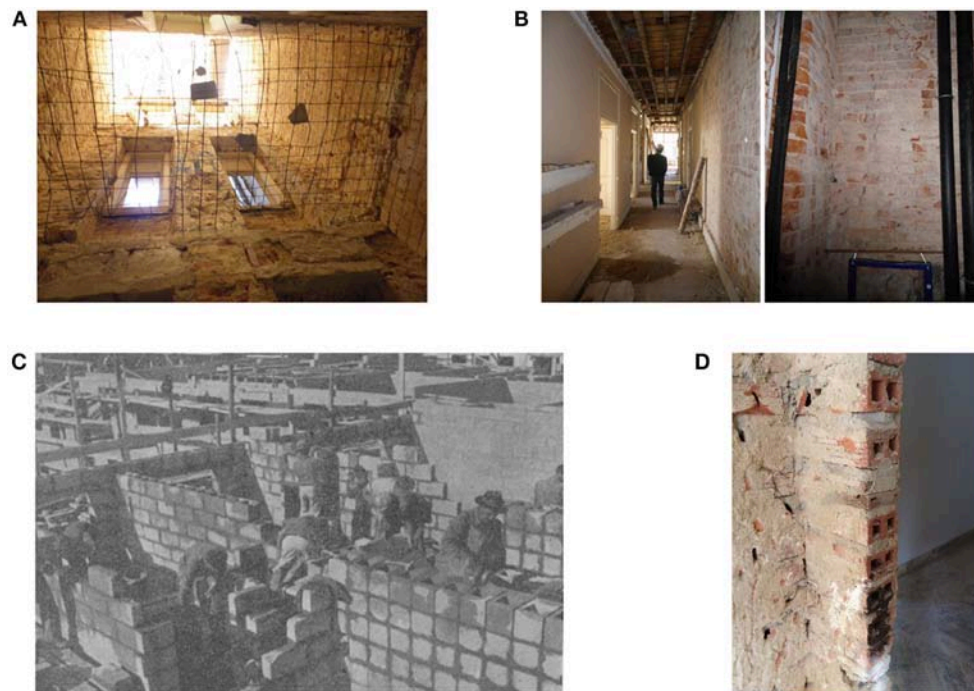
**FIGURE 6 |** Masonry walls with different type of materials: **(A)** Rubble stone, **(B)** Brick, and **(C)** Concrete block.

C16/20 and C20/25, whereas most steel corresponds to the class A235.

The most common types of roof are still the timber framed of Pinus pinaster Ait. **Figure 7**, as in the case of timber floors. The configuration of the timber frames consists of main beams (rafters), mainly disposed parallel to the façade and supported by vertical or diagonals timber elements (**Figure 7**), loading the main internal and side walls. A range of perpendicular beams, distancing from 0.40 to 0.60 m, was placed on top of the main beams to support the Portuguese roof tiles ("Telha Lusa" or "Marseille"). In these buildings started to appear RC roofs: flat roof and alongside the traditional solutions of sloping roof.

The main stairs were made with the concrete or wooden materials and are usually located in the middle of the building. Though, buildings with more than three floors have stairs preferably constructed in RC and with the capacity to install an elevator. On the other side, the buildings with more than four floors, next to the main stairs, have a service staircase with access from the street and built in RC or iron.

## SEISMIC BEHAVIOR OF LISBON MIXED MASONRY-RC BUILDINGS

For the global seismic behavior of buildings four main methods of structural analysis are proposed in more recent codes (e.g., EC8-3): linear static, linear dynamic response spectrum, nonlinear static (pushover) and nonlinear dynamic. Despite one can say that linear dynamic method and nonlinear static methods, are the ones that can be used in common practice, the former is still the most common in engineering offices. For the former, and according the EC8-3 classification, a q-factor approach is followed which request the use of a q-factor value.

In this section values of q-factors are defined for most representative type of mixed masonry-RC buildings. Thus, the case-study corresponds to buildings with rectangular shape, characterized by the similar type of material and similar structural elements (i.e., more standardized when compared with "Rabo de Bacalhau" type) and located mainly in Cell I and Cell II of "Alvalade" area.

The values of q-factors are defined from the pushover curves considering different sources of uncertainties that influence the global seismic behavior.

## Case Study

The case study consists of three floors, constant in the height, with two flats per floor. They are with rectangular shape with overall dimensions 17.50 m by 6.40 m. **Figure 8** illustrates some original archive drawings of the cut section and plan view of the building, together with the front and back façades. Façade walls thickness is 0.50 m on the ground floor, while they are thinner at the upper levels (walls thickness on the last floor is 0.40 m); side walls are with the thickness of 0.50 m without openings, constant in height. Rubble stone masonry and hydraulic mortar characterize the exterior walls (façades and side walls), whereas the interior walls were built mainly with hollow bricks and cement mortar. Only walls around the services stairs in the ground floor and intermediate walls of the stairs below the first floor were built with solid bricks.

The part on the façades below the window in each floor was constructed with hollow brick with 0.15 m thickness. RC elements are placed on the external walls, which are strengthened (belted) on all floors by RC beams at the height of the window lintels with the thickness of the wall and 0.20 m in height; small RC lintels were found of each doorway. There are two types of floor construction used in these buildings: timber floors in the rooms and concrete floors in the services areas. On the ground floor, below the part where the timber floor exists, there is the "ventilation box" in order to provide the air circulation and to avoid accumulation of moisture below the floor.

## Modeling and Definition of Uncertainties

For case study, only the global seismic response is considered, whereas the local flexural behavior of floors and the out-of-plane walls' response are not explicitly computed as, according to the authors opinion it is not relevant. This is due to the presence of RC ring beams which reduce the vulnerability to the out-of-plane failure modes of masonry walls.

The global response of the buildings is examined through the equivalent frame modeling approach, using 3Muri

**FIGURE 7 |** Timber roofs.
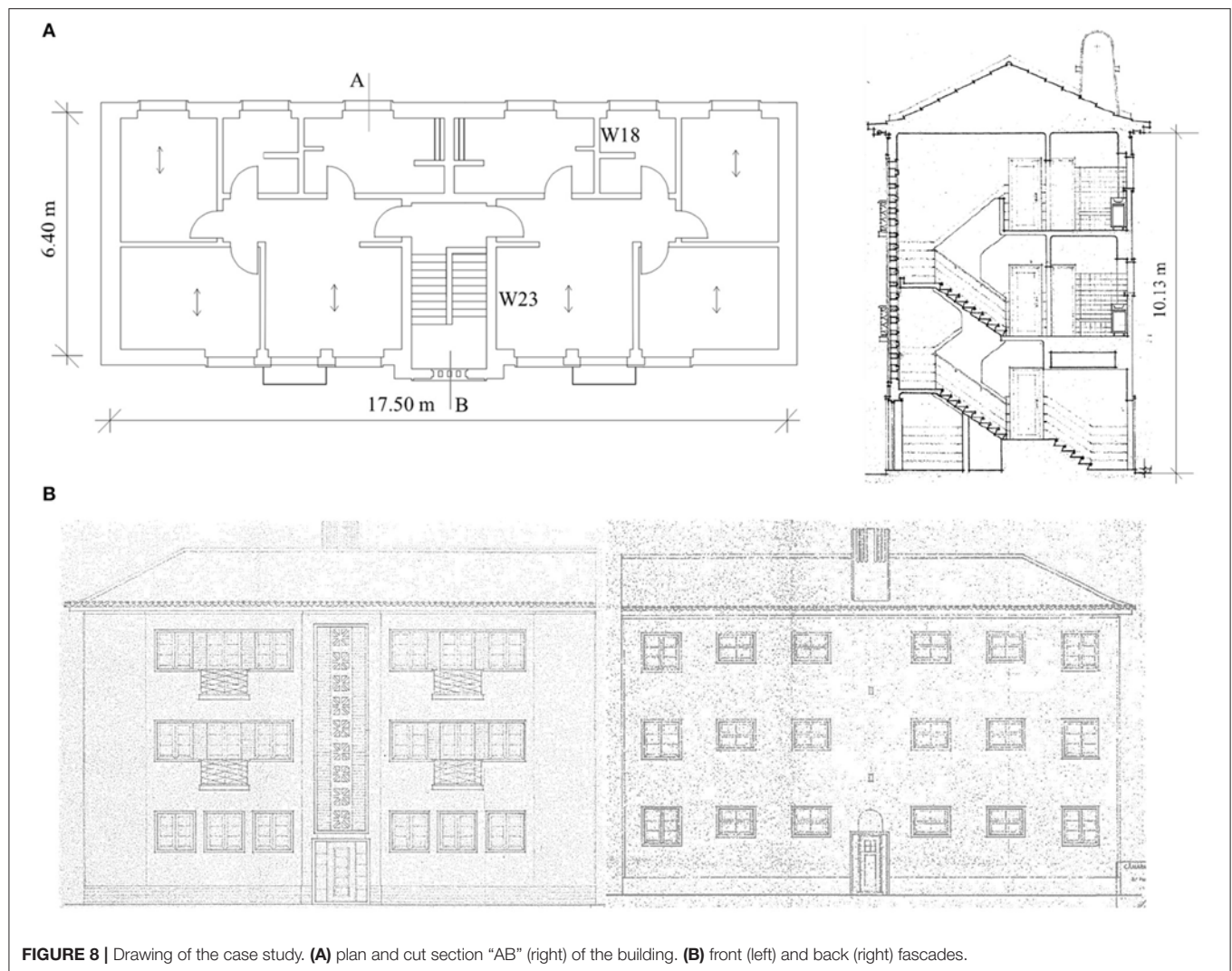


**FIGURE 8 |** Drawing of the case study. **(A)** plan and cut section "AB" (right) of the building. **(B)** front (left) and back (right) fascades.

Tremuri program (3Muri[2]; Lagomarsino et al., 2013) and by performing nonlinear static analysis. The nonlinear response of masonry panels, concentered at walls divided into piers and

spandrels, is described through nonlinear beams characterized by piecewise-linear law (Cattari and Lagomarsino, 2013a). For the definition of the backbone curve, the elastic response is described regarding to the beam theory by defining the initial Young (E) and Shear (G) modulus of masonry. Afterwards, the

---

[2]3Muri Program, S.T.A.DATA s.r.l., release 5.0.4.

**TABLE 1 |** Parameters adopted for sensitivity analyses in terms of aleatory uncertainties.

| Set Pk | Variable | $X_{min}$ | $X_{median}$ | $X_{max}$ |
|---|---|---|---|---|
| $X_1$ | E [GPa] | 0.69 | 0.82 | 0.98 |
| | G [GPa] | 0.23 | 0.27 | 0.33 |
| | $f_m$ [MPa] | 2.07 | 2.33 | 2.63 |
| $X_2$ | $\tau_0$ [MPa] | 0.064 | 0.077 | 0.092 |
| $X_3$ | E [GPa] | 2.3 | 2.95 | 3.73 |
| | G [GPa] | 0.77 | 0.98 | 1.24 |
| | $f_m$ [MPa] | 1.45 | 1.66 | 1.89 |
| $X_4$ | $\tau_0$ [MPa] | 0.24 | 0.28 | 0.32 |
| $X_5$ | $\theta_{P,S3}/\theta_{P,S4}/\theta_{P,S5}$ | 0.0023/0.0039/0.0056 | 0.0029/0.0049/0.0069 | 0.0037/0.0061/0.0084 |
| | $\theta_{P,F3}/\theta_{P,F4}/\theta_{P,F5}$ | 0.0046/0.0078/0.0120 | 0.0058/0.0098/0.0147 | 0.0074/0.012/0.01796 |
| | $\beta_{P,S3}/\beta_{P,S4}/\beta_{P,F3}$ | 0.6/0.25/0.8 | 0.7/0.4/0.85 | 0.8/0.55/0.9 |
| $X_6$ | $\theta_{S,S3}/\theta_{S,S4}/\theta_{S,S5}$ | 0.0015/0.0045/0.015 | 0.0019/0.0058/0.0194 | 0.0025/0.0075/0.025 |
| | $\theta_{S,F3}/\theta_{S,F4}/\theta_{S,F5}$ | 0.0015/0.0045/0.015 | 0.0019/0.0058/0.0194 | 0.0025/0.0075/0.025 |
| | $\beta_{S,S3}/\beta_{S,S4}/\beta_{S,F3}$ | 0.4/0.4/0.4 | 0.6/0.6/0.6 | 0.8/0.8/0.8 |
| $X_7$ | $k_0 - k_{el}$ | 0.5 – 1.25 | 0.65 – 1.50 | 0.8 – 1.75 |
| $X_8$ | $G_{timber}$/ [MPa] | 6.136 | 9.88 | 15.91 |
| $X_9$ | $G_{concrete}$ [MPa] | 1208.3 | 3820.98 | 12083 |
| $X_{10}$ | A [m$^2$] | 0.001 | 0.000282843 | 0.00008 |
| | I [m$^4$] | 0.0005 | 0.000141421 | 0.00004 |
| $X_{11}$ | $p_{floor}$ [kN/m$^2$] | 0.683 | 0.826 | 1 |

*E, Young Modulus; G, shear modulus; $f_m$, compressive strength; $\tau_0$, shear strength; $\theta_{(P, S/F)}$ and $\beta_{(P, S/F)}$, drift and residual strength for piers; $\theta_{(S, S/F)}$ and $\beta_{(S, S/F)}$, drift and residual strength for spandrels (shear, S and flexural, F); $k_0$ - value of the shear for which starts the degradation of stiffness, normalized to the ultimate shear and $k_{el}$ - the ratio between the initial and the secant stiffness; $G_{eq,timber\ floor}$ and $G_{eq,RC\ floor}$, equivalent shear modulus for timber and RC floor, respectively; A and I, area and moment of inertia of "equivalent" beam*

**TABLE 2 |** Gravity and variable loads.

| Gravity loads G  (*Variable loads Q) [kN/m$^2$] | |
|---|---|
| Timber floor | 1.10 (*2.0) |
| RC floor | 3.78 (*2.0) |
| RC staircase | 3.78 (*3.0) |
| Roof | 1.15 (*0.4) |
| Balcony | 3.78 (*5.0) |

progressive degradation is approximated using a secant stiffness. The elastic values are defined by multiplying the secant stiffness by a coefficient ($k_{el}$), which values are defined in **Table 1**. The progression of nonlinear response is associated with increasing levels of damage, by assigning progressive strength drops ($\beta_{Ei}$) at predetermined drift levels ($\theta_{Ei}$), associated with the achievement of reference damage levels (DL) (from 1 to 5, i.e., DL1–slight; DL2–moderate; DL3–extensive; DL4–near collapse; DL5–collapse).

The maximum shear and bending strength are defined assuming the criteria proposed in codes and literature by considering the occurrence of different failure modes: shear, flexural and mixed.

For the diagonal shear cracking, the criterion proposed by Turnšek and Sheppard (1980) is adopted, while for the flexural behavior, the one proposed in Lagomarsino et al. (2013) is considered, combining both, the compressive and bending failure. Reinforced concrete elements are modeled as nonlinear

beams by assuming elasto-perfectly plastic hinges concentrated at the end sections (Cattari and Lagomarsino, 2013b). Diaphragms are modeled as an equivalent membrane with an equivalent thickness of 0.022 m and characterized by normal stiffness represented by Young Modulus in the main warping direction $E_{1,eq}$ (29 GPa), and $E_{2,eq}$ in the perpendicular direction (12 GPa) and in-plane shear stiffness related to the shear modulus $G_{eq}$ (0.00988 GPa). For the RC slabs, the values adopted in the modeling are $E_{eq} = 29$ GPa, equal in both directions and $G_{eq} = 12$ GPa.

Concerning the uncertainties, two types are considered: aleatory (related to the mechanical parameters) and epistemic (related to the structural details). In terms of aleatory uncertainties, eleven variables are considered for the execution of the sensitivity analyses (2N+1, N corresponds to the number of variables or group of variables, defined in the following). These variables include mechanical properties in terms of Young modulus, shear modulus and compressive strength of rubble stone and hollow brick masonry (X1 and X3, respectively) and shear strength of rubble stone and hollow brick masonry (X2 and X4), then the parameters which control the drift and strength decay of piers and spandrels, respectively (X5 and X6), the parameters which control the degradation for the initial elastic stiffness (X7), the parameters connected to the stiffness of the timber and RC floor, respectively (X8 and X9), the parameters which control the connection between external walls (X10) and the parameters which control the different thickness of the reinforced concrete slab (X11). To each variable,

**FIGURE 9 |** Pushover curves: **(A)** Model A; **(B)** Model B.
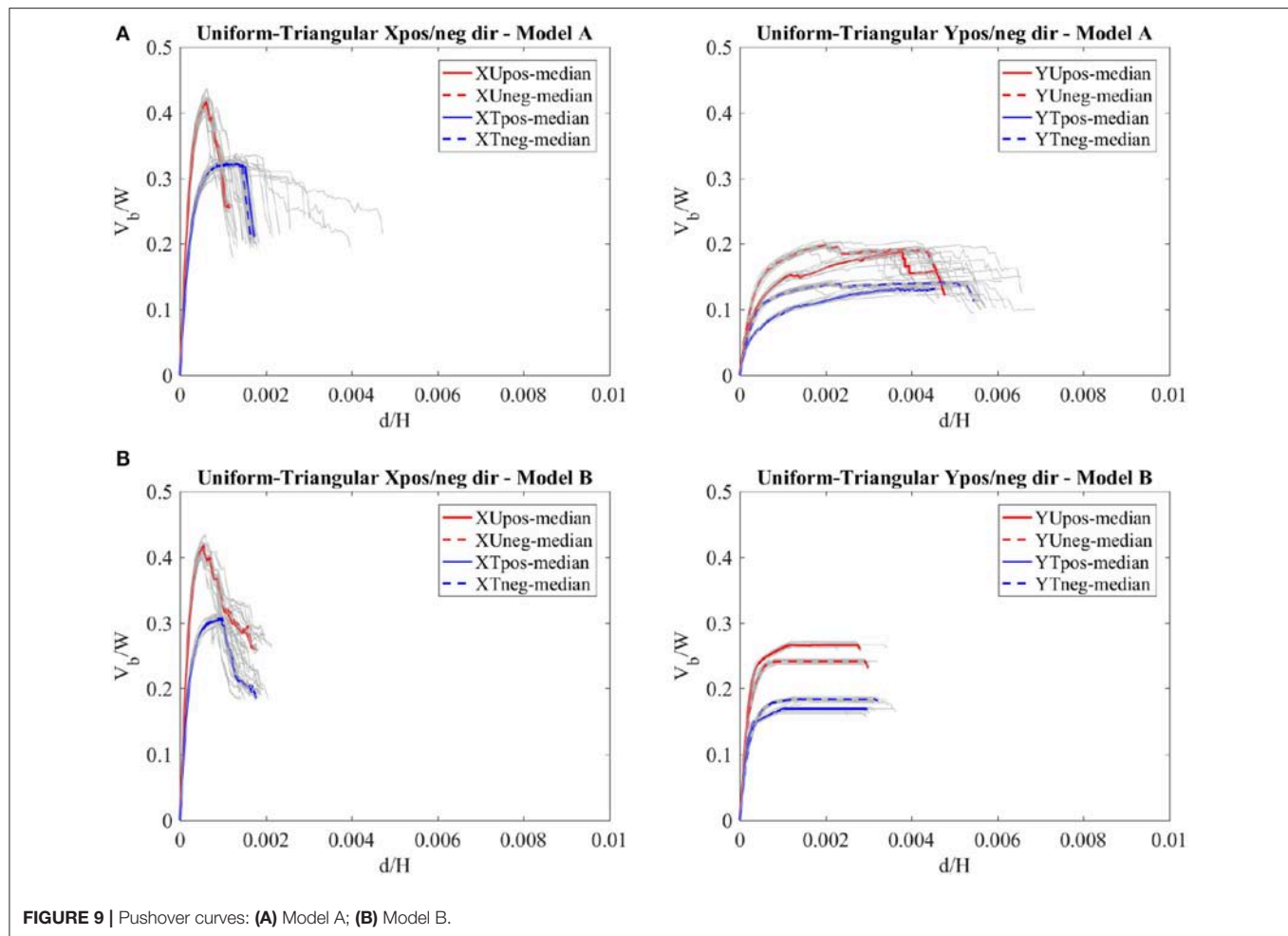
it is defined a plausible range of variation - a minimum value ($X_{low}$), a median one ($X_{mean}$) and maximum value ($X_{up}$) - used for the proceeding of the sensitivity analysis. The mechanical properties were defined based on the values from Italian standard and on the values obtained from experimental tests performed on the buildings, similar as the one under the examination. Detailed explanation about the procedure how the parameters were defined can be found in Milosevic et al. (2018a). **Table 1** represents the aleatory variables considered as the most relevant and included in the sensitivity analyses. **Table 2** includes the gravity and live loads adopted for the examined building. The values related to drift limit and strength degradation are adopted from the experimental tests available in the literature.

As referred in the previous section, one of the main problem for buildings from these typology is the connection between exterior/exterior and exterior/interior walls, as well as between walls and floors. Thus, epistemic uncertainties considered in this study are related on the connections between exterior/interior walls. Due to this, two models have been adopted: (i) model with bad connections between exterior/interior walls and intermediate connections between exterior/exterior walls

(model A) and (ii) model with good connections between walls (model B). In order to simulate bad connections between exterior/interior walls, the automatic mesh generated by 3Muri[2], was modified by introducing equivalent elastic beams connecting nodes at intersections. On the other hand, to model good connections between the walls, the equivalent beams assume values resembling a rigid link. It worth to mention that connection between exterior/exterior walls and between walls and floors, were considered as aleatory uncertainties, i.e., X10 and X8/X9, respectively. Detail description about the calibration of the effectiveness of the wall to wall connections could be found in Milosevic et al. (2018a,b). The model A is considered as more representative and realistic; nevertheless, the q-factor is provided for both models (see section Structural Behavior Factor).

## Pushover Curves

Nonlinear static (pushover) analyses were performed by considering each main direction (X and Y) in both senses (positive and negative) and two load patterns distributions (uniform, proportional to the mass, and triangular, proportional to the product between mass and height), as recommended in

**FIGURE 10 |** Example of the final position of DLi in the pushover curve in the X **(A)** and Y **(B)** directions (W23L3 stands for wall 23 in the 3rd floor and W18L1 for wall 18 1st floor–see **Figure 8A**).
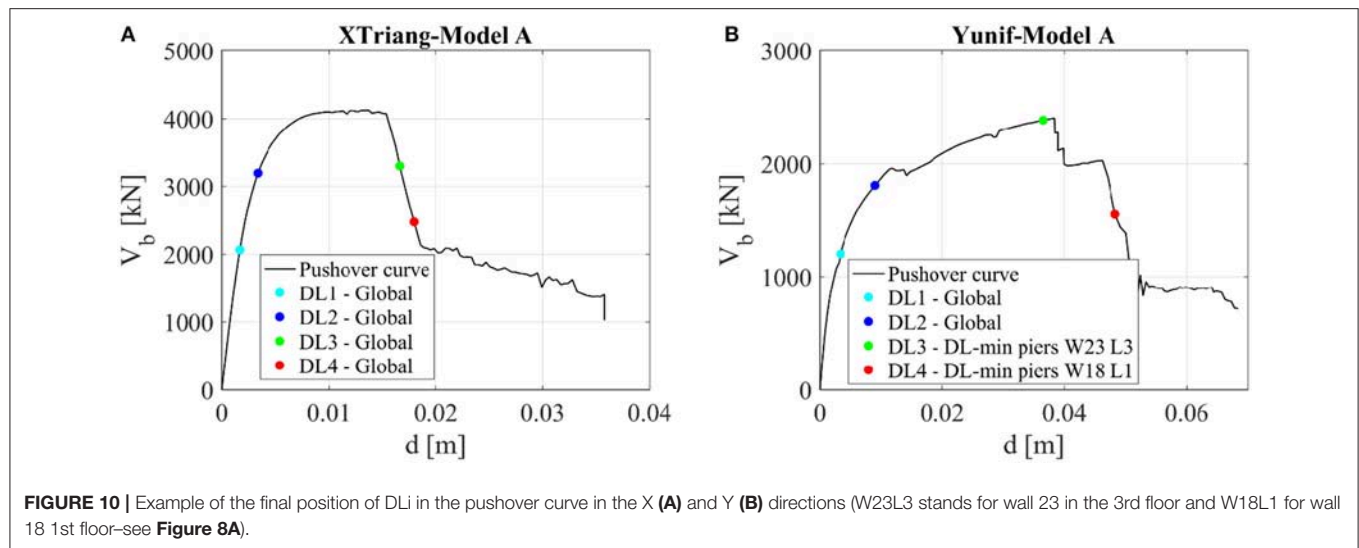
EC8 and NTC. The load distribution was adopted regarding the conclusions presented in the previous study performed on similar types of buildings (Cattari et al., 2015b). However, regarding the results obtained from nonlinear dynamic analyses, which is out of scope of this paper, the more comprehensible load patterns for buildings under study was defined for each direction, i.e., in case of the X direction the more appropriate load pattern is the triangular, whereas in the case of Y direction, uniform load pattern has better correspondence with nonlinear dynamic analyses. For detailed results see Milosevic et al. (2018b). Control node was selected at the top level in the wall that first collapses, as recommended in Lagomarsino and Cattari (2015).

**Figure 9** represents the normalized pushover curves in case of both analyzed models for each main direction and both load distributions. The overall base shear is normalized to the total weight W, while the top displacement d to the total height H of the buildings. The pushover curves depend, among others, on the material's strength, deformation capacity of each structural element and on the structural details. In the present study, the values of mechanical parameters are varied between min-median-max values, together with the two different models in terms of the connection between walls, series of the pushover curves are obtained (**Figure 9**). In total 184 analyses were performed for each defined model (A and B). Next to the pushover curves obtained by median values of mechanical parameters (red and blue for uniform and triangular load distribution, respectively), pushover curves obtained for all models (represented in gray color) considered in the sensitivity analysis are also presented; in this way, it is possible to observe the variability of the behavior of the structure, considering different values of mechanical parameters. According to **Figures 9A,B**), which refers to Model A, it is possible to observe that both, stiffness and base shear capacity are higher in case of the X direction for both load patterns, whereas the higher ductility is obtained for Y direction due to the flexural behavior (damage) of the walls in such direction. Comparing the two load patterns considered in the analysis, it is worth highlighting that in

both directions the uniform pattern distributions gives higher capacity, whereas the triangular pattern distributions leads to higher ductility, mainly in X direction. Concerning the median pushover curves obtained in positive and negative directions, there is no such a big difference, particularly in the X direction, due to the symmetry of the buildings. However, based on the results obtained for all performed analyses, the dispersion in the displacement is more emphasized in case of the triangular load distribution. Namely, the values adopted for drift in case of piers for different DLi (group X5, **Table 1**) are the ones that significantly affect the final ductility of the buildings (**Figure 9A**).

As concern the Model B, similar conclusion as to the Model A is reached: bigger strength is obtained in case of the uniform load pattern for both analyzed directions. Comparing the Model A and Model B, obtained base shear is higher for the latter one, particularly in case of the Y direction, where the bad connections between walls were mainly considered (Milosevic et al., 2018a). These results are showing: (i) the importance of improving the connections between exterior/exterior for this typology; and (ii) the need to perform the seismic analysis considering the bad connections between walls.

Based on the more appropriate load pattern defined for each direction (Milosevic et al., 2018b), only the correspondent results are presented in the following and, consequently, the behavior factor is obtained for such cases (see section Structural Behavior Factor).

It should be mentioned that pushover curves are presented only until the value of the ultimate displacement ($d_u$), i.e., displacement which corresponds to Damage Level 4 (see section Definition of Limit States).

## Definition of Limit States

The evaluation of damage levels (DLs) (assuming to have a direct relation to Limit States, LSs) from nonlinear static analysis is not an easy task, and different approaches may be adopted. For instance, in the Eurocode 8 (CEN Eurocode

**FIGURE 11 |** Parameters for the definition of the behavior factor q (F base shear, d displacement at a control point).
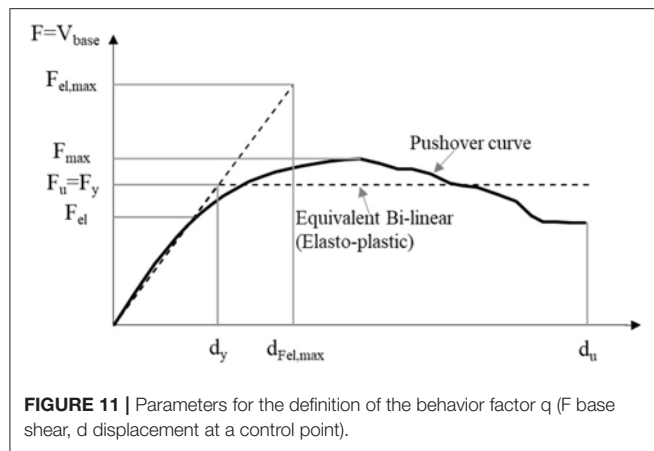
8, 2004) a heuristic approach is followed, where LSs are defined based on conventional limits directly defined on the pushover curve, usually in terms of decay percentage or reaching of the maximum value of the overall base shear.

Though, in case of existing old masonry or mixed masonry-timber and masonry-RC buildings, application of this approach may lead to untrustworthy results. In fact, while in case of a box-type behavior with in-plane almost rigid floor behavior it is realistic to assume that many structural elements and walls reach almost at the same time a certain damage level (DLi), in case of existing buildings with timber floors this condition is far to be true due to the existence of flexible floors. In fact, for unreinforced masonry buildings (URM) with flexible diaphragms, the limited load transfer between vertical elements leads to a more independent behavior of the walls. Consequently, the reaching of serious damage in a wall may not appear evident on the global pushover curve, when this wall offers a small contribution to the total base shear force.

Aiming to monitor the occurrence of significant damage in parts of the structure that may not be evident in the pushover curve, Lagomarsino and Cattari (2014) and Lagomarsino and Cattari (2015) proposed a multi-scale approach to define DLs on the pushover curve that defines the behavior of the buildings at three scales: (i) local, with damage on structural elements, piers and spandrels, (ii) macro-elements (like masonry walls or floors) and (iii) global (represented by the pushover curve).

In the presented work, damage levels (DLi, i = 1 … 4) are defined by taking into account the different scales considered. It may be mentioned that reference is made to the attainment of damage levels 2, 3, and 4 assumed to correspond respectively to the Damage Limitation, Life Safety and Near collapse as defined in the part 3 of Eurocode 8 (CEN Eurocode 8, 2005). According to the multi-scale approach, the DLi is defined by the minimum displacement threshold obtained from the verification of conventional limits at the three scales, explained briefly in the following:

i. Local scale: related with the assessment of the cumulative rate of damage in piers that reach DLi in accordance to the element multi-linear constitutive law (Lagomarsino and Cattari, 2015);

ii. Macro-element scale: comprehends the verification of inter-story drift limits in each wall and level ($\theta_{DLi}$) or the angular strain ($\gamma_F$) (in case of floors assumed as flexible);

iii. Global scale: described as a function of a rate ($k_G$) of the maximum base shear force ($V/V_{max}$). In this study, the following limits are considered: 0.5 for DL1, 0.75 for DL2, 0.8 for DL3 and 0.6 for DL4.

For the macro-element scale, a new formulation is adopted in this study, as proposed by Marino et al. (2018). It refers to the attainment of a given DL on all piers located on a story at a certain level with the aim of checking the occurrence of a soft-story mechanism.

**Figure 10** presents the final position of DLi in the pushover curve in X and Y directions for the Model A and the for the most representative cases in terms of load pattern distributions.

## Structural Behavior Factor

The determination of the expected behavior factor (q-factor according to the part 1 of Eurocode 8 (CEN Eurocode 8, 2004), for existing buildings is of great importance from the engineering point of view. Indeed, as linear analysis are still the most used in various countries and well-known among practicing engineers, suggesting adequate values of q-factors would contribute for a more predictable seismic structural performance of existing building stock.

According to EC8-1, the q-factor is a "factor used for design purposes to reduce the forces obtained from a linear analysis, in order to account for the non-linear response of a structure, associated with the material, the structural system and the design procedures." EC8-1 clear refers that q-factor is estimated approximately as "the ratio of the seismic forces that the structure would experience if its response was completely elastic with 5% viscous damping, to the seismic forces that may be used in the design, with a conventional elastic analysis model, still ensuring a satisfactory response of the structure." The evaluation of the behavior factors for different types of masonry buildings have been carried out by different authors (e.g., Benedetti and Castoldi, 1982; Benedetti et al., 1984, 1998; Tomaževič and Weiss, 1994; Tomaževič, 1999; Tomaževič et al., 2004) performing static and dynamic experimental tests. Moreover, considering the probabilistic approach Thomos and Trezos (2005) have been derived the behavior factor for reinforced concrete structures. However, neither of these structures correspond completely to the structures under investigation. Indeed, a lot of variety exist in terms of material and structural elements and in principle q-factor should be defined for each typology.

In the presented casestudy, q-factor is estimated based on nonlinear static sensitivity analysis. After having defined the pushover curves (section Pushover Curves), DLis (explained in section Definition of Limit States) were defined on each pushover curve. Then Intensity measure for each damage level (IM$_{DLis}$), in terms of the peak ground acceleration (IM$_{DLis}$ = a$_{g,DLis}$), were computed (adopting the capacity spectrum method) for each pushover curve and each damage level, defined on such pushover curve (as demonstrated in **Figure 10**). Finally, after the definition of all these data, the q-factor was calculated following different
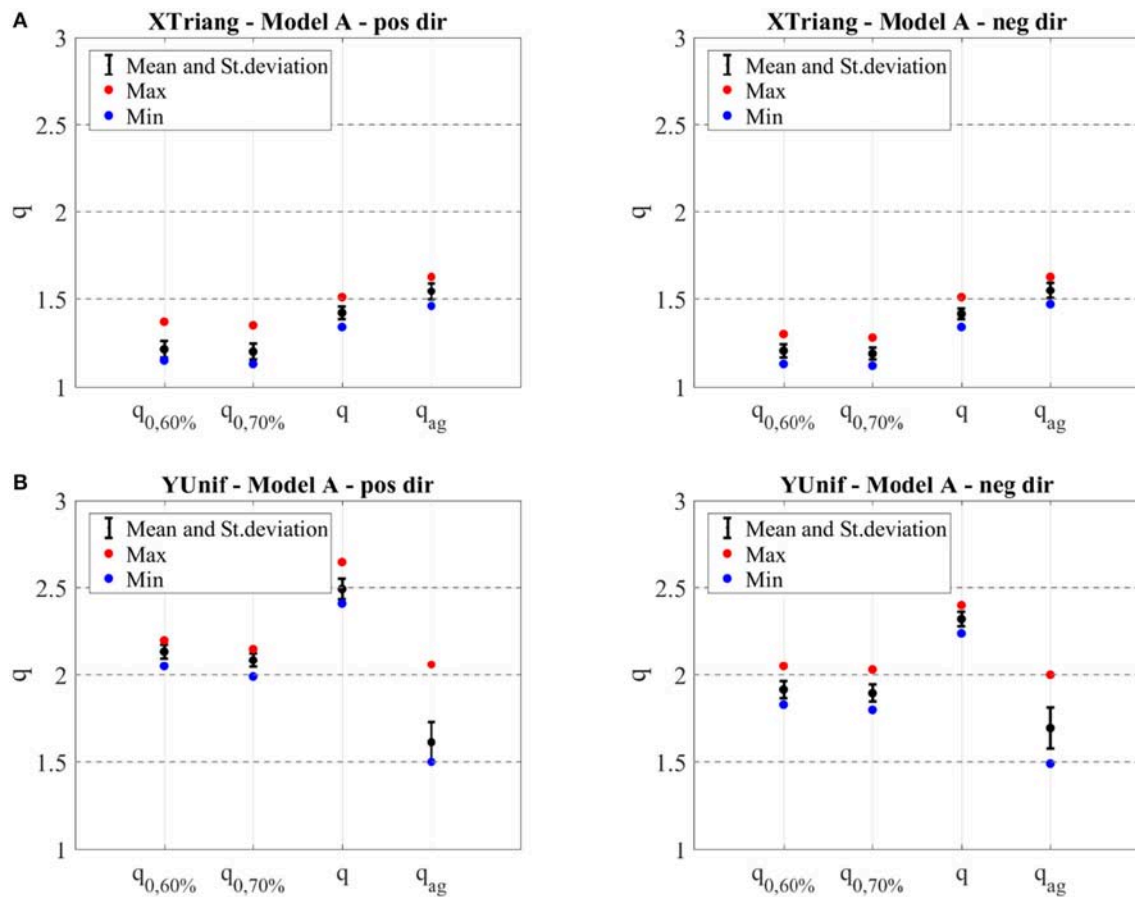
**FIGURE 12 |** Mean, maximum and minimum values and standard deviation of the behavior factor for X **(A)** and Y direction **(B)** for Model A. Doted lines represent the values proposed by NTC Italian Code for Structural Design (2008).

criteria. It should be mentioned that, despite all values have been evaluated, only median, min and max values (obtained between the analyzed models) for q-factors are presented (**Figure 12**).

In the following, adopted criteria are briefly explained:

● **Criterion 1:** The typicalcriterion to evaluate the q-factor is defined according to Equation (1) and the response of the structure is represented by a pushover curve F-d (base shear vs. control displacement).

$$q = \frac{F_{el,max}}{F_y} = q_0 \qquad (1)$$

$F_{el,max}$ is the ideal elastic base shear response and $F_y$ corresponds to the strength of an ideal bi-linear system equivalent to the "true" nonlinear behavior. The bilinear system is defined considering (i) an equivalent initial stiffness defined following the suggestion of Bondarabadi (2018) and NTC (NTC Italian Code for Structural Design, 2008), as the secant stiffness in the first point of the seismic resistance curve attaining 60% ($F_{y,60\%}$) and 70% ($F_{y,70\%}$), respectively, of the maximum lateral strength. This was adopted with the aim to

analyze how q-factor is influenced by the definition of $F_y$; (ii) the equal displacement rule (same $d_u$); and (iii) equal areas below idealized equivalent elastic-plastic relationship and the nonlinear pushover curve. With this equivalence criterion, the strength $F_y$ is usually slightly lower than the maximum resistance $F_{max}$ (**Figure 11**) but can be considered an estimate of the ultimate base shear capacity of the structure. $F_{el,max}$ is the maximum seismic base shear developed in a completely linear elastic structure.

Nevertheless, the definition of the q-factor should then consider an overstrength ratio (OSR). The force $F_{el}$ (**Figure 11**) represents the base shear at which the first structural element would reach its strength capacity (shear or flexural) according to a linear elastic analysis. Beyond this elastic limit, a restricted deformation capacity into the nonlinear regime is still available, sufficient to allow the structure to withstand an increasing seismic load, by increasing the forces on other structural elements (redistribution of seismic loads). Thus, ultimate strength capacity ($F_{max}$ or $F_y$ for a bilinear idealization of the response) is reached for values of base shear that are higher than $F_{el}$.
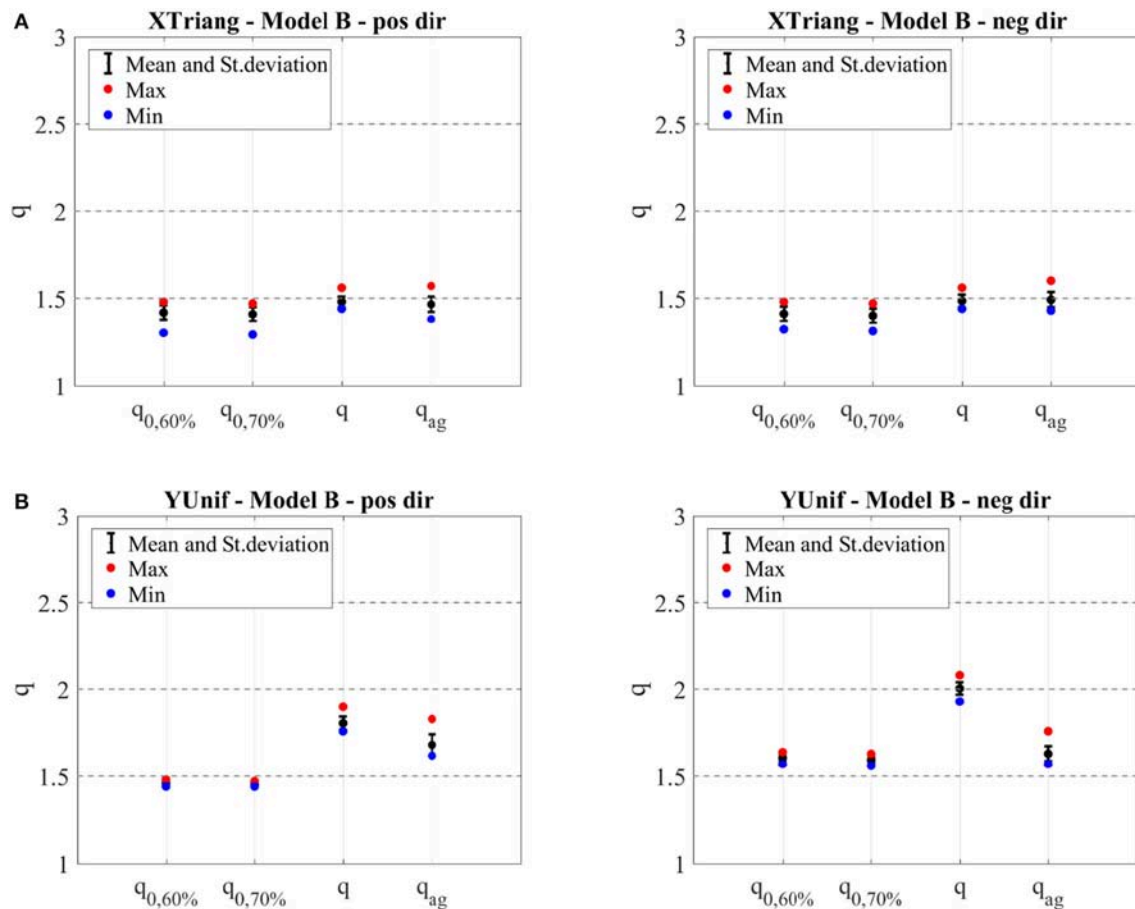
**FIGURE 13 |** Mean, maximum and minimum values and standard deviation of the behavior factor for X **(A)** and Y direction **(B)** for Model B. Doted lines represent the values proposed by NTC Italian Code for Structural Design (2008).

Then, a correct definition of q-factor would be then:

$$q = \frac{F_{el,max}}{F_{el}} = \frac{F_{el,max}}{F_y} \frac{F_y}{F_{el}} = q_0 \, OSR \qquad (2)$$

- **Criterion 2:** An alternative criterion to define q-factor consists of its identification with the ratio between the ground acceleration leading the structure to its ultimate limit state and the ground acceleration leading to the elastic limit. In the presented case study, the acceleration which correspond to the ultimate limit state is related to the value of DL4 ($a_{g,DL4}$, explained in the section Definition of Limit States), whereas the value of DL2 is considered as the acceleration to the elastic limit ($a_{g,DL2}$). The q-factor ($q_{ag}$) is calculated as it is presented in Equation 3:

$$q_{ag} = \frac{a_{g,DL4}}{a_{g,DL2}} \qquad (3)$$

It is worth noting that DL1 could also be considered for the definition of the elastic limit of the acceleration; indeed, it is more similar with the concept of the first element that attains the nonlinear behavior. Though, DL2 was adopted as will lead

to q-factor values on the safe side. A discussion about this issue will be presented at the end of the section.

**Figure 12** presents the values of the behavior factor for model A, obtained following the above- mentioned criteria. As can be observed, the values obtained for the examined type of buildings, in case of the X direction are smaller or in correspondence with the minimum value (depends on the criterion) proposed by NTC and EC8 ($q = 1.5$). On the other side, in case of the Y direction, q-factors values match well with the ones recommended by the seismic standards ($q = 1.5$–$2.5$). The values in X direction attained from different criteria are very close, opposite what was found in Y direction, particularly for Model A. Namely, as can be seen in **Figure 12B**), for Model A, in case of the Y direction it is clear a difference between the values obtained for q and $q_{ag}$. This difference is due to the fact that in the first criterion, the q-factor is calculated with the elastic force $F_{el,max}$ (defined for an elastic stiffness), while the values of the q-factor for the second criterion correspond to the stage of the buildings DL4 where the side walls, the structural elements which mainly contributed for the global building's behavior in the Y direction, are damaged. In case of the Model B, the significant difference between these two criteria,
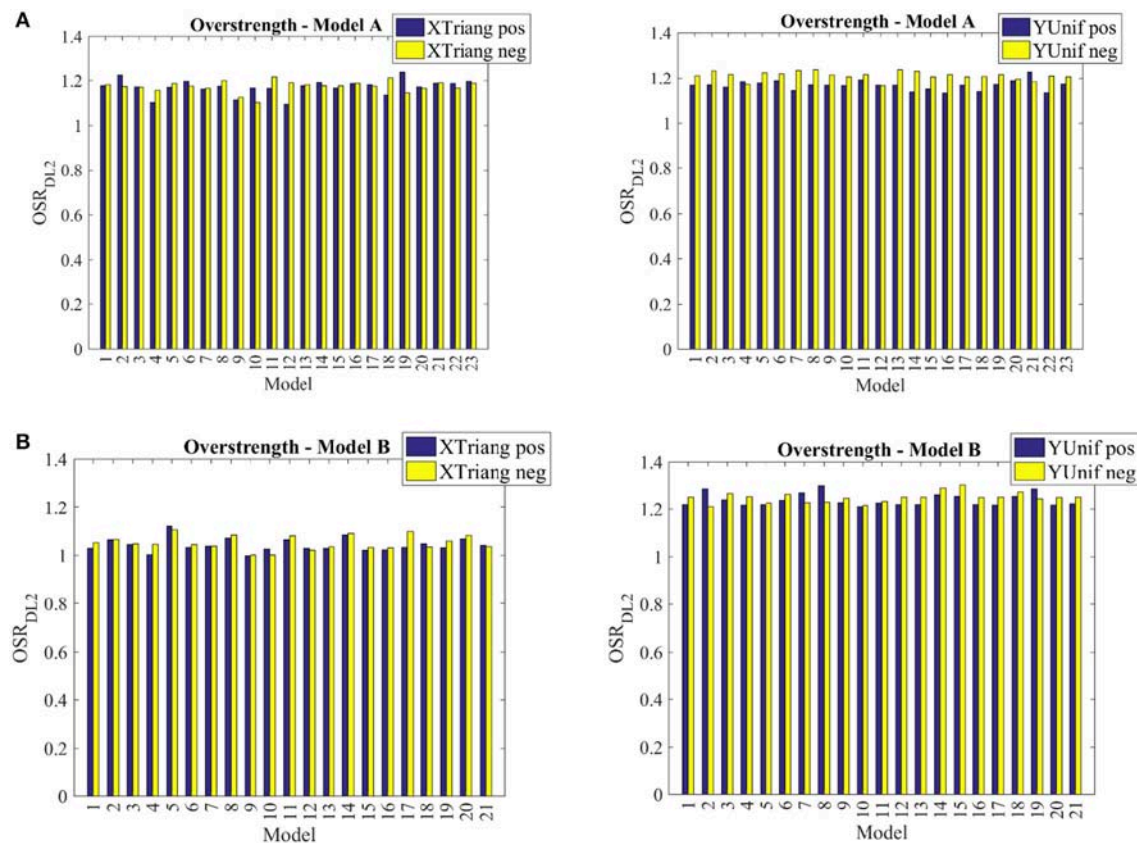
**FIGURE 14 |** Overstrenght for X and Y direction for Model A **(A)** and Model B **(B)** adopting DL2.

does not appear, since that most of the walls have influence on the total base shear and damage is spread through all the walls, even in the stage of DL4.

From the results of **Figure 12**, it is shown that the values of the standard deviation of the behavior factor are greater in Y than in X direction, particularly in case of the second criterion. This is related to the different behavior of the models analyzed in the current study varying the mechanical parameters as abovementioned. In fact, the higher dispersion in terms of capacity was likewise obtained for Y direction (Milosevic et al., 2018b). The difference between the values calculated with $F_{y,60\%}$ and $F_{y,70\%}$ is irrelevant for these typology, as is depicted in **Figure 12**. Finally, regarding all presented conclusions, the values of the behavior factor proposed for the typology under investigation, considering the bad connections between walls are 1.5 and 2 for X and Y direction respectively.

As concern the Model B, the values of the behavior factor are presented in **Figure 13**. The values of q-factor in the X direction are in range with the values defined by Model A. This similarity was expected, since bad connections between walls in such direction are not considered. On the other side, the values in Y direction are different, showing the higher values of q-factor for Model A; this is mainly since Model B (good connections) has higher values of maximum strength (i.e., higher values of

$F_y$), leading to smaller q-factor values. Concerning standard deviation values, higher values are obtained for Model A, as expected.

As it is considered as important parameter which influence the final definition of q-factor, overstrength (OSR) was calculated and the results presented for both models (A and B), and taken into account all the aleatory uncertainties. As known, the OSR depends on a series of factors varying from the structural configuration and associated redundancy to modeling assumptions (Magenes, 2006). In previous studies, OSR has been evaluated numerically (Magenes, 2004; Magenes and Morandi, 2006; Magenes and Menon, 2009), through nonlinear static analyses from nonlinear capacity curves, of several low-rise reinforced and unreinforced masonry buildings. Additionally, experimental evaluation of OSR have been also reported in the literature (Benedetti and Castoldi, 1982; Benedetti et al., 1984, 1998; Magenes and Menon, 2009).

In the current study OSR values were calculated numerically, for all models with good and bad connections for the most representative cases. As it can be noticed, the range of variation of the OSR is not significant (**Figure 14**): in case of the model with bad connections all values are around 1.2, whereas in case of the models with good connections, values are of 1 and 1.2 for X and Y direction respectively. It worth noting that typically,
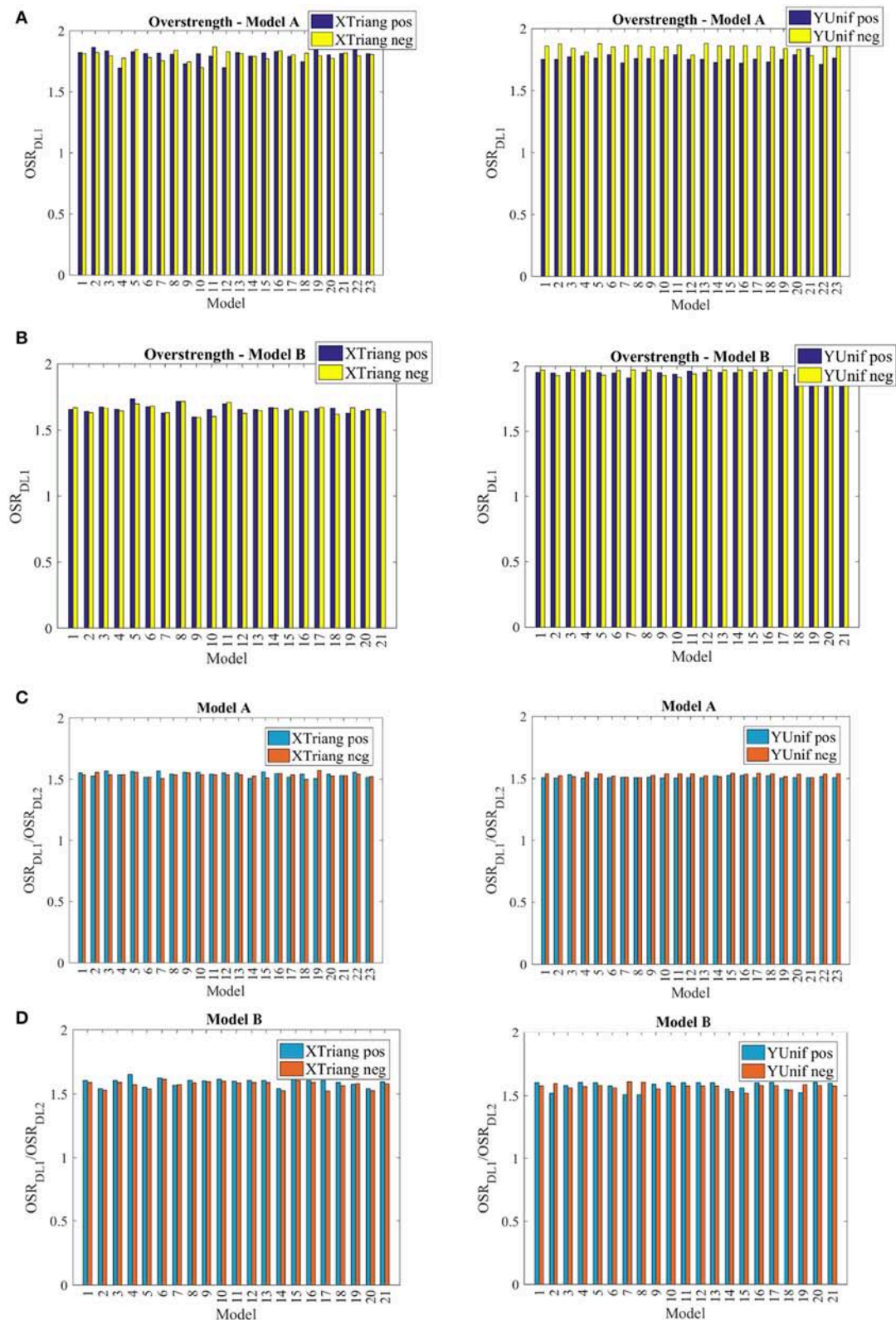
**FIGURE 15 |** Overstrenght for X and Y direction for Model A **(A)** and Model B **(B)** adopting DL1 and ratio between the overstrength defined for DL1 and DL2 for X and Y direction in case of Model A **(C)** and Model B **(D)**.

the unreinforced masonry structures are characterized by higher values of OSR (Magenes, 2006). However, the structures under study are mixed masonry-RC buildings and all reinforced elements are characterized for weak concrete and very low ratios of vertical and transversal steel reinforcement which can decrease, in average, the typical values of OSR in URM buildings (Magenes, 2006). Besides, it is clear that, for the typology under study, OSR does not depend on the variation of the mechanical parameters of the material for this typology.

Based on the results obtained, and according to all assumptions adopted, it is recommended to adopt an OSR = 1.2 for the mixed masonry-RC typology studied.

If DL1 was chosen to define the limit of the elastic behavior, higher values of OSR ($OSR_{DL1}$) are reached. In **Figure 15** the values of $OSR_{DL1}$ are presented, as well as the ratio of $OSR_{DL1}$ and $OSR_{DL2}$. Based on these results, one can say that the OSR would increase of about 1.5 times if DL1 is adopted. Thus, this way, a value of about 1.8 would be recommended for OSR.

## CONCLUSIONS

As well-known, each traditional building typology is unique and the need of an exhaustive understanding and knowledge on the materials of the building and structural details are crucial before performing any type of analysis. In addition, collecting accurate historical information, concerning the building construction chronology is also relevant. Due to this, the first step of the presented research was focused on the understanding the historical background of the typology under study, the mixed masonry-RC buildings existent in Lisbon. Afterwards, information about structural characterization of the buildings was collected and examined and the appropriate values of the mechanical parameters were defined. After collecting all important above-mentioned information seismic behavior of the buildings structures was assessed and the correspondent structural behavior factor defined.

Definition of adequate q-factors corresponds to an important step ahead in the seismic safety and preservation of our constructions, mainly as linear elastic methods are the ones most frequently used in engineering offices. Thus, in the presented paper, the q-factor was defined and values are proposed for the type of mixed masonry-RC building selected: the rectangular type shape mainly located in Cell I and II of "Alvalade" area in Lisbon. This configuration was chosen as it represents one of most representative of mixed buildings in Lisbon. Nevertheless, it is planned to evaluate q-factors to the other types, including all the "Rabo de Bacalhau" plan configurations.

The seismic behavior of the buildings was evaluated by using sensitivity nonlinear (pushover) static analysis, considering both aleatory and epistemic uncertainties, aiming to define, as accurate as possible, the q-factor values. In fact, the presented study indicates that values of structural behavior factor depend most on the type of connections between walls.

Behavior factor was defined considering two different criteria, as explained in section Structural Behavior Factor. Based on all results obtained and herein presented for rectangular shape of mixed masonry-RC buildings case study, one can recommend:

- a q-factor = 1.5 in the direction of façades (X direction) and equal to 2.0 in the direction of side-walls (Y direction);
- not to use the criterion 2 for the definition of q-factor of this type of buildings (this recommendation should be generalized for buildings with flexibles floors in plan but further studies are still required);
- a 1.2 for the OSR value in case when the DL2 is adopted.

It worth noting that the q-values and OSR herein suggested are in the range of the values proposed by EC8 and NTC. Though, if a different damage limit was chosen for the definition of the limit of elastic behavior (i.e., DL1 instead of DL2), the OSR would be of about 1.8. Lastly, it is recommended that the assessment of such factors, for a specific class and a particular structural building type should always be adequately evaluated.

Furthermore, it is worth to note in this work the conclusions are supported based on the results from nonlinear static analyses. However, additional confirmation may be derived by performing additional nonlinear dynamic analyses.

## AUTHOR CONTRIBUTIONS

JM, RB, and SC Contributed their research experience and knowledge to the seismic assessment of a mixed masonry-reinforced concrete structures with the final goal to define the structural behavior factor. It is a relevant work in the sense that linear analysis is still the most used procedure in the design engineering offices.

## FUNDING

## REFERENCES

Alegre, A., and Heitor, T. (2004). Flexibility in the first generation of reinforced concrete housing: a public housing estate in Lisbon. *J. Constr. Hist.* 20, 85–93. Available online at: https://www.jstor.org/stable/41613879

Benedetti, D., Benzoni, G. M., and Petrini, V. (1984), "Experimental evaluation of seismic provisions for stone masonry buildings," in *Proceedings 8th WCEE* (San Francisco, CA).

Benedetti, D., and Castoldi, A. (1982). "Dynamic and static experimental analysis of stone masonry buildings," in *Proceedings of 7th ECEE* (Athens).

Benedetti, D., Pezzoli, P., and Carydis, P. (1998). Shaking table tests on 24 simple masonry buildings. *J. Earthq. Engin. Struct. Dyn.* 27, 67–90. doi: 10.1002/(SICI)1096-9845(199801)27:1<67::AID-EQE719>3.0.CO;2-K

Bondarabadi, H. (2018). *Analytical and Empirical Seismic Fragility Analysis of Irregular URM Buildings With Box Behavior*. dissertation/Ph.D. Thesis, University of Minho (Minho).

Cattari, S., Lagomarsino, S., Bosiljkov, V., and D'Ayala, D. (2015a). Sensitivity analysis for setting up the investigation protocol and defining proper confidence factors for masonry buildings. *J. Bull. Earthq. Eng.* 13, 129–151. doi: 10.1007/s10518-014-9648-3

Cattari, S., Marino, S., and Lagomarsino, S. (2015b). "Seismic assessment of plan irregular masonry buildings with flexible diaphragms," in *Proceedings of the 10th Pacific Conference on Earthquake Engineering. Building an Earthquake-Resilient Pacific,* (Sydney, NSW)

Cattari, S., and Lagomarsino, S. (2013a). "Masonry structures," in *Developments in the Field of Displacement Based Seismic Assessment*, eds T. Sullivan and G. M. Calvi (Pavia: IUSS Press; Eucentre) 151–200.

Cattari, S., and Lagomarsino, S. (2013b). Seismic assessment of mixed masonry-reinforced concrete buildings by non-linear static analyses. *J. Earthq. Struct.* 4, 241–264, doi: 10.12989/eas.2013.4.3.241

CEN Eurocode 8 (2004). *Design of Structures for Earthquake Resistance - Part 1: General Rules, Seismic Actions and Rules for Buildings (EC8-1).* EN1998–1:2004, Comité Européen de Normalisation, (Brussels).

CEN Eurocode 8 (2005). *Design of structures for earthquake resistance – Part 3: Assessment and retrofitting of buildings (EC8-3).* EN1998-3:2005, Comité Européen de Normalisation, (Brussels).

Costa, J. (2005). *Bairro De Alvalade: Um Paradigma No Urbanismo Português.* Lisbon: Livros Horizonte.

ESRI (2014). *Online Documentation of Geographic Information System, Arcgis (Arcmap and Arccatalog).* Redlands, CA: EUA; ESRI. Available online at: http://esri.com/

Fernandez, P. (1943). *Memória Descritiva Do Edifício N° 3 Da Praça João Do Rio, Arquivo Municipal De Lisboa - Obra 4553-Proc 26322-Dag-Pg-1943.* Folha 8, Lisboa.

França, J. (1997). *Lisboa: Urbanismo E Arquitectura.* Lisbon: Livros Horizonte.

GRUC (1930). *Regulamento Geral da Construção Urbana, Lisboa Para a Cidade de Lisboa.* Lisbon: GRUC.

ICOMOS/ISCARSAH Committee (2003). *Recommendations for the Analysis, Conservation and Structural Restoration of Architectural Heritage.* ICOMOS International Committee for Analysis and Restoration of Structures of Architectural Heritage.

ISO 13822 (2010). *Basis for Design of Structures: Assessment of Existing Structures.* ISO 13822.

Lagomarsino, S., and Cattari, S. (2014). "Fragility functions of masonry buildings," in *SYNER-G: Typology Definition and Fragility Functions for Physical Elements at Seismic Risk: Elements at Seismic Risk,* Geotechnical, Geological and Earthquake Engineering 27, eds K. Pitilakis, H. Crowley, and A. M. Kaynia (Dordrecht: Springer Science+Business Media), 111–156.

Lagomarsino, S., and Cattari, S. (2015). "Seismic performance of historical masonry structures through pushover and nonlinear dynamic analyses," in *Perspectives on European Earthquake Engineering and Seismology. Geotechnical, Geological and Earthquake Engineering,* Vol. 39, ed A. Ansal (Cham: Springer), 455.

Lagomarsino, S., Penna, A., Galasco, A., and Cattari, S. (2013). TREMURI program: an equivalent frame model for the nonlinear seismic analysis of masonry buildings. *J. Eng. Struct.* 56, 1787–1799. doi: 10.1016/j.engstruct.2013.08.002

Magenes, G. (2004). *Prospects for the Revision of the National Seismic Code With Regard to Masonry Constructions.* Isola Vicentina: Assemblea ANDIL, sezione Murature (in Italian).

Magenes, G. (2006). "Masonry building design in seismic areas: recent experiences and prospects from a European standpoint," in *Proceedings of the 1st European Conference on Earthquake Engineering and Seismology*

(a joint event of the 13th ECEE and 30th General Assembly of the ESC) (Geneva).

Magenes, G., and Menon, A. (2009). A review of the current status of seismic design and assessment of masonry buildings in Europe. *J. Struct. Eng. SERC Madras* 35, 247–256.

Magenes, G., and Morandi, P. (2006). *National and European Masonry Codes: Eurocode 8 and Evolution of the OPCM 3274.* EUCENTRE Report, Pavia (in Italian).

Marino, S., Cattari, S., and Lagomarsino, S. (2018). "Use of non-linear static procedures for irregular URM buildings in literature and codes," in *Proceedings of the 16th European Conference on Earthquake Engineering* (Thessaloniki).

Milosevic, J., Cattari, S., and Bento, R. (2018a). Sensitivity analyses of seismic performance of masonry-RC buildings in Lisbon. *J. Masonry Res. Innov.* 3, 108–154. doi: 10.1504/IJMRI.2018.092459

Milosevic, J., Bento, R., and Cattari, S. (2018b). Definition of fragility curves through nonlinear static analyses: procedure and application to a mixed masonry-RC building stock. *J. Eng. Struct.*

NTC Italian Code for Structural Design (2008). *(Norme Tecniche per le Costruzioni – NTC) D.M. 14/1/2008.* Official Bulletin N° 29 of February 4, (In Italian).

RRCS (1935). *Regulamento De Estruturas De Betão Armado – Dec. 25948, Incm, 16 De Outubro De 1935,* Lisbon, Portuguese Standard.

Senaldi, I., Magenes, G., Penna, A., Galasco, A., and Rota, M. (2014). The effect of stiffened floor and roof diaphragms on the experimental seismic response of a full-scale unreinforced stone masonry building. *J. Earthq. Eng.* 18:407–443. doi: 10.1080/13632469.2013.876946

Thomos, G. C., and Trezos, C. G. (2005). *Behaviour factor of RC structures: a Probabilistic Approach, Earthquake Resistant Engineering Structures.* WIT Press WIT Transactions on The Built Environment. Vol. 81, Available online at: www.witpress.com, ISSN 1743-3509 (on-line).

Tomaževič, M. (1999). *Earthquake -resistant design of masonry buildings, Series on Innovation in Structures and Construction,* Vol. 1, (London: Imperial College Press).

Tomaževič, M., Bosiljkov, V., and Weiss, P. (2004). "Structural behavior factor for masonry structures," in *Proceedings of the 13th World Conference on Earthquake Engineering,* Paper no. *2642* (Vancouver, BC).

Tomaževič, M., and Weiss, P. (1994). Seismic behavior of plain and reinforced masonry buildings. *J. Struct. Eng. ASCE* 120, 323–338.

Turnšek, V., and Sheppard, P. (1980). "The shear and flexural resistance of masonry walls," in *Proceedings of the International Research Conference on Earthquake Engineering.* Skopje, Macedonia.

Check for updates

# Structural Assessment and Upgrading for an Old Building Belonging to an Historical Multi-Sports Center in Naples

Andrea Miano[1]*, Giovanni Chiumiento[1] and Angelo Saggese[2]

[1] Department of Structures for Engineering and Architecture, University of Naples Federico II, Napoli, Italy, [2] Independent Researcher, Salerno, Italy

A significant number of non-ductile existing reinforced concrete frame buildings, built in different seismic regions around the world but without adequate seismic detailing requirements, suffered damages, or collapse after past earthquakes. In fact, these reinforced concrete frame buildings are much more susceptible to high level of damage or to collapse than modern code-conforming frames. A crucial issue in the community of the earthquake engineering is the assessment and the upgrading of these non-ductile reinforced concrete structures. In particular, a careful assessment of the existing buildings is very important in order to understand the failure mechanisms that govern the achievement of predefined limit states or the collapse of the structures. Only after an in depth seismic assessment, the best upgrading/retrofit strategy can be designed and applied to the structure. In some cases, the historical value of these buildings makes the assessment procedure and the upgrading design more complicated due to the constraints related to the limited possibility of interventions. In this work, a building belonging to an old multi-sports center, is used as case study. The complex orbits around the soccer stadium called Collana and located in Naples. This soccer stadium was initially built in the late '20s and then it was completely rebuilt in the post-war period and used as a sports center for different sporting activities. Currently, the complex includes a soccer field, an athletic track, three indoor gyms, three tennis fields, a medical center sports, and the indoor pool building investigated herein. The analysis of seismic vulnerability implemented for the case study building shows an unsafe condition under both vertical and seismic loads. The building upgrading is provided choosing the best strategy among different options in order to achieve a certain predefined threshold of the seismic safety for the building. Definitively, the paper presents a real upgrading design case study for a building belonging to an historical complex. Assessment and upgrading are shown based both on linear and dynamic non-linear analyses procedures. Finally, the effectiveness of the structural interventions of upgrading is measured coherently with the new Italian guidelines for seismic risk classification of constructions.

**Keywords: structural upgrading, historical buildings, non-linear static analysis procedure, non-linear dynamic analysis procedure, seismic risk classification of the constructions**

# INTRODUCTION

The "Collana" football stadium was initially built in the late '20s and then be completely rebuilt in the post-war period and used as a multi-sports center together with other buildings intended for various sporting activities. Currently, the complex includes a soccer field, an athletic track, three indoor gyms, three tennis courts, a medical center sports, and the indoor pool under study. The present work concerns the description and verification of the structural upgrading design for the swimming pool building, realized inside the more general scope of the project of functional upgrading of the entire building, which at the moment of the design was unusable. In general, the assessment and upgrading/retrofit of existing structures in highly seismic zones are crucial issues in earthquake engineering. In fact, post-earthquake reconnaissance and recent research on seismic risk analysis have shown that non-ductile concrete frame structures are much more susceptible to collapse than modern code-conforming frames. In particular, a careful assessment of the existing buildings is fundamental for understanding the failure mechanisms that govern the collapse of the structure or the achievement of the recommended limit states. Based on the seismic assessment, the best upgrading/retrofit strategy can be designed and applied to the structure. Many conventional upgrading methods, such as concrete or steel jacketing of the columns, addition of shear walls and methods often based on new materials as fiber reinforced polymers (FRP), have been proposed and used (Moehle, 2000; Thermou and Elnashai, 2006; Calvi, 2013; Formisano and Sahoo, 2015a; Formisano et al., 2015, 2016, 2017a; Miano et al., 2017a). These methods can be applied considering the desired limit states/performance levels, using the requirements of new seismic codes or more advanced performance based approaches to measure the probability of collapse and quantify and minimize the costs and/or the losses with different approaches (Aslani and Miranda, 2005; Liel and Deierlein, 2013; Jalayer et al., 2015, 2017; Miano et al., 2018a). Non-linear static analysis procedure, also known as pushover, has been implemented in this work for seismic and vertical loads safety assessment and for measure the effectiveness of the different retrofit strategies. In particular, pushover analysis, can be used to calculate the vulnerability index indicator, also called seismic safety factor (Frascadore et al., 2015; NTC, 2018). Moreover, non-linear dynamic analysis procedures can be used to perform probabilistic seismic assessment using recorded ground motions. Cloud Analysis is chosen here by applying simple regression in the logarithmic space of non-linear dynamic structural response vs. seismic intensity for a set of ground motion records. Cloud Analysis is particularly efficient since it involves non-linear analyses of the structure subjected to a set of un-scaled ground motion time histories. The simplicity of its formulation makes it a quick and efficient analysis procedure for fragility assessment (Jalayer et al., 2007, 2015, 2017; Celik and Ellingwood, 2010; Miano et al., 2017b). The 3D model of the building is produced using the commercial software for structural calculation CDS (CDS, 2018). The analysis of seismic vulnerability carried out on the mentioned building highlights deficiencies in both vertical loads and seismic loads conditions.

The upgrading of the building is designed in order to solve the vertical load deficiency and to achieve a certain threshold of the seismic vulnerability index, as described in Italian code (NTC, 2018). The design solutions adopted and described below are based on a careful campaign of *in situ* investigations performed on the existing structure together with accurate measurements to represent the dimensional characteristics and the construction details of the building. Based on different considerations related to effectiveness, costs and invasive grade of the upgrading options, steel jacketing is chosen. The steel jacketing is realized through steel plates wrapped completely around the beams plus angular plates in the corners around the length of the members. In this upgrading option, all the reinforced concrete (RC) columns and beams are steel jacketed. Assessment and retrofit are shown both based on linear and dynamic non-linear analyses procedures. In particular, the achievement of an adequate value of seismic vulnerability index through non-linear static analysis, as required for buildings susceptible to crowding in the case of temporary use of the structure for purposes related to the management of the emergencies in general, is shown. Moreover, non-linear dynamic analyses are implemented to measure the probability of achieving predefined limit states before and after the upgrading. Finally, the seismic risk class is assigned before and after the upgrading according to two parameters (Guidelines, 2017; Cosenza et al., 2018). The first parameter is economic and is called expected annual mean losses (Perdite Annue medie, PAM). The second one is related to the safety of the structure and id called Life Safety Index (Indice di sicurezza della vita, IS-V).

# CASE STUDY

## Building Description

The building is roughly rectangular in plan and consists of a pool block of consistent height, equal to about 6.50 m, with a surface area of about 600 m$^2$. In adjacency on the two sides of the pool body there is the stripped area, with a plant area of 500 m$^2$, with a height of about 3.50 m above ground and, limited to one of the service areas, 5.30 m. The covered area of the entire structure is about 1,200 m$^2$ and, in addition to the two bodies described, there is also a technical room of about 60 m$^2$. Access to the pool, as well as from inside the stadium, is allowed directly from the street, with respect to which the footfall is slightly higher. There is also an underground floor, done with RC walls at different quotes and directly connected to the foundation system, but the design project regards only the upper floor. However, it was possible to note that no damages or cracks are present in the underground floor. **Figure 1** shows the lateral view of the building.

The process of knowledge for the building has been done following two different directions, e.g., respectively visual and in depth *in situ* surveys and tests and research of the technical, administrative and planning documentation referred to structure under study, as required by the Italian technical regulations for buildings existing (NTC, 2008, 2018). Considering the construction time of the building, dating back to the 60 s,

**FIGURE 1 |** Lateral view of the building.

and the lack of the obligation to deposit the project at the city offices, it was not possible to find any documentation useful for the knowledge of the structural characteristics of the building. Definitively, in this section, the visual structural relief is commented, while, in the next section, the *in situ* tests campaign is described. **Figure 2** shows the plan view of the building. Structurally, the building is done by frames of RC beams and columns. The slabs are made of prefabricated joists on the first level and of prefabricated RC concave tiles for the pool area. At the basement level, around the perimeter, there are RC walls, covered by the ground for three of the four sides of the building. The cross section of the beams is $400 \times 450$ mm, while the columns have two different cross sections, respectively $250 \times 500$ mm and $400 \times 400$ mm. The number of bars and stirrups is limited in all the sections. The bars are smooth, as in the most part of the buildings of the same construction age. The distribution of the frames is quite regular with the adoption of similar typologies referred to sections of beams and columns. However, the structural design of the building is affected by the era of realization of the works since there are no connecting elements between the supporting frames. It is clear that there is a lack of an earthquake-resistant design of the structure in this building, such as in numerous buildings of the period, designed only for vertical loads.

Figure 3 shows the typical structural designs of the layout of the cross sections of columns and beams (in cm). In particular, **Figures 3A,B** shows the cross sections of beams (a) and columns (b) before structural upgrading operations, while **Figures 3C,D** shows the cross sections of beams (c) and columns (d) after structural upgrading operations (for the details of the upgrading operations, see Section Building Structural Upgrading).

## *In situ* Tests Campaign and Materials Mechanical Characteristics

For the definition of the properties of the materials, reference has been made to the indications of point C8A.1B3 of the Italian code explanatory test (Circolare, 2009, **Table 1**). The goal has been to obtain the knowledge level 2 (*KL2*). Based on this consideration, extended *in situ* tests have been carried according to table C8A.1.3a of Circolare (2009), considering the absence of technical design documentation. The engineers have chosen to achieve *KL2*, also in order to use static non-linear analysis as procedure for the assessment, as shown in **Table 1**.

With respect to the determination of the mechanical characteristics of the concrete, direct (destructive), and indirect (non-destructive) tests have been carried out, according to Circolare (2009). The types of tests performed in structural elements in order to evaluate their compressive strength are, respectively, the compression breaking of cylindrical specimens of concrete and non-destructive tests (Sonreb tests). The mechanical characteristics of the steel have been determined based on destructive tests with the removal of bars from structural elements. In particular, the steel specimens have been taken from the columns. The cover of the designated element has been removed with the subsequent removal of a piece of length equal to about 1 m and re-insertion of a suitable replacement bar with subsequent restoration of the cover. In general, the choice of the elements to be investigated has been carried out in order to obtain a significant sample of elements, able to represent the average characteristics of the concrete and the steel. **Table 2** summarizes the recommended minimum requirements for different levels of testing for the number of concrete and steel tests. It is important to note that the Circolare (2009) allows to replace each destructive test with three non-destructive tests up to the 50% of all the required destructive tests.
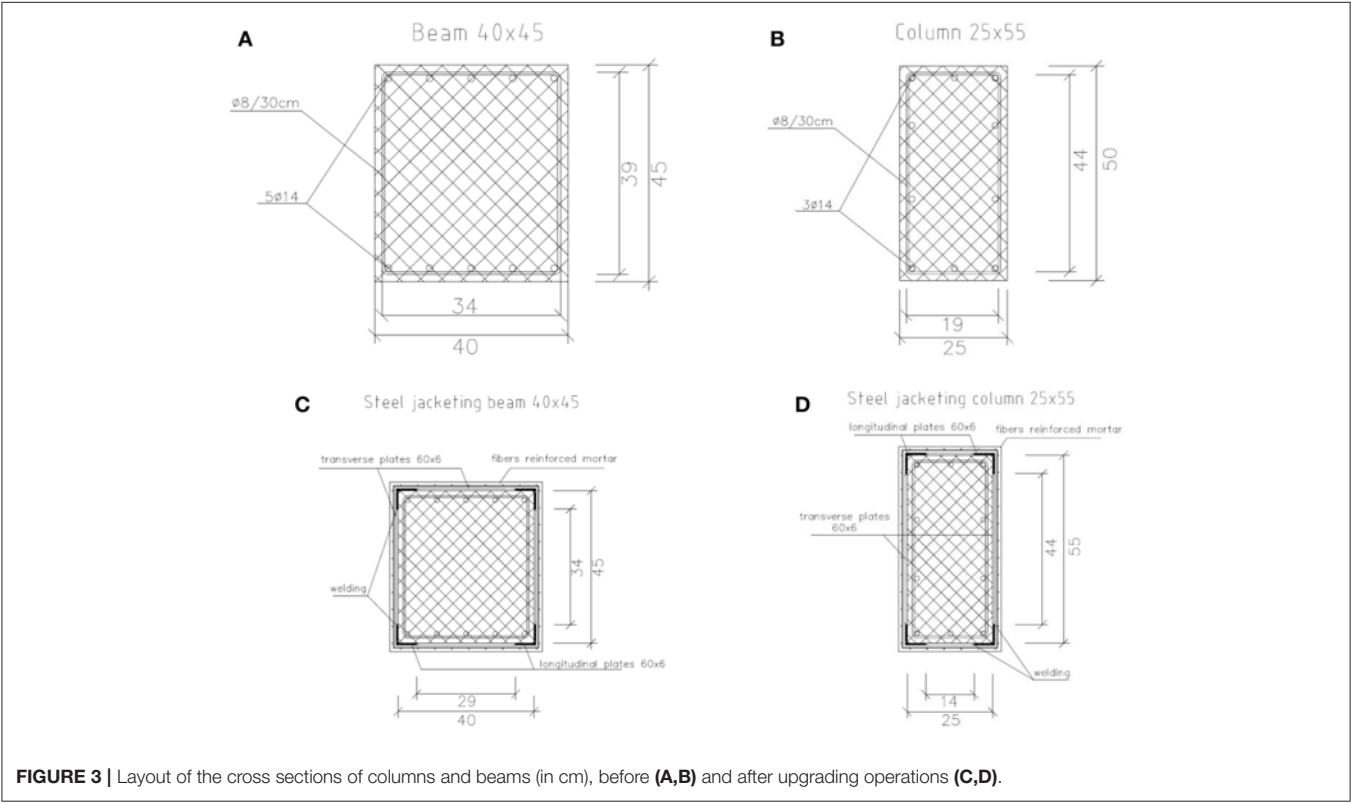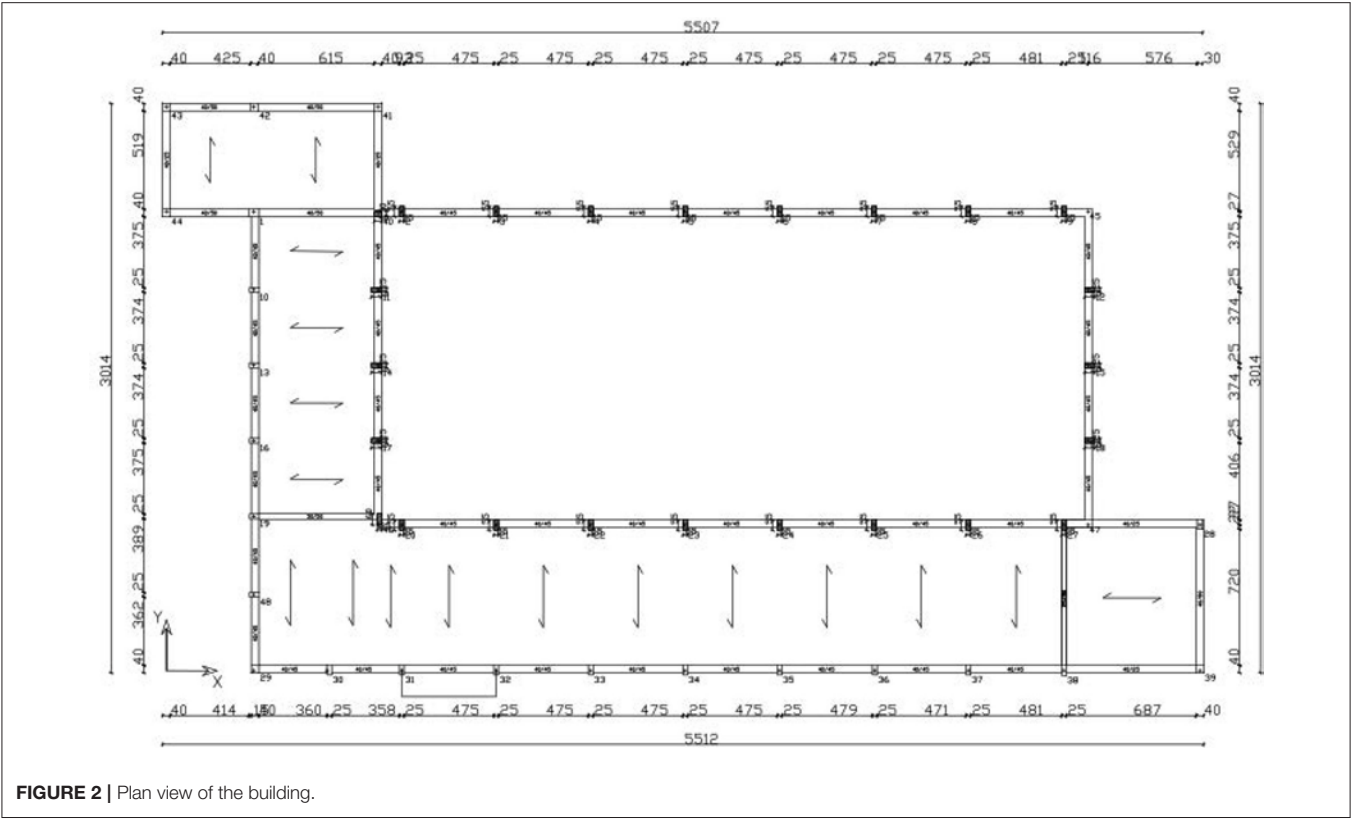
FIGURE 2 | Plan view of the building.



FIGURE 3 | Layout of the cross sections of columns and beams (in cm), before (A,B) and after upgrading operations (C,D).

| Knowledge level | Materials | Analysis | Coefficient |
|---|---|---|---|
| KL1 | Default values for the time of construction plus limited *in situ* tests | Lateral force procedure and Modal response spectrum analysis | 1.35 |
| KL2 | Original design specifications plus limited *in situ* tests or extended *in situ* tests | All | 1.20 |
| KL3 | Original test reports plus limited *in situ* tests or comprehensive *in situ* tests | All | 1.00 |

| Check type | Limited checks | Extended checks | Comprehensive checks |
|---|---|---|---|
| Tests on materials | 1 sample for each 300 m$^2$ of floor of the building for each structural member | 2 sample for each 300 m$^2$ of floor of the building for each structural member | 3 sample for each 300 m$^2$ of floor of the building for each structural member |
| Required tests for the case study structure | 2 sample for each floor for each structural member (floor area = 600 m$^2$) | 4 sample for each floor for each structural member (floor area = 600 m$^2$) | 6 sample for each floor for each structural member (floor area = 600 m$^2$) |

Based on the recommendations provided in **Table 2** line 1 and considering a surface of about 600 m$^2$ of the building, a number of four samples is required at each floor for each structural member in order to achieve extended checks and, then, *KL2* (**Table 2** Line 2). With reference to concrete, the performed tests have included a number of two destructive plus six non-destructive tests for each structural member at the floor under consideration. With reference to steel, only two destructive tests have been realized for each structural member. This is quite reasonable since the variability of the steel mechanical properties can be considered less than that the one affecting concrete specimens. Moreover, in same cases it is to consider the impossibility to perform *in situ* tests on steel samples for different reasons. For example, in some columns, only corner bars were found. Since this circumstance was judged dangerous from the structural designers, they decided to don't extract steel bars from the corners. Definitively, based on the analysis of the results of the tests carried out, the average compressive concrete and steel yielding strengths assumed in the modeling of the structural members are:

- concrete: $f_{cm} = 24.5$ Mpa;
- steel: $f_{ym} = 356.8$ Mpa.

# BUILDING STRUCTURAL ASSESSMENT

## Non-linear Static Analysis Procedure

Non-linear static analyses are presented in this section. They are implemented through the commercial software CDS (CDS, 2018). First, some basic information about the modeling is provided. The analysis for the combinations of permanent and variable actions is carried out in a linear elastic regime. The checks are carried out using the limit state method (Life Safety and Damage Limitation Italian Limit States), using the partial coefficients of the regulations as in NTC (2008, 2018). In particular, with reference to the Damage Limitation (DL) limit state, the limit state condition is represented by the attainment of the value of 0.005 of the height of the floor as maximum displacement in a floor. Instead, with reference to the Life Safety (LS) limit state, the limit state condition is represented by the attainment of the maximum shear strength (brittle safety checks) or the maximum rotational capacity (ductile safety checks). In addition, the joints safety verifications are carried out. With respect to the structure resolution method, the structure is modeled with the finite elements method. The constitutive laws for concrete and steel are presented in **Figure 4**. Concrete material behavior is modeled using a zero tensile strength and a parabolic compressive stress-strain behavior up to the point of maximum strength with a linear deterioration beyond peak strength, according to the Kent-Scott-Park model (CDS, 2018). Longitudinal steel behavior is simulated using a bilinear stress-strain envelope with the definition, respectively of a yielding and a rupture deformations, according to Fedeas model (CDS, 2018). Member force-deformation response is computed assuming that inelastic action occurs mainly at the member ends and that the middle of the member remains typically elastic. A sectional analysis is implemented to obtain the non-linear moment-curvature relation in the member ends. Plastic hinge integration methods are used to confine non-linear deformations in end regions of the element of specified length. The remainder of the element is assumed to stay linear elastic and it is assumed that the length of the plastic region is equal to the depth of the cross-section. The deformational contributions from shear and bar slip are neglected in the section analysis. In particular, it is to consider that slip of longitudinal column bars at column ends (i.e., from the footing or beam-column joint) causes rigid body rotation of the column. This rotation is not accounted for in flexural analysis, where the column ends are assumed to be fixed. Many studies have been proposed to taking into this deformational contribution (Sezen and Moehle, 2004; Braga et al., 2012, 2015; D'Amato et al., 2012; Caprili et al., 2015). Finally, it is to note that the shear safety checks are however performed as post-processing, comparing the maximum demand value with the capacity in terms of force.

Definitively, a moment curvature envelope is calculated based on section analysis and is assigned at the end of the members with a concentrated plasticity model. Pushover analysis
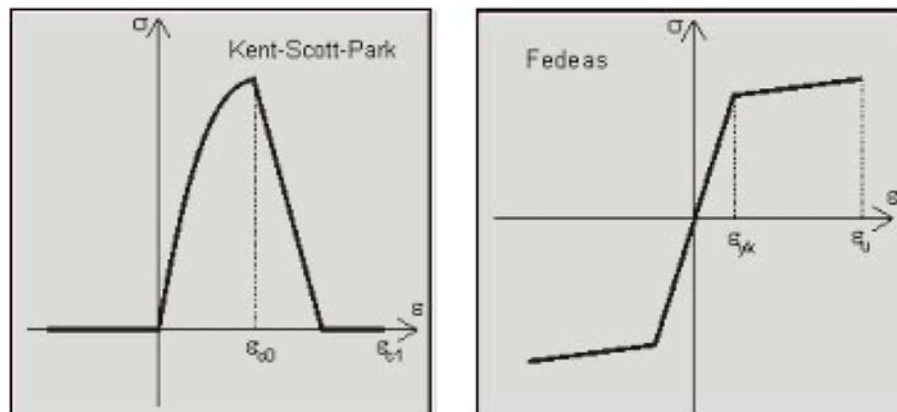
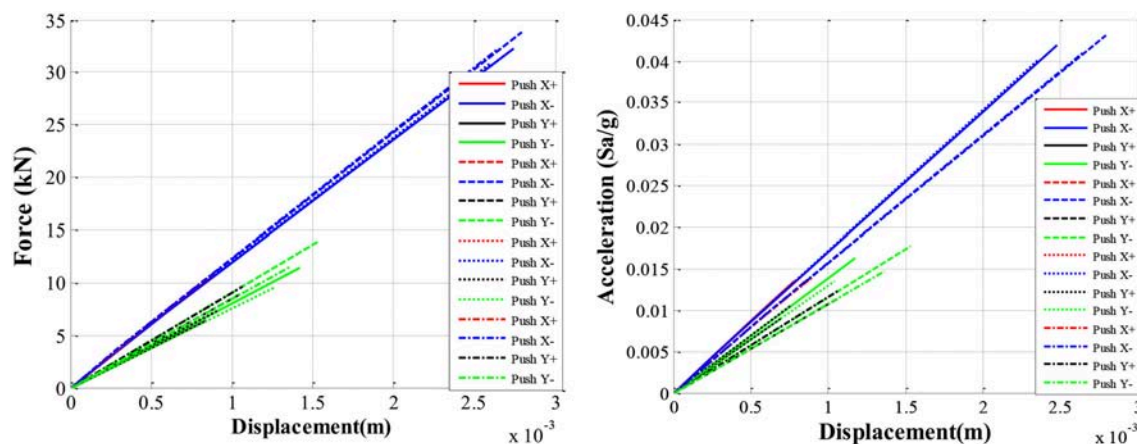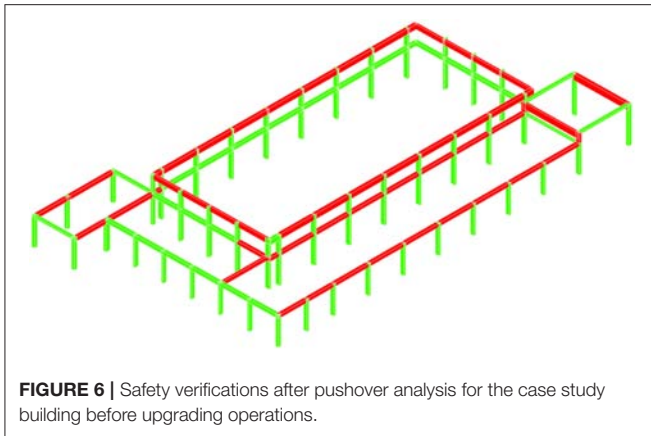**FIGURE 4 |** Concrete and steel constitutive laws.



**FIGURE 5 |** Pushover curves for the case study building before upgrading operations.

is carried out by following the Italian seismic code (NTC, 2008) for the case study building, based on the properties calculated with respect to KL2. Vertical loads analysis is implemented before pushover analysis. The safety verifications after vertical loads analysis show mainly premature shear failures in some beams. Then, a number of 16 pushovers is done, using two different distributions of forces and using a possible eccentricity of the 5% in each direction. The first forces distribution is proportional to the floor masses, while the second one is proportional to the shape of the first vibration mode (NTC, 2008 and Circolare, 2009). **Figure 5** shows the pushover results in terms of base shear/acceleration vs. top displacement. The 16 pushovers are differentiated by colors in group of four, where each group represent a certain direction of application of the forces, while the four pushovers for each direction are relative to the two distributions of forces suggested by Italian code and with the application of plus/minus 5% eccentricity with respect to the geometrical barycentre of the building. In particular, the red curves correspond to forces parallel to horizontal × positive

direction (see **Figure 3**); the blue curves correspond to forces parallel to horizontal × negative direction; the black curves correspond to forces parallel to horizontal y positive direction; the green curves correspond to forces parallel to horizontal y negative direction.

For the DL and LS limit states, the members verifications are provided, showing a situation of strong deficiency. It's interesting to show the safety verifications for the LS limit state. In particular, **Figure 6** shows for the LS limit state with red color the members for which the safety verifications are not satisfied and with green color the members for which the safety verifications are satisfied, showing that a high number of beams and columns result unsafe. The safety verifications are implemented also for the DL state, showing a lot of deficiencies in the structural members. In particular, there is the same configuration of the brittle failures of the beams as in the vertical loads analysis. These premature failures don't allow to the structure to reach a ductile behavior and to have excursions in plastic zone. The analysis is stopped when these premature failures are reached, as it is possible to see from the linear behavior in **Figure 5**.

**FIGURE 6 |** Safety verifications after pushover analysis for the case study building before upgrading operations.

It is to note that the first crises are related mainly to shear failures of the beams along the principal direction of the building. So, it is to consider that the most important deficiency is related to the unsafe verifications of the members against vertical loads (as it can be seen from the results of the pushovers and from the consideration that the capacity displacement is about the same for DL and LS limit states, based on the fact that there is no possibility to develop plastic dissipation, because in the first step of the pushover the vertical loads shear failures happen).

In order to measure the level of seismic safety before and after upgrading, the Italian code (NTC, 2008, 2018) suggests to verify the vulnerability index with reference to LS limit state. For this reason, the bare building and its upgraded versions are compared at the end of the process based on the vulnerability index calculated with respect to LS limit state, verifying a part in addition the condition of the members in the DL limit state. Definitively, in order to define if the building is safe with respect to seismic actions, the software (CDS, 2018) calculates the vulnerability index ($\zeta_E$), also called in literature seismic safety factor (Frascadore et al., 2015), that is a very useful parameter to measure the vulnerability of the structure. The pushover curve is an essential tool for the application of the capacity spectrum method (CSM; Vidic et al., 1994) that allows for the determination of the building response for earthquakes of a given spectral shape. All the steps of the procedure for calculate the $\zeta_E$ are well-described in Frascadore et al. (2015). The procedure starts from the pushover response in terms of the MDOF (Multi Degree of Freedom) system and passes to the response in terms of the corresponding SDOF (Singol Degree of Freedom). The parameters that characterize the SDOF, period $T^*$, yield strength $F_y^*$, and ultimate displacement $d_u^*$, allow to derive the return period capacity, and therefore the peak ground acceleration capacity, for which the crisis mechanism is reached. The procedure for the quantification of the $\zeta_E$ is implemented in the ADRS space (Acceleration Displacement Response Spectrum, Fajfar, 1999, 2000), in which the abscissas are the spectral displacements and the ordinates are the spectral accelerations. It consists in scaling the elastic spectrum of seismic demand, for small decrements of the return period $T_R$, until the

spectrum that contains the point performance (Sae; Sde) of the equivalent SDOF is found, identified by the line of inclination $T^*$ and the displacement $d_{maxSLV}^*$. Finally, $\zeta_E$ is defined as the ratio between the demand peak ground acceleration (PGA), based on the seismic actions prescribed from the code for the Life Safety limit state, and the capacity PGA of the building:

$$\zeta_E = \frac{PGA_{LS_{Capacity}}}{PGA_{LS_{Demand}}} \tag{1}$$

where $PGA_{LS\_Capacity}$ is the PGA corresponding to the achievement of the first crisis related to LS limit state inside the building, while $PGA_{LS\_Demand}$ is the PGA obtained from the elastic code spectrum for the specific site with reference to the LS limit state. It can be noted that this ratio between these two accelerations is directly related to the measurement of the seismic vulnerability of the structure with reference to the achievement of the crisis condition for the LS limit state. There are 16 SDOF systems associated to the 16 pushovers. The minimum value among the 16 values of the $\zeta_E$ related to the 16 SDOF systems is considered as $\zeta_E$ of the structure. The final value of the $\zeta_E$ is 0.23. Thus, the structure is not safe in terms of seismic actions. Moreover, also the verifications in terms of vertical loads are not satisfied. Definitively, it is clear that upgrading operations are needed for the structure.

## Non-linear Dynamic Analysis Procedure

In seismic assessment and upgrading procedures, it's crucial to have accurate evaluation of the seismic vulnerability. Fragility curves are the most common and useful way to have the measure of the vulnerability. Herein, analytical fragility curves are developed for the case study building with reference to the conditions before and after upgrading operations. The curves are based on the application of a set of 30 ground motion records to the SDOF system calculated from the software program (CDS, 2018). In particular, since 16 pushover curves are developed and so 16 SDOF systems are available, Cloud Analysis refers to the most penalized SDOF, the one that minimizes the value of $\zeta_E$. The methodology starts to the identification of the structural response parameter. As described in Jalayer et al. (2007), for each non-linear time-history analysis, the corresponding critical demand to capacity ratio ($DCR_{LS}$), for each limit state, equal to the mechanism that brings the structure closest to the onset of the specific limit state, is adopted as the structural response parameter. The $DCR_{LS}$ parameter, that is equal to unity at the onset of the limit state can be calculated for the SDOF systems analyzed here as the ratio between the maximum demand in terms of displacement for each record among all the steps of the non-linear dynamic analysis and the limit state capacity, calculated accordingly with Italian code (NTC, 2008, 2018). Obviously, the ratios between demand and capacity at the level of the SDOF and MDOF systems are equal because both the demand and the capacity have to be multiplied by the modal participation factor in order to pass from SDOF system to MDOF system. Two capacity values refer in this work to DL and LS limit states, but it's to note that the procedure can be used for any other prescribed performance levels or limit states. The record

selection is a very critical issue for have a good implementation of non-linear dynamic analysis procedures. Herein, a set of 30 strong ground-motion records is selected from the NGA-West2 database (see Jalayer and Ebrahimian, 2017 and Miano et al., 2018b for the details about the criteria for record selection) in order to implement Cloud Analysis. This suite of records covers a wide range of magnitudes between 5.6 and 7.2, and closest distance-to-ruptured area (RRUP) up to around 40 km. The shear wave velocity in upper 30 m of soil, Vs30, at the structure's site is in the range of 180–360 m/s (e.g., soil class C, accordingly to Italian code, NTC, 2018). Based on this information, the main part of the selected records are chosen to be on NTC (2018) site classes B and C. Only one of the two horizontal components of each recording. Finally, the records are selected to be free field or on the ground level. **Table 3** summarizes the most important information about the suite of ground motion records used in this study.

In order to estimate the structural fragility, Cloud analysis is adopted herein as non-linear dynamic analysis procedure. Cloud analysis is a procedure in which a structure is subjected to a set of ground motion records of different first-mode spectral acceleration, Sa(T), values. It is to note that Sa(T) or simply Sa is adopted herein as the IM. This intensity measure has been proved to be a relatively sufficient IM for moment-resisting frames with first-mode periods lying within the moderate range (Jalayer et al., 2012). Once the ground motion records are selected, they are applied to the structure and the resulting $DCR_{LS}$ is calculated. This provides a set of values that form the basis for the cloud-method calculations. In order to estimate the statistical properties of the cloud response, conventional linear regression is applied to the response on the natural logarithmic scale, which is the standard basis for the underlying log-normal distribution model. This is equivalent to fitting a power-law curve to the cloud response in the original (arithmetic) scale. This results in a curve that predicts the median drift demand for a given level of structural acceleration:

$$\eta_{DCR|Sa}{}^{(Sa)} = a \cdot Sa^b$$
$$\ln(\eta_{DCR|Sa}{}^{(Sa)}) = \ln(a) + b \cdot \ln(Sa) \qquad (2)$$

where ln(a) and b are regression constants. The logarithmic standard deviation $\beta_{DCR|Sa}$ is the root mean sum of the square of the residuals with respect to the regression prediction:

$$\beta_{DCR|Sa} = \sqrt{\frac{\sum{(\ln(DCR_i) - \ln(a \cdot S_{a,i}{}^b))^2}}{N-2}} \qquad (3)$$

where $DCR_i$ and $Sa_i$ are the demand over capacity ratio values and the corresponding Sa for record number i within the cloud response set and N is total number of records. The standard deviation of regression, as introduced in the preceding equation, is presumed to be constant with respect to Sa over the range of spectral accelerations in the cloud. Finally, the structural fragility

curves based on the Cloud Analysis can be expressed as:

$$P\left(DCR_{LS} > 1 \,|\, S_a\right) = P\left(\ln DCR_{LS} > 0 \,|\, S_a\right)$$
$$= 1 - \Phi\left(\frac{-\ln \eta_{DCR_{LS}|S_a}}{\beta_{DCR_{LS}|S_a}}\right) = \Phi\left(\frac{\ln \eta_{DCR_{LS}|S_a}}{\beta_{DCR_{LS}|S_a}}\right) \qquad (4)$$

**Figure 7A** presents the results of the Cloud linear logarithmic regression for the LS limit state with respect to the pre-upgrading building (it corresponds also the DL limit state as explained before). **Figure 7A** shows the scatter plots for Cloud Analysis data D = {($S_{a,i}$, $DCR_{LS,i}$), i = 1:30, where LS corresponds to Limit State} for the set of records outlined in **Table 3**. For each data point (cyan colored squares), the corresponding record number is shown. Moreover, the figure illustrates the Cloud Analysis regression prediction model (i.e., regression line and the estimated parameters, see Equation 2) fitted to the data. The line $DCR_{LS}$ =1 corresponding to the onset of limit state is also shown with red-dashed line. It can be noted that consistent with the recommendations provided in Jalayer et al. (2017), the Cloud Analysis data not only cover a vast range of Sa values but also provide data points both in the range of $DCR_{LS}$ >1 and in the range of $DCR_{LS}$ <1. **Figure 7B** shows the resulting Cloud Analysis-based fragility curve. The values of the statistics (e.g., median and the logarithmic standard deviation) associated with the Cloud Analysis based fragility curve are, respectively, 0.04 and 0.72.

# BUILDING STRUCTURAL UPGRADING

## Upgrading Operations

The main goal of the upgrading design is to prevent premature failure of non-ductile elements and to increase their ductility and strength. In addition, the lateral displacements need to be limited and as uniform as possible over the height of the structure to prevent soft story mechanism. To control lateral drift by keeping them below the target displacement, one effective strategy for concrete moment frame is to add lateral stiffness, e.g., by adding a shear wall, to reduce the period, and decrease the resulting displacements. Another effective way to improve ductility and strength of the frame is to increase flexural and shear strength and deformation capacity of lateral load resistant members by better confining the columns and shifting the failure mode from shear to flexural mode (e.g., by enlarging the cross section of concrete jacketing). In some cases, to avoid the restriction of use of building for a long time, methods based on a quick application, such as fiber reinforced polymers (FRP), can be useful. However, there are many practical upgrading options (Moehle, 2000; Thermou and Elnashai, 2006; Formisano et al., 2008; Calvi, 2013; Formisano and Mazzolani, 2015b; Bertolesi et al., 2017; Miano et al., 2018b). It's important to highlight that coherently with the actual Italian code, in case of seismic retrofit of a public building, the minimum value of the $\zeta_E$ after the upgrading operations should be 0.60. In this building, steel jacketing is chosen as upgrading technique. The reason for choosing this technique is that there was no possibility to change the dimensions of the cross sections, due to architectural recommendations. Moreover, there was a quite total absence

**TABLE 3 |** The suite of strong ground-motion records used in this study.

| Record number | NGA record number | Earthquake name | Station name | Horizontal component | Magnitude | RRUP (km) |
|---|---|---|---|---|---|---|
| 1 | 1103 | Northridge-01 | LA - Saturn St | 2 | 6, 69 | 27, 01 |
| 2 | 1126 | Kozani, Greece-01 | Kozani | 1 | 6.4 | 19.54 |
| 3 | 125 | Friuli, Italy-01 | Tolmezzo | 2 | 6.5 | 15.82 |
| 4 | 160 | Imperial Valley-06 | Bonds corner | 2 | 6, 53 | 2, 66 |
| 5 | 167 | Imperial Valley-06 | Compuertas | 1 | 6, 53 | 15, 3 |
| 6 | 176 | Imperial Valley-06 | El Centro Array #13 | 1 | 6, 53 | 21, 98 |
| 7 | 26 | Hollister-01 | Hollister City hall | 2 | 5, 6 | 19, 56 |
| 8 | 288 | Irpinia, Italy-01 | Brienza | 1 | 6.9 | 22.56 |
| 9 | 289 | Irpinia, Italy-01 | Calitri | 2 | 6.9 | 17.64 |
| 10 | 290 | Irpinia, Italy-01 | Mercato San Severino | 1 | 6.9 | 29.80 |
| 11 | 313 | Corinth, Greece | Corinth | 2 | 6.6 | 10.27 |
| 12 | 3605 | Lazio Abruzzo, Italy | Cassino-Sant' Elia | 1 | 5.8 | 24.40 |
| 13 | 4054 | Bam, Iran | Mohammad Abad- | 1 | 6.6 | 46.22 |
| 14 | 4284 | Basso Tirreno, Italy | Naso | 1 | 6.0 | 19.59 |
| 15 | 4316 | Umbria-03, Italy | Pietralunga | 2 | 5.6 | 25.33 |
| 16 | 4328 | Potenza, Italy | Brienza | 1 | 5.8 | 26.20 |
| 17 | 4335 | Umbria Marche (foreshock), Italy | Assisi-Stallone | 2 | 5.7 | 23.48 |
| 18 | 4336 | Umbria Marche (foreshock), Italy | Borgo-Cerreto Torre | 1 | 5.7 | 21.31 |
| 19 | 4345 | Umbria Marche, Italy | Assisi-Stallone | 1 | 6.0 | 16.55 |
| 20 | 4352 | Umbria Marche, Italy | Nocera Umbra | 2 | 6.0 | 8.92 |
| 21 | 4477 | L'Aquila, Italy | GRAN SASSO (Assergi) | 1 | 6.3 | 6.40 |
| 22 | 464 | Morgan Hill | Hollister diff. Array #3 | 1 | 6, 19 | 26, 43 |
| 23 | 477 | Lazio-Abruzzo, Italy | Atina | 2 | 5.8 | 18.89 |
| 24 | 522 | N. Palm Springs | Indio | 2 | 6, 06 | 35, 57 |
| 25 | 564 | Kalamata, Greece-01 | Kalamata (bsmt) | 2 | 6.2 | 6.45 |
| 26 | 754 | Loma Prieta | Coyote Lake dam (Downst) | 2 | 6, 93 | 20, 8 |
| 27 | 8164 | Duzce, Turkey | IRIGM 487 | 2 | 7, 14 | 2, 65 |
| 28 | 818 | Georgia, USSR | Iri | 1 | 6.2 | 31.47 |
| 29 | 901 | Big Bear-01 | Big Bear Lake-Civic Cent. | 1 | 6, 46 | 8, 3 |
| 30 | 93 | San Fernando | Whittier Narrows dam | 2 | 6, 61 | 39, 45 |

of steel in the structural members. The steel jacketing is less invasive with respect to other common upgrading strategies. The purpose of the steel jacketing is to increase the low shear strength of the elements (as a result of the lack of stirrups) and, in particular for the columns, to increase the bearing capacity due to the concrete confinement effect. It is to note

that also the FRP wrapping allows to have a good increase of confinement action (Formisano et al., 2006, 2017b; Laterza et al., 2017). However, the steel jacketing has been chosen because it allowed an higher increase of the flexural capacity of the members, given a fixed economical threshold. The steel jacketing is applied to the structural elements (e.g., columns and beams, see
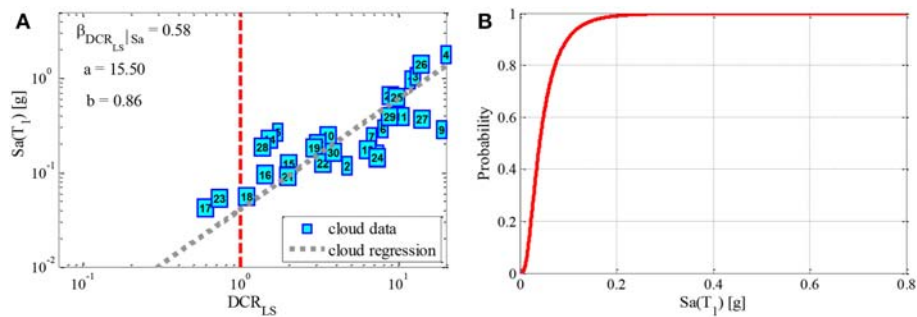
**FIGURE 7 |** Cloud regression **(A)** and fragility curve **(B)** for the *LS* limit state with respect to the bare building.
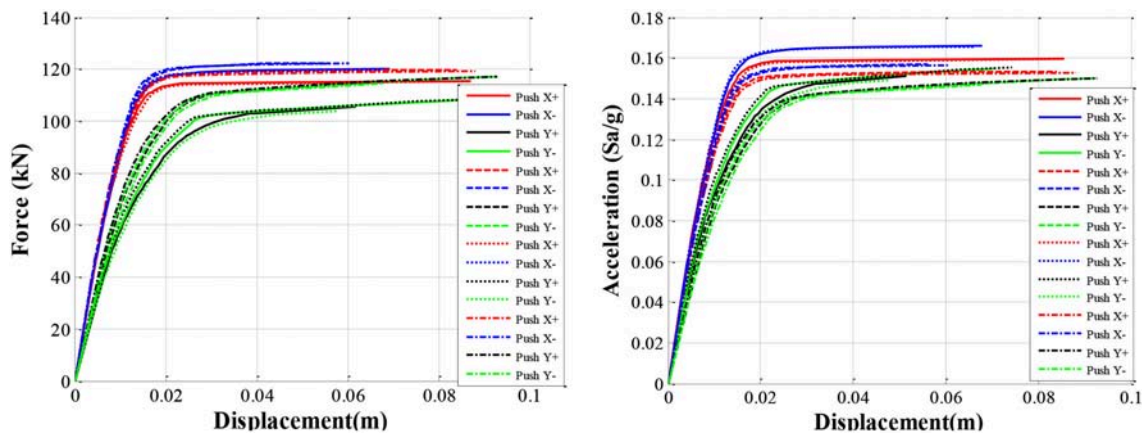


**FIGURE 8 |** Pushover curves for the case study building after steel jacketing.

**Figures 3C,D**) with a rectangular section. The jacket consists of four angular profiles (dimensions $60 \times 60 \times 6$ mm) connected by welded plates, with a width of 60mm and a thickness of 6 mm positioned with appropriate distance. The angular profiles are fixed to the element by epoxy resin, after preliminary treatment of the surface of the members, with protection of the bars, restoring of the concrete cover with cement mortar and cleaning of the surface.

## Non-linear Static Analysis Procedure

First, it is to note that the same modeling approach used for the bare building is used also for the upgraded building. As for the bare building, pushover analysis has been carried out by following the Italian seismic code (NTC, 2008) for the case study upgraded building. A number of 16 pushovers has been done, using two different distributions of forces and using a possible eccentricity of the 5% in each direction. **Figure 8** shows the pushover results in terms of base shear vs. top displacement. As explained for the pushovers of the bare building, the red curves correspond to forces parallel to horizontal × positive direction (see **Figure 1**); the blue curves correspond to forces parallel to horizontal × negative direction; the black curves correspond to forces parallel to horizontal y positive direction; the green curves correspond to forces parallel to horizontal y negative direction.

**Figure 9** shows for the LS limit state with red color the members for which the safety verifications are not satisfied and with green color the members for which the safety verifications are satisfied, showing that however a limited number of members result unsafe. It is to note that the unsafe members still present shear deficiencies and so the first crisis in the members is still related to possible shear failure. The reason is related to the impossibility to operate in that zone of the building, as consequence of the presence of the engine of the climate installations, that is fundamental to be preserved in a swimming pool. However, as general goal of the upgrading, a vulnerability index of 0.61 has been achieved.

## Non-linear Dynamic Analysis Procedure

**Figure 10** shows the scatter plots for Cloud Analysis data D = {(Sa,i, DCRLS,i), i = 1:30 for the set of records outlined in **Table 3**. For each data point (cyan colored squares), the corresponding record number is shown. Moreover, the figure illustrates the Cloud Analysis regression prediction model (i.e., regression line and the estimated parameters, see Equation 2) fitted to the data. The line $DCR_{LS} = 1$ corresponding to the onset of limit state (herein, DL in **Figure 10A** and LS in **Figure 10B**) is also shown with red-dashed line. **Figure 11** shows the resulting Cloud Analysis-based fragility curves for the pre e post upgrading

building with reference to the limit states of DL and LS. For DL limit state, the capacity is assumed as the displacement corresponding to the end of the bilinear system of the SDOF. The LS capacity, instead, is attained in correspondence of the ultimate displacement of the bilinear system of the SDOF. The values of the statistics (e.g., median and the logarithmic standard deviation) associated with the Cloud Analysis based fragility curve are, respectively, 0.51 and 0.66 (LS limit state) and 0.13 and 0.66 (DL limit state).

## CLASS OF RISK ACCORDING TO ITALIAN SEISMIC CLASSIFICATION BEFORE AND AFTER THE UPGRADING

In this last section, the class of risk (according to the Italian Guidelines on the seismic classification, Guidelines, 2017) is calculated for the case study building before and after the upgrading. Once the capacity of the structure is assessed, two parameters are calculated. The first parameter is economic and is called expected annual mean losses (Perdite Annue medie, PAM). The second one is related to the safety of the structure and id called Life Safety Index (Indice di sicurezza della vita, IS-V). The same calculation is repeated after the upgrading. It
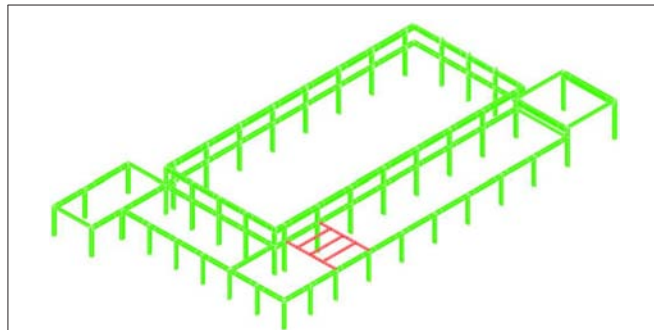
is to note that with the 2017 law (Italian Balance Law, 2017), a campaign has been launched for the seismic improvement of existing structures. This is the so-called "Sismabonus," an opportunity to stimulate a voluntary plan for the evaluation and prevention of seismic risk of buildings. In this context, the Italian guidelines have been conceived, with the goal of providing the operational tools for classifying the seismic risk of buildings; The document defines eight Classes of Risk, with increasing risk from letter A+ to G, and establishes two methods for determining the risk class of a building: the conventional method and the simplified one. The first one is conceptually applicable to any type of construction and is based on the application of the standard methods of analysis provided by the current codes (NTC, 2018) and allows the assessment of the class of risk of the construction both before and after upgrading. Instead, the simplified method, applicable only to masonry buildings, allows a reliable but simplified estimate. Herein, in the following seismic classification, the conventional method is used. As said, for the determination of the risk



FIGURE 9 | Safety verifications for the case study building after steel jacketing.
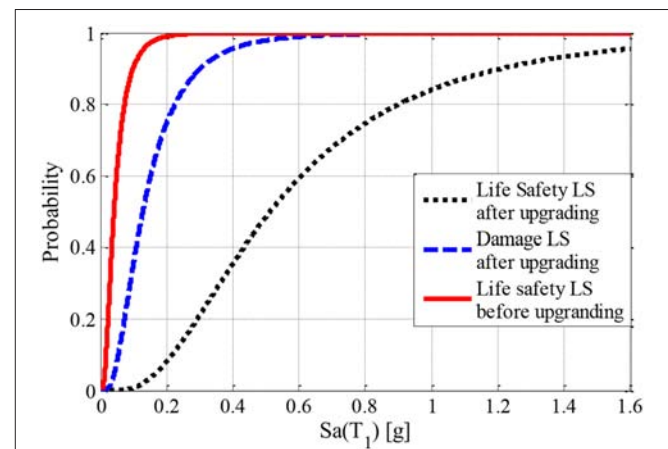


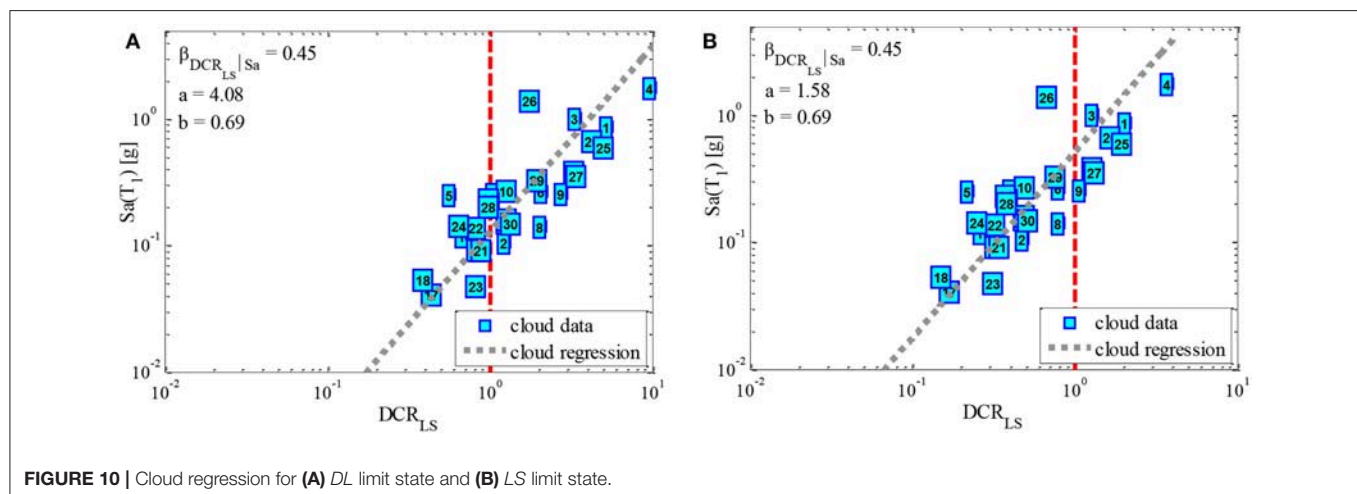FIGURE 11 | Fragility curves comparison before and after upgrading operations.



FIGURE 10 | Cloud regression for (A) DL limit state and (B) LS limit state.
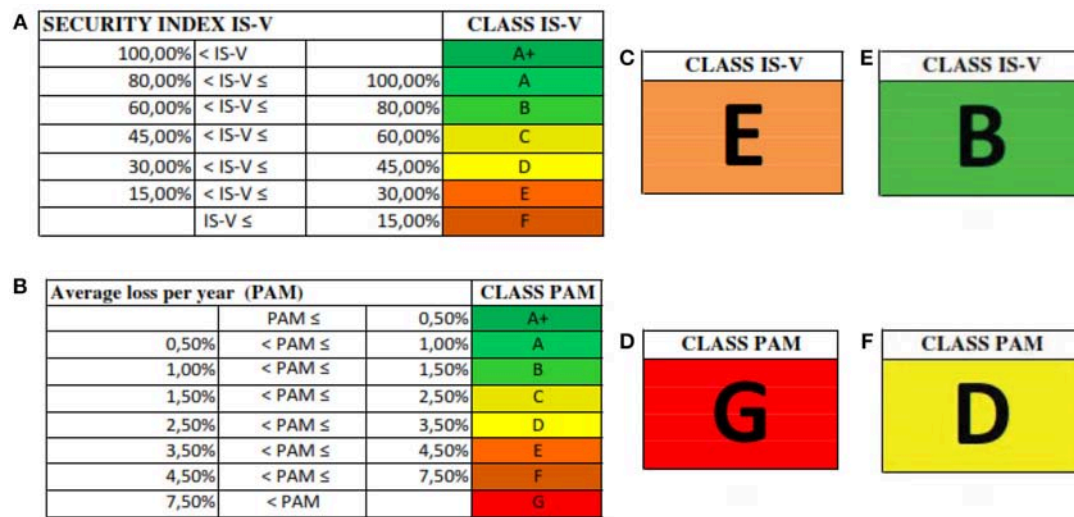
**FIGURE 12** | **(A)** Assignment of the IS-V risk class according to the size of the Security Index; **(B)** Attribution of the PAM risk class according to the magnitude of the expected annual average Losses; **(C)** IS-V class before upgrading; **(D)** PAM class before upgrading; **(E)** IS-V class after upgrading; **(F)** PAM class after upgrading.

class, reference is made to two parameters (e.g., the PAM, that takes into account the economic losses associated with damage to the elements, structural or not and the IS-V, that takes into account the safety of the structure or the safety index). The seismic risk class assessment procedure includes the following steps:

- PGA evaluation: with respect to the specific site, the peak ground accelerations, $PGA_D$, for reaching the different limit states are evaluated;
- Structural analysis: the values of the capacity peak ground accelerations, $PGA_C$, which induce the achievement of LS and DL limit states are calculated;
- Identification of the IS-V class, that is the relationship between the $PGA_C$ (for LS limit state) and the $PGA_D$ of the site where the construction is located. The percentage value obtained, through the table shown in **Figure 12A**, allows to identify the seismic risk class of the building according to the vulnerability index.
- Vulnerability analysis—which allows to quantify the structural and non-structural damage consequent to the achievement of certain levels by the response parameters, through the calculation of the following values: (a) return periods, $T_{rC}$, associated with the earthquakes that generate such accelerations; (b) value of the annual average frequency of exceeding λ (equal to the inverse of the return period); (c) the value of the reconstruction cost percentage (CR%) associated with the corresponding value of λ for each of the limit states considered;
- Identification of the PAM class as the area under the curve representing direct economic losses, obtained as function of the annual average frequency of exceeding the events that cause the achievement of a certain limit state for the

structure. The PAM Class is identified, using the table shown in **Figure 12B**.

Finally, the risk class is identified as the worst class between the PAM class and the IS-V class. **Figure 12** shows the results in terms of risk class before and after the upgrading operations for the case study building. It can be noted that before the upgrading operations the risk class was G, while after the upgrading operations, the risk class D is achieved.

## CONCLUSIONS

The "Collana" football stadium was initially built in the late '20s and then be completely rebuilt in the post-war period and used as a multi-sports center together with other buildings. The present work concerns the description and verification of the structural upgrading design for the swimming pool building, realized inside the more general scope of the project of functional upgrading of the entire building. The upgrading of the building is designed in order to solve the vertical loads deficiency and to achieve a certain threshold of the seismic vulnerability index, as described in Italian code. Based on different considerations related to effectiveness, costs and invasive grade of the upgrading options, steel jacketing is chosen. The steel jacketing is realized through steel plates wrapped completely around the beams plus angular plates in the corners around the length of the members. All the columns and the members are steel jacketed. Assessment and upgrading are shown both based on linear and dynamic non-linear analyses procedures. In particular, the achievement of an adequate value of seismic vulnerability index through non-linear static analysis, as required for buildings susceptible to crowding in the case of temporary use of the structure

for purposes related to the management of the emergencies in general, is shown. Moreover, non-linear dynamic analyses are implemented to measure the probability of achieving predefined limit states before and after the upgrading. Finally, the seismic risk class is assigned before and after the upgrading according to two parameters. The final results show the effectiveness of the structural interventions of upgrading with respect to the application of non-linear static and dynamic analyses procedures and based on the new Italian guidelines for seismic risk classification of construction.

## DATA AVAILABILITY

The datasets generated for this study are available on request to the corresponding author.

## AUTHOR CONTRIBUTIONS

AM is responsible for the organization and implementation of this research. GC is responsible for the structural calculations. AS is responsible for the architectural design project.

## REFERENCES

Aslani, H., and Miranda, E. (2005). *Probabilistic Earthquake Loss Estimation and Loss Disaggregation in Buildings*, Dissertation, Stanford University.

Bertolesi, E., Fabbrocino, F., Formisano, A., Grande, E., and Milani, G. (2017). FRP-strengthening of curved masonry structures: local bond behavior and global response. *Key Eng. Mat.* 747, 134–141. doi: 10.4028/www.scientific.net/KEM.747.134

Braga, F., Caprili, S., Gigliotti, R., and Salvatore, W. (2015). Hardening slip model for reinforcing steel bars. *Earthq. Struct.* 9, 503–539. doi: 10.12989/eas.2015.9.3.503

Braga, F., Gigliotti, R., Laterza, M., D'Amato, M., and Kunnath, S. (2012). Modified steel bar model incorporating bond-slip for seismic assessment of concrete structures. *ASCE J. Struct. Eng.* 138, 1342–1350. doi: 10.1061/(ASCE)ST.1943-541X.0000587

Calvi, G. M. (2013). Choices and criteria for seismic strengthening. *J. Earth Eng.* 17, 769–802. doi: 10.1080/13632469.2013.781556

Caprili, S., Moersch, J., and Salvatore, W. (2015). Mechanical Performance vs. corrosion damage indicators for corroded steel reinforcing bars. *Adv. Mater. Sci. Eng.* 2015:739625. doi: 10.1155/2015/739625

CDS (2018). *CDS Win, Computer Design of Structures*. Catania: Scientific and technical Software.

Celik, O. C., and Ellingwood, B. R. (2010). Seismic fragilities for non-ductile reinforced concrete frames–role of aleatoric and epistemic uncertainties. *Struct. Saf.* 32, 1–12. doi: 10.1016/j.strusafe.2009.04.003

Circolare (2009). Circolare 2 febbraio 2009 n. 617 del Ministero delle Infrastrutture e dei Trasporti (G.U. 26 febbraio 2009 n. 27 – Suppl. Ord.), Istruzioni per l'applicazione delle 'Norme Tecniche delle Costruzioni' di cui al D.M. 14 gennaio 2008.

Cosenza, E., Del Vecchio, C., Di Ludovico, M., Dolce, M., Moroni, C., Prota, A., et al. (2018). The Italian guidelines for seismic risk classification of constructions: technical principles and validation. *Bull. Earthq. Eng.* 16, 5905–5935. doi: 10.1007/s10518-018-0431-8

D'Amato, M., Braga, F., Gigliotti, R., Laterza, M., and Kunnath, S. (2012). Validation of a modified steel bar model incorporating bond-slip for seismic assessment of concrete structures. *ASCE J. Struct. Eng.* 138, 1351–1360. doi: 10.1061/(ASCE)ST.1943-541X.0000588

Fajfar, P. (1999). Capacity spectrum method based on inelastic demand spectra. *Earth Eng. Struct. Dyn.* 28, 979–994.

Fajfar, P. (2000). A nonlinear analysis method for performance-based seismic design. *Earth Spectr* 16, 573–592. doi: 10.1193/1.1586128

Formisano, A., Castaldo, C., and Chiumiento, G. (2017a). Optimal seismic upgrading of a reinforced concrete school building with metal-based devices using an efficient multi-criteria decision-making method. *Struct. Infrastruct. Eng.* 13, 1373–1389. doi: 10.1080/15732479.2016.1268174

Formisano, A., De Matteis, G., Panico, S., and Mazzolani, F.M. (2008). Seismic upgrading of existing RC buildings by slender steel shear panels: a full-scale experimental investigation. *Adv. Steel Constr.* 4, 26–45.

Formisano, A., Di Lorenzo, G., Iannuzzi, I., and Landolfo, R. (2017b). Seismic vulnerability and fragility of existing Italian industrial steel buildings. *Open Civil. Eng. J.* 11, 1122–1137. doi: 10.2174/1874149501711011122

Formisano, A., Faggiano, B., Landolfo, R., and Mazzolani, F. M. (2006). "Ductile behavioural classes of steel members for seismic design," in *Proceedings of the 5th International Conference on Behaviour of Steel Structures in Seismic Areas* (Yokohama), 225–232.

Formisano, A., Iaquinandi, A., and Mazzolani, F.M. (2015). Seismic retrofitting by FRP of a school building damaged by Emilia-Romagna earthquake. *Key Eng. Mat.* 624, 106–113. doi: 10.4028/www.scientific.net/KEM.624.106

Formisano, A., Lombardi, L., and Mazzolani, F. M. (2016). Perforated metal shear panels as bracing devices of seismic-resistant structures. *J. Constr. Steel Res.* 126, 37–49. doi: 10.1016/j.jcsr.2016.07.006

Formisano, A., and Mazzolani, F. M. (2015b). On the selection by MCDM methods of the optimal system for seismic retrofitting and vertical addition of existing buildings. *Comput. Struct.* 159, 1–13. doi: 10.1016/j.compstruc.2015.06.016

Formisano, A., and Sahoo, D. R. (2015a). Steel shear panels as retrofitting system of existing multi-story RC buildings: case studies. *Adv. Struct. Eng. Mech.* 1, 495–512. doi: 10.1007/978-81-322-2190-6_41

Frascadore, R., Di Ludovico, M., Prota, A., Verderame, G. M., Manfredi, G., Dolce, M., et al. (2015). Local strengthening of reinforced concrete structures as a strategy for seismic risk mitigation at regional scale. *Earth Spectr.* 31, 1083–1102. doi: 10.1193/122912EQS361M

Guidelines (2017). Guidelines for the seismic risk classification of constructions, Decreto del Ministero delle Infrastrutture e dei Trasporti 28 febbraio 2017, n. 58.

Italian Balance Law (2017). L.205/17, Balance Law 2018, Official Gazette n. 302 of 29/12/17, Ordinary Supplement n. 62 (in Italian).

Jalayer, F., Beck, J., and Zareian, F. (2012). Analyzing the sufficiency of alternative scalar and vector intensity measures of ground shaking based on information theory. *J. Eng. Mech.* 138, 307–316. doi: 10.1061/(ASCE)EM.1943-7889.0000327

Jalayer, F., De Risi, R., and Manfredi, G. (2015). Bayesian Cloud Analysis: efficient structural fragility assessment using linear regression. *Bull. Earth Eng.* 13, 1183–1203. doi: 10.1007/s10518-014-9692-z

Jalayer, F., and Ebrahimian, H. (2017). Seismic risk assessment considering cumulative damage due to aftershocks. *Earthq. Eng. Struct. Dyn.* 46, 369–389. doi: 10.1002/eqe.2792

Jalayer, F., Ebrahimian, H., Miano, A., Manfredi, G., and Sezen, H. (2017). Analytical fragility assessment using un-scaled ground motion records. *Earth Eng. Struct. Dyn.* 46, 2639–2663. doi: 10.1002/eqe.2922

Jalayer, F., Franchin, P., and Pinto, P. E. (2007). A scalar damage measure for seismic reliability analysis of RC frames. *Earthq. Eng. Struct. Dyn.* 36, 2059–2079. doi: 10.1002/eqe.704

Laterza, M., D'Amato, M., Braga, F., and Gigliotti, R. (2017). Extension to rectangular section of an analytical model for concrete confined by steel stirrups and/or FRP jackets. *Compos. Struct.* 176, 910–922. doi: 10.1016/j.compstruct.2017.06.025

Liel, A. B., and Deierlein, G. G. (2013). Cost-benefit evaluation of seismic risk mitigation alternatives for older concrete frame buildings. *Earth Spectr.* 29, 1391–1411. doi: 10.1193/030911EQS040M

Miano, A., Jalayer, F., Ebrahimian, H., and Prota, A. (2018a). Cloud to IDA: efficient fragility assessment with limited scaling. *Earth Eng. Struct. Dyn.* 47, 1124–1147. doi: 10.1002/eqe.3009

Miano, A., Jalayer, F., and Prota, A. (2017b). "Considering structural modeling uncertainties using bayesian cloud analysis," in *Proceedings of the 6th ECCOMAS Thematic Conference on Computational Methods in Structural Dynamics and Earthquake Engineering* (Rhodes).

Miano, A., Sezen, H., Jalayer, F., and Prota, A. (2017a). "Performance based comparison of different retrofit methods for reinforced concrete structures," in *Proceedings of the 6th ECCOMAS Thematic Conference on Computational Methods in Structural Dynamics and Earthquake Engineering* (Rhodes).

Miano, A., Sezen, H., Jalayer, F., and Prota, A. (2018b). "Performance based assessment and retrofit of non ductile existing reinforced concrete structures," in *Proceedings of the Structures Conference* (Fort Worth, TX).

Moehle, J.P. (2000). "State of research on seismic retrofit of concrete building structures in the US," in *US-Japan Symposium and Workshop on Seismic Retrofit of Concrete Structures.*

NTC (2008). - D. M. Infrastrutture Trasporti 14 gennaio 2008, Norme tecniche per le Costruzioni, G.U. 4 febbraio 2008 n. 29 - Suppl. Ord.Circolare 2009.

NTC (2018). - D. M. Infrastrutture Trasporti 17 gennaio 2018, Norme tecniche per le Costruzioni, G.U. 20 febbraio 2018 n. 42 - Suppl. Ord.

Sezen, H., and Moehle, J. P. (2004). Shear strength model for lightly reinforced concrete columns. *J. Struct. Eng.* 130, 1692–1703. doi: 10.1061/(ASCE)0733-9445(2004)130:11(1692)

Thermou, G. E., and Elnashai, A. S. (2006). Seismic retrofit schemes for RC structures and local-global consequences. *Prog. Struct. Eng. Mater.* 8, 1–15. doi: 10.1002/pse.208

Vidic, T., Fajfar, P., and Fischinger, M. (1994). Consistent inelastic design spectra: strength and displacement. *Earth Eng. Struct. Dyn.* 23, 507–521. doi: 10.1002/eqe.4290230504

# Dynamic Behavior of an Inclined Existing Masonry Tower in Italy

Angela Ferrante[1], Francesco Clementi[1]* and Gabriele Milani[2]

[1] Department of Civil and Building Engineering, and Architecture, Polytechnic University of Marche, Ancona, Italy,
[2] Department of Architecture, Built Environment and Construction Engineering ABC, Polytechnic of Milano, Milan, Italy

The renaissance bell tower of San Benedetto in Ferrara (Italy) has been investigated to understand its nonlinear dynamics correctly with the Non-Smooth Contact Dynamic (NSCD) method. The masonry structure has been modeled with the Discrete Element Methods (DEM), assuming rigid blocks and frictional joints, with the aim to recreate the tower in the actual configuration with the inclination and in a fictitious perfect vertical shape in order to assess the influence of the initial slope on its dynamics. The contacts between blocks are governed by the Signorini's impenetrability condition and by dry-friction Coulomb's law. Both configurations have been analyzed inducing real seismic excitations of various types and intensities, corresponding to the six main seismic events of the last few decades in Italy. Thus, the seismic vulnerability of the examined tower is clearly expressed in the numerical results, proving the effects due to the inclination on the amplification of the vulnerability and the several possible collapse mechanisms. Moreover, the NSCD has demonstrated to be a powerful numerical technique to obtain highly accurate results in the structural analyses of masonry structures in the nonlinear range.

Keywords: masonry tower, inclination effect, vulnerability, nonlinear dynamic analysis, non-smooth contact dynamic (NSCD)

## INTRODUCTION

A major research field in structural engineering concerns the structural safety and seismic assessment of the masonry buildings, especially historic structures, to preserve their main architectural features in the cultural heritage (Roca et al., 2013). In the last few decades, a significant number of structures was severely damaged, especially monumental buildings, churches and belfries, by the most recent Italian earthquakes such as Umbria-Marche 1997–1998, Abruzzo 2009, Emilia-Romagna 2012, Central Italy Earthquake 2016 (Lagomarsino and Podestà, 2004; Brandonisio et al., 2013; Milani, 2013; Clementi et al., 2017).

Among the buildings belonging to the heritage of Italian architecture, the masonry structures characterized by a predominantly vertical development, such as towers and belfries, are prevalent. In this context, the detailed analysis of interpretative models that can successfully define the effects of the earthquakes is an indispensable mean to know and predict the behavior of unplanned masonry buildings under seismic forces (Pellegrini et al., 2018).

The primary challenge is the mechanical behavior of the masonry structures which significantly depends on the complex nature of the masonry itself. Thus, an accurate numerical model has to take into account the discontinuity of ancient masonry structures, characterized by units, like bricks, stones, blocks, voids, and mortar. For this purpose, the constitutive laws and the material properties assume a relevant aspect in the model (Clementi et al., 2015; Terracciano et al., 2015; Valente and Milani, 2016; Formisano et al., 2017), to represent the proper quality of masonry walls, which decrease severely in case of poor material or incorrect construction techniques, and the different range of stresses that exist in masonry structures.

In general, experimental and numerical analyses of masonry are widely showed in literature, in particular with the finite element (Acito et al., 2014; Cavalagli and Gusella, 2015; Valente and Milani, 2016; Clementi et al., 2018a; Formisano et al., 2018; Giordano et al., 2019), that allows analyzing the dynamics beyond the elastic behavior, but it does not explicitly consider the interaction between the blocks. Furthermore, the non-smooth behavior near collapse, i.e., when the blocks slide and impact between them, is not introduced also in sophisticated analyses such as micro-modeling that distinguishes the elements of masonry. Hence, in this work, to study this high nonlinearity of the historic structures and to identify the typologies of collapse has been used the advance rigid-body dynamics formulation belonging to the distinct element method (DEM) (Poiani et al., 2018).

This approach can reproduce all the possible collapse mechanisms, peculiarities of historic masonry, large displacements and common contact phenomena such as the stick-slip transition, representing a sudden change in motion at the collision. Furthermore, the DEM is particularly successful since each masonry unit is individually modeled and the joints represent the natural planes of slip and crack. The number of blocks in the numerical model should be adjusted between computational cost and realistic structural behavior.

To the authors' knowledge, the non-smooth nature of the dynamic response of towers is not analyzed in depth. For this reason, in the present work, a DEM code which implements the Non-Smooth Contact Dynamics (NSCD) method (Moreau, 1988; Chetouane et al., 2005; Dubois et al., 2018) is used to analyze the dynamic behavior of an inclined existing masonry tower. The masonry is simulated using an assembly of rigid bodies approximately equal to the real geometry of bricks, but with greater dimensions to take into account the thickness of the mortar. The analyses are done with the LMGC90© code which works with a solver able to compute the nonlinear dynamics of complex masonry structures in the 3D space, and with a post-processing program allowing to plot all the quantities of interest, in order to compare the numerical predictions with the real damages.

Hence, in this work, to figure out the nonlinear dynamics of a renaissance bell tower, six different sets of ground accelerations related to most recent Italian earthquakes have been considered. The analyzed masonry bell tower belongs to the San Benedetto's complex in Ferrara (Italy) and presents an unusually high inclination, **Figure 1**. Therefore, for all cases, it is possible to evaluate a comparison between the inclined and vertical tower, in order to understand, in a qualitatively and quantitatively manner, the slope's influence on the dynamics and failure mechanisms.

## A BRIEF DESCRIPTION OF SAN BENEDETTO'S TOWER

The complex of San Benedetto in Ferrara goes back to the fifteenth century. The Church was built for the Benedictines of Pomposa between 1496 and 1553 and consecrated in 1563, while the bell tower was built in 1621. In 1611 Ludovico Ariosto was buried there, according to his will, where now there is the altar of the Madonna, to be then transferred to the Ariostea public library in 1801 at the behest of General de Miollis, at that time in Ferrara after the occupation of the city from the Napoleonic army. After being used as army camp and stable during the French Revolution, it was restored and reopened to worship in 1812. In 1944 the church was severely hit and destroyed in large part by the English bombing, as visible in **Figure 2A**. It was entirely rebuilt on the original design in 1954 (see **Figure 2B**).

On 15th June 2007, a great fire was developed in the central apse of the church, and the investigators have hypothesized it as a malicious cause. The fire was then quickly tamed without making any victims, but it damaged the whole church. Damages involve structures, installations, organ, works of art. The restoration is currently underway.

Differently, the masonry tower was built on the design of Giovan Battista Aleotti from 1621 and completed in 1646, due to the development of foundation settlements at a very early stage of the construction process. The bell tower is high about 55 m, and it has a square cross-section with a long side of 7.33 m. The structure is quite regular along the height, with the different upper part that is about 5.7 × 5.7 m, as in **Figures 3D,E**. There is only a floor at 32.0 m, where are located the bells, and another at 39.8 m, which consist of two cross vaults.

The vertical structure is characterized by massive regular brick walls, with internally visible reductions of thickness varying from 1.40 m at the base up to 0.65 m on the last floor, and a dome made by masonry bricks closing at the top. The belfry consists of large arches with measuring 1.65 × 3.91 m, and it is topped with a cell with smaller rectangular openings with dimensions 1.49 × 3.2 m. Lastly, the vertical connection is guaranteed only by steel stairs, consider as a load in the numerical model.

As consequence of a storm, in 1842 there was the collapse of the summit of the bell tower of Aleotti, that was particularly serious because it also damaged the covered church choir of San Benedetto, which then had to be repaired, as later was restored the bell cell. Subsequently, new damages were recorded due to fortuitous situations and storms, first in 1880 and then in 1933. These events, together with the nature of the ground and other static problems, meant that the high construction came out of its barycenter since the 1600s; so that the inclination was accentuated more and more in the following centuries, until the earthquake of 2012, after which the structure has suffered clearly cracks on North and South façade. Now the tower has a notable overhang in one of the geometrical directions.

The results of 2008 survey exhibit a horizontal displacement of the centroid of the top section of the structure (52.45 m from the base) equal to 0.50 m along the northward direction and almost 2.82 m along the westward direction, whereas in 1883 survey they were respectively equal to 0.40 and 2.50 m (see **Figure 3F**). The overhang values are gradually increasing (Pellegrinelli et al., 2014) and, recently, the equilibrium conditions have been assessed carefully in static conditions to have an insight into both the stability of the structure and the residual capacity against possible, albeit small, seismic events. Also a dynamic identification with a calibration of a first classical Finite Element Model (FEM) was also done in 2016 (Clementi et al., 2018b).

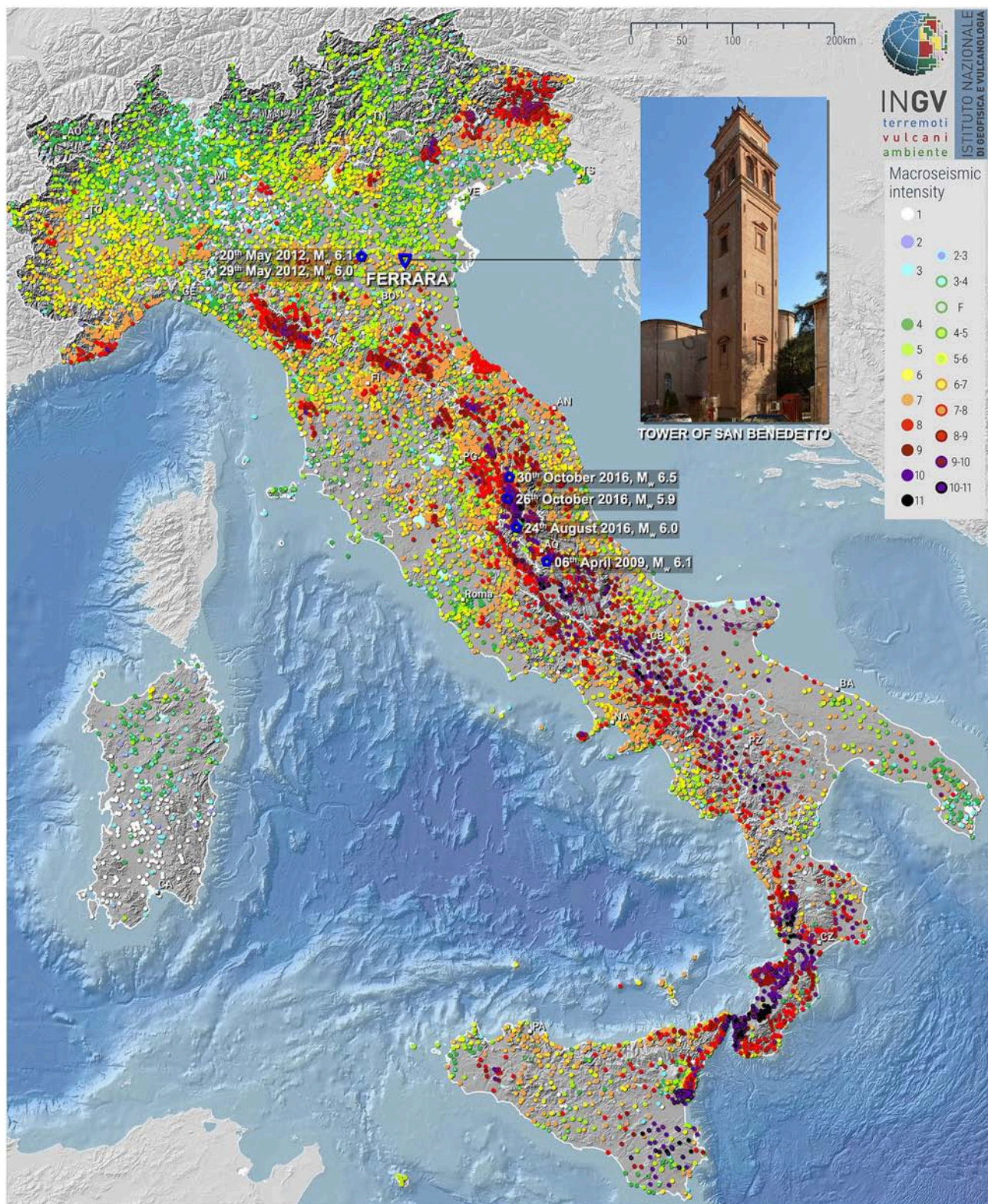**FIGURE 1 |** Maps of the geographical location of the bell tower of San Benedetto in Ferrara (Italy) and Italian Macroseismic intensity (https://emidius.mi.ingv.it/), with the position of the six main seismic events of the last few decades in Italy taken into account for analyses.
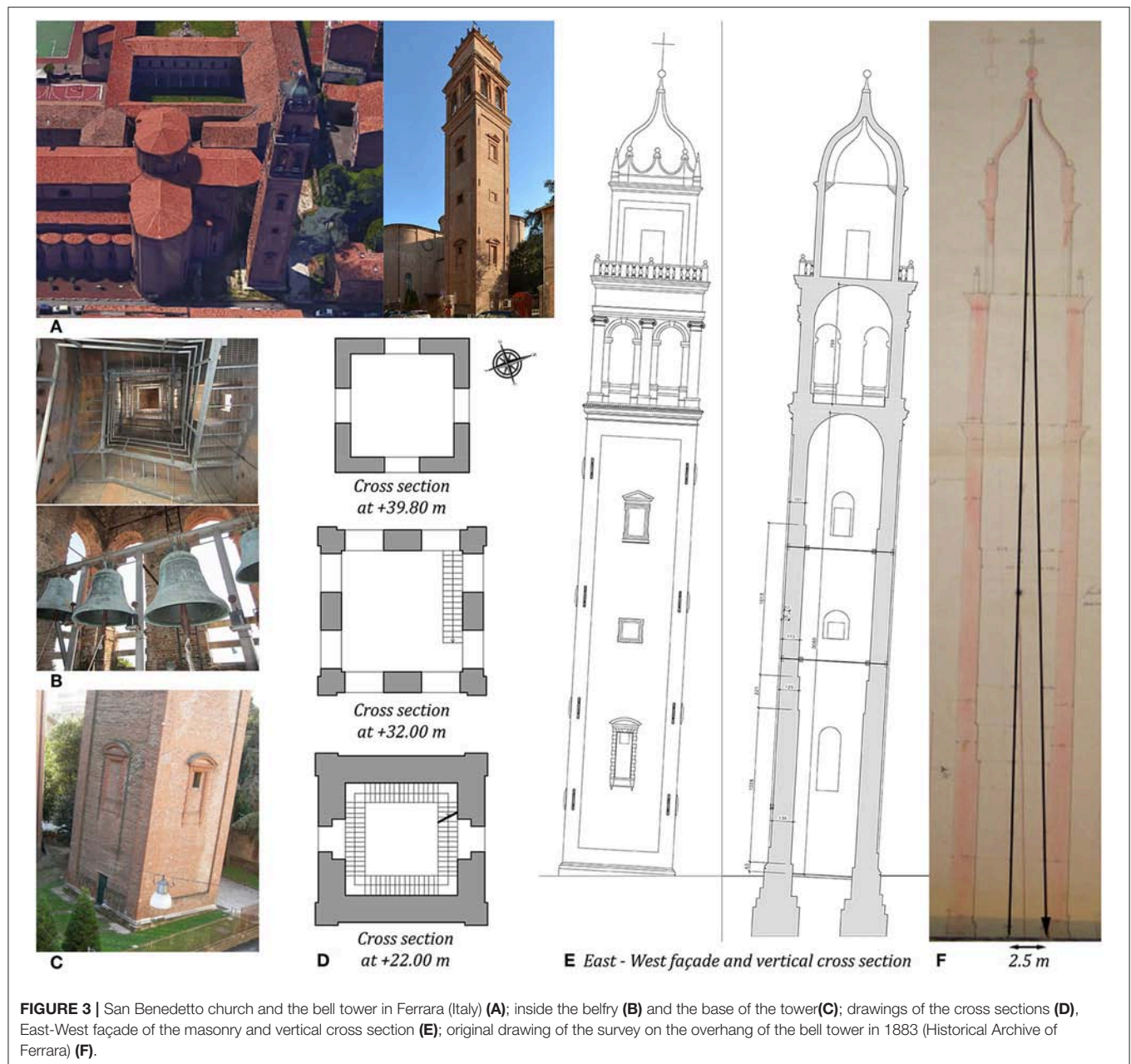
**FIGURE 2 |** Complex of San Benedetto in Ferrara (Italy) after the bombing of the World War in 1944 **(A)**, a view of the bell tower and the complex after rebuilding **(B)**.

## DISTINCT ELEMENT METHOD FOR HISTORICAL MASONRY

At present, the simulation of masonry structures does not have a straightforward or unified approach. Indeed, according to the required level of accuracy and computational cost, there are several numerical approaches in the current structural engineering's knowledge. In practice is commonly used the FEM, which takes into account the numerical model as a continuous medium (Betti et al., 2014; Pierdicca et al., 2016; Valente and Milani, 2016; Sarhosis et al., 2018) whose geometry and behavior are described using pre-defined finite elements. This approach allows to represent several masonry behaviors, nevertheless for an advanced numerical modeling of ancient structures view as discontinuous units, with stiff bodies and deformational

behavior at the joints, it is necessary the use of the Discrete Element Method (DEM). Concerning DEMs, the structure is characterized by an assembly of 3D separate bodies, deformable or stiff, and by points of contacts on the interfaces between the bodies, which represent the interaction at masonry's joints. The motion of the bodies is governed by contact laws (Lemos, 2007), that are different in order to estimate widespread interactions (Asteris et al., 2015).

Among the various approach, an NSCD method has been implemented in the LMGC90© software, which is an open source software, within a non-smooth dynamics framework, with an implicit time integration, and implicit contact solvers (i.e., nonlinear Gauss-Seidel (NLGS), preconditioned conjugate gradient with projection (PCGP), etc.). Furthermore, the applications with many interacting 3D

**FIGURE 3 |** San Benedetto church and the bell tower in Ferrara (Italy) **(A)**; inside the belfry **(B)** and the base of the tower**(C)**; drawings of the cross sections **(D)**, East-West façade of the masonry and vertical cross section **(E)**; original drawing of the survey on the overhang of the bell tower in 1883 (Historical Archive of Ferrara) **(F)**.

bodies are reachable through parallel computing (shared or distributed memory) and during computation, it is possible to check the relevance of the analysis through some global indicators (convergence norm, quality of interaction laws computation, etc.).

As a rule, the interaction between bodies, in DEM application, is examined in the contact localized at point assumption, in which the normal and shear stress vector are functions of the relative displacement and velocity of the contacting objects. This simplification, however, still allows right accuracy if a sufficient number of contact points is used.

## NSCD for Masonry Structures Modeling

The NSCD method is based on a particular formulation of the equation of motion, as firstly explained by Moreau (1988). The "non-smooth" regards to the specific laws used to model mechanical systems with unilateral contacts and friction. The second-order dynamics is characterized by velocity jumps due to the impacts, with unilateral kinematic constraints on the position, which introduce to non-smoothness in time and space.

The non-smoothness in the interaction laws are written as multi-valued mappings between contact reactions and the relative velocity, in the framework of the NSCD method (Dubois

et al., 2018). Fairly large time steps are permitted by this method. In fact, the multi-contact problem resolution consists in solving two groups of unknowns which are global ones, as kinematic space unknowns related to the blocks, and local ones as contact space unknowns, related to interactions, linked together thanks to kinematic and duality relationships.

Furthermore, the action and reaction law define the contact forces between two blocks in the NSCD method. Thus, to control the contact forces is necessary to compute the interaction of the antagonist body $A$ on the candidate body $C$ (see **Figure 4**), which is the force $r_\alpha$ acting at the contact point between these two bodies. At the contact, that is considered as punctual for simplifying, it is possible to set a local frame consisting of three vectors, in 3D model, including a normal vector $n_\alpha$ pointing from $A$ to $C$ and two tangential vectors $s_\alpha$ and $t_\alpha$, which define the tangential space by respecting this convention $s_\alpha \wedge t_\alpha = n_\alpha$. Moreover, the distance between body $A$ and $C$ along the normal direction is defined as the gap $g_\alpha$, which is positive for rigid bodies and there is not interpenetration between blocks.

Furthermore, it is required to correlate the local forces to the contribution of contact $\alpha$ to the resultant global force, using a linear mapping $H_\alpha$, by the following equation:

$$R_\alpha = H_\alpha(q)r_\alpha \quad (1)$$

where $H_\alpha(q)$ is a mapping which contains the local information about contactors, where $q$ is the configuration parameter which can represent the discretized displacement or any generalized coordinates of the rigid motion. Additionally, it is possible to calculate the global resultant contact forces exerted on objects with the relation

$$R = \sum_\alpha R_\alpha . \quad (2)$$

The velocity is analyzed with the same procedure. The relative velocity $u_\alpha$ at the contact point is defined for two bodies in contact by the following equation:

$$u_\alpha = H^T(q)v \quad (3)$$

where $H^T$ is the transpose of $H$, $v$ is the time derivative of $q$, and $t$ is the time. The relative velocity is decomposed in a normal component represented by $u_{\alpha,n}$ and a tangential component $u_{\alpha,T} = (u_{\alpha,s}, u_{\alpha,t})$. It should be noted that the derivative of the gap function $g$ is equal to the normal component of the relative velocity:

$$t \to g_\alpha(t), \quad \dot{g_\alpha} = u_{\alpha,n}. \quad (4)$$

During the evolution of the model, it is impossible to describe the acceleration as the usual second time derivative of the configuration parameter because it could be introduced shocks with multi-contact systems, which produce velocity discontinuities concerning time. Hence, the equation of motion will be written as

$$Mdv = F(q, v, t)dt + dI, \quad (5)$$

where $dt$ is the Lebesgue measure on $\mathbb{R}$, $dv$ is a differential measure of velocity denoting the acceleration measure and $dI$ is a differential measure of impulse representing forces. The matrix $M$ in the last equation is the mass matrix and the vector $F(q, v, t)$ is the vector of internal and external discretized forces acting on the system.

To determine the value of each component of $r_\alpha$ is important to have additional information about contact forces. These data are primordial to complete the Equation (5) and to describe the motion of the system. To simplify the writing, it is here considered the two-dimensional case, the $s$-components of $r_\alpha$ is disregard, the symbol $\alpha$ is omitted, and it is considered only $r_n$ and $r_T$ which represent the normal and tangential components of the force in the local frame, respectively. The reaction force always has a positive normal component or at least equal to zero when the contact disappears. In fact, it is not possible to have penetration between bodies in the system, as mentioned above with the impenetrability of contact, and there is not attraction among contacting bodies. This contact behavior is the so-called Signorini's condition or the first unilateral constraint:

$$g \geq 0, \quad r_n \geq 0 \ and \ g \cdot r_n = 0 \quad (6)$$

Regarding the cohesive contact instead, that is not the case considered here, the shifting can be applied to $r_n$ and $r_T$ and it assumes a value equal to zero if the contact is interrupted.

Concerning the case of Coulomb dry friction or the second unilateral constraint, it can be expressed by the equations below:

$$\begin{cases} if & \|u_T\| = 0, \|r_T\| \leq \mu r_n \\ if & \|u_T\| \neq 0, \|r_T\| = \mu r_n, \ u_T = -kr_T, \ k \geq 0 \end{cases} \quad (7)$$

As in Equation (7), the main features are that the friction force lies in Coulomb's cone, with $\|r_T\| \leq \mu r_n$ and $\mu$ friction coefficient, and, in the slip phase, the friction resultant force is opposed to the sliding velocity with value a equal to $\mu r_n$, when the sliding velocity $u_T$ is different from zero.

It is important to highlight that it is not necessary to manage explicitly the contact events in the time-stepping integration scheme, as in the case of the event-driven scheme. The time subdivision is done on intervals $[t_i, t_{i+1}]$ of length $h$ and it is fixed; consequently it is possible to deal with a great number of discontinuities during a one-time step, and the contact problem is solved over the range in terms of measures of this interval and not in a point-wise way. Thus, the equation is integrated on each time step, which involves to

$$\begin{cases} M(v_{i+1} - v_i) = \int_{t_1}^{t_{i+1}} F(q, v, t)dt + I_{i+1}, \\ q_{i+1} = q_i + \int_{t_1}^{t_{i+1}} v(t)dt, \end{cases} \quad (8)$$

where the variable $v_{i+1}$ denotes the approximation of the right limit of the velocity at the time $t_{i+1}$, and $q_{i+1} \approx q(t_{i+1})$. For impulse the $I$, it is integrated the measure $dI$ over the time interval $[t_i, t_{i+1}]$

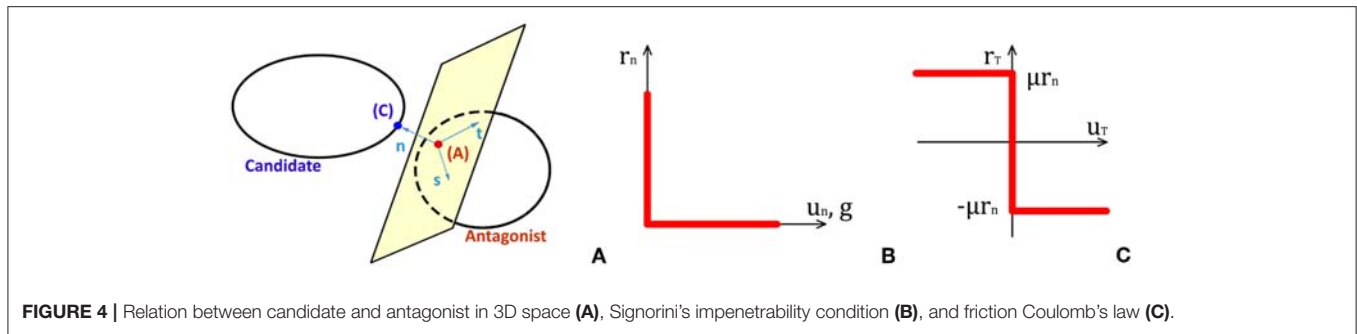$$I([t_i, t_{i+1}]) = \int_{[t_i, t_{i+1}]} I \cong I_{i+1}. \quad (9)$$

**FIGURE 4 |** Relation between candidate and antagonist in 3D space **(A)**, Signorini's impenetrability condition **(B)**, and friction Coulomb's law **(C)**.

Afterward, it is introduced the $\theta$-method as time-integration algorithm, that is an implicit scheme and it remains between 0.5 and 1 for the stability condition of the scheme, to approximate the two integrals of the system introduced before in Equation (8), which leads to the following equation:

$$\begin{cases} \int_{t_1}^{t_{i+1}} F\left(q,\,v,t\right) dt = h\theta F\left(q_{i+1}, v_{i+1},\, t_{i+1}\right) + h\left(1-\theta\right) F(q_i, v_i, t_i), \\ \qquad q_{i+1} = q_i + h\theta v_{i+1} + h\left(1-\theta\right) v_i. \end{cases}$$

$$(10)$$

Furthermore, the latter scheme in Equation (10) allows obtaining the energy balance analysis in the case of non-smooth motion with impact. To have a look on the total mechanical energy of the system, it is important to highlight that the dissipated energy of this system represents the work done by the contact impulse at the time of impact $t_i$. Note that completely inelastic impacts at contacts are assumed, leading to a loss of energy after each impact. Lastly, a detailed analysis of the energy balance for non-smooth systems can be found in Maschke et al. (2001).

Hence, it is essential to stress the fact that to investigate the ancient masonry towers it is necessary to do some observations on the NSCD method used here, which relies on modeling simplifications. The main assumption is that the blocks are stiff. Moreover, we add a perfectly plastic impact law to the contacts between blocks, in addition to the Signorini's impenetrability condition, i.e., Newton law with restitution coefficient equal to zero, which involves no bounces after collisions. According to this, there are valuable advantages regarding the contribution of impacts to the computational complexity, that is modest since they are modeled in a very basic and simple way, and about the perfectly plastic impact, which dissipates energy. Actually, regarding the integration, this dissipation improves the stability of the numeric computation and, from an engineering perspective, it is represented by the material failures and cracks of bricks after the impacts. Furthermore, another relevant aspect is the dissipation of energy that occurs using dry frictional joints and without viscous damping.

## THE MODELING OF THE TOWER

The main purpose of the modeling with the proposed approach is to recreate the geometrical and mechanical properties of the masonry in order to have the greatest resemblance with the complex configuration of the real structure and afterward
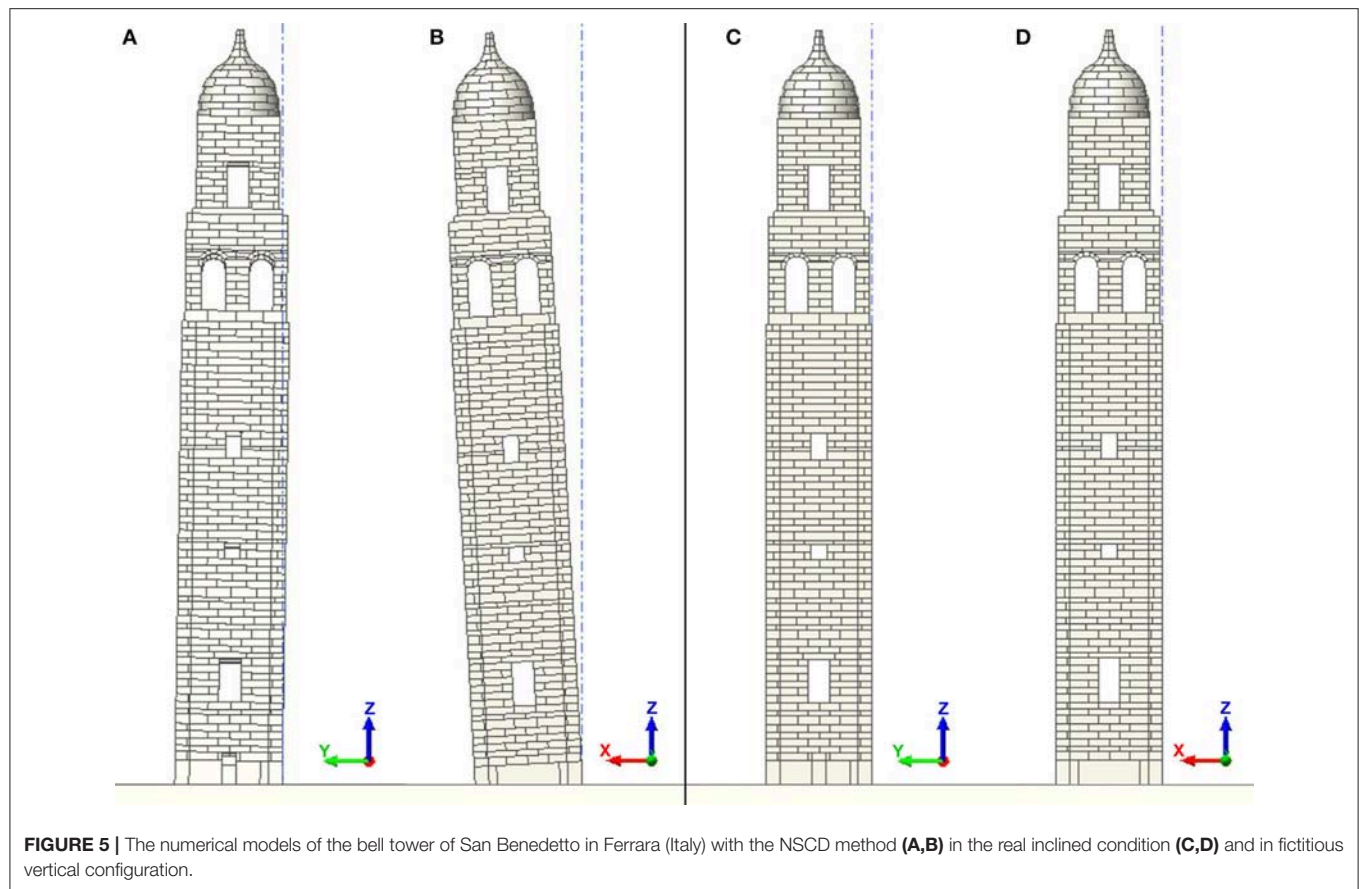
to highlight the influence of the inclination on the dynamic response of the tower.

To achieving this objective, the models follow the revealed measures in loco of the tower and the structure properties, according to the previous survey of the past in historical archive (see **Figure 3**). The discretization of masonry with rigid blocks is made as much as possible neat, by including the thickness of the mortar in the dimensions of the bricks and thus giving a zero dimension to the joints, as shown in **Figure 5**. Therefore, the blocks assume different dimensions, but they are clearly regular and convex objects. Concerning other parameters as the mass density, it is related to the existing masonry, and it assumes the specific value of 18 kN/m$^3$ as indicated in the (Circolare Ministeriale n., 617, 2009).

As a rule, in ancient structures, there are relevant phenomena of degradation, and thus the mortar loses its quality over time (Vasconcelos and Lourenço, 2009), reducing the friction coefficient until a value of 0.3 for a very poor kind. However, for a recent structure or a careful design of retrofitting, the friction can reach a value equal to 0.8. To define the frictional behavior of the structure, overlooking the interaction of the masonry with the foundation, it has been chosen a value equal to $\mu = 0.9$, for the relationship between structure and basement, and a value of $\mu = 0.5$, for the interaction between the blocks of the buildings.

Hence, for modeling of the tower of San Benedetto, it has been taken into account the condition of the structure with the benefits of the latest renovation and, at the same time, the degradation of material over time. This approach it has been followed for the real configuration of the tower with the actual inclination (in **Figures 5A,B**) and, also, for the vertical configuration (i.e., without the initial slope as reported in **Figures 5C,D**) in order to have an insight on the effect of the initial inclination on the seismic behavior of the tower, and on the possible activation of mechanisms.

Several analyses have been implemented applying to the system firstly the gravity loads and afterward the different ground accelerations: the dynamic behavior has been elaborate on shocks action of real events imported on the main directions of the base of the tower. The main shocks considered have various specifications; all of these are obtained by the records of seismic events occurred in the Italian territory. In particular, the recordings of velocities have been taken by the stations of the epicenters, and in this paper all three components, i.e., two on horizontal x and y and one on vertical z directions,

**FIGURE 5 |** The numerical models of the bell tower of San Benedetto in Ferrara (Italy) with the NSCD method **(A,B)** in the real inclined condition **(C,D)** and in fictitious vertical configuration.

are used. It has been considered two shocks events of a sequence of 2012 that took place in North-East of Italy, near Ferrara where is located the analyzed tower, and further four earthquakes of the highly active seismological area of the Central Italy, which belong to separate seismic sequences of 2009 and 2016:

(i)   06th April 2009 L'Aquila with $M_L = 5.9$ and $M_W = 6.1$ [AQV station in Italian Accelerometric Archive (ITACA)],
(ii)  20th May 2012 Mirandola with $M_L = 5.9$ and $M_W = 6.1$ (MRN station in ITACA),
(iii) 29th May 2012 Mirandola with $M_L = 5.8$ and $M_W = 6.0$ (MRN station in ITACA),
(iv)  24th August 2016 Amatrice with $M_L = 6.0$ and $M_W = 6.0$ (AMT station in ITACA),
(v)   26th October 2016 Campi with $M_L = 5.9$ and $M_W = 5.9$ (CMI station in ITACA),
(vi)  30th October 2016 Forca Canapine $M_L = 6.1$ and $M_W = 6.5$ (FCC in ITACA).

The location of epicenters are plotted in **Figure 1**, and the comparison between the characteristics of the seismic accelerations is reported in **Table 1**, where (Luzi et al., 2008, 2017; Pacor et al., 2011):

- $R_{jb}$, is the Joyner-Boore distance, known as the smallest spacing from the site to the surface projection of the rupture surface;
- $R_{rup}$, is the shortest distance between the site and the rupture surface;
- $R_{epi}$, is the distance estimated by the geometric swap.

## NUMERICAL RESULTS

The results of all numerical analyses performed on the bell tower of San Benedetto in Ferrara are shown in **Figure 6**, where are plotted the last configuration of the TH, obtained by the nonlinear dynamic simulations under shocks excitations.

All the events generate the activation of failure mechanisms of the upper part of the structures and cracks along the vertical dimension of the tower. Obviously, these results point out the adverse effects of the openings, distributed to different heights on the vertical walls, on the dynamic response of the considered tower. In particular, the most extensive damage -for both models of the tower- is due to the ground acceleration of the shock of 30th October 2016, which is the biggest and the most recent event in Italy. In **Figure 6**, it is already appreciable the increased vulnerability of the structure due to the inclination, but in order to have a clear picture of the numerical damage in **Figures 7**, **8** are also reported enlargements.

Firstly, it is necessary to pay attention to the damage mechanism of the upper part of the tower visible in **Figures 7**,

| Seismic event | $M_L$ | Depth (km) | Station | Class EC8 | $R_{jb}$ [km] | $R_{rup}$ [km] | $R_{epi}$ [km] | Channel NS PGA (cm/s²) | Channel EW PGA (cm/s²) | Channel UD PGA (cm/s²) |
|---|---|---|---|---|---|---|---|---|---|---|
| 06/04/2009 | 5.9 | 8.3 | AQV | B* | 0 | 5.43 | 4.90 | −535.20 | 644.25 | 486.65 |
| 20/05/2012 | 5.9 | 9.5 | MRN | C* | 4.34 | 8.97 | 16.10 | −258.79 | −257.23 | 297.30 |
| 29/05/2012 | 5.8 | 8.1 | MRN | C* | 0 | 3.86 | 4.10 | −288.63 | −218.58 | −840.74 |
| 24/08/2016 | 6.0 | 8.1 | AMT | B* | 1.38 | 4.62 | 8.50 | 368.39 | −850.80 | 391.37 |
| 26/10/2016 | 5.9 | 7.5 | CMI | C* | 2.53 | 7.44 | 7.10 | 302.56 | −638.31 | −468.28 |
| 30/10/2016 | 6.1 | 9.2 | FCC | A* | 0 | 5.55 | 11.00 | 843.73 | −931.14 | 893.5 |
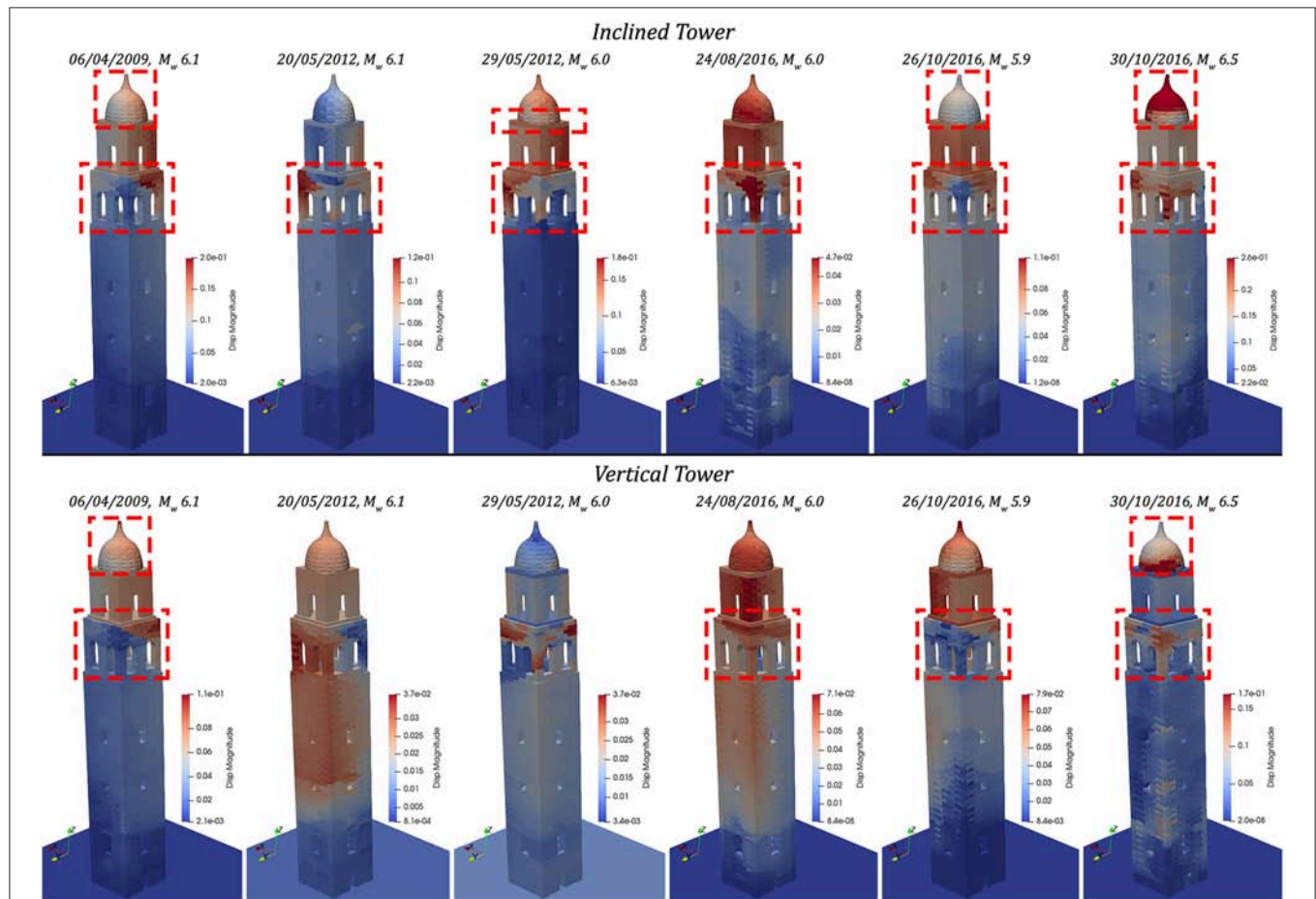


**FIGURE 6 |** Final configurations of the failure mechanisms of the bell tower of San Benedetto in Ferrara (Italy) under the six main seismic events of the last few decades in Italy, for the inclined real configuration and the other one vertical fictitious.

**8**, where it is evident the failure of the bell cell and the dome for every seismic load used in the 12 different simulations done. The main mechanism involves the mullioned windows of the belfry, which engender a vulnerability for the masonry walls with diffuse cracks on it and dislocations of blocks of the piers. These displacements are more highlighted on the results of earthquakes of 26 and 30th October 2016 (**Figure 8**), in particular for the inclined tower, which suffered the amplification of these movements.

Additionally, the failure of the dome arises in all results, and the activation of its mechanism is similar at varying of the different dynamic actions. Thus, it is more developed in simulations with the recorded velocities of 06th April 2009 (in **Figure 7**), 24th August 2016, 26th October 2016 and 30th October 2016 (in **Figure 8**). The damages consist of the massive displacements of the blocks at the base of the dome and the rotation of the pinnacle. Again, these motions are more significant in the cases of the inclined tower.
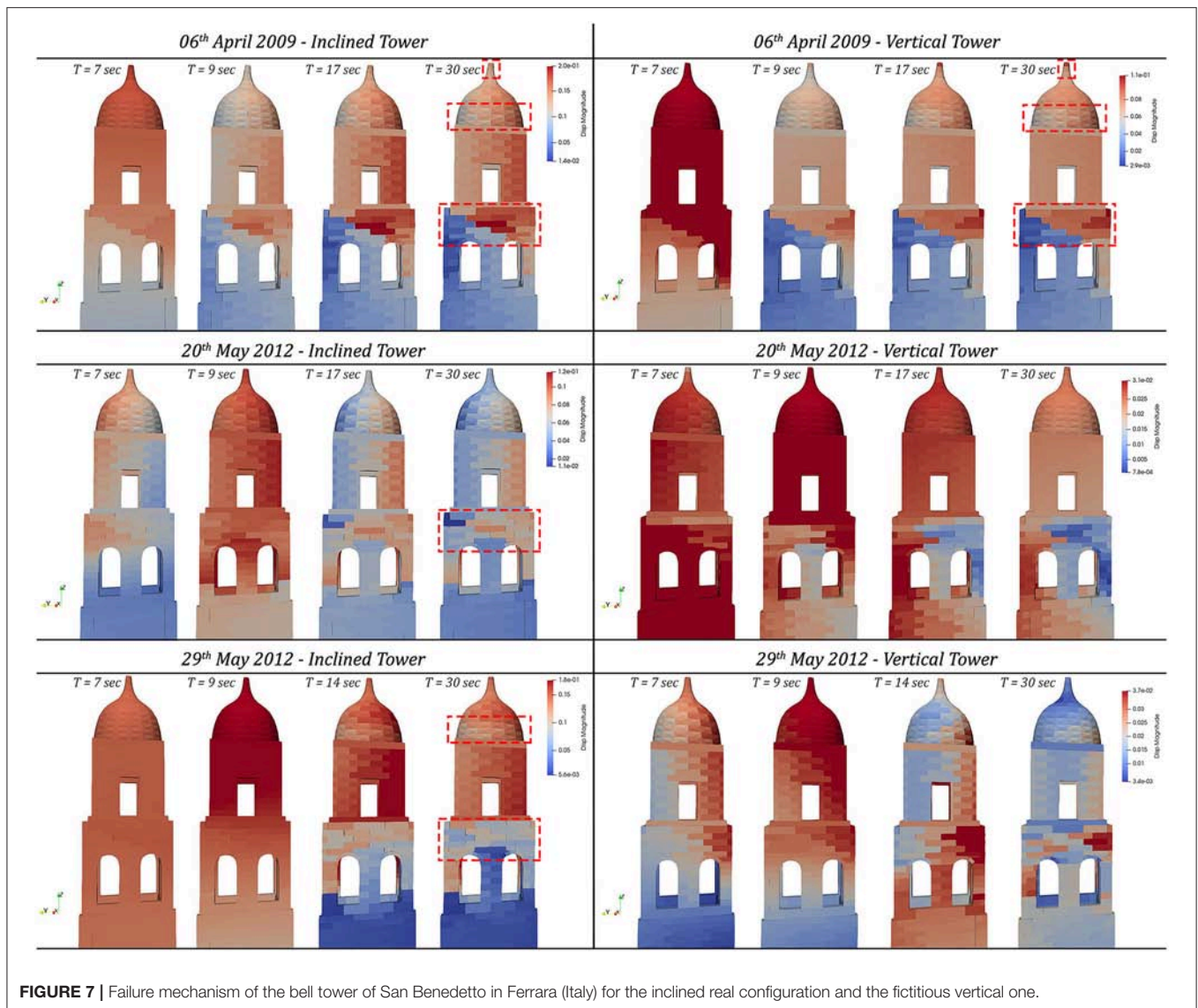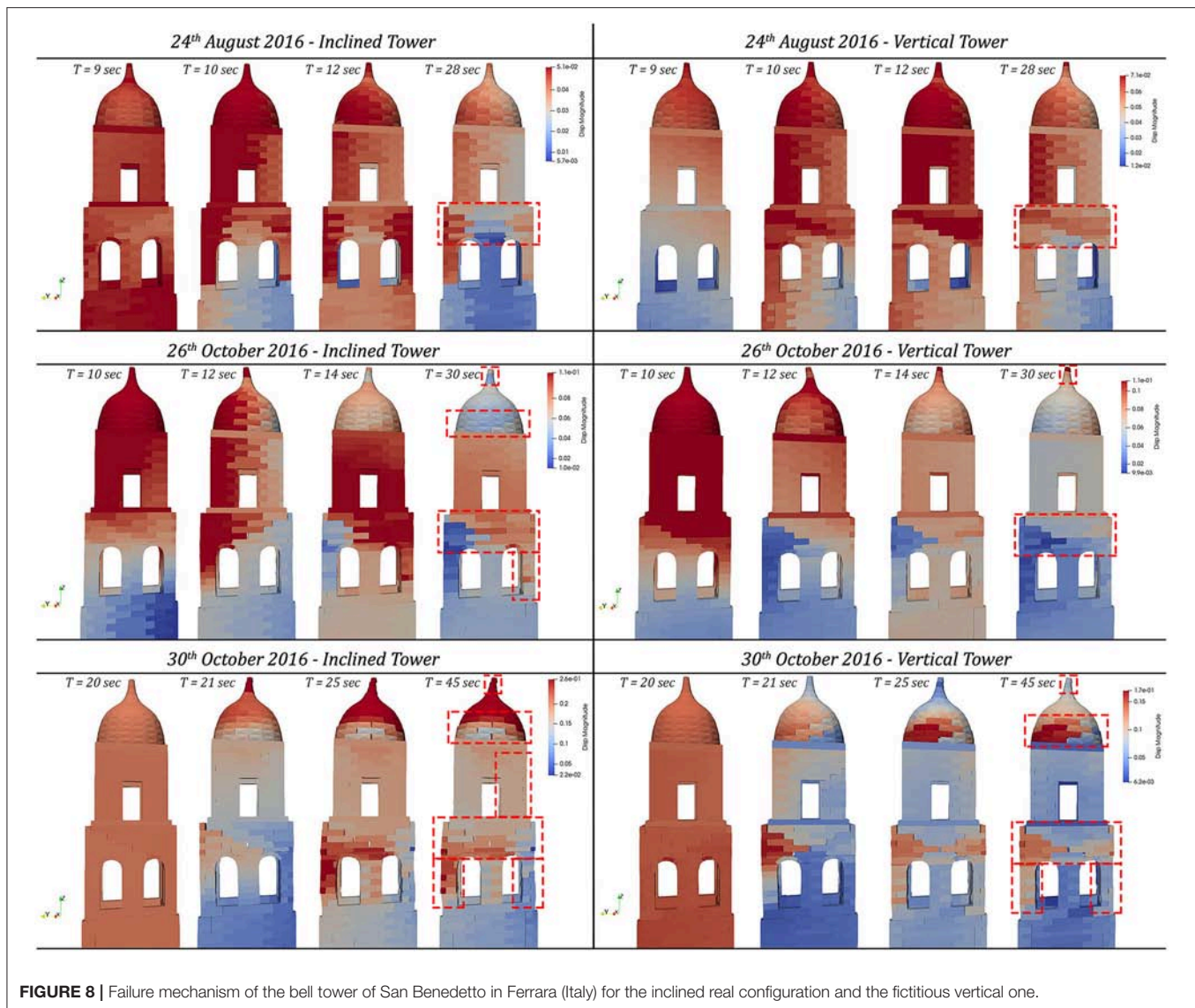
**FIGURE 7 |** Failure mechanism of the bell tower of San Benedetto in Ferrara (Italy) for the inclined real configuration and the fictitious vertical one.

To explain in detail the differences of the dynamic response between inclined and vertical towers and to highlight the effects of amplification of slope on the damage mechanism and on the vulnerability of the masonry, the displacements of several control points over time of both configurations of the bell tower are analyzed.

The displacements Time Histories (THs) related to the pinnacle of the dome, namely the control point #1, are reported in **Figure 9**, with the use of the solid line to plot the results of the inclined tower and the dotted line to show the results of the vertical structure. In this graph, at varying of the seismic actions, it is possible to observe that the resultant displacements of both models are similar, with bigger values in the inclined case. This permits a more precise reading of the damage reported in **Figures 7**, **8** concerning the activation of the mechanism of the dome for this event, in particular the overturning of the pinnacle, much more noticeable for

the model with the slope. Naturally, this result becomes more meaningful in the dynamic analyses with the earthquake of 30th October 2016, for which is plotted residual displacement for the point #1 of ∼45 cm for the inclined and of ∼10 cm for the vertical configurations. The same behavior is exhibited with the other earthquakes, with lower deviation from the values of the displacements of the two configurations considered for the tower.

Similarly, for the earthquakes of 24th August 2016 and of 26th October 2016 the main results related to the peak shifts show higher values for the control points #1 of the inclined model than of the vertical one. Instead, the residual displacement is noticeably lower for the inclined configuration than the second one. Hence, for these events, the pinnacle exhibits a more vulnerability in the case of the vertical tower, which has a higher resistance in the bottom part of the masonry.

**FIGURE 8 |** Failure mechanism of the bell tower of San Benedetto in Ferrara (Italy) for the inclined real configuration and the fictitious vertical one.

The dynamic responses of the control point #2, which is at the base of the dome, are pointed out in **Figure 10** where a comparison between both configurations of the tower for the six seismic events are reported. Also in this case, the displacements THs introduce higher values of the displacement's peak for the inclined model than of the vertical one. Similarly, the residual shift has higher values for the inclined tower than the vertical tower for the shocks of 06th April 2009, 20th May 2012 and 29th May 2012, and, on the other hand, it has lower values for the inclined than the vertical configurations for the earthquakes of 24th August 2016, 26th October 2016 and 30th October 2016. These last have a smaller gap between the values than the first three. In fact, for the events of 29th May 2012, the residual displacement is ∼12 cm for the inclined tower and ∼2 cm for the vertical one. Hence, these results correspond to an explicit activation of the in-plane mechanism with sliding of blocks at the base of the

dome for all the analyses of the inclined model, overall with greatest dislocations.

Regard to the displacements THs of the control point #3, belonging to the top of the tower, they present comparable values of displacement with those illustrated in **Figure 11** for all the seismic events. The resultant displacements are greater for the inclined tower than the vertical, except for the earthquakes of 24th August 2016 and 26th October 2016, in which the values are almost the same for both models. The main difference of the values regards to the residual displacement of the shocks of 29th May 2012, which is near to 15 cm for the inclined tower and between 3 and 4 cm for the vertical one, and of 30th October 2016 that is equal to 18 cm for the inclined configuration and near to 4 cm for the vertical one. There are other two results which are no doubt slightly less significant but nonetheless they are still of importance, such as the residual displacement of the dynamic actions of 06th April 2009, that is equal to 15 cm for the inclined
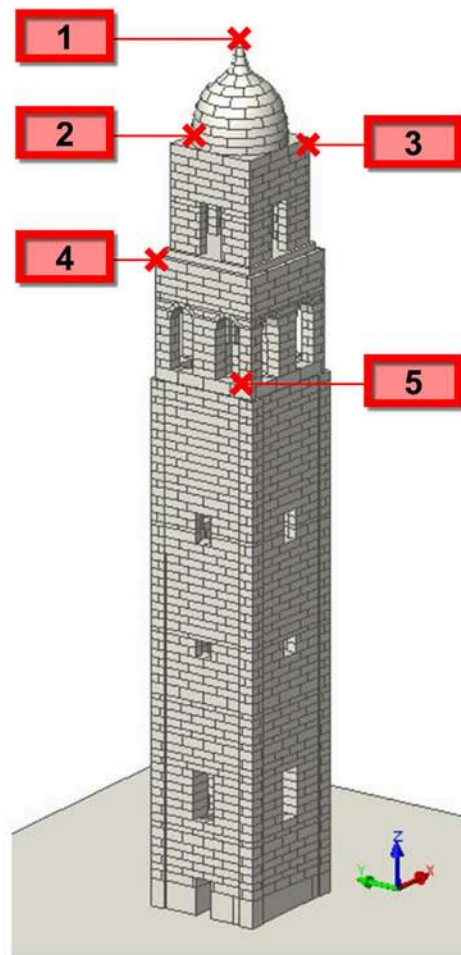
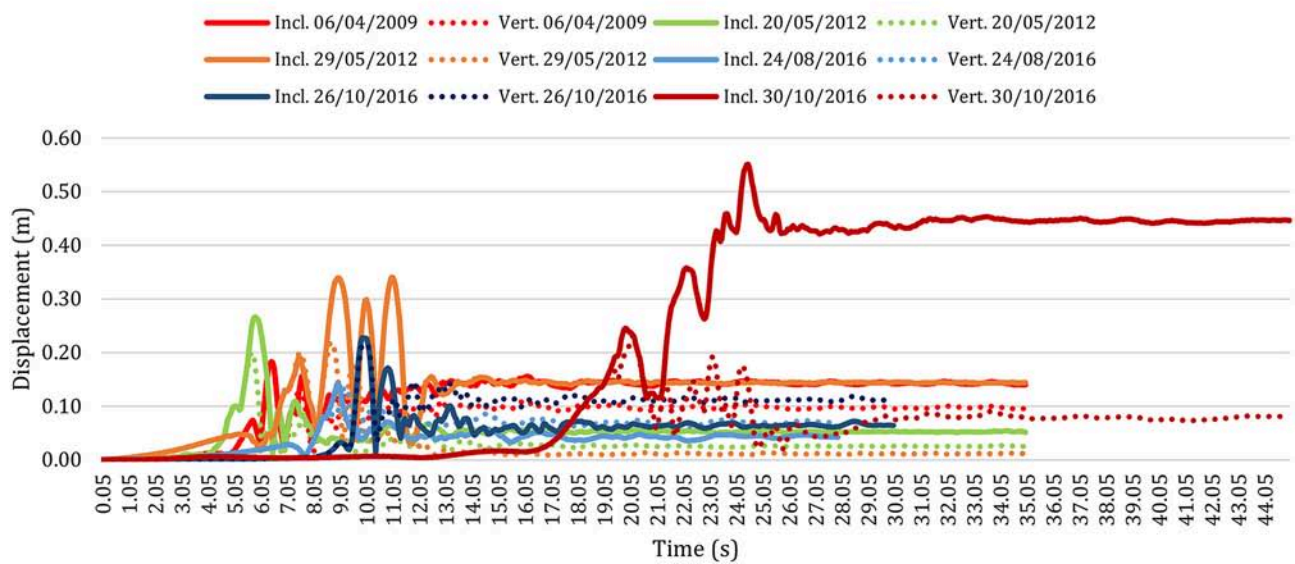**FIGURE 9 |** Displacements time histories of the control point #1 of the bell tower of San Benedetto in Ferrara (Italy) for the inclined real and the fictitious vertical configurations for the six main Italian earthquakes of the last few decades.

**FIGURE 10 |** Displacements time histories of the control point #2 of the bell tower of San Benedetto in Ferrara (Italy) for the inclined real and the fictitious vertical configurations for the six main Italian earthquakes of the last few decades.
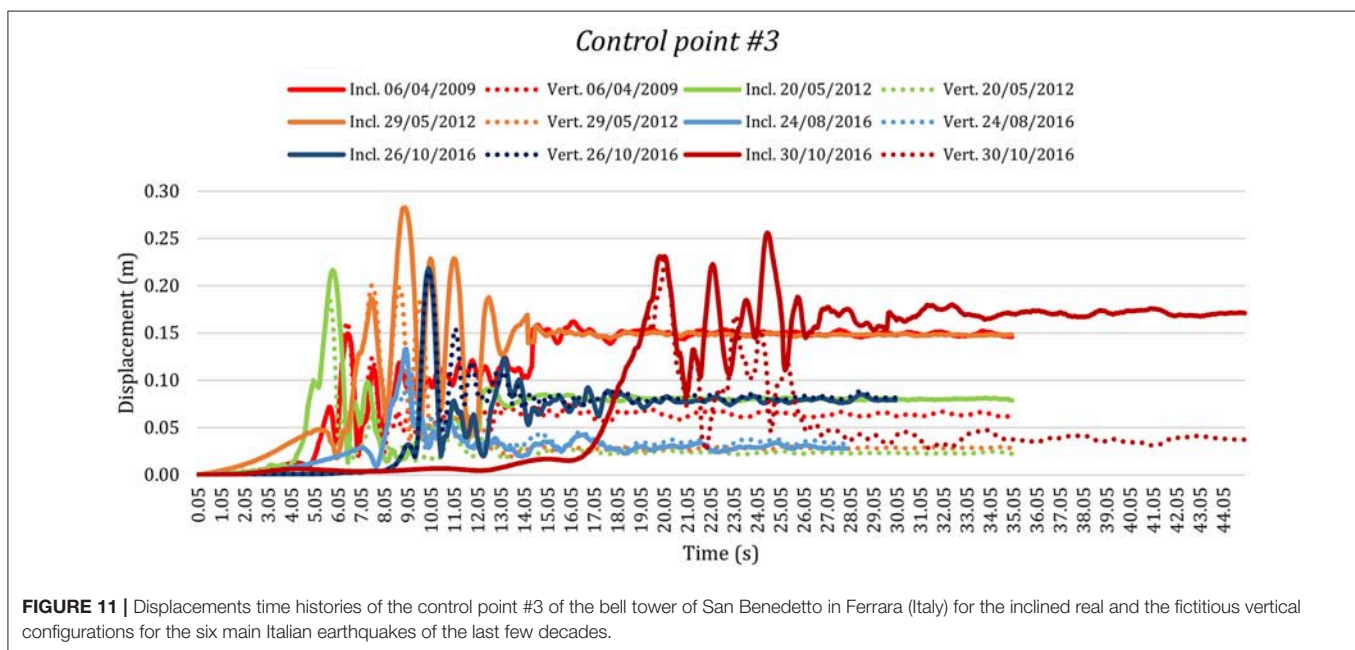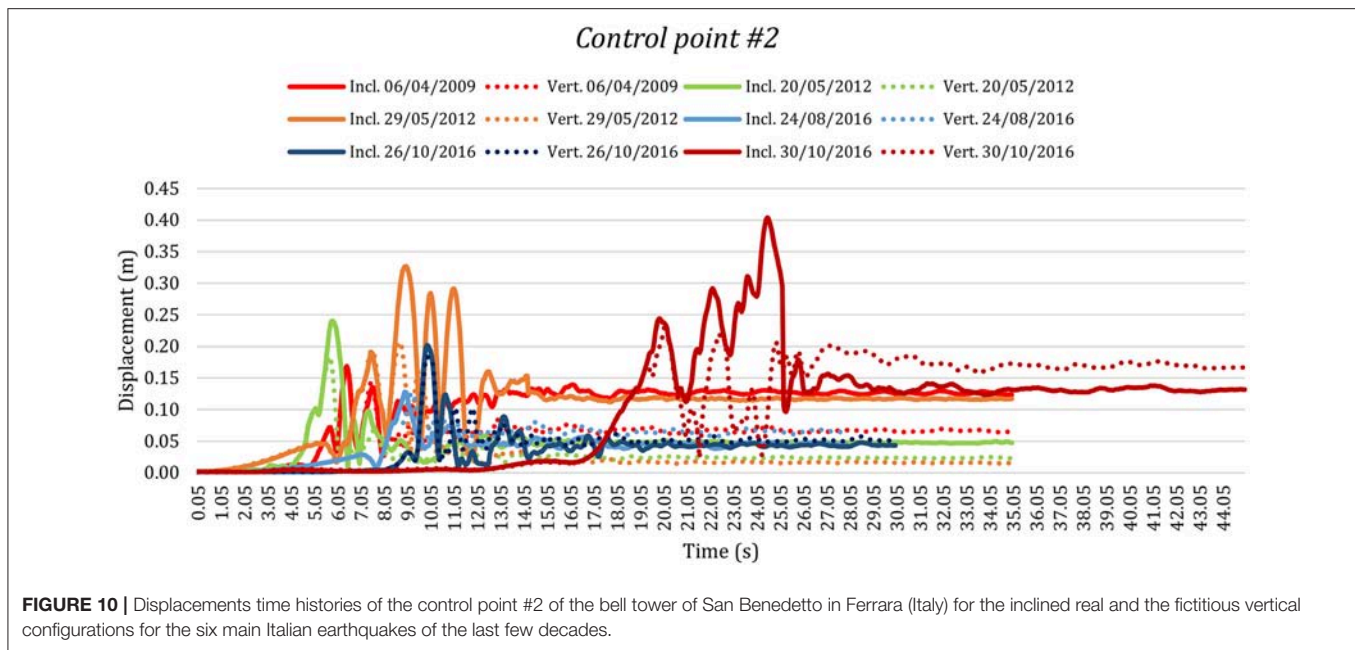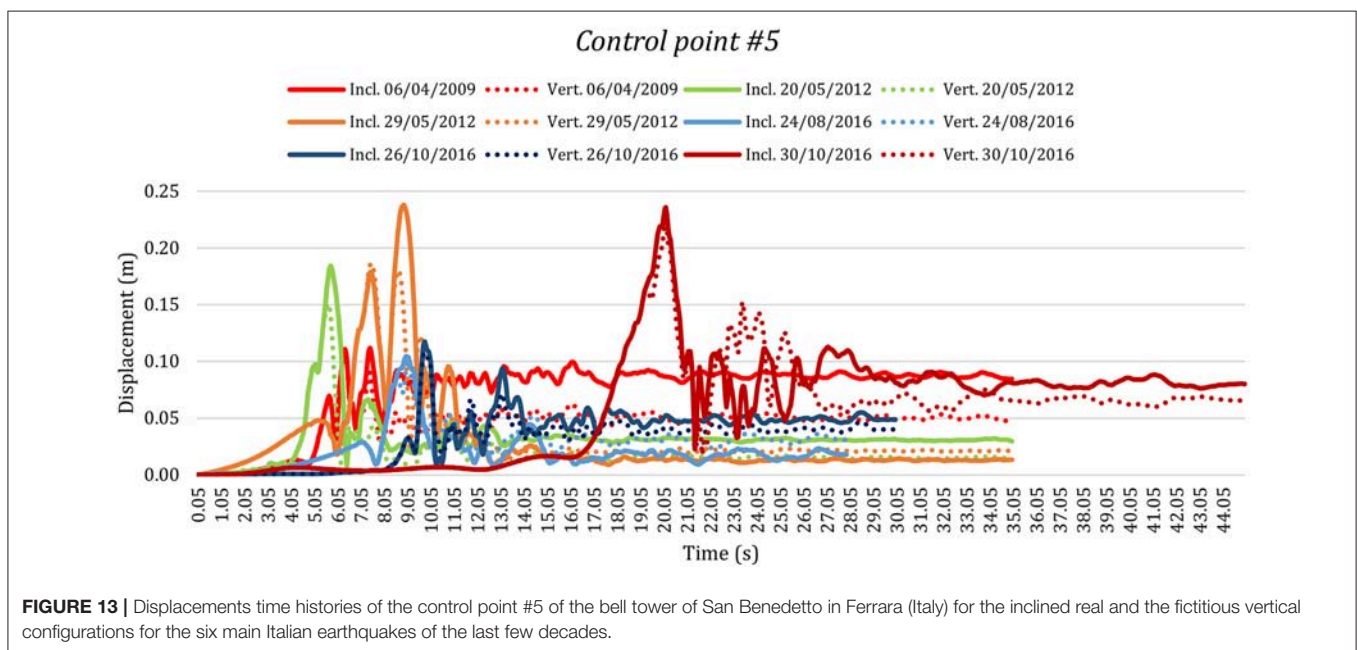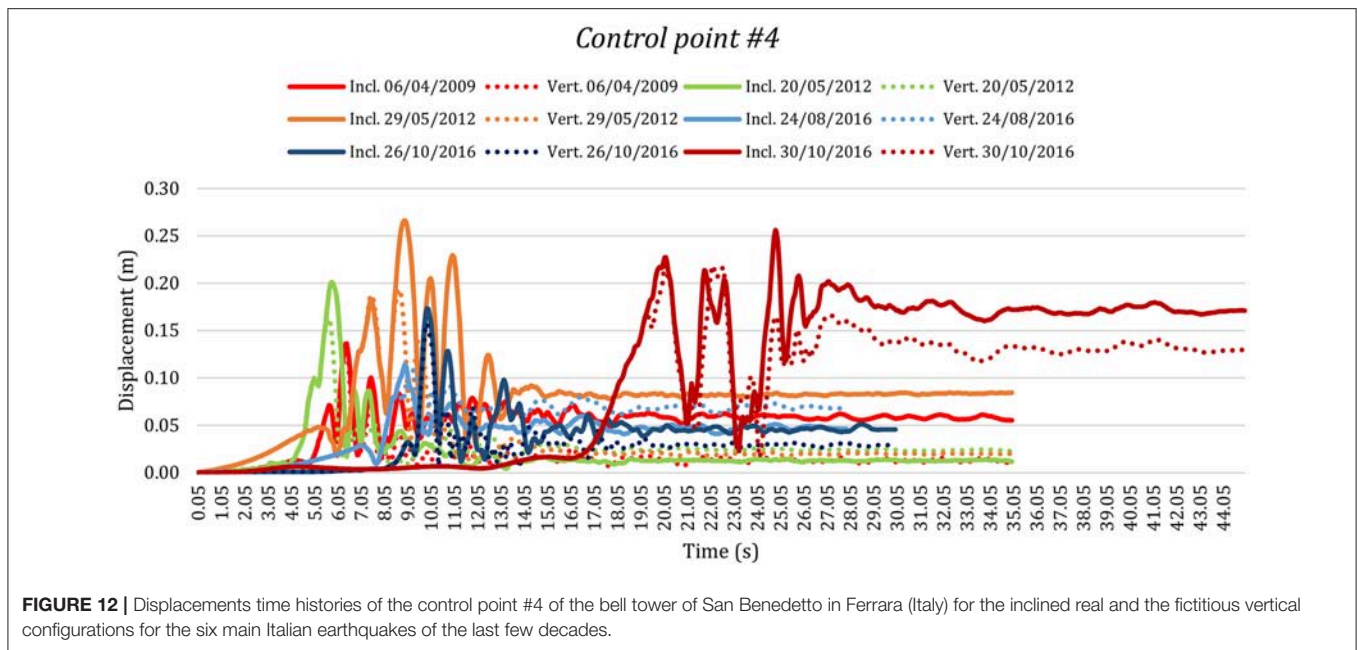


**FIGURE 11 |** Displacements time histories of the control point #3 of the bell tower of San Benedetto in Ferrara (Italy) for the inclined real and the fictitious vertical configurations for the six main Italian earthquakes of the last few decades.

configuration and near to 6 cm for the vertical one, and 20th May 2012, which is near to 8 cm for the inclined tower and near to 3 cm for the vertical one.

Looking at the displacements THs of the control point #4 plotted in **Figure 12**, it is noticeable that the overall behavior is similar in both cases for all dynamic actions. In particular, it is noticeable the activation of a damage mechanism for the event of 30th October 2016 for both the configurations, with the values of the residual displacement between 17 and 18 cm for the inclined tower and between 13 and 14 cm for the vertical tower. Otherwise, there is not an explicit activation of mechanism for

the shocks of 20th May 2012 for both models, remaining with residual displacements between 2 and 3 cm. Other and different considerations shall be made concerning the seismic analyses with recorded ground velocity of 06th April 2009, 29th May 2012 and 26th October 2016, in which the values of the residual displacement of the control point #4 for the inclined tower are respectively more or less equal to 6, 8, and 5 cm, and instead, for the vertical tower are correspondingly equal to 2, 3, and 4. Therefore, for these analyses there is a light amplification of sliding and damages for the tower with the slope. For the seismic event of 24th August 2016 a reversed situation compared to the

**FIGURE 12** | Displacements time histories of the control point #4 of the bell tower of San Benedetto in Ferrara (Italy) for the inclined real and the fictitious vertical configurations for the six main Italian earthquakes of the last few decades.



**FIGURE 13** | Displacements time histories of the control point #5 of the bell tower of San Benedetto in Ferrara (Italy) for the inclined real and the fictitious vertical configurations for the six main Italian earthquakes of the last few decades.
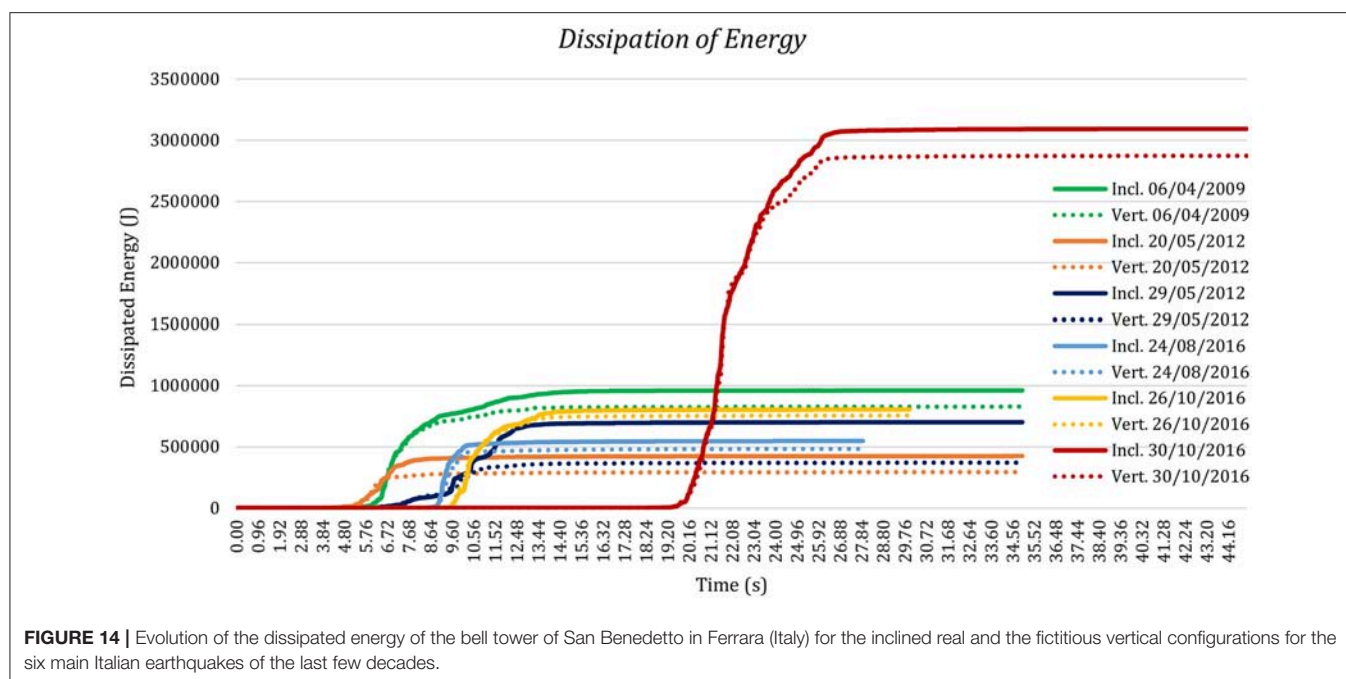
previous results is noticeable: the residual displacement has a bigger value (of about 7 cm) for the vertical than the inclined configurations (of about 5 cm).

Similar considerations can be done with regard to the control point #5, shown in **Figure 13**, which is the lowest one along the height of the structure. It presents similar resultant displacements for both configurations of the tower and, again, overall lesser values for the vertical configuration. This is especially highlighted for the events of 06th April 2009 and 30th October 2016, which have values of the residual displacement for the inclined tower more or less equal to 9 and 8 cm, respectively, and for the

vertical tower equal to 5 cm and between 6 and 7 cm, respectively. Otherwise, the events of 20th May 2012 and 26th October 2016 exhibit bigger values of the residual displacement for the inclined than the vertical one, but with small deviations between them. Whereas, the values of the residual displacement are higher for the vertical configuration than the inclined one for the shocks of 29th May 2012 for which are equal to 3 cm (inclined) and 2 cm (vertical), and of 24th August 2016 for which are 2÷3 (inclined) cm and 3÷4 cm (vertical).

Finally, in **Figure 14** is plotted the dissipated energy due to the friction at varying of the shocks for both the models. Hence,

**FIGURE 14 |** Evolution of the dissipated energy of the bell tower of San Benedetto in Ferrara (Italy) for the inclined real and the fictitious vertical configurations for the six main Italian earthquakes of the last few decades.

it is possible to observe that the dissipations of energy firstly have a high increase and then remain more or less unchanged during the velocity of the six main Italian earthquakes of the last few decades used for the dynamic analyses. Furthermore, the dissipated energy presents quite near values over the all-time for the different models, with increased values for the inclined tower (indicated with solid line) than the vertical one (indicated with dotted line), *consistent* with all *the* results of the analyses examined above.

It is possible to conclude that the initial inclination of the tower leads to greater damage in the area of the belfry and along the trunk and the damage is greater with the magnitude of the considered earthquake. Also, the non-symmetry of the damage is accentuated in the presence of an initial inclination. Otherwise the perfectly vertical tower amplifies the damage in the top area, leaving the rest of the structure undisturbed, unless there are very intense earthquakes.

## CONCLUSIONS

An inclined existing masonry tower has been modeled by means of the DEM and the NSCD method has been used to study its complex nonlinear behavior and the effect of an initial inclination on the seismic vulnerability.

The numerical models used do not reproduce the exact stone block shapes, but it preserves the real horizontality of the mortars joint with an average dimension of the units of the texture to have a rational compromise between the computational burden and the request of comprehensive description of the masonry of the tower. In fact, the models provided a fairly good representation of the observed displacements and near collapse modes.

The structural model of the existing tower has been carefully examined with the real inclined and a fictitious vertical configuration, under the action of the most six destructive Italian seismic events of the last 10 years.

In the case of the inclined structure, an obvious increment of the failure mechanisms has been remarked, compared to the structure without overhang. On the other hand, the dome introduces a well-known weakness to the assessment of the tower's vulnerabilities in both configuration, even if it is more damaged in the perfectly vertical configuration. Differently, the bell cell, another perfectly knows vulnerability of the masonry towers, it is more damaged in the presence of initial inclination.

As a result, the meaningful increased vulnerability of the inclined bell tower is demonstrated by the largest damages and the weakness along all height of the tower itself. At the same time, the greater values of the displacements and the dissipation of energy over time for the structure with slope under different dynamic input confirm the negative impact of the inclination on the tower, that makes it less durable respect to dynamic actions.

Finally, the DEM significantly has proving to be a powerful numerical approach to analyzed dynamics behavior of historic masonry structures in the nonlinear field, also by means of the NSCD method, that allows to point out in depth the masonry's vulnerabilities.

## AUTHOR CONTRIBUTIONS

AF created the numerical model, FC analyzed the results, GM supervised the research. All the authors contributed to the writing of the manuscript.

# REFERENCES

Acito, M., Bocciarelli, M., Chesi, C., and Milani, G. (2014). Collapse of the clock tower in Finale Emilia after the May 2012 Emilia Romagna earthquake sequence: numerical insight. *Eng. Struct.* 72, 70–91. doi: 10.1016/j.engstruct.2014.04.026

Asteris, P. G., Sarhosis, V., Mohebkhah, A., Plevris, V., Papaloizou, L., Komodromos, P., et al. (2015). "Numerical Modeling of Historic Masonry Structures," in *Handbook of Research on Seismic Assessment and Rehabilitation of Historic Structures*, eds. P. Asteris and V. Plevris (Hershey, PA: IGI Global), 213–256.

Betti, M., Galano, L., and Vignoli, A. (2014). Comparative analysis on the seismic behaviour of unreinforced masonry buildings with flexible diaphragms. *Eng. Struct.* 61, 195–208. doi: 10.1016/j.engstruct.2013.12.038

Brandonisio, G., Lucibello, G., Mele, E., and De Luca, A. (2013). Damage and performance evaluation of masonry churches in the 2009 L'Aquila earthquake. *Eng. Fail. Anal.* 34, 693–714. doi: 10.1016/j.engfailanal.2013.01.021

Cavalagli, N., and Gusella, V. (2015). Dome of the basilica of santa maria degli angeli in assisi: static and dynamic assessment. *Int. J. Archit. Herit.* 9, 157–175. doi: 10.1080/15583058.2014.951799

Chetouane, B., Dubois, F., Vinches, M., and Bohatier, C. (2005). NSCD discrete element method for modelling masonry structures. *Int. J. Numer. Methods Eng.* 64, 65–94. doi: 10.1002/nme.1358

Circolare Ministeriale n., 617 (2009). Cons. Sup. LL. PP., "Istruzioni per l'applicazione delle Nuove Norme Tecniche per le Costruzioni" di cui al decreto ministeriale del 14.01.2008. G.U. del 26.02.2009 n. 47, supplemento ordinario n. 27. (in Italian).

Clementi, F., Gazzani, V., Poiani, M., Mezzapelle, P. A., and Lenci, S. (2018a). Seismic assessment of a monumental building through nonlinear analyses of a 3D solid model. *J. Earthq. Eng.* 22, 35–61. doi: 10.1080/13632469.2017.1297268

Clementi, F., Pierdicca, A., Milani, G., Gazzani, V., Poiani, M., and Lenci, S. (2018b). "Numerical model upgrading of ancient bell towers monitored with a wired sensors network," in *10th International Masonry Conference (IMC_10)*, eds. S. Milani, G., Taliercio, A., Garrity (Milano), 1–11.

Clementi, F., Quagliarini, E., Maracchini, G., and Lenci, S. (2015). Post-world war II Italian school buildings: typical and specific seismic vulnerabilities. *J. Build. Eng.* 4, 152–166. doi: 10.1016/j.jobe.2015.09.008

Clementi, F., Quagliarini, E., Monni, F., Giordano, E., and Lenci, S. (2017). Cultural heritage and earthquake: the case study of "Santa Maria Della Carità" in Ascoli Piceno. *Open Civic Eng. J.* 11, 1079–1105. doi: 10.2174/1874149501711011079

Dubois, F., Acary, V., and Jean, M. (2018). The contact dynamics method: a nonsmooth story. *Comptes Rendus Mécanique* 346, 247–262. doi: 10.1016/j.crme.2017.12.009

Formisano, A., Di Lorenzo, G., Iannuzzi, I., and Landolfo, R. (2017). Seismic vulnerability and fragility of existing italian industrial steel buildings. *Open Civ. Eng. J.* 11, 1122–1137. doi: 10.2174/1874149501711011122

Formisano, A., Vaiano, G., Fabbrocino, F., and Milani, G. (2018). Seismic vulnerability of Italian masonry churches: the case of the Nativity of Blessed Virgin Mary in Stellata of Bondeno. *J. Build. Eng.* 20, 179–200. doi: 10.1016/j.jobe.2018.07.017

Giordano, E., Clementi, F., Nespeca, A., and Lenci, S. (2019). Damage assessment by numerical modeling of sant'agostino's sanctuary in offida during the central italy 2016–2017 Seismic Sequence. *Front. Built Environ.* 4:87. doi: 10.3389/fbuil.2018.00087

Lagomarsino, S., and Podestà, S. (2004). Damage and vulnerability assessment of churches after the 2002 Molise, Italy, Earthquake. *Earthq. Spectra* 20, S271?S283. doi: 10.1193/1.1767161

Lemos, J. V. (2007). Discrete Element Modeling of Masonry Structures. *Int. J. Archit. Herit.* 1, 190–213. doi: 10.1080/15583050601176868

Luzi, L., Hailemikael, S., Bindi, D., Pacor, F., Mele, F., and Sabetta, F. (2008). ITACA (ITalian ACcelerometric Archive): a web portal for the dissemination of italian strong-motion Data. *Seismol. Res. Lett.* 79, 716–722. doi: 10.1785/gssrl.79.5.716

Luzi, L., Pacor, F., and Puglia, R. (2017). *Italian Accelerometric Archive v 2.3*. Rome.

Maschke, R., Lozano, B., Brogliato, O., and Egeland, O. (2001). *Dissipative Systems Analysis and Control*. London, UK: Theory and Applications.

Milani, G. (2013). Lesson learned after the Emilia-Romagna, Italy, 20–29 May 2012 earthquakes: a limit analysis insight on three masonry churches. *Eng. Fail. Anal.* 34, 761–778. doi: 10.1016/j.engfailanal.2013.01.001

Moreau, J. J. (1988). "Unilateral Contact and Dry Friction in Finite Freedom Dynamics," in *Nonsmooth Mechanics and Applications* (Vienna: Springer Vienna), 1–82.

Pacor, F., Paolucci, R., Luzi, L., Sabetta, F., Spinelli, A., Gorini, A., et al. (2011). Overview of the Italian strong motion database ITACA 1.0. *Bull. Earthq. Eng.* 9, 1723–1739. doi: 10.1007/s10518-011-9327-6

Pellegrinelli, A., Furini, A., and Russo, P. (2014). Earthquakes and ancient leaning towers: geodetic monitoring of the bell tower of San Benedetto Church in Ferrara (Italy). *J. Cult. Herit.* 15, 687–691. doi: 10.1016/j.culher.2013.12.005

Pellegrini, D., Girardi, M., Lourenço, P. B., Masciotta, M. G., Mendes, N., Padovani, C., et al. (2018). Modal analysis of historical masonry structures: linear perturbation and software benchmarking. *Constr. Build. Mater.* 189, 1232–1250. doi: 10.1016/j.conbuildmat.2018.09.034

Pierdicca, A., Clementi, F., Isidori, D., Concettoni, E., Cristalli, C., and Lenci, S. (2016). Numerical model upgrading of a historical masonry palace monitored with a wireless sensor network. *Int. J. Mason. Res. Innov.* 1:74. doi: 10.1504/IJMRI.2016.074748

Poiani, M., Gazzani, V., Clementi, F., Milani, G., Valente, M., and Lenci, S. (2018). Iconic crumbling of the clock tower in Amatrice after 2016 central Italy seismic sequence: advanced numerical insight. *Procedia Struct. Integr.* 11, 314–321. doi: 10.1016/j.prostr.2018.11.041

Roca, P., Cervera, M., Pel,à, L., Clemente, R., and Chiumenti, M. (2013). Continuum FE models for the analysis of Mallorca Cathedral. *Eng. Struct.* 46, 653–670. doi: 10.1016/j.engstruct.2012.08.005

Sarhosis, V., Milani, G., Formisano, A., and Fabbrocino, F. (2018). Evaluation of different approaches for the estimation of the seismic vulnerability of masonry towers. *Bull. Earthq. Eng.* 16, 1511–1545. doi: 10.1007/s10518-017-0258-8

Terracciano, G., Di Lorenzo, G., Formisano, A., and Landolfo, R. (2015). Cold-formed thin-walled steel structures as vertical addition and energetic retrofitting systems of existing masonry buildings. *Eur. J. Environ. Civ. Eng.* 19, 850–866. doi: 10.1080/19648189.2014.974832

Valente, M., and Milani, G. (2016). Seismic assessment of historical masonry towers by means of simplified approaches and standard FEM. *Constr. Build. Mater.* 108, 74–104. doi: 10.1016/j.conbuildmat.2016.01.025

Vasconcelos, G., and Lourenço, P. B. (2009). Experimental characterization of stone masonry in shear and compression. *Constr. Build. Mater.* 23, 3337–3345. doi: 10.1016/j.conbuildmat.2009.06.045

# Comparative Seismic Assessment of Ancient Masonry Churches

*Michele D'Amato[1]\*, Rosario Gigliotti[2] and Raffaele Laguardia[2]*

[1] Department of European and Mediterranean Cultures (Architecture, Environment and Cultural Heritage), University of Basilicata, Matera, Italy, [2] DiSG – Department of Structural Engineering, Sapienza University of Rome, Rome, Italy

The seismic risk assessment of the historical and architectural heritage is, nowadays, a very relevant topic due the potential human and economic losses involved in case of global or partial collapse. In order to preserve the inestimable value of such heritage, the prevention and mitigation of the seismic risk is needed and it cannot be postponed. Among the several methods available in the literature to perform vulnerability assessment on cultural heritage, this study focuses on two simplified methods proposed by the current Italian Directive, containing the guide lines for assessment and reduction of cultural heritage seismic risk. Furthermore, a new simplified method is applied, capable at a territorial scale of quickly ranking the seismic behavior of ancient churches. In the paper, the considered evaluation methods are applied to the case study of the Matera Cathedral, named SS. Maria della Bruna. The obtained results are then compared with others of similar ancient churches, all belonging to the historical centre "Sassi of Matera," a site protected by UNESCO having a moderate seismic hazard.

Keywords: ancient churches, cultural heritage protection, masonry, seismic vulnerability, seismic risk

## INTRODUCTION

Natural disasters, such as volcanoes, floods, landslides, hurricanes, earthquakes, and climatic changes, represent a real danger for the conservation of the existing cultural heritage. Nevertheless, insufficient programs have been applied, aimed at reducing the vulnerability, and the related risk of cultural heritages. An idea of the problem dimensions is given by analyzing the costs required in the last natural disasters in order to manage the emergencies, repairs, and reconstruction. According to an estimation provided by World Bank (World Bank Indipendent Evaluation Group, 2006), natural disaster damage costs are increasing, and they have achieved about 652 billion US dollars in the 1990s. These costs result 15 times higher than the ones registered in the 1950s, even for natural disasters. Another piece of important information is obtained: if one considers that one-third of the cost to the global economy (about 50 billion US dollars) is spent on predicting, preventing, and mitigating disasters and the other two thirds represent the direct costs of the damage (Alexander, 2017).

   The ability to react to these disasters is directly related to the public awareness about the future destructive events that may occur. In this context, it is necessary to design and to apply prevention measures addressed for protecting the cultural heritage, where experts of different fields (engineering, statistics, chemistry, seismology, etc.) are involved. Thanks to this cooperation, different documents have been proposed such as, among the others, the Mexican risk identification atlas (CENAPRED, 2014), and the territorial information systems proposed in ISCR (2017).

   In line with these premises, this paper presents a comparative study of the seismic performance of ancient masonry churches. To this scope, the simplified methods reported within the Italian

Directive (GU. n. 47, 09/02/2011) are considered, with particular attention to *Level of Valuation 1* (*LV1*, for an evaluation at a territorial dimension) and *Level of Valuation 2* (*LV2*, considering the macro-elements approach). Furthermore, a new simplified method proposed in (CENAPRED, 2006) and validated in D'Amato et al. (2018), useful at a territorial scale for preliminary scoring and classifying the seismic behavior of churches, is applied. This methodology has also been recently validated for ancient adobe Chilean Churches (Fuentes et al., 2019).

The seismic performance evaluation in this study is conducted by considering in detail the case study of the Cathedral of Matera (Italy), an ancient masonry church dedicated to *SS Maria Della Bruna*. The obtained results are then compared with other churches, similar to the Cathedral with respect to materials, geometrical characteristics, and constructions details. All the churches considered fall within the historic centre of Matera, named "Sassi of Matera," recognized since 1993 as a World Heritage Site by UNESCO.

The main feature of the considered methods is that they can be used within a multilevel seismic vulnerability approach. In fact, they are based only on simple surveys characterized by visual and geometric detections, implying limited costs. Thus, these methods can also be applied as decision making tools in order to rank priorities and to proceed to further material and structural investigations for performing advanced structural analyses. Within this multi-level approach, the new simplified method recently proposed can be intended as a "*Level of Valuation 0*" ("*LV0 method*"), by allowing a very rapid seismic assessment, even at a larger territorial scale. Moreover, the comparisons among the obtained results show that the simplified methods may also overestimate the seismic actual response. Therefore, they remain useful for comparing and ranking the case studies, but they cannot substitute more refined methods for realistically simulating the seismic behavior of churches.

## SEISMIC ASSESSMENT METHODS INDICATED IN THE ITALIAN DIRECTIVE

The Italian directive, specific for Cultural Heritage (G. U. n. 47, 26/02/2011), defines three levels of valuation, namely the *LV1*, *LV2*, and *LV3* method for assessing the seismic performance of different historical constructions. These methods have an increasing complexity, requiring in parallel an increasing amount of information regarding structural details and materials properties.

As regards to the *LV1* method, it is suitable when a comparative seismic performance at a territorial level is conducted. Basically, the idea of this method is to relate the seismic performance to a global vulnerability index of a structure. No intervention may be designed with this method. Recent applications and similar approaches to this method may be found, for instance, in Lourenço and Roque (2006); Lourenço et al. (2013); Caprili et al. (2017); Formisano et al. (2017, 2018); Marotta et al. (2018); Sarhosis et al. (2018); Valente and Milani (2018a).

A more refined seismic performance evaluation may be obtained with the *LV2* method. It consists of evaluating the local mechanisms of architectural parts of a structure, named "*macro-elements*," and the global vulnerability corresponds to the activation of the most vulnerable mechanism considered. The macro-elements approach has been proposed after the damage surveys suffered by ancient churches during some recent Italian earthquakes. The conducted surveys have highlighted a systematic repetition of the detected damages, suggesting that the church structural system should be considered as a group of architectural parts, showing independent response mechanisms under seismic lateral loading. The macro-elements are identified as architectural parts (such as the main façade, lateral walls, longitudinal and transverse colonnade of main nave, triumphal arch, bell tower, dome, etc.), evaluating possible interactions with adjacent elements. Applications of this approach may be found, among the others, in Betti et al. (2018), Brandonisio et al. (2013), D'Ayala and Paganoni (2011), Doglioni et al. (1994), Formisano and Marzo (2017), Lagomarsino and Podestà (2004a,b), while a recent investigation on the estimation of main frequency of ancient masonry churches may be found in Lopez et al. (2019).

Non-linear finite element analyses are considered in the *LV3* method (G. U. n. 47, 26/02/2011), and they may regard limited parts or a whole structure. The adopted models must reproduce the real distribution of stiffness and mass, as well as the material non-linear behavior. Of course, the results obtained may realistically simulate the structural behavior only if the numerical assumptions made are true. This is strictly dependent on the knowledge of structural details (such as, for instance, wall connections, connections with the roof parts, and clear knowledge of the structure evolution during the past). The amount of these available data, and consequently, the reliability of the obtained results may increase if an in-depth and critical investigation campaign, through *in situ* tests and inspections, is performed. However, it should be carefully considered that *in-situ* tests should be focused at first on structural details more than on material mechanical properties, since the former dominate the response influencing the elements interaction more than the latter. Discussion about this issue may be found in Clementi et al. (2016), Castori et al. (2017), and Valente et al. (2017). In addition, the use of non-linear methods, such as the conventional pushover approach, implies the decisive choice of the control point on which the non-linear global response and the evaluation of the seismic performance depend. A discussion of this aspect may be found, among others, in Betti et al. (2018). While a general discussion on the application of non-linear analyses and the comparisons with the macro-element approach may be found in Castellazzi et al. (2013) and Valente and Milani (2018b).

Although it is the most simplified one, the *LV1* method is useful for evaluations at a territorial scale capable of providing, through a vulnerability index, an estimation of the ground acceleration related to the collapse. It requires only visual inspections and a qualitative judgment of some structural details. On the other hand, a local analysis may be performed with the *LV2* method (macro-element approach) also designing local interventions, where the potential interaction among the structural part may also be taken into account. The most refined

approach is represented, without any doubt, by the *LV3* method, where non-linear FE models are required. However, as discussed previously, this approach required a high amount of data and it may be extremely high time consuming from a computational point of view.

In the following, only the *LV1* and *LV2* methods are described in detail and, later on, are applied to some case studies. In addition, in this study a new simplified method for seismic assessment of the considered cases is also considered, proposed as *LV0* in continuity with the Italian Directive approach. The obtained results will be compared, in order to establish if a general correspondence in terms of the predicted seismic performance among the examined methods exists.

## LV1 Method

The LV1 method is the simplest method for assessing the seismic performance of a structure, revealing particularly adaptation for territorial scale evaluation (G. U. n. 47, 26/02/2011). The method requires defining, only through a visual survey, the global vulnerability index $i_v$ calculated as weighted combination of 28 possible damage mechanisms with the following relationship:

$$\mathbf{i_v} = \frac{1}{6} \frac{\sum_{k=1}^{28} \rho_k \left( v_{ki} - v_{kp} \right)}{\sum_{k=1}^{28} \rho_k} + \frac{1}{2} \tag{1}$$

where $i_v$ may vary between 0 and 1, and the other parameters may assume the following values:

$\rho_k$ is the response mechanism weight, varying from 0.5 to 1. If the considered mechanism is absent or not involved, it must be set equal to zero;

$v_{ki}$ and $v_{kp}$ measure, from the *k-th* response mechanism, the vulnerability and the efficiency of any possible seismic-resistant device. It is indicated to assume the value 1 for the most important response mechanisms, such as main façade overturning, triumphal arch response, longitudinal nave response, etc.; while, as for secondary mechanisms, such as mechanisms of transept and chapels, or prothyrum—narthex response, the value may range from 0.5 to 1.

Then, the ground acceleration corresponding to the attainment of Damage Limit State (*DLS*) and Life-Safety Limit State (*LSLS*) may be estimated by applying the following expressions:

$$a_{DLS}S = 0.025 \cdot 1.8^{2.75-3.44i_v} \ [g] \tag{2}$$
$$a_{LSLS}S = 0.025 \cdot 1.8^{5.1-3.44i_v} \ [g] \tag{3}$$

where $S$ is the stratigraphic amplification depending on the foundation soil. The previous equations have been established on a statistical basis starting from the surveys carried out in some recent Italian earthquakes.

By knowing $a_{LS}$, one may calculate the *safety index* $I_{LS}$:

$$I_{LS} = \frac{T_{LS}}{T_{R,LS}} \tag{4}$$

where $T_{LS}$ is related to the seismic action $a_{LS}$ for *LSLS* or *DLS* (that is the seismic capacity), and $T_{R,LS}$ is the expected reference return period for *LSLS* or *DLS* (that is the seismic demand). $T_{LS}$ may be calculated with the following expression (GU. n. 47, 09/02/2011):

$$T_{LS} = T_{R1} \cdot 10^{\log(T_{R2}/T_{R1}) \cdot \log(a_{LS}S/F_C a_1 S_1)/\log(a_2 S_2/a_1 S_1)} \tag{5}$$

where $a_1 S_1$ and $a_2 S_2$ define the interval of the seismic hazard in which $a_{LS}$ is included; $S$ is the stratigraphic amplification; $T_{R1}$ and $T_{R2}$ correspond to the return periods associated with $a_1$ and $a_2$, and $F_c$ represents the confidence factor depending on the knowledge level of the structure.

Whereas, as for the return period $T_{R,LS}$ associated to the expected seismic action, it is obtained through the Equation 6 depending on the reference period ($V_R$), and the probability of exceedance ($P_{VR}$) is associated with the considered limit state, having a $P_{VR}$ equal to 61 and 10%, respectively, for the DLS and LSLS.

$$T_{R,LS} = -\frac{V_R}{\ln\left(1 - P_{V_R}\right)} \tag{6}$$

Another ratio that may be particularly useful for seismic assessment is the *acceleration factor* $f_{a,LS}$, expressing the structure strength with respect to the seismic demand:

$$f_{a,LS} = \frac{a_{LS}}{a_{g,LS}} \tag{7}$$

where $a_{LS}$ corresponds to the achievement of the considered limit state and $a_{g,LS}$ is the expected one at the site, both referred to a rigid soil. It should be remarked that if a certain seismic protection level is satisfied, both $I_{LS}$ and $f_{a,LS}$ are major than unity.

## LV2 Method

This method is based on the analysis of rigid bodies by the means of the kinematic model (kinematic analysis). The failure mechanism considered may be schematized as a group of rigid blocks forming a kinematic chain, unstable with respect to the lateral actions, where all bodies are connected to each other with flexural hinges placed where the cracking likely occurs. The method is applied under the hypotheses (Heyman, 1966) that the masonry strength in compression is infinite and in tension is neglectable, and that any sliding between two adjacent blocks is restrained. It is suitable also for designing local interventions, if they do not modify the entire response of a structure.

The method involves an incremental approach, consisting of increasing a distribution of lateral forces, applied to the rigid blocks, proportional to the bodies mass. The lateral forces are increased until the failure arising when an inadmissible thrust line verifies. The beginning of the failure mechanism, according to Eurocode 8 (CEN, 2004) and Italian Design Code (Ministerial Decree, 14/01/2008), corresponds to the Damage Limit State (*DLS*) and it is associated with a lateral forces multiplier usually indicated as $\alpha_0$.

Certainly in this method, a primary importance is represented by the definition of the macro-elements that, as known,

are strictly dependent on manufacturing techniques and structural details such as, for instance, elements connections or existing cracks. Investigations in this regard may be found in Lagomarsino and Resemini (2009) as for the compressive strength influence, or in Lagomarsino (2012) for the no-tensile strength assumption. Whereas, as far as the influence of orthogonal walls connection in the overturning mechanism is concerned, it is worth noting the study carried out by de Felice and Giannini (2001), D'Ayala and Speranza (2003), and Lagomarsino (2012). To this regard, recently in Instructions for the application of the Ministerial Decree MD (17/01/2018), it is also recommended to take into account in the calculation of the wall overturning mechanism and the stabilizing friction contribution of the orthogonal walls due to an effective connection. As it will be shown later, this contribution is neglected in this paper, and, therefore, the so-found activation multipliers underestimate the real ones.

The failure mode activation multiplier $\alpha_0$ of a rigid block chain is defined according to the following expression, representing an application of the Theorem of Virtual Works (Instructions for the application of the Ministerial Decree MD, 14/01/2008):

$$\alpha_0 \left( \sum_{i=1}^{n} P_i \, \delta_{x,i} + \sum_{j=n+1}^{n+m} P_j \delta_{x,j} \right) - \sum_{i=1}^{n} P_i \delta_{y,i} - \sum_{h=1}^{o} F_h \delta_h = L_{fi} \quad (8)$$

where:

- $n$ is the rigid blocks number involved;
- $m$ is the forces number that do not directly act on the rigid blocks. Their masses are considered in the calculation of horizontal inertial forces under the seismic action;
- $o$ is the external force number applied to the different blocks and not associated to masses;
- $P_i$ is the dead weight of the generic rigid block;
- $P_j$ is the force that does not directly act on the rigid block. Its mass is considered producing a horizontal inertial force;
- $\delta_{x,i}$ and $\delta_{x,j}$ are the virtual displacements in the horizontal direction of the application points of $P_i$ and $P_j$, respectively. It is assumed as positive vs. associated to direction of the considered seismic action;
- $\delta_{y,i}$ is the virtual displacement in the vertical direction (positive is upward) of the application point $P_i$;
- $F_h$ is an external generic force (in absolute value) applied to a rigid block;
- $\delta_h$ is the application point virtual displacement of the $F_h$ force (positive if having discordant vs. from $F_h$);
- $L_{fi}$ corresponds to the internal forces virtual work, assumed equal to zero.

Subsequently, it is possible to determine the equivalent non-linear response of a single degree of freedom (SDOF) system, deriving the seismic spectral acceleration $a_0^*$ from the calculated activation multiplier $\alpha_0$. $a_0^*$, which may be calculated with the Equation (9), descending from the standard modal analysis principles:

$$a_0^* = \frac{\alpha_o \sum_{i=1}^{n+m} P_i}{M^* FC} = \frac{\alpha_o g}{e^* FC} \quad (9)$$

In the previous equation:

- $g$ is the gravity acceleration;
- $\sum_{i=1}^{n+m} P_i$ represents the dead weights sum. Their masses produce horizontal inertial force under seismic action to consider in the kinematic chain schematization;
- $FC$ indicates the Factor of Confidence;
- From $M^*$ representing the effective participating mass:

$$M^* = \frac{\left( \sum_{i=1}^{n+m} P_i \delta_{x,i} \right)^2}{g \sum_{i=1}^{n+m} P_i \delta_{x,i}^2} \quad (10)$$

it is possible to calculate $e^*$, that is the participating mass fraction related to $M^*$:

$$e^* = \frac{g M^*}{\sum_{i=1}^{n+m} P_i} \quad (11)$$

As for the DLS, $a_0^*$ has to be compared with the acceleration spectrum demand $a_g (P_{VR}) \cdot S$, that is the expected Peak Ground Acceleration:

$$a_0^* > a_g (P_{VR}) \cdot S \quad (12)$$

where $P_{VR}$ is the exceedance probability for considered limit state (in this case DLS) in the reference life ($V_R$), and $S$ is the soil stratigraphic amplification. The Equation (12) refers to the macro-elements that are directly connected at ground level, and it neglects the dynamic motion amplification due to structural deformability (Doherty et al., 2002).

Whereas, when they are considered macro-element responses that are not directly connected to the ground floor (as the gable overturning), the dynamic amplification of the response has to be considered, according to the Equation (13).

$$a_0^* > S_e (T_1) \cdot \psi (z) \cdot \gamma \quad (13)$$

where $z$ is the constraints barycenter height of rigid blocks considered; $S_e(T_1)$ is the spectral ordinate evaluated for $T_1$, that is the entire structure vibration period along the considered direction; $\psi(z)$ is the shape of the first vibration mode, normalized at the structure top. It may be assumed equal to $\psi(z) = z/H$, where $H$ is the structure height with respect to the foundation floor; $\gamma$ is the modal participating coefficient assumed in a simplified way equal to $\gamma = 3N/(2N+1)$ with $N$ the number of structure stories. The simplified relationship for estimating the churches fundamental period of oscillation $T_1$, proposed by Lagomarsino and Podestà (2005), should also be mentioned:

$$T1 = 0.07 H^{\frac{3}{4}} \quad (14)$$

where $H$ represents the structure height, measured up to the lowest point of the roof.

As regards to the LSLS, the behavior factor $q$ (Ministerial Decree, 14/01/2008) has to be considered in the previous

formulations. Therefore, in the case of ground-connected mechanisms, we have:

$$a_0^* > \frac{a_g\,(P_{VR}) \cdot S}{q} \tag{15}$$

where it is applied, in the case of not directly ground-connected mechanisms, the Equation (16).

$$a_0^* > \frac{S_e\,(T_1) \cdot \psi\,(Z) \cdot \gamma}{q} \tag{16}$$

In the previous equations, the behavior factor $q$ may be assumed equal to 2. The symbols used in Equations (15, 16) are the same as Equations (12, 13), respectively. It should be pointed out that, in the Instructions for the application of the Ministerial Decree MD (17/01/2018), a more refined approach for calculating the floor design spectra of the horizontal seismic action is indicated and, consequently, the seismic demand of the response mechanism is not directly ground connected (such as, for instance, the gable overturning). However, although more precise, this approach requires knowledge of the dynamic characteristics of the considered mechanism that, for the detail level of this work, are unknown. Therefore, the formulations reported in the Equations (13, 16) will be applied, indicated in the previous Instructions for the application of the Ministerial Decree MD (14/01/2008), where a first evaluation of the seismic demand may be done independently on the fundamental period of the response mechanism considered.

## A NEW SIMPLIFIED APPROACH FOR ASSESSING THE SEISMIC RISK

In Dìaz (2016), a new simplified methodology capable of assessing the seismic risk of ancient masonry churches has been proposed. Subsequently, this methodology has been preliminarily validated in D'Amato et al. (2018), and recently also extended to the case of Chilean Churches in Fuentes et al. (2019).

The simplified methodology provides a seismic risk score $R$, applying the known symbol equation (UNDRO, 1979; FEMA, 2004):

$$R = E \times H \times V \tag{17}$$

where $E$, $H$, and $V$ represent the exposure of elements or assets at risk, the seismic hazard, and the vulnerability, respectively.

The seismic risk score $R$ is obtained by multiplying the scores $E$, $H$, and $V$, separately evaluated by applying three different tools, that are:

- *Tool 1*: it provides a score associated to the exposition factor $E$, and accounting for the cultural value;
- *Tool 2*: with this tool a score it is calculated associated to the seismic hazard $H$. Different threats may be considered consulting, for example, published maps such as, for instance, the Italian *Risk Map* (CENAPRED, 2006; ISCR, 2017) and (Degg and Chester, 2005);
- *Tool 3*: the seismic vulnerability index $V$ is calculated considering additional information provided in some seismic vulnerability forms such as the DGPTA (2003) and Chilean Norm N. 3332 (2013).
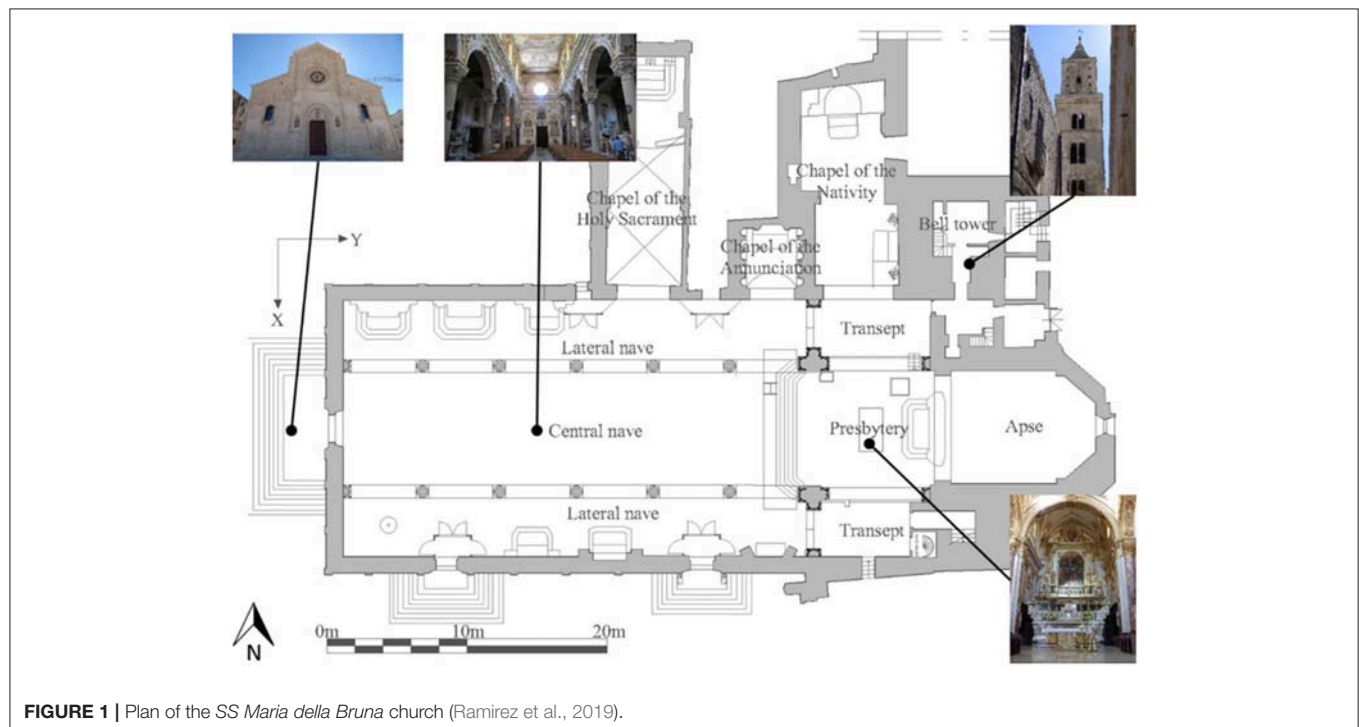


**FIGURE 1 |** Plan of the *SS Maria della Bruna* church (Ramirez et al., 2019).

As proposed in Dìaz (2016), the simplified method may also be applied as the scoring method by neglecting the exposition value, that is the *E* score within the Equation (17). Hence, the seismic score *R* is given by:

$$R = [H + 1] \, x \, V \qquad (18)$$

obtained by considering only the scores separately obtained with the *Tool 2* and the *Tool 3*. In the previous equation, *H* is increased as a unity for obtaining a seismic score *R* more major than 1. One may note that as *R* increases, the seismic risk also increases. The proposed method is particularly suitable for conducting, at a territorial scale, a seismic comparative analysis, with the simplicity of requiring few information to be applied. Instructions on how to calculate the vulnerability (*V*) and seismic hazard (*H*) scores may be found in Dìaz (2016) and in D'Amato et al. (2018).
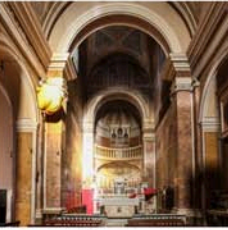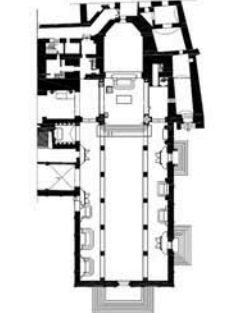
## CASE STUDIES

The city of Matera is located at the south of Italy, in the region of Basilicata. Specifically, the *SS Maria della Bruna* church is located in the city center, called "*Sassi of Matera*," consisting of two areas protected, since 1993, by UNESCO and reported within the World Heritage List. As shown in **Figure 1**, the church is characterized by a main body composed of three naves, having a latin cross configuration in plan. As in the Cristian tradition, the church main façade is oriented toward the west while the altar is oriented toward the east. The Cathedral construction started between 1226 and 1231 (Morelli, 1970). An inscription on the bell tower door reports that in 1270 the construction finished. Between the 15 and 16th c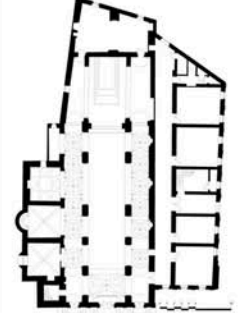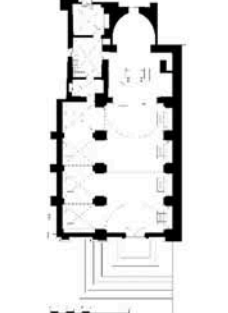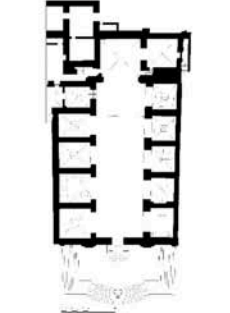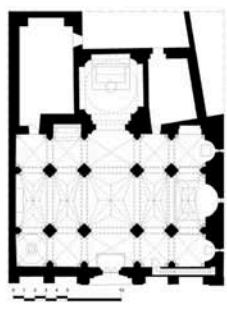enturies some chapels were annexed to the main body on the north side. As for the bell tower, two distinct parts may be clearly identified, since the upper zone was built later than the rest of the tower but not after 1709, given that this part appears in a fresco. The choir was originally completed in 1729 and, later, completely reconstructed in 1738. Additionally, it is supposed that due to a partial collapse, the dome was reconstructed. Regarding the bell tower, it is possible that the upper section was built later than the rest of the tower but not after 1709, given that this part appears in a fresco after this year (Ragone et al., 2017). The façade of the Cathedral presents several ornamental elements with religious meanings. Above the main entrance, a statue of *SS Maria della Bruna*, the Saint Patron of the City, is situated. At the top of the main façade, a finely decorated oculus is situated. A plan of the church is reported in **Figure 1**.

The results obtained from the considered case study are also compared in this work with four similar ancient masonry churches, all located within the "*Sassi of Matera*" area. The four additional churches, examined in a previous work (D'Amato et al., 2018) are: *San Pietro Caveoso, San Rocco, San Francesco*

**TABLE 1 |** Some views of the considered case studies.

*d'Assisi,* and *San Giovanni Battista*. The considered churches are illustrated in **Table 1**, where for each of them, the main facade, an interior view and the floor plan is reported. For each considered church, original drawings reporting the geometrical dimensions were retrieved. In addition, specific detailed surveys were conducted in order to control any possible existing cracking pattern, material deterioration or structural instability. No *in-situ* tests were carried out since the calculation methods applied in this study do not depend on the mechanical properties of the involved materials. In the following, a summary of the description of the considered churches is reported.

## San Pietro Caveoso Church

The church is placed in front of a large square, and along the canyon rocky ridge of Gravina river. The main façade is in baroque style, with three different portals, suggesting the subdivision of the internal structure into three naves. Above the portals, three semicircular niches contain the statues of Saints Peter and Paul, respectively to the left and to the right, with the Madonna della Misericordia in a central position. The façade is advanced with respect to its original position and connected to the internal longitudinal space through vaults in the Lecce style. Inside there are three naves and four of the eight original chapels overlooking the left nave. The original ceiling of the central nave is hidden today by a wooden false ceiling decorated with paintings. The main nave ends with a deep choir containing the presbytery with the eighteenth-century altar. On the left of the façade rises the bell tower with three orders, culminating with a pyramidal spire.

## San Rocco Church

The main entrance of the church is served by an imposing staircase. The internal layout has a division into two aisles: the largest exhibits a barrel-vaulted roof, supported by round arches crossing, and along the right side, niches with altars. The lateral aisle is made up of four quadrangular spans, covered by cross vaults with a slightly raised profile and accompanied by exquisite workmanship altars, embellished with paintings and sculptures from various eras. Through a triumphal arch it is possible to reach the presbytery area, covered by a pseudo-sail vault and concluded by a semicircular apse where the choir with the organ is placed.

## San Francesco d'Assisi Church

This church was built on top of the rupestrian church of Saints Peter and Paul. It presents an imponent façade and is divided into three distinct naves. On the lateral aisles are present nine chapels: four chapels on the right side and five chapels on the left side, with the characteristic that each of these is covered by a different vaulted system. Behind the presbytery there are additional spaces, among which sits the choir area hosting also a huge organ. On the right side, there is an environment linking the church with the bell cell.

## San Giovanni Battista Church

This church presents a basilica layout with three naves, with a Greek cross plan. The pillars delimiting the central nave have a cruciform plan, composed of four half-columns, of which only one supports the vault of the central nave. The church has a conspicuous development in height, with different vaulted systems, such as a star-shaped, Lecce-type, and cross-shaped, respectively. The aisles, delimited by cruciform pillars and columns projecting from the internal walls, intersect the transept and are divided into two equal parts, composed of two spans each with a cross-shaped roof.

After collecting all the main information, the principal characteristics of the considered churches may be summarized as follows:

> ***Configuration in plan***: *SS Maria della Bruna*, *San Giovanni Battista,* and *San Pietro Caveoso* are characterized by plan configuration with three naves, where *San Rocco* and *San Francesco d'Assisi* churches have a one-nave plan-configuration;
> ***Roof structures:*** *SS Maria della Bruna*, *San Rocco,* and *San Giovanni Battista* have a vaulted system, while roof structures of *San Pietro Caveoso* and *San Francesco d'Assisi* are made also by truss wooden structures in the central main nave;
> ***Configuration in elevation***: in all cases the roof structures are covering the main nave and the lateral ones. No additional floor was detected.
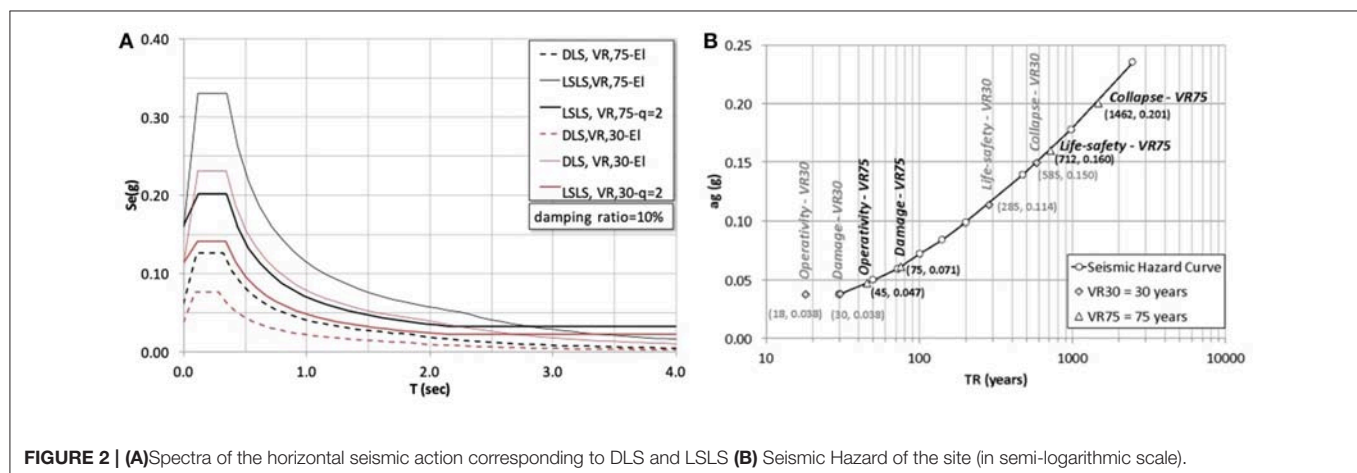


**FIGURE 2 | (A)** Spectra of the horizontal seismic action corresponding to DLS and LSLS **(B)** Seismic Hazard of the site (in semi-logarithmic scale).

The construction material for all the churches was represented by *tufo*, a local calcarenite rock. The state of conservation of masonry elements was good with a regular texture, and no cracking patter was encountered in each church. Similar approaches may be found in Laterza et al. (2016), D'Amato et al. (2017), and Fabbrocino et al. (2018). Whereas, a discussion of some critical aspects in investigating structural details may be found, among the others, in Krstevska et al. (2010); Luchin et al. (2018), and Marghella et al. (2016).

## DEFINITION OF PERFORMANCE LEVELS AND SEISMIC HAZARD

With the aim of requalifying the highest number of manufacts of the Italian cultural heritage, the Italian directive (G.U. n. 47, 26/02/2011) allows for improving the seismic performance without imposing a complete retrofitting. This consequently allows us to design small and cheap interventions, instead of

heavy, widespread and invasive ones. In this way each manufact can be considered as seismically protected for a lower action level (i.e., for a lower Return Period, $T_R$). In other words, it is permitted to reduce the observation time in which the seismic action is evaluated. This interval, defined as reduced nominal life $V_{N,Red}$, has to be assumed equal to or higher than 20 years (G.U. n. 47, 26/02/2011).

In line with this criterion, the seismic analyses presented herein are performed considering a reduced nominal life $V_{N,Red}$ assumed corresponding to 20 years, and a standard nominal life $V_N$=50 years, as requested for newly designed buildings. The coefficient of use adopted in both the cases is $C_U$=1.5, and, therefore, the observation time is adopted to define the seismic action results $V_R$=30 years for $V_{N,Red}$=20 years and $V_R$=75 years for $V_N$=50 years.

The city of Matera falls in a moderate seismicity zone, and many moderate seismic events hit it in the past years. Specifically, in the Italian historic catalog (CPTI, 2015), some events with macro-seismic intensity equal to 7 and many events

TABLE 2 | Scores obtained by applying the LV1 method.

| | | (v$_{ki}$-v$_{kp}$) | | | | |
|---|---|---|---|---|---|---|
| Macro-elements | ρk | SS Maria della Bruna | San Pietro Caveoso | San Rocco | San Francesco d'Assisi | San Giovanni Battista |
| 1 Façade overturning | 1 | 0 | −1 | 0 | 0 | 0 |
| 2 Mechanisms at the top of the façade | 1 | 2 | 2 | 0 | 0 | 3 |
| 3 Façade in-plane mechanisms | 1 | 1 | 2 | 0 | 3 | 1 |
| 4 Prothyrum-Narthex | 0.9 | 0 | 0 | 0 | 0 | 0 |
| 5 Main nave transversal response | 0.9 | 0 | 3 | 0 | 0 | 1 |
| 6 Lateral walls shear mechanism | 0.9 | 0 | −3 | 3 | 0 | −3 |
| 7 Colonnade longitudinal response | 1 | 0 | 0 | 3 | 0 | 3 |
| 8 Main nave vaults | 1 | 3 | 0 | 0 | 0 | 3 |
| 9 Lateral naves vaults | 0.5 | 0 | 3 | 3 | 0 | 3 |
| 10 Transept end wall overturning | 1 | 0 | 0 | 0 | 0 | 0 |
| 11 Transept walls shear mechanisms | 1 | 0 | 0 | 0 | 0 | 0 |
| 12 Transept vaults | 0.9 | 0 | 0 | 0 | 0 | 0 |
| 13 Triumphal arches | 1 | −3 | −3 | −3 | −3 | 0 |
| 14 Dome, drum/tiburium | 0.9 | −3 | 0 | 0 | 0 | −3 |
| 15 Lantern | 1 | 0 | 0 | 0 | 0 | 0 |
| 16 Apse overturning | 0.9 | 0 | −3 | 0 | 1 | 0 |
| 17 Presbytery/apse shear mechanism | 0.9 | 0 | 0 | 3 | 0 | 0 |
| 18 Presbytery/apse vaults | 0.9 | 0 | 0 | −3 | 3 | 0 |
| 19 Roof parts: main nave | 0.9 | 0 | −3 | −3 | −3 | 0 |
| 20 Roof parts: transept | 0.8 | 0 | 0 | 0 | 0 | 0 |
| 21 Roof parts: apse | 1 | 0 | 0 | −3 | 3 | 0 |
| 22 Chapels overturning | 1 | 0 | −1 | 2 | 0 | −3 |
| 23 Chapels shear mechanisms | 1 | 0 | −3 | 3 | 0 | −3 |
| 24 Chapels vaults | 1 | 0 | 0 | 3 | 3 | 0 |
| 25 Interactions next to plan/elevation irregularities | 1 | 0 | 3 | 0 | 2 | −3 |
| 26 Projections (spires, pinnacles, statues) | 0.9 | 0 | 0 | 0 | 0 | −1 |
| 27 Bell tower | 0.9 | 0 | 0 | 0 | 0 | 0 |
| 28 Bell cell | 0.9 | −1 | 0 | 0 | 0 | 0 |
| i$_v$ | | 0.47 | 0.44 | 0.62 | 0.68 | 0.49 |

with intensity equal to 6 are found. The seismic action is defined in accordance with the Italian seismic code (Ministerial Decree, 14/01/2008) by considering the Damage Limit State (*DLS*) and the Life Safety Limit state (*LSLS*). By assuming the observation periods discussed above, we obtain a return period $T_R$ equal to 30 and 75 years for the *DLS*, and $T_R$ equal to 285 and 712 years for the *LSLS*.

In **Figure 2** the considered elastic and design spectra for the horizontal component of seismic action are shown. It should be noted that, according to what observed in Paulay and Priestley (1992) for masonry structures, the elastic spectra is calculated by considering a damping ratio equal to 10%. Furthermore, a behavior factor $q=2$ is considered for the design spectra, according to the Italian code suggestions.

## APPLICATION OF LV1 METHOD

In order to apply the *LV1* method, **Table 2** numerically reports, for each macro-element considered, the score assigned to the actual vulnerability ($v_{ki}$) and seismic-resistant device ($v_{Kp}$). With these scores, it has been possible to calculate for each church the vulnerability index $i_v$ (Equation 1), and then the seismic capacity measured through $a_{LSLS}$ and $a_{DLS}$ (Equations 2, 3). The obtained results are summarized in **Table 3**, where they

**TABLE 3 |** Seismic assessment according to the LV1 method for LSLS and DLS.

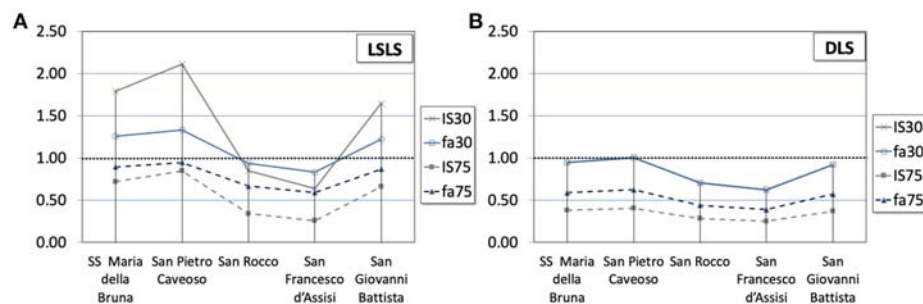| | LV1- Seismic assessment | | | | |
|---|---|---|---|---|---|
| | **SS Maria della Bruna** | **San Pietro Caveoso** | **San Rocco** | **San Francesco d'Assisi** | **San Giovanni Battista** |
| $a_{LSLS}S$ (g) | 0.193 | 0.204 | 0.144 | 0.127 | 0.187 |
| $a_{LSLS}/FC$ (g) | 0.143 | 0.151 | 0.106 | 0.094 | 0.139 |
| $T_{LSLS}$ (years) | 511 | 602 | 242 | 181 | 469 |
| $I_{S30}$ ($T_{LSLS}/T_{R,LSLS30}$) ($V_R$ = 30 years, $V_N$ = 20 years, $T_{R,LSLS30}$ = 285 years) | 1.79 | 2.11 | 0.85 | 0.64 | 1.65 |
| $I_{S75}$ ($T_{LSLS}/T_{R,LSLS75}$) ($V_R$ = 75 years, $V_N$ = 50 years, $T_{R,LSLS75}$ = 712 years) | 0.72 | 0.85 | 0.34 | 0.25 | 0.66 |
| $a_{g,LSLS30}$ - $V_R$ = 30 years | 0.114 | 0.114 | 0.114 | 0.114 | 0.114 |
| $a_{g,LSLS75}$ - $V_R$ = 75 years | 0.160 | 0.160 | 0.160 | 0.160 | 0.160 |
| $f_{a30}$ ($a_{LSLS}/a_{g,LSLS30}$) | 1.26 | 1.33 | 0.94 | 0.83 | 1.22 |
| $f_{a75}$ ($a_{LSLS}/a_{g,LSLS75}$) | 0.89 | 0.94 | 0.67 | 0.59 | 0.87 |
| $a_{DLS}S$ (g) | 0.048 | 0.051 | 0.036 | 0.032 | 0.047 |
| $a_{DLS}/FC$ (g) | 0.036 | 0.038 | 0.027 | 0.024 | 0.035 |
| $T_{DLS}$ (years) | 28 | 30 | 21 | 19 | 28 |
| $I_{S30}$ ($T_{DLS}/T_{R,DLS30}$) ($V_R$ = 30 years, $V_N$ = 20 years, $T_{R,DLS30}$ = 30 years) | 0.95 | 1.01 | 0.70 | 0.62 | 0.92 |
| $I_{S75}$ ($T_{DLS}/T_{R,DLS75}$) ($V_R$ = 75 years, $V_N$ = 50 years, $T_{R,DLS75}$ = 75 years) | 0.38 | 0.40 | 0.28 | 0.25 | 0.37 |
| $a_{g,DLS30}$ - $V_R$ = 30 years | 0.038 | 0.038 | 0.038 | 0.038 | 0.038 |
| $a_{g,DLS75}$ - $V_R$ = 75 years | 0.061 | 0.061 | 0.061 | 0.061 | 0.061 |
| $f_{a30}$ ($a_{DLS}/a_{g,DLS30}$) | 0.95 | 1.00 | 0.70 | 0.62 | 0.92 |
| $f_{a75}$ ($a_{DLS}/a_{g,DLS75}$) | 0.59 | 0.62 | 0.44 | 0.39 | 0.57 |



**FIGURE 3 |** Indexes calculated with the LV1 method for **(A)** LSLS and **(B)** DLS.
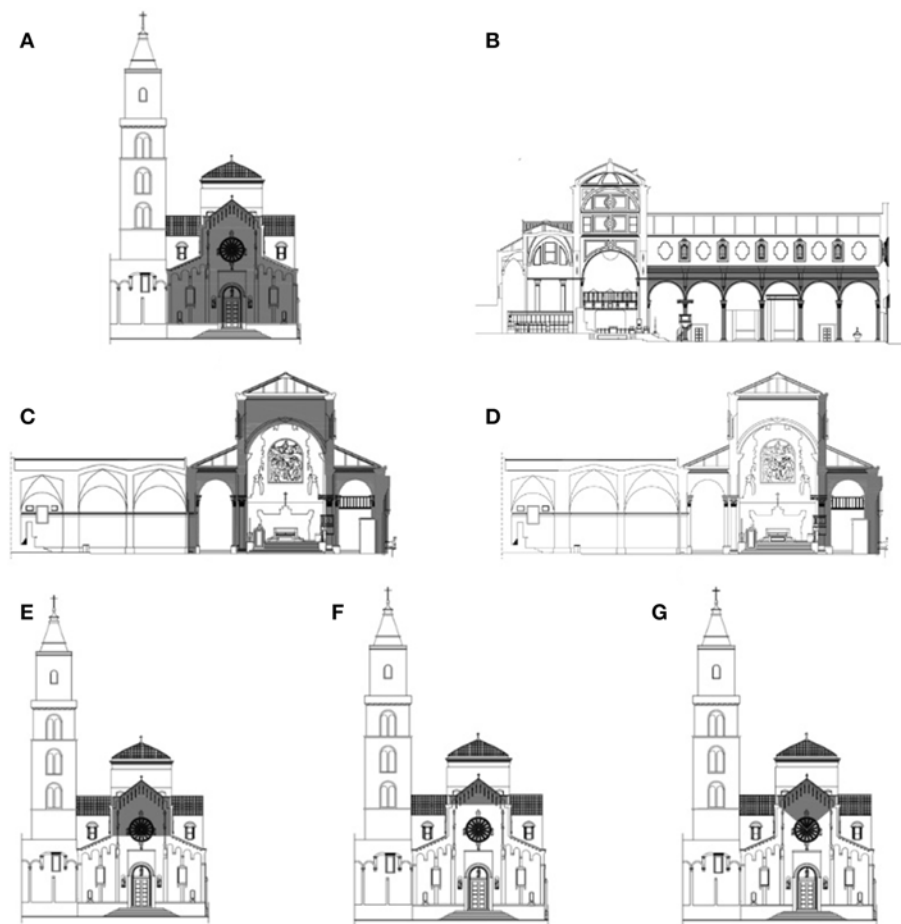
**FIGURE 4 |** *SS Maria della Bruna* church. Response mechanisms considered: **(A)** Façade simple overturning, **(B)** longitudinal response of the colonnade, **(C)** triumphal arch transversal response, **(D)** lateral nave transversal response, **(E)** top façade overturning, **(F)** gable simple overturning, **(G)** gable out-of-plane breakout.

**TABLE 4 |** Directly ground-connected response mechanisms.

| Macro-element | SS Maria della Bruna | San Pietro Caveoso | San Rocco | San Francesco d'Assisi | San Giovanni Battista |
|---|---|---|---|---|---|
| Façade simple overturning (g) | 0.078 | 0.065 | 0.050 | 0.059 | 0.162 |
| Colonnade longitudinal response (g) | 0.197 | 0.271 | 0.106 | 0.322 | 0.167 |
| Nave transversal response (g) | 0.179 | 0.071 | 0.108 | 0.046 | 0.185 |
| Triumphal arch transversal response (g) | 0.121 | 0.166 | – | 0.165 | – |
| **Minimum $a_0^*$ (g)** | **0.078** | **0.065** | **0.050** | **0.046** | **0.162** |
| **Life-Safety Limit State (LSLS)** | | | | | |
| $a_{g,LSLS30}$ S/q (g) | 0.057 | 0.057 | 0.057 | 0.057 | 0.057 |
| $a_{g,LSLS75}$ S/q (g) | 0.080 | 0.080 | 0.080 | 0.080 | 0.080 |
| $f_{a30}$ [$a_0^*/(a_{g,LSLS30}$ S/q)] | 1.374 | 1.145 | 0.881 | 0.810 | 1.338 |
| $f_{a75}$ [$a_0^*/(a_{g,LSLS75}$ S/q)] | 0.975 | 0.813 | 0.625 | 0.575 | 0.950 |
| **Damage Limit State (DLS)** | | | | | |
| $a_{g,DLS30}$ S (g) | 0.038 | 0.038 | 0.038 | 0.038 | 0.038 |
| $a_{g,DLS75}$ S (g) | 0.061 | 0.061 | 0.061 | 0.061 | 0.061 |
| $f_{a30}$ [$a_0^*/(a_{g,DLS30}$ S)] | 2.056 | 1.713 | 1.318 | 1.212 | 2.003 |
| $f_{a75}$ [$a_0^*/(a_{g,DLS75}$ S)] | 1.276 | 1.063 | 0.818 | 0.753 | 1.243 |

*Spectral acceleration $a_0^*$ and related indexes for LSLS and DLS according to the LV2 method.*

are reported as the a*cceleration factor* $f_a$ (Equation 7) and the *seismic safety index* $I_S$ (Equation 4). These parameters are calculated by considering two observation periods, that are $V_R=30$ years (obtaining $I_{s,30}$ and $f_{a,30}$) and $V_R=75$ years (obtaining $I_{S,75}$ and $f_{a,75}$). The seismic verifications are conducted by referring to both the *LSLS* (having a $P_{VR}=10$ %) and to the *DLS* (having instead a $P_{VR}=63$ %). Moreover, in comparing the results, the following additional assumptions have been made: FC =1.35 (factor of confidence), S=1 (soil stratigraphic factor).

Firstly, the results are presented in terms of return periods ($T_{LSLS}$ and $T_{DLS}$, for *LSLS* and *DLS*, respectively) obtained on the predicted accelerations ($a_{LSLS}/FC$ and $a_{DLS}/FC$) of each case study. It must be noted that the expected return period $T_{DLS}$ results are always, except for *San Pietro Caveoso* church, lower than 30 years, corresponding to the first point available of the site seismic hazard (**Figure 2B**). Therefore, in these cases, by following the Italian Design Code, $a_{g,DLS30}$ has been considered equal to the one provided for a return

period of 30 years (in this case it results $a_{g,DLS30}=0.038$g). For sake of completeness, Figure 3 illustrates the numerical results summarized in Table 3 for the two considered limit states.

**Figure 3A** shows the considered indexes obtained for *LSLS* (i.e., $I_s$ and $f_a$), evaluated for all the analyzed churches and for the two considered observation periods. For $V_R = 30$ years, the *SS Maria della Bruna* church shows a low vulnerability, having both indexes exceeding the unity: $I_{s30} = 1.65$ and $f_{a30} = 1.26$. On the contrary, these indexes are significantly lower than unity if the observation period is equal to 75 years: in this case it results as $I_{s75} = 0.66$, and $f_{a75} = 0.89$. It is worth noting that *SS Maria della Bruna* church shows a low vulnerability if compared with others, except for *San Pietro Caveoso* church, where it is found $I_{s30} = 2.11$ ($I_{s75} = 0.85$) and $f_{a30} = 1.33$ ($f_{a75} = 0.94$). In **Figure 3B**, the resulting indexes for *DLS* are shown. In this case, the *SS Maria della Bruna* church provides, in all cases, numerical values that are always lower than unity: $I_{s30} = 0.92$ ($I_{s75} = 0.37$) and $f_{a30} = 0.95$ ($f_{a75} = 0.59$), even though higher than the other ones, except
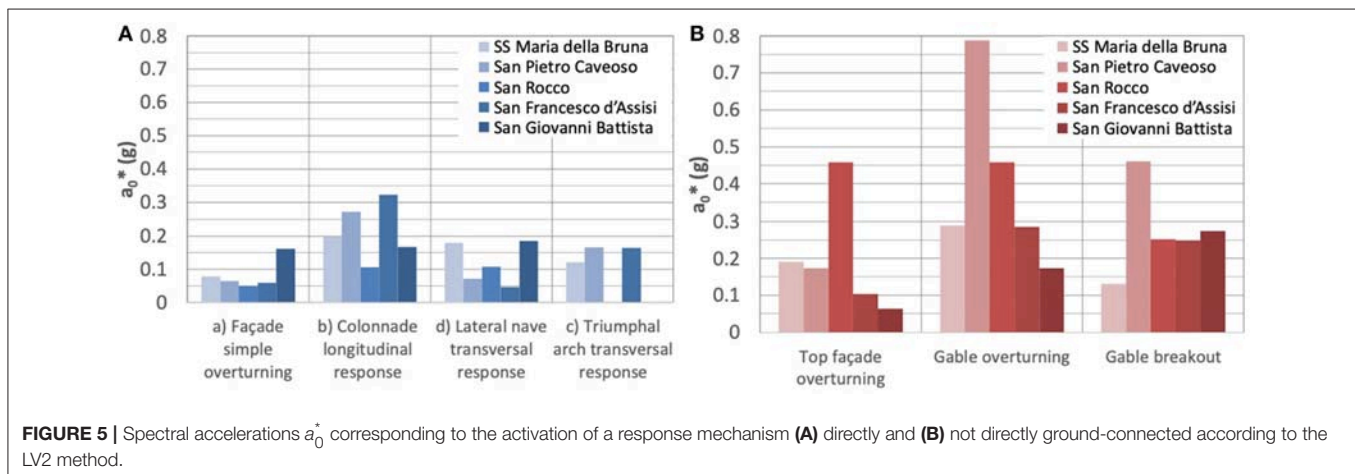


**FIGURE 5 |** Spectral accelerations $a_0^*$ corresponding to the activation of a response mechanism **(A)** directly and **(B)** not directly ground-connected according to the LV2 method.

**TABLE 5 |** Not directly ground-connected response mechanisms.

| Macro-element | SS Maria della Bruna | San Pietro Caveoso | San Rocco | San Francesco d'Assisi | San Giovanni Battista |
|---|---|---|---|---|---|
| Top façade overturning (g) | 0.191 | 0.173 | 0.458 | 0.103 | 0.064 |
| Gable overturning (g) | 0.289 | 0.788 | 0.458 | 0.286 | 0.173 |
| Gable breakout (g) | 0.131 | 0.460 | 0.252 | 0.248 | 0.274 |
| **Minimum $a_0^*$ (g)** | **0.131** | **0.173** | **0.252** | **0.103** | **0.064** |
| **Life-Safety Limit State (LSLS)** | | | | | |
| Se(T1) ψ(Z) γ/q - $V_R$ = 30 years (g) | 0.122 | 0.141 | 0.118 | 0.106 | 0.085 |
| Se(T1) ψ(Z) γ/q - $V_R$ = 75 years (g) | 0.178 | 0.202 | 0.173 | 0.153 | 0.124 |
| $f_{a30}$ [$a_0^*$/(Se(T1) ψ(Z) γ/q) - $V_R$ = 30 years] | 1.074 | 1.227 | 2.136 | 0.972 | 1.059 |
| $f_{a75}$ [$a_0^*$/(Se(T1) ψ(Z) γ/q) - $V_R$ = 75 years] | 0.736 | 0.856 | 1.457 | 0.673 | 0.726 |
| **Damage Limit State (DLS)** | | | | | |
| Se(T1) ψ(Z) γ - $V_R$ = 30 years (g) | 0.055 | 0.077 | 0.053 | 0.047 | 0.038 |
| Se(T1) ψ(Z) γ - $V_R$ = 75 years (g) | 0.102 | 0.127 | 0.103 | 0.087 | 0.072 |
| $f_{a30}$ [$a_0^*$/(Se(T1) ψ(Z) γ) - $V_R$ = 30 years] | 2.382 | 2.247 | 4.755 | 2.191 | 2.368 |
| $f_{a75}$ [$a_0^*$/(Se(T1) ψ(Z) γ) - $V_R$ = 75 years] | 1.284 | 1.362 | 2.447 | 1.184 | 1.250 |

*Spectral acceleration $a_0^*$ and related indexes for LSLS and DLS according to the LV2 method.*

again for *San Pietro Caveoso* church where it is found that $I_{s30} = 1.01$ ($I_{s75} = 0.40$) and $f_{a30} = 1.00$ ($f_{a75} = 0.62$).

One may note that, as for the *LSLS*, the seismic safety index $I_s$ constantly reduces by about 2.5 times in all the churches (about 1.4 times in the case of $f_a$), passing from $V_R = 30$ years to $V_R = 75$ years. This constant value may be justified by the fact that the ratio $I_{s30}/I_{s75}$ (or $f_{a30}/f_{a75}$) is dependent only on the return periods of the seismic actions expected on the site (accelerations expected on the site). The same conclusion may be done for the *DLS*, where $I_{s30}/I_{s75}$ results at about 2.5 ($f_{a30}/f_{a75} \cong 1.6$).

The results of **Figure 3** clearly show that all the plotted curves for *LSLS* and *DLS* have qualitatively the same shape. In other words, the ranking of the seismic performances is always the same independently from the Limit State and from the index considered.

## APPLICATION OF LV2 METHOD

Seven failure mechanisms have been considered in this study: four directly connected to the ground, and the other three are
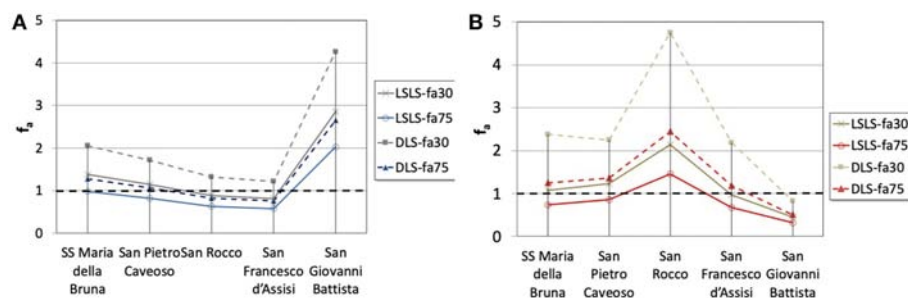


**FIGURE 6 |** LV2 method. **(A)** Acceleration factors $f_a$ of macro-elements mechanisms directly ground-connected and **(B)** not directly connected to the ground for LSLSL and DLS.
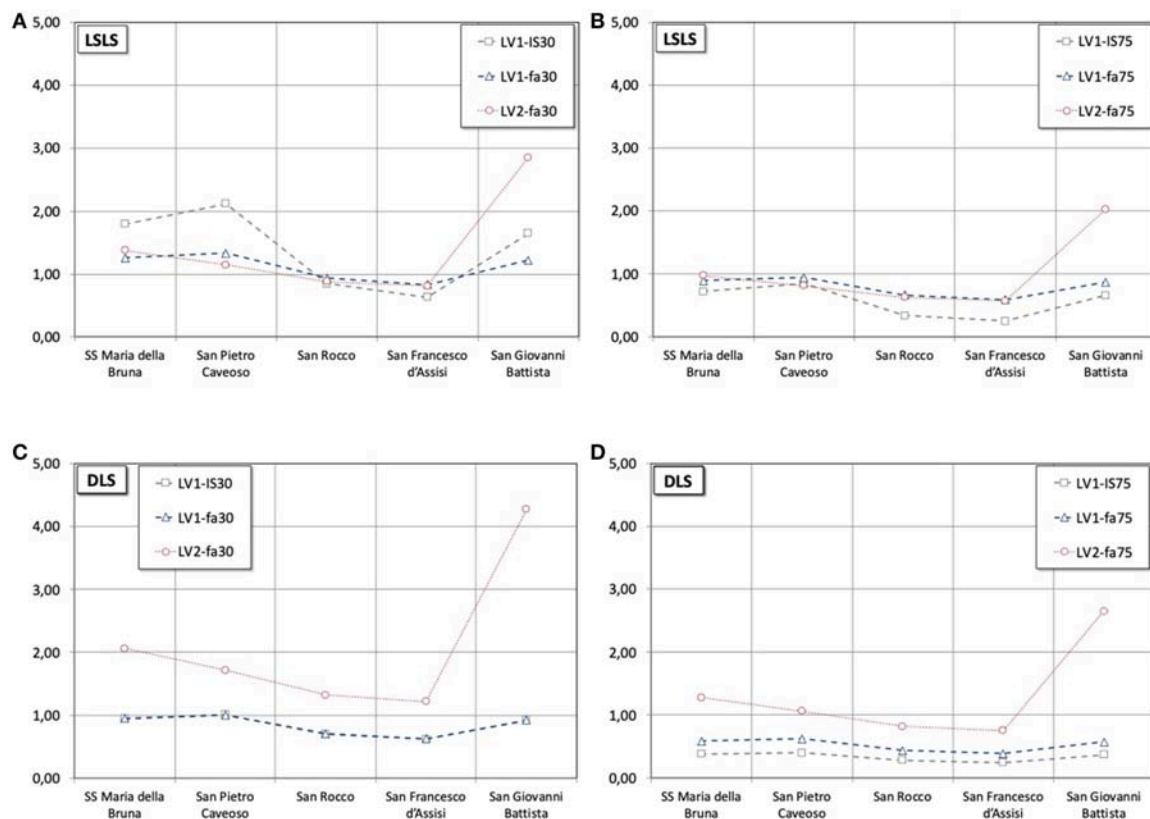


**FIGURE 7 |** LV1 and LV2 methods. LSLS: **(A)** $V_R = 30$ years and **(B)** $V_R = 75$ years. DLS: **(C)** $V_R = 30$ years and **(D)** $V_R = 75$ years.

not directly ground-connected. The considered mechanisms are the following:

- *Façade simple overturning*, where the stabilizing friction contribution of the orthogonal walls is neglected due to an effective connection;
- *Colonnade longitudinal response*, that is the macro-element separating the main nave from the lateral ones. It is composed of columns and arches placed in the longitudinal direction;
- *Transversal response of triumphal arch*, considering also (if present) the adjacent arches belonging to the lateral naves;
- *Transversal response of lateral nave*, that is an overturning mechanism considered separated from the main aula;
- *Top façade simple overturning*, façade portion overturning, starting from the highest point of lateral naves roof up to the façade peak;
- *Gable simple overturning*, simple overturning of the triangular portion placed at the façade top;
- *Gable out-of-plane breakout*, out-of-plane mechanism involving the triangular portion at the façade top activated by the means of three symmetrical cylindrical hinges.

For all the macro-elements, since the local masonry disintegration may be excluded, a monolithic behavior has been assumed. The macro-elements considered, as previously described, have been schematized starting from only visual investigations and geometric reliefs, since no clear cracking patterns have been encountered. In addition, no stabilizing contribution for each mechanism has been considered (such as interaction of transversal walls, or additional restrains). Therefore, the calculated activation multipliers underestimate the real ones. Furthermore, for simplicity, only the most vulnerable mechanisms have been considered in this study, not considering the in-plane response ones since they typically show higher activation multipliers.

**Figure 4** illustrates the failure mechanisms in the case of *SS Maria della Bruna* church. It must be clarified that, for the comparison with the other churches, in the case of *San Rocco* and *San Giovanni Battista* churches, the triumphal arch mechanism has not been considered due to the absence of this architectonic element.

The spectral accelerations $a_0^*$ (derived from $\alpha_0$ according to the Equation 9), related to the activation of the considered macro-elements mechanism connected to the ground are shown in **Table 4** and graphed in **Figure 5A**. Moreover, **Table 4** reported the acceleration factors $f_a$ for a $V_R = 30$ years and a $V_R = 75$ years, calculated as follows:

$$f_{a,LS} = \frac{a_0^*}{a_{demand}} \tag{19}$$

In Equation (19) for each church, it is considered the minimum values of $a_0^*$ for a given limit state (i.e., the most vulnerable failure mode). Whereas, $a_{demand}$ corresponds to the related expected seismic demand equal to: $a_{g,LSLS30}\ S/q$ (or $a_{g,LSLS75}\ S/q$), or to $a_{g,DLS30}\ S$ ($a_{g,DLS75}\ S$). Again, $S$ has been assumed equal to 1 and $q$ equal to 2.

**TABLE 6 |** New simplified seismic risk assessment scoring (Diaz, 2016).

|  | Macro-element | SS Maria della Bruna | San Pietro Caveoso | San Rocco | San Francesco d'Assisi | San Giovanni Battista |
|---|---|---|---|---|---|---|
| 1 | Position and foundations | A | A | B | A | A |
| 2 | Floor plan configuration | C | C | C | D | C |
| 3 | Elevation configuration | A | A | A | A | A |
| 4 | Distance between walls | C | D | D | D | D |
| 5 | Non-structural elements | C | D | D | D | D |
| 6 | Type-organization of R.S. | B | A | B | B | B |
| 7 | Quality of the R.S. | A | A | A | A | A |
| 8 | Horizontal structures | A | A | A | A | A |
| 9 | Roofing | C | C | C | C | C |
| 10 | Conservation status | A | A | A | B | A |
| 11 | Environmental alterations | A | B | A | A | A |
| 12 | Construction system alterations | A | A | A | A | A |
| 13 | Vulnerability to fire | B | B | B | B | B |
|  | **Seismic vulnerability score (V)** | **15.82** | **16.83** | **19.53** | **22.56** | **33.66** |
| 1 | Maximum Mercalli Intensity | 0.2 | 0.20 | 0.20 | 0.20 | 0.20 |
| 2 | Landslides/rock fracture | 0.05 | 0.15 | 0 | 0 | 0 |
| 3 | Erosion | 0.05 | 0.05 | 0 | 0.05 | 0.05 |
| 4 | Physical stress | 0 | 0 | 0 | 0 | 0 |
| 5 | Pollution | 0.05 | 0.05 | 0.05 | 0.05 | 0.05 |
| 6 | Socio-organizational | 0.05 | 0.05 | 0.05 | 0.05 | 0.05 |
| 7 | Demographic decline | 0 | 0 | 0 | 0 | 0 |
|  | **Seismic hazard score (H+1)** | **1.40** | **1.50** | **1.30** | **1.35** | **1.35** |
|  | **SEISMIC RISK [V x (H+1)]** | **22.15** | **25.25** | **25.39** | **30.46** | **25.00** |
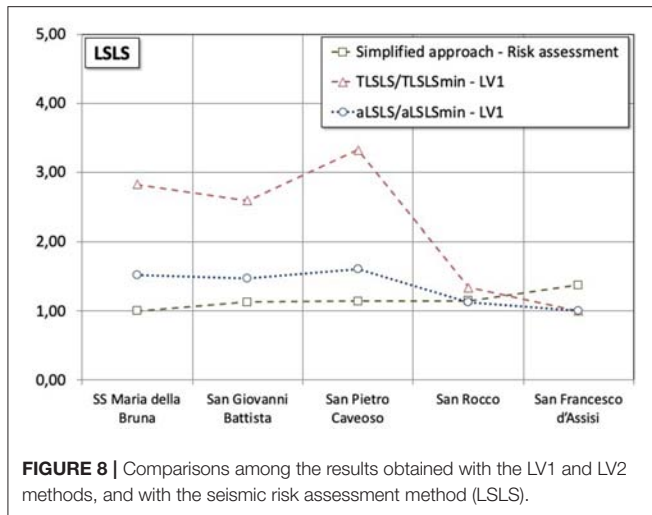
**FIGURE 8 |** Comparisons among the results obtained with the LV1 and LV2 methods, and with the seismic risk assessment method (LSLS).

The façade overturning results in the most vulnerable mechanism, with an activation acceleration of $a_0^* = 0.078$ g, while the others have acceleration significantly higher (i.e., transversal response of triumphal arch $a_0^* = 0.121$ g, about 55% higher than the value obtained for the façade overturning). It results that the most vulnerable mechanism for all churches is the simple overturning of the main façade, except for *San Francesco d'Assisi* church. In this case, the lowest spectral acceleration corresponds to the nave transversal response ($a_0^* = 0.046$ g). Furthermore, it should be remarked that in the case of *San Giovanni Battista* church, the accelerations obtained for all the mechanisms are significantly higher than the others, with a minimum value $a_0^*$ of 0.162 g that is more than twice of the one obtained for the *SS Maria della Bruna* Church. Moreover, **Table 5** and **Figure 6A** satisfy the seismic performance requirements in the case of $V_R = 30$ years for both *LSLS* and *DLS*, and in the case of $V_R = 75$ years for *DLS* only while for *LSLS* $f_{a75}$ it is slightly <1 (I.e. $f_{a75} = 0.975$). Again, as observed for the *LV1* method, the Cathedral is close to satisfying all the required seismic safety obtaining indexes, and this satisfaction level is similar or higher than the other considered churches, except for *San Giovanni Battista*.

In **Table 5** and **Figure 5B** the accelerations relative to the macro-elements that are not directly ground-connected are shown. For *SS Maria della Bruna* church, the most vulnerable mechanism is the gable breakout with an activation acceleration of 0.131 g. By comparing the results with the others, it should be noted that only *San Francesco d'Assisi* and *San Giovanni Battista* churches have low $a_0^*$, and therefore, the Cathedral is the third most vulnerable regarding these mechanisms. The seismic demand $a_{demand}$ is calculated in these cases as $S_e(T_1)_{30}\psi(Z)\gamma/q$ for $V_R = 30$ years [or $S_e(T_1)_{75}\psi(Z)\gamma/q$ for $V_R = 75$ years] for the *LSLS*, and as $S_e(T_1)_{30}\psi(Z)\gamma$ $V_R = 30$ years [or $S_e(T_1)_{75}\psi(Z)\gamma$ for $V_R = 75$ years] for the *DLS*. Given this seismic demand, the acceleration factors can be calculated as the ratio of $a_0^*$ and such demands (i.e., $f_{a30} = a_0^*/S_e(T_1)_{30}\psi(Z)\gamma/q$ and $f_{a75} = a_0^*/S_e(T_1)_{75}\psi(Z)\gamma/q$). By analyzing these acceleration factors (**Figure 6B**), it is worthy of noting that the *SS Maria della Bruna* church has values that are close or beyond the unity (i.e., for *LSLS*

$f_{a30} = 1.074$, $f_{a75} = 0.736$; while for *DLS* $f_{a30} = 2.382$, $f_{a75} = 1.284$), confirming the need for only light interventions in order to obtain the required seismic performances. Furthermore, it should be remarked that the most vulnerable church regarding these mechanisms is *San Giovanni Battista* (i.e., $a_0^* = 0.064$ g top façade overturning), which is less vulnerable regarding the mechanisms directly connected to the ground.

## COMPARATIVE SEISMIC ASSESSMENT

The comparisons of the results calculated with the *LV1* and *LV2* methods of the Italian directive (G.U. n. 47, 26/02/2011) are illustrated in **Figure 7**. It should be specified that, in the case of the *LV2* method, only the ground connected mechanisms are considered in these comparisons. Precisely, **Figures 7A,B** show the results for *LSLS* by referring to $V_R = 30$ years and $V_R = 75$ years, respectively. It is worth to note that for the Matera Cathedral the *LV1* method, which is simpler and less accurate, overestimates the results if compared with the *LV2* one. This trend is also found for *San Pietro Caveoso* church. However, for *SS Maria della Bruna* the scatter is low and, at least for $V_R = 30$ years, the ratios are always beyond the unity. Whereas, in **Figures 7C,D**, the comparisons between the two adopted methods for the considered *DLS* are shown. Contrarily to the *LSLS*, in this case the *LV1* method is, for the considered churches, always conservative with respect to the *LV2* one. With the *LV1* method only, the *San Pietro Caveoso* church exhibits, for $V_R = 30$ years, a seismic capacity closer to the demand. As for the *LV2* method, the capacity of all churches is always higher than demand except for *San Rocco* and *San Francesco d'Assisi* for $V_R = 75$ years. Anyway, it should be remarked that the vulnerability classification provided by considering the two methods separately would be very similar since, as illustrated in the **Figure 7**, the trends found are quite the same. Nevertheless, by increasing the detail level of the analysis (from *LV1* to *LV2*), it is found that in the analyzed cases, the *LV1* overestimates the seismic performance, as for *SS Maria della Bruna* and *San Pietro Caveoso* church. However, it should be kept in mind that in this study, for simplicity, the *LV2* results have been obtained by neglecting, as previously described, all the stabilizing contributions. Therefore, the actual results will be higher than those discussed here, and higher than the ones provided by the *LV1* method. This confirms that after a first and fast numerical evaluation, useful for classifying the case studies, there is always the need to implement more realistic numerical models that cannot be generalized since they are related to the boundary conditions of the analyzed problem.

Finally, in this study a comparison with the method proposed in (Dìaz, 2016) is illustrated and then validated in D'Amato et al. (2018). Its application is numerically reported in **Table 6**. With this method, the *SS Maria della Bruna* church obtains a score of $R = 22.15$, resulting as the lowest value. All the obtained results are compared in relative terms in **Figure 8**: at first, each seismic score ($R_i$) is divided by the minimum value found ($R_{min}$); then, all resulting ratios ($R_i/R_{min}$) are represented in ascending order. For comparison, in **Figure 8** the values calculated with

the *LV1* method are also reported. In detail, the dimensionless return period $T_{i,LSLS}/T_{LSLSmin}$, where $T_{i,LSLS}$ is the returning period corresponding to the *LSLS* achievement and $T_{LSLSmin}$ is the minimum value found among the churches (corresponding to 181 years for the *San Francesco d'Assisi* church), are plotted. In addition, in **Figure 8** the dimensionless ground acceleration capacity $a_{i,LSLS}/a_{LSLSmin}$ is also reported, where $a_{i,LSLS}$ is the ground acceleration related to the LSLS achievement and $a_{LSLSmin}$ is the lowest value found (that is 0.127 g corresponding, again, to the *San Francesco d'Assisi* church). One may consider these ratios as relative seismic vulnerability indexes: the ratio $T_{i,LSLS}/T_{LSLSmin}$ (or $a_{i,LSLS}/a_{LSLSmin}$) increases as the relative seismic vulnerability ($R_i/R_{min}$) decreases, where both indexes are calculated with respect to the most vulnerable church (in this case *San Francesco d'Assisi* church). The results found confirm the applicability of the new simplified method proposed in Dìaz (2016) and validated in D'Amato et al. (2018). This method may be intended, in a multi-level frame-work approach, as a "*Level of Evaluation 0*" (*LV0*) since it permits rapidly ranking the seismic performance at a territorial level. In this way, useful information for individuating the priorities may be found, to be investigated in more detail with more refined approaches (such as *LV1*, *LV2*, or *LV3*).

## CONCLUSIONS

In this work, it has been conducted as a comparative analysis among the seismic performances of ancient masonry churches, by the means of different simplified methods. At first, the seismic vulnerability of the Matera Cathedral, called *SS Maria della Bruna* of Matera, has been investigated, and then the obtained results have been compared with the ones of four churches located in the Matera city center. The great advantage of these methods is that they don't imply advanced structural analyses and investigations. Thus, they can be used as decision making tools for identifying the priorities, and

consequently, for performing further analyses and designing the potential interventions.

The analyses performed with the methods, indicated as *LV1* and *LV2* within the Italian directive (G.U. n. 47, 26/02/2011), have highlighted that, among the churches analyzed, the Matera Cathedral is one of the less vulnerable. Specifically, according to the *LV2* method, it satisfies the seismic protection level required in the case of $V_R$= 30 years, both for *LSLS* and for *DLS*. On the contrary, for $V_R$ = 75 years, few and light interventions are requested in order to achieve the required seismic demand for *LSLS*.

Finally, the comparisons with the new simplified method for seismic risk assessment confirm that it may be considered as a preliminary appraisal method for comparing the seismic performances of ancient churches at a territorial level. It may be proposed as a *LV0* approach, since it requires limited and qualitative information for ranking the seismic performance at a territorial scale. However, by analyzing the obtained results, it has emerged that, in general, simpler methods may overestimate the actual seismic performance of a church. Therefore, the simplified methods, although useful for comparing and ranking the churches seismic performances at a territorial level, cannot substitute the refined ones for realistically assessing the seismic behavior of a structure.

## DATA AVAILABILITY

All data generated or analyzed during this study are included in this published article.

## AUTHOR CONTRIBUTIONS

All authors listed have made a substantial, direct and intellectual contribution to the work, and approved it for publication.

## REFERENCES

Alexander, D. C. (2017). *Natural Disasters*. Routledge; Springer.

Betti, M., Boschi, S., Borghini, A., Ciavattone, A., and Vignoli, A. (2018). Comparative seismic risk assessment of basilica-type churches. *J. Earthquake Eng.* 22, 62–95. doi: 10.1080/13632469.2017.1309602

Brandonisio, G., Lucibello, G., Mele, E., and De Luca, A. (2013). Damage and performance evaluation of masonry churches in the 2009 L'Aquila earthquake. *Eng. Failure Anal.* 34, 693–714. doi: 10.1016/j.engfailanal.2013.01.021

Caprili, S., Mangini, F., Salvatore, W., Bevilacqua, M. G., Karwacka Codini, E., Squeglia, N., et al. (2017). A knowledge-based approach for the structural assessment of cultural heritage, a case study: La Sapienza Palace in Pisa. *Bull. Earthquake Eng.* 15, 4851–4886. doi: 10.1007/s10518-017-0158-y

Castellazzi, G., Gentilini, C., and Nobile, L. (2013). Seismic vulnerability assessment of a historical church: limit analysis and nonlinear finite element analysis. *Adv. Civil Eng.* 2013:517454. doi: 10.1155/2013/517454

Castori, G., Borri, A., Corradi, M., De Maria, A., and Sisti, R. (2017). Seismic vulnerability assessment of a monumental masonry building. *Eng. Struct.* 136, 454–465. doi: 10.1016/j.engstruct.2017.01.035

CEN, CE. (2004). *Design of Strctures for Earthquake Resistance. Part 3: Assessment and Retrofitting of Buildings*. Brussels: CEN, Comité Européen de Normalisation.

CENAPRED (2006). *Guía Básica Para la Elaboración de Atlas Estatales y Municipales de Peligros y Riesgos*. Conceptos básicos sobre peligros, riesgos y su representación geográfica. Mexico City.

CENAPRED (2014). *Diagnóstico de Peligros e Identificación de Riesgo de Desastres en México*. Centro Nacional de Prevención de Desaster, Coyoacán.

Chilean Norm N. 3332 (2013). *Estructuras - Intervención de Construcciones Patrimoniales de Tierra Cruda - Requisitos del Proyecto Estructural*. Santiago: INN, Instituto Nacional de Normalización Chile (in Spanish).

Clementi, F., Gazzani, V., Poiani, M., and Lenci, S. (2016). Assessment of seismic behaviour of heritage masonry buildings using numerical modelling. *J. Build. Eng.* 8, 29–47. doi: 10.1016/j.jobe.2016.09.005

CPTI (2015). *Parametric Catalogue of Italian Earthquakes*. Retrieved from: https://emidius.mi.ingv.it/CPTI15-DBMI15/index_en.htm

D'Amato, M., Laterza, M., and Casamassima, V. M. (2017). Seismic performance evaluation of a multi-span existing masonry arch bridge. *Open Civil Eng. J.* 11(Suppl. 5), 1191–1207. doi: 10.2174/1874149501711011191

D'Amato, M., Laterza, M., and Dìaz Fuentes, D. (2018). Simplified seismic analyses of ancient churches in matera's landscape. *Int. J. Architect. Heritage*. doi: 10.1080/15583058.2018.1511000. [Epub ahead of print].

D'Ayala, D., and Speranza, E. (2003). Definition of collapse mechanisms and seismic vulnerability of historic masonry buildings. *Earthquake Spectra* 18, 479–509. doi: 10.1193/1.1599896

D'Ayala, D. F., and Paganoni, S. (2011). Assessment and analysis of damage in L'Aquila historic city centre after 6th April 2009. *Bull. Earthquake Eng.* 9, 81–104. doi: 10.1007/s10518-010-9224-4

de Felice, G., and Giannini, R. (2001). Out of plane seismic resistance of masonry walls. *J. Earthquake Eng.* 5, 253–271. doi: 10.1080/136324601093 50394

Degg, M., and Chester, D. (2005). Seismic and volcanic hazards in Peru: changing attitudes to disaster mitigation. *Geogr. J.* 171, 125–145. doi: 10.1111/j.1475-4959.2005.00155.x

DGPTA (2003). *Rilevamento Della Vulnerabilità Sismica Degli Edifici in Muratura. Manuale Per la Compilazione Della Scheda GNDT/CNR di II Livello.* Roma: Direzione Generale delle Politiche Territoriali e Ambientali.

Dìaz, D. (2016). *Diseño de Herramientas de Evaluación del Riesgo Para la Conservación del Patrimonio Cultural Inmueble. Aplicación en dos Casos de Estudio del Norte Andino Chileno.* México: Publicaciones ENCRyM-INAH.

Doglioni, F., Moretti, A., and Petrini, V. (1994). *Churches and the Earthquake.* Trieste: Ed. LINT (in Italian).

Doherty, K., Griffith, M., Lam, N., and Wilson, J. (2002). Displacement-based seismic analysis for out-of-plane bending of unreinforced masonry walls. *Earthquake Eng. Struct. Dyn.* 31, 833–850. doi: 10.1002/eqe.126

Fabbrocino, F., Vaiano, G., and Formisano, A. (2018). "Parametric analysis on local collapse mechanisms of masonry churches,"in *16th International Conference of Numerical Analysis and Applied Mathematics - ICNAAM 2018.* Rhodes 13-18 September 2018: Proceedings of AIP Conference.

FEMA (2004). *Primer for Design Professionals (FEMA 389).* Washington, DC: Department of Homeland Security Emergency Preparedness and Response Directorate.

Formisano, A., Ciccone, G., and Mele, A. (2017). "Large scale seismic vulnerability and risk evaluation of a masonry churches sample in the historical centre of Naples," *13th International Conference of Computational Methods in Sciences and Engineering (ICCMSE 2017) - AIP Conference Proceedings 1906,* *1906.* Thessaloniki, 21-25 April 2017.

Formisano, A., and Marzo, A. (2017). Simplified and refined methods for seismic vulnerability assessment and retrofitting of an Italian cultural heritage masonry building. *Comput. Struct.* 180, 13–26. doi: 10.1016/j.compstruc.2016.07.005

Formisano, A., Vaiano, G., Fabbrocino, F., and Milani, G. (2018). Seismic vulnerability of Italian masonry churches: the case of the Nativity of Blessed Virgin Mary in Stellata of Bondeno. *J. Build. Eng.* 20, 179–200. doi: 10.1016/j.jobe.2018

Fuentes, D. D., D'Amato, M., and Laterza, M. (2019). "Seismic vulnerability and risk assessment of historic constructions: the case of masonry and adobe churches in Italy and Chile. SAHC 2018," *11th International Conference on Structural Analysis of Historical Constructions.* Cusco, 11-13 September 2018: RILEM Bookseries, 1127–1137.

GU. n. 47 (09/02/2011). *Directive of the Prime Minister dated on 09/02/2011.* Assessment and mitigation of seismic risk of cultural heritage with refeence to the technical code for the design of construction, issued by D.M. 14/01/2008 (in Italian).

Heyman, J. (1966). The stone skeleton. *Int. J. Solids Struct.* 2, 249–279. doi: 10.1016/0020-7683(66)90018-7

Instructions for the application of the Ministerial Decree MD (14/01/2008). "*Circolare 2 Febbraio 2009, n. 617 – Istruzioni per l'applicazione delle Nuove Norme Tecniche per le Costruzioni di cui al D.M. 14 Gennaio 2008*". S.O. n. 27 of the Official Gazette of the Italian Republic published on 26/02/2009, n. 47 (in Italian).

Instructions for the application of the Ministerial Decree MD (17/01/2018). "*Circolare 21 Febbraio 2019, n. 7 – Istruzioni per l'applicazione dell'Aggiornamento delle Nuove Norme Tecniche per le Costruzioni di cui al D.M. 17 Gennaio 2018.*" S.O. n. 8 of the Official Gazette of the Italian Republic published on 20/02/2018, n. 42 (in Italian).

ISCR, I. S. (2017). *Carta del Rischio.* Retrieved from: http://www.cartadelrischio.it/

Krstevska, L., Tashkov, L., Naumovski, N., Florio, G., Formisano, A., Fornaro, A., et al. (2010). "In-situ experimental testing of four historical buildings damaged during the 2009 L'Aquila earthquake,"in *COST ACTION C26: Urban Habitat Constructions under Catastrophic Events - Proceedings of the Final Conference* (Naples), 427–432.

Lagomarsino, S. (2012). Damage assessment of churches after l'Aquila earthquake (2009). *Bull. Earthquake Eng.* 10, 73–92. doi: 10.1007/s10518-011-9307-x

Lagomarsino, S., and Podestà, A. (2004a). Seismic vulnerability of ancient churches. Part 1: damage assessment and emergency planning. *Earthquake Spectra* 20, 377–394. doi: 10.1193/1.17 37735

Lagomarsino, S., and Podestà, S. (2004b). Seismic vulnerability of ancient churches. Part 2: statistical analysis of surveyed data and methods for risk analysis. *Earthquake Spectra* 20, 395–412. doi: 10.1193/1.1737736

Lagomarsino, S., and Podestà, S. (2005). *Inventario e Vulnerabilità del Patrimonio Monumentale dei Parchi dell'Italia Centro-Meridionale, Vol. III - Analisi di Vulnerabilità e Rischio Degli Edifici Monumentali.* L'Aquila: INGV/GNDT - Istituto Nazionale di Geofisica e Vulcanologia/Gruppo Nazionale per la Difesa dai Terremoti.

Lagomarsino, S., and Resemini, S. (2009). The assessment of damage limitation state in the seismic analysis of monumental buildings. *Earthquake Spectra* 25, 323–346. doi: 10.1193/1.3110242

Laterza, M., D'Amato, M., and Casamassima, V. M. (2016). "Seismic performance evaluation of multi-span existing masonry arch bridge," in *Proceedings of the 14th International Conference of Numerical Analysis and Applied Mathematics - ICNAAM 2016. 1863,* p. Article n. 450010. Rodos Palace Hotel, Rhodes, September 19th-25th 2016: AIP Conference Proceedings.

Lopez, S., D'Amato, M., Ramos, L., Laterza, M., and Lourenço, P. B. (2019). Simplified formulation for estimating the main frequencies of ancient masonry churches. *Front. Built Environ.* 5:18. doi: 10.3389/fbuil.2019.00018

Lourenço, P. B., Oliveira, D. V., Leite, J. C., Ingham, J. M., Modena, C., and da Porto, F. (2013). Simplified indexes for the seismic assessment of masonry buildings: international database and validation. *Eng. Failure Anal.* 34, 585–605. doi: 10.1016/j.engfailanal.2013.02.014

Lourenço, P. B., and Roque, J. A. (2006). Simplified indexes for the seismic vulnerability of ancient masonry buildings. *Construct. Build. Mater.* 20, 200–208. doi: 10.1016/j.conbuildmat.2005.08.027

Luchin, G., Luis, L. F., and D'Amato, M. (2018). Sonic tomography for masonry walls characterization. *Int. J. Architect. Heritage.* doi: 10.1080/15583058.2018.1554723 . [Epub ahead of print].

Marghella, G., Marzo, A., Carpani, B., Indirli, M., and Formisano, A. (2016). "Comparison between in situ experimental data and Italian code standard values,"in *16th International Brick and Block Masonry Conference, IBMAC 2016,* Padova, 1707–1714.

Marotta, A., Sorrentino, L., Liberatore, D., and Ingham, J. M. (2018). Seismic risk assessment of New Zealand unreinforced masonry churches using statistical procedures. *Int. J. Architect. Heritage* 12, 448–464. doi: 10.1080/15583058.2017.1323242

Ministerial Decree (14/01/2008). *Norme Tecniche per le Costruzioni.* S.O. n. 30 of the Official Gazette of the Italian Republic 2008, n. 29.

Morelli, M. (1970). *La cattedrale di Matera ha 700 anni.* Matera: Flli Montemurro (in Italian).

Paulay, T., and Priestley, M. (1992). *Seismic Design of Reinforced Concrete and Masonry Buildings.* New York, NY: John Wiley and Sons, Inc.

Ragone, A., Ippolito, A., Liberatore, D., and Sorrentino, L. (2017). "Emerging technologies for the seismic assessment of historical churches: the case of the bell tower of the Cathedral of Matera,"in *Handbook of Research on Emerging Technologies for Architectural and Archaeological Heritage* Hershey, PA: IGI Global, 159–196.

Ramirez, E., Lourenco, P. B., and D'Amato, M. (2019). "Seismic assessment of the matera cathedral,"in *SAHC 2018, 11th International Conference on Structural Analysis of Historical Constructions,* Cusco, 11-13 September 2018: RILEM Bookseries, 1346–1354.

Sarhosis, V., Milani, G., Formisano, A., and Fabbrocino, F. (2018). Evaluation of different approaches for the estimation of the seismic vulnerability of masonry towers. *Bull. Earthquake Eng.* 16, 1511–1545. doi: 10.1007/s10518-017-0258-8

UNDRO (1979). *Natural Disasters Vulnerability Analysis.* United Nations Disaster Relief Organisation.

Valente, M., Barbieri, G., and Biolzi, L. (2017). Seismic assessment of two masonry Baroque churches damaged by the 2012 Emilia earthquake. *Eng. Failure Anal.* 79, 773–802. doi: 10.1016/j.engfailanal.2017.05.026

Valente, M., and Milani, G. (2018a). Damage assessment and partial failure mechanisms activation of historical masonry churches under seismic actions: three case studies in Mantua. *Eng. Failure Anal.* 92, 495–519. doi: 10.1016/j.engfailanal.2018.06.017

Valente, M., and Milani, G. (2018b). Damage survey, simplified assessment, and advanced seismic analyses of two masonry churches after the 2012 Emilia earthquake. *Int. J. Architect. Heritage* doi: 10.1080/15583058.2018.1492646. [Epub ahead of print].

World Bank Indipendent Evaluation Group, (IEG). (2006). *Hazard of Nature, Risks to Development. An IEG Evaluation of World Bank Assistane for Natural Disasters*. Washington, DC: The World Bank.

**Conflict of Interest Statement:** The authors declare that the research was conducted in the absence of any commercial or financial relationships that could be construed as a potential conflict of interest.

# Knowledge-Based Approach for the Structural Assessment of Monumental Buildings: Application to Case Studies

Silvia Caprili[1]* and Irene Puncello[2]*

[1] Department of Civil and Industrial Engineering, University of Pisa, Pisa, Italy, [2] Department of Engineering of Energy, Systems, Territory and Construction, University of Pisa, Pisa, Italy

Historical buildings are characterized by a high level of complexity due to a long realization process often resulting in an overall lack of information and in a structural behavior that is more similar to a "structural aggregate" rather than to a "single building". The assessment of the static safety and seismic vulnerability then requires a multidisciplinary and multilevel approach including a deep and accurate preliminary knowledge phase before performing structural analyses. In the present paper, a consolidated knowledge-based procedure is presented and applied to four case studies in Italy. Interest is focused on the knowledge phase, combining critical–historical analysis to *in situ* architectural, geometrical, structural, material, and geotechnical aspects. The knowledge phase proves to be fundamental in understanding the structural behavior of cultural heritage, with special attention to the determination and analysis of local mechanisms and vulnerability elements and allowing to validate and give reason to numerical results.

Keywords: cultural heritage, historical buildings, masonry structures, multidisciplinary approach, structural assessment

## INTRODUCTION

The conservation of historical–monumental buildings represents a relevant topic in Italy and in all the Mediterranean countries. Earthquake events that recently struck central regions (as an example, Umbria e Marche 1997, Puglia-Molise 2002, Abruzzo 2009, Emilia Romagna 2012, Lazio–Umbria–Marche 2016–2017) were only the last evidence of the high seismic vulnerability of the national cultural and historical heritage. During the last decades, the need of elaborating and implementing a safeguard plan was faced, aiming to protect buildings from exceptional actions and following damages and, worse, local and global failures.

Current national technical standards (D. M., 2018) deal with high accuracy the precautions and the technical prescriptions to be adopted for the seismic protection of new constructions, as function of the structural typology, of the construction site, etc. Different is the case of existing structures and, even more, the one of historical and monumental buildings, realized according to common experience, following a process of progressive optimization of structural element proportions and mainly based on functional, architectural, and practical needs, neglecting consequences in terms of structural performance, resulting loads, and effects. Structures were sized to withstand static vertical loads and static horizontal thrusts of arcs and vaults, neglecting seismic action. Seismic horizontal forces, otherwise, highly alter the funicular polygon of thrusting elements, causing diffused cracks and, in worst cases, partial collapses. Therefore, historical

buildings are vulnerable, even if characterized by good quality materials, not always typical of constructions realized centuries ago (Lagomarsino, 2006; Castori et al., 2017). The constructive technique and the practical experience of a specific geographic area were strongly affected by the seismic hazard level and by the frequency of occurrence of earthquake events: in high-seismicity areas, their relevant occurrence led to the development of constructive solutions able to reduce the seismic vulnerability. This is, for example, the case of ties and buttresses adopted in the presence of arches and vaulted surfaces, which became an integral part of constructive methodology in seismic-prone areas, being otherwise used only for retrofit or in the presence of relevant damages in other cases or after several decades from the last seismic events (Lagomarsino, 2006).

Historical masonry buildings are characterized by very complex structures, not based on a uniform constructive process and developed thanks to subsequent modifications that occurred over centuries. As a result, they behave more similar to "structural aggregates," composed by several "structural units" than to unique buildings. It is thus important to carefully study the building construction process, the presence or the lack of adequate connections among structural units and vertical and horizontal elements, the cracking scenario to identify homogeneous portions for age of construction, the defined and ongoing relative displacements of elements and components, the structural system, materials, the floor and roof typology, the geometry, and so on (Binda et al., 1999b; Formisano et al., 2010; Cattari et al., 2014; Caprili et al., 2017; Baggio et al., 2018; Castellazzi et al., 2018). Structural elementary units can be, preliminarily, analyzed as isolated buildings, further considering their interaction and mutual interrelationship accounting possible restraints conditions, basing on the structural solution adopted and in situ investigated (Oliveira, 2003; Berto et al., 2017; Degli Abbati et al., 2019) The identification of the structural units highlights the constructive discontinuities that can represent weak areas of the structural aggregate to be in deep analyzed.

In relation to what the above presented, it is evident that the deep and accurate knowledge of construction is a crucial aspect to perform valid and representative assessment of existing buildings, especially in the case of architectural and historical relevance. To neglect the complexity of their evolution, in terms of morphological processes, structural features, and typologies of bearing elements and connections among structural units leads to wrong estimations of the structural safety and, therefore, to incorrect design of retrofit measurements (Oliveira, 2003). In the last decades, several methodologies were developed to assess the seismic vulnerability of existing buildings, according to different aims and different action ranges. The selection of the most feasible analysis approach depends on many factors, for example, the need to extend results at territorial scale, building complexity, accuracy needed of the results, time required, and resource demands. Methodologies based on the macro-seismic approach at the territorial scale, using data sheets concerning structural characteristics, maintenance status, damages, and other qualitative parameters, were elaborated for fast evaluations in both post- (GNDT I level—C.N.R., 1993) and pre-event phase (DPC, 2000) (AeDES—DPC 2000), (SISMA,

2007; Zuccaro et al., 2008; Zuccaro and Cacace, 2015), or to estimate the vulnerability index on the base of relevant parameters (GNDT II level—GNDT-SSN, 1994; Bernardini and Lagomarsino 2008). Such methods allowed the analysis of a wide quantity of constructions providing a "hierarchy" useful to assess the highest/lowest need of structural assessment or retrofit interventions and the following allocation of economic resources (Bernardini and Lagomarsino, 2008).

The adoption of simplified mechanical models able to provide a vulnerability estimation based on geometrical and material parameters or on in situ survey of the cracking scenario, without resorting to complex numerical models, was also considered at the urban or single scale level. Among them, the VM method (Dolce and Moroni, 2005), RE.SIS.TO® (Mazzotti et al., 2013), or the Lv1 Method (CdM, 2011) referred to the evaluation of the collapse acceleration, accounting only for the shear resistance of masonry piers (D'Amato et al., 2018; Fuentes et al., 2019). A macro-element approach simplifying the building as an "aggregation" of a reduced number of elements with assigned behavior was adopted by D'Ayala (2002) and Augusti et al. (2001). Displacement-based approaches, aimed at defining limit states on the acceleration/displacement plane, were also provided (Cattari et al., 2004; Kržan et al., 2015; Lagomarsino and Cattari, 2015). Macro-seismic and mechanical approaches were even combined, resulting in a mixed procedure such as in the case of the VULNUS method (Bernardini, 2000): critical values of the mean acceleration response, corresponding to defined collapse mechanisms, were combined with qualitative information on buildings and soil characteristics, resulting in the assessment of the collapse probability of a single building or groups of buildings. Lagomarsino (2006) highlighted the need to adopt a multistep methodology based on an in-depth study: starting from a widescale damage analysis based on building typology and using a macro-seismic approach characterized by a fast field survey, relevant "scored" parameters were defined to modify the vulnerability index and to assess the structural performance of critical single buildings or of macro-elements/components.

Complex methodologies based on the development of high-definition 3D numerical finite-element models were often adopted for the structural assessment of historical masonry buildings, despite the strong computational and time effort. Both linear and nonlinear analyses (Ramos and Lourenço, 2004; Chellini et al., 2014; Clementi et al., 2016; Miano et al., 2017; Ramírez et al., 2019) were used, according to the different aims and complexities. Each typology of analysis has, in fact, its own pros and cons: for example, nonlinear time–history analyses are commonly considered to better estimate the seismic demand but, at the same time, require a very strong computational effort, being not properly suited for masonry structures due to the fact that connections among elements are not easy to be represented despite their strong influence on dynamic behavior (Mallardo et al., 2008). The adoption of linear and nonlinear analyses is appealing since it allows to freely model each typology of geometry (for example, in the case of vaulted surfaces) and constitutive laws; beside, difficulties lie in the high computational effort, in the time required for modeling, and in the reliability of the model itself: geometry, construction materials, boundary
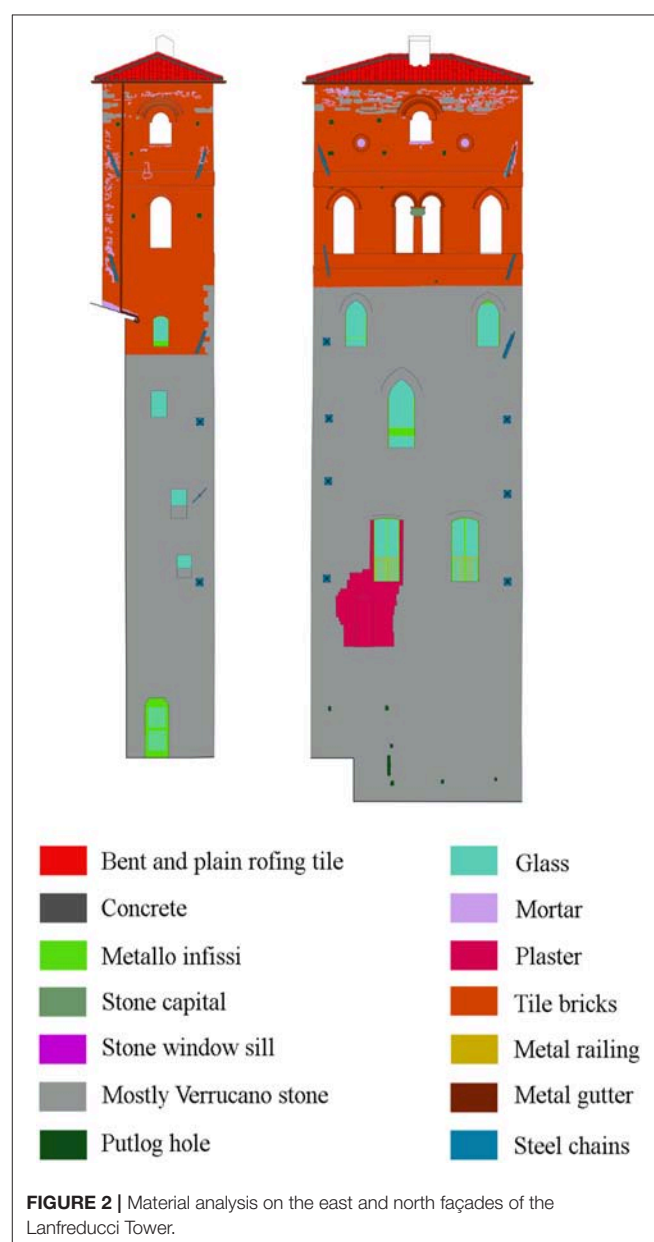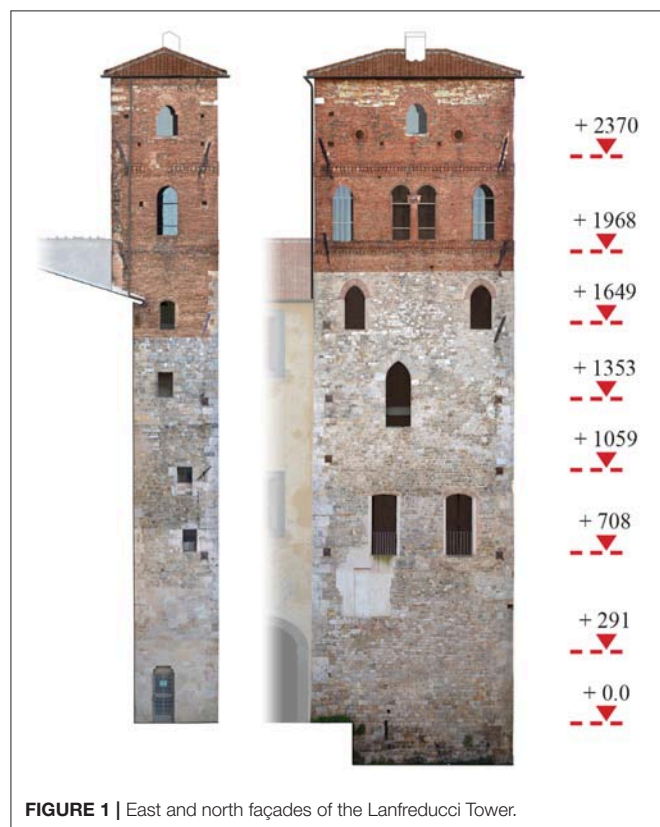
conditions, damages, and previous repairs strongly affect the results (Roca and Elyamani, 2018), these parameters being difficult to determine. Those models need then to be "combined" with accurate geometrical survey, even by means of a laser scanner, and deep investigations on structural details, material mechanical properties, and morphological evolution of the building (Caprili et al., 2017; Formisano et al., 2017).
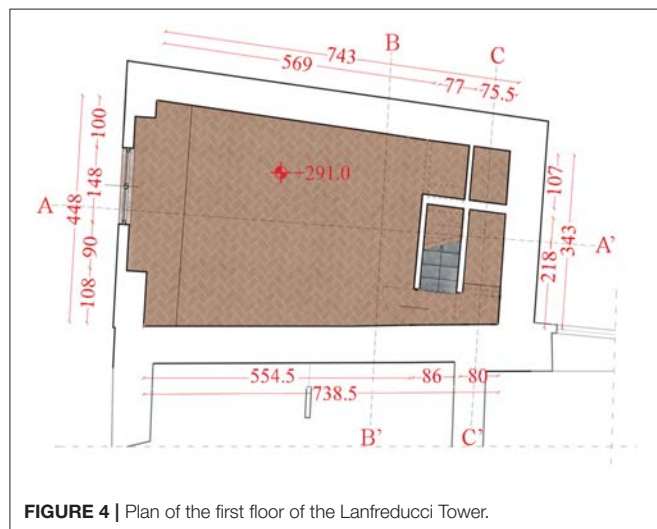
Regardless the chosen methodology, a proper multidisciplinary knowledge phase is essential to acquire information able to validate the results achieved. Hereinafter, a knowledge-based approach for the analysis of historical–monumental buildings is proposed with a specific focus on the knowledge phase. To highlight the possibility of directly applying the above-mentioned approach to cultural heritage, four different case studies are presented.

## KNOWLEDGE-BASED METHODOLOGY

A multilevel approach for the analysis of the seismic vulnerability of existing structures based on the accurate and reliable knowledge of the constructions themselves was proposed by Binda et al. (1999b), Binda and Saisi (2005) and applied to large-scale situations (e.g., historical city-centers), accounting for the collection of general information on different units, the execution of mechanical tests on materials, and, above all, the correlation between the *in situ* cracking scenario and the results of simplified macro-element analyses on relevant portions/units

of the aggregate. Even if characterized by several analogies, in terms of structural typologies, progressive modifications due to functional needs, coexistence of different construction techniques, etc., relevant differences exist for the case of historical masonry buildings; such differences lie in their structural nature and in the architectural relevance they own. The approach shall be well specified when applied to cultural heritage, allowing to preserve and highlight their architectural, historical, and artistic value. Barbieri et al. (2013) showed the "traditional" way to assess the structural performance of a historical masonry building starting from a real case study, presenting a typical example of how to behave with cultural heritage without defining a codified approach.



FIGURE 1 | East and north façades of the Lanfreducci Tower.



FIGURE 2 | Material analysis on the east and north façades of the Lanfreducci Tower.

**FIGURE 3 |** Sections of the Lanfreducci Tower.



**FIGURE 4 |** Plan of the first floor of the Lanfreducci Tower.



**FIGURE 5 |** Map of archaeological finds in the area of the tower (MappaGIS)[1].

In the case of cultural heritage, the key to success in achieving meaningful results close to reality is to develop an integrated approach that is a combination of "qualitative" and "quantitative" methods: the first ones are based on activities providing proper knowledge of the structure, allowing the deep understanding of the main structural and morphological features; the second ones are based on the application of one or more vulnerability assessing methodologies, including simplified mechanical methods and/or the use of numerical modeling and analysis. The qualitative approach is the fundamental part of structural assessment, needed to achieve reliable results and to identify the weakest areas of the buildings requiring an in-deep approach. The knowledge phase is the "framework" where the structural assessment is selected and organized, being fundamental the characterization of the constructive system, floor typologies, structural element geometry, information concerning foundation, geotechnical and geological characteristics of the soil, mechanical material properties, damages or restoration works that eventually happened in the past, local mechanisms that could be potentially activated (ICOMOS, 2005; D'Ayala et al., 2008; Bosiljkov et al., 2010; Caprili et al., 2015; Cattari et al., 2015; Castori et al., 2017). The degree of details of the knowledge phase and the typology of information collected should be calibrated based on the analysis that needs to be performed. Accounting for the peculiarities of historical–monumental buildings, a common knowledge multistep and multilevel procedure is defined, able to highlight criticisms and deficiencies fundamental for the organization of a reliable structural assessment.

## Historical Analysis

The genesis of a monumental building is a complex process taking place over centuries through modifications, alterations, aggregations of new portions, collapses, and rebuilding; these actions were not usually recorded in historical documents or drawings; sometimes their memory was lost over time
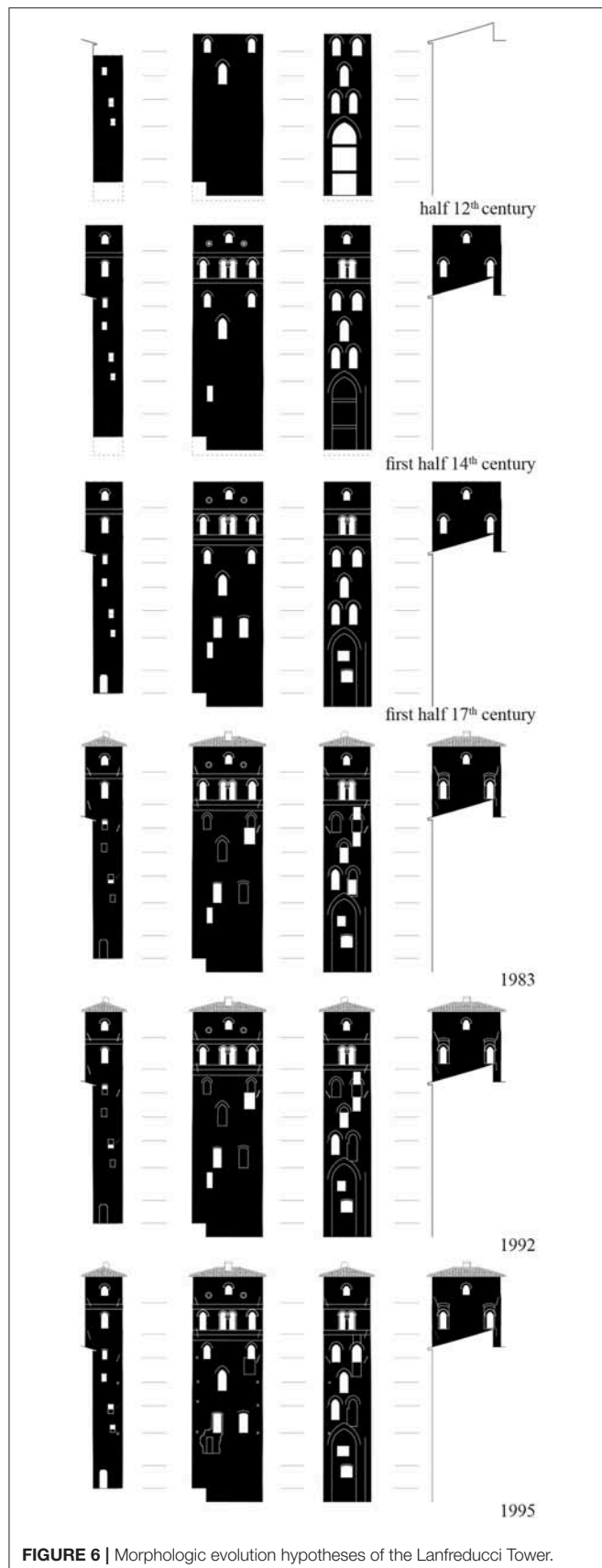
---

[1] MappaGIS, editor. *Ritrovamenti.*

FIGURE 6 | Morphologic evolution hypotheses of the Lanfreducci Tower.
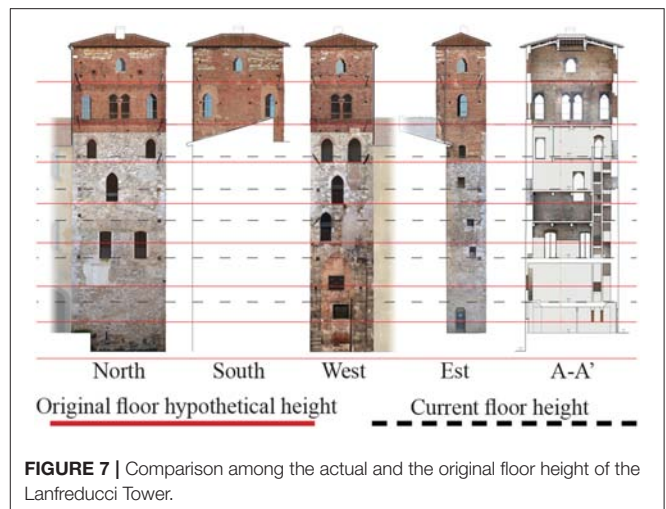


FIGURE 7 | Comparison among the actual and the original floor height of the Lanfreducci Tower.

as result of spontaneous and unplanned processes, making their presence not clearly recognizable. The critical–historical analysis allows the reconstruction of the construction and morphological evolution, pointing out areas of structural discontinuity and individuating past collapses or damages due to exceptional actions (e.g., past seismic event) or structural inadequacy, allowing to identify the weakest portions of the building or the mechanisms still ongoing. This result could be achieved crossing and comparing data coming from different sources such as bibliographic and archive research; study of historical documentations and cartography (e.g., cadastral maps, IGM maps); analysis of images of the building coming from paintings or frescoes, which could show, in a more or less reliable way, the characteristics of a specific historical period; critical analysis of masonry stratigraphy; and analysis of the architectonic features coming from *in situ* inspections (Augusti et al., 2001; Cattari et al., 2015; Berto et al., 2017). The critical–historical analysis allows to identify the structural units composing the overall aggregate, including the understanding of the mutual interrelationship resulting in different boundary conditions (Berto et al., 2017). By this way, it is possible to determine criticisms and vulnerabilities characterizing the building seen as a "structural aggregate" and analyze how the different structural units can influence each other in the whole performance (Caprili et al., 2017). The results of the morphological evolution are used to plan the *in situ* investigations in a rational and optimized way, deepen the efforts in correspondence with those areas affected by highest uncertainties, criticisms, overlapping of structural parts derived from different constructive phases, or evident structural weaknesses. The determination of past damages or previous restoration works could suggest structural deficiencies to be solved. Further, it helps in indentifying local mechanisms potentially activating, that cannot be adequately considered through global model and analysis (Binda and Saisi, 2005; Caprili et al., 2017).

The critical–historical analysis therefore allows to minimize the human impact on existing monumental buildings, where the artistic and architectural value shall be preserved (Cattari et al., 2015).
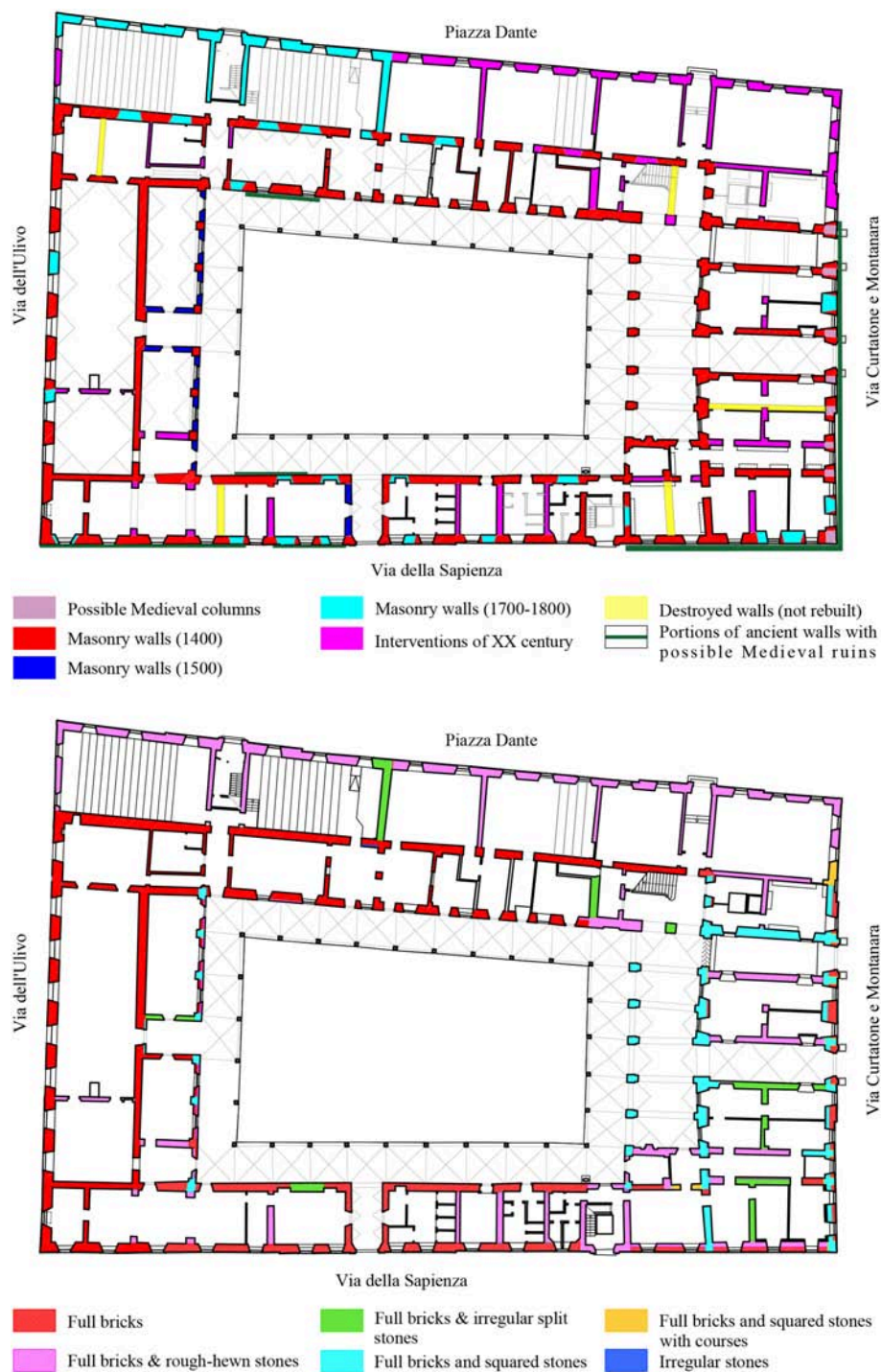
**FIGURE 8 |** Hypothesis of the evolutive development of the La Sapienza Palace and plan of ground floor with indications of the various types of masonry (Caprili et al., 2017).

## *In situ* Survey

The *in situ* survey includes several activities aimed at collecting information concerning the global geometry of the building (in plan and in elevation), the structural characteristics of elements and details, the mechanical characteristics of materials, and the geotechnical features. This information allows to recognize the bearing system of the building, determining the entity of loads acting on elements and understanding the structural performance toward vertical and horizontal actions. Direct survey of masonry walls, horizontal stories and roof
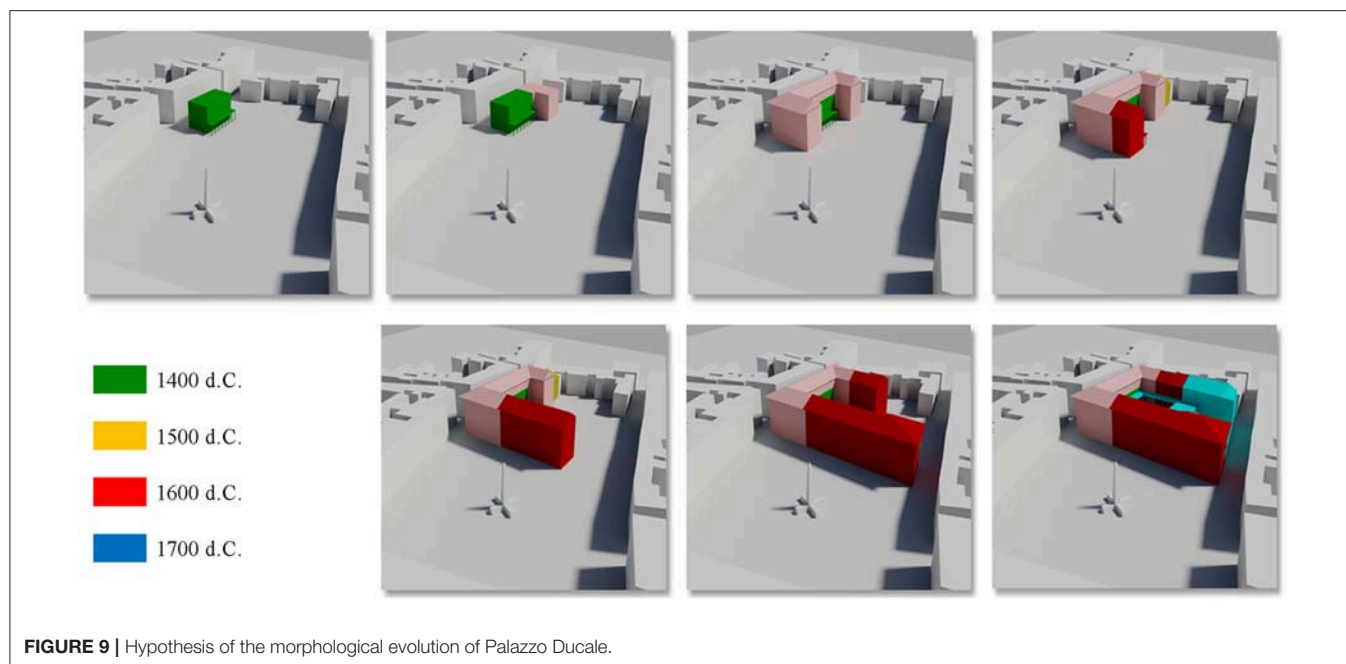
**FIGURE 9 |** Hypothesis of the morphological evolution of Palazzo Ducale.

stratigraphy, nonstructural elements including infills, structural asset, etc., is needed; data shall be collected by means of different tools, according to the budget available, the complexity of the structures, and the information coming from original documentation, allowing reduction of the *in situ* effort and minimizing the impact on cultural heritage.

Measurements can be made directly, as well as by means of tools such as a terrestrial laser scanner or drones, being as accurate as required in relation to the analysis that will be performed on the structure (Salonia et al., 2007; Fortunato et al., 2017). The analysis of the global geometry includes all the relevant aspects for the building structural response, such as the relationship with adjacent buildings—affecting the dynamic response and could cause building pounding, the presence of geometric irregularity in plan or elevation—influencing the irregular mass distribution, leading to an uneven dynamic response and the presence of thrusting structures—especially where ties are not introduced. Presence of untied mezzanines needs to be investigated because it is often characterized by lack of lateral force-resistant system, representing potential collapse elements whose stability needs to be checked. Irregular distribution of nonstructural elements, such as masonry partition walls and arcades or pillars alignments behaving as a soft story are surveyed (D'Ayala et al., 2008). Concerning structural details, as function of the complexity of the building, several information cannot be directly measured and needs to be defined based on reliable assumptions and considerations, also accounting for the information provided by the reconstruction of the morphological evolution process.

Masonry wall identification is performed by removing plaster portions to identify the masonry texture, its state of conservation, and the quality of the connection among perpendicular walls and among walls and floor, with attention to the eventual presence of artistic paintings to be protected. Endoscopic examinations allow the measurement of the wall thicknesses and the individuation of cavities, filling, metal insertions, or adjacent facings of different thicknesses or typologies (Roca et al., 2010; Caprili et al., 2017). The information achieved in this knowledge step should be compared and should integrate the results of the historical–critical analysis to reconstruct the building morphologic evolution (D'Ayala et al., 2008).

The material characterization can be achieved directly through the execution of *in situ* nondestructive or partially destructive tests, determining the mechanical properties (in terms of strength and elastic moduli) needed for structural assessment. The organization of experimental tests should take advantage of historical analyses, with the aim of characterizing all the relevant masonry typologies in relation to the age of construction. The determination of mechanical characterization based on results presented in the current scientific literature is also possible, if supported by adequate reasons (Binda et al., 1999a; Bosiljkov et al., 2005; Borri and De Maria, 2009; Magalhães and Veiga, 2009; Vasconcelos and Lourenço, 2009; Bosiljkov and Kržan, 2012). Geotechnical aspects are of relevant importance to characterize the foundation settlement and the types of soils and for the following analysis of seismic action and soil–structure interaction. The execution of local seismic response analysis could be performed as well, starting from the dynamic characterization of the foundation soil (Caprili et al., 2017).

## Analysis of the Cracking Scenario

The survey of the cracking scenario and of the deformation pattern includes information concerning type, geometry, and layout distribution of cracks in the building and presence

**FIGURE 10 |** Masonry typologies surveyed in Palazzo Ducale.

of cracks and out-of-plumbs. The identification of structural irregularities such as rotations, vertical deviations, or loss of horizontality in load-bearing elements is also needed, especially in a refined analysis (Binda and Saisi, 2005). These activities could be performed by means of inspections and, if needed, removal of plaster portion and are important to identify settlement movement of the structure or local mechanisms that can potentially activate. In the phenomenon-involved areas, the greater number of *in situ* investigations, with the aim of performing more accurate analysis, can be concentrated. By comparing the information collected with the historical–critical analysis (e.g., past collapses, damages, past seismic events) and that with the structural analysis (e.g., structural deficiency, lack of quoins), the understanding of the reasons of local failures

and collapses or damages is possible (Avorio and Cangi, 1999; Borri et al., 1999; Bartoli et al., 2000; Casarin and Modena, 2008), together with the organization of a continuous or step-by step monitoring system to analyze the development of relevant displacements (Binda and Saisi, 2005).

## Structural Analysis and Evaluation of Seismic Assessment

The knowledge phase represents the qualitative contribution to the vulnerability assessment procedure; once completed, enough information for the execution of the quantitative approach has been collected. The potentially achievable local mechanisms, previously identified combining the
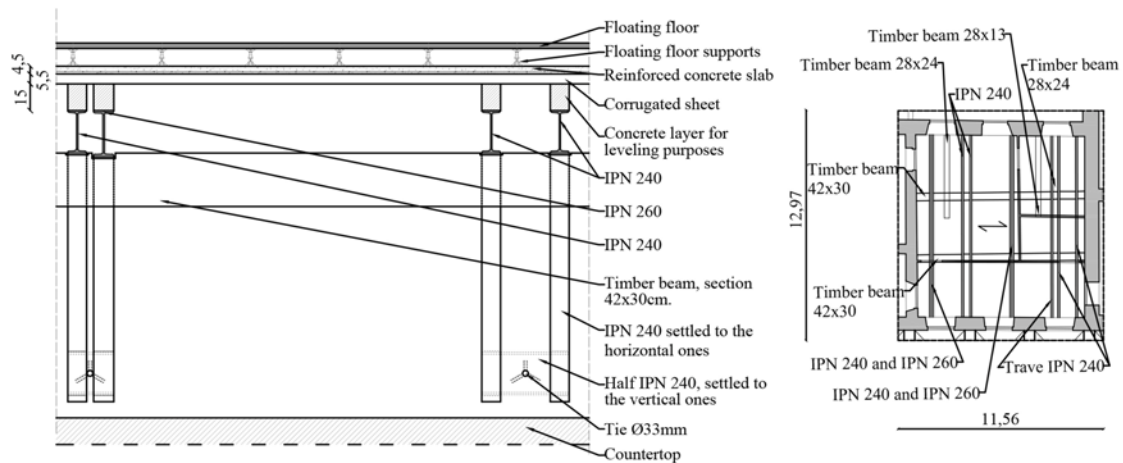
**FIGURE 11 | (A)** Floor typologies (flat or vaulted) surveyed in correspondence to the second level of Palazzo Ducale. **(B)** Floor typologies surveyed in correspondence to the third level of Palazzo Ducale.
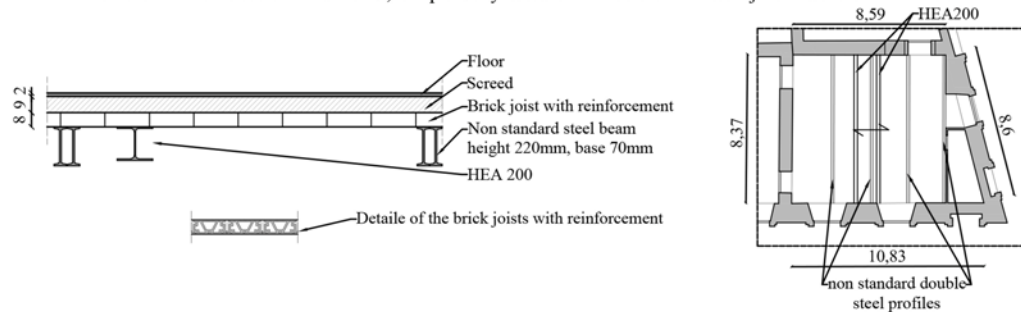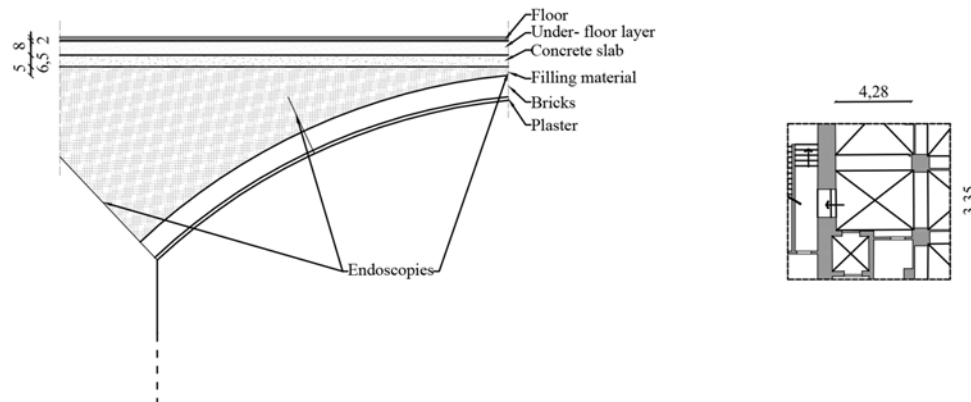
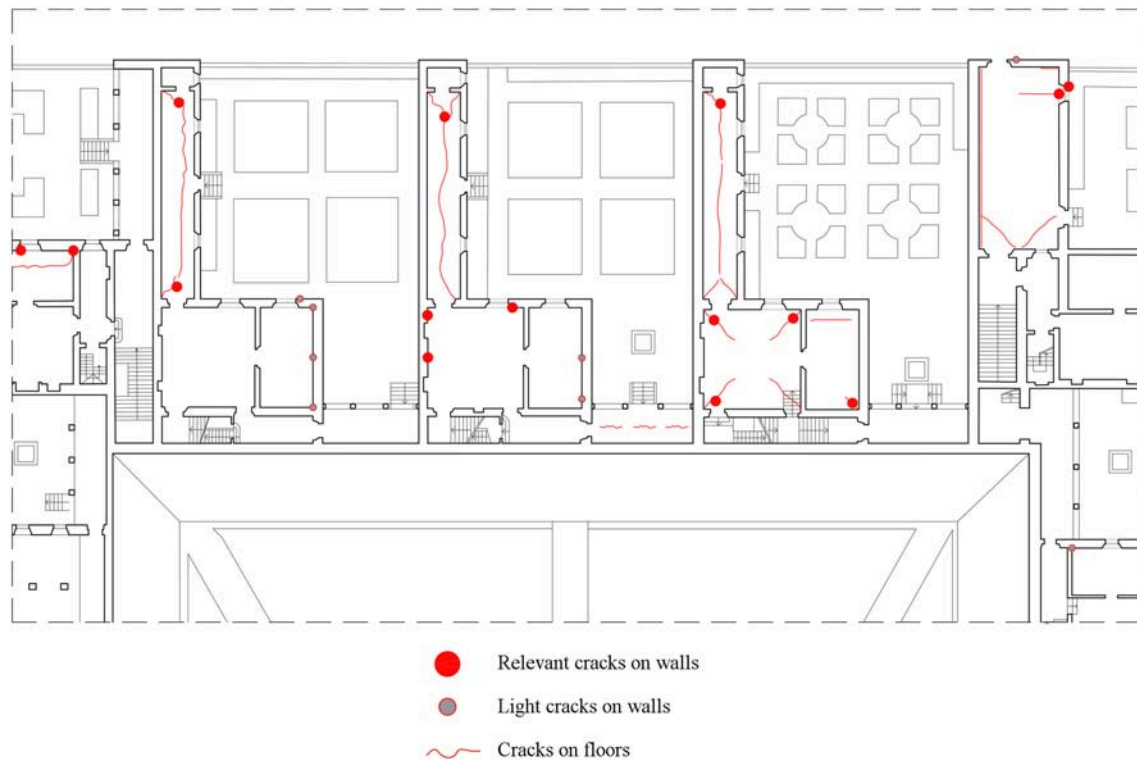**FIGURE 12 |** Examples of structural details surveyed in Palazzo Ducale.

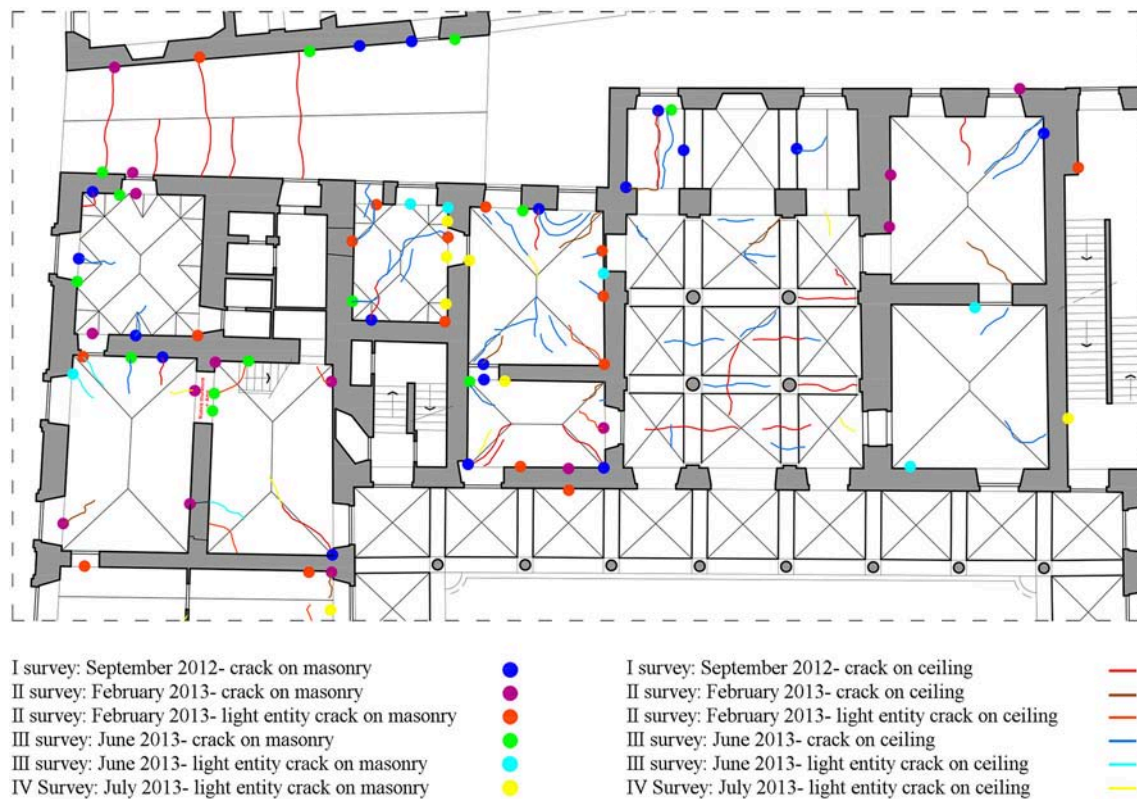FIGURE 13 | Cracking scenario of a portion of the clauster in the Certosa of Calci.
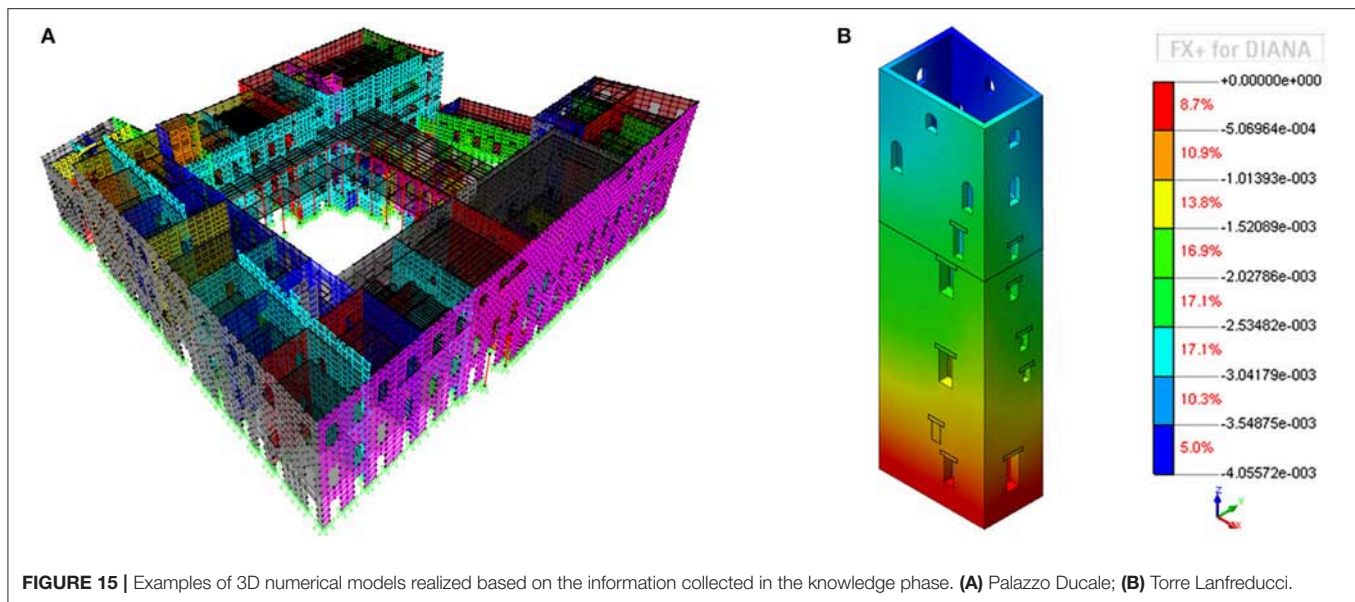


FIGURE 14 | Cracking scenario of a portion of the Palazzo Ducale.

**FIGURE 15 |** Examples of 3D numerical models realized based on the information collected in the knowledge phase. **(A)** Palazzo Ducale; **(B)** Torre Lanfreducci.

morphological evolution and the determination of independent structural units/portions/elements and the *in situ* survey of the evident cracking scenario, should be analyzed. Local problems can enable the development of a global building behavior, causing serious damage even for low-intensity earthquakes or, in general, in the presence of relevant quasi-static horizontal thrusts. Simplified techniques, such as the already mentioned macro-element analysis, linear or nonlinear kinematic analysis, or other procedures suggested in the current scientific literature (Borri et al., 1999; Orduña and Lourenço, 2001; Milani, 2013; Rossi et al., 2015; Circolare, 2019), can be adopted. Global analyses on the whole building, with numerical models realized based on the knowledge achieved according to the information previously collected, are meaningful only if the activation of local failures has been prevented, since otherwise the study of a global "box" behavior is not realistic.

## APPLICATION TO CASE STUDY BUILDINGS

The relevance of the proposed methodology was appreciated within the structural assessment of four historical case study buildings located in the Tuscany region: the Lanfreducci Tower (Pisa, Italy), the Palazzo La Sapienza (Pisa, Italy), the Palazzo Ducale (Massa, Italy), and the Certosa of Calci (Pisa, Italy).

The Lanfreducci Tower is a medieval masonry tower located in the most ancient area of the city of Pisa, directly connected to the building "Alla Giornata." The tower is known with the name of the family that owned it for several centuries: the building was officially mentioned for the first time in a will in 1348, and the Lanfreducci family owned it until the end of the Nineteenth century. There were no official documents concerning the construction of the tower, and very few were contained information concerning the modifications undergone

by the tower and by the whole surrounding urban area during the centuries. Palazzo La Sapienza is a monumental complex located in the city center of Pisa, very close to the Lanfreducci Tower. The structure was the result of the progressive aggregations of several masonry units or tower houses to the medieval structure of Piazza del Grano and of Dogana del Sale, due to the creation of the house seat of the University of Pisa in the Fifteenth century. Relevant structural modifications (e.g., demolition of internal bearing walls, super-elevations, realization of new slabs, etc.) were performed in the Nineteenth century to enlarge the space for hosting the books of the University Library, causing structural diseases.

The Certosa of Calci is a monumental complex in a valley close to Pisa, whose construction began in 1366. At the end of the Fourteenth century, the first nucleus, including all the functions needed for a monk's life, was completed. Interventions and modifications were continuously carried out until the Eighteenth century, aiming at enlarging the building, creating more comfortable spaces, and embellishing, decorating, and harmonizing the complex. In the Nineteenth and Twentieth centuries, retrofit was performed to adapt the building to new intended uses (e.g., military barracks, war hospital, and museum).

Palazzo Ducale is located in the center of Massa. The first unit of the building dates to the Fifteenth century with the construction of a small rectangular-shaped dwelling aimed at being a hunting residence for the Malaspina, a noble family that ruled around the town. During the Sixteenth century, several modifications, not well documented, enlarged the building size, up to the Seventeenth century when the palace reached the appropriate size for a noble residence and was supplied of representative rooms. In the following centuries, the works proceeded, giving the palace the actual configuration.

The drawings, the structural sections, and the plans of the different levels of the Lanfreducci Tower are presented in **Figures 1**–**4**. The architectural/geometrical survey was

performed using both traditional instruments and total station/theodolite technique, allowing to achieve an accurate and reliable organization of masonry walls and horizontal stories both in plan and in elevation. The information coming from the historical analyses, mainly concerning the construction phases, was validated using the results of the *in situ* surveys. Archaeological findings (**Figure 5**) as well as cadastral maps were analyzed to date back the construction birth and to understand the influence of the urban area on the buildings' evolution. Based on the historical information and architectural features—e.g., materials, windows' shape, typological characteristics of medieval towers, presence and typology of decorations, etc.—hypotheses about the morphological evolution of the tower were formulated (**Figure 6**), allowing to reconstruct the original stories' height (**Figure 7**). Masonry typologies were visible from the outside, differently with respect to the other cases, well highlighting the different construction phases and their correspondence with historical findings.

In the cases of more complicated buildings, such as, for example, the Palazzo La Sapienza or the Palazzo Ducale, masonry typologies were not directly visible, and more investigations were needed to allow the correspondence among construction phases and mechanical characteristics of materials to be used in the numerical modeling and structural assessment (**Figures 8**–**10**). More invasive techniques, such as removal of plastic portions, were adopted beyond the visual inspections, and, in both cases, the surveys were spread all over the buildings to have an overall idea of the masonry typologies, concentrating actions where the historical analysis located discontinuity areas, criticisms, etc.

Similar considerations shall be made concerning horizontal stories, whose bearing capacity is an important parameter for the structural assessment of the whole structure, taking also into account that the knowledge of their characteristics (in terms of thickness and weight of different layers) is needed for the numerical modeling. In the case of the Palazzo Ducale di Massa, a lot of different floor typologies were found due to the great interventions' stratification. In the first and second building levels, there was a prevalence of vaulted surfaces: barrel or pavilion vaults were detected mainly in wide spaces, while cross vaults characterized little spaces (**Figure 11**). An irregular stone-brick masonry bearing layer characterized most of the vaults on the first level, while a one-brick-thick bearing layer characterized most of the vaults on the second level. Endoscopic investigations, performed in different vault sections, allowed to define the thickness of the bearing layer and of the filling material, which changed significantly according to the different vaults. The density of the filling material was opportunely measured not to under(or over)estimate permanent loads. In the third and fourth levels, horizontal stories with different bearing elements were found, such as steel frames, timber frames, and precast reinforced concrete, introduced as a consequence of different retrofit operations. For example, steel frames were often introduced in timber frame structures to increase the bearing capacity and/or to limit high deflections. Interest was paid to brittle elements, which could represent a criticism, such as brick

joists with or without reinforcement, as well to identify frames with insufficient support length in the wall. An extended *in situ* survey campaign was planned to investigate all the typologies of horizontal structures by defining the floor stratigraphy, the geometrical size, and the structural characteristics of elements. For each investigation, structural sections (**Figure 12**), useful for the modeling, were provided.

Information resulting from the cracking scenario survey joined with other indications coming from old documents, structural retrofit, etc., leads to the identification of local mechanisms and to the comprehension of the possible causes of the detected phenomena. The cracks' layout represents a valid tool to understand the structural behavior and to recognize phenomena such as vertical wall overturning, collapse of the upper portion of the facade, separation and expulsion of the corners, and so on. For instance, in the case of the Certosa of Calci, the analysis of the cracking scenario in the cluster cells had highlighted a crack prevalence in the long rectangular body instead of in the smallest ones (**Figure 13**). That difference was probably since the two bodies of the cells were not built in the same period and with the same masonry typology and since there was a phenomenon of subsidence of the land that facilitates a rotational phenomenon. Land subsidence phenomenon, when detected, need to be investigated in-depth because it could seriously affect the structural response of the building. The visual recognition performed for the Lanfreducci Tower did not highlight important cracks, resulting in a nonsignificant cracking scenario, a possible consequence of recent maintenance operations carried out over the past decades, being the Tower was used as headquarters of the rectorate of the University of Pisa. Palazzo La Sapienza, as evidenced in Caprili et al. (2017), highlighted a cracking scenario characterized by an irregular distribution of medium-high damages mainly located in correspondence with those areas where the highest modifications toward the centuries took place: as an example, the corner between Via Curtatone e Montanara and Via della Sapienza suffered from the differential displacements caused by different settlement of foundations and from the presence of different masonry typologies (e.g., stone columns of ancient tower houses, masonry panels, etc.). This situation evidenced the strict relationship existing between the morphological and historical development of the aggregate and its structural response. A periodical monitoring of the cracking scenario was performed for Palazzo Ducale, because of the small damages and cracks that became visible after the earthquake event of May 2012. This procedure was adopted to understand if the building was—or not—subjected to ongoing phenomena, potentially representing a structural problem since connected to in-progress relative displacements. As presented in **Figure 14**, four survey campaigns were executed from September 2012 to July 2013, highlighting an ongoing crack phenomenon, probably a consequence of the earthquake of Emilia Romagna and still in progress.

The application of the proposed multistep procedure granted reliability to the 3D numerical finite element models, realized for the execution of the analyses, adopting, for example, the models represented in **Figure 15** based on a deep and *in situ* knowledge of the construction analyzed.

## CONCLUSIONS

In the present paper, a knowledge-based approach for the analysis of historical–monumental buildings is presented and applied to four case studies of relevant importance located in the Tuscany region. Historical–monumental buildings are generally characterized by great complexity due to a long and not homogeneous constructive process, which results in the buildings being characterized by the interaction of several "structural units" whose behavior determines the structural response of the overall complex. Because of this complexity and to the general lack of information typical of this kind of buildings, all the methods for the evaluation of the seismic vulnerability should be associated to a deep and accurate knowledge phase in order to provide reliable results when structural assessment is performed.

A multidisciplinary and multilevel knowledge procedure has been proposed and tested on case studies with the aim of providing a tool easy to adapt in all typologies of monumental buildings, respecting their peculiarities and their uniqueness. The procedure is based on three main steps able to achieve information concerning morphological evolution, geometry, structural details and typologies, material mechanical characteristics, ground characteristics, possible local mechanisms, and deformation. In this way, it is possible to reconstruct a geometrical–structural model of the building able in pointing out structural units, in comprehending the typology of connections among them, and in recognizing the weakest areas of the overall building, which needs to be investigated and analyzed in-depth. In the framework provided by the knowledge procedure, it is possible then to develop numerical models for carrying out complex analyses or to perform simplified analyses, according to one of the several methodologies provided by the current scientific literature, obtaining reliable results representative of the reality.

## DATA AVAILABILITY

All datasets generated for this study are included in the manuscript and/or the supplementary files.

## AUTHOR CONTRIBUTIONS

SC and IP contributed to the design and implementation of this research, to the planning and survey of the *in situ* investigations, to the analysis of the results and to the writing of the manuscript.

## REFERENCES

Augusti, G., Ciampoli, M., and Giovenale, P. (2001). Seismic vulnerability of monumental buildings. *Struct. Saf.* 23, 253–274. doi: 10.1016/S0167-4730(01)00018-2

Avorio, A. B., and Cangi, G. (1999). "Meccanica del danneggiamento negli edifici storici: dall'osservazione diretta all'interpretazione strutturale," in *Assisi '99 Seminario Internazionale e Workshop Il Comportamento Sismico del Patrimonio Edilizio nei Piccoli Centri Storici* (Assisi), 22–24.

Baggio, S., Berto, L., Rocca, I., and Saetta, A. (2018). Vulnerability assessment and seismic mitigation intervention for artistic assets: from theory to practice. *Eng. Struct.* 167, 272–286. doi: 10.1016/j.engstruct.2018.03.093

Barbieri, G., Biolzi, L., Bocciarelli, M., Fregonese, L., and Frigeri, A. (2013). Assessing the seismic vulnerability of a historical building. *Eng. Struct.* 57, 523–535. doi: 10.1016/j.engstruct.2013.09.045

Bartoli, G., Casamaggi, C., and Spinelli, P. (2000). "Numerical modelling and analysis of monumental buildings: a case study," in *5th International Congress on Restoration of Architectural Heritage* (Florence).

Bernardini, A. (ed). (2000). *La vulnerabilità Degli Edifici: Valutazione Ascala Nazionale Della Vulnerabilità Sismica Degli Edifici Ordinary*. Rome: CNR-Gruppo Nazionale per la Difesa dai Terremoti.

Bernardini, A., and Lagomarsino, S. (2008). The seismic vulnerability of architectural heritage. *Struct. Build.* 4, 171–181. doi: 10.1680/stbu.2008.161.4.171

Berto, L., Doria, A., Faccio, P., Saetta, A., and Talledo, D. (2017). Vulnerability analysis of built cultural heritage: a multidisciplinary approach for studying the Palladio's Tempietto Barbaro. *Int. J. Archit. Heritage* 11, 773–790. doi: 10.1080/15583058.2017.1290853

Binda, L., Baronio, G., Penazzi, D., Palma, M., and Tiraboschi, C. (1999a). "Caratterizzazione di murature in pietra in zona sismica: data-base sulle sezioni murarie e indagini sui materiali," in *Atti del 9 Convegno Nazionale: L'ingegneria Sismica in Italia*, 20–23 *Settembre 1999* (Turin).

Binda, L., Gambarotta, L., Lagomarsino, S., and Modena, C. (1999b). "A multilevel approach to the damage assessment and seismic improvement of masonry buildings in Italy," in *Seismic Damage to Masonry Buildings* (Rotterdam: Balkema), 170–195. doi: 10.1201/9780203740040-17

Binda, L., and Saisi, A. (2005). Research on historic structures in seismic areas in Italy. *Prog. Struct. Eng. Mater.* 7, 71–85. doi: 10.1002/pse.194

Borri, A., Avorio, A., and Cangi, G. (1999). "Considerazioni sui cinematismi di collasso osservati per edifici in muratura", in *IX Convegno Nazionale "L'ingegneria Sismica in Italia"* (Turin: ANIDIS).

Borri, A., and De Maria, A. (2009). "L'indice di qualità muraria (IQM): evoluzione ed applicazione nell'ambito delle norme tecniche per le costruzioni del 2008,"

in *Proceedings of 13th Italian National Conference for Earthquake Engineering* (Bologna).

Bosiljkov, V., Bokan-Bosiljkov, V., Strah, B., Velkavrh, J., and Cotič, P. (2010). Review of innovative techniques for the knowledge of cultural assets (geometry, technologies, decay), *PERPETUATE (EC-FP7 project), Deliverable D* 62.

Bosiljkov, V., and Kržan, M. (2012). Results of laboratory and *in-situ* tests on masonry properties and tables with mechanical parameters to be adopted in numerical modelling. *PERPETUATE (ECFP7 project), Deliverable D* 15.

Bosiljkov, V. Z., Totoev, Y. Z., and Nichols, J. M. (2005). Shear modulus and stiffness of brickwork masonry: an experimental perspective. *Struct. Eng. Mech.* 20, 21–44. doi: 10.12989/sem.2005.20.1.021

C.N.R. (1993). "Assessment of the exposure and the seismic vulnerability of buildings: instructions for making out the 1st level form," in *Seismic Risk of Public Buildings* (Rome: National Research Council—National group for the Defence from Earthquake).

Caprili, S., Mangini, F., Paci, S., Salvatore, W., Bevilacqua, M. G., Karwacka, E., et al. (2017). A knowledge-based approach for the structural assessment of cultural heritage, a case study: La Sapienza Palace in Pisa. *Bull. Earthquake Eng.* 15, 4851–4886. doi: 10.1007/s10518-017-0158-y

Caprili, S., Mangini, F., and Salvatore, W. (2015). "Numerical modelling, analysis and retrofit of the historical masonry building" La Sapienza"", in *COMPDYN 2015, 5th ECCOMAS Thematic Conference on Computational Methods in Structural Dynamics and Earthquake Engineering.* Pisa: Institute of Structural Analysis and Antiseismic Research School of Civil Engineering National Technical University of Athens (NTUA), 772–787.

Casarin, F., and Modena, C. (2008). Seismic assessment of complex historical buildings: application to Reggio Emilia Cathedral, Italy. *Int. J. Archit. Heritage* 2, 304–327. doi: 10.1080/15583050802063659

Castellazzi, G., D'Altri, A. M., de Miranda, S., Chiozzi, A., and Tralli, A. (2018). Numerical insights on the seismic behavior of a non-isolated historical masonry tower. *Bull. Earthquake Eng.* 16, 933–961. doi: 10.1007/s10518-017-0231-6

Castori, G., Borri, A., De Maria, A., Corradi, M., and Sisti, R. (2017). Seismic vulnerability assessment of a monumental masonry building. *Eng. Struct.* 136, 454–465. doi: 10.1016/j.engstruct.2017.01.035

Cattari, S., Curti, E., Giovinazzi, S., Lagomarsino, S., Parodi, S., and Penna, A. (2004). "Un modello meccanico per l'analisi di vulnerabilitá del costruito in muratura a scala urbana," in *11th Conference "L'ingegneria Sismica in Italia"* (Genova).

Cattari, S., Degli Abbati, S., Ferretti, D., Lagomarsino, S., Ottonelli, D., and Tralli, A. (2014). Damage assessment of fortresses after the 2012 Emilia earthquake (Italy). *Bull. Earthquake Eng.* 12, 2333–2365. doi: 10.1007/s10518-013-9520-x

Cattari, S., Lagomarsino, S., Bosiljkov, V., and D'Ayala, D. (2015). Sensitivity analysis for setting up the investigation protocol and defining proper confidence factors for masonry buildings. *Bull. Earthquake Eng.* 13, 129–151. doi: 10.1007/s10518-014-9648-3

CdM (2011). "Linee guida per la valutazione e la riduzione del rischio sismico del patrimonio culturale con riferimento alle Norme Tecniche per le costruzioni di cui al decreto del Ministero delle Infrastrutture e dei trasporti del 14 gennaio 2008," in *Supplemento Ordinario Alla Gazzetta Ufficiale* (Rome: Istituto Poligrafico e Zecca dello Stato).

Chellini, G., Nardini, L., Pucci, B., Salvatore, W., and Tognaccini, R. (2014). Evaluation of seismic vulnerability of Santa Maria del Mar in Barcelona by an integrated approach based on terrestrial laser scanner and finite element modeling. *Int. J. Archit. Heritage* 8, 795–819. doi: 10.1080/15583058.2012.747115

Circolare (2019). *Istruzioni per l'applicazione dell'«Aggiornamento Delle "Norme Tecniche per le Costruzioni" di cui al Decreto Ministeriale 17 Gennaio 2018.*

Clementi, F., Gazzani, V., Poiani, M., and Lenci, S. (2016). Assessment of seismic behaviour of heritage masonry buildings using numerical modelling. *J. Build. Eng.* 8, 29–47. doi: 10.1016/j.jobe.2016.09.005

D'Amato, M., Laterza, M., and Diaz Fuentes, D. (2018). Simplified seismic analyses of ancient churches in Matera's landscape. *Int. J. Archit. Heritage* 13, 1–20. doi: 10.1080/15583058.2018.1511000

D'Ayala, D., Carriero, A., Sabbadini, F., Fanciullacci, D., Ozelik, P., Akdogan, M., et al. (2008). "Seismic vulnerability and risk assessment of cultural heritage buildings in Istanbul, Turkey," in *14th World Conference of Earthquake Engineering* (Beijing).

D'Ayala, D. and Speranza, E. (2002). "An Integrated Procedure for the Assessment of SeismicVulnerability of Historic Buildings," in *Proceedings of the 12th European Conference on Earthquake Engineering* (London), 561.

Degli Abbati, S., D'Altri, A. M., Ottonelli, D., Castellazzi, G., Cattari, S., de Miranda, S., and Lagomarsino, S. (2019). Seismic assessment of interacting structural units in complex historic masonry constructions by nonlinear static analyses. *Comp. Struc.* 213, 51–71. doi: 10.1016/j.compstruc.2018.12.001

D. M. (2018). *Norme Tecniche per le Costruzioni*, ed M.d.I.e.d. Trasporti. (Rome).

Dolce, M., and Moroni, C. (2005). "La valutazione della Vulnerabilità e del Rischio Sismico degli Edifici Pubblici mediante le procedure VC e VM," in *Atti del Dipartimento di Strutture* (Geotecnica: Geologia applicata all'ingegneria), 4.

DPC (2000). *Manuale per la Compilazione Della Scheda di Primo Livello di Rilevamento Danno, Pronto Intervento e Agibilità per Edifici Ordinari Nell'emergenza Post- sismica.* ed D.d.P. Civile (DPC).

Formisano, A., Chiumiento, G., Fabbrocino, F., and Landolfo, R. (2017). "Comparative seismic evaluation between numerical analysis and Italian guidelines on cultural heritage applied to the case study of a masonry building compound," in *Proceedings of the AIP Conference* (Rhodes).

Formisano, A., Mazzolani, F., Florio, G., and Landolfo, R. (2010). "A quick methodology for seismic vulnerability assessment of historical masonry aggregates," in *Proceedings of the COST Action C26 Final Conference "Urban Habitat Constructions under Catastrophic Events"* (Naples), 577–582.

Fortunato, G., Funari, M. F., and Lonetti, P. (2017). Survey and seismic vulnerability assessment of the Baptistery of San Giovanni in Tumba (Italy). *J. Cult. Heritage* 26, 64–78. doi: 10.1016/j.culher.2017.01.010

Fuentes, D. D., Laterza, M., and D'Amato, M. (2019) "Seismic vulnerability and risk assessment of historic constructions: the case of masonry and adobe churches in italy and chile," in *Structural Analysis of Historical Constructions*, Vol. 18 RILEM Bookseries, eds R. Aguilar, D. Torrealva, S. Moreira, M. A. Pando, and L. F. Ramos (Cham: Springer). doi: 10.1007/978-3-319-99441-3_122

GNDT-SSN (1994). *Scheda di Esposizione e Vulnerabilità e di Rilevamento Danni di Primo Livello e Secondo Livello (Muratura e Cemento Armato)*, GNDT-SSN.

ICOMOS (2005). *Recommendations for the Analysis, Conservation and Structural Restoration of Architectural Heritage.* International scientific committee for analysis and restoration of structures and architectural heritage. ed ISCARSAH (Barcelona: ICOMOS).

Kržan, M., Gostič, S., Cattari, S., and Bosiljkov, V. (2015). Acquiring reference parameters of masonry for the structural performance analysis of historical buildings. *Bull. Earthquake Eng.* 13, 203–236. doi: 10.1007/s10518-014-9686-x

Lagomarsino, S. (2006). On the vulnerability assessment of monumental buildings. *Bull. Earthquake Eng.* 4, 445–463. doi: 10.1007/s10518-006-9025-y

Lagomarsino, S., and Cattari, S. (2015). PERPETUATE guidelines for seismic performance-based assessment of cultural heritage masonry structures. *Bull. Earthquake Eng.* 13, 13–47. doi: 10.1007/s10518-014-9674-1

Magalhães, A., and Veiga, R. (2009). Physical and mechanical characterisation of historic mortars. Application to the evaluation of the state of conservation. *Mater. Const.* 59, 61–77.

Mallardo, V., Malvezzi, R., Milani, E., and Milani, G. (2008). Seismic vulnerability of historical masonry buildings: a case study in Ferrara. *Seismic Reliab. Anal. Prot. Historic Build. Heritage Sites* 30, 2223–2241. doi: 10.1016/j.engstruct.2007.11.006

Mazzotti, C., Savoia, M., Chinni, C., and Perri, G. (2013). Una metodologia speditiva per la valutazione di vulnerabilitá sismica di edifici in muratura e calcestruzzo armato. *Progettazione Sismica* 4:2. doi: 10.7414/PS.4.2.95-112

Miano, A., Jalayer, F., Ebrahimian, H., and Prota, A. (2017). Cloud to IDA: efficient fragility assessment with limited scaling. *Earthquake Eng. Struct. Dyn.* 2017, 1–24. doi: 10.1002/eqe.3009

Milani, G. (2013). Lesson learned after the Emilia-Romagna, Italy, 20–29 May 2012 earthquakes: a limit analysis insight on three masonry churches. *Eng. Fail. Anal.* 34, 761–778. doi: 10.1016/j.engfailanal.2013.01.001

Oliveira, C. S. (2003). Seismic vulnerability of historical constructions: a contribution. *Bull. Earthquake Eng.* 1, 37–82. doi: 10.1023/A:1024805410454

Orduña, A., and Lourenço, P. B. (2001). "Limit analysis as a tool for the simplified assessment of ancient masonry structures," in *Historical Constructions* (Guimarães: University of Minho), 511–520.

Ramírez, E., Lourenço, P. B., and D'Amato, M. (2019). "Seismic assessment of the matera cathedral," in *Structural Analysis of Historical Constructions*, Vol. 18 RILEM Bookseries, eds R. Aguilar, D. Torrealva, S. Moreira, M. A. Pando, and L. F. Ramos (Cham: Springer). doi: 10.1007/978-3-319-99441-3_144

Ramos, L. F., and Lourenço, P. B. (2004). Modeling and vulnerability of historical city centers in seismic areas: a case study in Lisbon. *Eng. Struct.* 26, 1295–1310. doi: 10.1016/j.engstruct.2004.04.008

Roca, P., Cervera, M., Gariup, G., and Pelá, L. (2010). Structural analysis of masonry historical constructions. Classical and advanced approaches. *Arch. Comput. Methods Eng.* 17, 299–325. doi: 10.1007/s11831-010-9046-1

Roca, P., and Elyamani, A. (2018). A review on the study of historical structures using integrated investigation activities for seismic safety assessment. Part II: model updating and seismic analysis. *Sci. Cult.* 4, 29–51. doi: 10.5281/zenodo.1048243

Rossi, M., Cattari, S., and Lagomarsino, S. (2015). Performance-based assessment of the Great Mosque of Algiers. *Bull. Earthquake Eng.* 13, 369–388. doi: 10.1007/s10518-014-9682-1

Salonia, P., Bellucci, V., Scolastico, S., Marcolongo, M., and Leti Messina, T. (2007). "3D survey technologies for reconstruction, analysis and diagnosis in the conservation process of cultural heritage," in *Proceedings of CIPA*, (Athens).

SISMA (2007). *System Integrated for Security Management Activities in Cultural Heritage* (2000–2006). ed c.i.I.I.B.C. 3B035 (Perugia: Petruzzi).

Vasconcelos, G., and Lourenço, P. (2009). Experimental characterization of stone masonry in shear and compression. *Constr. Build. Mater.* 23, 3337–3345. doi: 10.1016/j.conbuildmat.2009.06.045

Zuccaro, G., Albanese, V., Cacace, F., Mercuri, C., Papa, F., Pizza, A. G., et al. (2008). "Seismic vulnerability evaluations within the structural and functional survey activities of the COM bases In Italy," in *AIP Conference Proceedings*, 1665–1674. doi: 10.1063/1.2963797

Zuccaro, G., and Cacace, F. (2015). Seismic vulnerability assessment based on typological characteristics. The first level procedure "SAVE". *Soil Dyn. Earthquake Eng.* 69, 262–269. doi: 10.1016/j.soildyn.2014.11.003

**frontiers**
in Built Environment

Check for
updates

# Fatigue Assessment and Deterioration Effects on Masonry Elements: A Review of Numerical Models and Their Application to a Case Study

Vito Michele Casamassima* and Michele D'Amato

*DICEM, Department of European and Mediterranean Cultures (Architecture, Environment and Cultural Heritage), University of Basilicata, Matera, Italy*

Safety assessment with respect to seismic and vertical loads of existing and very old masonry structures is currently a central topic for the scientific engineering community. In particular, there are many ancient bridges still in service that are subjected to higher and more frequent cyclic loads. For these structures, it is important to determine the actual fatigue strength, rather than the ultimate carrying capacity. In this way the remaining service life, with possible traffic load limitations, may be estimated. This paper reports an updated review of the state-of-the art on recently published fatigue models that account for deterioration effects under cyclic loads. In addition, results related to fatigue performance of a bridge are shown and comments are provided. The numerical comparisons among existing fatigue models reveal that the application of the available fatigue models is particularly problematic for ancient masonry elements, where appropriate stress-life curves are required.

Keywords: masonry, fatigue assessment, fatigue deterioration, residual service life, stress-life curves

## INTRODUCTION

To date, there have been conspicuous advances in simulating the response of ancient masonry structures, mainly with the aim of determining the ultimate vertical loads and capacity with respect the lateral seismic actions. For example, among other studies, modeling criteria for ancient bridges may be found in Laterza et al. (2017b) and D'Amato et al. (2017), while for ancient churches they are reported in Pelà et al. (2009); Formisano and Marzo (2017); Betti et al. (2018); D'Amato et al. (2018), Formisano et al. (2018); Fuentes et al. (2019); Ramirez et al. (2019), and Lopez et al. (2019), and they are discussed for towers in Shakya et al. (2016); Bartoli et al. (2018) and Sarhosis et al. (2018). Models of general historical buildings are discussed in Caprili et al. (2017) and Milani et al. (2018), while detailed study on *in-situ* tests may be found, among the others, in Krstevska et al. (2010); Bartoli et al. (2013), and Luchin et al. (2018).

Nowadays, the study of ancient masonry structures' responses is a relevant topic since most of them are still in service without any kind of limitation.

By contrast, in the scientific community there is not yet the same level of interest for a correct understanding of fatigue effects and the prediction of the remaining service life of masonry elements under cyclic compressive loads. Among ancient masonry structures, it is known that arch bridges are affected by fatigue problems. This is due to the fact that they are currently subjected to higher and more frequent cyclic loads due to population growth, resulting in premature cracking and deterioration. As such, the available fatigue strength, that is the maximum stress acting in cyclic conditions, is significantly lower than the one obtained under quasi static loading conditions. Therefore, rather than the ultimate carrying capacity, it is important to know the actual fatigue strength, starting from which useful indications on the remaining service life with a possible traffic load limitation may be established. Moreover, the deterioration of materials and cyclic action may accelerate masonry deterioration and reduce carrying capacity. Clark (1994) and Roberts et al. (2006) performed cyclic tests on brick masonry columns and concluded that the stress limit of dry specimens was about 50% of the static compressive strength, whereas Choo and Hogg (1995) and Schueremans and Van Gemert (2001) instead suggested limiting the applied load to <50% of the ultimate vertical load. Furthermore, in Melbourne et al. (2004) the cyclic vertical load capacity of multi-ring masonry arches varied between 37 and 57% of the static load carrying capacity. This significant reduction was due to a separation of rings, which was provoked by a shear failure mode among bricks and mortar joints instead of a four-hinge failure mechanism. Finally, in Melbourne et al. (2007), a unitary assessment procedure (named *SMART* procedure) was proposed for evaluating fatigue performance of masonry arches, involving the application of the fatigue model reported in Roberts et al. (2006).

Stress-life curves for masonry elements, indicated as *S-N* curves, are usually established in a limited number of experimental tests and, very often, are not adequate to reproduce the elements of ancient masonry. Moreover, in many of the actual design codes—among which are (Ministerial Decree D.M. 14/01/2008 (NTC-08), 2008), with the related (Italian Design Code Instructions (NTC-08 Instructions), 2009), and Eurocode 3 (EC3, 2003)—appropriate indications for evaluating the fatigue strength of masonry elements are still missing, contrarily to steel elements. Nevertheless, as highlighted from laboratory tests carried out on prototype models cast in a reduced scale, cycling loads related to in-service conditions may provoke fatigue failure for a vertical load significantly lower than the one related to the ultimate condition (Melbourne et al., 2004).

In this study, an updated review is provided for the main stress-life curve models available in the literature for estimating the fatigue strength of masonry elements. In particular, the models proposed by Ronca et al. (2004), Roberts et al. (2006), Casas (2009), Tomor and Verstrynge (2013), and Koltsida et al. (2018a) are considered. At first, they are separately described and shown. Then, the considered models are applied to a case study, an ancient masonry arch bridge. In particular, the main arch fatigue

strength is assessed by considering the numerical simulations for repeated vertical loads reported in a previous study (Laterza et al., 2017a).

## MODELS TO PREDICT THE MASONRY FATIGUE LIFE UNDER COMPRESSIVE LOADING

### Ronca et al. (2004)

Ronca et al. (2004) conducted, in accordance with BS EN998-2 (2003), a series of tests applying repeated vertical loads on masonry specimens that contained M4 mortar, with an average strength in compression of 48.86 N/mm$^2$ and an average ultimate strength in compression ranged between 10 and 13 MPa. The tests were performed in order to evaluate the role of loading rate on material response, with the aim of deriving a fatigue model in terms of *S-N* curves. In the tests, the specimens were subjected to heavy sustained loads with small perturbations, mostly due to environmental conditions (for example traffic vibrations and thermal excursion, among others). The brickwork prisms were tested under very high vertical loads applied axially (65–80% of the ultimate compressive strength) and by imposing a small variation of the alternating loads with three different frequencies: 1, 5, and 10 Hz.

**Table 1** summarizes the ratios $S_{min}/S_{max}$, and $S_a/S_u$ reached in each test, where $S_a$ is the stress induced with the alternating load (in absolute value); $S_u$ is the compressive strength of the investigated masonry; $S_{max}$ and $S_{min}$ are the maximum and the minimum stresses induced during the cycle, respectively; $R$ is a parameter given by the ratio of $S_{min}$ to $S_{max}$; while $S$ is the ratio of $S_{max}$ to $S_u$, measuring how far the maximum stress is cyclically induced from the monotonic masonry compressive strength. In particular, during the tests the $R$ ratio ranged from 0.73 to 0.88, while the $S$ ratio ranged from 0.7 to 0.90. **Figure 1** shows, in the semi-logarithmic plane $logN$-$S_a/S_u$, the experimental values obtained from each test together with the stress-life curves proposed by the same authors. It is important to note that fatigue strength increases as the number of cycles, $N$, decreases.

### Roberts et al. (2006)

Roberts et al. (2006) conducted experimental tests on different types of masonry prisms considering also different levels of water saturation degree. Starting from the obtained results, Equation (1) was proposed, representing a lower bound for the fatigue strength:
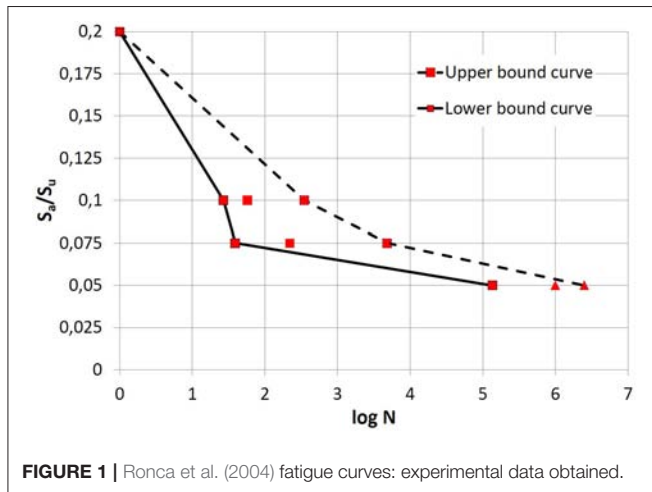
$$F(S) = \frac{(\triangle SSmax)^{0,5}}{Su} = 0.7 - 0.05 logN \tag{1}$$

where $F(S)$ is the function of the induced stress range, $S_{max}$ is the maximum stress amplitude, $\triangle S$ is the difference between $S_{max}$ and $S_{min}$, $S_u$ is the compressive strength and $N$ is the number of cycles to failure.

Three types of specimens were tested for simulating more closely the masonry arch barrels, while considering both dry and saturated conditions. A vertical load eccentricity ratio $e/d$ ranging from 0 to 0.256 (where $e$ is the vertical load eccentricity and $d$

| Number of samples | f (Hz) | Sa/Su | R=Smin/Smax | S = Smax/Su |
|---|---|---|---|---|
| 3 | 1 | 0.1 | 0.78 | 0.90 |
| 3 | 1 | 0.075 | 0.83 | 0.88 |
| 3 | 1 | 0.05 | 0.88 | 0.85 |
| 1 | 1 | 0.1 | 0.73 | 0.75 |
| 2 | 5 | 0.1 | 0.73 | 0.75 |
| 1 | 10 | 0.05 | 0.86 | 0.70 |

| Pb | 0.95 | 0.90 | 0.80 | 0.70 | 0.60 | 0.50 |
|---|---|---|---|---|---|---|
| A | 1.106 | 1.303 | 1.458 | 1.494 | 1.487 | 1.464 |
| B | 0.0998 | 0.110 | 0.109 | 0.102 | 0.094 | 0.087 |

levels was proposed for masonry under compressive loading, in accordance with Equation (3):

$$S = \frac{Smax}{Su} = AN^{-B(1-R)} \tag{3}$$

where $N$ is the number of cycles to failure, $R = S_{min}/S_{max}$ is the ratio between minimum and maximum induced stresses, and $S = S_{max}/S_u$ is the ratio between the maximum induced stress and compressive strength of the masonry. The coefficients $A$ and $B$ are reported in **Table 2**, defined as a function of the survival probability levels, while **Figure 2** shows the stress-life curves obtained with Equation (3) by varying the stress ratio $R$ from 0 to 0.9.

Starting from the Casas (2009) formulation, Tomor and Verstrynge (2013) proposed a probabilistic fatigue model, introducing the correction coefficient $C$ set equal to 0.62 for accounting for the joined fatigue and creep deterioration simultaneously. In this model the material deterioration due to fatigue damage is more relevant for lower stress, while the creep effects dominate the cyclic response at higher stresses. In accordance with this work, Equation (4) was proposed, where the values of $A$ and $B$ are equal to 1 and 0.04, respectively:

$$Smax = AN^{-B(1-CR)} \tag{4}$$

For completeness, **Figure 3** illustrates a series of fatigue curves obtained according to the model proposed by Tomor and Verstrynge (2013) by considering 5% of failure probability.



FIGURE 1 | Ronca et al. (2004) fatigue curves: experimental data obtained.

the specimen depth) was applied. The load frequency was kept constant to 5 Hz until failure. The test series indicated that the high cycle fatigue strength of wet and submerged brick masonry specimens was only slightly less than that of dry specimens. The mortar was mixed in order to reproduce the representative mortar used for ancient brick masonry arches. It was shown that the compressive strength measured at 28 days ranged between 0.45 MPa and 2.78 MPa. The masonry compressive strength, determined by assuming a linear stress distribution along the specimens, varied between 6 and 14 MPa.

By introducing in Equation (1) the stress ratio $R=S_{min}/S_{max}$, and substituting $\Delta S$ for the difference $S_{max}-S_{min}$, the formulation proposed by Roberts et al. (2006) may be rewritten in the familiar form of stress-life curve $logN$- $S_{max}/S_u$ as follows:

$$S = \frac{Smax}{Su} = \frac{1 - 0.05 logN}{\sqrt{1 - R}} \tag{2}$$

In Equation (2), the fatigue strength $S$ depends only on the imposed number of cycles $N$ and on the amplitude of the induced stresses range $R$ (the lower the $R$ ratio the higher the interval amplitude of stresses).

## Casas (2009)

Based on the test results from Roberts et al. (2006) , Casas (2009) post-processed the experimental results using a probabilistic approach. A new stress life curve for different survival probability

## Koltsida et al. (2018a)

In order to develop new stress life curves for masonry under compressive loading, Koltsida et al. (2018a) performed a series of experimental fatigue tests on low-strength masonry prisms under compressive cyclic load, proposing stress-life curves for different values of survival probability. They tested 64 brick full-size masonry prisms according to ASTM (2014) . Static and cyclic tests were performed with a frequency of 2 Hz. The tests showed an average compressive strength of 4.86 MPa for bricks and of 2.94 MPa for the masonry. The minimum induced stress during the tests was set to 10% of the masonry compressive strength, while the maximum induced stress ranged between 55 and 80%. The limit on the number of cycles up to failure was fixed as $10^7$. For a given survival probability $L$, the fatigue curve may be described as follows (Koltsida et al., 2018a):

$$L = 10^{-0.1127(Smax\Delta S)^{3.9252}(logNf)^{3.8322}} \tag{5}$$

In **Figure 4**, Equation 5 is reported by considering different values of R ratios, assuming L = 0.05 (i.e., by assuming a 5% failure probability).
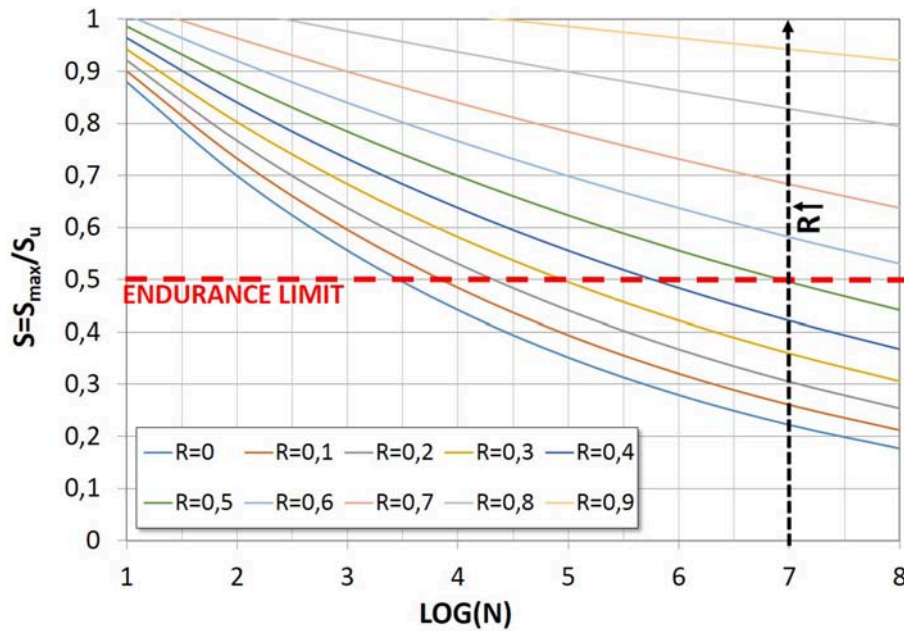
**FIGURE 2 |** Casas (2009) fatigue curves, referred to a 5% of failure probability.
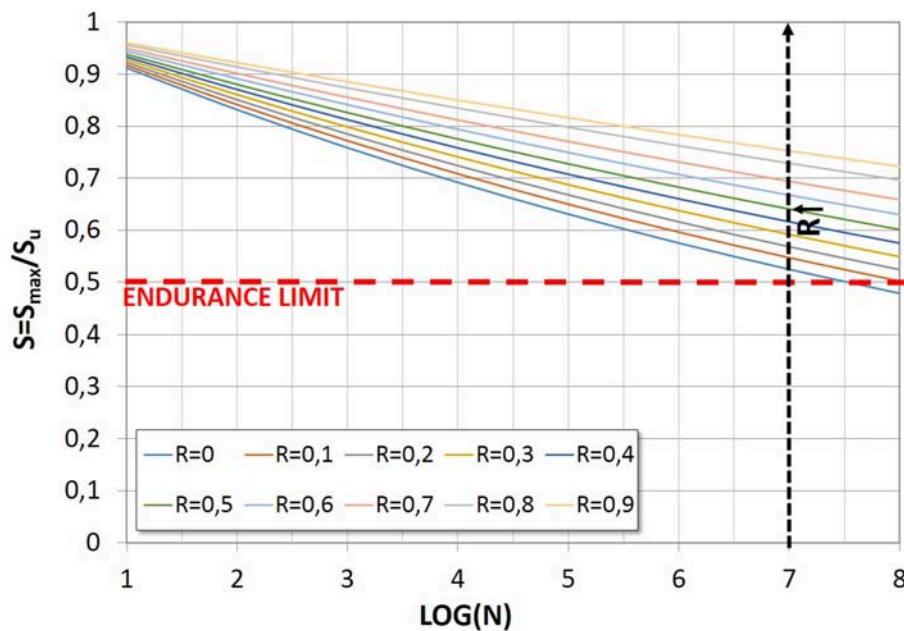


**FIGURE 3 |** Tomor and Verstrynge (2013) fatigue curves, referred to a 5% of failure probability.

# DETERIORATION OF THE ELASTIC MODULUS IN MASONRY ELEMENTS UNDER COMPRESSIVE LOADS

Koltsida et al. (2018b) investigated deterioration of the elastic modulus of masonry during compressive cyclic loading. This study was conducted starting from similar studies regarding concrete specimens, as reported in Crumley and Kennedy (1977); Holmen (1982); Cachim et al. (2002); Mu and Shah (2005); Breitenbucher and Ibuk (2006); Zanuy et al. (2011);Vicente et al. (2014).

Specifically, Crumley and Kennedy (1977) in their tests concluded that the elastic modulus decreased by about 40% over the concrete usable life, and that a remarkable reduction of elastic
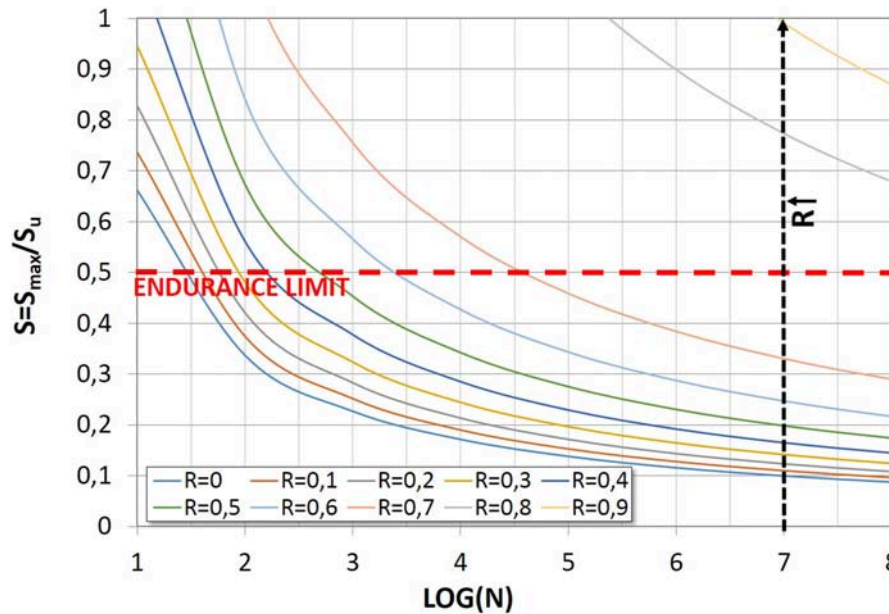
**FIGURE 4 |** Koltsida et al. (2018a) fatigue curves, referred to a 5% of failure probability.

modulus arose often at 75% of the fatigue life. In Holmen (1982) the elastic modulus of concrete cylinders consisted of three different phases: a first rapid decrease from 0 to about 10% of the number of failure cycles, a constant decrease from 10 up to 80% of the number of failure cycles, and then a sudden decrease until the specimen's fatigue failure. These reductions resulted from increasing the number of cycles up to the failure. In addition, during the performed tests it was found that the absorbed energy at failure was the same for static and fatigue loads with different intensities. Mu and Shah (2005) performed experimental fatigue tests on the concrete cylinders to evaluate the damage evolution in the case of biaxial fatigue loading, compression and torsion. The results showed that the evolution of cracks in the material may be divided into two phases: the first phase was characterized by a deceleration of the crack, and the second one by a sudden acceleration. The authors proposed the following relationship:

$$\log(Nf) = -0.82 \cdot \log\left(\frac{dk}{dN}\right) + 2.8 \quad (6)$$

where $k$, $N$ and $N_f$ are the elastic modulus, cycle and fatigue life, respectively. It should be noted that this relationship is independent of the fatigue load range. A different approach for predicting the elastic modulus of concrete under repeated compressive loads was proposed by Zanuy et al. (2011). In accordance with this model, the maximum strain ($\varepsilon_{max}$) and the elastic modulus ($E$) were directly related to the number of cycles:

$$\varepsilon_{\max} = \varepsilon_{\max}\left(\frac{N}{Nf}\right) \quad (7)$$

$$E = E\left(\frac{N}{Nf}\right) \quad (8)$$

The deterioration influence on Equation (7) and Equation (8) depends on the maximum and the minimum stresses ($\sigma_{max}/f_c$, $\sigma_{min}/f_c$). In particular, the authors defined three different deterioration stages. In Stage 1, concrete deterioration was due to micro-cracks forming at the aggregate-paste interface. This stage covered approximately 10–15% of the fatigue life. In Stage 2, micro-cracks grew steadily, with a constant reduction of the elastic modulus. This stage covered about 80–90% of the fatigue life. In Stage 3, micro-cracks converged to form a macro-crack causing specimen failure. The expressions proposed to determine elastic modulus in the transition from Stage 1 to Stage 2 and the rate of modulus decline in fatigue Stage 2 were as follows (Zanuy et al., 2011):

$$E = (N = 0.1Nf) = \left[\left(0.09 + 8.19 + \frac{\sigma min}{fc}\right) + \left(0.84 + 8.19\frac{\sigma min}{fc}\right)\frac{\sigma max}{fc}\right]Ec \leq 0.93Ec \quad (9)$$

$$\frac{dE}{d\left(\frac{N}{Nf}\right)} = \left(0.1 < \frac{N}{Nf} < 0.8\right) = \frac{0.25}{0.61 - \frac{\sigma min}{fc}}$$
$$\left(0.39 + \frac{\sigma min}{fc} - \frac{\sigma max}{fc}\right)Ec \leq 0 \quad (10)$$

where $E_c$ is the static modulus of deformation.

Starting from the previous studies, a few research groups have proposed similar formulations by considering, instead of concrete, the masonry material. Among these groups, it is worth mentioning the studies conducted by (Alshebani and Sinha, 2001). In this work, the authors concluded that deterioration
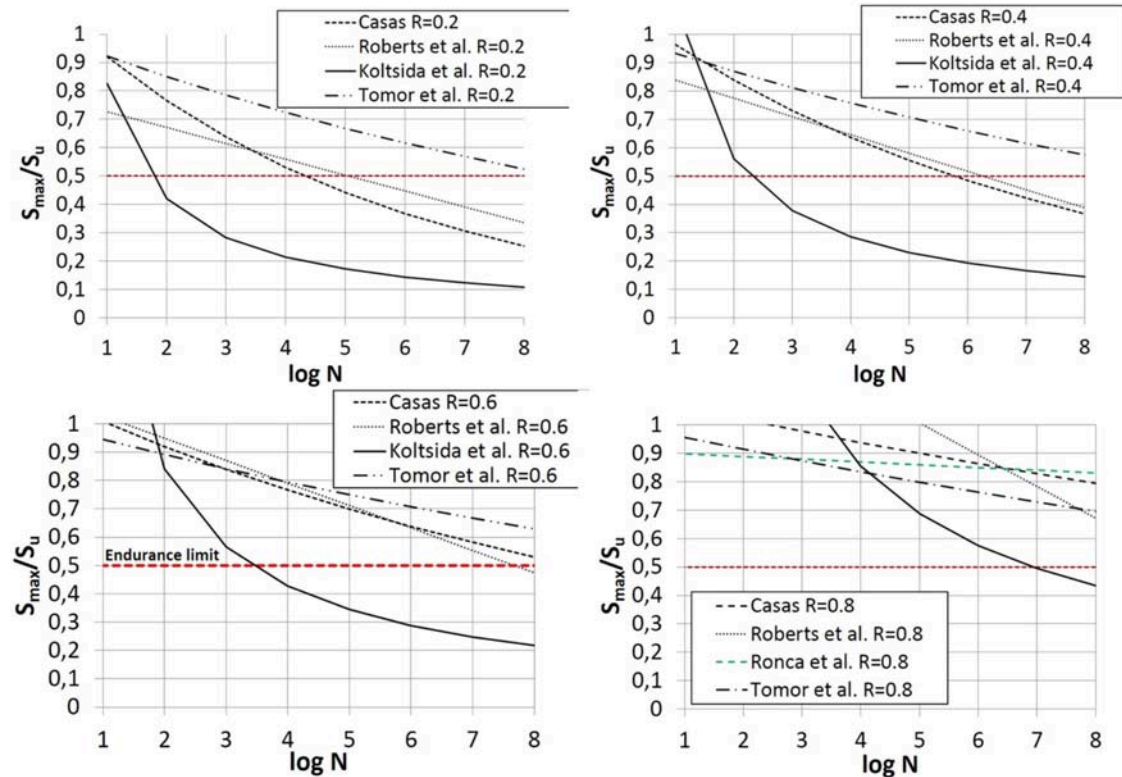
**FIGURE 5 |** Comparisons between stress life curves for different values of the ratio R, referred to the 5% of failure probability.

of the elastic modulus began at 20% of the compressive load capacity. Moreover, the strength and stiffness deterioration depended on the number and intensity of cyclic loads, and in particular the degradation increased as the load and number of cycles increased.

As mentioned above, Koltsida et al. (2018b) recently proposed a different formulation to describe the evolution of the stiffness degradation under cyclic loading. The tests highlighted that until 95% of the fatigue life, the variation of the elastic modulus remained constant, while beyond the 95% mark it rapidly decreased until failure. To describe the evolution of the elastic modulus during cyclic loading, a linear model was proposed as described by Equation 11 and Equation 12, where $E/E_0$ represents the ratio between the elastic modulus and initial elastic modulus, and $N/N_f$ is the ratio between the number of cycles and the number of cycles to failure. In Equation 12 the coefficient $a$ is the gradient coefficient, while $b$ is the intercept coefficient of the linear equation:

$$\frac{E}{E_0} = a\frac{N}{Nf} + b \quad (11)$$

$$\frac{d\frac{E}{E_0}}{d\frac{N}{Nf}} = a \quad (12)$$

In Koltsida et al. (2018b) the following function was found as the best fit curve of the maximum

induced stress:

$$\frac{d\frac{E}{E_0}}{d\frac{N}{Nf}} = a = -3.0181S_{max}^3 + 5.6894S_{max}^2 - 3.5118S_{max} \quad (13)$$

By substituting the previous Equation (13) into Equation (11), the following relationship describing the reduction of the elastic modulus under cycling loading was proposed:

$$\frac{E}{E_0} = 1 - (3.0181S_{max}^3 - 5.6894S_{max}^2 + 3.5118S_{max} - 0.6175)$$

$$(\frac{N}{N_f}) \quad (14)$$

## COMPARISON AMONG THE STRESS-LIFE CURVES CONSIDERED

In **Figure 5** the comparisons among the stress–life curves considered in this work are reported and illustrated in the semi-logarithmic plane *Log N- S*. In the comparisons the following values of the ratio $R=S_{min}/S_{max}$ are considered: 0.2, 0.4, 0.6, and 0.8. Moreover, the curves proposed by Casas (2009) and Koltsida et al. (2018a) are drawn by referring to the 5% of failure probability, as considered by the EC3 and NTC-08 for the material nominal compressive strength. Also, **Figure 5** reports the Tomor and Verstrynge (2013) stress life curves, and the ones
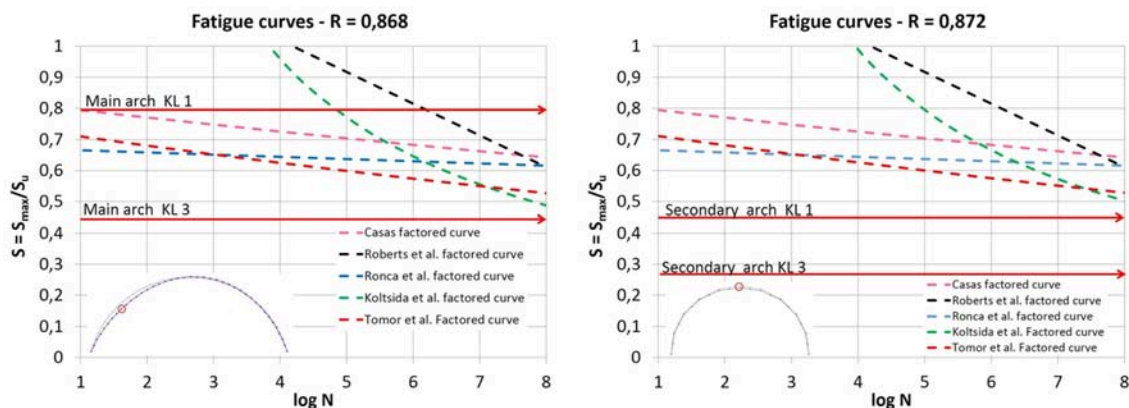
**FIGURE 6 |** Main arch (left) and secondary arch (right): calculation of the life cycles at the failure.

proposed by Ronca et al. (2004), related to the ratio *R* equal to 0.8, since 0.8 is approximately the average value of the imposed *R* in all the performed tests. In all the graphs, the fatigue endurance limit *S=0.5* is also highlighted. It is important to outline that all the considered models may predict a low number of cycles at failure, even lower than the stress level corresponding to the classic endurance limit. From the comparisons, it is possible to highlight that when the stress ratio *R* decreases, i.e., the stress fluctuation between the minimum and maximum compressive stress increases, the number of cycles to failure decreases for any value of ratio $S=S_{max}/S_u$. Moreover, it can be observed that for *R* equal to 0.6 and 0.8, the fatigue strength becomes significantly higher than the endurance limit, very high also for a number of cycles. Finally, the curves proposed by Tomor and Verstrynge (2013) indicated very different values for the number of cycles to failure compared to the other curves, especially for high values of ratio *S*, where the effect of the plastic deformations are more influent.

## APPLICATION TO A CASE STUDY

In this paper fatigue assessment related to a case study is discussed. In particular, the results related to the main and secondary arches of an ancient masonry arch bridge are shown.

The case study, "Cavone Bridge," was built in Italy before the Second World War and is currently still open to the traffic. It takes its name from the river it crosses and consists of seven arches of brick masonry. The bridge is 140 m in length and 5.6 m wide, and it is composed of three main arches with span lengths of 22 m and three secondary arches with span lengths of 10 m. The arches are supported by two piers of which 14 m are outside the riverbed. The piers have a total height from the foundation plane of about 24 m.

The bridge serves a provincial road according to the Italian Transport Classification (1992). The bridge was subjected to some *in situ* tests to identify the typology and the thickness of all its elements and components. The tests showed that the piers, abutments and spandrel walls consist of an external

leaf of regular stone blocks. The piers have a core of cohesive backfill, while the bridge deck is formed by an incoherent backfill that has the function of spreading the traffic loads to the supporting arches. More details about numerical investigations carried out on this bridge for fatigue and seismic performance may be found performance in Laterza et al. (2017a,b) and D'Amato et al. (2017). In particular, in this section the numerical investigations illustrated in Laterza et al. (2017a) regarding the most unfavorable section for fatigue assessment verifications are discussed.

As for the load scheme, in this study *Fatigue Model 3*, which has two axles with a load of 120 kN/axle, is used. In accordance with Eurocode 1 (EC1, 2003) the considered fatigue model is more appropriate for typical heavy traffic on European main roads or motorways. In addition, a *Traffic Category 2* has been assumed, resulting in $5 \times 10^5$ passages for the year ($N_{cat}$). Since there is an absence of a relative procedure for masonry elements, in this study the fatigue assessment for steel elements has been applied, as proposed in the Italian Design Code Instructions (NTC-08 Instructions) (2009) and EC3 (2003), while applying fatigue stress-strain curves for masonry.

In accordance with the Italian Design Code Instructions (NTC-08 Instructions) (2009), two different values for the masonry compressive strength associated with *Knowledge Level 1* (*KL1*) and *Knowledge Level 3* (*KL3*) have been considered for the arches (NTC-08). Precisely, the compressive strength of masonry is assumed equal to 2.4 MPa for *KL1* and 3.2 MPa for *KL3*. The strength is further reduced by a confidence factor *FC* =1.35 for *KL1* and *FC*=1 for *KL3*.

**Figure 6** reports the comparisons of the fatigue curves considered in this study, plotted for main and secondary arches. It should be noted that, in accordance with the NTC-08 and EC3 methods, all the curves are factorized, i.e., the fatigue strength is divided by $\gamma_{Mf}$ (fatigue strength partial factor), assumed in this case equal to 1.35 by supposing a high consequence of arch failure due to the fatigue strength achievement. Meanwhile, the stress range $\Delta\sigma_i$, due to the stresses fluctuation resulting from the transit of the load along the arch, is amplified by $\gamma_{Ff} = 1$, where

**TABLE 3 |** Residual service life evaluation of the main arches.

| S-N curve<br>$R = 0.868$ | $S_{max}/S_u$<br>KL1 | $S_{max}/S_u$<br>KL3 | logN | N | Ncat traffic category 2 | Residual life (years) N/Ncat |
|---|---|---|---|---|---|---|
| (Casas, 2009) | 0.790 | 0.440 | 1.17 | 14.63 | $5 \times 10^5$ | $\approx 0$ |
| (Roberts et al., 2006) | 0.790 | 0.440 | 6.25 | $1.78 \times 10^6$ | $5 \times 10^5$ | 3.56 |
| (Koltsida et al., 2018a) | 0.790 | 0.440 | 4.8 | $6.31 \times 10^4$ | $5 \times 10^5$ | $\approx 0$ |
| (Tomor and Verstrynge, 2013) | 0.790 | 0.440 | NA | - | $5 \times 10^5$ | - |
| (Ronca et al., 2004) | 0.790 | 0.440 | NA | - | $5 \times 10^5$ | - |

**TABLE 4 |** Residual service life evaluation of the secondary arches.

| S-N curve<br>$R = 0.872$ | $S_{max}/S_u$<br>KL1 | $S_{max}/S_u$<br>KL3 | logN | N | Ncat traffic category 2 | Residual life (years) N/Ncat |
|---|---|---|---|---|---|---|
| (Casas, 2009) | 0.494 | 0.275 | NA | - | $5 \times 10^5$ | - |
| (Roberts et al., 2006) | 0.494 | 0.275 | NA | - | $5 \times 10^5$ | - |
| (Koltsida et al., 2018a) | 0.494 | 0.275 | NA | - | $5 \times 10^5$ | - |
| (Tomor and Verstrynge, 2013) | 0.494 | 0.275 | NA | - | $5 \times 10^5$ | - |
| (Ronca et al., 2004) | 0.494 | 0.275 | NA | - | $5 \times 10^5$ | - |

$\gamma_{Ff}$ is the partial factor for equivalent constant amplitude stress range $\Delta\sigma_i$.

As far as the stress fluctuation is concerned, three different sections (2 haunches section, and 1 key section) for each arch have been numerically investigated in Laterza et al. (2017a) by means of FEM models. However, in this study only the most unfavorable section for fatigue assessment in terms of $\Delta\sigma_i$ fluctuation is considered, which is the haunch section for the main arches and the key for the secondary ones. For these sections the ratio $S_{min}/S_{max}$ results in value equal to 0.868 for the main arches and to 0.872 for the secondary ones, where $S_{min}$ and $S_{max}$ are the minimum and maximum axial stresses. In **Tables 3**, **4**, the numerical results are summarized for the main and secondary arches, reporting the ratios $S_{max}/S_u$ (maximum stress $S_{max}$ over the ultimate strength in compression $S_u$) for both KL1 and KL3.

The fatigue performance is evaluated through the calculation of the residual service life, expressing the residual time (in year) before the failure to fatigue. This is given by the following ratio:

$$Residual\ Service\ Life = \frac{N}{N_{cat}}\ (years) \quad (15)$$

where $N$ is the cycle number to failure obtained from the stress-life curve and $N_{cat}$ is the number of passages per year assumed for the category of the bridge ($N_{cat} = 5 \times 10^5$ passages/year).

It should be noted that for KL3, by referring to the main arches, and for KL1 and KL3 in the case of secondary ones, the cycles' number to failure $N$ are always very high (greater than $10^8$) so that, substantially, the residual life may be considered infinite.

On the other hand, the fatigue assessment results drastically change if the KL1 is considered for main arches. In this case, the models of Tomor and Verstrynge (2013) and Ronca et al. (2004) are not applicable, since the stress level $S_{max}/S_u = 0.790$

falls beyond the stress-life curves for any value of logN. As for the model proposed by Casas (2009) and Koltsida et al. (2018a), the residual life is <1 year. Meanwhile, according to the Roberts et al. (2006) model, the residual life is about 3.5 years.

By comparing the chosen models, it is possible to conclude that the models proposed by Koltsida et al. (2018a), Tomor and Verstrynge (2013) and Casas (2009) actually represent the most complete models, since they have been derived from experimental results considered with a probabilistic approach. Differently from the Ronca et al. (2004) model (derived by imposing a small variation of the alternating loads), both the Roberts et al. (2006) and Casas (2009) models estimate, at a number of cycles that is not too high, fatigue strength ratios ($S_{max}/S_u$) significantly lower than 0.5, which is the value usually indicated as the fatigue endurance limit. This demonstrates the importance of an appropriate evaluation of the fatigue strength that may lead, if simplified methods are applied (such as the endurance limit criterion), to an overestimation of the actual fatigue strength.

## CONCLUSIONS

In this paper, a critical review has been made and we have applied some fatigue models to a case study, considering also the deterioration of the masonry due to the effect of the cyclic loads.

In particular, different fatigue curves have been considered for evaluating the damage accumulation due to traffic load, in compliance with the procedure proposed by the EC3 (2003) and NTC-08 (2008). Since in the examined codes no clear indication is reported for masonry elements, the fatigue performance approach has been applied similarly to the one proposed for steel elements, with masonry fatigue curves.

Different stress-life curves have been considered in accordance with the models proposed by Ronca et al. (2004), Roberts et al. (2006), Casas (2009), Tomor and Verstrynge (2013) and Koltsida et al. (2018a), which are also capable of estimating the degradation of the material due to fatigue.

By comparing the chosen models, it possible to conclude that the models proposed by Casas (2009), Tomor and Verstrynge (2013), and Koltsida et al. (2018a) actually represent the most complete models, since they have been derived from the experimental results considered with a probabilistic approach. It must be remarked, however, that they have been derived from laboratory tests performed on masonry specimens having compressive strength values higher than the usual ones encountered in existing masonry. To this aim, particular attention should be also paid to the influence on the fatigue capacity of the cyclic load frequency. As a matter of fact, the fatigue models examined in this study have been proposed for cycled loads having frequencies (more than 1 Hz) higher than the ones associated with traffic loads indicated in the considered codes (for example, in the case analyzed the traffic load frequency results equal to 0.015 Hz). A first approach has been adopted to evaluate the degradation of the material due to the fatigue effects by using the recent model proposed by Koltsida et al. (2018b).

Finally, new laboratory tests focused on ancient masonry specimens will permit researchers to study in a more in-depth manner the fatigue behavior and the evolution of the material degradation of masonry, which have not yet been fully detailed.

## DATA AVAILABILITY

The datasets generated for this study are available on request to the corresponding author.

## AUTHOR CONTRIBUTIONS

All authors listed have made a substantial, direct and intellectual contribution to the work, and approved it for publication.

## REFERENCES

Alshebani, M. M., and Sinha, N. S. (2001). *Stiffness Degradation of Brick Masonry Under Cyclic Compressive Loading, Vol. 15*. Masonry International, 13–16.

ASTM (2014). "Standard test method for compressive strength of masonry prisms," in *Annual Book of ASTM Standards*, *Vol. 4.05*, eds ASTM (West Conhohocken, ASTM International), 889–895.

Bartoli, G., Betti, M., Galano, L., and Zini, G. (2018). Numerical insights on the seismic risk of confined masonry towers. *Eng. Struct.* 180, 713–727. doi: 10.1016/j.engstruct.2018.10.001

Bartoli, G., Betti, M., and Giordano, S. (2013). *In situ* static and dynamic investigations on the "Torre Grossa" masonry tower. *Eng. Struct.* 52, 718–733. doi: 10.1016/j.engstruct.2013.01.030

Betti, M., Borghini, A., Boschi, S., Ciavattone, A., and Vignoli, A. (2018). Comparative seismic risk assessment of basilica-type churches. *J. Earthq. Eng.* 22 (supp1), 62–95. doi: 10.1080/13632469.2017.1309602

Breitenbucher, R., and Ibuk, H. (2006). Experimentally based investigations on the degradation-process of concrete under cyclic loading. *Mater. Struct.* 39, 717–724. doi: 10.1617/s11527-006-9097-9

BS EN998-2 (2003). *Specification for Mortar for Masonry. Masonry Mortar*. London, UK: British Standard Institution.

Cachim, P., Figueiras, J., and Pereira, P. (2002). Fatigue behaviour of fiber reinforced concrete in compression. *Cement Concrete Composites* 24, 211–217. doi: 10.1016/S0958-9465(01)00019-1

Caprili, S., Mangini, F., Salvatore, W., Bevilacqua, M. G., Karwacka Codini, E., Squeglia, N., et al. (2017). A knowledge-based approach for the structural assessment of cultural heritage, a case study: la Sapienza Palace in Pisa. *Bull. Earthq. Eng.* 15, 4851–4886. doi: 10.1007/s10518-017-0158-y

Casas, J. R. (2009). A probabilistic fatigue strength model for brick masonry under compression. *J. Construct. Build. Mater.* 23, 2964–2972. doi: 10.1016/j.conbuildmat.2009.02.043

Choo, B. S., and Hogg, V. (1995). "Determination of the serviceability limit state for masonry arch bridges," in *Arch Bridges*, ed C. Melbourne (London, UK: Thomas Telford), 529–536.

Clark, G. W. (1994). *Bridge Analysis Testing and Cost Causation Project: Serviceability of Brick Masonry*. British Rail Research Report LR CES 151.

Crumley, J., and Kennedy, W. (1977). *Fatigue and Repeated-load Elastic Characteristics of Inservice Portland Cement Concrete*. Texas, USA: *Center of Highway* Research, The University of Texas.

D'Amato, M., Laterza, M., and Casamassima, V. M. (2017). Seismic performance evaluation of a multi-span existing masonry arch bridge. *Open Civil Eng. J.* 11 (Suppl. 5) M11, 1191–1207. doi: 10.1063/1.4992619

D'Amato, M., Laterza, M., and Diaz Fuentes, D. (2018). Simplified seismic analyses of ancient churches in matera's landscape. *Int. J. Architect. Heritage*. doi: 10.1080/15583058.2018.1511000. [Epub ahead of print].

EC1 (2003). *EN 1991-2:2003. Eurocode 1. Actions on structures – Part 2: Traffic Loads on Bridges*.

EC3 (2003). *EN 1993-1-9:2003. Eurocode 3. Design of steel structures – Part 1-9: Fatigue*.

Formisano, A., and Marzo, A. (2017). Simplified and refined methods for seismic vulnerability assessment and retrofitting of an Italian cultural heritage masonry building. *Comput. Struct.* 180, 13–26. doi: 10.1016/j.compstruc.2016.07.005

Formisano, A., Vaiano, G., Fabbrocino, F., and Milani, G. (2018). Seismic vulnerability of italian masonry churches: the case of the nativity of blessed virgin mary in stellata of bondeno. *J. Build. Eng.* 20, 179–200. doi: 10.1016/j.jobe.2018

Fuentes, D. D., Laterza, M., and D'Amato, M. (2019). "Seismic vulnerability and risk assessment of historic constructions: the case of masonry and adobe churches in Italy and Chile,"in *Proceedings of SAHC 2018, 11th International Conference on Structural Analysis of Historical Constructions. RILEM Bookseries 18* (Cusco), 1127–1137.

Holmen, J. (1982). Fatigue of concrete by constant and variable amplitude. *ACI J.* 75, 71–110.

Italian Design Code Instructions (NTC-08 Instructions) (2009). *Circolare 2 Febbraio 2009, n. 617 – Istruzioni per l'Applicazione Delle Nuove Norme Tecniche per le Costruzioni di cui al D.M. 14 gennaio 2008*. Pubblicata su S.O. n. 27 alla G.U.

Italian Transport Classification (1992). *Nuovo Codice Della Strada." Pubblicato sul supplemento ordinario n.74 alla "Gazzetta Ufficiale" n. 114 del 18 Maggio 1992 – Serie Generale Quanto Definito Da: "Nuovo Codice Della Strada"*.

Koltsida, I. S., Tomor, A. K., and Booth, C. A. (2018a). Probability of fatigue failure in brick masonry under compressive loading. *Int. J. fatigue.* 112, 233–239. doi: 10.1016/j.ijfatigue.2018.03.023

Koltsida, I. S., Tomor, A. K., and Booth, C. A. (2018b). Experimental evaluation of changes in strain under compressive fatigue loading of brick masonry. *Construct. Build. Mater.* 162, 104–112. doi: 10.1016/j.conbuildmat.2017.12.016

Krstevska, L., Tashkov, L., Naumovski, N., Florio, G., Formisano, A., Fornaro, A., et al. (2010). "In-situ experimental testing of four historical buildings damaged during the 2009 L'Aquila earthquake," in *COST ACTION C26: Urban Habitat Constructions under Catastrophic Events - Proceedings of the Final Conference* (Naples), 427–432.

Laterza, M., D'Amato, M., and Casamassima, V. M. (2017a). Stress-life curves method for fatigue assessment of ancient brick arch bridges. *Int. J. Archit. Heritage* 11. 843–858. doi: 10.1080/15583058.2017.1315621

Laterza, M., D'Amato, M., and Casamassima, V. M. (2017b). "Seismic performance evaluation of multi-span existing masonry arch bridge," in *AIP Conference Proceedings, 1863, art. no. 450010. International Conference of Numerical Analysis and Applied Mathematics 2016, ICNAAM 2016* (Rhodes).

Lopez, S., D'Amato, M., Ramos, L., Laterza, M., and Lourenço, P. B. (2019). Simplified formulation for estimating the main frequencies of ancient masonry churches. *Front. Built Environ.* 5:18. doi: 10.3389/fbuil.2019.00018

Luchin, G., Ramos, L. F., and D'Amato, M. (2018). Sonic tomography for masonry walls characterization. *Int. J. Architec. Heritage.* doi: 10.1080/15583058.2018.1554723. [Epub ahead of print].

Melbourne, C., Tomor, A. K., and Wang, J. (2004). "Cyclic load capacity and endurance limit of multi-ring masonry arches," in *Arch Bridge '04" Conference Proceedings* (Barcelona), 375–384.

Melbourne, C., Wang, J., and Tomor, A. K. (2007). "A new masonry arch bridge assessment strategy (SMART)," in *Proceedings of the Institution of Civil Engineers-Bridge Engineering, 160* (London, UK).

Milani, G., Formisano, A., and Fabbrocino, F. (2018). Design of new structures and vulnerability reduction of existing buildings in presence of seismic loads: Open challenges. *AIP Conf. Proceed.* 1978:450001. doi: 10.1063/1.5044055

Ministerial Decree D.M. 14/01/2008 (NTC-08) (2008). *Norme Tecniche per le Costruzioni. S.O. n. 30 of the Official Gazette of the Italian Republic.*

Mu, B., and Shah, S. (2005). Fatigue behavior of concrete subjected to biaxial loading in the compression region. *Mater. Struct.* 38, 289–298. doi: 10.1007/BF02479293

Pelà, L., Aprile, A., and Benedetti, A. (2009). Seismic assessment of masonry arch bridge. *Eng. Struct.* 31, 1777-1788. doi: 10.1016/j.engstruct.2009.02.012

Ramirez, E., Lourenço, P. B., and D'Amato, M. (2019). "Seismic assessment of the Matera Cathedral," in *Proceedings of SAHC 2018, 11th International Conference on Structural Analysis of Historical Constructions. RILEM Bookseries 18* (Perù), 1346–1354.

Roberts, T. M., Hughes, T. G., Dandamudi, V. R., and Bell, B. (2006). Quasi-static and high-cycle fatigue strength of brick masonry. *J. Constr. Build. Mater.* 20, 603–614. doi: 10.1016/j.conbuildmat.2005.02.013

Ronca, P., Franchi, A., and Crespi, P. (2004). "Structural failure of historic buildings: masonry fatigue tests for an interpretation model," in *Proceeding Paper of the Fourth International Conference on Structural Analysis of Historical Constructions* (Bologna), 273–279.

Sarhosis, V., Milani, G., Formisano, A., and Fabbrocino, F. (2018). Evaluation of different approaches for the estimation of the seismic vulnerability of masonry towers. *Bull. Earthq. Eng.* 16, 1511–1545. doi: 10.1007/s10518-017-0258-8

Schueremans, L., and Van Gemert, D. (2001). "Assessment of existing structures using probabilistic methods-state of the art, Computer methods in structural masonry-5," in *Proc. Fifth Int. Symp. Computer Methods in Structural Masonry* (Rome), 255–262.

Shakya, M., Varum, H., Vicente, R., and Costa, A. (2016). Empirical formulation for estimating the fundamental frequency of slender masonry structures. *Int. J. Architect. Heritage* 10, 55–66. doi: 10.1080/15583058.2014.951796

Tomor, A., and Verstrynge, E. (2013). A joint fatigue–creep deterioration model for masonry withacoustic emission based damage assessment. *Construct. Build. Mater.* 43, 575–588.

Vicente, M., Gonzalez, D., Minguez, J., and Martinez, J. (2014). Residual modulus of elasticity and maximum compressive strain in HSC and FRHSC after high-stress-level cyclic loading. *Struct. Concrete.* 15, 210–218. doi: 10.1016/j.conbuildmat.2013.02.045

Zanuy, C., Albajar, L., and De la Fuente, P. (2011). The fatigue process of concrete and its structural influence. *Mater. de Constr.* 61, 385–399. doi: 10.3989/mc.2010.54609

# Seismic Vulnerability Analysis and Retrofitting of the SS. Rosario Church Bell Tower in Finale Emilia (Modena, Italy)

Antonio Formisano[1]* and Gabriele Milani[2]

[1] Department of Structures for Engineering and Architecture, School of Polytechnic and Basic Sciences, University of Naples "Federico II", Naples, Italy, [2] Department of Architecture, Built Environment and Construction Engineering, Politechnic of Milan, Milan, Italy

The Italian territory is rich of constructions belonging to the architectural heritage which deserve to be protected against earthquakes. In seismic prone areas ecclesiastic complexes, including churches, bell towers, monasteries, basilicas, synagogues, cathedrals and so on, have shown to be very susceptible at damage, even with partial or total collapses, when undergoing earthquakes. Indeed, these constructions, which are usually designed to withstand gravity loads only, are characterized by slender walls, lack of horizontal floors, bad quality of the masonry apparatus, ineffective connections among walls and between roofs and walls and absence of tie-beams absorbing the thrusts of arches and vaults. All these issues are responsible of the damages suffered by these structures, as detected after the last Italian earthquakes, such as those occurred in L'Aquila (2009), Emilia-Romagna (2012), Central Italy (2016), and Ischia (2017). In the current paper the seismic vulnerability assessment of the bell tower of the SS. Rosario ecclesiastic complex in Finale Emilia (district of Modena, Italy) is presented and discussed. After the geometrical and structural surveys of the whole masonry structure have been performed, the global seismic analysis of the bell tower by the 3Muri analysis software has been done. In particular, the behavioral differences between the isolate condition of the tower and the case within the ecclesiastic complex have been highlighted, showing the aggregate beneficial effect. Finally, proper retrofitting interventions have been designed and applied to the masonry bell tower, considered both as isolate construction and aggregate one, and the different benefits deriving from these interventions in the two inspected cases have been emphasized.

Keywords: masonry church, masonry bell tower, Emilia-Romagna earthquake, aggregate condition, collapse mechanisms, non-linear static analyses, upgrading and retrofitting interventions

## INTRODUCTION

Italy is rich of masonry constructions belonging to the architectural heritage, but the majority of them require to be protected against earthquakes. In seismic areas, religious complexes, such as churches, bell towers, monasteries, etc., have shown to be very vulnerable, experiencing partial or total collapses (Doglioni et al., 1994; Krstevska et al., 2010; Tashkov et al., 2010; Lagomarsino, 2012; Brandonisio et al., 2013; Criber et al., 2015; D'Amato et al., 2018; Formisano et al., 2018b).

Indeed, these constructions, which are usually designed to withstand gravity loads, are sometimes characterized by slender walls, flexible floors, bad quality of the masonry material, bad interlocking among perpendicular walls and between roof and walls and absence of tie-beams able to absorb the thrusts of arches and vaults. All these issues are responsible of critical damages suffered by such structures, as observed during the last Italian earthquakes, such as those occurred in L'Aquila (2009), Emilia-Romagna (2012), Central Italy (2016), and Ischia (2017). The evaluation of masonry seismic vulnerability is still an open issue, despite advanced research became popular in the last few years. Italy—as the country most reach in monumental churches and bell towers - has conceived *ad-hoc* Guidelines for the built heritage (DPCM, 2011), a code which provides dedicated methodologies mostly for churches, palaces and towers. Such methodologies are simplified by purpose, because they must be handled by common practitioners, which will produce quick assessments of the seismic vulnerability case by case. Whilst such Guidelines are probably one of the most advanced assessment method, they still exhibit important critical issues to be further improved or refined. Alternative approaches foresee large scale seismic vulnerability evaluation methods based on survey forms related to the main features of religious constructions and their damages suffered under last earthquakes (Criber et al., 2015; De Matteis et al., 2016; Formisano et al., 2017).

Limiting the discussion to churches, the ultimate load carrying capacity under horizontal loads, i.e., the ratio between horizontal failure acceleration and gravity acceleration, is estimated using the kinematic theorem of limit analysis on so called pre-assigned failure mechanisms, which are macro-blocks forming a kinematic chain. The material is assumed, on the safe side, as unable to withstand tensile stresses, so that internal power dissipation (which favors equilibrium) on cracks or yield lines is disregarded.

Since the actual failure mechanism activating is in principle unknown, an abacus of the most probable mechanisms as observed during past earthquakes is provided with exemplificative sketches on generic geometries. They are 28, all local, and the most common include façade and tympanum overturning, apse shear and rocking failure, triumphal arch four-hinges mechanisms, etc. (Casolo et al., 2000; Casolo and Uva, 2013; Casolo, 2017).

The repeated application of the kinematic theorem of limit analysis on the different mechanisms allowed to collect a database of normalized accelerations at collapse ($a_g/g$) with their corresponding failure mechanism. The mechanism associated to the smallest collapse acceleration is that collapsing first with the highest probability. The classification of the most dangerous mechanisms is also important for an effective strengthening intervention; as a matter of fact, it is not sufficient to increase the load carrying capacity of the most critical mechanism, because it may happen that other local mechanisms, geometrically far from the previous one, exhibit load carrying capacities slightly larger. The resultant seismic improvement for the whole structure would be totally ineffective, because limited to the worst case without considering the other (almost) critical conditions.

Limit analysis on pre-assigned failure mechanisms appears therefore to the Authors rather appealing, because it can be applied immediately by users not familiar with structural analyses

and earthquake engineering. However, there are also some limitations that one should point out, the most important being to limit the research of the active mechanism to only 28 different configurations. Designers are nowadays familiar with 3D geometric modelers integrating with Finite Element (FE) codes, a trend going exactly on the opposite direction. Limit analysis by Italian Guidelines requires at hand or semi-automatic calculations, or procedures that are still far to be fully automated, where the exact geometries and position of the loads in the church are unavoidably lost to simplify the approach.

The presence of complex clusters of arches, vaults and roofs cannot be handled manually if the problem is the passage between a 3D detailed model and limit analysis calculations. Then, the application of the gravity loads is done basically in an isostatic fashion, again disregarding the complex interaction in terms of thrust lines between vaults and columns at the intersection region. Typically, the collapse loads obtained with limit analysis result very conservative and very sensible to the assumptions done on the interlocking between perpendicular walls. However, to propose sophisticated nonlinear 3D FE approaches is not possible for common design studies (Betti and Vignoli, 2011; Milani and Venturini, 2011; Brando et al., 2015; Milani and Valente, 2015; Clementi et al., 2017; Giordano et al., 2019).

To assume masonry behaving as a no-tension material is certainly done on the safe side, but some important features of the masonry material are neglected, such as orthotropy, limited compressive strength and shear-normal stress interaction (Milani et al., 2006).

For towers, it is intuitive that the most accurate approach to deal with the analysis under horizontal loads should require specific *ad-hoc* FE approaches, because the extreme level of complexity necessitates a certain accuracy. Again however, to use non-linear methods and full 3D Finite Element models is quite uncommon, requires powerful and expensive FE codes and skilled users. Alternative effective investigations are provided by structural health monitoring analyses (Ubertini et al., 2017, 2018). Using the same philosophy adopted for churches, the Italian code for the built heritage (DPCM, 2011) allows to utilize a simplified model which considers the tower as a cantilever beam, where only flexural failure is possible. The advantage is again the utilization of a method that can be handled without a FE code and with no particular structural expertise, whereas the disadvantage is here the impossibility to account for a combined shear and flexural failure of the towers, which in practice is common in case of low slenderness (Milani et al., 2018). In the case of towers, this is a major limitation, because the risk is to identify possible zones of weakness on the base of a wrong failure mode, with the subsequent implementation of an ineffective strengthening intervention.

In this scenario, where Italian Guidelines push the research forward on simplified methods and the most diffused international trend is to use very sophisticated FE codes (Milani et al., 2011; Casolo et al., 2013; Acito et al., 2014; Valente and Milani, 2016; Marra et al., 2017; Sarhosis et al., 2018), a research lying in between such two extreme positions is needed.

In particular, in the present paper, the capabilities and limitations of a simplified modeling technique based on the "Equivalent Frame" are discussed on a historical masonry church

severely damaged by an earthquake. The substitution of piers and spandrels with an equivalent frame made by non-linear beams proved to be effective also for historical buildings, at least in presence of generally regular walls, giving thus the possibility to all practitioners working in the safety assessment of historical buildings, to perform easily pushover analyses. However, also in case of regular constructions, it could be questionable to use this approach, regularly applied to framed structures, for masonry church characterized by massive piers and spandrels not comparable to slender columns and beams composing RC and steel frames. Moreover, the poor performances exhibited by historical and monumental masonry constructions during the last earthquakes required the use of proper upgrading and retrofitting interventions, whose effectiveness has been investigated by many researchers (Faggiano et al., 2009; Grande et al., 2011; Grande and Milani, 2016, 2018; Formisano and Marzo, 2017; Mosoarca et al., 2017; Formisano et al., 2018a, 2019), also with reference to large scale applications on whole historical centers (Brando et al., 2017; Rapone et al., 2018; Chieffo et al., 2019).

The meaningful case under study is the SS. Rosario church located in Finale Emilia with particular reference to its bell tower. The aim is to provide conclusions and recommendations that could hold also in different cases, using as base a simple numerical model that can be used by anyone. After the geometrical and mechanical characterization of the masonry complex, first the global seismic analysis of the bell tower by the 3Muri software is done. In particular, the behavioral differences between the isolate condition of the tower and the case when the whole neighboring complex is modeled, show that the presence of the aggregate has a beneficial effect on the tower. Finally, proper retrofitting interventions are designed and applied to the masonry bell tower, considered both as isolate or not; the different benefits deriving from these interventions in the two inspected cases are also emphasized.

## THE EMILIA-ROMAGNA EARTHQUAKE

On 2012 May 20th and 29th two earthquakes with local magnitude (ML) of 5.9 and 5.8 on the Richter scale, respectively, struck the Emilia-Romagna region of Italy. The first mainshock had epicenter between Mirandola and Finale Emilia, in the district of Modena, and hypocentre at about 6.3 km. It was followed by several aftershocks, also with magnitude greater than 5. The second mainshock had epicenter at Medolla, very close (about 10 Km west) to the first mainshock location, and hypocentre at about 10.2 km. Also this earthquake was followed by numerous aftershocks (http://ambiente.regione.emilia-romagna.it/en/geologia/temi/sismica/earthquake-20-may-2012).

The performed analyses (Galli et al., 2012) classified the largest shocks (seven with magnitude greater or equal than 5 in the period May-June 2012) as very strong with levels VII-VIII on the MCS intensity scale. The same intensity was also recorded in this area in 1346, in 1570 and in 1796 (Locati et al., 2011). In particular, the 2012 earthquakes had many analogies with the 1570 seismic event occurred in Ferrara.

From the geological point of view, the territory struck by the seismic sequence belongs to the Po Plain and is morphologically uniform, whereas the subsoil is rather more complex, with a series of geological structures, running parallel to the Apennines, which are seismically active.

Peak Ground Acceleration (PGA) values recorded during the 2012 earthquakes were rather high in some areas, in some cases also over 20% the gravity acceleration. Contrary, the ground accelerations expected on the basis of the Italian seismic hazard map were equal to about 0.15 g. This significant acceleration increase can be attributed to the subsoil local characteristics, leading to the so-called site effects connected to the lithological and geomorphologic features. In particular, loose, and poorly consolidated terrains (i.e. recent alluvial sediment, lacustrine and marine deposits, etc.) can modify the propagation of seismic waves upwards, amplifying the shaking extent and duration.

This amplification effect in the subsoil upper portion was also one of the causes of the liquefaction, that is the most striking environmental phenomenon observed during the Emilia-Romagna seismic sequence. The liquefaction is connected to different physical phenomena, such as cyclic mobility, cyclic and flow liquefactions, observed in saturated sandy deposits during strong earthquakes and extending in some cases for tens of meters. The phenomenon occurs when some conditions (uncemented and loose sand at a depth of less than15-20 m, depth of water table less than 15 m, size of sand grains from 0.02 to 2 mm and fine sediment content less than 15%) meet given earthquake properties (magnitude above 5.5, PGA equal to 15% of g and duration of shaking at least 15-20 s).

In the Po plain area the occurred strong earthquakes released the energy required to activate the liquefaction phenomenon. While in the past earthquakes liquefaction occurred away from built areas, during the 2012 seismic events the phenomenon involved several urbanized zones (especially S. Carlo, a hamlet of S. Agostino, and Mirabello, both in the district of Ferrara), causing extensive damages, such as rigid translation settlements of constructions, in some cases with a slight rotational component, and shear failure of joints, occurred in structurally weak buildings (garages, sheds, etc.), which were demolished after the earthquake.

The combined effect of high magnitude earthquakes with liquefaction phenomena gave rise to a long seismic sequence causing heavy damages and collapses (partial or total) especially to cultural heritage constructions, namely castles and towers, churches, bell towers and palaces. In the paper the case study of a masonry bell tower affected by the 2012 earthquake has been faced with the purpose of highlighting its seismic behavior as a part of an ecclesiastic complex.

## THE SS ROSARIO ECCLESIASTIC COMPLEX
### Knowledge Phase and Historical Information

The knowledge of historical masonry constructions is a fundamental prerequisite both for the purpose of a reliable seismic safety evaluation and the choice of effective upgrading

or retrofitting interventions. The problems are those common to all the existing buildings even if, in the case of the cultural heritage to be protected, even more important is to know the original characteristics of the construction, the changes occurred during the time, the damage phenomena caused by anthropic transformations, the aging of materials and the occurred hazardous events. It is, therefore, necessary to refine analysis techniques and interpretation of historical artifacts through cognitive phases of different reliability degree also in relation to their impact. The knowledge can be achieved with different levels of deepening in terms of survey operations accuracy, historical researches and experimental investigations.

The study of the construction features is aimed at the definition of an interpretative model that allows for both a qualitative interpretation of the structural functioning and the structural analysis for a quantitative seismic evaluation. The degree reliability of this model will be closely related to the used deepening level and to the available data. From this point of view, different knowledge levels, namely limited, adequate and accurate according to increasing information levels, can be attained, they being linked to corresponding confidence factors [Ministerial Decree (NTC), 2008, 2018; Ministerial Circular (MC), 2009]. The knowledge path can be traced back to the following activities:

- Identification of the construction, its localization in relation to particular areas at risk and its relationship with the urban context. In particular, the analysis consists on the schematic survey of the artifact and the identification of any valuable elements (fixed decorative apparatus, movable artistic goods, etc.) that can affect the level of risk; geometric survey of the construction in the present state, including any cracks and deformation phenomena; relief of materials to completely identify the resistant structure of the artifact, keeping in mind their quality and preservation state.
- The evolution of the construction, understood as a sequence of transformation phases from the hypothetical original configuration to the present state;
- The identification of seismic-resistant elements, with particular attention to the erection techniques, to the constructive details and to the connections among elements;
- The recognition of materials, together with their state of decay and mechanical properties;
- Knowledge of the subsoil and of the foundation structures, also with reference to the changes and failures that took place during the time.

The knowledge phase activities above listed have been used to characterize the SS. Rosario ecclesiastic complex placed in Finale Emilia, that is the most eastern municipality of the province of Modena, in the corner between Andrea Costa street and Guglielmo Oberdan one (**Figure 1A**).

The Church of the Rosary was built around 1580. The original structure, built on the ground of the old ditch of the northern walls, was originally smaller and simpler than the current one, which dated back to the second half of the seventeenth century, when behind the main altar there was probably also a sacristy compartment. A century later, the altar was set back and a compartment of octagonal shape, housing the sacristy, was

created (**Figure 1B**). In 1646 the carved altars made of timber were manufactured and the ground was acquired to obtain a forecourt. Probably, in that time the church was enlarged. In the first decades of the nineteenth century, with the Napoleon's government, the church passed to the demesne and it was used as a barracks for the French soldiers under the orders of General Montrizard. Such a condition caused enormous damage to the building. With the fall of Napoleon and after the request of the bishop, the confreres of the Rosary resumed possession of their ancient seat, restored the Brotherhood and undertook to reopen the church, which was however deprived of many of its assets. In 1814 the sacristy modified its shape from octagonal to rectangular, also annexing the rectory and the stairs for access to the upper floor (**Figure 2A**). The bell tower was built only in 1856 and later on, in 1890, the façades were also transformed in the neoclassical style (**Figure 2B**). Starting from 1928, the church and the bell tower were restored. Damaged during the bombardments of the Second World War, the bell tower was again restored in 1955. In 1975 the building was closed to the faithful cult to eliminate the problems of humidity by means of both the total renovation of the roof and floor and the renovation of walls. Suspended and resumed several times during 90s, the restoration interventions ended in 1997.

## Geometrical and Structural Surveys

The church can be considered as composed, both from the purely geometrical point of view and the structural one, of two in-plane rectangles. In fact, thinking to the different "stratifications" followed during the time, the construction can be divided into two structural bodies:

- part A, understood as the original body of the complex, containing the central nave and the altar;
- part B, considered as the most recent structure, containing the sacristy, the dormitory and the hospitalization.

The structural part A (**Figure 3**) has plan measures of $24.00 \times 11.20$ m, excluding ornamental elements, and develops on a maximum total height (at the ridge) of 16.50 m. The coverage is represented by a pitched roof made of timber beams with pushing actions. On the long side of the church there are numerous shelters in the masonry walls in order to host the altars and the chapels, as well as two openings, one on the street side and the other toward the inner courtyard.

The structural part B (**Figure 4**), instead, has plan dimensions of $26.50 \times 7.30$ m and develops on two levels, one at the ground floor with height of 3.70 m and the other at the first floor with height equal to 4.60 m. The total height at the ridge of this structural part is 10.70 m. On the facades there are several openings with arched shape. Vaulted floors, which in some cases are masked by false ceilings, represent the horizontal structures.

From the structural point of view, since walls are covered by plaster, it is not simple to evaluate, on the basis of a visual investigation only, the typology of the load-bearing vertical structure.

Nevertheless, from the historical analysis of the artifact, it is possible to assume that the major structural criticisms are relative to the poor connections among masonry walls in the
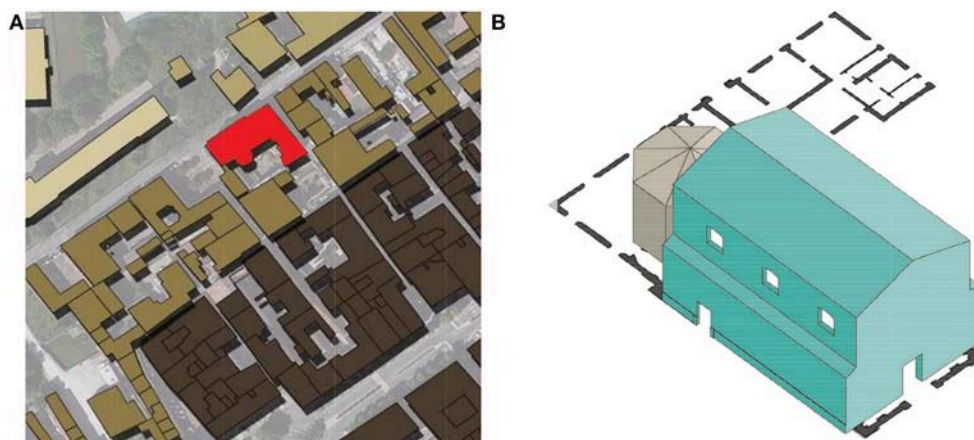
**FIGURE 1 |** Bird-eye-view (highlighted in red) **(A)** and original configuration **(B)** of the SS. Rosario ecclesiastic complex in Finale Emilia.
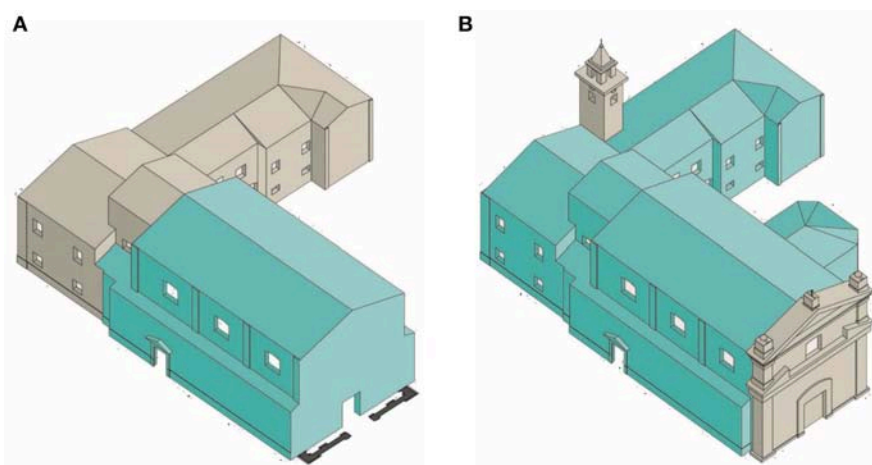


**FIGURE 2 |** Transformed configuration dated back to the 1814 of the SS. Rosario church **(A)** and renovation intervention of the façade in 1890 **(B)**.

zone between body A and body B, which were erected in different historical periods.

The vertical structures able to withstand loading actions are made of masonry bricks held together by lime mortar joints according to the constructive techniques of that erection time. In order to acquire these information so to eliminate some sources of initial uncertainty, it is usually made recourse to non-destructive indirect investigation techniques (thermography, georadar, sonic tomography, etc.) or weakly destructive direct inspections (endoscopies, peeling of plasters, essays, etc.) to be performed in significant points of the structure. In the case under study, unfortunately, since it has not been possible to carry out any kind of investigation tests, only a limited knowledge level has been attained and assumptions on the safe side both in terms of masonry mechanical properties and confidence factor have been used. Therefore, the knowledge level LC1 according to the provisions of the current Italian technical code [Ministerial Decree (NTC), 2018] has been taken

into account. This knowledge status has been attained since survey of the ecclesiastic complex (church, sacristy and bell tower) has been done and some limited visual observations on the quality of masonry and effectiveness of connections among walls have been carried out. As a consequence, the minimum levels of stresses and the average elastic modules for brick masonry deduced from the table reported in the Ministerial Circular 2 February 2009 [Ministerial Circular (MC), 2009], an explicative code of the NTC 2008 standard, have been considered.

No specific geological and geotechnical tests have been performed to know in detail the subsoil stratigraphy and the physical-mechanical characteristics of the soil. However, from a significant number of geotechnical investigations in areas close to the church one, it has been possible to identify from the seismic point of view, according to the NTC 2008, a soil of type D, that is "deposits of coarse-grained soils, sparsely thickly or poorly sizeable fine grained soils, with thicknesses exceeding
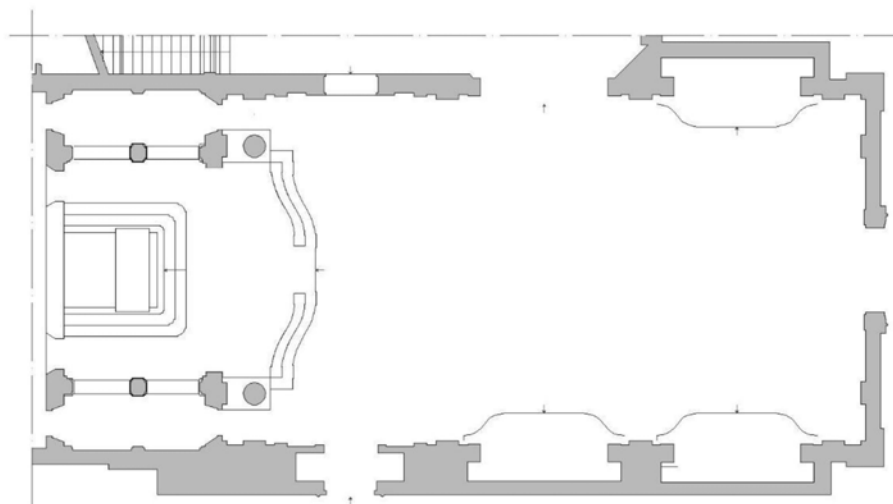
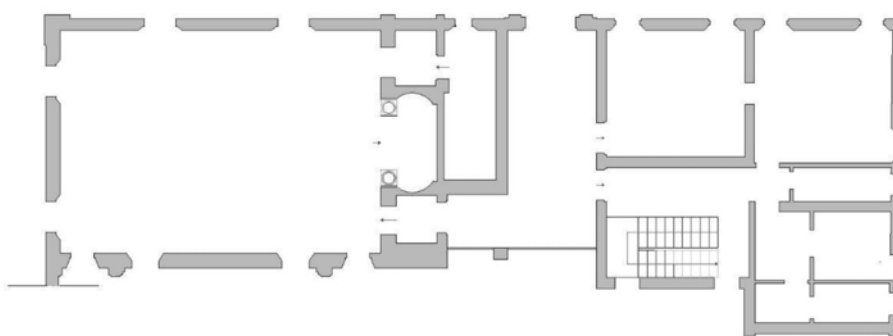**FIGURE 3 |** Structural Part A of the church.



**FIGURE 4 |** Structural Part B of the church.

30 m, characterized by a gradual improvement of the mechanical properties with the depth".

## SEISMIC VULNERABILITY ASSESSMENT

### Foreword

Seismic vulnerability analyses have been performed by using the 3Muri software, which uses the well-known Frame-by-Macro-Element (FME) approach to model masonry walls (S.T.A.DATA srl, 2018). In this software piers and spandrels are modeled as deformable macro-elements, while the nodes between vertical elements and horizontal ones are considered as rigid parts, considering that they exhibited very few damages under earthquakes. After the whole macro-elements structural model is setup, it is transformed into the classic Equivalent Frame Model (EFM), used to seismically analyse framed structures. On this EFM, dynamic linear and static non-linear analysis are carried out in the two main analysis directions aiming at evaluating the probable seismic damages.

In the case under study, the bell tower has been modeled as isolate structure and, subsequently, as a part of the ecclesiastic complex in order to evaluate the behavioral differences under seismic actions in the non-linear static field between the two modeling approaches. Based on the vulnerability assessment analysis results, proper seismic upgrading and retrofitting interventions have been considered and applied to both analysis models in order to increase the seismic performance of the inspected bell tower.

### The Isolate Bell Tower

Initially, the masonry bell tower has been modeled as isolate structure. Geometrical and mechanical features of the structure have been taken according to the information achieved from the historical-critical analysis of the artifact. The geometrical layout and the FME model of this structure modeled with the 3Muri software are shown in **Figure 5**. Seismic actions have been taken according to the response spectra given by \$\$NTC 2008 at the Collapse, Life Safety, Operational and Damage Limit States for constructions of class

II (use coefficient of 1.0) placed in Finale Emilia (district of Modena), founded on a soil type D with topographic class T1 (amplification coefficient equal to 1) and having nominal life of 50 years. The fundamental parameters used to characterize the elastic spectra at different limit states are depicted in **Table 1**.

24 pushover analyses, different for analysis direction (x and y), loading type (proportional either to masses or to the first vibration mode) and eccentricities (positive and negative) between centroid and stiffness center, have been performed (**Table 2**). The pushover analysis results showed that, since the seismic risk coefficients α are always less than 1, all seismic checks are not satisfied. The worst results are related to the analyses n. 12 and n. 24 in directions x and y, respectively, which are highlighted with bold text in **Table 2**. The final deformed shapes of the masonry bell tower at the end of these pushover analyses are plotted in **Figures 5C,D**, where it is apparent that failure mechanisms are concentrated at the ground level in direction x and at the penultimate level in direction y. The MDOF pushover curves related to the main analysis directions are plotted in **Figure 6**. In **Table 3** the seismic verifications in terms of displacements, leading to the so-called Vulnerability Index (VI), are reported. In this table $D_{max}$ and $D_u$ are the seismic demand displacement and the capacity one, respectively, while $q^*$ is the ratio between the elastic response resistance and the yielding resistance of the SDOF system. Also, comparing the results in terms of displacements, it is achieved that the bell tower is not able to resist the standard seismic actions and that the worst result is obtained in the direction y.

## The Aggregate Bell Tower

The seismic behavior of the bell tower has been also investigated when it is included in the aggregate of constructions given by the ecclesiastic complex, whose 3D geometrical and macro-element models are depicted in **Figure 7**.

In this case the pushover curves of the bell tower have been reconstructed starting from those of the ecclesiastic complex by monitoring step-by-step both the base shear of own masonry walls (considering the influence of loads transmitted by the adjacent parts of the church) and the displacements of the top level centroid. For the sake of comparison, the MDOF bi-linear pushover curve of the bell tower related to the analysis n. 24 in direction y, which corresponds the worst result to, has been plotted and compared to that of the isolate structure, as reported in **Figure 8A**.

The final deformation of the structure corresponding to this analysis is shown in **Figure 8B**, where it is noticed that, differently from the isolate case, the bending-compression failure of the top level occurs.

TABLE 1 | Seismic parameters of elastic spectra according to the NTC 2008 standard.

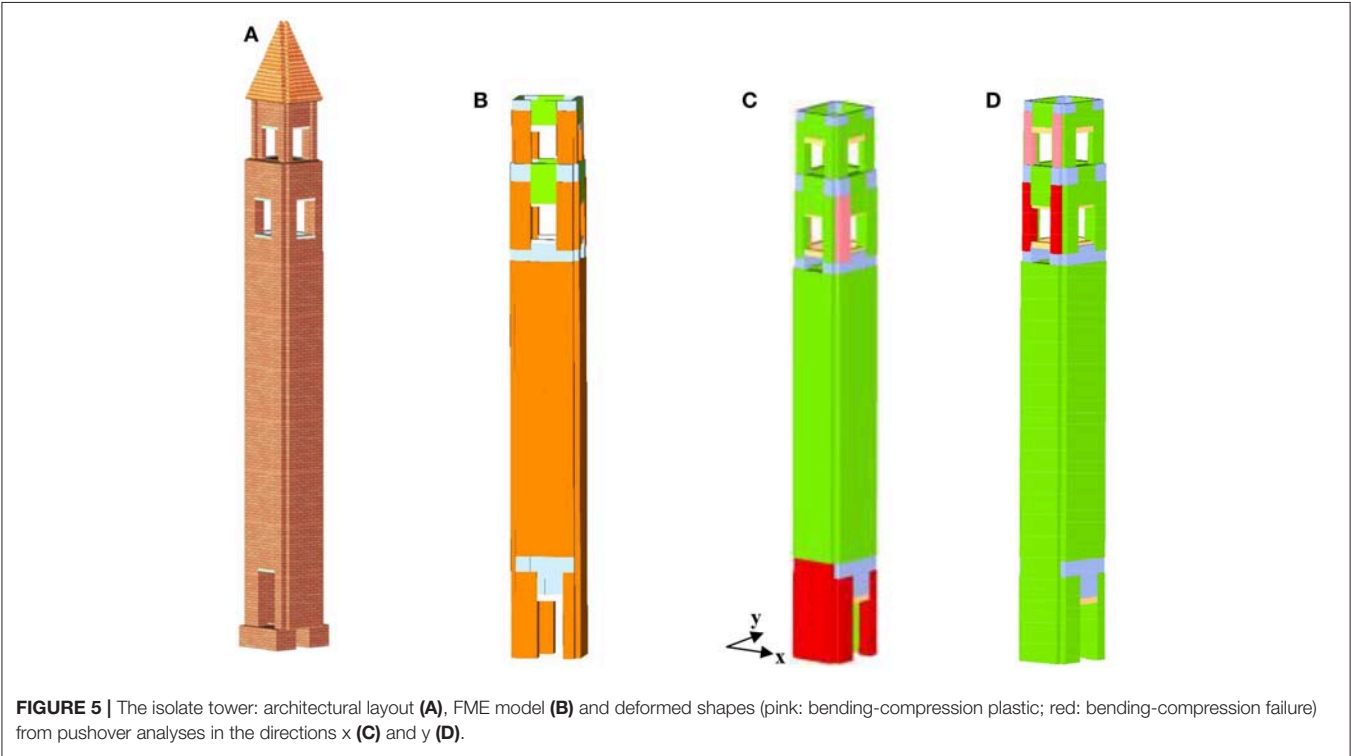| Limit state | Return period $T_R$ [years] | $a_g$ [g] | $F_0$ [–] | $T_C^*$ [s] |
|---|---|---|---|---|
| Operational (OLS) | 30 | 0.039 | 2.562 | 0.253 |
| Damage (DLS) | 50 | 0.051 | 2.475 | 0.268 |
| Life safety (LSLS) | 475 | 0.149 | 2.589 | 0.270 |
| Collapse (CLS) | 975 | 0.200 | 2.537 | 0.277 |



FIGURE 5 | The isolate tower: architectural layout **(A)**, FME model **(B)** and deformed shapes (pink: bending-compression plastic; red: bending-compression failure) from pushover analyses in the directions x **(C)** and y **(D)**.

| No. | Analysis direction | Type of seismic loading | Eccentricity [cm] | $\alpha_{LSLS}$ | $\alpha_{DLS}$ | $\alpha_{OLS}$ |
|---|---|---|---|---|---|---|
| 1 | +X | Mass | 0.0 | 0.308 | 0.720 | 0.606 |
| 2 | +X | 1st mode | 0.0 | 0.297 | 0.573 | 0.481 |
| 3 | −X | Mass | 0.0 | 0.324 | 0.815 | 0.743 |
| 4 | −X | 1st mode | 0.0 | 0.441 | 0.668 | 0.596 |
| 5 | +Y | Mass | 0.0 | 0.431 | 0.697 | 0.635 |
| 6 | +Y | 1st mode | 0.0 | 0.256 | 0.566 | 0.505 |
| 7 | −Y | Mass | 0.0 | 0.389 | 0.567 | 0.476 |
| 8 | −Y | 1st mode | 0.0 | 0.254 | 0.468 | 0.387 |
| 9 | +X | Mass | 8.4 | 0.306 | 0.716 | 0.603 |
| 10 | +X | Mass | −8.4 | 0.304 | 0.724 | 0.609 |
| 11 | +X | 1st mode | 8.4 | 0.310 | 0.569 | 0.478 |
| **12** | **+X** | **1st mode** | **−8.4** | **0.280** | **0.576** | **0.503** |
| 13 | −X | Mass | 8.4 | 0.386 | 0.811 | 0.739 |
| 14 | −X | Mass | −8.4 | 0.302 | 0.819 | 0.746 |
| 15 | −X | 1st mode | 8.4 | 0.507 | 0.664 | 0.593 |
| 16 | −X | 1st mode | −8.4 | 0.374 | 0.671 | 0.600 |
| 17 | +Y | Mass | 10.7 | 0.408 | 0.701 | 0.639 |
| 18 | +Y | Mass | −10.7 | 0.364 | 0.678 | 0.632 |
| 19 | +Y | 1st mode | 10.7 | 0.270 | 0.568 | 0.524 |
| 20 | +Y | 1st mode | −10.7 | 0.263 | 0.549 | 0.502 |
| 21 | −Y | Mass | 10.7 | 0.382 | 0.570 | 0.479 |
| 22 | −Y | Mass | −10.7 | 0.401 | 0.564 | 0.473 |
| 23 | −Y | 1st mode | 10.7 | 0.267 | 0.471 | 0.390 |
| **24** | **−Y** | **1st mode** | **−10.7** | **0.248** | **0.465** | **0.385** |



**FIGURE 6 |** Capacity curves of the isolate bell tower.
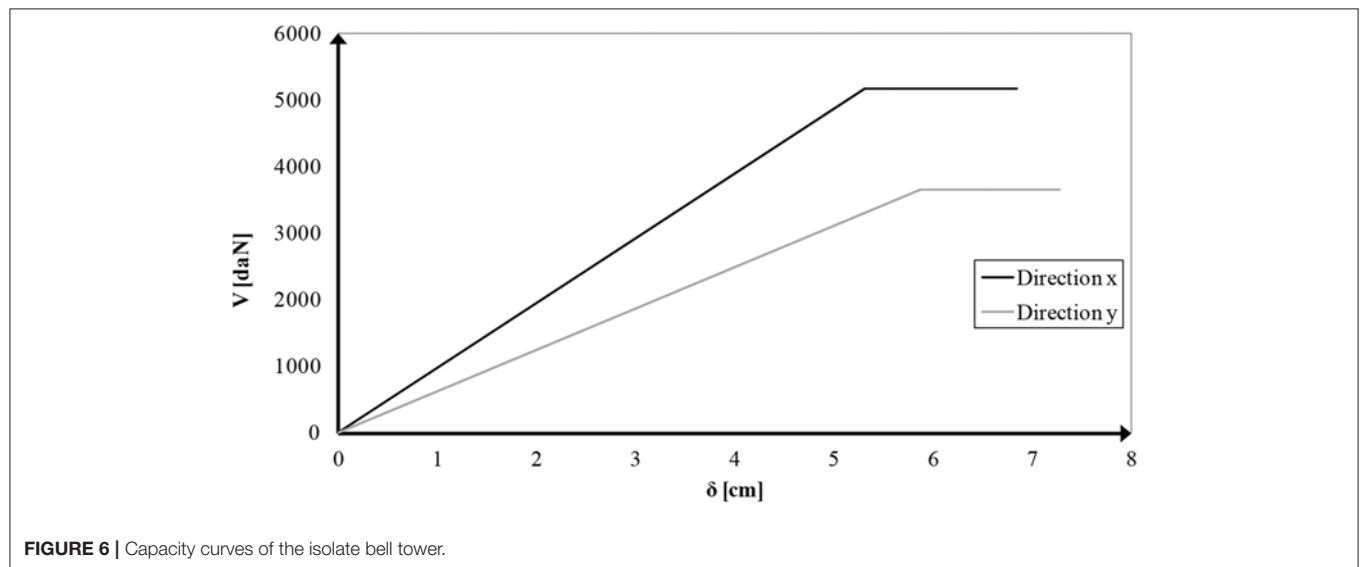
From the comparison with the isolate condition it appears that, when the bell tower is inserted in the building aggregate, the base shear is basically unaltered, while the stiffness and ultimate displacement are reduced of about 80 and 65%, respectively.

Moreover, the comparison among the isolate case and the aggregate one has been performed in the ADRS format, providing the capacity curves of **Figure 9**. The vulnerability index, intended as the ratio between the demand displacement and the capacity one, assumes values of about 4.03 and 3.15 in the cases of the isolate tower and of the aggregate one, respectively. This means that the aggregate condition reduces the seismic vulnerability of more than 20%.

**TABLE 3 |** Vulnerability indexes related to the worst pushover analyses.

| N. | Analysis direction | Type of seismic loading | Eccentricity [cm] | $D_{max}$ [cm] | $D_u$ [cm] | $V_I = D_{max}/D_u$ |
|----|--------------------|--------------------------|---------------------|-----------------|--------------|----------------------|
| 12 | +X | 1st mode | −8.4 | 24.47 | 6.85 | 3.57 |
| 24 | −Y | 1st mode | −10.7 | 29.37 | 7.28 | 4.03 |
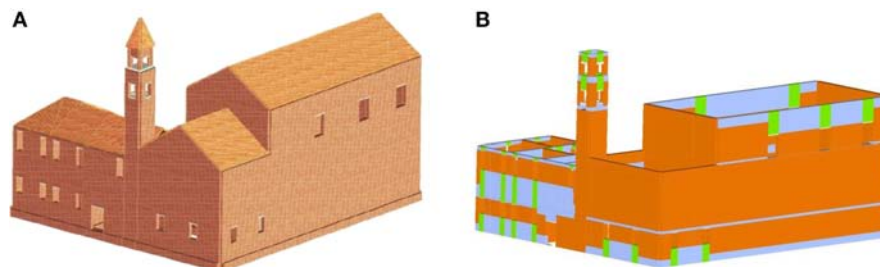


**FIGURE 7 |** 3D geometrical **(A)** and macro-element **(B)** models of the whole church.
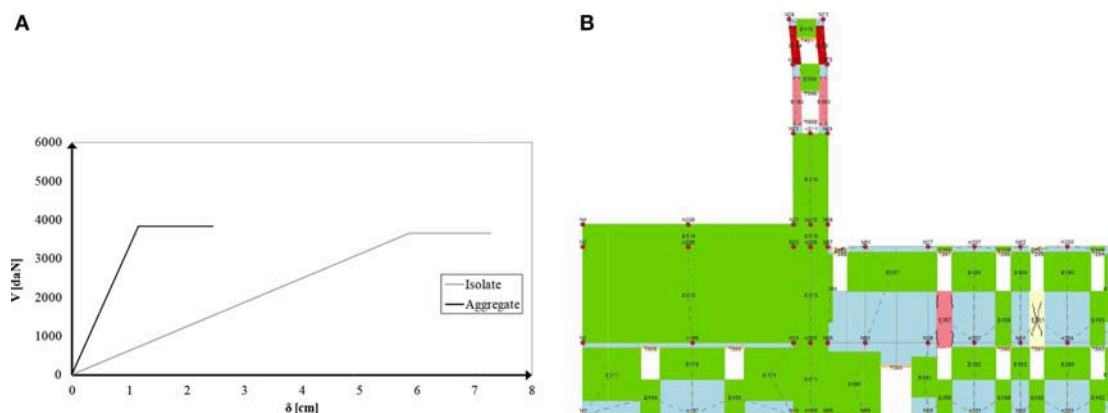


**FIGURE 8 |** Comparison between bi-linear pushover curves in direction y (analysis n. 24) of the bell tower in the two structural configurations considered **(A)** and deformed shape of the church at the end of this pushing phase **(B)**.

# ANTI-SEISMIC INTERVENTIONS

The insufficient results deriving from seismic checks have required interventions on the masonry bell tower with the purpose to be economic and easy to be implemented. In the case under study, two different interventions based on the use of either glass fibers sheets, having acronym of G-FRP, or reinforced plaster have been foreseen. In both cases they have been applied at the two last levels together with the confinement of existing openings with portals made of steel profiles. All the above interventions have been applied both to the isolate tower and to the aggregate one. In particular, two layers of glass fibers sheets, having thickness of 0.035 mm, mesh of 25 × 25 mm, elastic modulus of 72 GPa and ultimate strain of 1.8%, have been used as jacketing system of the inadequate masonry walls. These sheets have been applied on both sides of the walls between two layers of mortars and they have been connected to each other by means of appropriate glass fibers connectors. On the other hand,

reinforced plaster has been based on the use of two reinforced concrete jacketing walls armed with φ12 bars made of B450C steel arranged in meshes of 50 × 50 cm. The two reinforced walls have been connected to each other by means of φ12 steel bars placed each 50 cm in horizontal and vertical directions.

The application of the above mentioned reinforcing interventions has provided the capacity curves in the ADRS format of **Figure 10**, where the comparison with the seismic response of the isolate tower has been also reported.

From the comparison it has been achieved that the vulnerability index passes from 4.03 (isolate tower) to about 1.55 and 1.70 in the cases of interventions with G-FRP and reinforced plaster, respectively. This means that in both cases the seismic upgrading of the bell tower is achieved. Nevertheless, from the seismic point of view, intervention with G-FRP is slightly preferable to that with reinforced plaster. In fact, in the former case a reduction of seismic vulnerability of about 62% is attained, whereas in the latter one the vulnerability decrease
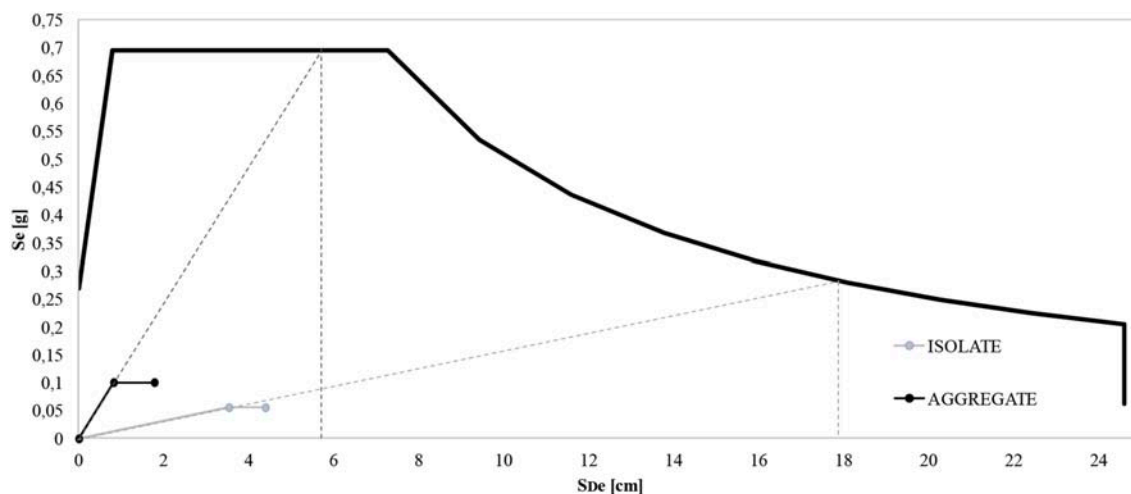
**FIGURE 9** | Comparison between capacity curves of the bell tower in the ADRS format.
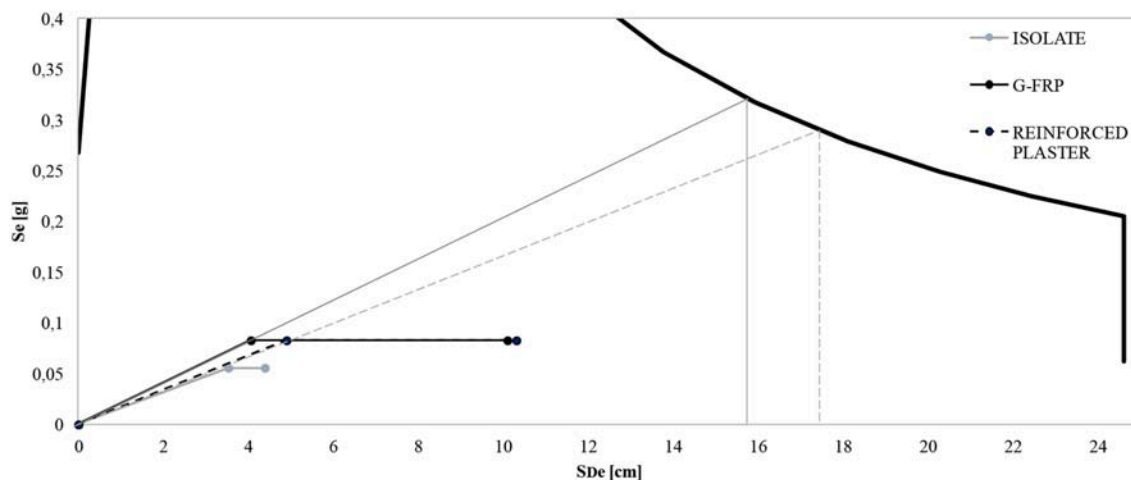


**FIGURE 10** | Comparison between capacity curves of the isolate bell tower in the ADRS format before and after retrofitting interventions.

is about 58%. Contrary, a strong preference toward G-FRP is recognized in terms of Life Cycle Assessment, since glass fibers have environmental impact lower than that of plasters reinforced with steel bars.

Finally, the same interventions above described have been applied to the case of the aggregate bell tower and the comparison among capacity curves has been done, as depicted in **Figure 11**.

From the analysis results it is obtained that the vulnerability index is changed from 3.15 (aggregate condition) to 0.85 and 0.65 in case of interventions with G-FRP and reinforced plaster, respectively. This means that, since vulnerability indexes are lower than one, both considered interventions are able to retrofit seismically the bell tower. In addition, vulnerability indexes provided by interventions with G-FRP and reinforced plaster are about 27 and 21% of the index achieved on the aggregate tower, respectively. Finally, even if more impacting from the

environmental point of view, reinforced plaster represents the best intervention, since it provides the lowest vulnerability index and it is less expensive than G-FRP.

## CONCLUDING REMARKS

The current paper has estimated the seismic vulnerability of a masonry bell tower located in the municipality of Finale Emilia, in the district of Modena (Italy), hit by the 2012 Emilia-Romagna earthquake. In particular, the difference of behavior between the isolate case and the aggregate one, the latter when the bell tower is inserted in the constructions compound, has been evaluated. From analysis results it has been seen that, in both cases, the seismic checks are not satisfied. The comparison of results in terms of pushover curve has shown that, when the tower is in aggregate, the stiffness and ultimate displacement
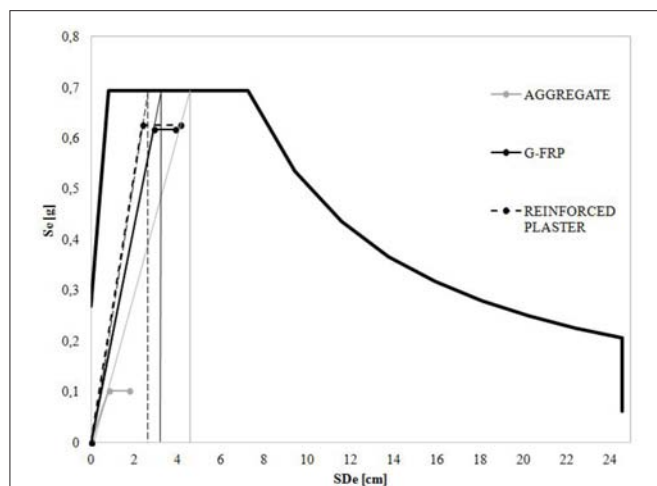
**FIGURE 11** | Comparison between capacity curves of the aggregate bell tower in the ADRS format before and after retrofitting interventions.

are reduced of about 80% and 65%, respectively, with respect to the case of the isolate structure. Besides, the aggregate condition reduces the tower seismic vulnerability of more than 20%. In the two analysis cases the same compression-bending damage mechanisms have been detected, but at different levels, i.e. the penultimate level for the isolate tower and the top level for the aggregate one.

Considering the bad seismic performance of the tower, two different interventions based on the use of either glass fibers (G-FRP) sheets or reinforced plaster have been foreseen. In both cases they have been applied at the two last levels together with the confinement of existing openings with portals made of steel profiles. These interventions have been considered both in the isolate case and in the aggregate one. From numerical

analyses, it has been shown that both interventions are able to seismically upgrade the bell tower. When the isolate tower is taken into account, intervention with G-FRP, which gives a reduction of seismic vulnerability of about 62%, is slightly preferable to that with reinforced plaster, which corresponds a vulnerability decrease of about 58% to. Moreover, G-FRP is strongly preferred to reinforced plaster if Life Cycle Assessment issues are of concern, since the former technique has a lower impact on the environment.

Contrary, the same interventions applied to the aggregate tower have lead toward the seismic retrofitting of the structure, since the achieved vulnerability indexes are lower than one. In particular, vulnerability indexes provided by interventions with G-FRP and reinforced plaster are about 27 and 21%, respectively, of the index achieved on the basic aggregate tower. As conclusion, reinforced plaster intervention, while having a higher environmental impact, has represented the best retrofitting solution, since it has provided the lowest vulnerability index, allowing also to save money with respect to applications with G-FRP.

However, the results herein presented are related to the case study examined only and, therefore, in order to generalize the obtained outcomes, parametric analyses on other masonry bell towers with different geometrical and mechanical features should be performed as a further development of the current research.

## DATA AVAILABILITY

All datasets generated for this study are included in the manuscript and/or the supplementary files.

## AUTHOR CONTRIBUTIONS

AF setup the methodology and elaborated the paper draft. GM revised the paper.

## REFERENCES

Acito, M., Bocciarelli, M., Chesi, C., and Milani, G. (2014). Collapse of the clock tower in Finale Emilia after the May 2012 Emilia Romagna earthquake sequence: numerical insight. *Eng. Struct.* 72, 70–91. doi: 10.1016/j.engstruct.2014.04.026

Betti, M., and Vignoli, A. (2011). Numerical assessment of the static and seismic behaviour of the basilica of Santa Maria all'Impruneta (Italy). *Constr. Build. Mater.* 25, 4308–4324. doi: 10.1016/j.conbuildmat.2010.12.028

Brando, G., Criber, E., and De Matteis, G. (2015). The effects of L'Aquila earthquake on the St. Gemma church in Goriano Sicoli: part II - fem analysis. *Bull. Earthquake Eng.* 13, 3733–3748. doi: 10.1007/s10518-015-9793-3

Brando, G., De Matteis, G., and Spacone, E. (2017). Predictive model for the seismic vulnerability assessment of small historic centres: application to the inner Abruzzi Region in Italy. *Eng. Struct.* 153, 81–96. doi: 10.1016/j.engstruct.2017.10.013

Brandonisio, G., Lucibello, G., Mele, E., and De Luca, A. (2013). Damage and performance evaluation of masonry churches in the 2009 L'Aquila earthquake. *Eng. Fail. Anal.* 34, 693–714. doi: 10.1016/j.engfailanal.2013.01.021

Casolo, S. (2017). A numerical study on the cumulative out-of-plane damage to church masonry façades due to a sequence of strong ground motions. *Earthquake Eng. Struct. Dyn.* 46, 2717–2737. doi: 10.1002/eqe.2927

Casolo, S., Milani, G., Uva, G., and Alessandri, C. (2013). Comparative seismic vulnerability analysis on ten masonry towers in the coastal Po Valley in Italy. *Eng. Struct.* 49, 465–490. doi: 10.1016/j.engstruct.2012.11.033

Casolo, S., Neumair, S., Parisi, M. A., and Petrini, V. (2000). Analysis of seismic damage patterns in old masonry church facades. *Earthquake Spectra* 16, 757–773. doi: 10.1193/1.1586138

Casolo, S., and Uva, G. (2013). Nonlinear analysis of out-of-plane masonry façades: full dynamic versus pushover methods by rigid body and spring model. *Earthquake Eng. Struct. Dyn.* 42, 499–521. doi: 10.1002/eqe.2224

Chieffo, N., Formisano, A., and Miguel Ferreira, T. (2019). Damage scenario-based approach and retrofitting strategies for seismic risk mitigation: an application to the historical Centre of Sant'Antimo (Italy). *Eur. J. Environ. Civ. Eng.* doi: 10.1080/19648189.2019.1596164. [Epub ahead of print].

Clementi, F., Quagliarini, E., Monni, F., Giordano, E., and Lenci, S. (2017). Cultural heritage and earthquake: the case study of "Santa Maria della Carità" in Ascoli Piceno. *Open Civ. Eng. J.* 11, 1079–1105. doi: 10.2174/1874149501711011079

Criber, E., Brando, G., and De Matteis, G. (2015). The effects of L'Aquila earthquake on the St. Gemma church in Goriano Sicoli: part I - damage

survey and kinematic analysis. *Bull. Earthquake Eng.* 13, 3713–3732. doi: 10.1007/s10518-015-9792-4

D'Amato, M., Laterza, M., and Diaz Fuentes, D. (2018). Simplified seismic analyses of ancient churches in Matera's landscape. *Int. J. Archit. Herit.* 1–20. doi: 10.1080/15583058.2018.1511000. [Epub ahead of print].

De Matteis, G., Criber, E., and Brando, G. (2016). Damage probability matrices for Three-Nave Masonry Churches in Abruzzi after the 2009 L'Aquila Earthquake. *Int. J. Archit. Herit.* 10, 120–145. doi: 10.1080/15583058.2015.1113340

Doglioni, F., Moretti, A., and Petrini, V. (1994). *Churches and Earthquake*. Rome: GNDT, Lint Press.

DPCM 9/2/2011 (2011). *Italian Guidelines for The Evaluation and The Reduction of The Seismic Risk for The Built Heritage With Reference to The Italian Norm of Constructions*. Rome: Decree of the Ministries Council Presidency.

Faggiano, B., Marzo, A., Formisano, A., and Mazzolani, F. M. (2009). Innovative steel connections for the retrofit of timber floors in ancient buildings: a numerical investigation. *Comput. Struct.* 87, 1–13. doi: 10.1016/j.compstruc.2008.07.005

Formisano, A., Ciccone, G., and Mele, A. (2017). "Large scale seismic vulnerability and risk evaluation of a masonry churches sample in the historical centre of Naples," in *AIP Conference Proceedings* (Thessaloniki), 1906. doi: 10.1063/1.5012360

Formisano, A., Di Lorenzo, G., Landolfo, R., and Mazzolani, F. M. (2018a). Seismic-volcanic vulnerability and retrofitting of a cultural heritage masonry palace in the Vesuvius area. *Int. J. Masonry Res. Innov.* 3, 244–268. doi: 10.1504/IJMRI.2018.093485

Formisano, A., and Marzo, A. (2017). Simplified and refined methods for seismic vulnerability assessment and retrofitting of an Italian cultural heritage masonry building. *Comput. Struct.* 180, 13–26. doi: 10.1016/j.compstruc.2016.07.005

Formisano, A., Vaiano, G., and Fabbrocino, F. (2019). Seismic and energetic interventions on a typical south Italy residential building: cost analysis and tax detraction. *Front. Built Environ.* 5:12. doi: 10.3389/fbuil.2019.00012

Formisano, A., Vaiano, G., Fabbrocino, F., and Milani, G. (2018b). Seismic vulnerability of Italian masonry churches: the case of the Nativity of Blessed Virgin Mary in Stellata of Bondeno. *J. Build. Eng.* 20, 179–200. doi: 10.1016/j.jobe.2018.07.017

Galli, P., Castenetto, S., and Peronace, E. (2012). The MCS macroseismic survey of the Emilia 2012 earthquakes. *Ann. Geophys.* 55, 663–672. doi: 10.4401/ag-6163

Giordano, E., Clementi, F., Nespeca, A., and Lenci, S. (2019). Damage assessment by numerical modelling of Sant'Agostino's sanctuary in Offida during the central Italy 2016-2017 seismic sequence. *Front. Built Environ.* 4:87. doi: 10.3389/fbuil.2018.00087

Grande, E., Imbimbo, M., and Sacco, E. (2011). Bond behaviour of CFRP laminates glued on clay bricks: experimental and numerical study. *Compos. B* 42 , 330–340. doi: 10.1016/j.compositesb.2010.09.020

Grande, E., and Milani, G. (2016). Modeling of FRP-strengthened curved masonry specimens and proposal of a simple design formula. *Compos. Struct.* 158, 281–290. doi: 10.1016/j.compstruct.2016.09.017

Grande, E., and Milani, G. (2018). Interface modeling approach for the study of the bond behavior of FRCM strengthening systems. *Compos. B* 141, 221–233. doi: 10.1016/j.compositesb.2017.12.052

Krstevska, L., Tashkov, L., Naumovski, N., Florio, G., Formisano, A., Fornaro, A., et al. (2010). "*In-situ* experimental testing of four historical buildings damaged during the 2009 L'Aquila earthquake," in *COST ACTION C26: Urban Habitat Constructions Under Catastrophic Events - Proceedings of the Final Conference* (Naples), 427–432.

Lagomarsino, S. (2012). Damage assessment of churches after L'Aquila earthquake (2009). *Bull. Earthquake Eng.* 10, 73–92. doi: 10.1007/s10518-011-9307-x

Locati, M., Camassi, R., and Stucchi, M. (eds). (2011). *DBMI11, Italian Macroseismic Database, 2011 Version*. Milano and Bologna. Available online at: http://emidius.mi.ingv.it/DBMI11

Marra, A. M., Salvatori, L., Spinelli, P., and Bartoli, G. (2017). Incremental dynamic and nonlinear static analyses for seismic assessment of Medieval Masonry Towers. *ASCE J. Perf. Constr. Facil.* 31, 1–10. doi: 10.1061/(ASCE)CF.1943-5509.0001022

Milani, G., Casolo, S., Naliato, A., and Tralli, A. (2011). Seismic assessment of a medieval masonry tower in northern Italy by limit, nonlinear static, and full dynamic analyses. *Int. J. Archit. Herit.* 6, 37–41. doi: 10.1080/15583058.2011.588987

Milani, G., Lourenço, P. B., and Tralli, A. (2006). Homogenised limit analysis of masonry walls, Part I: failure surfaces. *Comput. Struct.* 84, 166–180. doi: 10.1016/j.compstruc.2005.09.005

Milani, G., Shehu, R., and Valente, M. (2018). A kinematic limit analysis approach for seismic retrofitting of masonry towers through steel tie-rods. *Eng. Struct.* 160, 212–228. doi: 10.1016/j.engstruct.2018.01.033

Milani, G., and Valente, M. (2015). Comparative pushover and limit analyses on seven masonry churches damaged by the 2012 Emilia-Romagna (Italy) seismic events: possibilities of non-linear finite elements compared with pre-assigned failure mechanisms. *Eng. Fail. Anal.* 47, 129–161. doi: 10.1016/j.engfailanal.2014.09.016

Milani, G., and Venturini, G. (2011). Automatic fragility curve evaluation of masonry churches accounting for partial collapses by means of 3D FE homogenized limit analysis. *Comput. Struct.* 89, 1628–1648. doi: 10.1016/j.compstruc.2011.04.014

Ministerial Circular (MC) (2009). *Instructions for the Application of the ≪New Technical Standards for Buildings≫ Referred to in the Ministerial Decree of 14 January 2008 (in Italian)*. Official Gazette n.47 of 26/02/2009, Ordinary Supplement n.27, Rome.

Ministerial Decree (NTC) (2008). *New Technical Codes for Constructions (in Italian)*. Official Gazette n. 29 of 04/02/08, Ordinary Supplement n. 30, Rome.

Ministerial Decree (NTC) (2018). *Updating of Technical Codes for Constructions (in Italian)*. Rome: Official Gazette n. 42 of 20/02/18, Ordinary Supplement n. 8.

Mosoarca, M., Apostol, I., Keller, A., and Formisano, A. (2017). Consolidation methods of Romanian historical building with composite materials. *Key Eng. Mater.* 747, 406–413. doi: 10.4028/www.scientific.net/KEM.747.406

Rapone, D., Brando, G., Spacone, E., and De Matteis, G. (2018). Seismic vulnerability assessment of historic centers: description of a predictive method and application to the case study of Scanno (Abruzzi, Italy). *Int. J. Archit. Herit.* 12 , 1171–1195. doi: 10.1080/15583058.2018.1503373

S.T.A.DATA srl (2018). *3Muri 10.9.0 - User's Manual*. Turin.

Sarhosis, V., Milani, G., Formisano, A., and Fabbrocino, F. (2018). Evaluation of different approaches for the estimation of the seismic vulnerability of masonry towers. *Bull. Earthquake Eng.* 16, 1511–1545. doi: 10.1007/s10518-017-0258-8

Tashkov, L., Krstevska, L., Naumovski, N., De Matteis, G., and Brando, G. (2010). "Ambient vibration tests on three religious buildings in Goriano Sicoli damaged during the 2009 L'Aquila earthquake," in *COST ACTION C26: Urban Habitat Constructions under Catastrophic Events - Proceedings of the Final* Conference, 427-432; 433–438.

Ubertini, F., Cavalagli, N., Kita, A., and Comanducci, G. (2018). Assessment of a monumental masonry bell-tower after 2016 Central Italy seismic sequence by long-term SHM. *Bull. Earthquake Eng.* 16, 775–801. doi: 10.1007/s10518-017-0222-7

Ubertini, F., Comanducci, G., Cavalagli, N., Pisello, A. L., Materazzi, A. L., and Cotana, F. (2017). Environmental effects on natural frequencies of the San Pietro bell tower in Perugia, Italy, and their removal for structural performance assessment. *Mech. Syst. Signal Process.* 82, 307–322. doi: 10.1016/j.ymssp.2016.05.025

Valente, M., and Milani, G. (2016). Seismic assessment of historical masonry towers by means of simplified approaches and standard FEM. *Constr. Build. Mater.* 108, 74–104. doi: 10.1016/j.conbuildmat.2016.01.025

# Seismic Vulnerability of Buildings in Historic Centers: From the "Urban" to the "Aggregate" Scale

*Giulia Cocco, Andrea D'Aloisio, Enrico Spacone and Giuseppe Brando\**

*Department of Engineering and Geology (INGEO), University "G. D'Annunzio" of Chieti-Pescara, Pescara, Italy*

Seismic vulnerability assessment of urban centers is a challenging issue that needs to be faced accurately for the earthquake risk of large territorial areas. The selection of suitable methods is a crucial aspect that must be treated according to different evaluation processes, depending on the size of the problem and on the available calculation capacities. A possible strategy consists in analyzing large stocks of buildings, so to include in the analyses all those structural parameters that characterize their response and to involve the variability of the considered features. This would require a high computational effort that should be addressed to the investigation of the response of a large number of models. For this reason, simplified procedures based on engineeristic judgements, are commonly considered a viable way to be undertaken in order to predict damage scenarios. Alternatively, the attention could be focused on a limited number of buildings that are judged to be representative of the whole stock. In this case, more sophisticated analyses could be carried out and the obtained results could be extended to the whole urban center. Based on this premise, this paper presents the results obtained through the application of two different seismic vulnerability methodologies on the historic center of Campotosto, in Italy, which was hit by the last 2016 Central Italy earthquake. The first is an empirical method, applied considering a large stock of 130 buildings, which was calibrated by the authors after the 2009 L'Aquila earthquake for historical centers that are similar to the one studied in this paper. The latter, is a method based on analytical formulations dealt with by the Vulnus software, developed at the University of Padua in Italy, which was used for evaluating the seismic vulnerability of an aggregate building, which has been considered representative of the historic center. The final aim is to compare, also in the light of the damage provoked by the 2016 earthquake, the observed post-seismic scenarios, expressed in terms of fragility curves, derived from the two applied methodologies, in order to prove their reliability and to stress the possible issues related to their implementation at different scales.

Keywords: historic centers, aggregate buildings, seismic vulnerability assessment, damage scenarios, masonry buildings, empirical methods, analytical methods, 2016 Central Italy earthquake

# INTRODUCTION

The seismic activity that hit the central area of Italy in 2016 stresses, once again, the fragility of those territories characterized by the presence of small medieval historic centers made of poor masonry structures (Fiorentino et al., 2018; Sorrentino et al., 2018). For this reason, their seismic vulnerability assessment is a very timely topic that needs to be faced urgently.

Seismic vulnerability evaluation is a process that can be implemented at different levels. The selection of a proper method is a crucial issue that depends on the accuracy of the targeted results, as well as on the sustainability of the analyses that have to be carried out owing to the scale to which the evaluation itself is addressed (Formisano and Marzo, 2017).

When the goal is to quantitatively detect the vulnerability at the building level, traditional methods of structural analysis, based on the use of sophisticate Finite Element (Brando et al., 2015) or numerical (Clementi et al., 2017; Portioli and Cascini, 2017; Cascini et al., 2018) models, properly calibrated on the basis of tests (Krstevska et al., 2010; Tashkov et al., 2010; Anastasopoulos et al., 2018), can be used. This often entails a careful knowledge of the construction details and a significant effort devoted to capture the most relevant behaviors of the structures during an earthquake.

Conversely, when the objective is to examine a population of buildings and to establish priorities of interventions for mitigating the seismic risk of the whole urban center they form, rapid methods based on engineering judgements are often the most viable way (Vicente et al., 2011; Ferreira et al., 2013). In this case, empirical methods can be applied for assessing the potential damage (expressed in terms of percentages of buildings that would experience certain limit states) under different earthquake intensities. The engineering judgements should be given for those structural characteristics that contribute positively or negatively to the buildings response, also in view of the observations carried out after earthquakes of the past on buildings that are similar to the ones of the studied stock (Brando et al., 2017b; Sorrentino et al., 2019).

A compromise strategy is to select, among the buildings of the urban centers, few typologies that are representative of the whole population under examination and to carry out analyses of intermediate complexity that are more manageable. For example, for masonry buildings, kinematic analyses (Criber et al., 2015) are often implemented, looking at those out-of-plane mechanisms that are more dangerous for the building stability. These types of analyses are particularly indicated when aggregates buildings are analyzed. In fact, for these types of constructions (Formisano, 2017a,b), numerical FEM model would result too much heavy and would need a large number of information on the structural details. Moreover, within the kinematic analyses, the interaction forces between the buildings in the same aggregate can be taken into account too.

On the basis of this premises, this paper deals with the seismic vulnerability assessment of the historic center of Campotosto, in Abruzzi region. To this purpose, two methodologies are applied at different scales. The first is an empirical method developed by the Authors after the 2009 L'Aquila earthquake and validated on historic centers that are similar to the one dealt with in this paper. The latter consists in the application of kinematic analyses on an aggregate building that has been judged to be representative of the whole historic center. To this aim the Vulnus software, developed at the University of Padua in Italy, has been used.

The final aim is to compare the fragility curves derived from the two applied methodologies, in order to prove their reliability and to stress the possible issues related to their implementation at different scales.

The paper is organized as follows. In section The Historic Center of Campotosto, a brief description of the historic center of Campotosto is given. In section The methodologies Applied for the Seismic Vulnerability Assessment, the considered procedures that have been implemented at the "urban" and at the "aggregate" scales are presented. Finally, in section The Seismic Vulnerability of the Historic Center of Campotosto, the results obtained by applying the two methodologies are presented and the corresponding fragility curves are compared.

It must be pointed out that the results reported in the paper are the base for a more comprehensive study that has to be developed in the future accounting for larger stocks of buildings that have to be analyzed through the here presented procedures. Moreover, some issues that are only briefly mentioned in this paper, such as the one related to the site effects due to the soil typology, are worthy of being deepening, as they could influence significantly the proposed outcomes.

# THE HISTORIC CENTER OF CAMPOTOSTO
## General

Campotosto is a town of about 730 inhabitants in the province of L'Aquila, located at 1,420 m on the sea level. It is part of the so-called "Amiternina" mountain community and gives its name to a lake, in the hearth of the homonymous natural park.

The urban articulation of Campotosto is characterized by a main core in the top and most ancient part of the town, which had its spatial development, during the centuries that followed its foundation (XIII century), until the lake. The urban organization is articulated around a series of minor roads arranged like a comb, which has in the main street, Via Castello, its rib (**Figure 1A**).

The historical center was divided in three areas (**Figure 1B**). The first is located on the top of the hill and is labeled, in **Figure 1B**, with the letter C. The second mainly extends in the central area of Campotosto, along the western side of an embankment (Area B). The third (Area A) is situated closed to the lake.

This formal division was used to optimize the survey actions and the subsequent data elaboration. It was proposed in the reconstruction plan according to an historical analysis (Ponzi et al., 2013), and was accepted for carrying out the analyses presented in this paper, because the areas present different lithological features that will not dealt here, but that the authors are deepening for future more comprehensive analyses. However,
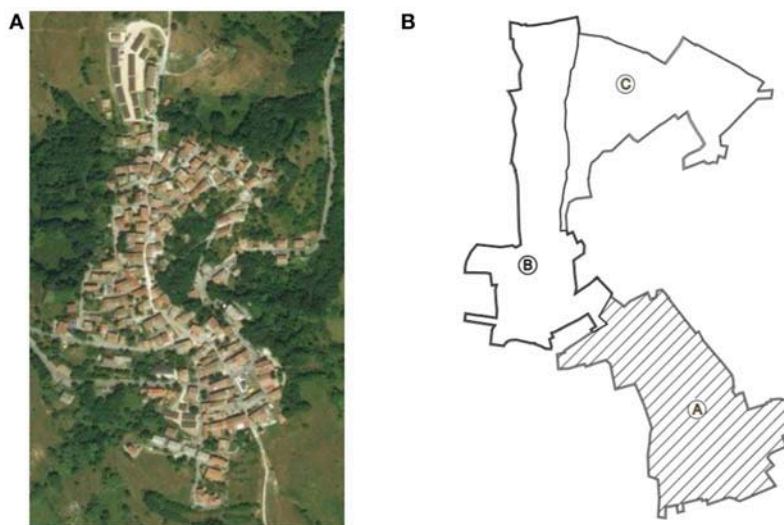
**FIGURE 1 |** Historic center of Campotosto: **(A)** Aerial photo (source: Google Earth) and **(B)** Territorial subdivision in areas according to the reconstruction plan of Campotosto drafted after 2009 L'Aquila earthquake (Ponzi et al., 2013).

the buildings of the three area present similar features and can be seen as a unique vulnerability class.

## Historical and Recent Seismicity

The territory of Campotosto was characterized in the past by a relevant earthquake activity, which found in the last 2016 seismic sequence, culminated in the most destructive shaking for Campotosto of January 2017, one of the most tragic episodes.

The main historical earthquakes occurred in 1639 (Mw 6.2), in 1646 (Mw 5.9) and in 1703 (Mw 6.9). They caused severe damage and implied several reconstruction processes that shaped the historic center up to the current aspect. Indeed, the original medieval plants of several buildings were completely demolished and replaced by more modern masonry buildings.

This historic center was also affected by the 2009 L'Aquila earthquake. The main shock of this earthquake was followed by two significant aftershocks of magnitudes 5.3 Mw (7 April) and 5.1 Mw (9 April), that provoked a severe state of damage, in particular the latter.

Finally, the last 2016 Central Italy earthquake affected almost the 70% of the buildings, provoking several collapses, in particular in the zone A of **Figure 1B**, near the lake.

The damage survey presented in this paper was carried out after the seismic event occurred on the 18th of January 2017, with epicenter in Montereale (L'Aquila). The accelerogram of this earthquake, recorded by the station of Mascioni, 19 km far from the epicenter and 14 km from Campotosto, is shown in **Figure 2A**. The 5% damped elastic spectrum shown in **Figure 2B** shows a maximum spectral acceleration of 0.72 g for short period buildings such as the ones studied in this paper.
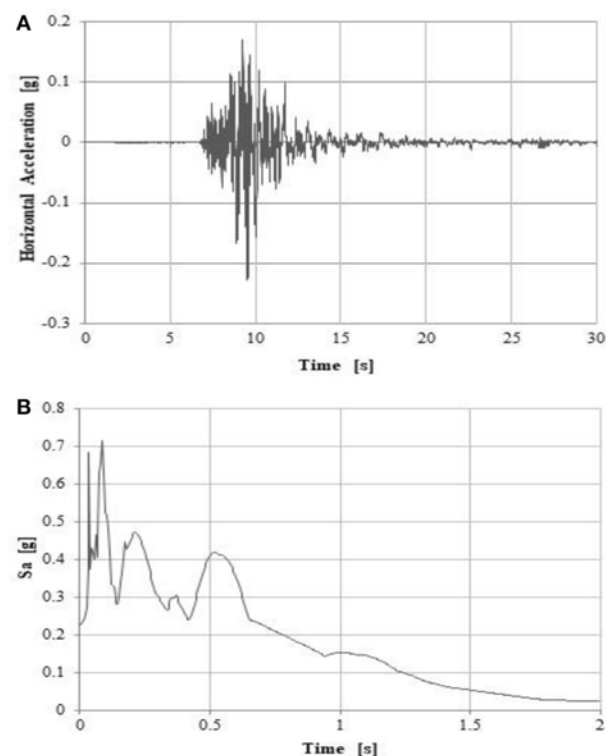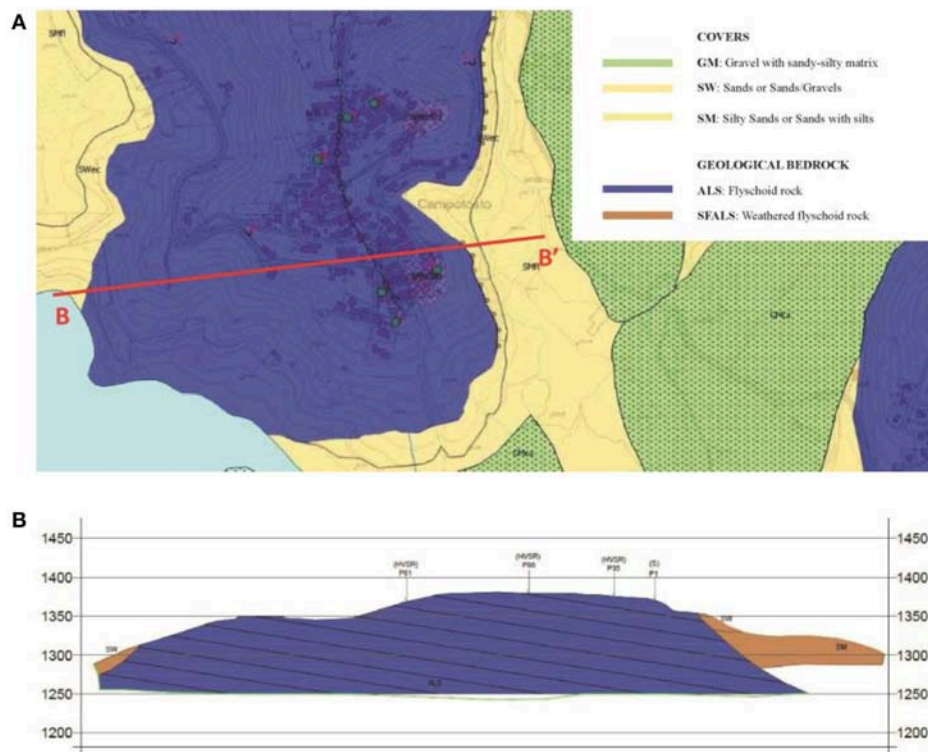


**FIGURE 2 | (A)** The accelerogram recorded by the station of Mascioni (18th of January 2017). **(B)** The corresponding 5% damped elastic spectrum.

Recent geological studies carried out in Campotosto confirm that the medium-high seismic hazard of the Campotosto basin is due to the presence of an active fault, the Monte

**FIGURE 3 |** Morphological and geological outlines: **(A)** Geological map of the historic center of Campotosto and **(B)** Geological section of the most critic area of the historic center (D'Onofrio and Tatoni, 2017).

Gorzano–Campotosto fault, also known as Monti della Laga fault, whit an extent of almost 30 km.

As mentioned before, this hazard can be exacerbated by the presence of side effects. In fact, as it is shown in **Figure 3**, extracted from a recent investigation carried out for achieving a third-level microzonation of the area (D'Onofrio and Tatoni, 2017), Campotosto is located at the top of a small ridge consisting of a flyschoid or turbiditic rock.

This rock is highly weathered in the upper portion leading to possible stratigraphic amplification phenomena, in addition to the site effects related to the topographical configuration described in section General. Gravelly and sandy covers can be found on the flanks of the ridge. Thus, amplification factors of 1.9, 2.0 are possible, as shown in the microzonation map in **Figure 4**.

## Main Features and Fragilities of Buildings

As mentioned before, the reconstructions that were carried out on the historic center of Campotosto, after the several earthquakes of the past, have led to the loss of the original urban configuration, as well as of the original building plant. However, the current layout of the built environment appears to be very uniform, except for few cases of reinforced concrete buildings, with recurrent typologies that can be seen as a unique vulnerability class.
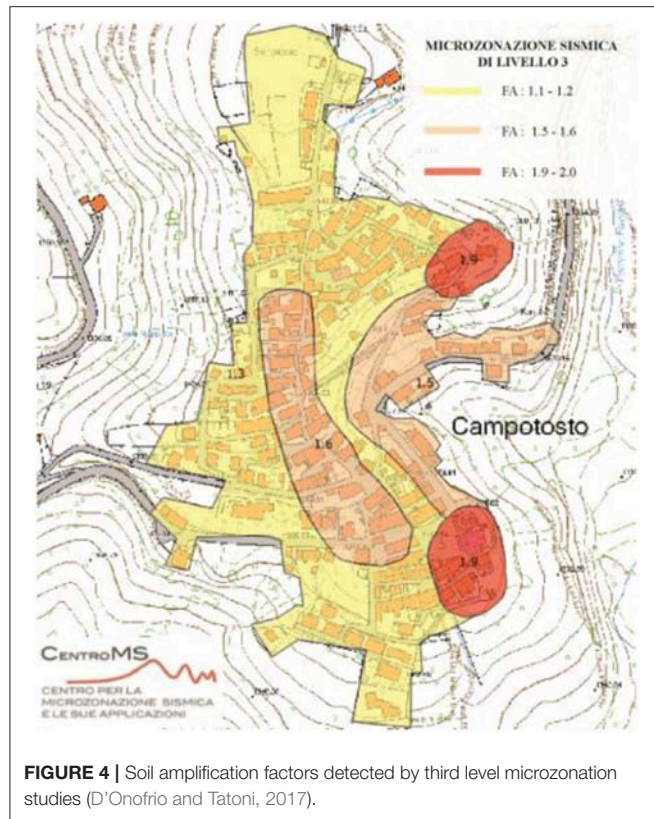
The settlement consists of stone masonry buildings that mostly are undergrounded for one or more stories, at least on

one side, where, at the top of the underground floors, on one of the perimeter edges, the main entrances overlook on minor roads. In this way, buildings form a series of "terraces" laid on the sloped terrain, so to accompany the orographic configuration of the site.

Focusing the attention on the masonry buildings, mainly organized on 2 or 3 stories above the ground, they are made of sandstone—the typical stone of L'Aquila province, where several mines are still present- with extremely varied size and assembled with weak and thin layers of lime mortars, as shown in **Figure 5**.
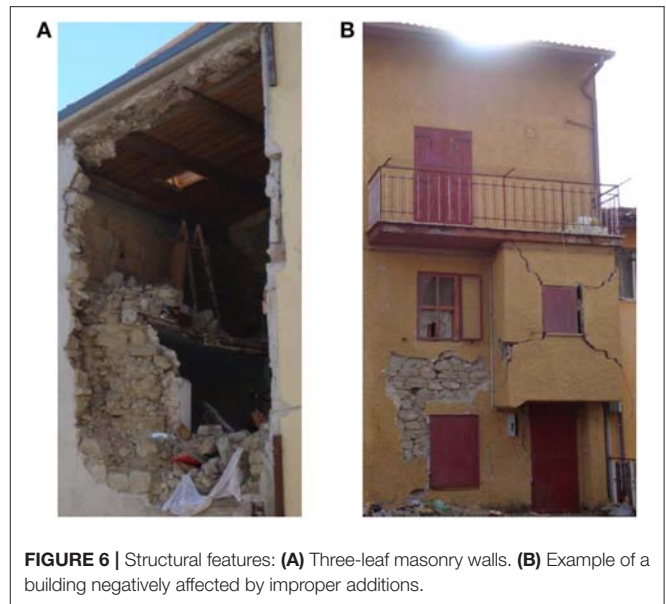
Observing the damaged buildings it has been possible, after the earthquake, to identify the characteristics of the three-leaves masonry wall sections, which have a thickness of about 80 cm and have inner core composed of poor filling material (**Figure 6A**). This kind of masonry is widely used in Abruzzi region and it results extremely dangerous for the stability of the wall when the internal core is degraded and there are no transversal connections between the two outer leaves.

Also, it has been observed that the walls are scarcely connected each other, as well as that the connection between the orthogonal walls is basically absent or not effective. These lacks were responsible of several out-of-plane mechanisms that were observed after both the 2009 and the 2016 seismic events. Roofing system are mainly made of timber elements.

FIGURE 4 | Soil amplification factors detected by third level microzonation studies (D'Onofrio and Tatoni, 2017).



FIGURE 5 | Masonry typology mainly presents in Campotosto.

Moreover, several buildings and aggregates show signs of transformation over time that worsened their original structural behavior, such as additions in plan (**Figure 6B**) and elevation, new or enlarged openings and use of materials that are not homogeneous with respect to the original ones, such as reinforced concrete used for horizontal slabs, ring beam, lintels and roofs.

Only the buildings renovated in more recent times are characterized by walls of good quality and are equipped with anti-seismic provisions as tie rods.



FIGURE 6 | Structural features: (A) Three-leaf masonry walls. (B) Example of a building negatively affected by improper additions.

## THE METHODOLOGIES APPLIED FOR THE SEISMIC VULNERABILITY ASSESSMENT

### The Method Used at the Urban Scale

The seismic vulnerability at large scale of Campotosto was evaluated through the application of an empirical method that was calibrated in order to reproduce the damage observed on the masonry structures of the minor historic centers of Abruzzi after the 2009 L'Aquila earthquake, as it is fully explained in Brando et al. (2017a).

It is a predictive method based on the fundamental hypothesis that, for each seismic intensity $I$, the probability $p[k|I]$ of attaining a certain limit state, evaluated according to the five damage levels of the EMS-98 macroseismic scale (Grünthal, 1998), can be interpreted by the binomial probability distribution given in Equation (1).

$$p[k|I] = \frac{5!}{k! \cdot (5-k)!} \cdot \left(\frac{\mu_D}{5}\right)^k \cdot \left(1 - \frac{\mu_D}{5}\right)^{5-k} \quad (1)$$

where $k$ is an integer score, ranging between 0 and 5, corresponding to the damage grade $D_k$ that the earthquake may potentially provoke:

- $D_0$: no structural damage ($k = 0$);
- $D_1$: negligible damage. Slight cracks on the walls, fall of small pieces of plaster, fall of tiles $k = 1$);
- $D_2$: moderate damage. Cracks in many walls, fall of large pieces of plaster, partial collapse of the chimney ($k = 2$);
- $D_3$: substantial damage. Large cracks in the walls, failure of non-structural elements, activation of out-of-plane mechanisms ($k = 3$);
- $D_4$: serious damage. Serious cracks, development of out-of-plane mechanisms with partial collapses that interest the horizontal structures and the walls ($k = 4$);
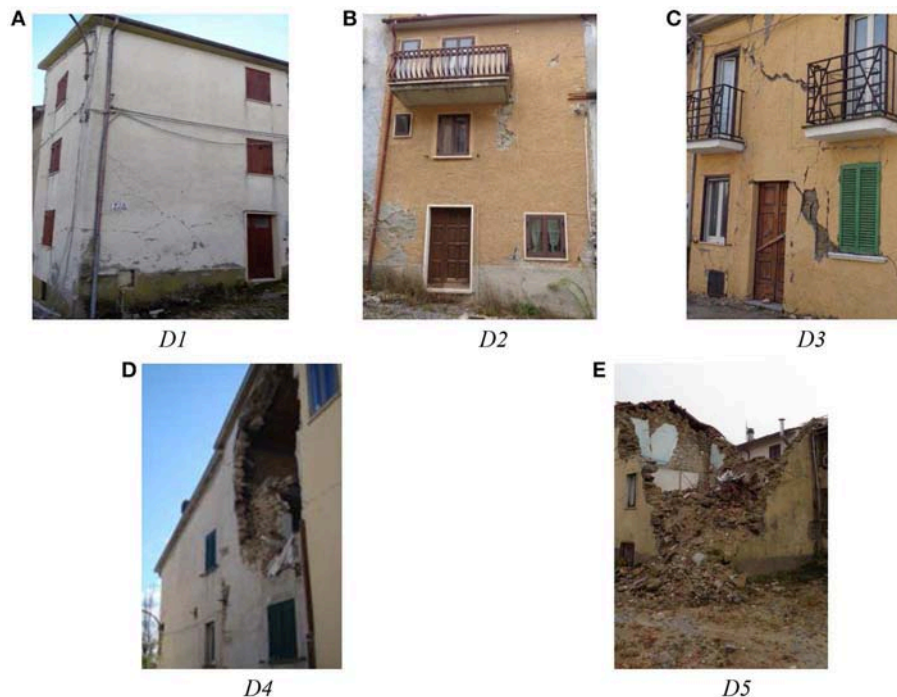
**FIGURE 7 |** Examples of the observed damage grades in Campotosto after the 2016 seismic event. **(A)** Negligible damage; **(B)** Moderate damage; **(C)** Substantial damage; **(D)** Serious damage; **(E)** Collapse.

- $D_5$: collapse. Notable collapses affecting more than 50% of the structure ($k = 5$).

$\mu_D$ is the mean of the expected damage grades, according to Equation (2).

$$\mu_D = \frac{\sum\limits_{i=1}^{n} D_{k,i}}{n} \qquad (2)$$

where $n$ is the number of buildings of the analyzed stock.

In **Figure 7**, some example of damage grades observed after the January 2017 earthquake are shown. As it is possible to observe, buildings having more or less the same types of plants presented different types of damage because of the different number and position of opening (see for example the different behavior of the buildings that experienced damage grades $D_1$, $D_2$, and $D_3$), the different position in the aggregate (see the building that experienced a damage grade $D_5$) and, also, because of other factors discussed previously, such as site effects.

On the other hand, the hypothesis related to the reliability of the binomial probability function was proved to be well-founded also in the light of the damage observed in the studied historic center after the 2016 Cental Italy Earthquake. As it is shown in **Figure 8A**, where the observed frequencies of the several damage grades are represented in terms of Damage Probability Matrix (DPM), the binomial probability function well approximate the damage grade $D_1$, $D_3$, and $D_4$, even if the damage grade $D_2$ is overestimated and $D_5$ is underestimated. As for these discrepancies, some ongoing studies, that the authors are carrying out by relating the spatial damage distribution

(**Figure 8B**) to the soil conditions, are proving that the excessive number of buildings experiencing a damage level $D_5$, which lead to an overestimation of buildings that, instead, would be characterized by a damage level $D_2$, collapsed because of some site effects, concentrated in the area $A$ of **Figure 1A**, closed to the lake. This aspect is surely to be deepened in the future.
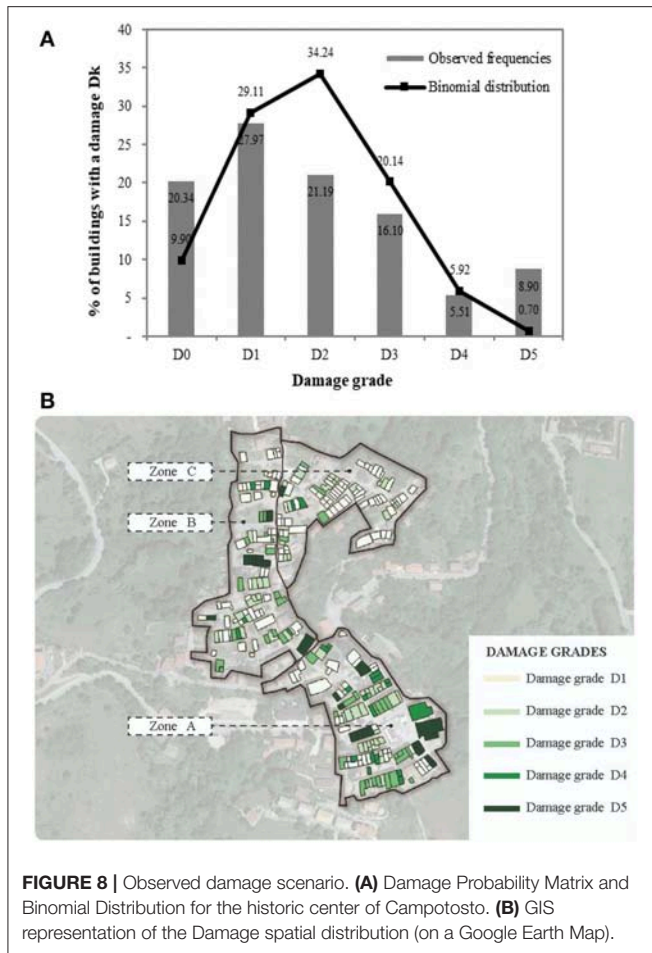
It must be finally pinpoint that the discrepancies corresponding to the damage level $D_0$ are quite expectable, as they are likely due to the ambiguities that usually characterize the pre-existing and the seismic induced damage.

The reliability of the binomial distribution for representing damage scenarios means that any type of predictive model has to target to provide, for each earthquake intensity, an estimation of the mean damage to be considered in Equation (1).

The method that has been considered in the present study, which was calibrated in the light of the damage scenarios observed on similar historic centers after the 2009 L'Aquila earthquake, is based on the evaluation, for each building of the historic center, of the structural features that characterize the 14 potential vulnerability sources $P_m$ (with $m = 1{:}14$) listed in **Table 1**.

Each of these features are then judged through the application of two scores $v_{mf}$ and $v_{mp}$. The first, named "fragility score," is higher as the structural features makes the vulnerability sources $P_m$ more severe. On the contrary, $v_{mp}$, named "protection score," represents a judgment on the type and the effectiveness of the possible anti-seismic devices applied in order to contrast the development of the vulnerability source "$P_m$."

Details on how to assign the scores to each vulnerability sources, are given in Rapone et al. (2018). According to the

**FIGURE 8** | Observed damage scenario. **(A)** Damage Probability Matrix and Binomial Distribution for the historic center of Campotosto. **(B)** GIS representation of the Damage spatial distribution (on a Google Earth Map).

**TABLE 1** | The 14 vulnerability sources taken into account for the vulnerability index method.

| Vulnerability source | Vulnerability type | $r_k$ |
|---|---|---|
| $P_1$ | Position in the cluster | 1.5 |
| $P_2$ | Number of stories | 1.5 |
| $P_3$ | 1st mode mechanism | 1.5 |
| $P_4$ | 2nd mode mechanism | 1.0 |
| $P_5$ | Arches | 1.0 |
| $P_6$ | Vaults | 1.0 |
| $P_7$ | Slabs | 1.0 |
| $P_8$ | Thrusting forces | 0.8 |
| $P_9$ | Presence of added structures | 0.5 |
| $P_{10}$ | Stairs | 1.0 |
| $P_{11}$ | Irregularities | 0.8 |
| $P_{12}$ | Non-structural elements | 0.5 |
| $P_{13}$ | Site effects | 1.5 |
| $P_{14}$ | Non seismic external hazard | 0.3 |

In this equation, the factors *a*, *b*, *c*, *d* have been calibrated on the basis of the observations carried out after the 2009 L'Aquila earthquake, as reported in Brando et al. (2017a).

The vulnerability factor *V* is then used in order to assess the mean damage by applying Equation (6):

$$\mu_D = 2.5 \cdot \left[ 1 + \tanh \left( \frac{I + 6.25 \cdot V - 13.1}{Q} \right) \right] \qquad (6)$$

where *I* is the expected macro seismic intensity, expressed in the Mercalli-Cancani-Sieberg scale (MCS), while *Q* is a coefficient that takes into account the ductility that characterizes the type of analyzed buildings, which, conventionally, also considering studies of the past [see for example (Lagomarsino and Giovinazzi, 2006)], has been imposed to be equal to 2.3.

## The Method Used at the Aggregate Scale

Alternatively to the empirical method dealt with in Section The Method Used at the Urban Scale, the vulnerability assessment of the urban center has been analyzed focusing the attention on one aggregate of Campotosto. It was selected in order to be representative of the great part of the buildings forming the stock analyzed with the empirical method dealt with in the previous Section, according to the masonry texture, the number of stories, the number of buildings forming the aggregate itself.

The Vulnus software (Bernardini et al., 2009), developed at the University of Padua in Italy, has been used in order to draw the fragility curve related to the attainment of a condition of severe damage/collapse, namely that fragility curve giving back, consistently with the damage grades provided by the EMS98 macroseismic scale, the probability of attaining a damage grade higher than D3.

In its latest version, the software allows to give an evaluation of the vulnerability of the aggregate by properly combining three indices, named $I_1$, $I_2$, and $I_3$, which can be computed for the single structural units.
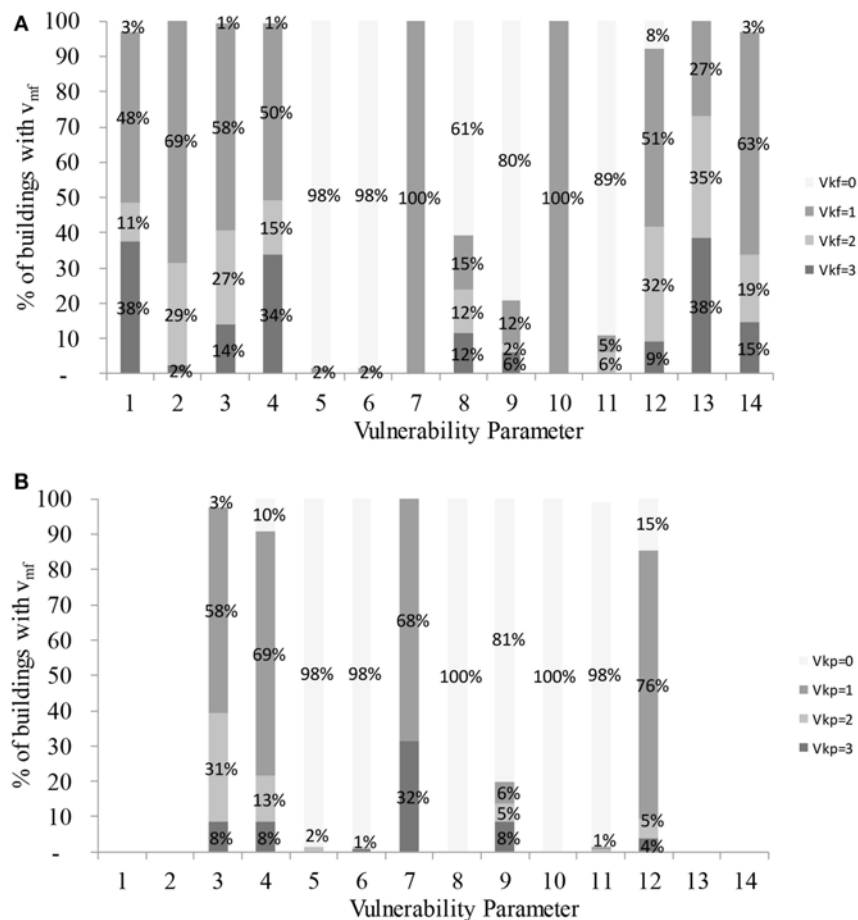
methodology, the two scores have been used, for each building of the stock, to find a vulnerability index $i_v$, given in Equation (3):

$$i_v = \frac{1}{6} \cdot \frac{\sum_{m=1}^{14} \rho_m \cdot \left( v_{mf} - v_{mp} \right)}{\sum_{m=1}^{14} \rho_m} + 0.5 \qquad (3)$$

where $\rho_m$ factor, also reported in **Table 1**, accounts for the influence that the source of vulnerability $P_m$ has on the overall stability of the structure.

All the vulnerability indices calculated according to Equation (3) are then used in order to find the mean index $i_v^*$, according to Equation (4).

$$i_v^* = \frac{\sum_{i=1}^{n} i_v}{n} \qquad (4)$$

$i_v^*$ is therefore used to calculate the vulnerability factor *V* of Equation (5):

$$\begin{aligned} V &= a + b \cdot i_v^* + c \cdot i_v^{*2} + d \cdot i_v^{*3} \\ &= 0.53 + 1.16 \cdot i_v^* - 4.00 \cdot i_v^{*2} + 4.21 \cdot i_v^{*3} \end{aligned} \qquad (5)$$

**FIGURE 9** | Distribution of the **(A)** fragility and **(B)** protection scores for the buildings of Campotosto.

$I_1$ is the ratio between the sum of the walls in-plane shear strengths, computed along the weakest direction of the building, and the weight of the building itself. In other words, $I_1$ accounts for the in-plane shear strength of the walls, which are expressed according the well-known Turnsek-Cacovic formulation (Turnsek and Cacovic, 1971), properly modified in order to account for potential sources of non-regularity in plan and/or in elevation.

$I_2$ is the ratio between the acceleration able to provoke the most critical out-of-plane mechanism and the acceleration of gravity. In order to compute this index, the software considers several mechanisms that can be triggered on the perimeter walls

$I_3$ is the weighted sum of the scores of the partial vulnerability factors applied in the second level GNDT form (GNDT, 1994) and not involved in the evaluation of $I_1$ and $I_2$ (only seven of the 11 factors of the GNDT form are taken into account). It adjusts the evaluation based on the $I_1$ and $I_2$ indices and accounts for those sources of vulnerability or of mitigation which are not directly included in the calculations described previously.

# THE SEISMIC VULNERABILITY OF THE HISTORIC CENTER OF CAMPOTOSTO

## Results Obtained by Applying the Empirical Method

Following an inspection of the typological and structural features of about 130 buildings belonging to the historical center of Campotosto (equally distributed in the three areas shown in **Figure 1B**), the related fragility ($v_{mf}$) and protection ($v_{mp}$) scores have been assigned.

In this way, it has been possible to identify and to classify the most influential fragilities (**Figure 9A**) and mitigation measures (**Figure 9B**) that characterize the analyzed buildings.

Also, possible interventions to be implemented for pursuing a risk mitigation have been preliminarily determined. As it can be observed in **Figure 9A**, the fragilities related to the potential trigger of the out-of-plane (Vulnerability source n° 3) and in-plane mechanisms (Vulnerability source n° 4) are particularly relevant. Moreover, a low percentage of buildings with effective anti-seismic preventive measures have been observed, as it is shown in **Figure 9B**.
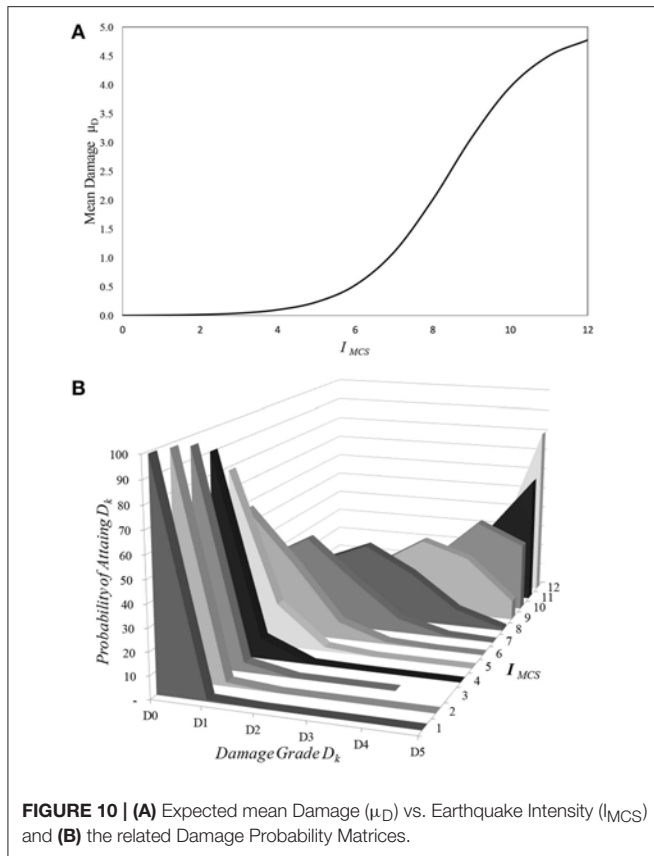
FIGURE 10 | (A) Expected mean Damage ($\mu_D$) vs. Earthquake Intensity ($I_{MCS}$) and (B) the related Damage Probability Matrices.
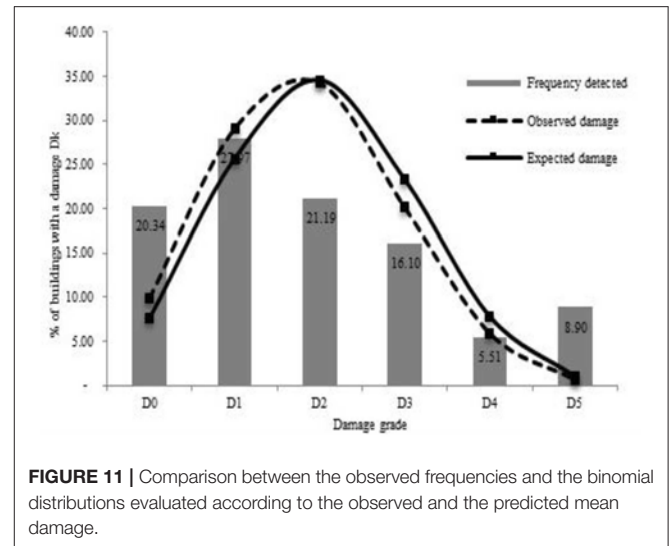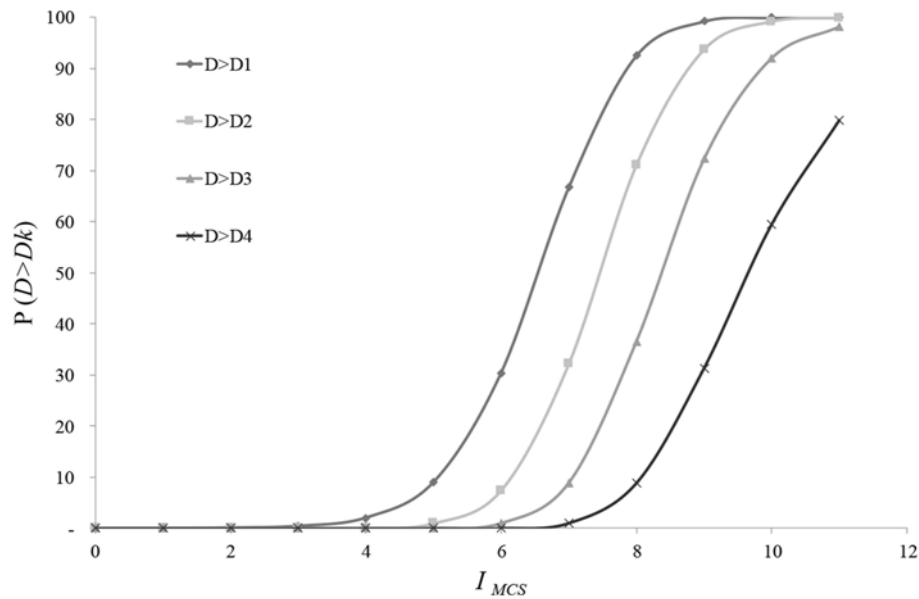


FIGURE 11 | Comparison between the observed frequencies and the binomial distributions evaluated according to the observed and the predicted mean damage.

Then, the scores have been used in order to apply the methodology presented in section 3.1, for obtaining an evaluation of the mean damage $\mu_D$ values that have to be expected for each earthquake intensity (**Figure 10A**). These mean values have been therefore used in order to forecast the damage probability matrices, shown in **Figure 10B**, corresponding to the binomial distribution expressed in Equation (1).

To demonstrate the accuracy of the vulnerability index methodology and its validity in predicting the vulnerability of the considered stock of buildings, the binomial function obtained from the expected mean damage $\mu_D$ for an earthquake intensity $I_{MCS}$ =VIII, that one recorded after the seismic event of 2017, has been superimposed to the binomial distribution obtained through the observed mean $\mu_D$.

As it is possible to observe in **Figure 11**, the two distribution perfectly match each other, this proving the reliability of the proposed empirical method.

By cumulating the probabilities shown in **Figure 10B**, the fragility curves for representing the expected damage scenarios for several earthquake intensities, which give the probability of exceeding the several damage grades, have been obtained. These are shown in **Figure 12**.

## Results by Applying the VULNUS Methodology

The aggregate considered as representative of the built environment of Campotosto is located in the area A shown

in **Figure 1B**. The plan of the building and its cadastral identification are depicted in **Figure 13**, whereas in **Figure 14** the front and the back are shown. The aggregate develops mainly along one longitudinal axis with a length of about 24 meters and a width of about 6 meters. It consists of 3-storeis buildings with an average height of 7.4 meters.

Given the impossibility of obtaining detailed historical documents, hypotheses concerning the development of the aggregate during the centuries have been done, mainly based on the analysis of the opening misalignments in the façade. Four structural units have been therefore detected (**Figure 15**).

Vertical walls are made of rubble stones kept together by thin layer of air lime mortar and are organized according to a three leaf layout, with a total thickness of about 60 cm. According to the Italian Provisions "Circolare"[1], this type o masonry is characterized (for a knowledge level LC1) by a compressive strength of $f_m$=2,0 MPa, a shear stress, in absence of axial stress, of 0,035 MPa, elastic normal and tangential moduli of 1,020 MPa and 340 MPa, respectively. The weight per unit of volume is 20 kN/m³.

Floors and roofs are made of timber elements.

A first evaluation of the $I_1$ and $I_2$ indices has been carried out for the maximum ground acceleration recorded at the Mascioni acceleration station, the closest among the ones belonging to the Italian Accelerometric network [RAN (Paolucci et al., 2011)], of 0.279g. This acceleration is very close to the ground acceleration given by the Italian Technical Standards for Construction of 2018 (NTC 2018)[2], for a soil type A and a probability of exceedance of 10% in 50 years (0.258g).

The obtained results are given in **Figure 16** for the four structural units. Broadly speaking, all the structural units present in both the in-plane and the out-of-plane directions safety factors

---

[1]Circolare n. 7 21/01/2019. Istruzioni per l'applicazione delle "Norme tecniche per le costruzioni, di cui al D.M. 17/01/2018" [Italian].

[2]D.M. 17/01/2018N. NTC 2018. Norme tecniche per le costruzioni [Italian].

**FIGURE 12 |** Comparison between the observed frequencies and the binomial distributions evaluated according to the observed and the predicted mean damage.
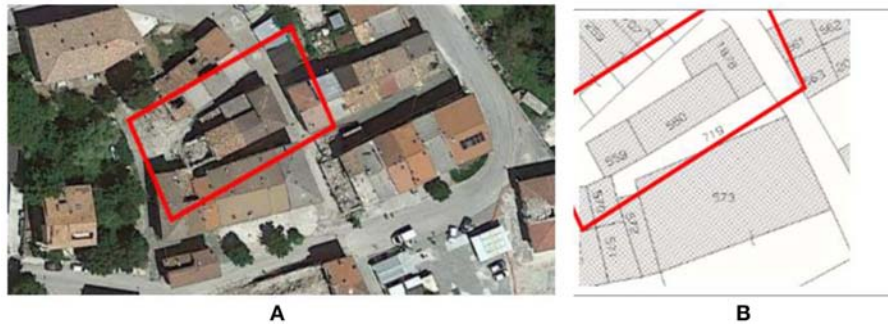


**FIGURE 13 |** The considered aggregate. **(A)** Satellite view (Source: Google Earth) and **(B)** Cadastral map.

lower than 1, with a minimum of 0.243 for the out of plane mechanism of the Building 2. This result was actually confirmed by analyzing the damage provoked by the earthquake occurred in January 2017. In fact, several cracks and some triggered out-of-plane mechanisms were observed, with a general state of damage that in the EMS-98 scale can be classified with a grade $D_3$.

It is interesting to note that the $I_2$ indices are lower than $I_1$, this stressing the higher sensitivity of the aggregate to experience out-of-plane mechanisms.

Once that all the information required for the definition of the $I_3$ index have been imputed in the software, fragility curves have been generated. In particular, the software combines the three indices $I_1$, $I_2$, and $I_3$ for different ground accelerations, and gives the probability of attaining a state of severe damage/collapse, or rather, consistently with the EMS-98 macro

seismic scale, the probability of attaining a damage level $D_4$ or $D_5$ (namely the probability of exceeding a damage level $D_3$).

In **Figure 17**, the obtained fragility curves are shown. In the same figure, two other fragility curves, named "Lower Bound" and "Upper Bound," are represented. They can be considered as a lower and an upper bound of the fragility and are obtained by Vulnus through a proper modification of the curve "Mean," once that uncertainties, related to those parameters that cannot determined accurately, on the indices $I_1$, $I_2$, and $I_3$ are properly accounted for. Also, the curves corresponding to the vulnerability classes "A" (curve "EMS98 LOW") and "B" (curve "EMS98 UP"), according to the macroseismic scale EMS-98 are reported. It is possible to observe that, considering the mean curve, the buildings of the aggregate have to be assimilated to a vulnerability class "A."
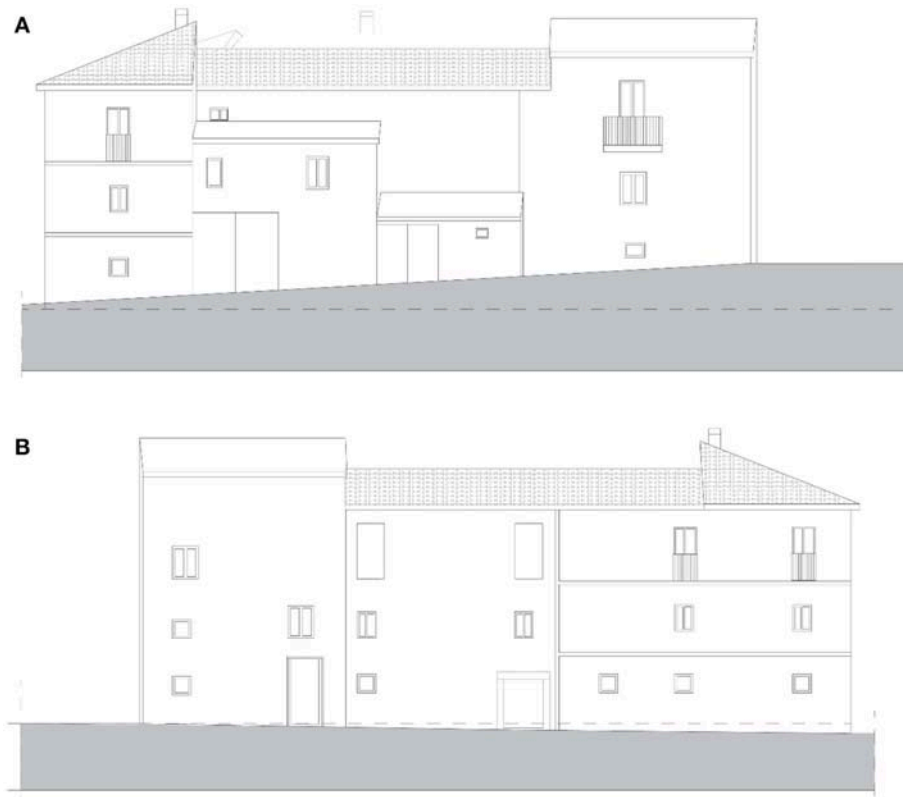
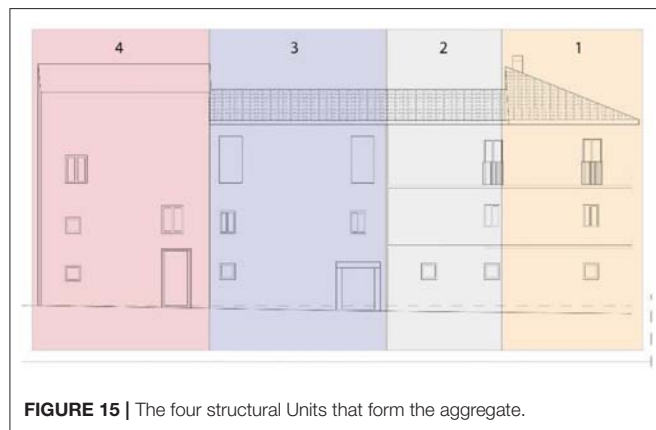FIGURE 14 | (A) Front and (B) back of the considered aggregate.


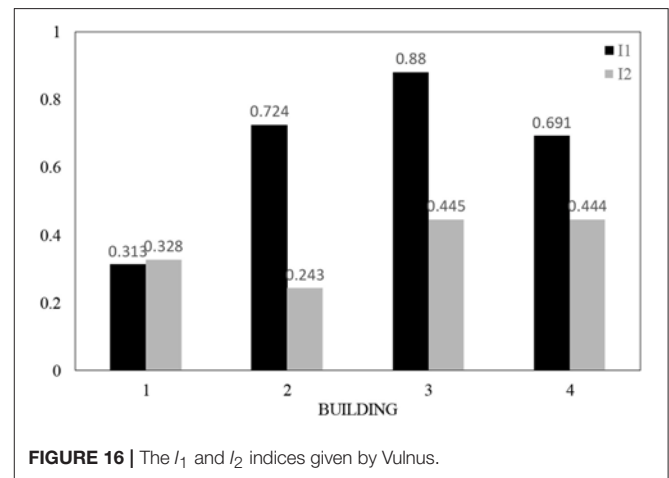FIGURE 15 | The four structural Units that form the aggregate.


FIGURE 16 | The $I_1$ and $I_2$ indices given by Vulnus.

## CONCLUSION

In this paper, the vulnerability assessment of the historic center of Campotosto, in the district of L'Aquila (Italy), has been dealt with.

The investigated historic center was hit by the 2016 Central Italy earthquake and reported several damage that have been represented by means of a Damage Probability Matrix, as well through a GIS map.

The vulnerability evaluation has been performed through the application of two simplified methods.

The first is an empirical method calibrated by the authors after the 2009 L'Aquila earthquake, based on observations carried out on similar historical centers. It has been applied on 130 buildings of the historic center of Campotosto, for which the main structural features have been identified.
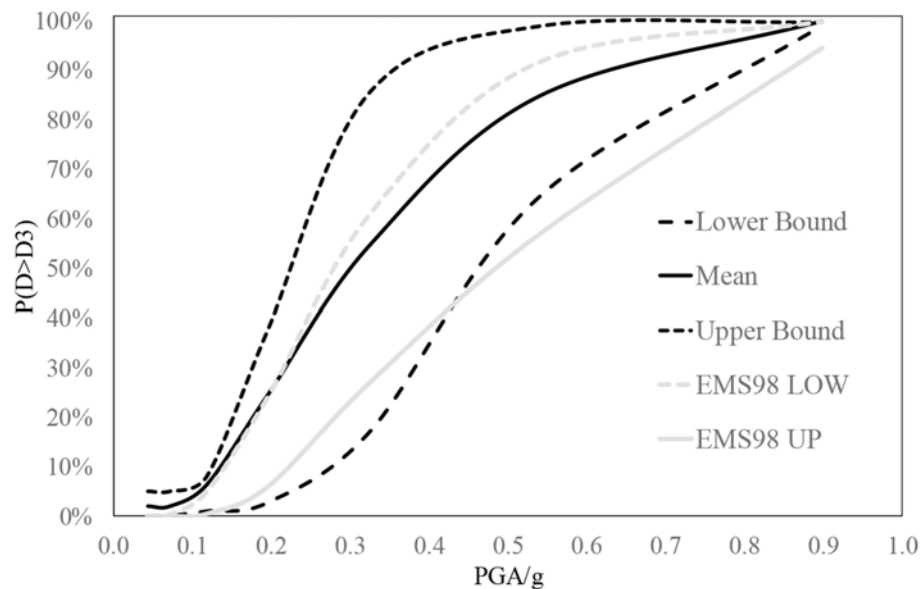
**FIGURE 17 |** The fragility curves given by Vulnus for a damage grade higher than D3.
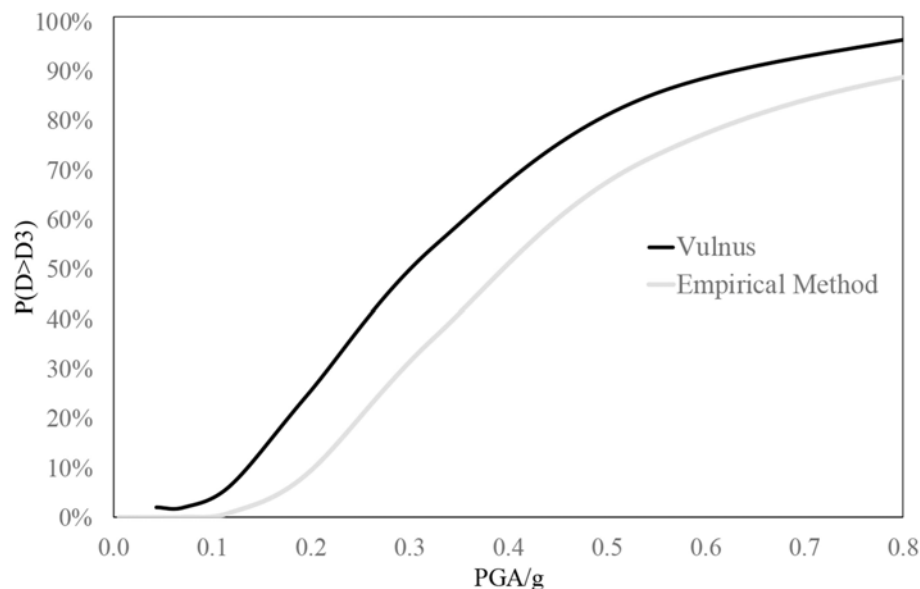


**FIGURE 18 |** Comparison between the fragility curves given by Vulnus and by the empirical method for a damage grade higher than D3.

The latter, is a methodology based on the use of the Vulnus software, developed at the University of Padua. It has been applied on a clustered building formed by four structural units, which has been considered as representative of the whole built environment.

The main conclusions of the study can be summarized as follows:

● The reconnaissance activity carried out after the 2016 Central Italy earthquake proved that the damage distribution can be

satisfyingly interpreted by a binomial probability function, which entails that the proposed empirical method for the vulnerability evaluation can be applied.

● The considered clustered building is characterized by a fragility curve for severe damage (damage grade higher than $D_3$) that well fit the fragility curve given by the EMS-98 macroseismic scale for a Vulnerability Class A.

● The fragility curve given by the analytical method based on the Vulnus evaluation is higher than the one provided by the

empirical method [given by transforming the $I_{MCS}$ intensity in the ground acceleration according to Margottini et al. (1987)], as it is shown in **Figure 18**. However, the registered scatters are quite acceptable (about 15%) for ground acceleration higher than 0.4 g.

● The high scatters for ground accelerations that are lower than 0.4 g can be justified by the fact that a unique cluster buildings is not sufficient to well esteem the vulnerability. For this reason, in the future, evaluations about the minimum number of aggregated buildings to be considered for the assessment have to be carried out.

It must be pointed out that, apart from the limited number of clustered buildings considered for the evaluation, other issues that have been only briefly mentioned in the paper, such as the one related to the site effects due to the soil typology, are worthy of being deepening, as they could influence significantly the proposed outcomes.

## DATA AVAILABILITY

The datasets generated for this study are available on request to the corresponding author.

## AUTHOR CONTRIBUTIONS

All authors listed have made a substantial, direct and intellectual contribution to the work, and approved it for publication.

## ACKNOWLEDGMENTS

## REFERENCES

Anastasopoulos, D., De Smedt, M., Vandewalle, L., De Roeck, G., and Reynders, E. P. B. (2018). Damage identification using modal strains identified from operational fiber-optic Bragg grating data. *Struct. Health Monitor.* 17, 1441–1459. doi: 10.1177/1475921717744480

Bernardini, A., Gori, R., Modena, C., Valluzzi, M. R, Benincà, G., Barbetta, E., et al. (2009). *Vulnus Vb 4.0: Procedura Automatica per Analisi di Vulnerabilità Sismica di Edifici in Muratura.* Available online at: http://hdl.handle.net/11577/3150148

Brando, G., Criber, E., and De Matteis, G. (2015). The effects of L'aquila earthquake on the St. Gemma church in Goriano Sicoli: part II—fem analysis. *Bull. Earthquake Eng.* 13, 3733–3748. doi: 10.1007/s10518-015-9793-3

Brando, G., De Matteis, G., and Spacone, E. (2017a). Predictive model for the seismic vulnerability assessment of small historic centers: application to the inner Abruzzi Region in Italy. *Eng. Struct.* 153, 81–96. doi: 10.1016/j.engstruct.2017.10.013

Brando, G., Rapone, D., Spacone, E., O'Banion, M. S., Olsen, M. J., Barbosa, A. R., et al. (2017b). Damage reconnaissance of unreinforced masonry bearing wall buildings after the 2015 Gorkha, Nepal, Earthquake. *Earthquake Spectra* 33(Special issue 1), S243–S273. doi: 10.1193/010817EQS009M

Cascini, L., Gagliardo, R., and Portioli, F. (2018). LiABlock,_3D: a software tool for collapse mechanism analysis of historic masonry structures. *Int. J. Archit. Herit.* doi: 10.1080/15583058.2018.1509155. [Epub ahead of print].

Clementi, F., Pierdicca, A., Formisano, A., Catinari, F., and Lenci, S. (2017). Numerical model upgrading of a historical masonry building damaged during the 2016 Italian earthquakes: the case study of the Podestà palace in Montelupone (Italy). *J. Civil Struct. Health Monitor.* 7, 703–717. doi: 10.1007/s13349-017-0253-4

Criber, E., Brando, G., and De Matteis, G. (2015). The effects of L'Aquila earthquake on the St. Gemma church in Goriano Sicoli: part I—damage survey and kinematic analysis. *Bull. Earthquake Eng.* 13, 3713–3732. doi: 10.1007/s10518-015-9792-4

D'Onofrio, K., and Tatoni, S. (2017). Third *Level Micro-zonation of the Municipality of Campotosto (Italian).* Available online at: https://www.comune.campotosto.aq.it/microzonazione-sismica/

Ferreira, T. M., Vicente, R., Mendes da Silva, J. A. R., Varum, H., and Costa, A. (2013). and Seismic vulnerability assessment of historical urban centers: case study of the old city center in Seixal Portugal. *Bull. Earthquake Eng.* 11, 1753–1773. doi: 10.1007/s10518-013-9447-2

Fiorentino, G., Forte, A., Pagano, E., Sabetta, F., Baggio, C., Lavorato, D., et al. (2018). Damage patterns in the town of Amatrice after August 24th 2016 Central Italy earthquakes. *Bull. Earthquake Eng.* 16, 1399–1423. doi: 10.1007/s10518-017-0254-z

Formisano, A. (2017a). Local- and global-scale seismic analyses of historical masonry compounds in San Pio delle Camere (L'Aquila, Italy). *Nat. Hazards* 86, 465–487. doi: 10.1007/s11069-016-2694-1

Formisano, A. (2017b). Theoretical and numerical seismic analysis of masonry building aggregates: case studies in San Pio Delle Camere (L'Aquila, Italy). *J. Earthquake Eng.* 21, 227–245. doi: 10.1080/13632469.2016.1172376

Formisano, A., and Marzo, A. (2017). Simplified and refined methods for seismic vulnerability assessment and retrofitting of an Italian cultural heritage masonry building. *Comput. Struct.* 180, 13–26. doi: 10.1016/j.compstruc.2016.07.005

GNDT (1994). *Scheda di Vulnerabilità di 2° Livello (Muratura).* Available online at: https://emidius.mi.ingv.it/GNDT2/Pubblicazioni/Lsu_96/vol_1/schede.pdf

Grünthal, G. (1998). *Ed European Macroseismic Scale 1998.* Luxembourg: Cahiers du Center Europèen de Gèodynamique et de Seismologie. Conseil de l'Europe.

Krstevska, L., Tashkov, L., Naumovski, N., Florio, G., Formisano, A., Fornaro, A., et al. (2010). "*In-situ* experimental testing of four historical buildings damaged during the 2009 L'Aquila earthquake," in *COST ACTION C26: Urban Habitat Constructions Under Catastrophic Events - Proceedings of the Final Conference,* ed Mazzolani (London: Taylor & Francis Group), 427–432.

Lagomarsino, S., and Giovinazzi, S. (2006). Macroseismic and mechanical models for the vulnerability and damage assessment of current buildings. *Bull. Earthquake Eng.* 4, 415–443. doi: 10.1007/s10518-006-9024-z

Margottini, C., Molin, D., Narcisi, B., and Serva, L. (1987). "Intensity vs. acceleration: Italian data," in *Proceedings of the Workshop on Historical Seismicity of Central-Eastern Mediterranean Region* (Roma: ENEA-IAEA), 213–226.

Paolucci, R., Pacor, F., Puglia, R., Ameri, G., Cauzzi, C., and Massa, M. (2011). "Record processing in ITACA, the new Italian strong motion database," in *Earthquake Data in Engineering Seismology, Geotech- nical, Geological and Earthquake Engineering Series, Vol. 14,* eds S. Akkar, P. Gulkan, and T. Van Eck (Berlin: Springer Science + Business Media B.V.), 99–113.

Ponzi, A., Tempesta, G., Di Napoli, E., Colasante, P., Limiti, F., Limiti, P., et al. (2013). *Reconstruction Plan of the di Campotosto Municipality Following the Seismic Event of the 6th of April 2009 (Italian).* Available online at: https://www.comune.campotosto.aq.it/vecchio/index.php?option=com_content&view=article&id=79&Itemid=200

Portioli, F., and Cascini, L. (2017). Large displacement analysis of dry-jointed masonry structures subjected to settlements using rigid block modelling. *Eng. Struct.* 148, 485–496. doi: 10.1016/j.engstruct.2017.06.073

Rapone, D., Brando, G., Spacone, E., and De Matteis, G. (2018). Seismic vulnerability assessment of historic centers: description of a predictive method

and application to the case study of Scanno (Abruzzi, Italy). *Int. J. Archit. Herit.* 12, 1171–1195. doi: 10.1080/15583058.2018.1503373

Sorrentino, L., Cattari, S., da Porto, F., Magenes, G., and Penna, A. (2018). Seismic behaviour of ordinary masonry buildings during the 2016 central Italy earthquakes. *Bull. Earthquake Eng.* 33, 1–25. doi: 10.1007/s10518-018-0370-4

Sorrentino, L., Doria, M., Tassi, V., and Liotta, M. (2019). Performance of a far-field historical church during the 2016-2017 central Italy earthquakes. *J. Performance Constructed Facil.* 33:04019016. doi: 10.1061/(ASCE)CF.1943-5509.0001273

Tashkov, L., Krstevska, L., Naumovski, N., De Matteis, G., and Brando, G. (2010). "Ambient vibration tests on three religious buildings in Goriano Sicoli damaged during the 2009 L'Aquila earthquake," in *COST ACTION C26: Urban Habitat Constructions Under Catastrophic Events - Proceedings of the Final Conference* (London), 433–438.

Turnsek, V., and Cacovic, F. (1971). "Some experimental results on the strength of brick masonry walls," in *Proceedings of 2nd International Brick Masonry Conference* (Stoke on Trent).

Vicente, R., Parodi, S., Lagomarsino, S., Varum, H., and Silva, J. A. R. M. (2011). Seismic vulnerability and risk assessment: case study of the historic city center of Coimbra, Portugal. *Bull. Earthquake Eng.* 9, 1067–1096. doi: 10.1007/s10518-010-9233-3

Check for updates

# Simplified and Refined Analyses for Seismic Investigation of Historical Masonry Clusters: Comparison of Results and Influence of the Structural Units Position

Giovanni Chiumiento* and Antonio Formisano

Department of Structures for Engineering and Architecture, University of Naples Federico II, Naples, Italy

The goal of this work is the assessment of the seismic vulnerability of building clusters within the historical center of Arsita (Teramo, Italy), damaged by the 2009 L'Aquila earthquake, by comparing two different analysis procedures applied to a construction compound case study. First, the seismic vulnerability of structural units of the building compound, has been appraised using a vulnerability evaluation quick form, appropriately conceived for masonry clusters. In particular, heading and intermediate structural units, having different geometrical configuration and seismic behaviors, have been inspected using the aforementioned form, which allowed for the calculation of a synthetic vulnerability index. Starting from these indices, the probable damage suffered by the examined structural units under different grade earthquakes, have been estimated. Later, both the single structural units and the whole construction compound were modeled using the macro-element refined method provided by the 3Muri non-linear analysis software. Static non-linear analyses performed on the above-mentioned structures have provided related pushover curves, used to estimate, using the N2 method, the damage suffered under seismic actions expected at that site. Therefore, the damage of single structural units have been compared to those experienced by the same structures within the building aggregate. Finally, the results derived from the two analysis methodologies considered were compared, confirming the effectiveness of the simplest technique to predict the seismic damage and vulnerability of investigated structures.

Keywords: masonry clusters, vulnerability assessment, L'Aquila earthquake, macroelement method, pushover curves, survey form, vulnerability index method

## INTRODUCTION

The assessment of the seismic vulnerability of existing buildings is a problem of particular relevance for the Italian territory, where a large part of the built heritage was not erected using anti-seismic criteria. Most of the ancient buildings in Italy are made of masonry materials with low mechanical properties, which also diminish over time due to both age and environmental factors. In addition, the rapid growth in buildings built after the Second World War, which represent the major part of Italian built heritage, was often not accompanied by planned urban development plans. It is also important to note that many Italian historical centers are often composed of clustered buildings

resulting from several planned and vertical additions made of different materials and constructive techniques. Since they are highly exposure as cultural, architectural and historical values and are placed into medium-high hazard zones, significant social and economic losses could occur in case of earthquakes.

For these reasons, the study of historical centers in terms of seismic actions is a key issue in the field of Civil Engineering and the individuation of possible protection strategies is becoming a pressing need for administrations and designers.

Current Italian technical standards [D.M. 17/01/2018; Ministerial Decree (M.D.), 2018] deal with the high accuracy of technical prescriptions that need to be adopted for seismic protection of new constructions. On the contrary, for existing structures and even more so for historical clustered buildings, seismic behavior assessment has been only been investigated systematically a few times. In fact, such structures were mainly designed to withstand static vertical loads and static horizontal thrusts of arches and vaults, neglecting seismic actions which can provoke diffused cracks and, in worst cases, partial or global collapse. Therefore, clustered buildings are vulnerable to earthquakes and this issue should be treated in much more detail within standard building codes. Nowadays, complex methodologies based on the development of high-definition 3D numerical FEM models are often adopted for the structural assessment of historical masonry buildings (Mallardo et al., 2008; Clementi et al., 2016; Miano et al., 2017, 2018; Ramírez et al., 2019). Nevertheless, non-linear time-history analyses, commonly considered to better estimate the seismic response of buildings, require a very strong computational effort. For this reason, the current standard provides a simplified method to evaluate the seismic behavior of clustered buildings, which is only effective in cases of intermediate structural units with rigid diaphragms, where pushover analyses can be performed for each building story. This vulnerability assessment method for historical clustered buildings provided for in the building code, is often not applicable due to the lack of some important prerequisites, such as the effective connections among masonry walls and the presence of rigid horizontal floors able to distribute seismic forces uniformly among seismic-resistant elements. Indeed, in most cases flexible floors are detected, and this requires the analysis of single walls instead of the whole building. In addition, in the case of heading or angle structural units, the effects of accidental torsion should be considered. In these two latter cases, no specific provisions are provided for by the standards. Therefore, the scientific community is being pushed to find simplified applicative methods to evaluate the seismic response of structural units in masonry building clusters.

Moreover, in the case of the seismic vulnerability assessment of large urban habitats, considering that sophisticated analysis on single constructions are not required, a lot of *in-situ* surveys should be performed and a lot data on buildings should be acquired. Effective analysis procedures, used at a territorial scale, should be quick and should employ information from similar buildings damaged by past seismic events (Caprili et al., 2017; D'Amato et al., 2018; Fuentes et al., 2019). Therefore, three different seismic vulnerability evaluation approaches, namely Damage Probability Matrices (DPM) (Whitman et al., 1973; Grunthal, 1998; Lagomarsino and Giovinazzi, 2006;

Formisano et al., 2017a), Vulnerability Indices (VI) (Benedetti and Petrini, 1984; GNDT, 1993; Bernardini, 2000; Formisano et al., 2011; Formisano, 2017a), and Capacity Curves (CC) (ATC, 1996; Kircher et al., 1997; Magenes, 2000; Formisano, 2017b; Formisano et al., 2017b), are typically used (Calvi et al., 2006). In particular, DPM and VI methods have been validated in the damage which occurred in several areas hit by earthquakes. Some other methods based on kinematics models, involving the equilibrium of macro-elements composed of single walls or sub-assemblages (Bernardini et al., 1990; Giuffrè, 1993), are also used for predicting the damage to buildings within historical centers. Nevertheless, clear numerical calculation methods of clustered buildings are not provided for by the standard codes, even if in the last few years some attempts have been made to solve this problem from a theoretical-numerical (Ramos and Lourenco, 2004; Valluzzi et al., 2007; Senaldi et al., 2010; D'Ayala and Paganoni, 2011; Da Porto et al., 2013; Formisano et al., 2016; Brando et al., 2017; Cara et al., 2018; Formisano and Massimilla, 2018; Chieffo et al., 2019; Mosoarca et al., 2019; Valente et al., 2019) and experimental (Senaldi et al., 2019) point of view.

Starting from these premises, the attention of the current paper is focused on the urban center of Arsita, located in the district of Teramo, within the Abruzzo region of Italy, with the target to find a useful and reliable tool to investigate the seismic behavior of structural units within historical masonry clusters. Two different analysis procedures based on VI and CC methods have been applied to a case study of clustered buildings. The analysis methodologies considered have been compared, in order to evaluate the effectiveness of the simplest VI technique to predict the seismic damage and vulnerability of the investigated structures.

## THE MUNICIPALITY OF ARSITA: DATA AND POST-EARTHQUAKE RECONSTRUCTION PLAN

Arsita (**Figure 1**) is a town with 889 inhabitants, located in the district of Teramo (the Abruzzo region of Italy) at about 470 m above sea level. It is placed in the upper valley of the Fino river, near the Gran Sasso massif. Arsita is part of the mountain community of Vomano, Fino, and Piomba and it is also located within the Laga Mountains National Park. The municipal territory extends over about 30 km$^2$ and, therefore, the population density is about 30 inhabitants per km$^2$. The historic center and the four isolated hamlets of Bivio Arsita, Colle dei Cerri, Colle Mesole and Pantane are part of the municipality of Arsita, where pre-Roman remains from the eighth century B.C., and Roman coins, floors of buildings and small statues of the early Christian era are found.

Called *Bacucco* until 1905, Arsita emerged in the later Middle Ages around a fortified castle called *Castello Bacucco*, which originally belonged to the Count of Chieti, then to the monks of Montecassino and finally to the Casa d'Este. The village was sold in 1583 to Margaret of Austria Farnese. Other historians claim that Bacucco took its name from the Roman word for the God Bacchus.

**FIGURE 1 |** Birds-eye view of the municipality of Arsita (source: Google maps).

In the twelfth century the town was owned by the ruling Acquaviva family. Its current urban configuration can be traced back to the late Middle Ages-early Renaissance. In 1806, the town came under the rule of the town of Penne. During the Napoleonic period a good number of brigands held the territory in and around Arsita. A series of skirmishes occurred during this period. In the early nineteenth century the waters from a spring in this area were said to have healing powers. Nowadays, Arsita founds its richness on agriculture, sheep-farming and local craft activities. On the night of April 6th 2009 the municipality was affected by an earthquake of magnitude ($M_w$) 6.3, which hit a very large area of the Abruzzo region with an epicenter at low focal depth (9.5 km, coordinates 42,348 N, 13,380 E) very close to the city of L'Aquila (about 7 km SO). This main event was the strongest of a sequence initiated a few months earlier, consisting of 23 seismic shocks of magnitude 4 between March 30th and April 23rd and two significant aftershocks ($M_w$ 5.6 on April 7th and $M_w$ 5.4 on April 9th). The consequences of this seismic sequence were very serious, with 18,000 damaged buildings, 305 casualties, about 1,500 injured and 70,000-80,000 residents temporarily evacuated in the first months after the disaster.

About 2 years after the L'Aquila seismic sequence, a scientific team set up by ENEA (Italian National Agency for New Technologies, Energy and Sustainable Economic Development), with the Universities of Pescara-Chieti "G. D'Annunzio," Naples "Federico II" and Ferrara, were tasked with a post-earthquake reconstruction plan for the Municipality of Arsita, whose contents can be found at a dedicated website (http://www.pdr-arsita.bologna.enea.it/).

The small and nice historic center of Arsita presents a very inhomogeneous built heritage with regards to earthquake damage, vulnerability, past interventions, maintenance, and signs of past seismic events. The ancient nucleus consisted of a fortified

construction (a masonry tower now in ruins), due to its strategic importance in the territory, providing for its present wonderful position in the landscape. Furthermore, the historic center is enshrined with notable palaces and churches (**Figures 2A,B**). Other than these important cultural heritage sights, the historical center includes a series of articulated building compounds typical of the Abruzzo region (**Figure 2C**).

Although the Intensity level (VI MCS) of the L'Aquila earthquake which affected Arsita was considered moderate, the combination of several factors (mainly high potential vulnerability, particular topographic and soil conditions) led to non-negligible widespread damage. Therefore, first, the Arsita Technical Office defined that the building clusters (depending on their structural continuity) needed to be either repaired or rehabilitated. Thus, the investigation of the historical center was focused on the effectiveness of a multidisciplinary approach based on the simultaneous application of Remote Sensing techniques, GIS (Geographical Information System) tools, DGPS and Laser Scanner surveys. In particular, the data acquisition was based first on direct visual surveys of the external and internal parts of all concerned constructions, including the measurement of the main geometric characteristics and the assessment of structural parts (walls, floors, roofs, etc.), materials, construction details and techniques. Samples of the most important materials (stone, brick, mortar, etc.) were collected, with the aim to perform characterization laboratory tests.

At the same time, the (AeDES, 2000), filled in by the Civil Protection expert teams during the emergency phase for the evaluation of seismic damage and safety, were studied, verified and digitized. Moreover, urban planning, architectonic, and energetic forms were also filled in order to investigate building descriptions and energetic aspects.
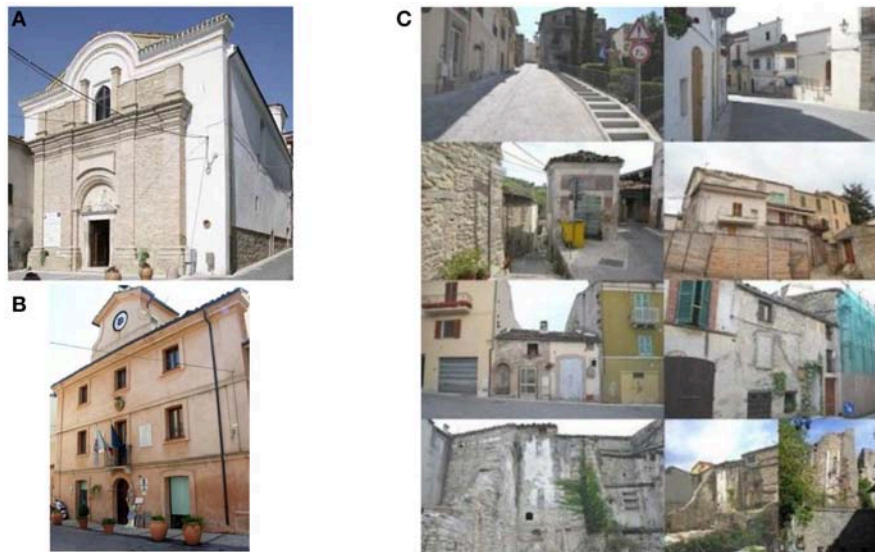
**FIGURE 2 |** Cultural and residential heritages of the historical center of Arsita: Santa Vittoria church **(A)**, Wolf Museum **(B),** and some clustered buildings **(C)** (source: personal archive).

After this phase, some quick and more refined procedures for vulnerability evaluation, namely Famive (D'Ayala and Speranza, 2002), GNDT (1993), a vulnerability assessment form purposely conceived for masonry clusters (Formisano et al., 2011, 2015) and MEDEA (Papa and Zuccaro, 2004), were applied to the structural units of examined masonry clusters in order to have a clear picture of their weak points from a seismic perspective. This activity was very important to define precise guidelines for the rehabilitation of the structural typologies of clustered buildings within these historical centers.

## SELECTION AND MAIN PROPERTIES OF THE CLUSTERED BUILDINGS UNDER STUDY

In the framework of the post-earthquake reconstruction plan of Arsita *in-situ* investigations were performed in order to subdivide the historical center of masonry clusters, in which appropriate seismic vulnerability analyses and retrofitting interventions were executed on. Therefore, 17 masonry clusters, made up of a total of 91 structural units, were individuated (**Figure 3A**).

The case study herein considered is a masonry cluster identified as number 8 and composed of four structural units (S.U.) named 8A, 8B, 8C, and 8D (**Figure 3B**).

The building aggregate, erected earlier than 1919, is characterized by a discrete architectural value and has both residential and productive uses. The constitutive materials are masonry stones typical of the Abruzzo region. Horizontal structures are made of steel beams and hollow slab blocks. Timber beams, which sustain overlying timber planks and tiles, are the load-bearing members of roofing. Regarding the morphology, the cluster is rather regular in plan, while the major discontinuities

are detected in elevation, with the presence of staggered floors and floors at different heights due to the soil slope. Plan layouts, vertical sections and external views of the inspected clustered buildings are shown in **Figures 4–6**, respectively.

In this study the intermediate (8B) and head (8C) structural units, characterized by different structural behaviors deriving from the dissimilar geometric conformations and in-plane location, are examined in detail.

## MACROELEMENT MODELING AND PUSHOVER ANALYSIS

Macro-element models of both the whole building cluster and single S.U. have been implemented by means of the 3Muri calculation software (Lagomarsino et al., 2013; STA DATA srl., 2018).

Through the guidelines delivered by the Italian Ministry of Cultural Heritage and Activities (Ministry of Cultural Heritage and Activities (MiBAC), 2011) concerning the assessment, prevention, and mitigation of the seismic risk, it has been possible to identify the constructive type of the investigated cluster, useful for modeling issues in the 3Muri program. In this calculation software the so-called macro-elements method is used. This modeling technique sees masonry walls as an assemblage of masonry piers, spandrels and rigid nodal panels. The masonry walls are then transformed into equivalent frames aiming at running pushover analyses. To this purpose, initially, all the geometric and mechanical information on the structures under study have been collected. Plan layouts of the S.U. in dxf format have been imported into the program and, after the walls, floors, and roofs have been modeled, mechanical features of materials have been assigned to the structural components on the basis of the standard provisions in the case of LC1 knowledge level, since
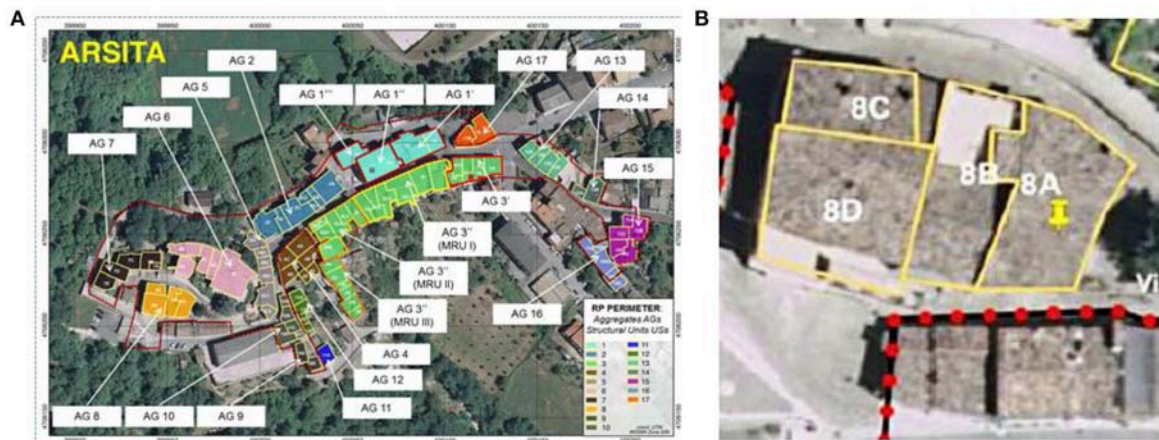
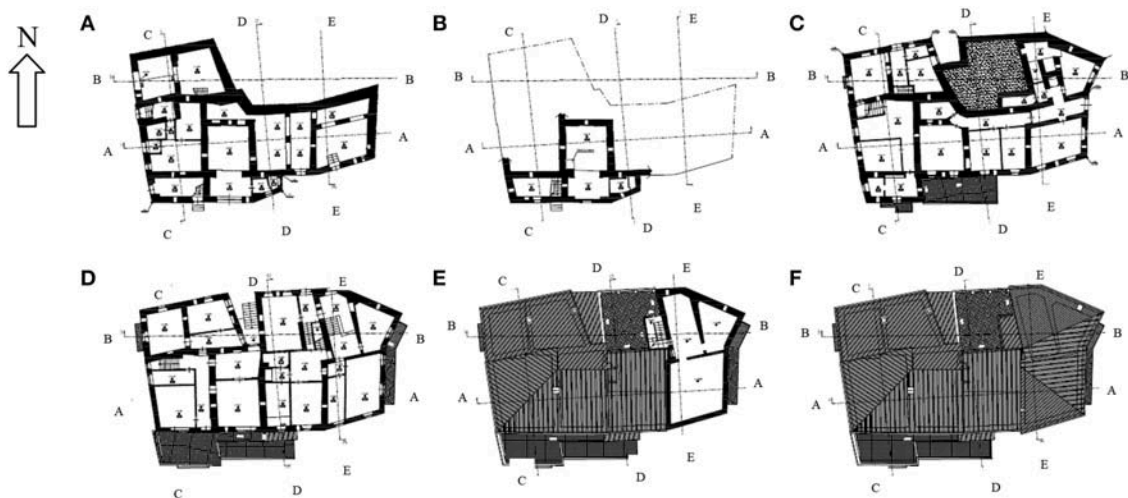**FIGURE 3 |** Masonry compounds of the historical center of Arsita **(A)** and the clustered buildings under study **(B)** (source: http://www.pdr-arsita.bologna.enea.it/).



**FIGURE 4 |** Plan layouts of the building cluster under study: ground **(A)**, mezzanine **(B)**, first **(C)**, second **(D)**, attic **(E)**, and roof floors **(F)**.

in this case no destructive and non-destructive tests on materials have been performed. Subsequently, the loads applied to floors and roofs have been assigned and the presence of staircases, due to the impossibility of the program to proceed with their explicit modeling, has been taken into account, applying the dead weight and relative loads to the supporting masonry walls.

Therefore, based on the above modeling approach, the macro-element models of both the whole buildings cluster (**Figure 7A**) and the S.U. 8B and 8C have been set up (**Figures 7B,C**).

In particular, it has been chosen to inspect in detail head and intermediate S.U. in order to show their different seismic behaviors due to the dissimilar in-plane positions they have in the compound of constructions. All of the above macro-element models have been analyzed by pushover analysis, which is the most common method proposed by the current standard for non-linear seismic analysis of existing structures. The method consists of applying some distributions of gradually increasing

forces to the structure, to attain the local or global collapse. In this way the damaging effect of the earthquake is known, starting from the MDOF structure capacity curve, which is then transformed into the bi-linear curve representative of the SDOF equivalent system.

Non-linear static analyses have been carried out, considering the units both individually and within the cluster, in order to compare their seismic behavior in terms of base shear-displacement curves on the basis of a simple vulnerability index.

First, from the analysis carried out using the 3Muri software, the MDOF pushover curves of isolated S.U. have been plotted in directions X and Y together with the main damage states detected for increasing displacement levels up to the collapse (**Figures 8–11**).

From the analysis results it appears that S.U. B and C suffered plastic and failure states due to compression-bending mechanisms being more than shear in both analysis directions.
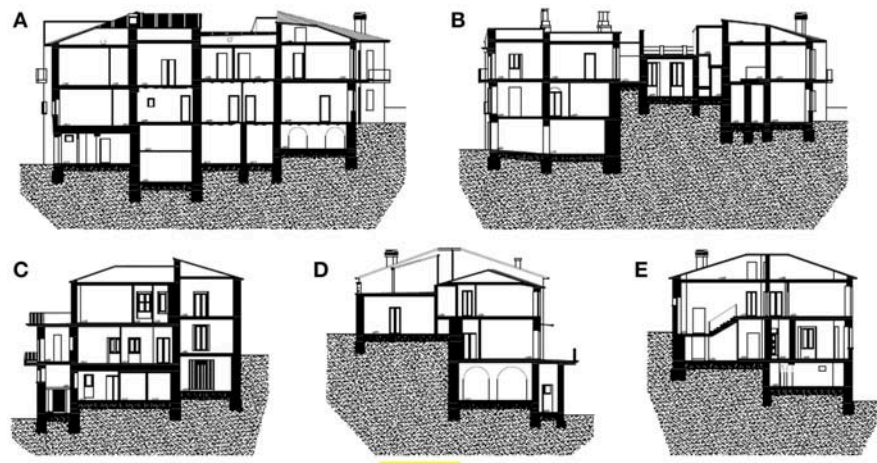
**FIGURE 5 |** Vertical sections of the building cluster under study: A-A **(A)**, B-B **(B)**, C-C **(C)**, D-D **(D)**, and E-E **(E)**.
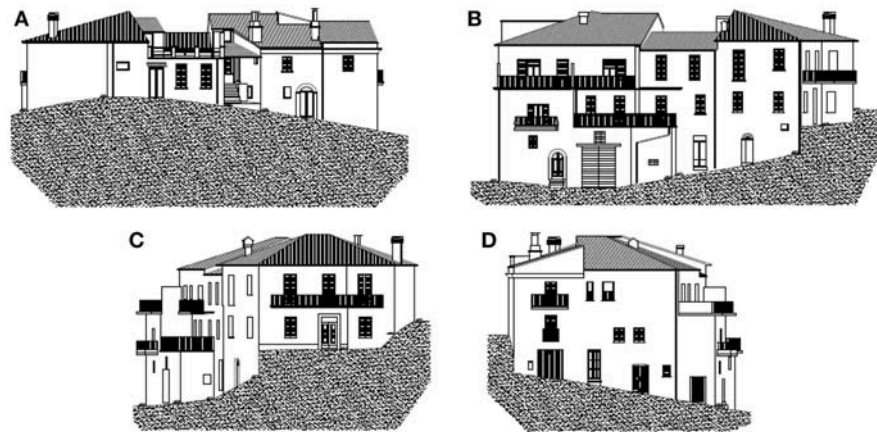


**FIGURE 6 |** External views of the building cluster under study: north **(A)**, south **(B)**, east **(C)**, and west **(D)**.
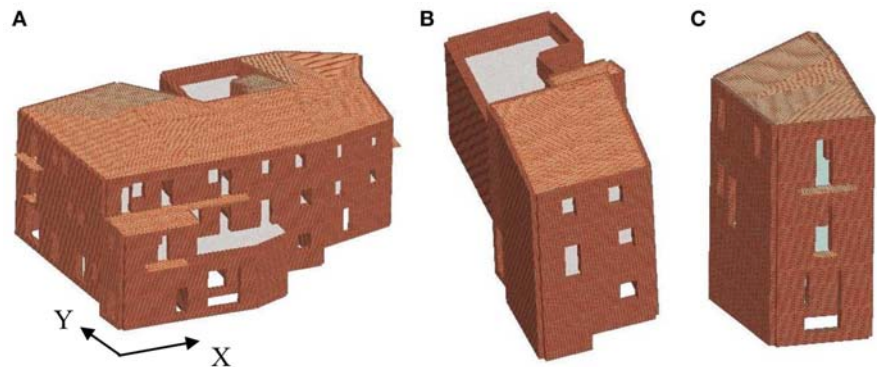


**FIGURE 7 |** Macro-element modeling: the whole cluster **(A)** and S.U. 8B **(B)** and 8C **(C)**.
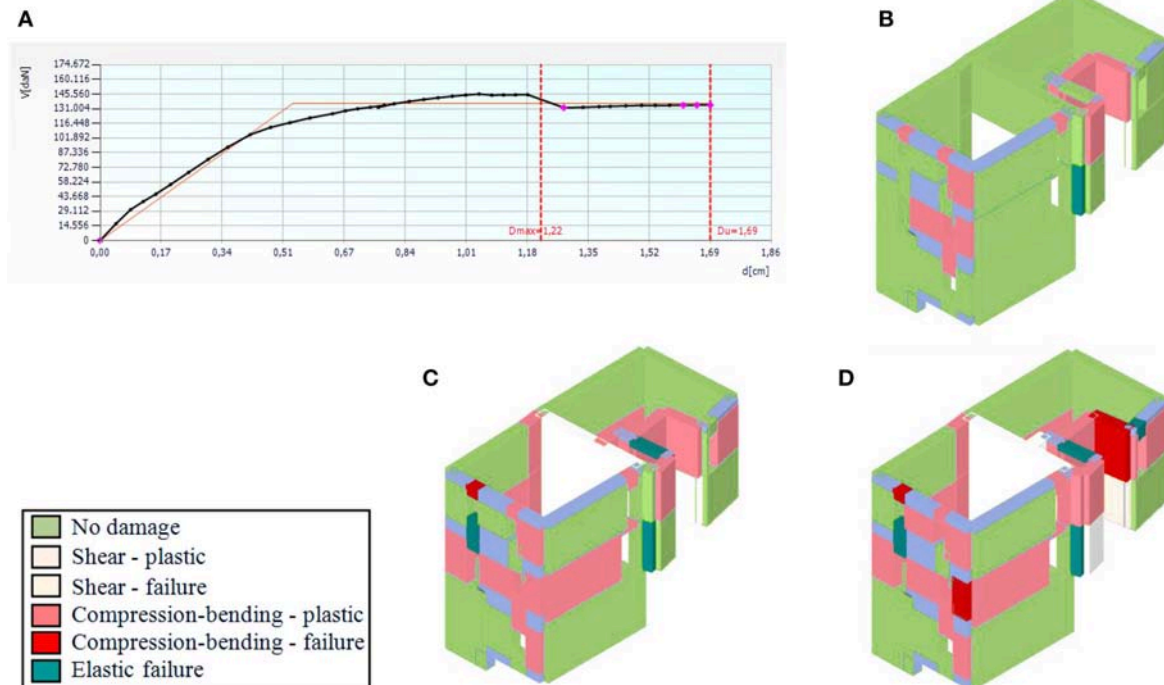
**FIGURE 8** | Seismic behavior in direction X of the isolated S.U. type B: MDOF pushover curve **(A)** and damage patterns related to the conventional yielding limit **(B)**, maximum base shear **(C)**, and ultimate displacement $D_U$ **(D)**.
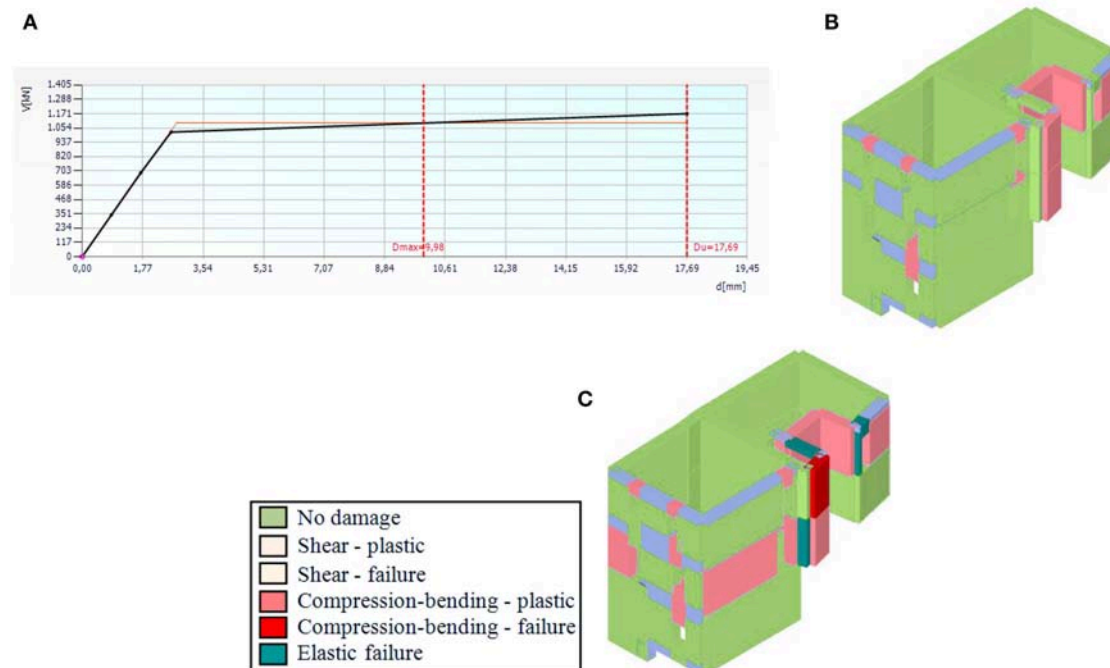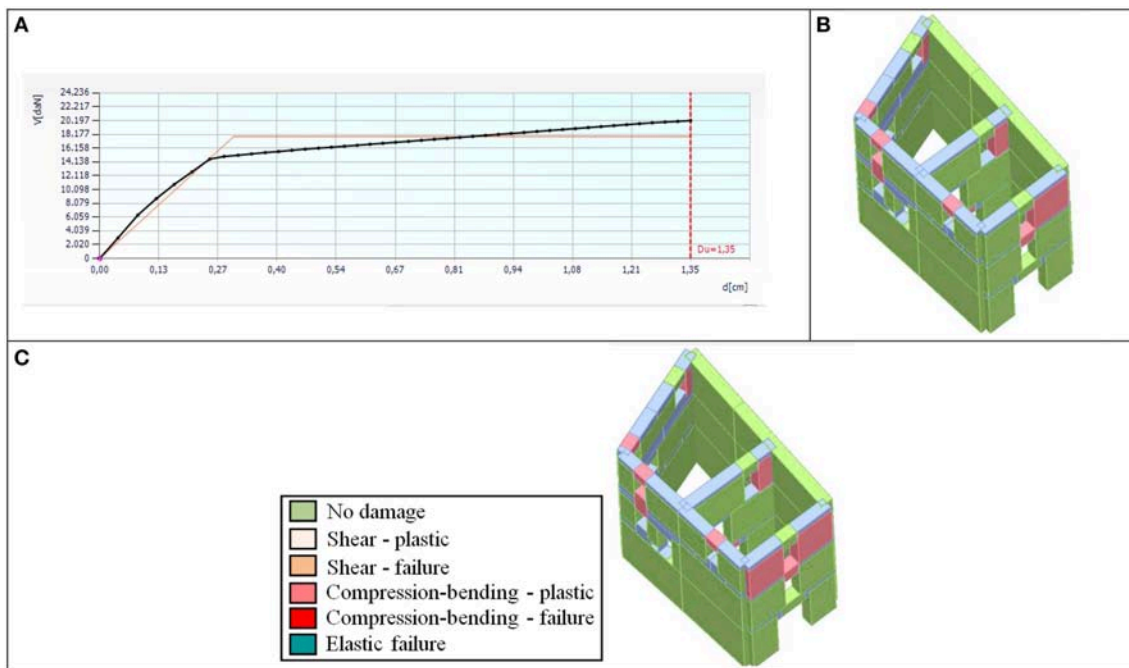


**FIGURE 9** | Seismic behavior in direction Y of the isolated S.U. type B: MDOF pushover curve **(A)** and damage patterns related to the conventional yielding limit **(B)** and ultimate displacement $D_U$ **(C)**.
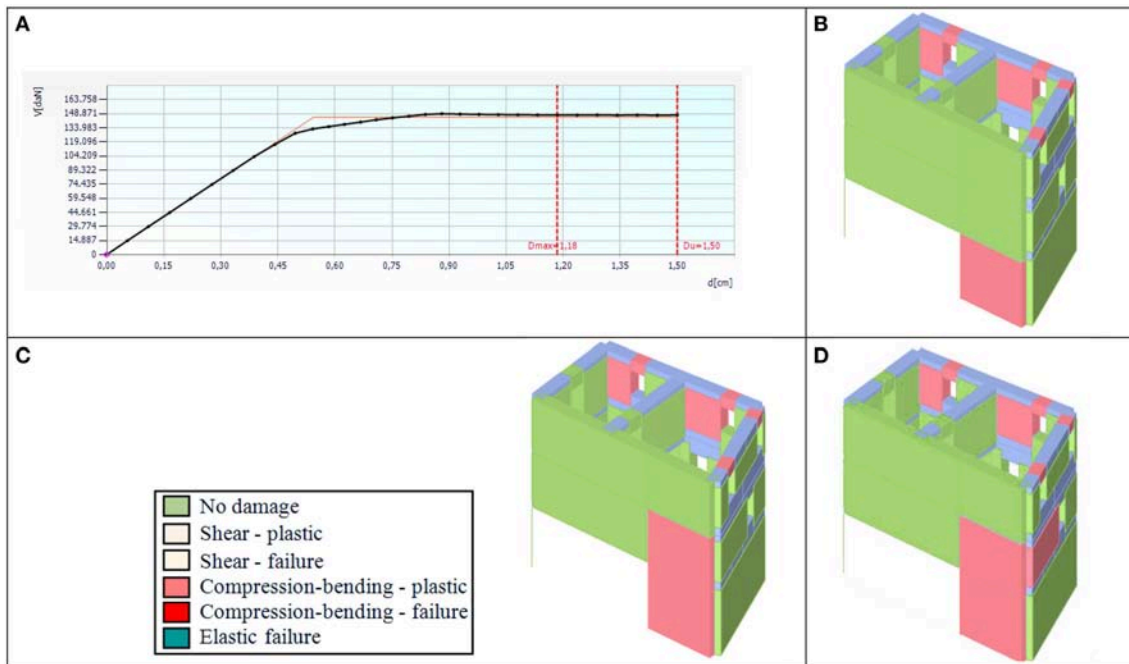
**FIGURE 10 |** Seismic behavior in direction X of the isolated S.U. type C: MDOF pushover curve **(A)** and damage patterns related to the conventional yielding limit **(B)**, maximum base shear **(C)**, and ultimate displacement $D_U$ **(D)**.



**FIGURE 11 |** Seismic behavior in direction Y of the isolated S.U. type C: MDOF pushover curve **(A)** and damage patterns related to the conventional yielding limit **(B)** and ultimate displacement $D_U$ **(C)**.

Subsequently, it has been possible, through the theory of the equivalence of areas, to pass from the MDOF curves to the SDOF bi-linear curves of S.U. 8B and 8C.

On the other hand, the curves of these S.U. have been directly obtained from the analysis results on the global cluster by considering their interaction with other units

in calculating the base shear and in estimating the top displacement. In particular, for a given analysis direction and for each loading step, the base shear has been calculated as the algebraic sum of all shears of masonry walls in that direction, taking into account the loads deriving from adjacent S.U., while the top displacement has been determined as the average value among displacements of all nodes of the last story.

So, in both cases (isolated structures and clustered ones), the maximum displacements required by the earthquake ($D_{max}$) have been estimated and, consequently, the related vulnerability indices have been computed. The bi-linear curves of single S.U and clustered ones in directions X and Y, together with the comparisons in terms of vulnerability indices, have been reported for S.U. 8B and 8C in **Figure 12**.

From the results collected, it is clear that the structural units in cluster conditions have, in all cases, vulnerability indices lower than those achieved when they are considered as isolated buildings. This effect is more clearly marked in direction X. for S.U. 8C, which has a vulnerability index lower than the one attained in direction Y. On the contrary however, for S.U. 8B vulnerability indices in both analysis directions are comparable to each other.

## QUICK SEISMIC VULNERABILITY ASSESSMENT

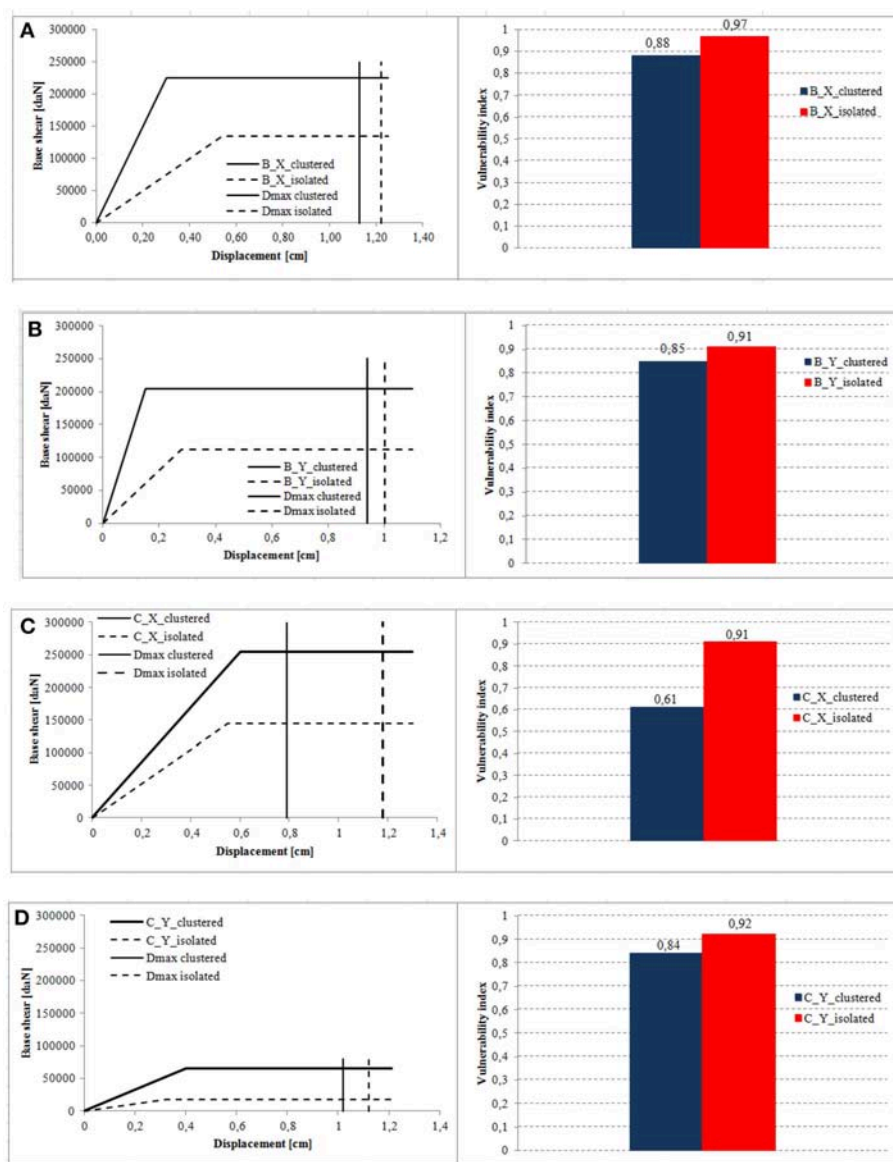An additional seismic evaluation methodology has herein been used to evaluate, through a simple vulnerability



**FIGURE 12 |** Pushover curves and comparison in terms of vulnerability indices for S.U. 8B in directions X **(A)** and Y **(B)** and for S.U. 8C in directions X **(C)** and Y **(D)**.

**TABLE 1 |** Quick form based vulnerability index of the S.U. type B.

**Cluster N° 8 Building B**

| | Classification | | | | Weight | Vulnerability index |
|---|---|---|---|---|---|---|
| **Parameter** | **A** | **B** | **C** | **D** | **W** | **Iv** |
| **BUILDING-SPECIFIC** | | | | | | |
| 1. Organization of vertical structures | 0 | 5 | 20 | 45 | 1 | 45 |
| 2. Nature of vertical structures | 0 | 5 | 25 | 45 | 0,25 | 6,25 |
| 3. Location of the building and type of foundations | 0 | 5 | 25 | 45 | 0,75 | 33,75 |
| 4. Distribution of resistant elements in plan | 0 | 5 | 25 | 45 | 1,5 | 37,5 |
| 5. Plan regularity | 0 | 5 | 25 | 45 | 0,5 | 12,5 |
| 6. Elevation regularity | 0 | 5 | 25 | 45 | 0,8 | 20 |
| 7. Horizontal structures | 0 | 5 | 25 | 45 | 0,8 | 20 |
| 8. Coverage | 0 | 15 | 25 | 45 | 1 | 45 |
| 9. Particular | 0 | 0 | 25 | 45 | 0,25 | 6,25 |
| 10. Current status | 0 | 5 | 25 | 45 | 1 | 5 |
| **Summation of first 10 parameters** | | | | | | 231,25 |
| **CLUSTER-SPECIFIC** | | | | | | |
| 11. Altimetric interaction | −20 | 0 | 15 | 45 | 1 | 0 |
| 12. Planimetric interaction | −45 | −25 | −15 | 0 | 1,5 | −37,5 |
| 13. Presence of staggered floors | 0 | 15 | 25 | 45 | 0,5 | 12,5 |
| 14. Typological and structural discontinuities | −15 | −10 | 0 | 45 | 1,2 | −18 |
| 15. Percentage difference of the holes in the façade | −20 | 0 | 25 | 45 | 1 | 25 |
| **Summation of last 5 parameters** | | | | | | −18 |
| **Summation of all 15 parameters** | | | | | | 213,25 |

*For each structural unit the colored values are the classes attributed to the parameters.*

form appropriately conceived for S.U. of masonry clusters, the seismic behavior of the inspected masonry building compound no.8.

The applied procedure is based on the (Benedetti and Petrini, 1984), elaborated about 35 years ago to estimate the seismic vulnerability of single constructions using 10 building-specific parameters. The 10 parameters are representative of the buildings structural behavior, they concern the organization and nature of vertical structures, the location of the building and type of foundations, the distribution of seismic-resistant elements, the in-plan and in-elevation irregularities, the type of floors and roofs, the structural details and the maintenance state. For each of the 10 parameters a class score, from A, the best, to D, the worst, is assigned. In addition, a weight is provided for each parameter. The weights take into account the minor or major importance that the various parameters have on the seismic behavior of the structure. They are characterized by a number varying from 0.25 to 1.50. Scores and weights were determined through the statistical analysis of damage data collected during recent earthquakes. Therefore, the vulnerability index is defined as the sum of the class score of each parameter multiplied by the respective weight. This index is then normalized into a range [0–1], where 0 indicates buildings complying with current seismic regulations, while 1 is representative of buildings with poor seismic behavior.

Starting from this study and according to recent research (Formisano et al., 2015, 2017b), five new cluster-specific parameters (in-plane and in-elevation interactions, staggered floors, typological and structural discontinuities, and difference of opening areas among adjacent facades) have been added to the original form in order to consider the interactions among S.U. when grouped in clusters. It is worth noting that the class scores of some of the new parameters assume negative values when they reduce the seismic vulnerability. Therefore, the final result is a modified form with 15 parameters capable of estimating, in quick and simple way, the seismic vulnerability of S.U. in historical centers. As in the original form, in the extended form the vulnerability index can be normalized in the range [0–1].

The vulnerability form for masonry cluster buildings has been filled in for S.U. 8B and 8C, providing the results illustrated, respectively, in **Tables 1**, **2**, where it is evident that the investigated buildings have an almost equal vulnerability index.

Finally, in **Figure 13** the comparison between vulnerability indices derived from 3Muri analyses and the simplified form ones are made.

From this comparison it has been shown that:

- The macro-element method provides indices higher than those of the vulnerability form. However, the two methods can be compared to each other only in qualitative terms, since the parameters considered for seismic vulnerability assessment (qualitative judgements in case of the form and quantitatively measured displacements in case of the macro-element analysis) are different.
- Structural units 8B and 8C have similar seismic vulnerability indices in both analysis directions. This is achieved using both analysis methods.

**TABLE 2 |** Quick form based vulnerability index of the S.U. type C.

**Cluster N° 8 Building C**

| Parameter | Classification | | | | Weight | Vulnerability index |
|---|---|---|---|---|---|---|
| | A | B | C | D | W | Iv |
| **BUILDING-SPECIFIC** | | | | | | |
| 1. Organization of vertical structures | 0 | 5 | 20 | 45 | 1 | 45 |
| 2. Nature of vertical structures | 0 | 5 | 25 | 45 | 0,25 | 6,25 |
| 3. Location of the building and type of foundations | 0 | 5 | 25 | 45 | 0,75 | 33,75 |
| 4. Distribution of resistant elements in plan | 0 | 5 | 25 | 45 | 1,5 | 67,5 |
| 5. Plan regularity | 0 | 5 | 25 | 45 | 0,5 | 2,5 |
| 6. Elevation regularity | 0 | 5 | 25 | 45 | 0,8 | 4 |
| 7. Horizontal structures | 0 | 5 | 25 | 45 | 0,8 | 20 |
| 8. Coverage | 0 | 15 | 25 | 45 | 1 | 45 |
| 9. Details | 0 | 0 | 25 | 45 | 0,25 | 6,25 |
| 10. Current status | 0 | 5 | 25 | 45 | 1 | 5 |
| **Summation of first 10 parameters** | | | | | | 235,25 |
| **CLUSTER-SPECIFIC** | | | | | | |
| 11. Altimetric interaction | −20 | 0 | 15 | 45 | 1 | 0 |
| 12. Planimetric interaction | −45 | −25 | −15 | 0 | 1,5 | −37,5 |
| 13. Presence of staggered floors | 0 | 15 | 25 | 45 | 0,5 | 7,5 |
| 14. Typological and structural discontinuities | −15 | −10 | 0 | 45 | 1,2 | −18 |
| 15. Percentage difference of the holes in the façade | −20 | 0 | 25 | 45 | 1 | 25 |
| **Summation of last 5 parameters** | | | | | | −23 |
| **Summation of all 15 parameters** | | | | | | 212,25 |

*For each structural unit the colored values are the classes attributed to the parameters.*
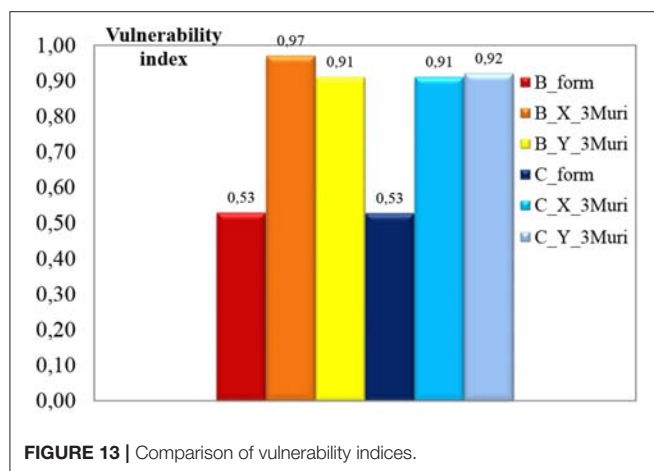


**FIGURE 13 |** Comparison of vulnerability indices.

- The simple and quick vulnerability assessment method is then able to predict, in relative terms, the same results of more refined analyses. In fact, the spirit of application of the simplest method is not to quantitatively evaluate the vulnerability indices of the two investigated S.U., but to compare their seismic indicators in a relative way, in order to evaluate what is the most vulnerable S.U. In the case under study, the two form vulnerability indices are equal, confirming that the two S.U. have the same seismic

vulnerability. The same result is achieved for numerical analyses, where the vulnerability indices of two S.U. in both analysis directions are basically the same. This confirms the reliability of the quick survey form in predicting the seismic vulnerability of structural units of masonry building clusters.

## CONCLUSIONS

In the current paper the seismic vulnerability of a masonry building compound in the historical center of Arsita (district of Teramo) damaged by the 2009 L'Aquila earthquake was assessed. Two structural units placed in intermediate and head positions were investigated by means of two analysis methods. The first method was based on pushover analysis results obtained on the basis of macro-element models, implemented through the 3Muri analysis program, of the two buildings both considered as isolated structures and within the construction compound. The second method was instead founded on a simple and quick vulnerability form appropriately conceived for structural units of masonry building clusters.

The comparison of results derived from numerical modeling showed that buildings considered as isolated structures have a strength and stiffness lower than those of the same structures grouped in aggregate. Moreover, from the comparison, in terms of vulnerability indices, it was found that the cluster condition

reduces the seismic vulnerability of both structural units and that this effect is more marked for S.U. 8C in direction X.

On the other hand, the comparison of results derived from filling the vulnerability form in for the two buildings provided almost equal indices.

Finally, macro-element indices were compared to vulnerability form indices. The comparison showed that structural units 8B and 8C have similar seismic vulnerability indices in both analysis directions, independent of the analysis method used. Therefore, as a conclusion, the vulnerability assessment form method was able to predict, in relative terms, the same results of more refined analyses. This confirmed the effectiveness of the survey form for cluster structural units to estimate, in a simple and rapid way, the seismic vulnerability of buildings within Italian historical centers.

## DATA AVAILABILITY

The datasets generated for this study are available on request to the corresponding author.

## AUTHOR CONTRIBUTIONS

GC performed numerical analyses and filled the vulnerability forms. AF conceived the analysis methodology and wrote the paper.

## REFERENCES

AeDES (2000). *First Level Form for Safety Assessment, Damage Investigation, Prompt Intervention for Ordinary Buildings in the Post-Earthquake Emergency (in Italian)*. Rome: Civil Defense Department.

ATC (1996). *Seismic Evaluation and Retrofit of Concrete Buildings*. ATC-40 Report, Redwood City, CA: Applied Technology Council.

Benedetti, D., and Petrini, V. (1984). On the seismic vulnerability of masonry buildings: proposal of an evaluation method (in Italian). *L'Industria delle Costruzioni*. 149, 66–74.

Bernardini, A. (2000). *The Vulnerability of Buildings: Evaluation at National Scale of Seismic Vulnerability of Ordinary Buildings (in Italian)*. Research Report, Rome: CNR-National Group for Defence against Earthquakes.

Bernardini, A., Gori, R., and Modena, C. (1990). "An application of coupled analytical models and experiential knowledge for seismic vulnerability analyses of masonry buildings," in *Engineering Aspects of Earthquake Phenomena*, Vol. 3, eds A. Koridze (Oxon: Omega Scientific), 161–180.

Brando, G., De Matteis, G., and Spacone, E. (2017). Predictive model for the seismic vulnerability assessment of small historic centres: application to the inner Abruzzi Region in Italy. *Eng. Struct.* 153, 81–96. doi: 10.1016/j.engstruct.2017.10.013

Calvi, G. M., Pinho, R., Magenes, G., Bommer, J. J., Restrepo-Vélez, L. F., and Crowley, H. (2006). Development of seismic vulnerability assessment methodologies over the past 30 years. *ISET J. Earthquake Technol.* 43, 75–104.

Caprili, S., Mangini, F., Salvatore, W., Bevilacqua, M. G., Karwacka Codini, E., Squeglia, N., et al. (2017). A knowledge-based approach for the structural assessment of cultural heritage, a case study: La Sapienza Palace in Pisa. *Bull. Earthquake Eng.* 15, 4851–4886. doi: 10.1007/s10518-017-0158-y

Cara, S., Aprile, A., Pelà, L., and Roca, P. (2018). Seismic risk assessment and mitigation at emergency limit condition of historical buildings along strategic urban roadways. Application to the "Antiga Esquerra de L'Eixample" neighborhood of Barcelona. *Int. J. Arch. Heritage* 12, 1055–1075. doi: 10.1080/15583058.2018.1503376

Chieffo, N., Mosoarca, M., Formisano, A., and Apostol, I. (2019). "Seismic vulnerability assessment and loss estimation of an urban district of Timisoara," in *IOP Conference Series: Materials Science and Engineering* (Prague), 471.

Clementi, F., Gazzani, V., Poiani, M., and Lenci, S. (2016). Assessment of seismic behaviour of 490 heritage masonry buildings using numerical modelling. *J. Build. Eng.* 8, 29–47. doi: 10.1016/j.jobe.2016.09.005

Da Porto, F., Munari, M., Prota, A., and Modena, C. (2013). Analysis and repair of clustered buildings: case study of a block in the historic city centre of L'Aquila (Central Italy). *Construct. Build. Mater.* 38, 1221–1237. doi: 10.1016/j.conbuildmat.2012.09.108

D'Amato, M., Laterza, M., and Diaz Fuentes, D. (2018). Simplified seismic analyses of ancient churches in Matera's landscape. *Int. J. Arch. Heritage.* doi: 10.1080/15583058.2018.1511000. [Epub a head of print].

D'Ayala, D., and Paganoni, S. (2011). Assessment and analysis of damage in L'Aquila historic city centre after 6th April 2009. *Bull. Earthquake Eng.* 9, 81–104. doi: 10.1007/s10518-010-9224-4

D'Ayala, D., and Speranza, E. (2002). "An integrated procedure for the assessment of seismic vulnerability of historic buildings," in *Proceedings of the 12th European Conference on Earthquake Engineering* (London).

Formisano, A. (2017a). Local- and global-scale seismic analyses of historical masonry compounds in San Pio delle Camere (L'Aquila, Italy). *Nat. Hazards* 86, 465–487. doi: 10.1007/s11069-016-2694-1

Formisano, A. (2017b). Theoretical and numerical seismic analysis of masonry building aggregates: case studies in San Pio Delle Camere (L'Aquila, Italy). *J. Earthquake Eng.* 21, 227–245. doi: 10.1080/13632469.2016.1172376

Formisano, A., Chieffo, N., Monaco, D., and Fabbrocino, F. (2016). "On the influence of the aggregate condition on the vibration period of masonry buildings: a case study in the district of Naples," in *AIP Conference Proceedings* (Athens), 1790.

Formisano, A., Chieffo, N., and Mosoarca, M. (2017a). Seismic vulnerability and damage speedy estimation of an urban sector within the municipality of San Potito Sannitico (Caserta, Italy). *Open Civ. Eng. J.* 11, 1106–1121. doi: 10.2174/1874149501711011106

Formisano, A., Chiumiento, G., Fabbrocino, F., and Landolfo, R. (2017b). "Comparative seismic evaluation between numerical analysis and Italian guidelines on cultural heritage applied to the case study of a masonry building compound," in *AIP Conference Proceedings* (Rhodes), 1863.

Formisano, A., Florio, G., Landolfo, R., and Mazzolani, F. M. (2011). "Numerical calibration of a simplified procedure for the seismic behaviour assessment of Masonry building aggregates," in *Proceedings of the 13th International Conference on Civil, Structural and Environmental Engineering Computing* (Stirlingshire).

Formisano, A., Florio, G., Landolfo, R., and Mazzolani, F. M. (2015). Numerical calibration of an easy method for seismic behaviour assessment on large scale of masonry building aggregates. *Adv. Eng. Softw.* 80, 116–138. doi: 10.1016/j.advengsoft.2014.09.013

Formisano, A., and Massimilla, A. (2018). A novel procedure for simplified nonlinear numerical modeling of structural units in Masonry aggregates. *Int. J. Archit. Herit.* 12, 1162–1170. doi: 10.1080/15583058.2018.1503365

Fuentes, D. D., Laterza, M., and D'Amato, M. (2019). "Seismic vulnerability and risk assessment of historic constructions: the case of masonry and adobe churches in Italy and Chile," in *Proceedings of the 11th International Conference on Structural Analysis of Historical Constructions* (Cusco: RILEM Bookseries).

Giuffrè, A. (1993). *Safety and Conservation of Historical Centres. The Case of Ortigia (in Italian)*. Bari: Laterza.

GNDT (1993). *Seismic Risk of Public Buildings, Part I: Methodological Issues (in Italian)*. Rome: CNR-National Group for Defence against Earthquakes.

Grunthal, G. (1998). *European Macroseismic Scale 1998*. Cahiers du Centre Européen de Géodynamique et de Séismologie, 101.

Kircher, C. A., Nassar, A. A., Kustu, O., and Holmes, W. T. (1997). Development of building damage functions for earthquake loss estimation. *Earthquake Spectra* 13, 663–682. doi: 10.1193/1.1585974

Lagomarsino, S., and Giovinazzi, S. (2006). Macroseismic and mechanical models for the vulnerability assessment of current buildings. *Bull. Earthquake Eng.* 4, 415–443. doi: 10.1007/s10518-006-9024-z

Lagomarsino, S., Penna, A., Galasco, A., and Cattari, S. (2013). TREMURI program: an equivalent frame model for the nonlinear seismic analysis of masonry buildings. *Eng. Struct.* 56, 1787–1799. doi: 10.1016/j.engstruct.2013.08.002

Magenes, G. (2000). "A method for pushover analysis in seismic assessment of masonry buildings," in *Proceedings of the 12th World Conference on Earthquake Engineering*. Paper No. 1866 (on CD). (Auckland).

Mallardo, V., Malvezzi, R., Milani, E., and Milani, G. (2008). Seismic vulnerability of historical masonry buildings: a case study in Ferrara. *Eng. Struct.* 30, 2223–2241. doi: 10.1016/j.engstruct.2007.11.006

Miano, A., Jalayer, F., Ebrahimian, H., and Prota, A. (2018). Cloud to IDA: efficient fragility assessment with limited scaling. *Earthquake Eng. Struct. Dyn.* 47, 1124–1147. doi: 10.1002/eqe.3009

Miano, A., Sezen, H., Jalayer, F., and Prota, A. (2017). "Performance based comparison of different retrofit methods for reinforced concrete structures," in *Proceedings of the 6th ECCOMAS Thematic Conference on Computational Methods in Structural Dynamics and Earthquake Engineering (COMPDYN 2017)* (Rhodes).

Ministerial Decree (M.D.) (2018). Updating of Technical Codes for Constructions (in Italian). *Official Gazette* no. 42 (Rome).

Ministry of Cultural Heritage and Activities (MiBAC) (2011). *Guidelines for the Seismic Risk Evaluation and Reduction of the Cultural Heritage - Alignment to the Technical Standards for Constructions (in Italian)*. Rome.

Mosoarca, M., Onescu, I., Azap, B., Onescu, E., Chieffo, N., and Szitar-Sirbu, M. (2019). Seismic vulnerability assessment for the historical areas of the Timisoara city, Romania. *Eng. Fail. Anal.* 101, 86–112. doi: 10.1016/j.engfailanal.2019.03.013

Papa, F., and Zuccaro, G. (2004). *MEDEA: A Multimedia and Didactic Handbook for Seismic Damage Evaluation*. Potsdam: European Seismological Commission.

Ramírez, E., Lourenço, P. B., and D'Amato, M. (2019). "Seismic assessment of the Matera Cathedral," in *SAHC 2018 - 11th International Conference on Structural Analysis of Historical Constructions* (Cusco: Springer), 1346–1354.

Ramos, L. F., and Lourenco, P. B. (2004). Modeling and vulnerability of historical city centers in seismic areas: a Case Study in Lisbon. *Eng. Struct.* 26, 1295–1310. doi: 10.1016/j.engstruct.2004.04.008

Senaldi, I., Magenes, G., and Penna, A. (2010). Numerical investigations on the seismic response of masonry building aggregates. *Adv. Mater. Res.* 133–134, 715–720. doi: 10.4028/www.scientific.net/AMR.133-134.715

Senaldi, I. E., Guerrini, G., Comini, P., Graziotti, F., Penna, A., Beyer, K., et al. (2019). Experimental seismic performance of a half-scale stone masonry building aggregate. *Bull. Earthquake Eng.* 1–35. doi: 10.1007/s10518-019-00631-2

STA DATA srl. (2018). *3Muri User Manual*. Turin.

Valente, M. V., Milani, G., Grande, E., and Formisano, A. (2019). Historical masonry building aggregates: advanced numerical insight for an effective seismic assessment on two row housing compounds. *Eng. Struct.* 190, 360–379. doi: 10.1016/j.engstruct.2019.04.025

Valluzzi, M. R., Munari, M., Modena, C., Binda, L., Cardani, G., and Saisi, A. (2007). Multilevel approach to the vulnerability analysis of historic buildings in seismic areas-Part 2: analytical interpretation of mechanisms for the vulnerability analysis and the structural improvement. *Int. J. Restor. Build. Monum.* 13, 427–441. doi: 10.1515/rbm-2007-6172

Whitman, R. V., Reed, J. W., and Hong, S. T. (1973). "Earthquake damage probability matrices," in *Proceedings of the Fifth World Conference on Earthquake Engineering, Vol. 2.* (Rome).

# Seismic Isolation for Protecting Historical Buildings: A Case Study

*Michele D'Amato [1], Rosario Gigliotti [2] and Raffaele Laguardia [2]\**

[1] *Department of European and Mediterranean Cultures (Architecture, Environment and Cultural Heritage), University of Basilicata, Matera, Italy,* [2] *Department of Structural and Geotechnical Engineering, Sapienza University of Rome, Rome, Italy*

The protection of cultural heritage from seismic risk is an open issue due to the difficulties in finding technical solutions allowing a balance between their effectiveness and invasiveness. Among the available protection techniques, seismic isolation is one of the most suitable obtaining a significant performance improvement by acting on a limited portion of the structure. In this paper, it is shown an application of such technique on a reinforced concrete frame building cataloged as of historical interest by Italian Ministry of Cultural Heritage. It was realized in 30's representing the "Modern Style" of Italian Architecture, also known as Italian Rationalism, and designed only for vertical loads without any specific regulation for lateral loads. Geometry, material properties and reinforcements characteristics have been derived from an extensive investigation campaign. By the means of a FEM 3D model they are simulated among them the seismic responses of both existing and retrofitted building through a seismic isolation system composed by elastomeric and sliding isolators. Furthermore, a new methodology for estimating the seismic capacity exhibited by the structure in the past is presented and applied.

Keywords: cultural heritage, monuments, reinforced concrete, seismic vulnerability, seismic retrofit, seismic isolated buildings

## INTRODUCTION

To date, the strategy of seismic isolation as earthquake-resistant technique applied on existing buildings is become very common all over the World. It is based on the concept of lengthening the natural period of the structure from the predominant frequency of the ground motions, significantly reducing the transmitted acceleration to the superstructure (Kelly, 1986; Alhan and Gavin, 2004; Ibrahim, 2008). The isolation plane is generally realized above the foundation and it consists of devices capable of reducing the lateral stiffness of the superstructure combing re-centering and energy dissipation action. In this way, the seismic demand on the superstructure is drastically reduced and the performance requirements are satisfied by strongly limiting or nullifying the elements damage. In addition, this strategy requires spaces of small dimensions to be realized, and in many cases not even requiring the evacuation of the occupants.

In Italy, during the last 30 years, the seismic isolation applications have been increased more and more representing, nowadays, a common technique of structural design. A proof of this is given by the fact that the Italian Design Code (NTC, 2008) and its recent update (NTC, 2018) recognize the

seismic isolation as standard application in buildings design. First applications of this strategy may be found in Mokha et al. (1996), Martelli and Forni (1998), Kawamura et al. (2000), Luca et al. (2001), Kelly (2002), Braga et al. (2005), Tomazevic et al. (2009), and Lignola et al. (2016).

Commonly, seismic isolation is used for retrofitting of Reinforced Concrete (RC) existing buildings, since very often they were designed only for vertical loads without any detailing rule for ductility, as highlighted in some recent studies such as, among the others, (Laterza et al., 2017a). In these cases, the seismic isolation is preferred to widespread and more invasive local interventions, consisting in strengthening and improving the confinement of the elements (Braga et al., 2006; D'Amato et al., 2012a,b; Laterza et al., 2017b; Caprili et al., 2018; Faqeer et al., 2018), or consisting in adding new structural elements in order to carry the seismic loads and dissipate energy (Ciampi et al., 1995; Di Sarno and Manfredi, 2010, 2012; Mazza and Vulcano, 2014; Laguardia et al., 2017; Braga et al., 2019).

This paper presents the application of the seismic base isolation for retrofitting an existing RC building, in accordance to the Italian Design Code (NTC, 2008). The case study chosen is the public building named "*Archivio di Stato*" (State Archive) designed and built during the 30's in Potenza, a city located along the Apennine chain with the highest seismic hazard in Italy. Moreover, due to its architectural importance, the considered building is protected by the Italian Ministry of Cultural Heritage. Indeed, it is representative of the "Modern Style" of Italian Architecture, also known as Italian Rationalism. The numerical simulations are obtained through response spectrum analyses for Fixed-Base (FB) and Base-Isolated (BI) model, considering also the impact of the variability of the friction coefficient of sliding devices.

In this article, it is therefore highlighted the effectiveness of the isolating system in order to retrofit historical buildings. In the case analyzed, several local reinforcements are required to gain the assumed seismic performance level, given the need to reduce the invasiveness of the intervention, the number and the impact of these interventions by varying the retrofit strategy is discussed. Moreover, in this study it is proposed a new and simplified methodology to estimate the structural capacity on the basis of the seismic performances exhibited by the building in the past occurred earthquakes. Precisely, the estimation of the occurred seismic action at building base stems from ground motions (GMs) available and recorded in the site surrounding area. The main idea of the proposed simplified methodology is the following: if a fixed base-building has experienced an earthquake in the past with negligible or limited damages, the seismic intensity of that earthquake may be intended as an experimental proof related to the building capacity, or rather, to the capacity of the superstructure portion of the base-isolated building. The new methodology can be used as a fast and useful tool to roughly assess the seismic performances of buildings sample in a certain area, identifying the most suitable ones for a seismic isolation strategy, implying negligible or limited damages of the superstructure. The so-estimated seismic capacity can

be also used as an experimental threshold to be considered in validating implemented numerical models for seismic assessment of a structure.

## CASE STUDY—"ARCHIVIO DI STATO" OF POTENZA, ITALY (1930)

The "*Archivio di Stato*" (State Archive) was designed and realized in the 30's by the architect Ernesto Puppo (1904–1987), one of the principal exponents of Italian Rationalism Movement. It is located in the city of Potenza along a hillside on a steep slope toward the City center and used as State Archive. The building consists of RC frame structures composing three intersecting volumes with a markedly non-symmetric geometry. In **Figure 1** are shown some views and technical drawings of the considered buildings. In particular, in **Figure 1A** they are reported a transversal and a longitudinal section of the building, where it can be appreciated the hillside disposition and the relevant irregularity in elevation. The Italian Ministry of Cultural Heritage has recently added this building among those to be protected due to its architectural relevance, even considering the construction period and the urban context in which it is inserted, that can be appreciated in the photos of **Figure 1B**. **Figure 1C** shows the current abandonment state of the building due to the slight damages suffered during the Irpinia earthquake on 23/11/1980, after that it was closed.

This building is of considerable importance also because it was one of the first realized in Italy with RC frame-resisting structure by the "*Cooperativa Muratori e Cementisti di Ravenna*" construction company between 1936 and 1939. The frame structure is characterized by columns with square or rectangular sections with deep or flat beams, the floors slabs are made of reinforced concrete with predominant unidirectional warping. The building has three underground floors and six floors above ground with an average interstory height of about 4.5 m. Due to the strong architectural variations in height, the floors surfaces significantly vary with height. **Table 1** summarizes these geometrical details, where the *Level 0* corresponds to the floor accessible from the main street facing the building. Moreover, each column is founded on a deep well-foundation and connected by a beam gridwork placed at a height of −9.6 m, while no connection is present for the columns of the lower part of the building, founded at −13.80 m. Finally, infills are made of bricks and placed both in the external frames and in some internal frames.

## Materials Properties and Concrete Elements Details

In order to characterize this building, in addition to an in-depth geometrical investigation, it has been also necessary to perform an extensive investigation campaign on material properties and structural reinforcement detailing disposition. To this regard, it should be noted that, at the time of construction, there were few code indications for reinforced concrete constructions or available consolidated calculation schemes. Therefore, the survey campaign has played an important role to define the structural
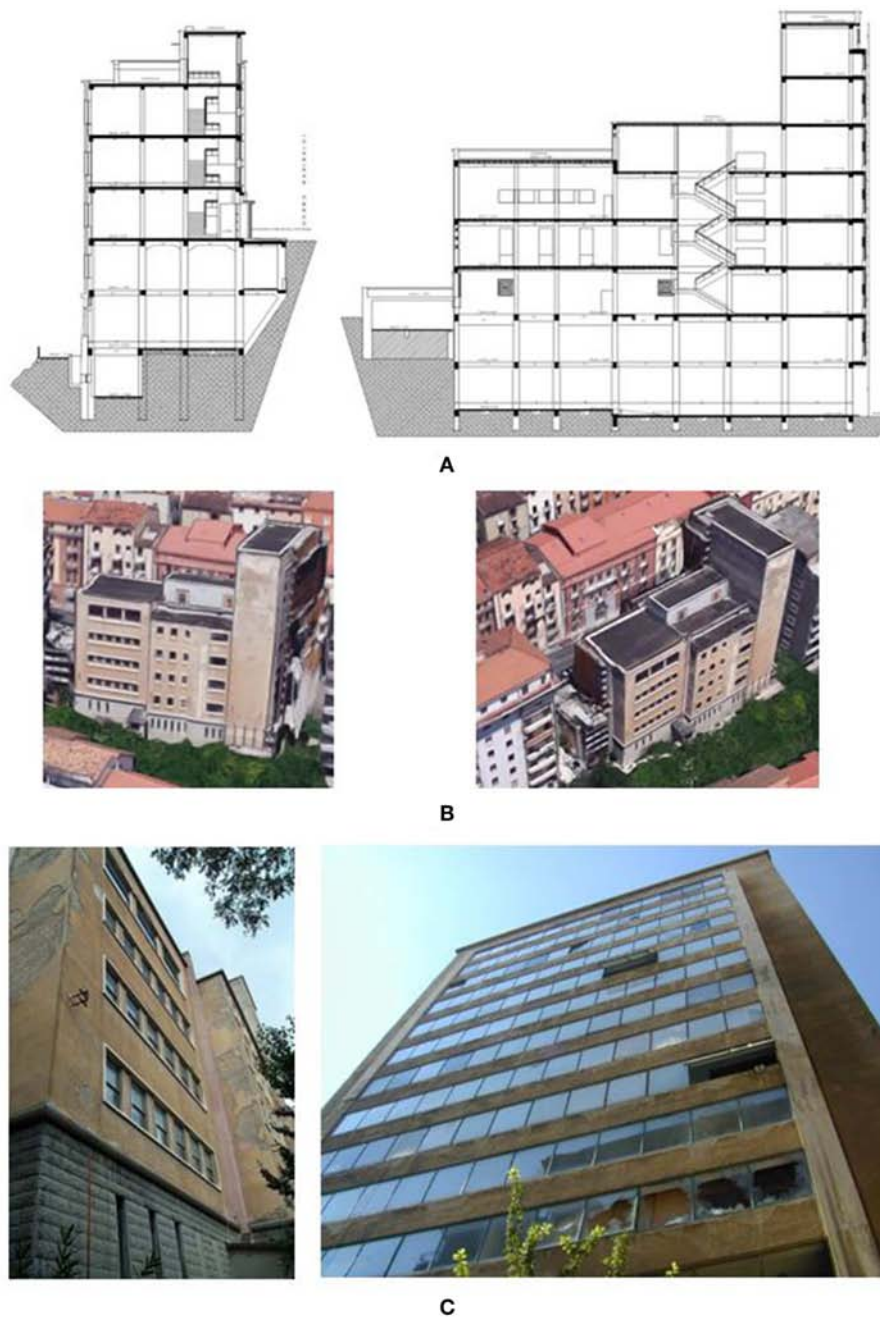
**FIGURE 1 |** Some images of the considered case study. **(A)** Transversal and longitudinal section of the building, **(B)** images from Google Maps (2019), and **(C)** current conditions of the building.

characteristics of the case study. Totally, the investigations campaign consisted of sampling of 13 reinforcing steel bars specimens, 21 concrete core drilled, 62 SONREB tests, and over 300 sections pacometric investigations for construction details. In this study, since the elaboration data is still in progress, only the results of the material properties measured with laboratory tests on concrete and rebars samples are illustrated. More in detail, laboratory tests on concrete samples (**Figure 2B**) extracted from

beams and columns were performed to evaluate the compressive strength of concrete. The mean values of compressive strength ($f_{cm}$) and the coefficient of variation (CV) of the sample are reported in **Figure 2A**. Since a different homogeneity along the building height was observed, the measured compressive strengths were divided in two different groups (**Figure 2A**): *Group 1* from height of −9.6–0.0 m, having an average value of 24.2 MPa measured on n. 11 concrete core samples; and

| Level | Relative height [m] | Interstory height [m] | Floor area [m²] |
|---|---|---|---|
| Level −3 | −13.80 | 4.20 | ≅ 113 |
| Level −2 | −9.60 | 5.10 | ≅ 648 |
| Level −1 | −4.50 | 4.50 | ≅ 648 |
| Level 0 | 0.00 | 4.50 | ≅ 648 |
| Level +1 | 4.50 | 4.50 | ≅ 648 |
| Level +2 | 9.00 | 4.50 | ≅ 648 |
| Level +3 | 13.50 | 4.50 | ≅ 648 |
| Level +4 | 18.00 | 4.50 | ≅ 190 |
| Level +5 | 22.50 | 5.00 | ≅ 114 |
| Level +6 | 27.50 | – | ≅ 114 |

*Group 2*, having a compressive strength of 18.8 MPa, from floor having 4.5 m height up to the roof. The so obtained compressive strengths, given the height differentiation, have been used for both beams and columns.

As regards the steel reinforcements, *in situ* investigations showed that, according to the RC existing buildings realized in 30's, only smooth bars were applied. A total of 13 samples were extracted (**Figure 2C**), 3 from hoops of 6 mm diameter, and 15 from longitudinal bars having a diameter between 8 and 16 mm. **Figure 2A** reports also the average tensile strength of the steel samples measured with laboratory tests. The values are separately reported for longitudinal bars and for hoops. The obtained average values are compatible with the Steel strength class Aq 42, very common in the construction period of the building (Verderame et al., 2001).

Construction details of beams and columns were measured with *in situ* pacometric measurements and visual inspections of reinforcements by locally removing the concrete cover. A simulated design in accordance with the design practice of that period was also performed in order to compare the obtained results with those measured through the experimental campaign. Since a good agreement was obtained, the simulated design was extended to all RC elements of the building. More in detail, 2.5 and 6 kN/m² were used as variable loads acting at the different floors for designing the reinforcements of decks and beams in according to simple schemes of continuous beams, as usual in the design practice. On the contrary, for columns no specific design scheme was adopted, since they were designed only for vertical loads without any lateral action for taking into account the earthquake effects. Therefore, it has been reasonable to design longitudinal and transverse reinforcements by assuming the detailing rules provided in the Italian Royal Decree (R.D., 1939), that is the design code temporally closer to the years of construction of the building. In particular, it gave the provision of assigning to RC columns an amount of longitudinal bars equal to 0.8% of $A_c$ if $A_c < 2,000$ cm², and equal to 0.5% of $A_c$ if $A_c > 5,000$ cm², where $A_c$ is the column gross area. Between $A_c = 2,000$ cm² and $A_c = 5,000$ cm² a linear interpolation was allowed. As for the hoops, on the basis of the obtained measurements with the pacometric tests, the spacing has been considered equal to 25 cm, slightly higher than the minimum requirements of R.D. (1939).

For completeness sake, **Figure 3** illustrates the reinforcement details obtained for some columns and beams.

## NUMERICAL MODELS

**Figure 4A** depicts the FEM model implemented in SAP 2000 software (Computers Structures Inc, 2015) for the numerical simulations of the existing building fully fixed at the base. Specifically, beams and columns have been modeled using linear elastic frames, while the decks have been modeled with shell elements having orthotropic stiffness to consider the actual heights, while the soil pressure of the underground building portions have been neglected. Finally, in order to take account of the section cracking occurring during the seismic excitation, the flexural and shear stiffness of primary columns and beams have been both reduced of 50%, in accordance with the maximum cracking level allowed by the Italian code (NTC, 2008).

In **Figure 4B** the base-isolated model is reported. The added elements, such as the rigid steel deck placed above the devices and the others beams, have been modeled also with linear elastic frames. The isolating system, as illustrated and detailed later in **Figure 9**, is composed by elastomeric and friction isolators, both modeled as linear link elements, whose stiffness corresponds to the secant one at the design displacement for the considered design limit state.

## SITE SEISMIC HAZARD AND RESPONSE SPECTRA

The site seismic hazard and response spectra considered in the numerical simulations are shown in **Figure 5**. Precisely, **Figure 5A** reports the parameters defining the seismic action in terms of seismic spectra referred to a rigid soil (*Type A*) for each Limit State considered by the Italian design code (NTC, 2008), that are: Operativity Limit State (*OLS*), Damage Limit State (*DLS*), Life-SafetyLimit State (*LSLS*), Collapse Limit State (*CLS*). The site seismic hazard is considered for a reference period of $V_R$ of 50 years (Nominal Life $V_N = 50$ years and Coefficient of Use $C_U = 1$), where: $T_R$ is the return period, $a_g$ is the maximum soil accelerations in the case of rock soil, $F_0$ is the maximum amplification of the spectrum, $T_c^*$ is the transition period between constant acceleration and constant velocity part of the spectrum.

In **Figure 5B** are reported the elastic response spectra according to NTC (2008) for the case analyzed, by considering a ground of *Type C* and a conventional viscous damping ratio $\xi = 5\%$. In order to perform linear analyses, the Italian code (NTC, 2008) suggests to keep in count the energy dissipated by the isolating system using an appropriate design spectrum. This spectrum is obtained by reducing of a factor $\eta = \sqrt{\frac{10}{(5+\xi_{esi})}}$ the spectral ordinates with period higher than $0.8*T_{is}$ (that is the range of isolating system vibrations periods), where $\xi_{esi}$ is the equivalent viscous damping ratio of the isolating system for the design horizontal displacement. In accordance with this, **Figure 5C** reports the so-obtained design spectra, where the equivalent $\xi_{esi}$ for each limit state is numerically reported in **Figure 9**.

**FIGURE 2 |** Investigation campaign: **(A)** Material properties derived from extracted samples. N, number of samples; CV, coefficient of variation; $f_{cm}$, average compressive strength; $f_{ym}$, average tensile strength; **(B)** steel reinforcements disposition obtained through pacometric investigations and sampling of concrete specimen, **(C)** steel samples collected.
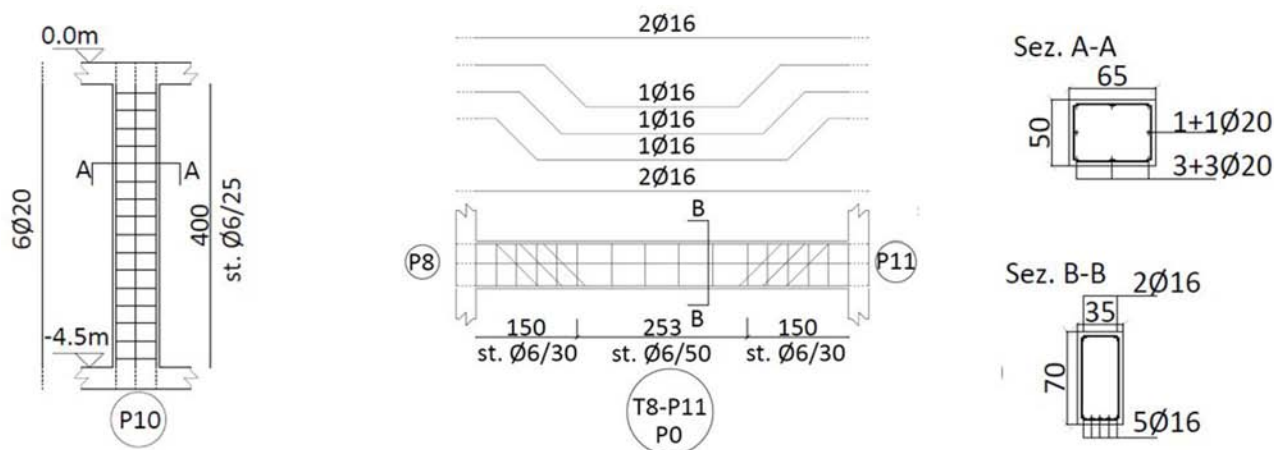


**FIGURE 3 |** Typical reinforcement details of columns and beams.

# NUMERICAL RESULTS

In this section are illustrated and commented the results obtained with the implemented FEM models where, as described in the previous section, linear elastic frames are used. In the case of base-isolated building, the seismic devices are modeled as linear links, where friction sliders have a linear stiffness corresponding to the secant one at the considered design limit state. In all the analyses performed, the horizontal seismic action effects are evaluated with a modal analysis with response spectra, where the modal effects are combined with CQC combination rule.
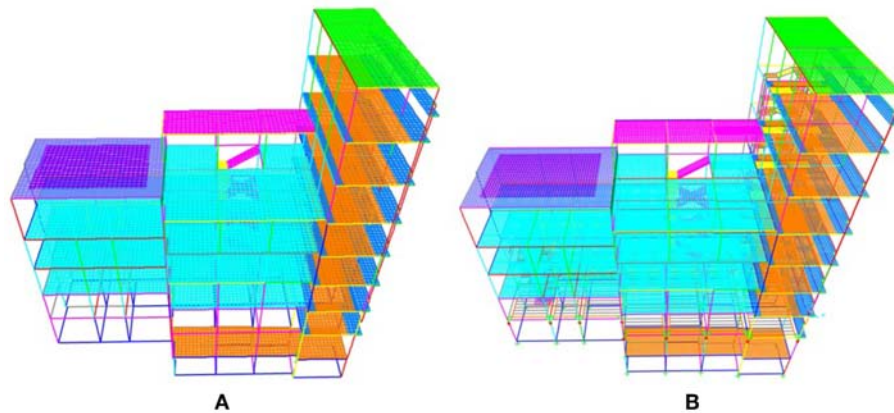
**FIGURE 4 |** 3D views of the implemented FEM model for fixed-base structure **(A)** and for base-isolated structure **(B)**.



| $V_R = 50\ years$ | $T_R\ (years)$ | $a_g\ (m/s^2)$ | $F_0$ | $T_C^*\ (sec)$ |
|---|---|---|---|---|
| **OLS** | 30 | 0.055 | 2.331 | 0.285 |
| **DLS** | 50 | 0.073 | 2.327 | 0.313 |
| **LSLS** | 475 | 0.205 | 2.449 | 0.362 |
| **CLS** | 975 | 0.267 | 2.442 | 0.405 |
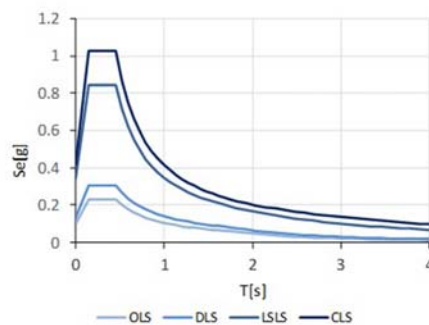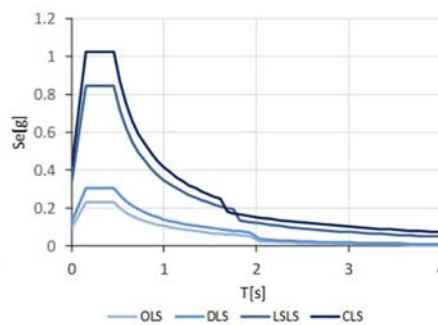
**FIGURE 5 |** Site seismic hazard and response spectra considered. **(A)** Parameters defining the seismic action referred to a rigid soil (Type A) for each limit state. **(B)** Elastic response spectra ($\xi = 5\%$) for a soil Type C. **(C)** Design spectra for isolated system for a soil type C.

## Seismic Response of Fixed-Base Building

The results of the modal analysis in the case of fixed-base building are reported in **Figure 6** where, for brevity, are reported only the first three vibration modes. The figure illustrates the shape of each vibration mode, and reports the related vibration period $T$, the translational modal participating mass ratios along $X$ and $Y$ ($U_X$ and $U_Y$), and the rotational one around $Z$ ($R_Z$). It is found that the first mode arises mainly along the $X$ direction, that is the direction along which the structure is more flexible and exhibits a more regular response. On the contrary, the second and the

third modes are both roto-translational, involving a coupling of a translation along $Y$ and a rotation along $Z$.

It is interesting, for the purposes of this work, to compare the floor shear distribution over the building height as illustrated in **Figure 7A**, obtained by considering the seismic action acting for Life-Safety Limit State. Along both the directions the shear distribution is regular and linear as demonstrated by the high mass participation ratio of the first mode. Moreover, also a study of the shear distribution at a certain level may be done. For instance, in **Figure 7B** the shear distribution at *Level 0* among
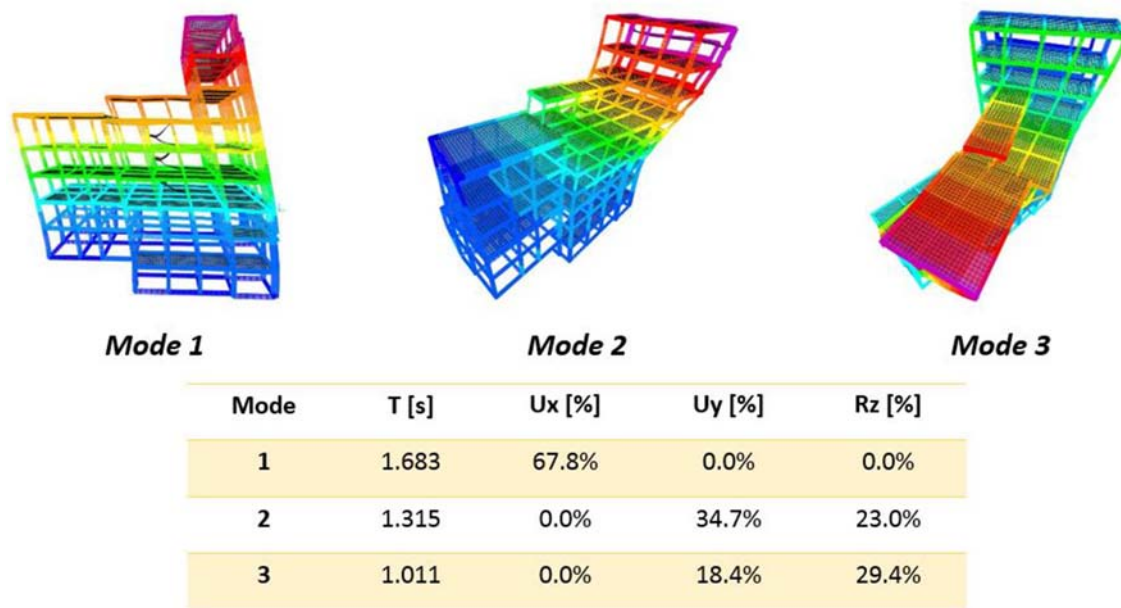
**FIGURE 6 |** Fixed-base model. Shapes and dynamic properties of the first three vibration modes.

the resistant frame is illustrated. As it is easy to note, the response is quite symmetric along the *X* direction, where the only two central vertical frames (having y = 8.5 m e y= 13.5 m) absorb more than 50% of the total shear at *Level 0*. By contrast, along the *Y* direction a consistent irregularity in the response is observed. The two higher frames (x = 0 m e x= −6 m), representing the building tower, are stiffer, bearing a considerable amount of the floor shear. Besides the shear global distribution, in order to verify the performances for ultimate limit states, local checks of demand/capacity ratios for ductile and fragile mechanisms have been performed, according to the requirements of Italian design code (NTC, 2008). By performing these checks, it emerges that about the 15% of beams and 2% of columns don't have enough flexural or shear capacity, by considering only gravity loads. Moreover, by considering the seismic loads, almost all the columns and the 30% of beams don't have enough shear capacity.

Finally, in **Figure 7C** the floor drifts obtained by considering the expected horizontal seismic action for the Damage Limit State are also plotted. For brevity, in this study the maximum horizontal drifts distribution is illustrated, arising along only the Y direction. Again, as observed for the shear forces, the distribution is quite regular above the height of the building and in any case the maximum values don't exceed the 0.5%, that is the limit for damage limit state indicated by the (NTC, 2008).

## Seismic Response of Base-Isolated Building

The structural intervention of seismically isolating the super-structure allows a global retrofit and, simultaneously, the respect of the architectural constraints on the building, related to its historical interest. Basically, the design criterion was of reducing as much as possible the seismic action and the number of

local reinforcements on the structural elements. The solution adopted is relatively easy to realize, given the fact that at a height of −4.5 m the building has an existing grid of RC beams completely free from constraints, below which the insertion of the isolation devices may be done. Then, a rigid deck may be realized above the isolation devices and among the beams grid, to provide stiffness at the base of the so-obtained superstructure, and to achieve a correct behavior of devices with respect to the lateral actions. In addition, interventions are also planned for the substructure. Specifically, all sections of existing columns will be increased to permit the allocation of devices, guaranteeing adequate stiffness and providing the required resistance by also introducing additional reinforcements. Finally, also the foundation plan will be significantly strengthened with the insertion, among the base of columns, of a RC plate. **Figure 8** reports a plan and an image of the chosen floor for inserting the isolation system.

As far as the base isolation system is concerned, it will be realized by the combination of two different devices, consisting of reinforced rubber elastomeric devices and flat low-friction sliders. Their arrangement and characteristics have been chosen to minimize the eccentricity between center of mass and stiffness, and to optimize both the equivalent viscous damping ratio and the system stiffness, to reduce as much as possible the seismic demand transmitted to the superstructure. In **Figure 9** the schematic layout of the isolation system and the devices details are shown. Three different rubber devices are considered (Type *A2*, *A3*, and *A4*) as function of the maximum vertical load capacity ($P_{E,max}$) required, having different lateral stiffness ($k_H$) and for an equivalent damping ratio ($\xi_H$) of 10%, evaluated in correspondence of the maximum displacement capacity ($v_{max}$) equal to 400 mm. Totally, 54% of devices are in rubber.
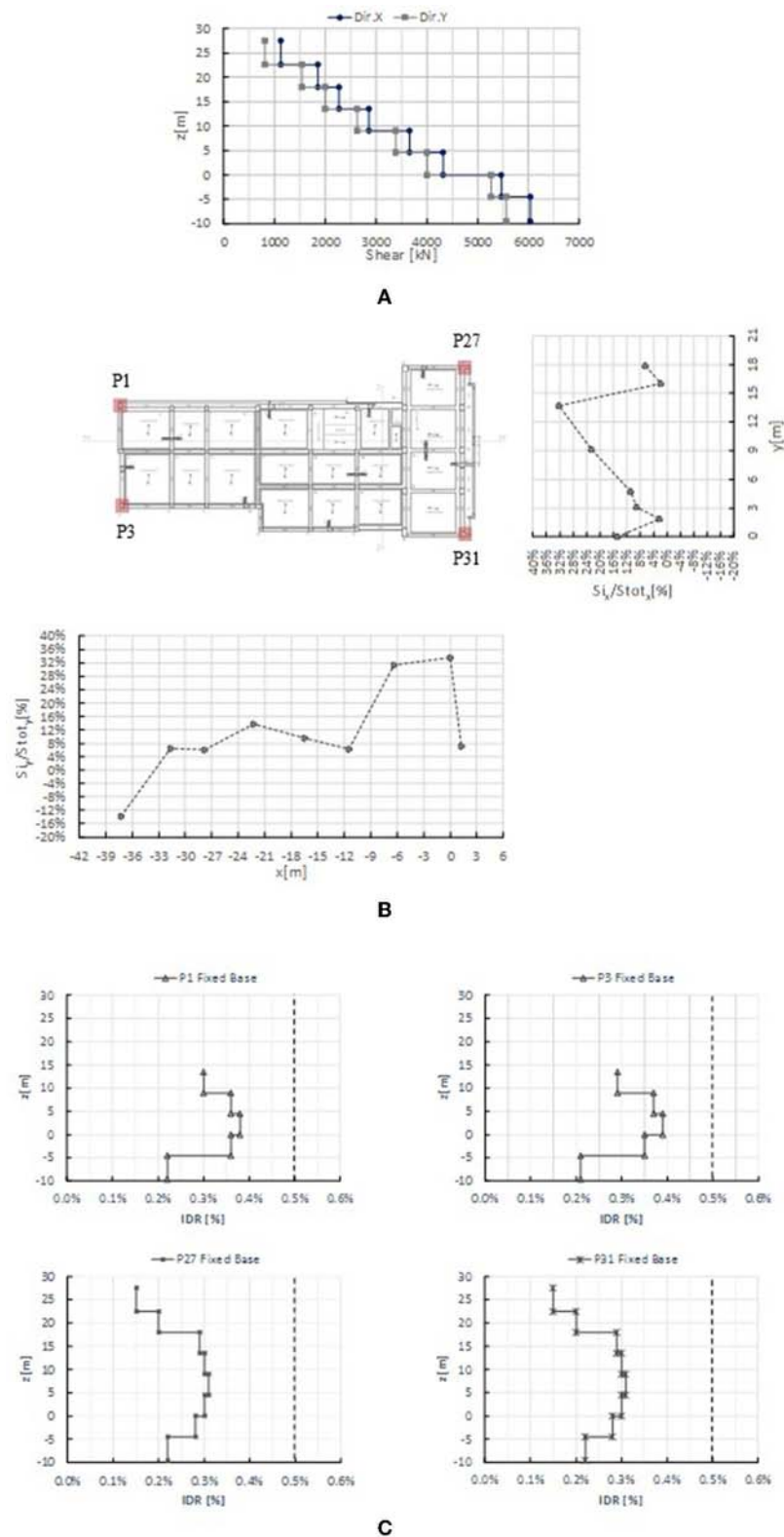
**FIGURE 7 |** Fixed-base model. Shear and drift distribution. **(A)** Shear distribution over the building height for Life-Safety Limit State, **(B)** shear distribution among the frames at Level 0 for Life-Safety Limit State, **(C)** drifts distribution over the building height in the y-direction for Damage Limit State.
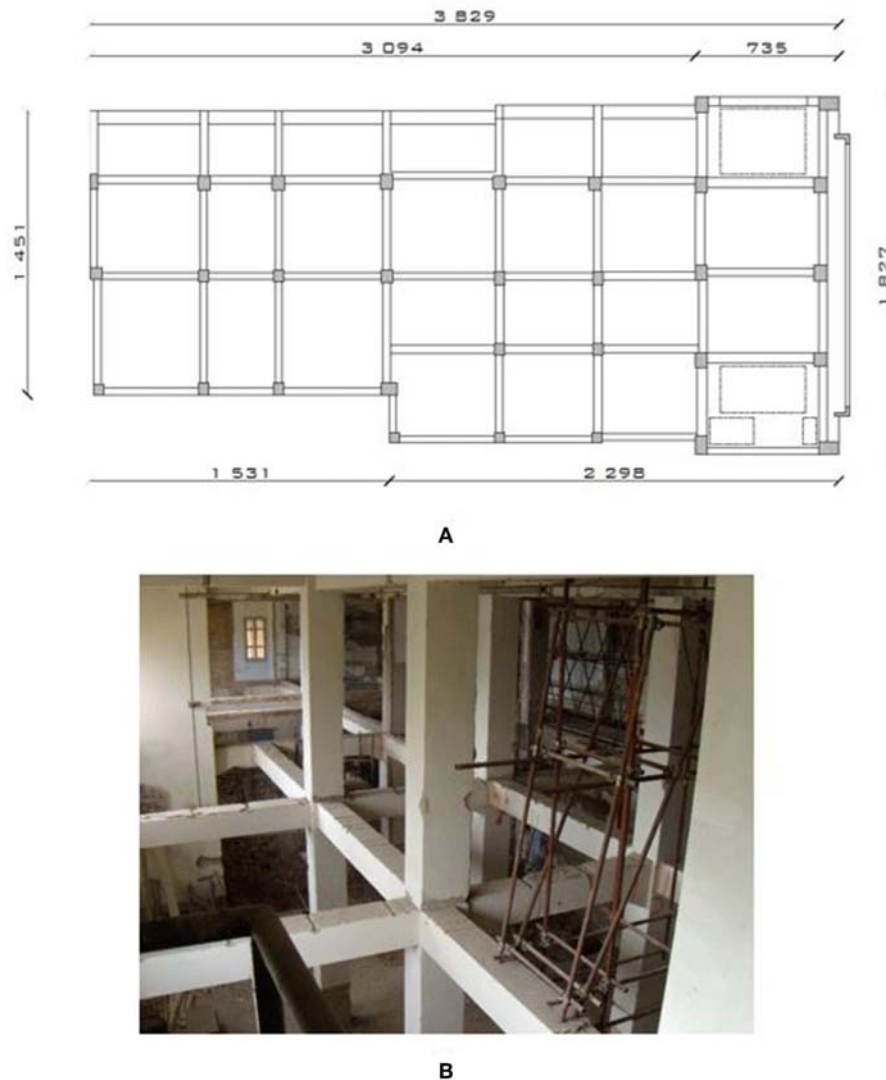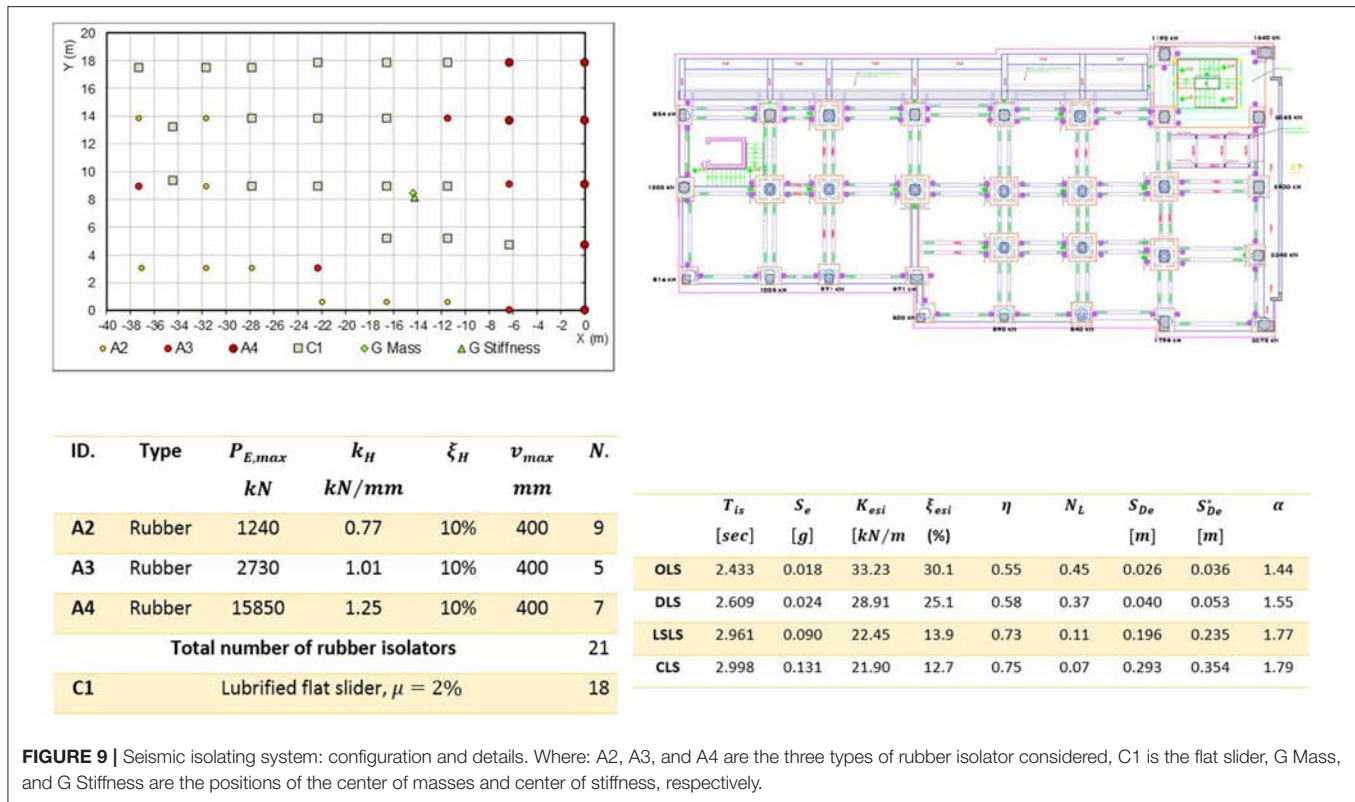
**FIGURE 8 |** Existing grid of RC beams. **(A)** Plan configuration (dimensions in centimeters), **(B)** view of current conditions.

The remaining devices are low-friction sliders with a friction coefficient $\mu$ equal to 2%, modeled as equivalent visco-elastic devices, having a secant stiffness and a viscous damping ratio related to the entire energy dissipated, both calculated in correspondence of maximum design displacement. In order to maximize the system torsional stiffness, the rubber devices, where possible, have been perimetrically positioned. The **Figure 9** also summarizes the equivalent linear characteristics of the isolation system for each limit state considered. More in detail, $T_{is}$ is the period of the isolated building, $S_e$ is the spectral acceleration for the period $T_{is}$, $K_{esi}$ is the secant stiffness of the system, $\xi_{esi}$ is the equivalent viscous damping ratio, $\eta$ is the reduction factor for the design spectra, $N_L$ is the Non-Linearity factor (Skinner et al., 1993), $S_{De}$ is the maximum horizontal displacement of the isolation system, $S_{De}^*$ is the maximum displacement of the devices assessed by considering torsional effects due to accidental

eccentricity by using the expressions of Italian design code (NTC, 2008) (i.e., by multiplying the displacement obtained through response spectrum analysis by a factor $\delta = 1 + e/r^2 \cdot x_p$ where $e$ is the considered eccentricity, $r$ is the torsional radius of the system and $x_p$ is the position of the device) and $\alpha$ is the isolation grade of the system (i.e., $T_{IS}/T_{FB}$).

It should be remarked that the equivalent linear characteristics of the isolation system indicated in the **Figure 9** are strongly dependent on the effective properties of the isolation devices and, in particular, on the friction coefficient of the flat sliders. As known, it is strictly related to several factors such as, among the others, the axial pressure, the sliding velocity, operating temperature, consumption of the material (Mokha et al., 1988; Constantinou et al., 1990). To this aim, a series of numerical analyses have been carried out in order to evaluate the sensitivity of the seismic response by varying $\mu$ between the values $\mu$

**FIGURE 9 |** Seismic isolating system: configuration and details. Where: A2, A3, and A4 are the three types of rubber isolator considered, C1 is the flat slider, G Mass, and G Stiffness are the positions of the center of masses and center of stiffness, respectively.

$= 1\%$ and $\mu = 6\%$. **Figure 10** shows the following obtained results by varying $\mu$: the resulting fundamental period $T_{is}$, the equivalent viscous damping ratio of the isolation system $\xi_{esi}$, the demand in terms of spectral ordinate in acceleration $S_e(T_{is})$ and maximum displacement of devices $S_{De}(T_{is})$. All these parameters are calculated with a FEM model implemented as described before, by considering the secant stiffness and by referring to the seismic action expected at the Collapse Limit State. As it is easy to observe by examining the obtained results, by increasing the friction coefficient $\mu$ from 1 to 6%, although the equivalent isolation system stiffness increases (i.e., $T_{is}$ reduces) the lateral acceleration $S_e(T_{is})$ transmitted to the superstructure is almost constant. This is because if $\mu$ increases also the dissipation expressed through $\xi_{esi}$ increases. Whereas, the expected maximum displacement $S_{De}(T_{is})$ tends gradually to reduce, increasing the capacity/demand ratio and thus increasing the safety factor.

In **Figure 11** the results of modal analyses obtained in the case of base-isolated model are reported. It is noted that the dynamic response is significantly modified with respect to the fixed-base model. In particular, thanks to the balanced arrangement of the seismic devices reducing the eccentricity between the center of mass and stiffness, a regular dynamic behavior is obtained, by activating about the 90% of mass participating with the first three modes. It is also useful, in order to quantify the benefits of the applied strategy, to compare in **Figure 12** the resulting floor shears and drifts over the height with the ones obtained with the fixed-base model.

**Figures 12A,B** report the comparisons in terms of floor shear over the height between the fixed-base and isolated model for the LSLS action level. It can be noted that the shear demand in the case of base-isolated model is reduced more than the 70% at each level. While, in **Figures 12C,D** the comparisons in terms of interstory drift ratio for the DLS action level are shown. In this case the drift is reduced by over 80% between the two models, giving evidence of the effectiveness of the isolation system to contain also the non-structural damage. On this aspect, it should be observed that linear analyses do not allow to consider the impact of the effect of the of higher modes participation due to non-linearity effects, that could significantly change the shear and drift values, as observed in Braga et al. (2005). However, given the limited value of the Non-Linearity factor (Skinner et al., 1993) for the proposed system, these effects have not been taken into consideration herein.

Despite of a consistent seismic demand reduction reached with the isolation system, additional local interventions are needed in the case analyzed herein. Precisely, concrete jacketing interventions are foreseen to improve shear and flexural resistance on columns, while interventions with steel jacketing with CAM system (Dolce et al., 2001) and composite material (i.e., FRP) are foreseen as shear and flexural reinforcements on beams. **Figure 13** depicts the number of local reinforcements required by increasing the level of the designing seismic action, represented as the ratio between the capacity ($a_{gC}$) and the demand ($a_{gD}$), expressed in terms of ground acceleration at the LSLS. In the case analyzed, by considering a full seismic
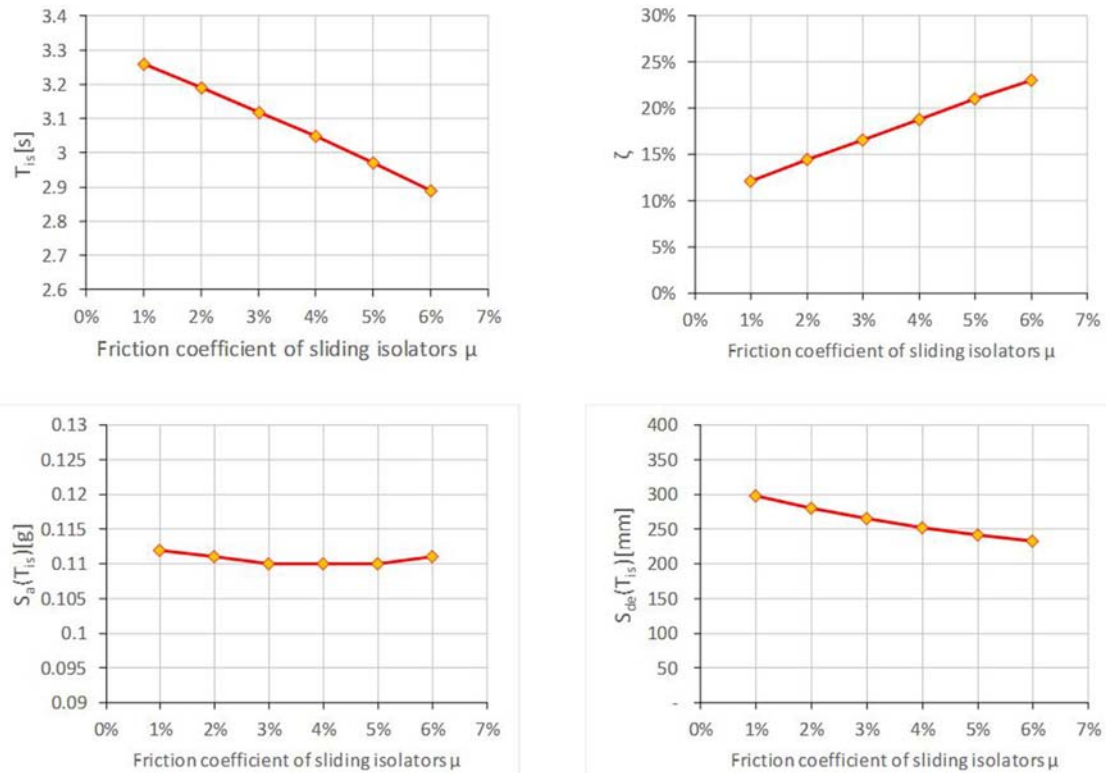
**FIGURE 10 |** Sensitivity analyses with the base-isolated FEM model by varying the friction coefficient of flat friction sliders.
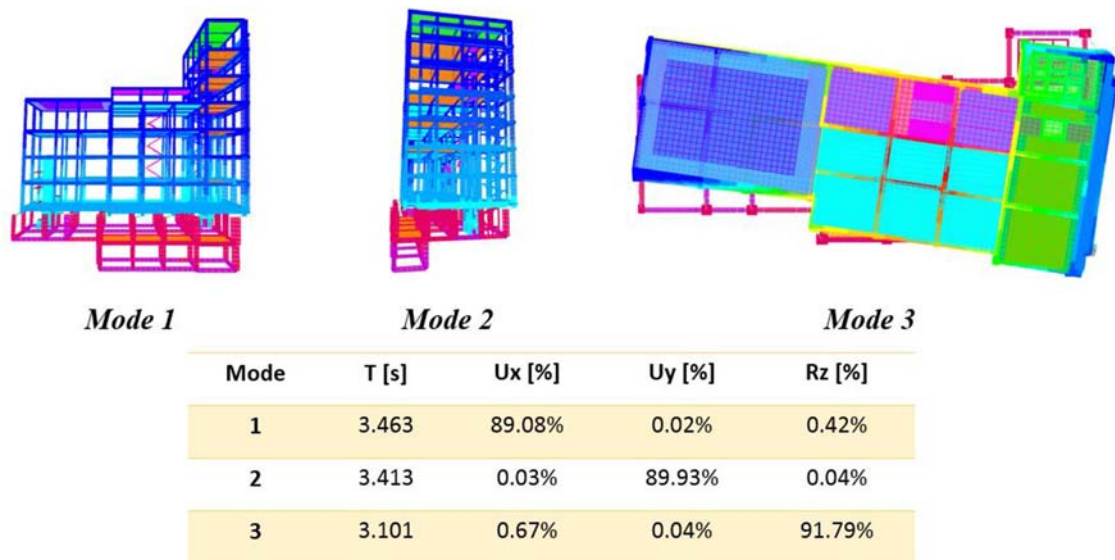


| Mode | T [s] | Ux [%] | Uy [%] | Rz [%] |
|------|-------|--------|--------|--------|
| 1 | 3.463 | 89.08% | 0.02% | 0.42% |
| 2 | 3.413 | 0.03% | 89.93% | 0.04% |
| 3 | 3.101 | 0.67% | 0.04% | 91.79% |

**FIGURE 11 |** Base-isolated model. Shapes and dynamic properties of the first three vibration modes.

retrofit (i.e., when $a_{gC}/ a_{gD} =100\%$), 19 interventions on columns are needed. More in detail, 12 columns need of interventions to improve shear resistance and 7 columns need

of interventions to improve the flexural capacity, in both cases the intervention consists in increasing of the column section and adding of longitudinal and transverse reinforcements. Similarly,
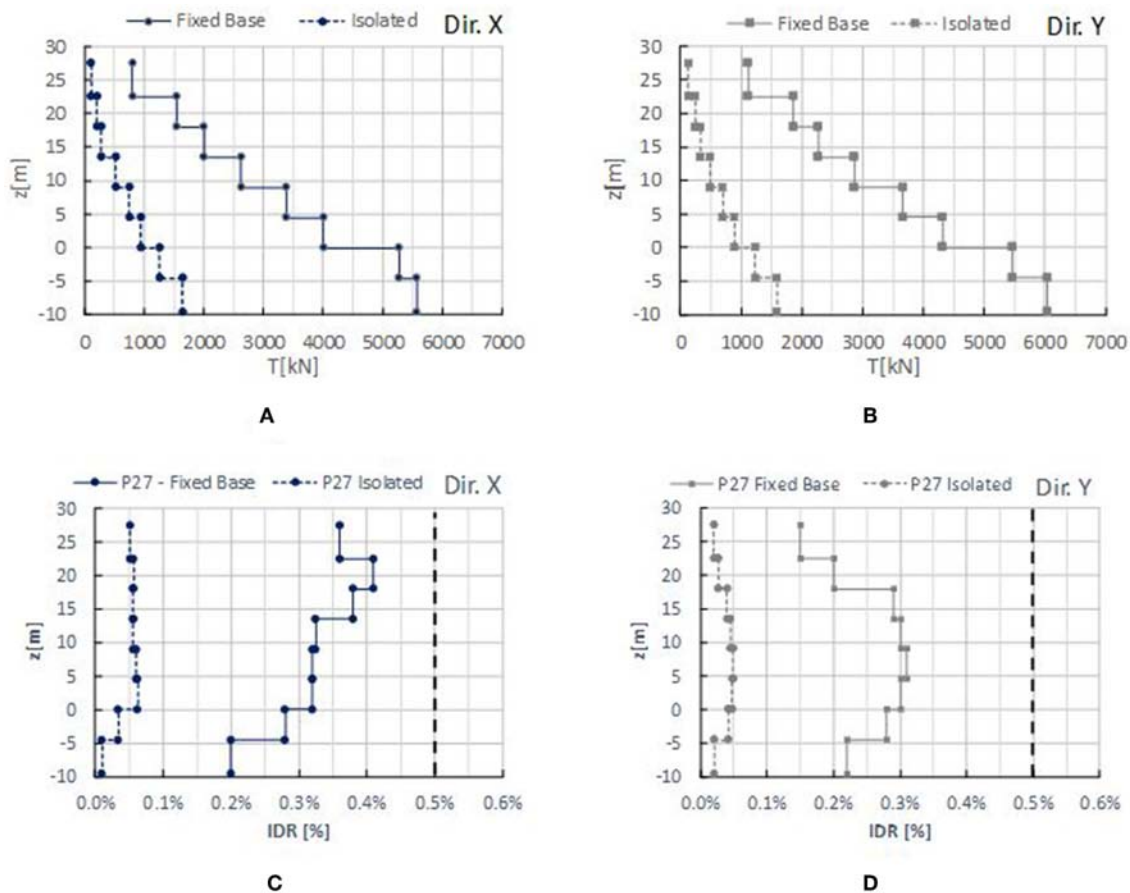
**FIGURE 12** | Fixed-base vs. base-isolated model. Comparison over the height of floor shears (at Life Safety Limit State) for the X-direction **(A)** and Y-direction **(B)** and of Drift Ratios (at Damage Limit State) for Column 27 for the X-direction **(C)** and Y-direction **(D)**.

55 interventions are needed on beams, 37 of them to improve shear resistance and 18 to improve flexural capacity. Specifically, the shear and flexural reinforcements in the support zones are provided by steel jacketing, while flexural reinforcements in the mid-span zones are provided by using FRP stripes. Three different load combinations are examined: only gravity loads, only seismic load, and both gravity and seismic loads. In **Figure 13A** the reinforcements needed on beams are shown, while **Figure 13B** reports the ones needed for columns. As it is clear to note, in this case many local reinforcements (45 reinforcements on beams and 4 reinforcements on columns) are mainly requested in order to carry on the gravity loads. Whereas, few interventions, are required for completely retrofitting the building with respect to the seismic action (i.e., obtaining a ratio $a_{gC}/a_{gD} = 100\%$). In detail, they are 10 for beams and 15 for columns.

The global cost of the intervention is about $330e$/sm (total 1.5 milion €). It should be observed that in these costs the realization of new structural elements are included (such as new stairs, new concrete wall systems and new decks) finalized to the architectural and functional rearrangement of the building, as foreseen in the project. The cost estimated

in order to retrofit the building through traditional methods (only local reinforcements) is almost the same (about 1.5 million $e$). Notwithstanding the two alternative solution have the same costs, the intervention through seismic isolation is less invasive, because it drastically reduces the need of local intervention in elevation. Moreover, it guarantees a higher reliability in estimating the structural response. Furthermore, the isolating system may induce many other advantages by adopting new assessment methodologies, as proposed herein in the following.

# A NEW METHODOLOGY FOR ASSESSMENT OF SEISMIC RESPONSE OF A BUILDING

In this study, it is also performed a preliminary seismic assessment of the case study with the following new methodology proposed. It is based on the idea of estimating, starting from the seismic events occurred in the past, the highest seismic action experienced by the building to which negligible or very limited damages are related. This action would become the minimum
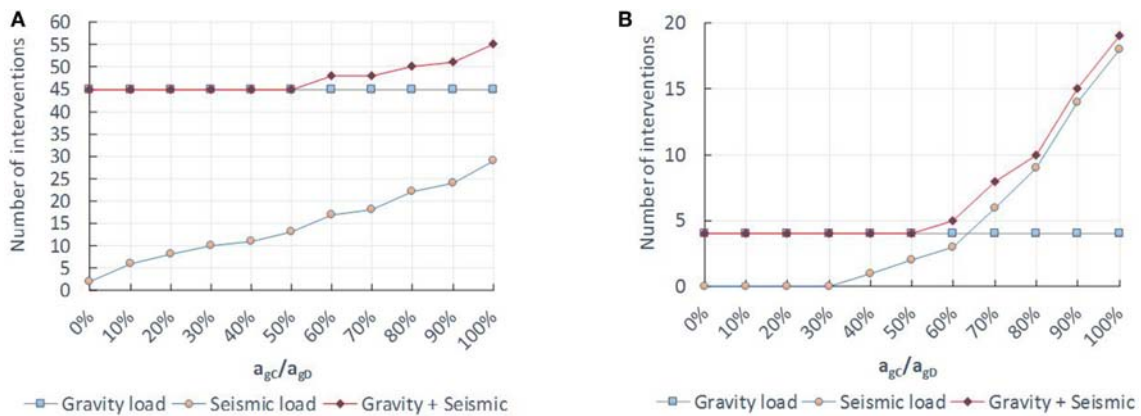
**FIGURE 13 |** Retrofitted structure: Number of local reinforcements on structural elements. Beams **(A)**, columns **(B)**.
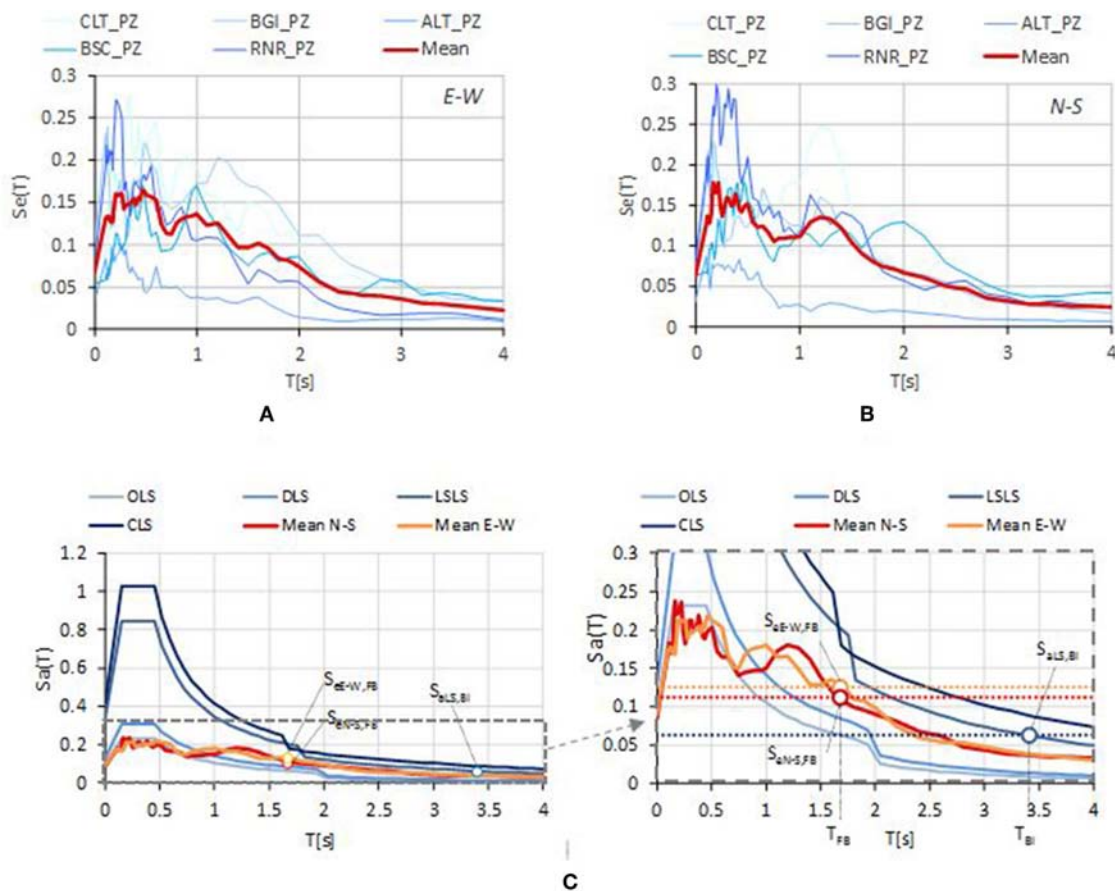


**FIGURE 14 |** Expected demand of Irpinia earthquake for the site of Potenza. **(A)** Recorded GMs spectra scaled for the site of Potenza in the E-W direction, **(B)** Recorded GMs spectra scaled for the site of Potenza in the N-S direction, **(C)** Mean spectra of GMs and code spectra for a soil type C.

seismic action, experimentally experienced, for which the ideal superstructure of a base-isolated building would suffer negligible or very limited damages. Thus, it would represent the minimum capacity of the base isolated building.

With the aim of identifying this minimum action, an accelerometric record at the site would be ideal, even if in many cases such record is not available. Therefore, the seismic action occurred at the site should be estimated in alternative as herein

proposed. The proposed procedure implies of using the Ground Motion Prediction Equations (GMPEs) together with the Ground Motions (GMs) recorded in the surrounding area to take into account the real characteristics of the considered seismic event and, in particular, the frequencies content actually involved. Then, the GMs records are scaled in the considered site by the means of proportioning factors, assessed by using the GMPE relationships. In this way, a rough assessment of the response spectra at the site for a certain earthquake is obtained.

In the considered case study, the procedure is applied by using the GMs record available in the ESM database (Luzi et al., 2016) and by using the GMPE proposed by Ambraseys et al. (1996). The reference earthquake is the Irpinia earthquake ($M_L$= 6.9) arisen in 1980, where the structure experienced very limited damages.

By considering the magnitude of the Irpinia earthquake ($M_L$ = 6.9) and the epicentral distance of each accelerometric station, the elastic spectral accelerations expected at the i-th station, $S_{a,i}^{GMPE}$, can be estimated through the GMPE proposed by Ambraseys et al. (1996) as follows:

$$\log(S_{a,i}^{GMPE}(T, R_i, M_L) = C_1(T) + C_2(T) \times M_L + C_3(T) \\ \times r_i + C_4(T) \times \log(r_i) \quad (1)$$

$$r_i(T) = \sqrt{R_i^2 + h_0^2(T)} \quad (2)$$

where $T$ is the oscillation period, $R_i$ is the epicentral distance, $C_h$ and $h_0$ are coefficients given by Ambraseys et al. (1996).

Among the several records available, it has been chosen to refer to only the GMs of sites with an epicentral distance lower than the one of Potenza (epicentral distance of Potenza, $R_{PZ}$ = 45 km). Therefore, the following 5 records are available: Calitri (CLT) (epicentral distance $R_{ep}$=18.9 km, maximum ground acceleration $a_g$ = 0.175 g), Bagnoli Irpino (BGL) ($R_{ep}$= 21.9 km, $a_g$= 0.187 g), Rionero in Vulture (RNR) ($R_{ep}$= 35.5 km, $a_g$= 0.096 g), Bisaccia (BSC) ($R_{ep}$= 28.3 km $a_g$ = 0.096 g), and Auletta (ALT) ($R_{ep}$= 23.4 km, $a_g$= 0.057 g). Then, the expected spectral accelerations for the site of Potenza, $S_{a,PZ}^{GMPE}$, can be assessed with the previous equations as follows:

$$\log(S_{a,PZ}^{GMPE}(T, R_{PZ}, M_L) = C_1(T) + C_2(T) \times M_L + C_3(T) \\ \times r_{PZ} + C_4(T) \times \log(r_{PZ}) \quad (3)$$

$$r_{PZ}(T) = \sqrt{R_{PZ}^2 + h_0^2(T)} \quad (4)$$

Consequently, for each oscillation period, the ratio of the spectral accelerations estimated through GMPE equations is calculated, given by the ratio of $S_{a,PZ}^{GMPE}$, for the considered site of Potenza, and $S_{a,i}^{GMPE}$, referred to the i-th accelerometric station having a $R_i$ epicentral distance:

$$\alpha_i(T, R_{PZ}, R_i, M_L) = \frac{S_{a,PZ}^{GMPE}(T, R_{PZ}, M_L)}{S_{a,i}^{GMPE}(T, R_i, M_L)} \quad (5)$$

For each accelerometric station considered, the so-obtained scale factor may be interpreted as a relative measure of the

amplification (or de-amplification) of the spectral ordinate occurred in Potenza site with respect to the i-th site. Thus, it can be used as a scaling factor to de-amplify (or amplify) the spectral accelerations recorded (i.e., derived from the recorded GMs) at the i-th site in order to estimate the spectral accelerations occurred at Potenza during the seismic event. Then, the spectral accelerations for the city of Potenza are obtained as follows

$$S_{a,i,PZ}^{GM}(T) = S_{a,i,PZ}^{GM}(T) \times \alpha_i(T) \quad (6)$$

where $S_{a,i}^{GM}$ is the spectral ordinate for the i-th recorded ground motion.

**Figures 14A,B** show the response spectra for bed-rock estimated for the site of Potenza starting from each of the 5 GMs chosen, scaled with the proposed $\alpha_i$ coefficient of the Equation (5). The spectra are separately reported for the East-West (E-W) and North-South (N-S) directions, considering also the mean spectrum for each direction considered. The latter, are compared in **Figure 14C** with the design spectra proposed by the Italian code (NTC, 2008) for different limit states, and by considering a sub-soil of Type C (i.e., when the velocity of propagation of seismic waves $V_{s30}$ is 180<$V_{s30}$[m/s]<360). In doing so, also each mean spectrum is amplified by the stratigraphic factor proposed in the Italian code (NTC, 2008) for a soil type C. As it is possible to note, the derived mean spectra are quite similar in the two directions and lower than the one of LSLS proposed by the Italian code. By considering that the fundamental vibration period of the fixed-base building is equal to $T_{FB}$ = 1.683 s (indicated in the **Figure 6**), the spectral accelerations estimated through the derived spectra starting from the recorded GMs result equal to 0.13 g for the E-W direction and 0.11 g for the N-S direction. These spectral accelerations, according to the new seismic methodology here presented, may be intended as the highest seismic action to date suffered in reality by the structure, and therefore experimentally experienced, for which the ideal superstructure of the base-isolated building would suffer negligible or very limited damages.

The so-estimated spectral accelerations are higher than the one experienced by the superstructure of the isolating building (i.e., $S_{a,LS,BIS}$ = 0.061 g by considering the fundamental period of the building related to the Life safety Limit state), that represents the spectral acceleration considered to design the base-isolated building. It must however be observed that the estimation of the mean spectra is affected by a considerable uncertainty, due to the high variability among the scaled GMs spectra of each site, as shown in the **Figures 14A,B**. Nevertheless, only the record of Auletta (ALT) has spectral accelerations lower than $S_{aLS,BI}$, while all the others considered records exhibit higher values.

The proposed new methodology may be intended as a preliminary assessment of the building seismic capacity, through an analysis of its capacity exhibited during previous earthquakes, without any numerical model of the structure. Therefore, with this approach, it is possible to estimate the seismic demand to which no one or very limited interventions are required, reducing significantly their invasiveness and the structural investigations. To this regard, it should be remarked that, this design philosophy is adopted by the Italian national directive for reducing the

seismic risk of cultural heritage (G.U. N. 47, 2011), where light interventions are permitted even in the absence of a total retrofit of the building.

## CONCLUSIONS

In this paper a seismic isolation intervention on the historical building of the "*Archivio di Stato*" of Potenza has been illustrated. The case study is one of the first reinforced concrete buildings built in Italy, having an architectural value such that it has been included in the list of protected properties by the Italian Ministry of Cultural Heritage. This building has several architectural constraints and strong irregularities in plan and elevation. Thus, among the various available intervention techniques, seismic isolation has been chosen because it allows a strong reduction of demand on structural elements with a minimal impact on the architectural components.

The comparison between structural responses of fixed-base and isolated building has been pointed out that, despite of the low values of isolating grade (i.e., $\alpha = 1.77$ for the LSLS), the isolating system is effective in order to reduce the seismic demand on the building. Specifically, the floor shear for LSLS have been reduced by over 70%, while the interstory drift ratios for DLS have been reduced by over 80% at each floor. However, the strong reduction of seismic demand results not sufficient to ensure a complete retrofit of the building, requiring several local interventions.

On this aspect, it has been proposed a new and fast methodology for estimating the seismic capacity exhibited by the building during the "Irpinia earthquake" of 1980. This methodology is based on a combined use of the recorded GMs of the surrounding area in conjunction with the attenuation law (GMPE). The methodology, by avoiding an implementation of a numerical model, allows to estimate the testing seismic action occurred in reality for the superstructure of the base-isolated building to which negligible or very limited damages are related. The application of this method has shown that the spectral acceleration transmitted to the superstructure with the design Italian spectra (i.e., $S_e = 0.061\,g$) would result lower than the one experienced by the ideal superstructure during the "Irpinia earthquake" (i.e., $S_{eN-S} = 0.11\,g$, $S_{eE-W} = 0.13\,g$), where the building exhibited very limited damages. Thus, this methodology has confirmed and certified the effectiveness of the isolating system demonstrating, in addition, that no local intervention would be necessary. In the future, the new methodology here presented may be also improved by accounting for the uncertainties such as, at first, the dispersion of the recorded GMs.

## DATA AVAILABILITY

The raw data supporting the conclusions of this manuscript will be made available by the authors, without undue reservation, to any qualified researcher.

## AUTHOR CONTRIBUTIONS

All authors listed have made a substantial, direct and intellectual contribution to the work, and approved it for publication.

## REFERENCES

Alhan, C., and Gavin, H. (2004). A parametric study of linear and non-linear passively damped seismic isolation systems for buildings. *Eng. Struct.* 26, 485–497. doi: 10.1016/j.engstruct.2003.11.004

Ambraseys, N. N., Simpson, A., and Bommer, J. J. (1996). Prediction of horizontal response spectra. *Earthq. Eng. Struct. Dyn.* 25, 371–400. doi: 10. 1002/(SICI)1096-9845(199604)25:4<371::AID-EQE550>3.0.CO;2-A

Braga, F., Faggella, M., Gigliotti, R., and Laterza, M. (2005). Nonlinear dynamic response of HDRB and hybrid HDRB-friction sliders base isolation systems. *Bull. Earthq. Eng.* 3, 333–353. doi: 10.1007/s10518-005-1242-2

Braga, F., Gigliotti, R., and Laguardia, R. (2019). Intervention cost optimization of bracing systems with multiperformance criteria. *Eng. Struct.* 182, 185–197. doi: 10.1016/j.engstruct.2018.12.034

Braga, F., Gigliotti, R., and Laterza, M. (2006). Analytical Stress – Strain Relationship for Concrete Confined by Steel Stirrups and / or FRP Jackets. *J. Struct. Eng.* 132, 1402–1416. doi: 10.1061/(ASCE)0733-9445(2006) 132:9(1402)

Caprili, S., Mattei, F., Gigliotti, R., and Salvatore, W. (2018). Modified cyclic steel law including bond-slip for analysis of RC structures with plain bars. *Earthquakes Struct.* 14, 187–201. doi: 10.12989/eas.2018.14.3.187

Ciampi, V., De Angelis, M., and Paolacci, F. (1995). Design of yielding or friction-based dissipative bracings for seismic protection of buildings. *Eng. Struct.* 17, 381–391. doi: 10.1016/0141-0296(95) 00021-X

Computers and Structures Inc (2015). *SAP2000 Integrated Solution for Structural Analysis and Design.* Berkeley, CA.

Constantinou, M., Mokha, A., and Reinhorn, A. (1990). Teflon bearings in base isolation II: modeling. *J. Struct. Eng.* 116, 455–474. doi: 10.1061/(ASCE)0733-9445(1990)116:2(455)

D'Amato, M., Braga, F., Gigliotti, R., Kunnath, S., and Laterza, M. (2012a). A numerical general-purpose confinement model for non-linear analysis of R/C members. *Comput. Struct.* 102–103, 64–75. doi: 10.1016/j.compstruc.2012.03.007

D'Amato, M., Braga, F., Gigliotti, R., Kunnath, S., and Laterza, M. (2012b). Validation of a modified steel bar model incorporating bond-slip for seismic assessment of concrete structures. *J. Struct. Eng.* 138, 1351–1360. doi: 10.1061/(ASCE)ST.1943-541X.00 00588

Di Sarno, L., and Manfredi, G. (2010). Seismic retrofitting with buckling restrained braces: application to an existing non-ductile RC framed building. *Soil Dyn. Earthq. Eng.* 30, 1279–1297. doi: 10.1016/j.soildyn.2010. 06.001

Di Sarno, L., and Manfredi, G. (2012). Experimental tests on full-scale RC unretrofitted frame and retrofitted with buckling-restrained braces. *Earthq. Eng. Struct. Dyn.* 41, 315–333. doi: 10.1002/eqe.1131

Dolce, M., Gigliotti, R., Laterza, M., Nigro, D., and Marnetto, R. (2001). "Il rafforzamento dei pilastri in c. a. mediante il sistema CAM," in *10th ANIDIS Conference L'ingegneria Sismica in Italia* (Potenza-Matera).

Faqeer, A., Faggella, M., Gigliotti, R., and Spacone, E. (2018). Effects of bond-slip and masonry in fi lls interaction on seismic performance of older R/C frame structures. *Soil Dyn. Earthq. Eng.* 109, 251–265. doi: 10.1016/j.soildyn.2018.02.027

G.U. N. 47 (2011). *Valutazione e Riduzione del Rischio Sismico del Patrimonio Culturale con Riferimento alle Norme tecniche per le Costruzioni di cui al Decreto del Ministero delle Infrastrutture e dei Trasporti del 14 Gennaio 2008.* Italian Presidency of the Council of Ministry.

Google Maps, (2019). *Google Maps.* https://goo.gl/maps/BdyEstNhfyp

Ibrahim, R. A. (2008). Recent advances in nonlinear passive vibration isolators. *J. Sound Vib.* 314, 371–452. doi: 10.1016/j.jsv.2008.01.014

Kawamura, S., Sugisaki, R., Ogura, K., Maezawa, S., and Tanaka, S. (2000). "Seismic isolation retrofit in Japan," in *12 th World Conference of Earthquake Engineering* (Auckland).

Kelly, J. M. (1986). Aseismic base isolation : review and bibliography. *Soil Dyn. Earthq. Eng.* 5, 202–216. doi: 10.1016/0267-7261(86)90006-0

Kelly, J. M. (2002). Seismic isolation systems for developing countries. *Earthq. Spectra* 18, 385–406. doi: 10.1193/1.1503339

Laguardia, R., Gigliotti, R., and Braga, F. (2017). "Optimal design of dissipative braces for seismic retrofitting through a multi- performance procedure," in *17th ANIDIS Conference "L'ingegneria Sismica in Italia* (Pistoia).

Laterza, M., D'Amato, M., Braga, F., and Gigliotti, R. (2017b). Extension to rectangular section of an analytical model for concrete confined by steel stirrups and/or FRP jackets. *Compos. Struct.* 176, 910–922. doi: 10.1016/j.compstruct.2017.06.025

Laterza, M., D'Amato, M., and Gigliotti, R. (2017a). Modeling of gravity-designed RC sub-assemblages subjected to lateral loads. *Eng. Struct.* 130, 242–260. doi: 10.1016/j.engstruct.2016.10.044

Lignola, G. P., Di Sarno, L., Di Ludovico, M., and Prota, A. (2016). The protection of artistic assets through the base isolation of historical buildings: a novel uplifting technology. *Mater. Struct. Constr.* 49, 4247–4263. doi: 10.1617/s11527-015-0785-1

Luca, A., De Mele, E., Molina, J., Verzeletti, G., and Pinto, A. V. (2001). Base isolation for retrofitting historic buildings : evaluation of seismic performance through experimental investigation. *Earthq. Eng. Struct. Dyn.* 1145, 1125–1145. doi: 10.1002/eqe.54

Luzi, L., Puglia, R., Russo, E., and Clara D'amico, M. (2016). Engineering strong motion database, version 1.0. *Seismol. Res. Lett.* 87, 987–997. doi: 10.1785/0220150278

Martelli, A., and Forni, M. (1998). Seismic isolation of civil buildings in Europe. *Prog. Struct. Eng. Mater.* 1, 286–294. doi: 10.1002/pse.2260010310

Mazza, F., and Vulcano, A. (2014). Equivalent viscous damping for displacement-based seismic design of hysteretic damped braces for retrofitting framed buildings. *Bull. Earthq. Eng.* 12, 2797–2819. doi: 10.1007/s10518-014-9601-5

Mokha, A., Constantinou, M., and Reinhorn, A. M. (1988). *Teflon Bearings in Aseismic Base Isolation: Experimental Studies and Mathematical Modeling.* Technical report, NCEER, Buffalo: NY.

Mokha, A., Navichandra, A., Constantinou, M. C., and Zayas, V. (1996). Seismic isolation of large historic building. *J. Struct. Eng.* 122, 298–308. doi: 10.1061/(ASCE)0733-9445(1996)122:3(298)

NTC (2008). *Norme Tecniche per le Costruzioni D.M. 14 Gennaio 2008.* Rome: Italian Ministry of Infrastructure.

NTC (2018). *D.M. 17.01.18 Aggiornamento delle 'Norme Tecniche per le costruzioni.'* Rome: Italian Ministry of Infrastructure.

R.D. (1939). *Norme per l'esecuzione di Opere in Conglomerato Cementizio Semplice o Armato - R.D. 16.11.1939 n 2229.* Rome: Regno d'Italia.

Skinner, R. I., Robinson, W. H., and McVerry, G. H. (1993). *An Introduction to Seismic Isolation.* Chichester: John Wiley & Sons.

Tomazevic, M., Klemenc, I., and Weiss, P. (2009). Seismic upgrading of old masonry buildings by seismic isolation and CFRP laminates : a shaking-table study. *Bull. Earthq. Eng.* 2009, 293–321. doi: 10.1007/s10518-008-9086-1

Verderame, G. M., Stella, A., and Cosenza, E. (2001). "Le proprietà meccaniche degli acciai impiegati nelle strutture in c. a. realizzate negli anni 60" in *10th ANIDIS Conference "L'ingegneria Sismica in Italia* (Potenza-Matera).

Check for updates

# Large-Scale Seismic Vulnerability and Risk of Masonry Churches in Seismic-Prone Areas: Two Territorial Case Studies

Francesco Fabbrocino[1], Generoso Vaiano[1], Antonio Formisano[2]* and Michele D'Amato[3]

[1] Department of Engineering, Pegaso University, Naples, Italy, [2] Department of Structures for Engineering and Architecture, University of Naples "Federico II", Naples, Italy, [3] Department of European and Mediterranean Cultures, University of Basilicata, Matera, Italy

In this paper, seismic vulnerability and risk assessment of two samples of churches, located in Teramo and Ischia island (Naples gulf), both affected by the most recent earthquakes that occurred in Italy, are presented. To this aim, we applied a simplified method particularly suitable for seismic evaluations at a territorial scale, providing a global resulting score to be compared among the cases analyzed. The data obtained allowed us to provide vulnerability maps and a seismic risk index for all the considered churches. In addition, the calculated indexes permit a preliminary health state evaluation of the inspected churches, for ranking the priorities and planning additional in-depth evaluations.

Keywords: seismic vulnerability, seismic risk, masonry church, L'Aquila earthquake, Ischia earthquake, large-scale analysis method, damage index

## INTRODUCTION

The structural analysis of monumental buildings belongs to a multidisciplinary study, where different types information are converging, such as construction history (year of erection, possible transformations, traumatic events), geometrical and structural critical survey, materials features and degradation, and the detection of crack patterns. In this way, it is possible to firstly diagnose the causes that produce instability and/or degradation of structural elements, which are very often multiple and generally act simultaneously. In general, these causes can be classified as intrinsic or extrinsic: the former refers to the origin and nature of the monumental buildings and, therefore, to their vulnerability; the latter is related to the site geographic conditions.

The Italian territory is characterized by a high seismicity level, demonstrated by the last earthquakes that occurred in the recent past such as in Irpinia (1980), San Giuliano of Puglia (2002), L'Aquila (2009), Emilia-Romagna (2012), Central Italy (2016), and Ischia (2017). These events unfortunately gave rise to serious consequences in terms of death and damage to historical buildings. Therefore, from an engineering point of view, appropriate numerical, experimental, and theoretical procedures are required in order to assess the seismic vulnerability of the structures and to design specific interventions useful for repairing the damages or avoiding future ones.

Recently, simplified models useful to preliminarily assess the seismic performance and the related risk at a territorial level have been proposed (Lourenço and Roque, 2006; Directive of the Italian Prime Minister, 2011; Lourenço et al., 2013). These methods are useful for ranking the priorities and for planning further analyses, to be conducted with more refined numerical

models, which may regard some construction parts or the entire structure. To this aim, the second-level vulnerability forms developed by the Italian National Group for Earthquakes Defense (GNDT) (Benedetti and Petrini, 1984; GNDT, 1994), which are useful for screening the structures through systematic surveys, are worth noting. Among these simplified models, a new and simplified procedure, developed, and validated at the University of Basilicata, has been recently proposed. This procedure may also be applied to ancient masonry churches, and it is useful to evaluate the seismic risk at a territorial scale including natural threats due to the geographical surrounding context. This methodology, described and validated in Dìaz Fuentes (2016), D'Amato et al. (2018), and D'Amato et al. (2019), and extended also to Chilean adobe churches in Fuentes et al. (2019a), is being applied in this paper to analyze the seismic vulnerability of two samples of Italian churches. In particular, the considered churches are located in two different geographical areas: in Teramo (Central Italy) and in Ischia island, located in the Naples gulf (Southern Italy). Both areas were affected by recent earthquakes and the considered churches suffered different structural damages. Initially, an international overview is shown on some researches devoted to the preservation of cultural heritage buildings through the proposal of manuals and principles for risk management, not limited to the seismic hazard. Later on, the simplified method considered in Dìaz Fuentes (2016) and D'Amato et al. (2018) is described and applied to the two church samples, after collecting all information (structural and related to potential threats in the area) necessary for evaluating seismic vulnerability and the resulting risk indexes. Finally, the achieved results are compared and discussed. The obtained results show that the considered methodology is also useful for comparison of the seismic risk of different geographical areas. Moreover, a new territorial seismic risk score is also proposed.

## SEISMIC VULNERABILITY AND RISK OF HISTORICAL CONSTRUCTIONS

Seismic vulnerability influences how damage caused by an earthquake in a given area is assessed from a construction point of view. The causes of high vulnerability even at very low levels of seismic forces may be different due, for instance, to structural irregularities, inadequate design, poor quality of materials, absence of constructive details, and scarce maintenance (Krstevska et al., 2010; Betti and Vignoli, 2011; Milani and Valente, 2015a; Clementi et al., 2017a,b; Fonti et al., 2017; Formisano et al., 2017, 2018; Milani et al., 2017a; Valente et al., 2017; Luchin et al., 2018; Valente and Milani, 2018a,b,c). After the recent seismic events, many efforts of the scientific community have been done in order to develop appropriate procedures for implementing seismic vulnerability analysis (Formisano, 2017; Formisano and Marzo, 2017; Laterza et al., 2017; Lopez et al., 2019) and specific retrofitting interventions (Faggiano et al., 2009; Terracciano et al., 2015; D'Amato et al., 2017; Milani et al., 2017b, 2018). In particular, as previously introduced, recurrent seismic damages were observed in historic masonry buildings characterized by local out-of-plane and

in-plane response mechanisms regarding one or more isolated structure portions (Lagomarsino and Podestà, 2004; Formisano et al., 2010; Leite et al., 2013; Gattulli et al., 2014; Milani and Valente, 2015b; Stockdale, 2016; Valente et al., 2016; Betti et al., 2018; De Matteis et al., 2019; Fuentes et al., 2019b; Penna et al., 2019; Ramirez et al., 2019).

In order to assess the seismic performance of an existing structure, the current Italian Design Code (Ministry of Infrastructures and Transports, 2008a,b; Cecchi and Calvi, 2010; Directive of the Italian Prime Minister, 2011; Ministry of Infrastructures Transports, 2018) defines the design criteria and the performance targets to be satisfied under an earthquake action. These indications are useful for assessing vulnerability combined with the seismic hazard for evaluating the resulting seismic risk as well as all the possible effects in terms of expected damage that an earthquake can produce in a determined time and area.

With regard to cultural heritage conservation in the international scenario, various principles and manuals for risk management, such as those delivered by the United Nations Educational, Scientific and Cultural Organization (UNESCO), the International Council of Monuments and Sites (ICOMOS, 2008), the International Centre for the Study of Conservation and Restoration of Cultural Heritage (ICCROM), and the Getty Conservation Institute (UNESCO World Heritage Centre, 2002; ICOMOS, 2008), were developed. In addition, innovative prevention programs, such as the Risk Maps of different countries and the Disaster Prevention Program on Cultural Heritage (INAH, 2013), have been set up. However, the principles proposed found rare applications, because they did not take into account the different cultural, social, and economic values among countries. In this context, the ICCROM and the Getty Conservation Institute, with the publication "Between Two Earthquakes" in 1987 (Feilden, 1987), were the first to propose guidelines for prevention of disaster risks. These guidelines focused on two constructive vulnerability aspects, namely, the intrinsic structure, and vulnerability due to building location. In 1998, the first risk management manual for the world cultural heritage was developed (Stovel, 1998), whose most important proposals concerned both threats and the cultural heritage value for the community. This document was updated in 2009, when the United Nations Office for Disaster Reduction (UNISDR) published "Terminology on disaster risk reduction" (UNISDR, 2009). Subsequently, in 2010, UNESCO, ICCROM, ICOMOS, and the World Union for Conservation of Nature (IUCN) developed the Managing Disaster Risks for World Heritage (UNESCO/ICCROM/ICOMOS/IUCN, 2010), a document integrating Stovel's manual and introducing physical nature threats caused by climatic factors and chemical nature hazards.

## SIMPLIFIED METHODOLOGY FOR SEISMIC RISK ASSESSMENT (Dìaz Fuentes, 2016; D'Amato et al., 2018)

Seismic risk is the measurement of the expected damage of buildings placed at a specified site in a given time interval. It is

considered as the combination of three factors, namely, hazard, vulnerability, and exposure. Therefore, in order to assess the seismic risk of a built area, knowledge of only the hazard is not enough, since it is also necessary to carefully estimate the different construction vulnerabilities present during the seismic event and the related economic and social value of their content.

In this paper, the methodology applied refers to a recent work carried out by the University of Basilicata for providing territorial risk maps for planning useful intervention plans also addressed to increase cultural heritage resilience (D'Amato et al., 2018; Fuentes et al., 2019a). This simplified method may be applied, in general, in a multi-risk evaluation procedure, by considering both natural and anthropic threats. In this work, the method is applied only for a seismic risk analysis, involving the application of three distinct tools, each of which assigns a specific score:

1. *Tool 1*: Priority attention on actions related to the buildings according to their exposure value (*E*);
2. *Tool 2*: Description, classification, and mapping of seismic hazard (*H*);
3. *Tool 3*: Evaluation and quantification of the seismic vulnerability level (*V*).

The choice of this simplified method is due to the fact that it allows assessment of seismic risk at a territorial scale before a real seismic event, just supposing different earthquake magnitudes. On the contrary, other methods, such as the ones proposed by the GNDT or Italian civil protection, are based on a post-earthquake survey of damages with visual analyses. Moreover, the method permits a fast appraisal of a large number of ancient churches in a certain area requiring very simple information about dimensional features, environmental characteristics, and site morphology. Once the first seismic risk screening is conducted, it is possible to carry out more in-depth analyses in order to program retrofitting interventions. However, the present simplified model does not take into account the cumulative damage due to repeated shocks (for example, during a typical seismic sequence, or due to a series of events acting on unrepaired buildings) that influences the vulnerability of the buildings investigated and, therefore, may vary seismic risk ranking.

In this study, the simplified method considered is applied, as it will be discussed later on, to two different samples of churches located in two distinct geographical areas: it allows one to perform comparative seismic risk analyses at a territorial scale.

## Description

The simplified procedure allows one to separately score exposure value (application of *Tool 1*), seismic hazard (*Tool 2*), and seismic vulnerability (*Tool 3*). Then, the so-obtained scores are multiplied in accordance with the relationship (UNDRO, 1979; FEMA, 2004):

$$R = E \times H \times V \qquad (1)$$

*Tool 1* estimates the cultural values, divided into socio-cultural, and economic values. Socio-cultural values include antiquity, historical, symbolic, and aesthetic values. Economic values

concern the value in use, as well as financial and scientific values. In this study, seismic risk assessment has been performed unless the score *E* is assigned by means of *Tool 1*.

## Hazard Scoring (*H*)

*Tool 2* provides the *H* score. It considers the risk from different points of view, with the aim of conducting a qualitative analysis that leads to the identification of threats conditioning the performances of buildings. Threats are divided into two categories, namely, sporadic events and continuous processes, depending on their occurrence probability. In particular, they can be grouped into three families:

- Natural threats, configured as sporadic events with catastrophic, or serious consequences;
- Physical threats, configured as continuous processes, whose consequences are generally low, even if they gradually increase;
- Anthropogenic, chemical, and electrochemical threats, generally corresponding to continuous processes with low or gradual consequences, except for the cases of sporadic events (i.e., fires caused by industrial activities and forest fires) with catastrophic consequences.

The risk scenarios are divided into the best, the most probable, and the worst. They are determined on the basis of the statistical principle that considers a higher probability of catastrophic events in areas already affected by earthquakes. The main natural threats are earthquakes and tsunami, landslides and floods, hydro-meteorological hazards, and volcanic phenomena. Physical threats are represented by water, terrestrial hazards, thermal risks, and dangers due to atmospheric environment. For these threats, the erosion index and the physical stress ones are defined.

The anthropogenic, chemical, and electrochemical threats are of the following different nature:

- Chemical: fires, explosions, radiation, toxic losses;
- Health-ecological: epidemics or parasites, air, soil, or water pollution;
- Socio-organizational: wars; social hardship manifestations; terrorism; vandalism; tourist pressure; population overload; relative humidity increase; air, marine, or terrestrial accidents; and forest fires;
- Severe demographic decline with consequent building abandonment and consequent lack of maintenance: material deterioration, loss of water (due to broken pipes, drainage problems, water protection, etc.).

Among these threats, those that influence cultural heritage the most are air and water pollution, which cause deterioration of materials and the environment.

All the above parameters are analyzed to determine the worst possible situation, based on historical information. They are subsequently classified according to the severity of the potential damage to monumental buildings. Damage can be absent, low or gradual, and catastrophic. These damage typologies are characterized by a given score assigned to each parameter on the basis of the threat influence on the building seismic behavior (**Table 1**). The resulting seismic hazard index

**TABLE 1** | Scenario description and classification of threats according to damage severity.

| Parameters | | Damage gravity | | |
|---|---|---|---|---|
| | | Absence of damage | Middle damage | Catastrophic damage |
| Sporadic Events | Earthquake and tsunami threat | 0 | 0.2 | 0.4 |
| | Landslides | 0 | 0.15 | 0.25 |
| | Volcanic threat | 0 | 0.2 | 0.4 |
| | Hydro-methodological threat | 0 | 0.15 | 0.25 |
| | Chemical–technological threat | 0 | 0.15 | 0.25 |
| | Forest fires | 0 | 0.15 | 0.25 |
| Continuous Events | Erosion threat | 0 | 0.05 | 0.1 |
| | Physical stress of threat | 0 | 0.05 | 0.1 |
| | Air pollution | 0 | 0.01 | 0.05 |
| | Socio-organizational threat | 0 | 0.01 | 0.05 |
| | Demographic decline | 0 | 0.01 | 0.05 |

**TABLE 2** | Parameter evaluation and quantification in order to calculate the vulnerability index.

| | Parameters | Class ($v_i$) | | | | Weight ($p_i$) |
|---|---|---|---|---|---|---|
| | | A | B | C | D | |
| 1 | Position of the building and foundations | 0 | 1.35 | 6.73 | 12.12 | 0.75 |
| 2 | In-plane configuration | 0 | 1.35 | 6.73 | 12.12 | 0.50 |
| 3 | In-elevation configuration | 0 | 1.35 | 6.73 | 12.12 | 1.00 |
| 4 | Distance among walls | 0 | 1.35 | 6.73 | 12.12 | 0.25 |
| 5 | Non-structural elements | 0 | 1.35 | 6.73 | 12.12 | 0.25 |
| 6 | Resistant system type and organization | 0 | 1.35 | 6.73 | 12.12 | 1.50 |
| 7 | Resistant system quality | 0 | 1.35 | 6.73 | 12.12 | 0.25 |
| 8 | Floors | 0 | 1.35 | 6.73 | 12.12 | 1.00 |
| 9 | Roofs | 0 | 1.35 | 6.73 | 12.12 | 1.00 |
| 10 | Conservation state | 0 | 1.35 | 6.73 | 12.12 | 1.00 |
| 11 | Environmental alterations | 0 | 1.35 | 6.73 | 12.12 | 0.25 |
| 12 | Construction system negative alterations | 0 | 1.35 | 6.73 | 12.12 | 0.25 |
| 13 | Fire vulnerability | 0 | 1.35 | 6.73 | 12.12 | 0.25 |

($H$), obtained by summing the singular threats scores, may assume a value ranging from 0 and 1. More details about the $H$ scoring may be found in Dìaz Fuentes (2016) and D'Amato et al. (2018).

## Vulnerability Scoring (*V*)

The application of *Tool 3* provides the vulnerability score *V*. This tool aims at evaluating the seismic vulnerability of the considered church, and it is based on the assessment of 13 vulnerability parameters related to various construction aspects. Specifically, 10 of these 13 parameters are derived from the Italian second-level GNDT vulnerability datasheet (GNDT, 1994). Each parameter has a different weight $p_i$, and is characterized by four different scores $v_i$ associated to four possible classes (*A*, *B*, *C*, and *D*). The values of $p_i$ and $v_i$ are reported in **Table 2**.

Finally, according to the considered method, the vulnerability index *V* may be evaluated with the following relationship:

$$V = \sum_{i=1}^{13} v_i p_i \qquad (2)$$

where, the sum is extended to all possible parameters considered. In particular, as it is worthy to note, the higher the *V* score, the higher the seismic vulnerability of a structure, which may fall within the following ranges:

- Low vulnerability: $0 < V \leq 10.81$;
- Medium vulnerability: $10.81 < V \leq 55.52$;
- High vulnerability: $55.52 < V \leq 100$.

In the following, each parameter considered is described in detail. More information may be found in Dìaz Fuentes (2016) and D'Amato et al. (2018).

## Position of the Building and Foundations

By indicating as $\Delta h$ the foundation difference altitude, the four considered classes are as follows:

Class A:

- Buildings placed on rocky terrain with slopes equal to or lower than 10% and any $\Delta h$;
- Buildings placed on loose ground with slopes lower than or equal to 10% and $\Delta h = 0$.

Class B:

- Buildings placed on rocky terrain with a slope of 10–30% and any $\Delta h$;
- Buildings placed on loose ground with $\Delta h \leq 1$ m and in the absence of unbalanced pressures due to embankments also verifying one of the following conditions:

1. A ground slope lower than 10% and $0 < \Delta h \leq l$;
2. A ground slope of 10–30% and $\Delta h \leq l$;
3. Building without foundations, a ground slope of 10–30% and $\Delta h \leq l$.

Class C:
- Buildings placed on rocky terrain with a slope of 30–50% and any $\Delta h$;
- Buildings on loose ground and $\Delta h \leq l$, which verifies one of the following conditions:

1. Absence of unbalanced thrusts due to embankments, the building has foundations, a ground slope of 30–50%, and $\Delta h \leq l$;
2. Absence of unbalanced thrusts due to embankments, the building has no foundations, the ground has a slope of 20–30%, and $\Delta h \leq l$;
3. Presence of unbalanced thrusts due to embankments, the building has foundations, the ground has a slope <50%, and $\Delta h \leq l$;
4. Presence of unbalanced thrusts due to embankments, the building has no foundations, the ground has a slope <30%, and $\Delta h \leq l$.
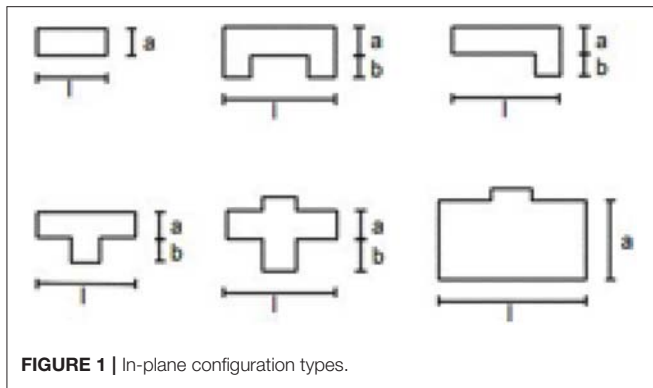
**FIGURE 1 |** In-plane configuration types.

Class D:
All the other cases that do not fall into the previous classes.

## In-plane Configuration

In the case of a rectangular building, a significant parameter is the ratio between the dimensions of minor and major sides $\beta_1 = a/l \times 100$ (**Figure 1**). In case of plan layouts with different shapes, in addition to the $\beta_1$ parameter, it is necessary to take into account another parameter $\beta_2 = b/l \times 100$, which is the ratio between the deviation size and the larger dimension (**Figure 1**).

The assignment to a given class is made on the basis of the most unfavorable conditions set by the $\beta_1$ and $\beta_2$ parameters as follows:
Class A:
$\beta_1 \geq 80$ and $\beta_2 \leq 10$
Class B:
$60 \leq \beta_1 < 80$ and $10 < \beta_2 \leq 20$
Class C:
$40 \leq \beta_1 < 60$ and $20 < \beta_2 \leq 30$
Class D:
$\beta_1 < 40$ and $\beta_2 > 30$

## In-elevation Configuration

It is necessary to take into account the presence of porticoes having a significant surface compared to that of the building, as well as towers of significant height and mass compared to the remaining part of the building. For the mass variation evaluation, the $\pm \Delta M/M$ ratio is considered, where:

- $\Delta M$ is the mass variation between two successive levels;
- $M$ is the mass of the lower floor.

Percentage variations <10% can be considered negligible. As a rule, the $\Delta M/M$ ratio can be replaced by the $\pm \Delta A/A$ ratio, where $A$ and $\Delta A$ are the plan covered surface and its variation, respectively. The four classes to be considered are as follows:
Class A:

- Buildings with uniform mass distribution over the whole height;
- Buildings with mass continually decreasing.

Class B:

- Buildings with porticoes and loggias of modest size;
- Buildings that present backwardness resulting in a decrease of the floor area >10 and <20%;
- Buildings with towers with a height <10% of the total building.

Class C:

- Buildings with porticoes or loggias having surface >10% and equal to or <20% of the total covering floor area;
- Buildings with retractions involving a reduction of the floor area more than 20%;
- Buildings with towers with a height more than 10 and <40% of the total building.

Class D:
All the other cases that do not fall into the previous classes.

## Distance Among Walls

The aim of this parameter is to evaluate the presence of walls (without considering partition walls) intersected by transverse ones that are able to constitute an efficient constraint to prevent the development of out-of-plane overturning mechanisms. The vulnerability classes are the following.
Class A:
Buildings having the following geometrical features:

- Slenderness (height/thickness) <8;
- The internal room width should not be more than 2.5 times the wall thickness;
- Door and window must be located at a distance from the nearest free edge almost three times the wall thickness;
- The distance between the wall bracing axes must be <6 times the wall thickness;
- The wall relative verticality must not be >10% of its height.

Class B:

- Buildings with only three of the Class A geometric features.

Class C:

- Buildings with only two of the Class A geometric features.

Class D:

- Buildings that do not have the geometrical features described in class A.

## Non-structural Elements

In this parameter, all the non-structural elements, such as fixtures, appendices, and projections that can cause damage to people or things, are considered. The classes are defined as follows:
Class A and Class B:

- Buildings without windows, appendices, overhangs, or false ceilings;
- Buildings with windows and fixtures well-connected to the walls;
- Buildings with balconies that are an integral part of the horizontal structures.

Class C:

- Buildings with external fixtures poorly bounded to the walls and with small false ceilings not well-connected.

Class D:
All the other cases that do not fall into the previous classes.

## Resistant System Type and Organization

The organization of the vertical elements is evaluated regardless of the material characteristics of walls. The significant element is the presence and effectiveness of the connections among orthogonal walls in order to ensure box structure behavior efficiency. The four classes are as follows:

Class A:

- Existing buildings consolidated or repaired according to the actual seismic rules.

Class B:

- Buildings with good connections among orthogonal walls.

Class C:

- Buildings that do not have adequate connections between walls and upper floors;
- Buildings with orthogonal walls having a good connection at all levels and floors built up with materials different from the original ones;
- One-story buildings composed of orthogonal walls not adequately connected, which instead have a good connection between the walls and the roofing system thanks to continuous horizontal structures made of original materials or materials compatible to the existing ones in terms of strength and stiffness.

Class D:
All the other cases that do not fall into the previous classes.

## Resistant System Quality

It depends on the material and masonry type. The four classes are as follows:

Class A:

- Square stone masonry having a good-quality mortar;
- Tuff masonry with low porosity and a good-quality mortar;
- Masonry composed of solid bricks having a good-quality mortar;
- Retrofitted masonry according to the current seismic rules.

Class B:

- Stone masonry composed of non-homogeneous elements having a good-quality mortar;
- Masonry composed of solid bricks having a medium-quality mortar.

Class C:

- Squared masonry stones with irregularities having plaster and medium-quality mortar;

- Non-squared masonry stones having plaster and medium-quality mortar
- Sack masonry stones having plaster and medium-quality mortar;
- Squared masonry stones having plaster and medium-quality mortar;
- Masonry bricks having low-quality mortar.

Class D:
Masonry types that do not fall within the previous classes.

## Floors

This parameter expresses the type and properties of horizontal structures. The four classes are defined as follows:

Class A:
Rigid slabs having:

a) Negligible in-plane deformability;
b) Effective floor–wall connections;
c) Absence of staggered floors.

Class B:

- Buildings that do not satisfy the third requirement of the previous class.

Class C:

- Deformable floor having good connections among walls.

Class D:

- Buildings that do not fall within the previous classes.

## Roof

The roof elements influencing the building's seismic behavior are as follows: thrusts on the perimeter walls, connections between roof and walls, seismic mass, stiffness, and strength difference with respect to the masonry building. The four classes are as follows:

Class A:

- Buildings with non-thrusting roofs having edge beams and/or metal tie rods.

Class B:

- Buildings with non-thrusting roofs without edge beams and/or metal tie rods;
- Buildings with non-thrusting roofs having edge beams and/or metal tie rods with the absence of efficient connections between the roof and walls.

Class C:

- Buildings with thrusting roofs made of the original building materials or materials compatible to the original ones in terms of strength and stiffness and without edge beams and/or metal tie rods;
- Buildings with non-thrusting roofs made of the original building materials or materials compatible to the original ones in terms of strength and stiffness and without edge beams and/or metal tie rods.

Class D:

- Buildings that do not fall within the previous classes.

## Conservation State

This parameter considers the actual building status. The four classes are as follows:

Class A:

- Walls in good condition without visible cracks.

Class B:

- Buildings with no diffused cracks, but with possible lesions generated by earthquakes.

Class C:

- Buildings with medium-size cracks (width of the lesion: 2–3 mm);
- Buildings without cracks, but with walls having a conservation status leading toward a significant resistance decrease.

Class D:

Buildings that do not fall within the previous classes.

Cracks and deformations can derive from different causes, such as construction defects, humidity presence, earthquakes, etc. The analyzed damage allows the interpretation of possible collapse mechanisms. In the vulnerability general form, it is necessary to identify in the appropriate section the type of existing damage (structural, non-structural, or humidity) and to express the percentage extension on the structural elements. The possible collapse mechanisms are illustrated in **Figure 2**.

## Environmental Alterations

The parameters useful for the vulnerability evaluation are as follows:

- Accessibility: in case of a catastrophic event, buildings have no accessibility to roads and/or infrastructures;
- Abandonment: the building is in an abandoned context;
- Population density: the building is located in a densely populated area;
- Isolation: the building is located at a considerable distance from the city center;
- Relationship with the geographical context: the building is in a situation of conflict with the site;
- Relationship with the built context: the building is in a situation of conflict with the adjacent constructions;
- Community relationship: the building is in a situation of conflict with the social context;
- Disinterest: the physical and social environments have no relationship with the building.

The classification is as follows:

Class A:

- Buildings that do not have any of the above conditions.

Class B:

- Buildings that have almost three of the above conditions.

Class C:

- Buildings that have almost six of the above conditions.

Class D:

- Buildings that have more than six of the above conditions.

## Constructive System Negative Alterations

Some interventions on buildings are useful for improving the response toward seismic events. However, following recent earthquakes, it was observed that invasive interventions with materials different from building original ones cause high vulnerabilities, leading to collapse in some cases. The classification is as follows:

Class A:

- Structures without interventions to the building system;
- Structures with modifications to the building system by reversible interventions made of materials compatible to the original ones in terms of strength and stiffness.

Class B:

- Structures with modifications to the building system by non-reversible interventions made of materials compatible to the original ones in terms of strength and stiffness.

Class C:

- Structures with interventions made of materials compatible to the existing ones that have modified the building mass.

Class D:

- Structures with interventions made of materials incompatible to the existing ones in terms of strength and stiffness.

## Fire Vulnerability

The parameters affecting fire resistance are as follows:

- Presence of ornaments and flammable materials;
- Roofs or cellars dust accumulation;
- Walls, floors, and doors with low fire resistance;
- Lack of compartmentation;
- Inadequate exits through doors, corridors, or stairs;
- Faulty electrical systems;
- Faulty fireplaces with soot and grease accumulation;
- Low standard in organization of fire drills;
- Fire danger due to smoking or kitchen operations.

## Seismic Risk Scoring (*R*)

The resulting seismic risk score (*R*) may be calculated, in accordance with the simplified method considered, as follows (D'Amato et al., 2018):

$$R = V \times (H + 1) \qquad (3)$$

where the $H$ score is increased to unity for having a resulting score higher than 1. As it is easy to understand, the seismic risk
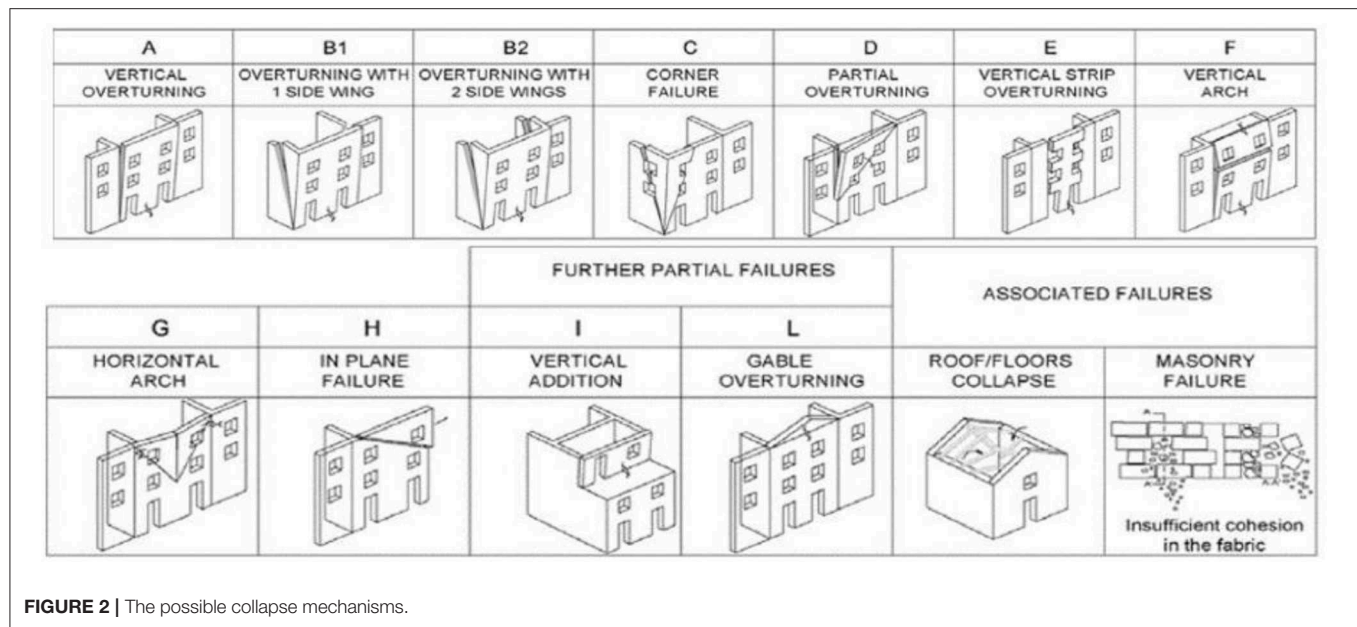
**FIGURE 2 |** The possible collapse mechanisms.

score $R$ increases as the vulnerability $V$ and/or the hazard scoring $H$ increases.

## CASE STUDIES

As previously introduced, in this paper, the vulnerability and the risk assessment of two samples of churches are presented. In particular, the chosen churches are located in two different geographical areas, both struck by recent Italian earthquakes. The first group of churches is located in Teramo, in central Italy, hit by the L'Aquila earthquake in 2009. The second group of churches falls within the Ischia island, in the province of Naples, which was hit by an earthquake in 2017.

### Teramo Churches

Teramo is the provincial capital of the homonymous province, located in the northern area of Abruzzo. It is placed within the Tordino Valley, a hilly area near the Gran Sasso Mountain, which extends toward the coast with a rich vegetation of vineyards and olive groves. It is the third most populous town of the Abruzzo region and has an area of about 10 km². The churches investigated, distributed within the Teramo area as reported in **Figure 3**, are 12 in total and listed as follows, indicating also the city hamlets where they are located:

1. Saint John church (Teramo);
2. Saint Anastasio church (Poggio Cono, hamlet of Teramo);
3. Holy Mary of Carmine church (Cavuccio, hamlet of Teramo);
4. Saint Nicola church (Cavuccio, hamlet of Teramo);
5. Saint Catherine of Alexandria church (Teramo);
6. Saint Luca church (Teramo);

7. Saint Mary de Praediis church (Pantaneto, hamlet of Teramo);
8. Saint Michael Archangel church (Magnanella, hamlet of Teramo);
9. Saint Francis of Assisi church (Villa Romano, hamlet of Teramo);
10. Saint John in Pergulis church (Valle San Giovanni, hamlet of Teramo);
11. Most Holy Salvatore church (Frondarola, hamlet of Teramo);
12. Saint Stephen church (Rapino, hamlet of Teramo).

Some images of the considered churches are reported in **Table 3**. For sake of completeness, the main geometric features of each church are reported in **Table 4**. In this table, the major and minor dimensions and the height of the hall and of the apse (if present) are reported. In addition, information about the presence of the bell tower and its estimated height are given as well.

### Ischia Churches

Ischia is an Italian island belonging to the *Flegree* islands archipelago in the Naples province. The island, which is the largest of the *Flegree* islands, is located in the northern area of the Gulf of Naples and not far from the Procida island in the Tyrrhenian Sea. Ischia is about 18 nautical miles from Naples; it extends 10 and 7 km from east to west and from north to south, respectively, and has a coastline of 34 km and a surface area of about 46.3 km². The island has a volcanic character, formed by several eruptions since about 150,000 years ago. The oldest parts of the island, which dates back to between 147,000 and 100,000 years ago, are recognizable along the southern coastlines. The following 10 churches are considered,
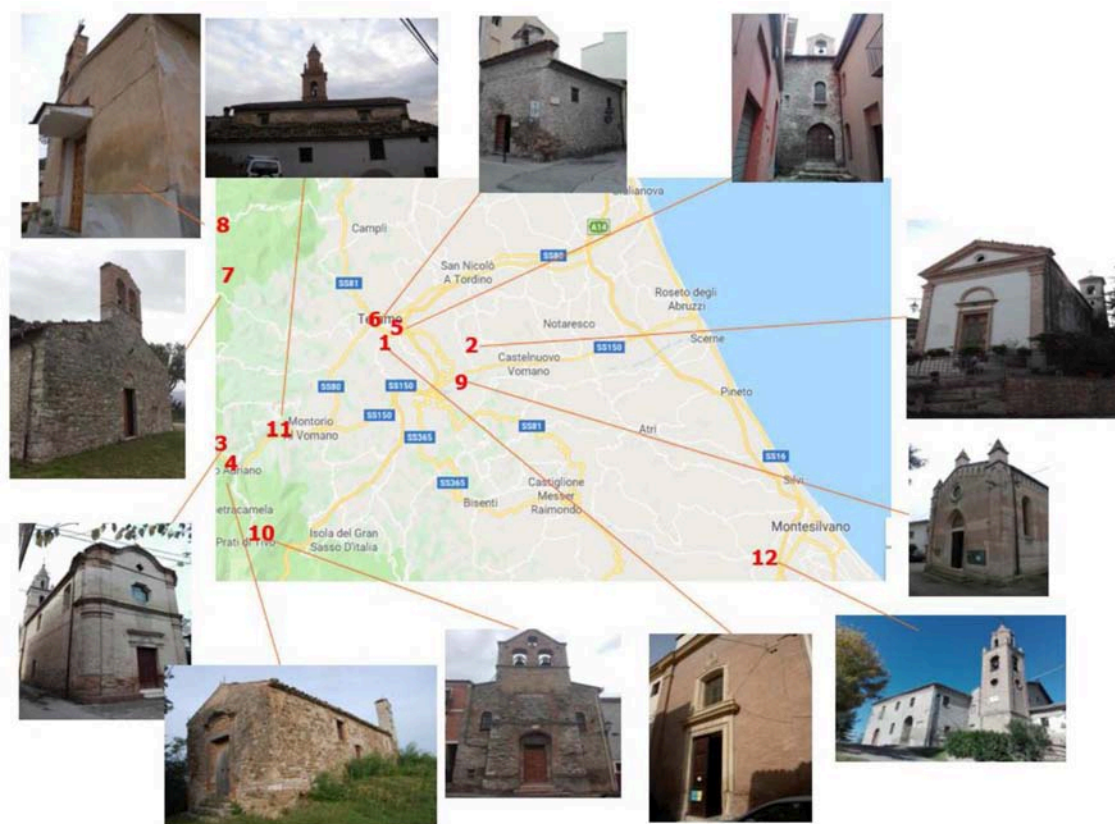
**FIGURE 3 |** Location of investigated churches in the city of Teramo.

located within the municipality indicated within parentheses, as illustrated in **Figure 4**:

1. Saint Francis of Paola church (Forio municipality);
2. Saint Vito church (Forio municipality);
3. Most Holy Annunciation church (Lacco Ameno municipality);
4. Saint Sebastiano church (Barano d'Ischia municipality);
5. Saint Michael Archangel church (Forio municipality);
6. Saint Mary of Loreto church (Forio municipality);
7. Saint Francis of Assisi church (Forio municipality);
8. Most Holy Annunciation coven (Forio municipality);
9. Saint Mary of Soccorso church (Forio municipality);
10. Saint Gaetano church (Forio municipality).

**Table 5** depicts some images of the considered church samples, while the main geometric features of each church are reported in **Table 6**.

## APPLICATION OF THE METHODOLOGY

### Application of *Tool 2*

From the analysis of all the collected information related to sporadic and continuous events [described in the section *Hazard Scoring (H)*], it has been possible to qualitatively evaluate

the potential damage severity that could affect the examined churches. The evaluations are numerically reported in **Table 7**, where the damage assigned for each event is in bold and underlined. One can easily note that the investigated area of Ischia has a hazard score $H$ greater than that of Teramo. This is due to the fact that, in the island, the potential threats that could produce damages are greater than those in the Teramo area.
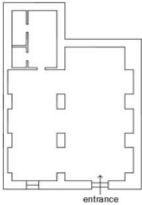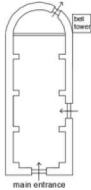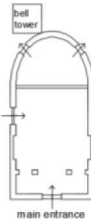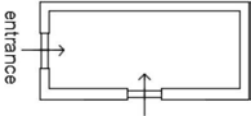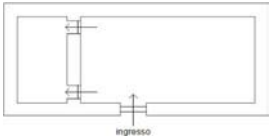
### Application of *Tool 3*

In order to apply the analysis with *Tool 3*, it has been necessary to carry out physical observations and detailed historical researches for each considered church, with the aim of acquiring as much information as possible. **Table 8** and **Figure 5** summarize the evaluation of the seismic risk score for the churches studied. In particular, in **Table 8**, the $R$ score is evaluated in accordance with the proposed (Equation 3), while in the **Figure 5**, a comparison between vulnerability and seismic risk score for each church is represented in the form of a histogram.

**Table 9** shows, for the Teramo and Ischia samples, the number of churches falling into each class (from $A$ to $D$) for a given vulnerability parameter. In this way, the distribution of the classes may be observed.

In the Teramo churches, there is a prevailing class for some of the vulnerability parameters, such as *position of the building*

**TABLE 3 |** Geometrical features of churches investigated in Teramo.

| Church name | External view | Internal view | Plan |
|---|---|---|---|
| 1. Saint Giovanni |  |  |  |
| 2. Saint Anastasio |  |  |  |
| 3. Holy Mary of Carmine |  |  |  |
| 4. Saint Nicola |  | |  |
| 5. Saint Catherine of Alexandria |  |  |  |
| 6. Saint Luca |  |  |  |

*(Continued)*

| Church name | External view | Internal view | Plan |
|---|---|---|---|
| 7. Saint Mary de Praediis | | | |
| 8. Saint Michael Archangel | | | |
| 9. Saint Francis of Assisi | | | |
| 10. Saint John in Pergulis | | | |
| 11. Most Holy Salvatore | | | |
| 12. Saint Stephen | | | |

**TABLE 4 |** Geometrical features of churches investigated in Teramo.

| Church | Hall | | | Apse | | | Bell Tower | |
|---|---|---|---|---|---|---|---|---|
| | Major side [m] | Minor side [m] | Average height [m] | Major side [m] | Minor side [m] | Average height [m] | Yes/no | Estimated height [m] |
| 1. Saint John | 16.50 | 14.30 | 10.00 | | – | | No | – |
| 2. Saint Anastasio | 14.70 | 7.20 | 6.70 | 7.50 | 3.50 | 7.15 | Yes | 10.00 |
| 3. Holy Mary of Carmine | 11.30 | 6.20 | 7.20 | 6.45 | 5.00 | 7.00 | Yes | 15.00 |
| 4. Saint Nicola | 11.00 | 4.60 | 3.50 | | – | | No | – |
| 5. Saint Catherine | 13.40 | 6.50 | 7.50 | | – | | No | – |
| 6. Saint Luca | 8.00 | 4.00 | 6.00 | | – | | No | – |
| 7. Saint Mary de Praediis | 14.50 | 9.00 | 5.00 | 3.00 | 1.50 | 5.00 | No | – |
| 8. Saint Michael Archangel | 16.20 | 5.30 | 5.00 | | – | | No | – |
| 9. Saint Francis of Assisi | 11.40 | 7.00 | 7.80 | 5.85 | 5.80 | 6.00 | Yes | 13.00 |
| 10. Saint John in Pergulis | 14.90 | 9.30 | 8.00 | | – | | Yes | 12.90 |
| 11. Most Holy Salvatore | 10.70 | 7.20 | 8.00 | | – | | Yes | 18.00 |
| 12. Saint Stephen | 14.40 | 5.25 | 5.85 | 3.40 | 5.25 | 3.50 | Yes | 15.00 |



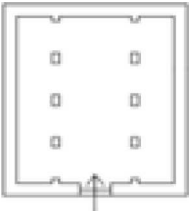**FIGURE 4 |** Location of churches investigated in the island of Ischia.
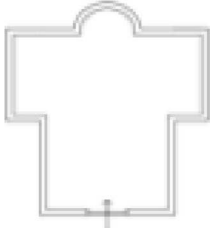
*and foundation* (no. 1), *non-structural elements* (no. 5), *resistant system type and organization* (no. 6), *floors* (no. 8), and *fire vulnerability* (no. 12).

On the other hand, in the Ischia church samples, a prevailing class for each parameter is observed in almost all cases, with the exception of the parameter *distance among walls* (no. 4), where classes *A* and *B* have been assigned to the same number of churches.

Finally, by observing the obtained results, the following considerations can be remarked:
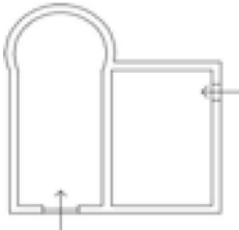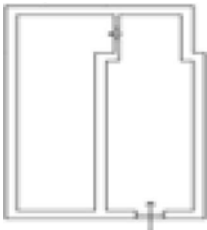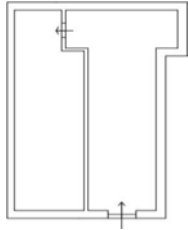
1. Class A of the parameter *position of the building and foundations* (no. 1) has been assigned to almost all the churches, since they are located on loose ground with a slope not higher than 10% and with discrete geotechnical properties. However, it has not been possible to detect the in-elevation differences of the foundations due to the absence of appropriate geological analyses;
2. Class *D* of the parameter *floors* (no. 8) has been attributed to all churches since rigid floors have never been observed;

**TABLE 5 |** Geometrical features of churches investigated in Ischia.

| Church name | External view | Internal view | Plan |
|---|---|---|---|
| 1. Saint Francis of Paola |  |  |  |
| 2. Saint Vito |  |  |  |
| 3. Most Holy Annunciation |  |  |  |
| 4. Saint Sebastiano |  |  |  |
| 5. Saint Michael Archangel |  |  |  |
| 6. Saint Mary of Lorero |  |  |  |

*(Continued)*

**TABLE 5 |** Continued

| Church name | External view | Internal view | Plan |
|---|---|---|---|
| 7. Saint Francis of Assisi |  |  |  |
| 8. Most Holy Annunciation |  |  |  |
| 9. Saint Mary of Soccorso |  |  |  |
| 10. Saint Gaetano |  |  |  |

3. It has not been possible to give objective judgments on the connection quality among orthogonal walls and between walls and horizontal structures because of the presence of frescos and decorations. However, the experience suggests neglecting a good level of connection among walls because, in the past, orthogonal walls were generally simply juxtaposed to each other, showing in most of the cases overturning mechanisms, especially in the façade elements;

4. Almost all roofs are made of timber elements that have, depending on the case, pushing or no-pushing structures. In general, it is rare to find edge beams with the exception of those where the roof was built in recent times. Even the presence of metal tie rods is quite rare: they are absent in the majority of cases;

5. The churches located in Teramo have a vulnerability index ranging from 21.22 to 66.32, with an average value of 45.68;

6. The churches located in Ischia have a vulnerability index ranging from 25.93 to 46.46, with an average value of 30.13;

7. The Ischia island hazard index ($H = 1.31$) is greater than that of Teramo ($H = 0.78$).

In order to determine the church sample and, consequently, the geographical area that are subjected to the highest seismic risk, in this paper, a new territorial seismic risk index $\rho$ is proposed as follows:

$$\rho = \sum S_j R_j / \sum S_j \qquad (4)$$

where $S_j$ is the $j$th church area, $R_j$ is the $j$th church seismic risk index, and $\Sigma S_j$ is the total area of investigated churches. Precisely, in the two geographical areas analyzed, the $\rho$ index is equal to 63.13 for Teramo churches and to 67.47 in the case of Ischia churches. The higher $\rho$ value in the case of Ischia churches is probably due to their higher vulnerability with respect to Teramo churches.

**TABLE 6 |** Geometrical features of churches investigated in Ischia.

| Church | Hall | | | Apse | | | Bell tower | |
|---|---|---|---|---|---|---|---|---|
| | Major side [m] | Minor side [m] | Average height [m] | Major side [m] | Minor side [m] | Average height [m] | Yes/no | Estimated height [m] |
| 1. Saint Francis of Paola | 19.50 | 3.30 | 7.00 | 3.40 | 3.30 | 8.50 | Yes | 18.00 |
| 2. Saint Vito | 22.00 | 4.80 | 7.10 | 4.80 | 2.80 | 10.00 | Yes | 27.00 |
| 3. Most Holy Annunciation | 6.50 | 3.90 | 6.55 | 4.80 | 4.00 | 6.55 | No | – |
| 4. Saint Sebastiano | 17.30 | 6.30 | 12.30 | 6.30 | 4.60 | 8.00 | Yes | 17.00 |
| 5. Saint Michael Archangel | 8.60 | 5.20 | 8.00 | 5.20 | 4.70 | 8.00 | No | – |
| 6. Saint Mary of Loreto | 30.00 | 5.80 | 11.00 | 8.15 | 5.80 | 10.00 | Yes | 17.00 |
| 7. Saint Francis of Assisi | 21.00 | 8.40 | 10.00 | 9.00 | 6.80 | 12.00 | No | – |
| 8. Most Holy Annunciation coven | 11.00 | 5.60 | 7.00 | 6.00 | 5.50 | 7.40 | Yes | 15.00 |
| 9. Saint Mary of Soccorso | 14.80 | 6.80 | 7.50 | 4.60 | 4.10 | 8.50 | Yes | 12.00 |
| 10. Saint Gaetano | 17.00 | 5.80 | 13.70 | 4.70 | 1.70 | 7.15 | No | – |

**TABLE 7 |** Scenarios description and classification of threats for church samples.

| | | | Damage gravity | | |
|---|---|---|---|---|---|
| | | Parameters | Absence of damage | Middle damage | Catastrophic damage |
| Churches located in the Teramo area | Sporadic Events | Earthquake and tsunami threat | 0 | 0.2 | 0.4 |
| | | Landslides | 0 | 0.15 | 0.25 |
| | | Volcanic threat | 0 | 0.2 | 0.4 |
| | | Hydro-methodological threat | 0 | 0.15 | 0.25 |
| | | Chemical–technological threat | 0 | 0.15 | 0.25 |
| | | Forest fires | 0 | 0.15 | 0.25 |
| | Continuous Events | Erosion threat | 0 | 0.05 | 0.1 |
| | | Physical stress of threat | 0 | 0.05 | 0.1 |
| | | Air pollution | 0 | 0.01 | 0.05 |
| | | Socio-organizational threat | 0 | 0.01 | 0.05 |
| | | Demographic decline | 0 | 0.01 | 0.05 |
| | | *Resulting Hazard score* | | *H = 0.78* | |
| Churches located in the Ischia area | Sporadic Events | Earthquake and tsunami threat | 0 | 0.2 | 0.4 |
| | | Landslides | 0 | 0.15 | 0.25 |
| | | Volcanic threat | 0 | 0.2 | 0.4 |
| | | Hydro-methodological threat | 0 | 0.15 | 0.25 |
| | | Chemical–technological threat | 0 | 0.15 | 0.25 |
| | | Forest fires | 0 | 0.15 | 0.25 |
| | Continuous Events | Erosion threat | 0 | 0.05 | 0.1 |
| | | Physical stress of threat | 0 | 0.05 | 0.1 |
| | | Air pollution | 0 | 0.01 | 0.05 |
| | | Socio-organizational threat | 0 | 0.01 | 0.05 |
| | | Demographic decline | 0 | 0.01 | 0.05 |
| | | *Resulting Hazard score* | | *H = 1.31* | |

# CONCLUSIONS

In this paper, a simplified method recently developed and validated for ancient masonry churches has been applied to case studies. The proposed method separately evaluates hazard ($H$) and vulnerability ($V$) in order to assess the seismic risk at a territorial scale. The method is a very useful tool because it quickly provides a territorial preliminary ranking for screening the intervention priorities and for considering different earthquake scenarios as well. The method is also versatile for comparing seismic risk evaluations performed in different geographical areas.

The case studies examined involved two samples of churches located in Teramo and in the Ischia island in the gulf

**TABLE 8 |** Seismic risk evaluation.

|  | Churches | Hazard, *H* | Vulnerability, *V* | Seismic risk, *R* |
|---|---|---|---|---|
| Churches located in the Teramo area | 1. St. John | 0.78 | 21.22 | 37.78 |
|  | 2. St. Anastasio |  | 51.52 | 91.70 |
|  | 3. Holy Mary of Carmine |  | 31.32 | 55.74 |
|  | 4. St. Nicola |  | 53.18 | 94.67 |
|  | 5. St. Catherine of Alexandria |  | 66.32 | 118.05 |
|  | 6. St. Luca |  | 22.23 | 39.57 |
|  | 7. St. Mary de Praediis |  | 39.06 | 69.53 |
|  | 8. St. Michael Archangel |  | 37.37 | 66.53 |
|  | 9. St. Francis of Assisi |  | 22.23 | 39.58 |
|  | 10. St. John in Pergulis |  | 28.96 | 51.55 |
|  | 11. Most Holy Salvatore |  | 45.44 | 80.89 |
|  | 12. St. Stephen |  | 30.64 | 54.54 |
| Churches located in the Ischia area | 1. St. Francis of Paola | 1.31 | 25.93 | 59.90 |
|  | 2. St. Vito |  | 25.93 | 59.90 |
|  | 3. Most Holy Annunciation |  | 38.64 | 89.26 |
|  | 4. St. Sebastiano |  | 34.33 | 79.30 |
|  | 5. St. Michael Archangel |  | 46.46 | 107.32 |
|  | 6. St. Mary of Loreto |  | 32.66 | 75.44 |
|  | 7. St. Francis of Assisi |  | 24.25 | 56.02 |
|  | 8. Most Holy Annunciation coven |  | 21.56 | 49.80 |
|  | 9. St. Mary of Soccorso |  | 23.24 | 53.68 |
|  | 10. St. Gaetano |  | 32.33 | 74.68 |



**FIGURE 5 |** Vulnerability (*V*) and the resulting seismic risk (*R*) scores.
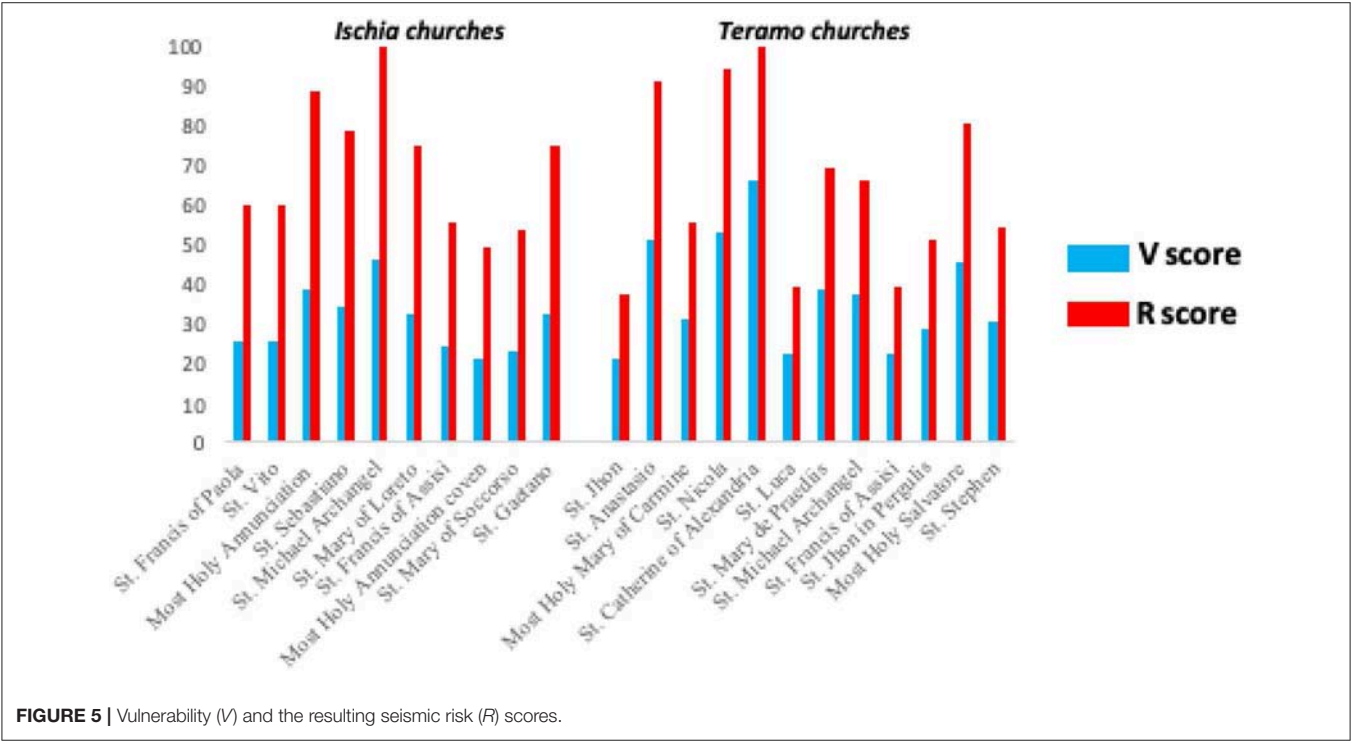
of Naples, both affected by recent seismic events. The territories of churches have many features in common, but there are some differences modifying the vulnerability index calculations. In particular, the analysis of results shows that all the churches of Teramo have a medium vulnerability index. The most vulnerable church is the Saint Catherine of Alexandria, which is, in fact, actually unusable. Even the Ischia churches have a medium vulnerability index, with

TABLE 9 | Distribution of parameter classes for Teramo churches.

| Parameters | | Teramo churches | | | | Ischia churches | | | |
|---|---|---|---|---|---|---|---|---|---|
| | | Classes | | | | Classes | | | |
| | | A | D | C | D | A | D | C | D |
| 1 | Position of the building and foundations | 11 | – | 1 | – | 10 | – | – | – |
| 2 | In-plane configuration | – | 2 | 6 | 4 | 1 | 2 | 5 | 2 |
| 3 | In-elevation configuration | 5 | 4 | 3 | – | 9 | 1 | – | – |
| 4 | Distance among walls | 5 | 6 | 1 | – | 5 | 5 | – | – |
| 5 | Non-structural elements | 7 | 1 | 1 | 3 | 1 | 2 | 6 | 2 |
| 6 | Resistant system type and organization | – | 8 | 2 | 2 | – | 9 | 1 | – |
| 7 | Resistant system quality | – | 6 | 5 | 1 | – | 9 | 1 | – |
| 8 | Floors | – | – | – | 12 | – | – | – | 10 |
| 9 | Roofs | 1 | 6 | – | 5 | – | 7 | 2 | 1 |
| 10 | Conservation state | – | 7 | 3 | 2 | – | 3 | 6 | 1 |
| 11 | Environmental alterations | 5 | 7 | – | – | – | 10 | – | – |
| 12 | Construction system | 6 | 1 | 5 | – | 7 | – | 2 | 1 |
| 13 | Fire vulnerability | – | 12 | – | – | – | 10 | – | – |

the highest value found in the case of the Saint Michael Archangel church.

Finally, it has been possible to estimate the vulnerability of inspected church areas by means of a new territorial seismic risk index ρ, which depends on the territory area covered by the churches and on their seismic risk index $R$. This new introduced index, useful for territorial comparisons, may be applied for globally evaluating the seismic risk of a certain area, representing a unique parameter taking into account all the constructions built and the related seismic risk scores.

## DATA AVAILABILITY

All datasets generated or analyzed for this study are included in the manuscript.

## AUTHOR CONTRIBUTIONS

All authors listed have made a substantial, direct and intellectual contribution to the work, and approved it for publication.

## REFERENCES

Benedetti, D., and Petrini, V. (1984). On the seismic vulnerability of masonry buildings: an assessment method (in Italian). *L'industria delle Costruzioni* 149, 66–74.

Betti, M., Borghini, A., Boschi, S., Ciavattone, A., and Vignoli, A. (2018). Comparative seismic risk assessment of basilica-type churches. *J. Earthq. Eng.* 22, 62–95. doi: 10.1080/13632469.2017.1309602

Betti, M., and Vignoli, M. (2011). Numerical assessment of the static and seismic behaviour of the basilica of Santa Maria all'Impruneta (Italy). *Constr. Build. Mater.* 25, 4308–4324. doi: 10.1016/j.conbuildmat.2010.12.028

Cecchi, R., and Calvi, M. (2010). "Guidelines for evaluation and mitigation of seismic risk to cultural heritage with reference to technical standard for construction (In Italian)," in *Ministry for Cultural Heritage and Activities*, ed G. Gangemi (Rome: Department of Civil Protection Agency).

Clementi, F., Gazzani, V., Poiani, M., Mezzapelle, P. A., and Lenci, S. (2017a). Seismic assessment of a monumental building through nonlinear analyses of a 3D solid model. *J. Earthq. Eng.* 22, 35–61. doi: 10.1080/13632469.2017.1297268

Clementi, F., Pierdicca, A., Formisano, A., Catinari, F., and Lenci, S. (2017b). Numerical model upgrading of a historical masonry building damaged during the 2016 Italian earthquakes: the case study of the Podestà palace in Montelupone (Italy). *J. Civil Struct. Health Monit.* 7, 703–717. doi: 10.1007/s13349-017-0253-4

D'Amato, M., Gigliotti, R., and Laguardia, R. (2019). Comparative seismic assessment of ancient masonry churches. *Front. Built Environ.* 5:56. doi: 10.3389/fbuil.2019.00056

D'Amato, M., Laterza, M., and Casamassima, V. M. (2017). Seismic performance evaluation of a multi-span existing masonry arch bridge. *Open Constr. Build. Technol. J.* 11, 1191–1207. doi: 10.2174/1874149501711011191

D'Amato, M., Laterza, M., and Diaz Fuentes, D. (2018). Simplified seismic analyses of ancient churches in Matera's landscape. *Int. J. Archit. Herit.* doi: 10.1080/15583058.2018.1511000

De Matteis, G., Brando, G., and Corlito, V. (2019). Predictive model for seismic vulnerability assessment of churches based on the 2009 L'Aquila earthquake. *Bull. Earthq. Eng.* 17, 4909–3. doi: 10.1007/s10518-019-00656-7

Dìaz Fuentes, D. A. (2016). *Diseño de herramientas de Evaluación del Riesgo Para la Conservación del Patrimonio Cultural Inmueble: Aplicación en dos Casos de Estudio del Norte Andino Chileno (in Spanish)*. Mexico: Publicaciones Digitales ENCRYM – INAH.

Directive of the Italian Prime Minister (2011). *Directive of the Prime Minister Dated on 09/ 02/2011*. Assessment and mitigation of seismic risk of cultural heritage with reference to the technical code for the design of construction, issued by D. M. 14/ 01/2008 (in Italian).

Faggiano, B., Marzo, A., Formisano, A., and Mazzolani, F. M. (2009). Innovative steel connections for the retrofit of timber floors in ancient buildings: a numerical investigation. *Comput. Struct.* 87, 1–13. doi: 10.1016/j.compstruc.2008.07.005

Feilden, B. (1987). *Between Two Earthquakes: Cultural Property in Seismic Zones*. Roma: ICCROM/Getty Conservation Institute.

FEMA (2004). *Primer for design professionals (FEMA 389)*. Washington, DC: Department of Homeland Security Emergency Preparedness and Response Directorate.

Fonti, R., Borri, A., Barthel, R., Candela, M., and Formisano, A. (2017). Rubble masonry response under cyclic actions: experimental tests and theoretical models. *Int. J. Mason. Res. Innov.* 2, 30–60. doi: 10.1504/IJMRI.2017.082391

Formisano, A. (2017). Local- and global-scale seismic analyses of historical masonry compounds in San Pio delle Camere (L'Aquila, Italy). *Nat. Hazards* 86, 465–487. doi: 10.1007/s11069-016-2694-1

Formisano, A., Ciccone, G., and Mele, A. (2017). Large scale seismic vulnerability and risk evaluation of a masonry churches sample in the historical centre of Naples. *AIP Conf. Proc.* 1906:090003. doi: 10.1063/1.5012360

Formisano, A., Di Feo, P., Grippa, M. R., and Florio, G. (2010). "L'Aquila earthquake: a survey in the historical centre of Castelvecchio Subequo," in *COST ACTION C26: Urban Habitat Constructions under Catastrophic Events - Proceedings of the Final Conference* (Naples), 371–376.

Formisano, A., and Marzo, A. (2017). Simplified and refined methods for seismic vulnerability assessment and retrofitting of an Italian cultural heritage masonry building. *Comput. Struct.* 180, 13–26. doi: 10.1016/j.compstruc.2016.07.005

Formisano, A., Vaiano, G., Fabbrocino, F., and Milani, G. (2018). Seismic vulnerability of Italian masonry churches: the case of the Nativity of Blessed Virgin Mary in Stellata of Bondeno. *J. Build. Eng.* 20, 179–200. doi: 10.1016/j.jobe.2018.07.017

Fuentes, D. D., Baquedano, J. P. A., D'Amato, M., and Laterza, M. (2019b). Preliminary seismic damage assessment of Mexican churches after September 2017 earthquakes. *Int. J. Archit. Herit.* doi: 10.1080/15583058.2019.1628323

Fuentes, D. D., Laterza, M., and D'Amato, M. (2019a). "Seismic vulnerability and risk assessment of historic constructions: the case of masonry and adobe churches in Italy and Chile (2019) RILEM Bookseries, 18," in *11th International Conference on Structural Analysis of Historical Constructions* (Cusco), 1127–1137. doi: 10.1007/978-3-319-99441-3_122

Gattulli, V., Antonacci, E., and Vestroni, F. (2014). Field observations and failure analysis of the Basilica S. Maria di Collemaggio after the 2009 L'Aquila earthquake. *Eng. Fail. Anal.* 34, 715–734. doi: 10.1016/j.engfailanal.2013.01.020

GNDT (1994). *(National Group for Earthquakes Defense) First and Second Level Form for Exposure, Vulnerability and Damage Survey (Masonry and Reinforced Concrete)* (in Italian). Rome: GNDT.

ICOMOS (2008). *Charter on the Interpretation and Presentation of Cultural Heritage Sites*.

INAH (2013). *Programa de Prevención de Desastres en Materia de Patrimonio Cultural*. México.

Krstevska, L., Tashkov, L., Naumovski, N., Florio, G., Formisano, A., Fornaro, A., et al. (2010). "*In-situ* experimental testing of four historical buildings damaged during the 2009 L'Aquila earthquake," in *COST ACTION C26: Urban Habitat Constructions under Catastrophic Events - Proceedings of the Final Conference* (Naples), 427–432.

Lagomarsino, S., and Podestà, S. (2004). Seismic vulnerability of ancient churches: II. Statistical analysis of surveyed data and methods for risk analysis. *Earthq. Spectra* 20, 395–412. doi: 10.1193/1.1737736

Laterza, M., D'Amato, M., and Casamassima, V. M. (2017). "Seismic performance evaluation of multi-span existing masonry arch bridge," in *Proceedings of the 14th International Conference of Numerical Analysis and Applied Mathematics - ICNAAM 2016 AIP Conference Proceedings* (Rhodes), 1863:art. no. 450010. doi: 10.1063/1.4992619

Leite, J., Lourenco, P. B., and Ingham, J. M. (2013). Statistical assessment of damage to churches affected by the 2010–2011 Canterbury (New Zealand) earthquake sequence. *J. Earthq. Eng.* 17, 73–97. doi: 10.1080/13632469.2012.713562

Lopez, S., D'Amato, M., Ramos, L., Laterza, M., and Lourenço, P. B. (2019). Simplified formulation for estimating the main frequencies of ancient masonry churches. *Front. Built Environ.* 5:18. doi: 10.3389/fbuil.2019.00018

Lourenço, P. B., Oliveira, D. V., Leite, J. C., Ingham, J. M., Modena, C., and Da Porto, F. (2013). Simplified indexes for the seismic assessment of masonry buildings: International database and validation. *Eng. Fail. Anal.* 34, 585–605. doi: 10.1016/j.engfailanal.2013.02.014

Lourenço, P. B., and Roque, J. A. (2006). Simplified indexes for the seismic vulnerability of ancient masonry buildings. *Constr. Build. Mater.* 20, 200–208. doi: 10.1016/j.conbuildmat.2005.08.027

Luchin, G., Ramos, L. F., and D'Amato, M. (2018). Sonic tomography for masonry walls characterization. *Int. J. Archit. Herit.* doi: 10.1080/15583058.2018.1554723

Milani, G., Shehu, R., and Valente, M. (2017a). Role of inclination in the seismic vulnerability of bell towers: FE models and simplified approaches. *Bull. Earthq. Eng.* 15, 1707–1737. doi: 10.1007/s10518-016-0043-0

Milani, G., Shehu, R., and Valente, M. (2017b). Possibilities and limitations of innovative retrofitting for masonry churches: advanced computations on three case studies. *Constr. Build. Mater.* 147, 239–263. doi: 10.1016/j.conbuildmat.2017.04.075

Milani, G., Shehu, R., and Valente, M. (2018). A kinematic limit analysis approach for seismic retrofitting of masonry towers through steel tie-rods. *Eng. Struct.* 160, 212–228. doi: 10.1016/j.engstruct.2018.01.033

Milani, G., and Valente, M. (2015a). Failure analysis of seven masonry churches severely damaged during the 2012 Emilia-Romagna (Italy) earthquake: non-linear dynamic analyses vs conventional static approaches. *Eng. Fail. Anal.* 54, 13–56. doi: 10.1016/j.engfailanal.2015.03.016

Milani, G., and Valente, M. (2015b). Comparative pushover and limit analyses on seven masonry churches damaged by the 2012 Emilia-Romagna (Italy) seismic events: possibilities of non-linear finite elements compared with pre-assigned failure mechanisms. *Eng. Fail. Anal.* 47, 129–161. doi: 10.1016/j.engfailanal.2014.09.016

Ministry of Infrastructures and Transports (2008a). *Ministerial Decree 14 January 2008 "Technical codes for constructions"* (in Italian). Official Gazette n. 29.

Ministry of Infrastructures and Transports (2008b). *Ministerial Circular 2 February 2008 n. 617 "Instructions for the Application of New Technical Codes for Constructions"* (in Italian). Official Gazette n. 47.

Ministry of Infrastructures and Transports (2018). *Ministerial Decree 17 January 2018, Updating of Technical Codes for Constructions* (in Italian). Official Gazette n. 42 of 20/02/18, Ordinary Supplement n. 8.

Penna, A., Calderini, C., Sorrentino, L., Carocci, C. F., Cescatti, E., Sisti, R., et al. (2019). Damage to churches in the 2016 central Italy earthquakes. *Bull. Earthq. Eng.* 1–28. doi: 10.1007/s10518-019-00594-4

Ramirez, E., Lourenco, P. B., and D'Amato, M. (2019). "Seismic assessment of the Matera Cathedral. SAHC 2018," in *11th International Conference on Structural Analysis of Historical Constructions* (Cusco: RILEM Bookseries), 1346–1354. doi: 10.1007/978-3-319-99441-3_144

Stockdale, G. (2016). Reinforced stability-based design: a theoretical introduction through a mechanically reinforced masonry arch. *Int. J. Mason. Res. Innov.* 1, 101–141. doi: 10.1504/IJMRI.2016.077469

Stovel, H. (1998). *Risk Preparedness: A Management Manual for World Cultural Heritage*. Roma: ICCROM/ UNESCO, WHC/ICOMOS.

Terracciano, G., Di Lorenzo, G., Formisano, A., and Landolfo, R. (2015). Cold-formed thin-walled steel structures as vertical addition and energetic retrofitting systems of existing masonry buildings. *Eur. J. Environ. Civ. Eng.* 19, 850–866. doi: 10.1080/19648189.2014.974832

UNDRO (1979). *Natural Disasters Vulnerability Analysis*. United Nations Disaster Relief Organisation.

UNESCO World Heritage Centre (2002). *Managing Tourism at World Heritage Sites: A Practical Manual for World Heritage Site Managers*.

UNESCO/ICCROM/ICOMOS/IUCN (2010). *Managing Disaster Risks for World Heritage*.

UNISDR (2009). *Terminology on Disaster Risk Reduction*. Ginevra: UNISDR.

Valente, M., Barbieri, G., and Biolzi, L. (2016). Damage assessment of three medieval churches after the 2012 Emilia earthquake. *Bull. Earthq. Eng.* 15, 2939–2980. doi: 10.1007/s10518-016-0073-7

Valente, M., Barbieri, G., and Biolzi, L. (2017). Seismic assessment of two masonry Baroque churches damaged by the 2012 Emilia

earthquake. *Eng. Fail. Anal.* 79, 773–802. doi: 10.1016/j.engfailanal.2017.05.026

Valente, M., and Milani, G. (2018a). Effects of geometrical features on the seismic response of historical masonry towers. *J. Earthq. Eng.* 22, 2–34. doi: 10.1080/13632469.2016.1277438

Valente, M., and Milani, G. (2018b). Damage assessment and partial failure mechanisms activation of historical masonry churches under seismic actions: three case studies in Mantua. *Eng. Fail. Anal.* 92, 495–519. doi: 10.1016/j.engfailanal.2018.06.017

Valente, M., and Milani, G. (2018c). Damage survey, simplified assessment, and advanced seismic analyses of two masonry churches after 2012 Emilia earthquake. *J. Archit. Herit.* 13, 901–924. doi: 10.1080/15583058.2018.1492646

# Assessment and Restoration of an Earthquake-Damaged Historical Masonry Building

Chrysanthos Maraveas [1,2*]

[1] Department of Civil Engineering, University of Patras, Patras, Greece, [2] C. Maraveas and Associates P.C. – Consulting Engineers, Athens, Greece

This paper presents an assessment of the capacity and enhancement of the seismic performance of a historical masonry structure in Plomari, a town on the south coast of Lesbos island in Greece. Owing to uncertainties regarding the properties of the material and the effectiveness of the members in providing lateral resistance, the study was particularly challenging. In addition, the fact that the structure consisted of a variety of structural element types, e.g., unreinforced masonry from natural stones, timber-framed masonry (with burned clay masonry units), and timber girders, while lacking horizontal diaphragms, introduced complexities to the response of the structure in both directions. In the design of the retrofit, the need to preserve the building's architectural and historical value by minimizing interventions posed several problems. To solve them, conventional as well as state-of-the-art strengthening methods are proposed. Moreover, the procedures of these methods are in accordance with the Greek seismic design code of 1959 and European standards (Eurocodes) related to earthquake-resistant masonry as well as guidelines for the design of timber and reinforced concrete. Seismic analyses of the structure were carried out with two different methods (statically applied load and time history analysis) for comparison. The results verify the improvement in its behavior in response to earthquakes as a result of the proposed strengthening methods.

Keywords: historical structures, masonry, earthquake resistance, strengthening, restoration, retrofit, rigid diaphragm

## INTRODUCTION

Assessment of the seismic performance of historical buildings is an important subject owing to the risk of casualties as well as the potential impact on culture and the economy in case of a global or partial collapse. Therefore, to preserve such structures, the prevention of extended damage during earthquakes is necessary. State-of-the-art assessment methods of historic buildings can be found in the literature. More specifically Boscato et al. (2010) employed dynamic monitoring in order to assess the structural behavior of Rialto Bridge in Venice. Moreover, advanced assessment techniques like ground penetrating radar and endoscopic test were employed by Boscato et al. (2014) and Sciarretta et al. (2018) and in order to investigate the medieval façades of Palazzo Ducale in Venice.

The building examined in this study was built in the first half of the nineteenth century. It is a traditional mansion that is an exemplar of Greek heritage, and has been declared a protected monument—building (listed as protected—heritage structure) by the Greek Government.

Similarly, as emphasized in previous studies of the restoration of traditional buildings (Maraveas et al., 2015), the preservation of the traditional architectural characteristics is of paramount importance in these projects. All retrofitting solutions thus need to ensure the preservation of the external and internal appearance of the building.

This study proposes the structural restoration of the historical masonry structure described above. First, a reliable assessment of its load-carrying capacity is performed and used to create a finite element model with the aid of the Robot Structural Analysis software (Autodesk Robot Structural Analysis Professional, 2016) in order to assess static and seismic demands on the various elements of the structure. Furthermore, a realistic simulation of the mechanical properties is crucial for minimizing uncertainties in the properties of the material. Accurate modeling of the geometry of the building and the analyses employed led to the identification of structural deficiencies. More importantly, the results of analyses of the simulated damage were compared with the actual damage recorded on a visit to the site. Strengthening solutions based on non-destructive methods are proposed. Finally, the effectiveness of these solutions is evaluated.

Scope of this study is to show the effectiveness of rigid diaphragms on the improvement of the performance of masonry structures under earthquake loading for various safety levels. Furthermore, this study shows that simplified linear analysis can give realistic—even conservative—results and advanced analysis methods (Syrmakezis et al., 1995; Asteris et al., 2005; Kyriakides et al., 2016, 2018; Caddemi et al., 2017; Casamassima and D'Amato, 2019), as well as advanced material models (Asteris et al., 2005, 2014; Asteris and Giannopoulos, 2012; Apostolopoulou et al., 2017) are not always needed, as they require extensive experimental investigations (Chronopoulos et al., 2012; Lysandrou et al., 2017) and time consuming analysis validation (Asteris et al., 2017, 2019).

## THE JUNE 2017 EARTHQUAKE IN LESVOS ISLAND, GREECE

An earthquake measuring 6.3 on the Richter scale struck under the sea between the islands of Lesbos and Chios in the East Aegean Sea on June 12, 2017, with tremors felt as far as Istanbul and Athens (BBC website, 2017). The epicenter of the earthquake was 5 km south of Plomari and had a focal depth of 10 km. Several buildings were damaged by the earthquake; in addition, the major road from the island's capital, Mytilene, to Plomari was damaged by a landslide. In the village of Vrisa, ~25 km northeast of Plomari, 10 people were taken to hospital with injuries due to the earthquake. **Figure 1** (Lekkas et al., 2017) shows several buildings in Plomari that were severely damaged under the induced seismic loads.

## DESCRIPTION OF GEOMETRY

The building studied covered an area of ~160 m$^2$, and had a rectangular layout with approximate dimensions of 18.5 × 8.5 m; therefore, the walls along one of the main directions were nearly two times longer than those in the other main direction. Therefore, lateral stiffness and mass were not symmetrically distributed. The building had three floors with heights of 2.9, 5.75, and 4.7 m with a roof 1.4 m high. Owing to the architectural requirement of daylighting, each wall consisted of several large openings with dimensions of 1.2–1.5 × 1.2–4.2 m, occupying ~45% of the surface of each wall. This, of course, reduced the strength of the walls. Their thickness varied from 0.50 m at the top to 0.80 m at the base. Photographs of the exterior of the building (façade) are shown in **Figures 2A,B** while a typical plan of the building is presented in **Figure 2C**.

## PROPERTIES OF MATERIAL AND STRUCTURAL BEHAVIOR

### Material Properties

As is the case for most historical structures, sufficient information on the properties of the materials of the present masonry building was not available. Hence, tests were conducted by the contractor on samples taken from different locations of the building to assess the mechanical properties of the materials. More specifically, as shown in **Figure 3A**, six cylindrical masonry samples (see **Figures 3B,C**) were extracted from different locations and levels of the building which were then taken to the lab and subjected to monoaxial compression test. Three of these samples were also employed in order to estimate the compressive strength of the mortar. In addition to the laboratory tests, 12 Schmidt hammer tests were performed (their locations was not recorded) as well as four ultrasonic tests with their location presented in **Figure 3A**. A similar approach was used by Maraveas and Tasiouli (2015). Six core samples were extracted from various locations of the building's ground floor.

The results of the aforementioned tests are summarized in **Table 1** accompanied with the calculation of the average value and standard deviation of each testing. Specifically, the normalized mean compressive strength of the units in the direction of the applied action, $f_b$, and the compressive strength of the mortar, $f_m$, were defined as 43 and 1.19 MPa, respectively. Once these two properties have been obtained, the characteristic compressive strength, $f_k$ and shear strength of masonry, $f_{vk0}$ can be easily calculated through equations provided in EN 1996-1-1 (2005).

Note that the tests characterized the mortar as weak. However, it should be mentioned that in some cases of historical masonry buildings, the equations described in EN 1996-1-1 (2005) may not be applicable due to peculiar block arrangement, aging etc. In this study, the state of the masonry blocks and mortar allowed the use of the provided in EN 1996-1-1 (2005).

### Structural Behavior Under Seismic Loads

Similarly to most historical structures, the timber floors and roof of the masonry building were assumed to be inadequate to act as diaphragms. This mainly a matter of poor connection between the floor and the walls. This connection is rather difficult to be achieved since the huge lateral stiffness of the masonry walls makes the in-plane stiffness of the floor insignificant. The

**FIGURE 1 |** Typical damage to unreinforced masonry buildings that underwent partial or global collapse during the 2017 Lesvos earthquake (Lekkas et al., 2017; Reproduced with the permission of the authors). **(A)** The masonry failed under out-of-plane bending due to lack of a rigid diaphragm at the top. **(B)** The longitudinal masonry walls failed under out-of-plane bending due to their poor connection to the transverse walls. **(C,D)** Failures attributed to poor material properties and construction techniques.

walls were thus not expected to have effective lateral support perpendicular to the applied seismic load. That is, there was not adequate support to distribute the horizontal forces to the walls parallel to them; as a result, the walls experienced an excessive out-of-plane response.

A discussion of some critical aspects related to the effect of the diaphragm on the seismic behavior of masonry buildings can be found in Simsir et al. (2001) and Langroudi et al. (2011). **Figures 4A,B** illustrate the contribution of floor diaphragms to the flow of forces in unreinforced masonry buildings and the damage to these buildings without diaphragms, respectively.

The key weakness of the unreinforced masonry member is its behavior under bending due to its inability to resist tension. Furthermore, it is widely recognized that unreinforced masonry leads to a brittle structure that fails when the maximum applied actions exceed the strength of the system. In the event of failure under shear, the masonry walls exhibit limited capacity for energy dissipation, especially when subjected to high compression stresses that are typical when the walls are heavy (Tomaževič, 1999).

The existence of timber elements (timber members supporting steel members under window bite) with masonry infills further complicates the seismic assessment of the examined structure. It is typical of historical buildings that the connections between timber elements and unreinforced masonry are weak (lack of shear connection), which leads to the separation of single parts from the rest of the building and causes them to behave as independent structural elements (Gabellieri et al., 2012). The seismic behavior of timber walls with masonry infills is a complex topic in earthquake engineering. The most important parameter of the seismic response of such structures is the connection between the different materials (Dutu et al., 2017). Even in cases where the interaction between timber and masonry is limited, overall seismic behavior improves. The timber carries the horizontal forces induced by the earthquake while the masonry carries mainly the gravitational loads, also dissipating energy through joints sliding after the cracking of mortar (Dutu et al., 2012). As shown in **Figures 5A–D**, the connection between the timber frames and the masonry is practically absent, leading to damage in specific regions under seismic loads.

Moreover, as shown in **Figures 5E,F**, damage during the 2017 earthquake revealed cracks inside the masonry, which verifies the characterization of mortar as weak during the laboratory tests.

**FIGURE 2 | (A)** Front view, **(B)** rear view, **(C)** typical plan.

## DESIGN PRINCIPLES

The First Greek Seismic Code (Royal Decree on the Seismic Code for Building Structures, 1959) was initially implemented to assess the seismic response of buildings. According to this code, seismic loads can be applied horizontally to the center of mass of each floor, and are proportional to the total vertical load of the floor. The constant of this proportionality depends on the seismic zone and type of soil, and it was calculated 0.12. The total horizontal load at the top of each floor is divided by the number of nodes at the respective level and applied as the concentrated force at each node. Subsequently, on the basis of EN 1998-1-1 (2003), an inelastic response spectrum was adopted for soil type C (soil factor $S = 1.15$ and characteristic response spectrum periods $T_B = 0.2$ s, $T_C = 0.6$ s, and $T_D = 2.0$ s), design ground acceleration $a_g = 0.24$ g, importance factor $\gamma_I = 1.20$, and behavior factor $q = 1.50$. Finally, dynamic time history analysis was employed based on three

accelerograms. For each of the abovementioned analyses, design checks according to EN 1996-1-1 (2005) were performed on the masonry members.

In addition to the weight of the structure itself, distributed dead loads of 0.5 and 1.0 kN/m$^2$ were considered for the floors and the roof, respectively. The live load of the floor was 3.0 kN/m$^2$. The abovementioned values are proposed by the Greek Loading Code (1945). Similarly to the approach used for the assignment of horizontal loads to the structure, vertical loads were applied as nodal forces.

## NUMERICAL ANALYSES

### Finite Element Model

The performed analyses were linear in terms of both material and displacements. In case of masonry buildings, shell elements are necessary to effectively capture the in-plane and out-of-plane bending of walls because they account for flexural deformation
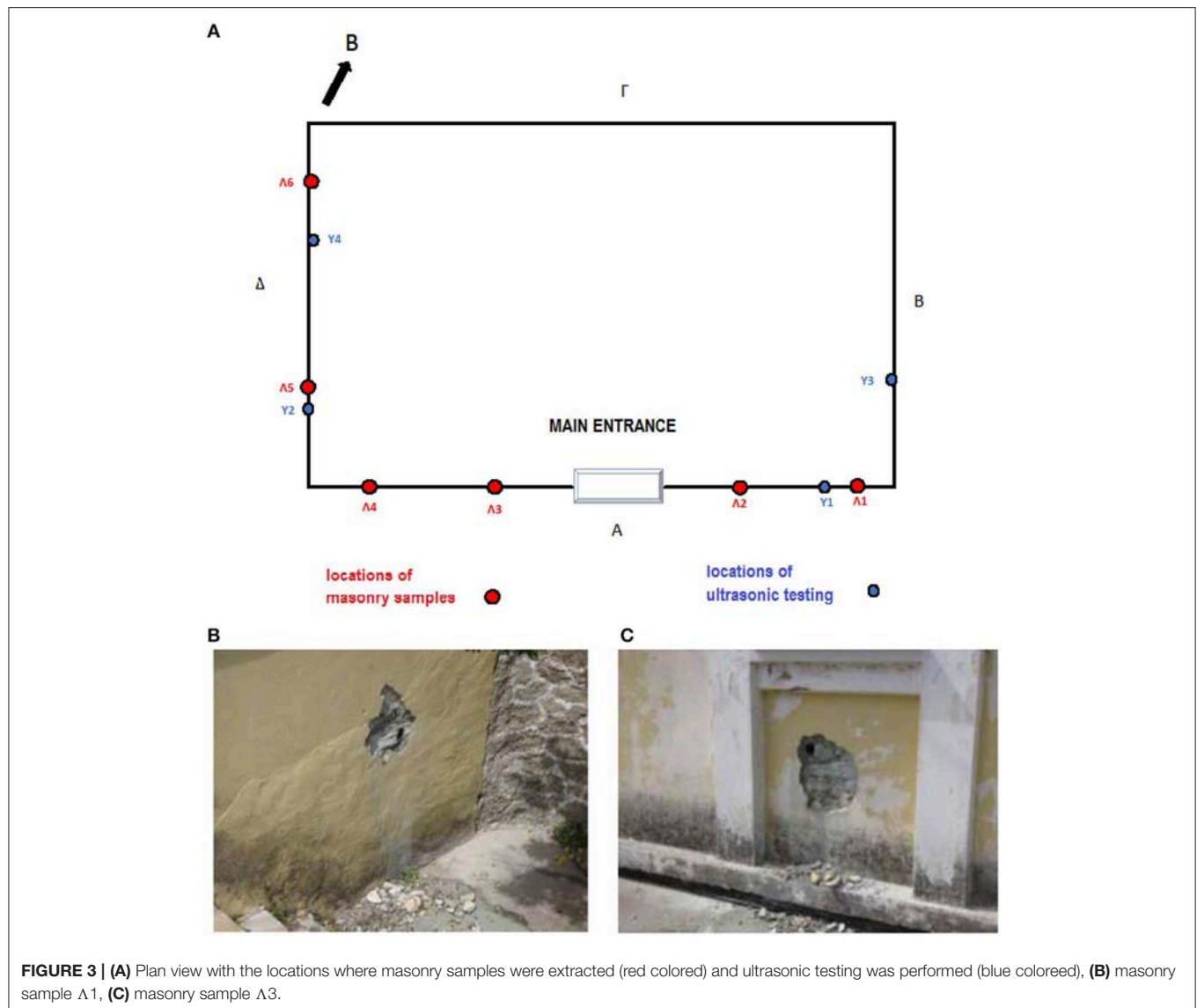
FIGURE 3 | (A) Plan view with the locations where masonry samples were extracted (red colored) and ultrasonic testing was performed (blue coloreed), (B) masonry sample Λ1, (C) masonry sample Λ3.

in addition to membrane forces. In this study, 4-noded shell elements were employed with 0.50 m thickness, a Young's Modulus, $E$, of 6,610 MPa and a Poisson's ratio, $v$, of 0.30. A sensitivity analysis was also performed to define the finite element mesh size. In **Figure 6**, a 3D view of the model along with the meshing consisting of shell elements is presented. In regard to the boundary conditions at the ground level, fixed connections were considered in depth of 1.5 m as the foundation is deep. After sensitivity analysis, of fixed boundary conditions at −1.5 m and hinged at 0.00 m, it has been found that the results were the same (except of local stresses at supports). As shown in **Figure 6**, the timber roof was not included in the model because the connection between the roof and the masonry structure was considered weak, thus making interaction unlikely. Moreover, the timber-framed masonry elements were conservatively considered as unreinforced masonry elements.

## Validation of Finite Element Model

The results of the analysis were validated by comparison with damage recorded during a visit to the site. **Figure 7** shows the results for seismic forces acting in the y direction according to the First Greek Seismic Code (Royal Decree on the Seismic Code for Building Structures, 1959), while **Figure 8** show some damage recorded at the site. The stress concentrations of **Figure 7** match the recorded damages in **Figure 8**, and are indicated by circles or ellipses of varying color. Specifically, the black circles indicate stress concentrations at the corners of the openings for walls parallel to the seismic action and the associated damage at those regions, green ellipses highlight stress concentrations approximately at the middle of the walls perpendicular to the seismic action (out-of-plane behavior) and the resulting cracks in masonry, and brown ellipses indicate the different behaviors of intersecting walls, where one of them was under tensile and

**TABLE 1 |** Material properties determined by the performed tests.

| Schmidt hammer test (on site) | | Ultrasonic testing (on site) | | Strength of mortar (in Lab) | | Point load test (in Lab) | |
|---|---|---|---|---|---|---|---|
| Sample ID | Compressive strength (MPa) | Sample ID | Compressive strength (MPa) | Sample ID | Compressive strength (MPa) | Sample ID | Is-50 strength (MPa) |
| K1_GF | 44.3 | Y1 | 49.4 | K1_GF | 0.97 | Λ1 | 6.03 |
| K2_GF | 43.4 | Y2 | 29.4 | K9_GF | 1.84 | Λ2 | 4.60 |
| K3_GF | 40.8 | Y3 | 45.7 | K8_FL1 | 0.76 | Λ3 | 1.40 |
| K9_GF | 46.4 | Y4 | 53.2 | | | Λ4 | 8.18 |
| K10_GF | 42.9 | | | | | Λ5 | 11.1 |
| K4_FL1 | 42.4 | | | | | Λ6 | 10.98 |
| K6_FL1 | 42.9 | | | | | | |
| K8_FL1 | 43.6 | | | | | | |
| K11_FL1 | 41.0 | | | | | | |
| K12_FL1 | 42.4 | | | | | | |
| K13_FL2 | 44.1 | | | | | | |
| K15_FL2 | 42.9 | | | | | | |
| Average compressive strength (MPa) | 43.09 | | 44.43 | | 1.19 | | 7.05 |
| Standard deviation (MPa) | 1.49 | | 10.47 | | 0.57 | | 3.79 |
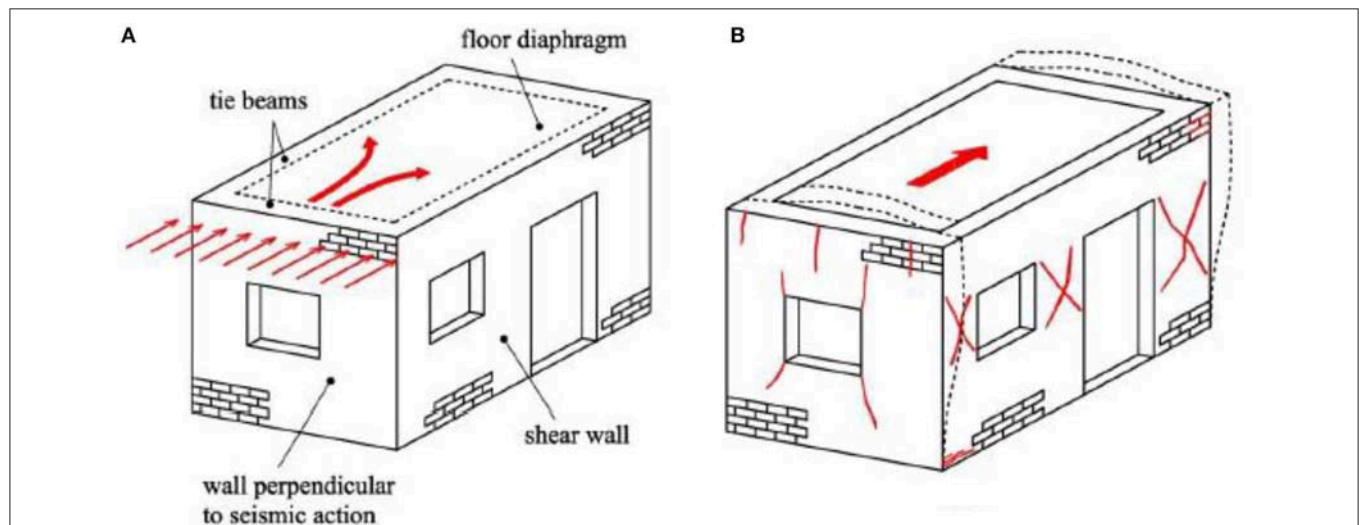


**FIGURE 4 | (A)** Flow of forces in an unreinforced masonry building with rigid diaphragm. **(B)** Failure mechanisms to be considered when rigid diaphragm is absent (Tomaževič, 1999; Reproduced with the permission of the authors).

the other under compressive stresses, and the associated vertical crack was at the intersection of the walls.

## Time History Analysis for EN1998-1 Response Spectra

A spectral analysis of modal response should be preceded by a modal analysis as this can be an issue in masonry buildings. In reinforced concrete and steel structures, it is reasonable to assume that the total weight of the floor is at the center of the slab. Moreover, the modeling of such structures with beam elements is usually sufficient to capture the structural response, while the existence of slabs provides diaphragm action. This leads to a uniform response of the structural members that constitute the building. As a result, in modal analysis of buildings such as the one considered in the present study, only a few modes are usually sufficient for mobilizing 90% of the total mass in lateral translation.

The above does not apply to masonry buildings with flexible diaphragms or no diaphragm at all, where the largest part of the total weight is distributed on the walls and realistic modeling of their response requires the use of shell elements, which results in more degrees of freedom than in a model consisting of beam elements. As noted in a study by Pantazopoulou (2013), the total number of degrees of freedom in the structure significantly
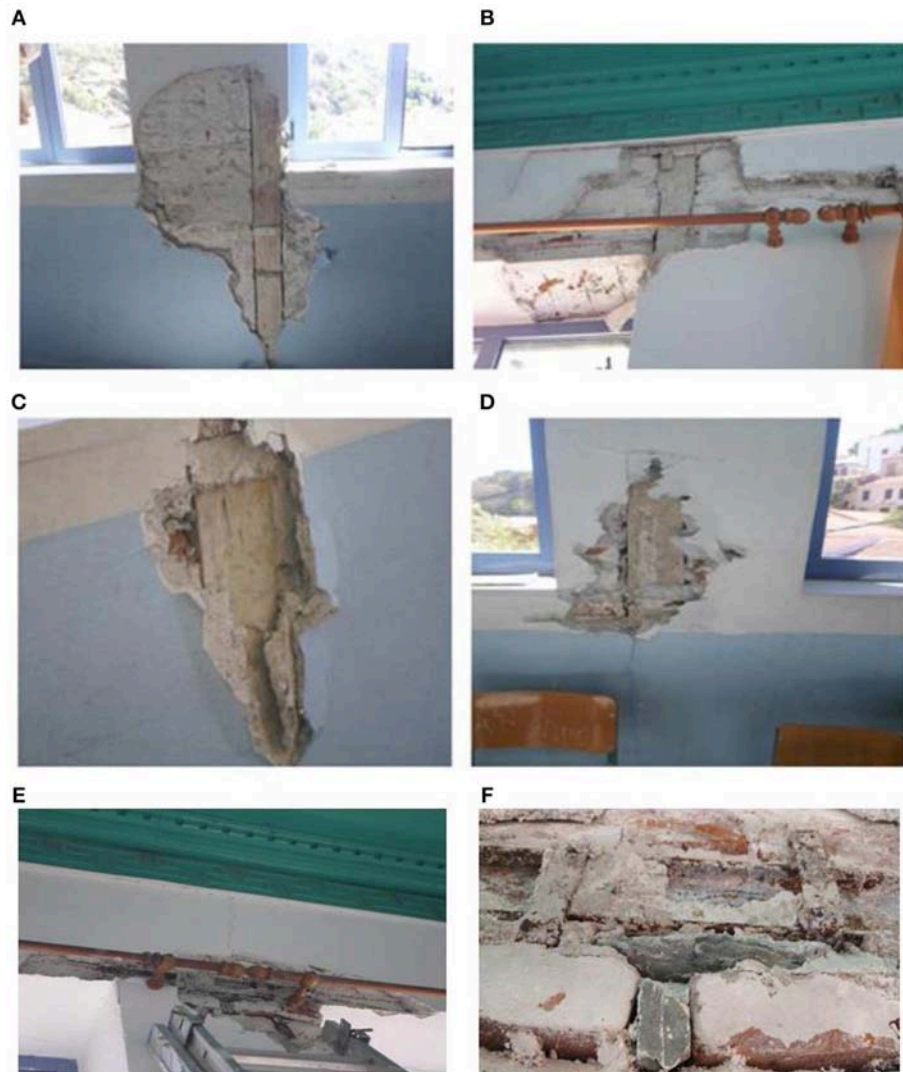
**FIGURE 5 | (A–D)** Damages indicating weak connections between timber frames and masonry. **(E,F)** Damages attributed to weak mortar and the presence of voids inside the masonry panels.

affects the number of modes generated during modal analysis. As mentioned in the same study (Pantazopoulou, 2013), in case of masonry buildings with flexible diaphragms or no diaphragm at all, several hundred modes are sometimes needed for the modal analysis to mobilize as much as 70% of the total mass in lateral translation. In this study, more than 100 modes were used so that an effective modal mass equal to 90% of the total mass could be activated. **Table 2** presents the results of the modal analysis which verify the abovementioned studies. As it can be seen, 124 modes were required in order for the activation of the 90% of the total mass criterion to be satisfied in both orthogonal directions.

Similarly to previous studies on the restoration of traditional buildings (Maraveas et al., 2014), seismic action was examined in terms of the time histories of ground accelerations for comparison. To this end, recordings of accelerations during three

earthquake events (Loma Prieta, 1989; Northridge, 1994; Kocaeli, 1999) provided by the SeismoMatch software were considered (SeismoMatch, 2018). The original accelerograms were scaled using the software to adjust the ground motion records to the spectrum defined in the design code (target spectrum; Eurocode 8, 2003) using the wavelets' algorithm (Abrahamson, 1992; Hancock et al., 2006).

Although according to the literature (Oyarzo-Vera and Chouw, 2008), there is no uniform set of criteria for record scaling, EN 1998-1-1 (2003) suggests that artificial records be generated from the scaling of at least three real records.

From the time history analysis the most unfavorable time step considered.

**Figures 9A,B** present the response spectra of the initial records and the matched spectra, respectively, along with the target spectrum. The original (blue) and scaled (red)
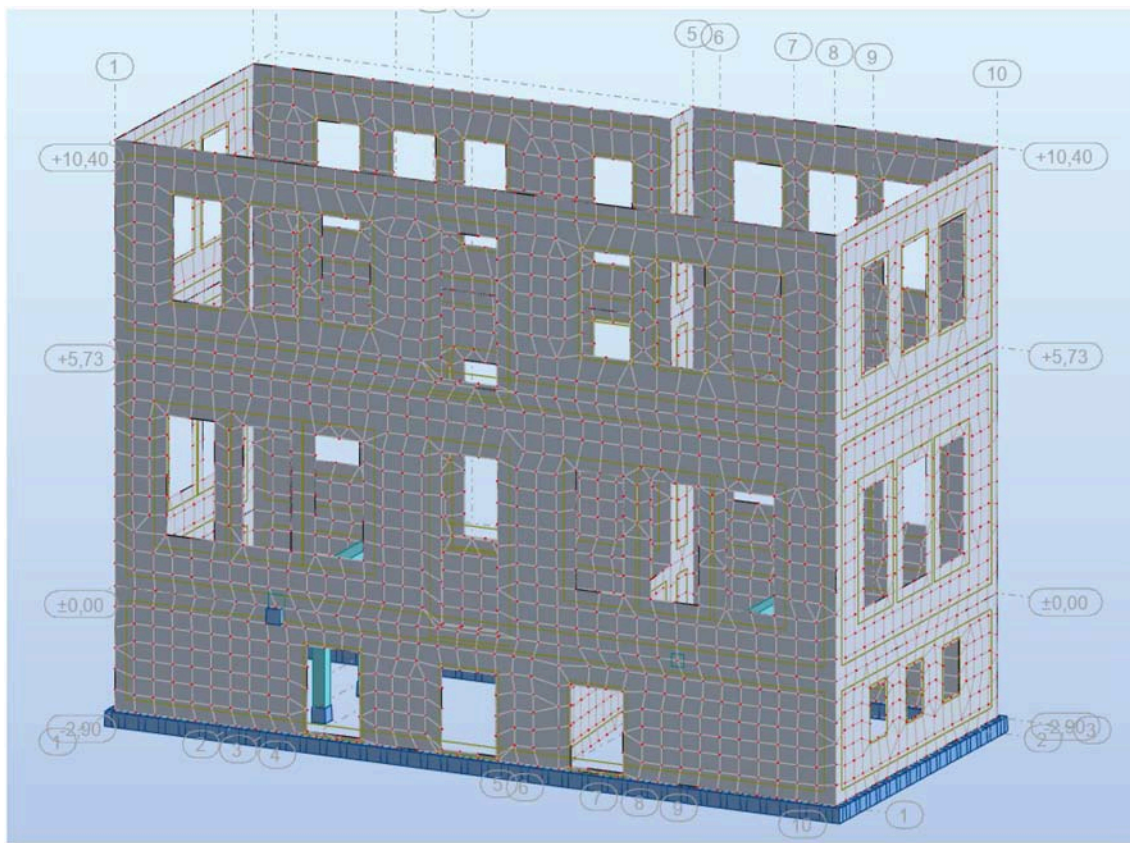
**FIGURE 6 |** Finite element model in Robot Structural Analysis software (Autodesk Robot Structural Analysis Professional, 2016).

accelerograms corresponding to the employed seismic motions are presented in **Figure 10**.

## STRUCTURAL EVALUATION OF THE BUILDING

The design resistances of unreinforced masonry according to EN 1996-1-1 (2005) were employed to check the results of the analyses, and are summarized below (Equations, 1–4):

$$N_{\text{Rd}} = \frac{\Phi t f_k}{\gamma_{\text{M}}} \tag{1}$$

$$V_{\text{Rd1}} = \frac{f_{\text{vk0}} + 0.4\sigma_0}{\gamma_{\text{M}}} bt \tag{2}$$

$$V_{\text{Rd2}} = \frac{1.5 f_{\text{vk0}} bt}{\gamma_{\text{M}}} \sqrt{1 + \frac{\sigma_0}{1.5 f_{\text{vk0}}}} \tag{3}$$

$$M_{\text{Rd}} = \frac{\sigma_0 b^2 t}{2} (1 - \frac{\sigma_0}{0.85 f_d}) \tag{4}$$

The results of the modal response spectrum analysis indicated that the absence of rigid diaphragms at floor levels leads to serious damages. Its deformed shape under horizontal load was similar to that of a 10.5 m cantilever owing to the absence of a horizontal diaphragm. The stability of the unreinforced masonry could thus

not be ensured because of a combination of large out-of-plane bending moments and slenderness ratios approximately equal to eight.

## STRENGTHENING PROPOSAL

The most important step in the process of retrofitting a masonry building involves the elucidation of its pathology. Thus, the main goal of the retrofit was to restore the lateral stability of the walls. According to Fardis (2009), the aim of retrofitting is to modify the seismic demands $E_d$, and/or capacities, so that all relevant elements of the strengthened building satisfy the general verification inequality, $E_d \leq R_d$, under the specified seismic action. This goal can be achieved by following one of the strategies below, or even a combination of them:

1. by reducing seismic demands on the members and the structure as a whole; and
2. by increasing the capacity of the members.

Bearing this in mind, the following retrofitting solutions are proposed:

a. *Building rigid diaphragms at floor level*. This method provides an effective way of distributing the horizontal
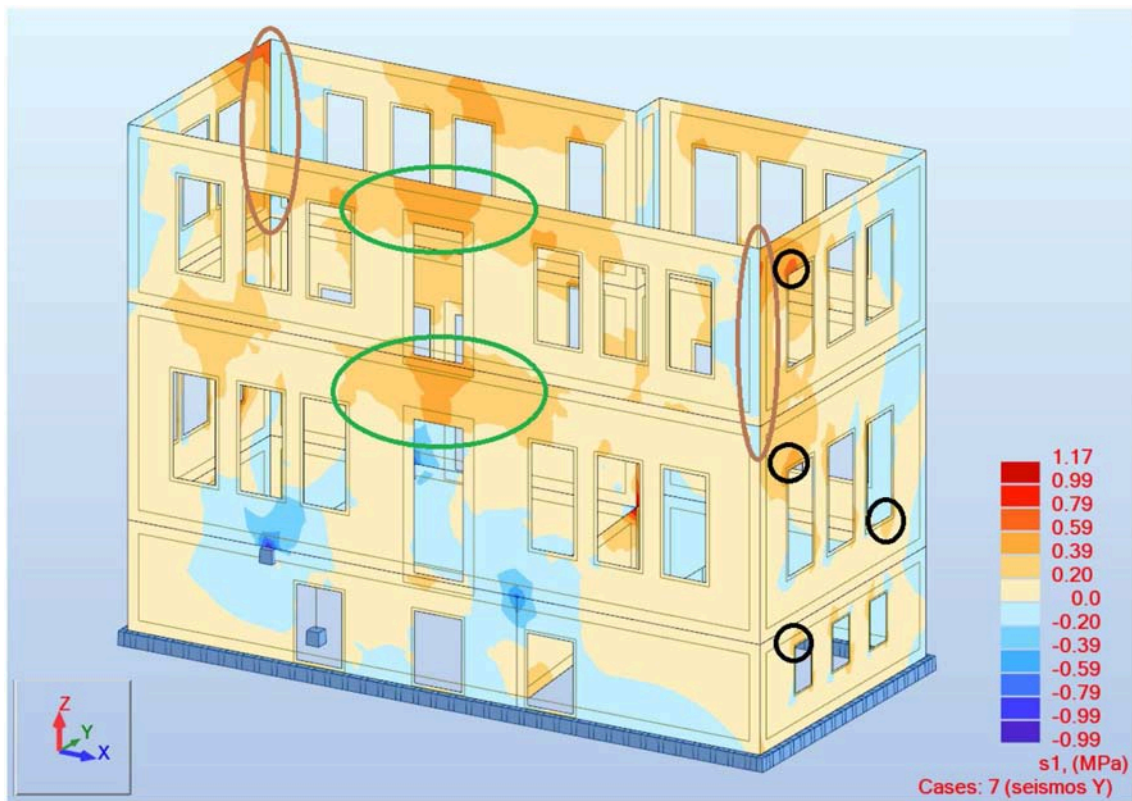
**FIGURE 7 |** Results of principal stresses (MPa) for seismic action in the y direction according to the First Greek Seismic Code (Royal Decree on the Seismic Code for Building Structures, 1959).
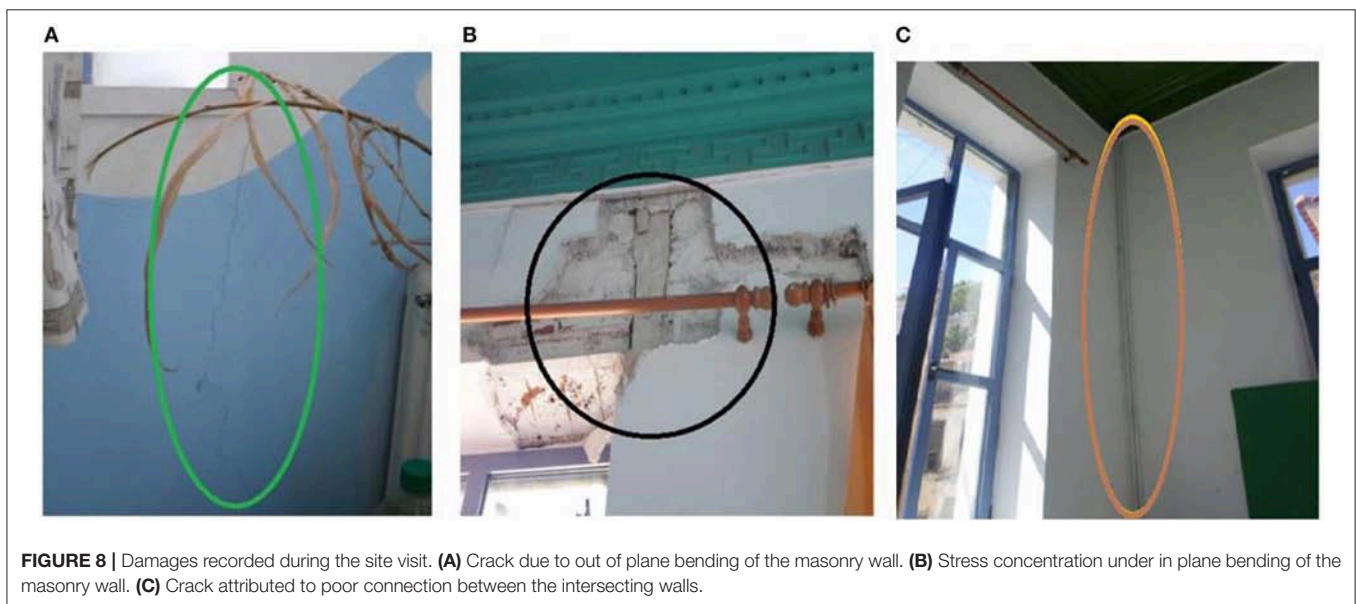


**FIGURE 8 |** Damages recorded during the site visit. **(A)** Crack due to out of plane bending of the masonry wall. **(B)** Stress concentration under in plane bending of the masonry wall. **(C)** Crack attributed to poor connection between the intersecting walls.

forces induced by the earthquake to all masonry walls, thus diminishing the detrimental out-of-plane response of the walls perpendicular to the seismic action. Thus, the separation of the walls along the vertical

joints and excessive cracking in general is expected to be resolved.

b. *Repointing*. As mentioned above, the mortar was found to be weak. Therefore, it was considered

**TABLE 2 |** Results of modal analysis.

| Mode | Period (s) | Total activated mass in X direction (%) | Total activated mass in Y direction (%) |
|------|-----------|------------------------------------------|------------------------------------------|
| 1 | 0.32 | 0.16 | 33.23 |
| 2 | 0.20 | 0.67 | 33.85 |
| 3 | 0.18 | 1.20 | 33.86 |
| 4 | 0.13 | 23.55 | 39.06 |
| 5 | 0.13 | 30.28 | 56.40 |
| 6 | 0.11 | 31.20 | 60.06 |
| 7 | 0.11 | 33.47 | 60.06 |
| 8 | 0.10 | 38.33 | 62.91 |
| 9 | 0.10 | 54.68 | 63.50 |
| 10 | 0.09 | 56.52 | 63.51 |
| **108** | 0.02 | 87.86 | **90.09** |
| **124** | 0.01 | **90.23** | 91.53 |

*Bold values represent the number of modes that satisfy the 90% of mass participation criterion.*

necessary to replace part of the existing mortar with mortar of significantly better quality, e.g., cement mortar.

c. *Cement grouting.* When the examined structure was built, the method of construction of unreinforced masonry usually led to the development of voids over their entire volume. Hence, filling the voids by injecting cementitious grout can be an adequate solution for retrofitting.

d. *External bonding of timber members with masonry and improvement of shear connection.*

Of the aforementioned retrofitting solutions, only (a) belongs to strategy 1, whereas (b), (c), and (d) belong to strategy 2. Another key parameter regarding methods of restoration is the preservation of characteristics of the traditional architecture. This requirement is assumed to be satisfied because it is clear that none of the abovementioned strengthening solutions affect the historical value and aesthetic appearance of the building. In the following section, solutions (a) and (d) are discussed because methods (b) and (c) are used frequently to improve the seismic performance of masonry piers.

## Building Rigid Diaphragms at Floor Levels

For rigid diaphragm action, the boards of the timber floor were temporarily removed after being counted, and two plywood boards, each 10 mm thick, were placed in both orthogonal directions at the top of the timber joists. The removed boards were then placed exactly in their initial positions and the entire system was fastened together using wood screws (**Figure 11A**). A similar approach has been suggested by Tomaževič (1999), according to whom rigid horizontal diaphragm action is obtained by nailing boards in both orthogonal directions at the top of the timber joists. Of course, this method assumes that the timber joints are effectively connected to the walls through steel anchors.

Therefore, holes should be bored to allow steel anchors to penetrate the walls and then be bolted to the timber joints. The holes are then filled with non-shrinking grout and the anchors are anchored at the external surface of the walls through steel plates. A schematic of this method is presented in **Figure 11B**.

## External Bonding of Timber Walls With Infilled Masonry

As described by Triantafillou (2016), the textile-reinforced mortar (TRM) system is an ideal retrofitting solution for connecting different structural members. Accordingly, this method was selected for bonding the masonry units with the adjacent timber elements.

The effectiveness of this method in comparison with similar strategies has been previously investigated in studies such as those by Papanicolaou et al. (2007) and Tetta et al. (2015), where a comparison between TRM and fiber-reinforced polymers (FRP) as strengthening material was drawn. This method was only implemented on panels between openings, for two reasons: first, these represent the positions where the related damage was detected; second, the application of the specific method, as detailed below, is much easier in such positions.

As shown in **Figure 11C**, to enhance the response of the specific elements, the existing plaster was removed and a first layer of mortar (5 mm thick) was placed. A fiberglass mesh was then installed and covered with a second 5-mm-thick mortar layer while the first layer was wet. The total thickness of the strengthening system was approximately the same as that of the initial plaster.

It must be noted that the effect of TRM has been considered in the analysis of the retrofitted model. The effect on the overall response was negligent, as the thickness of the TRM is just 1 cm, the Young's modulus is similar to masonry (for compatibility issues), and the retrofit was local, only around the windows of the A' floor level. So, the effect of TRM was considered mainly in terms of improved masonry capacity.

## COMPARATIVE RESULTS

A schematic of the results (in terms of principal bending moments) of time history analyses for the initial and the retrofitted model (including diaphragms) is presented in **Figures 12A,B,** respectively. In the absence of diaphragms, the bending moments spread freely from the foundation to the top of the building, while for the strengthened model, the bending moments were limited to low values with the exception of walls of the top floor, which act as cantilevered walls.

**Table 3** lists a comparison of various results obtained from the analysis of both the existing and the retrofitted structures. The results refer to the maximum bending moment, shear force, and top displacement on the structure.

In regard to the values under the "Before Retrofit" row, only those related to the Royal Decrees of 1959 satisfied the design checks provided by EN 1996-1-1 (2005) presented earlier (section Structural Evaluation of the Building) in this study.
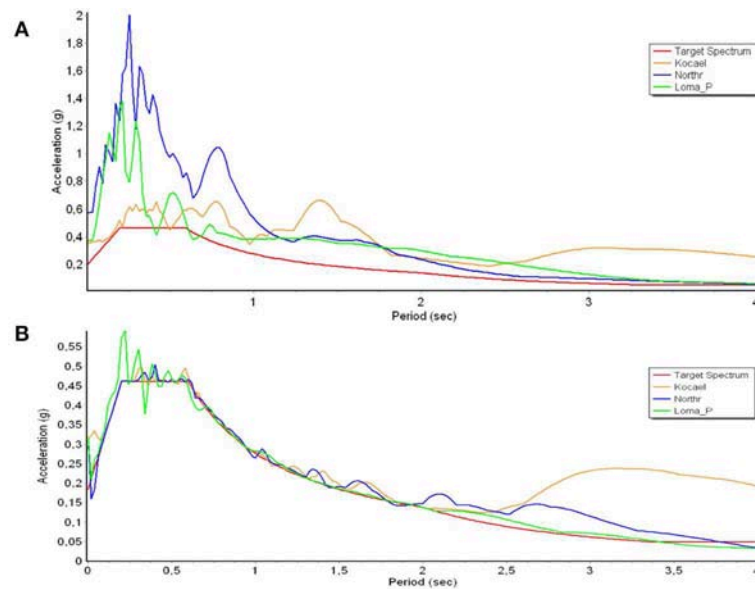
**FIGURE 9 |** **(A)** Response spectra of the original accelerograms, and **(B)** response spectra of the matched accelerograms.
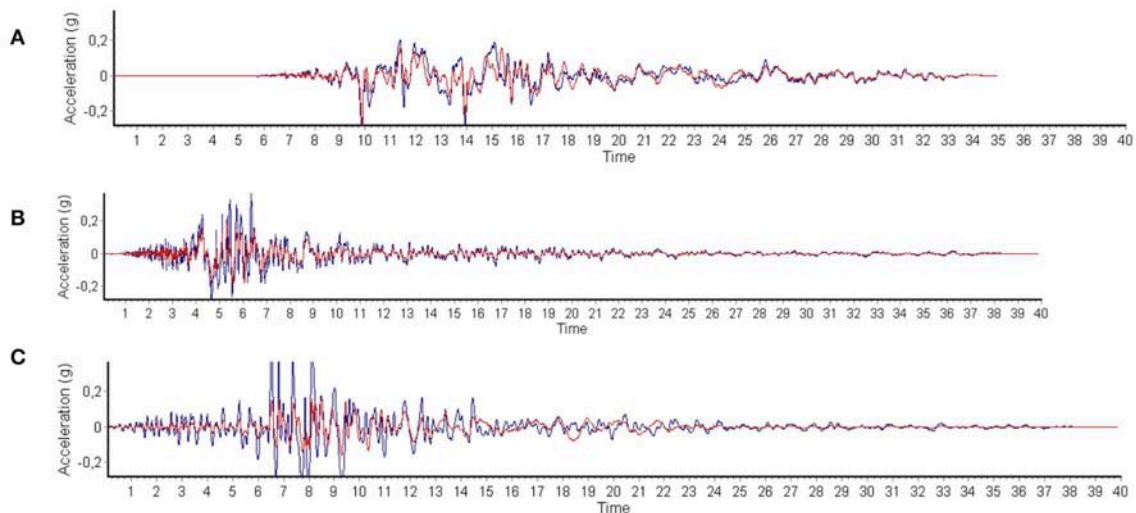


**FIGURE 10 |** Time histories used for dynamic analyses: **(A)** Kocaeli (1999), **(B)** Northridge (1994), and **(C)** Loma Prieta (1989), with blue and red indicating the original and the scaled accelerograms, respectively.

However, all values under the retrofitted section satisfied the same design checks.
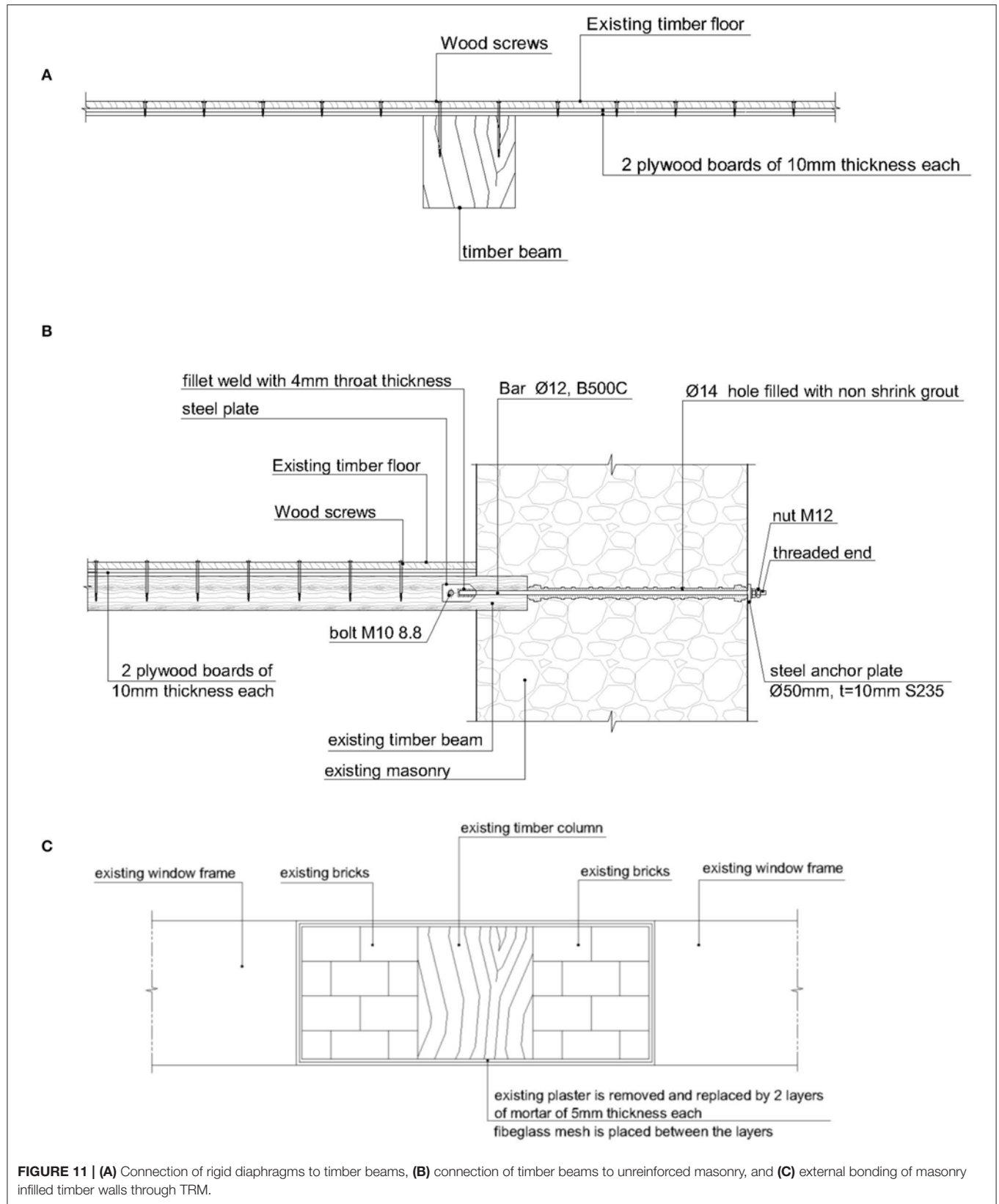
It should additionally be noted that the modal frequencies of the retrofitted building were higher than those of the existing building owing to an increase in stiffness associated with the presence of floor diaphragms.

## CONCLUSIONS

1. Comparison of the results revealed that the simpler method of analysis proposed in the first Seismic Greek

Code (Royal Decree on the Seismic Code for Building Structures, 1959) may underestimate the seismic behavior of masonry buildings. The response spectrum analysis yielded the most unfavorable results, with dynamic time history analysis resulting in a slightly more favorable seismic response.

2. Although it has been stated that traditional lateral load-resisting systems were conceived to sustain seismic forces (Syrmakezis et al., 2005; Vintzileou et al., 2007), this seems to apply only to cases where the seismic response was evaluated based on previous design codes (Royal
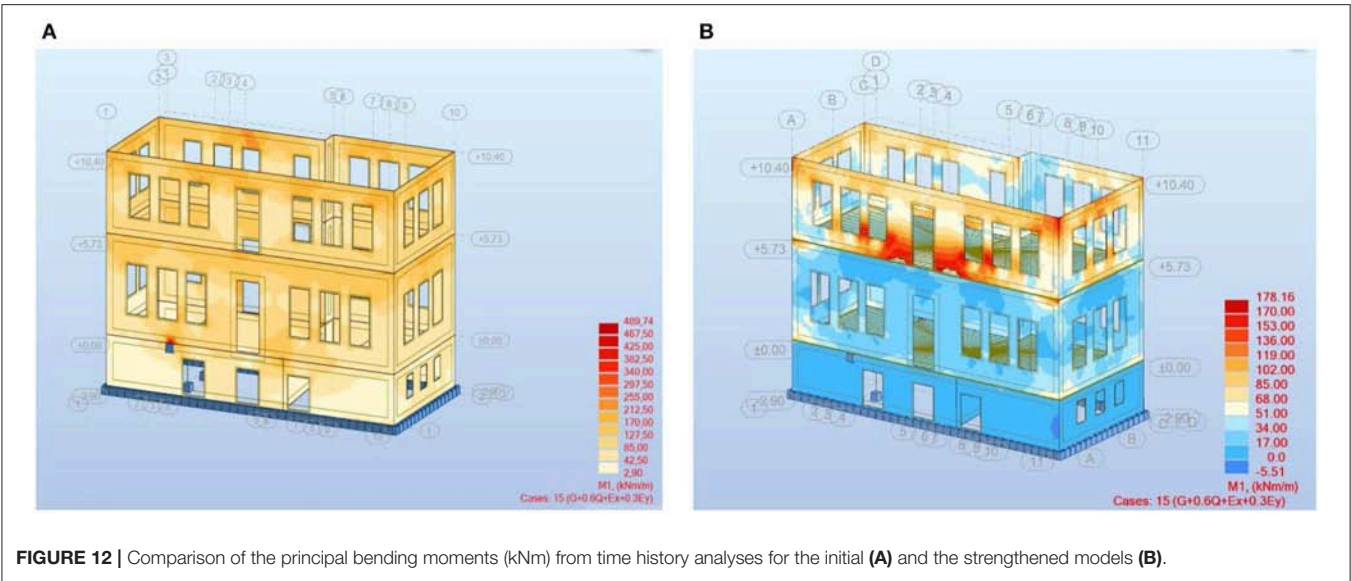
**A**

Wood screws

Existing timber floor

2 plywood boards of 10mm thickness each

timber beam

**B**

fillet weld with 4mm throat thickness

steel plate

Existing timber floor

Wood screws

Bar Ø12, B500C

Ø14 hole filled with non shrink grout

nut M12

threaded end

bolt M10 8.8

2 plywood boards of 10mm thickness each

existing timber beam

existing masonry

steel anchor plate Ø50mm, t=10mm S235

**C**

existing window frame

existing bricks

existing timber column

existing bricks

existing window frame

existing plaster is removed and replaced by 2 layers of mortar of 5mm thickness each

fibeglass mesh is placed between the layers

**FIGURE 11 | (A)** Connection of rigid diaphragms to timber beams, **(B)** connection of timber beams to unreinforced masonry, and **(C)** external bonding of masonry infilled timber walls through TRM.

**FIGURE 12 |** Comparison of the principal bending moments (kNm) from time history analyses for the initial **(A)** and the strengthened models **(B)**.

**TABLE 3 |** Comparison of forces and displacements for the studied cases of seismic analysis, while moment capacity is of the range of 250 kN m/m and shear capacity is of the range of 120 kN/m (depends of the exact dimensions of each masonry unit).

|  | Analysis | Max. moment in masonry (kNm/m) | Max. shear in masonry (kN/m) | Max. displacement at the top of masonry (mm) |
|---|---|---|---|---|
| Before Retrofit | Royal Decrees 1959 | 63.88 | 249.79 | 8.13 |
|  | Time history analysis (scaled to EN1998-1) (most unfavorable time step) |  |  |  |
|  | Kocaeli | 739.21 | 1259.29 | 24.83 |
|  | Northridge | 768.96 | 1118.53 | 23.06 |
|  | Loma Prieta | 799.18 | 1191.62 | 23.69 |
| After Retrofit | Royal Decrees 1959 | 40.01 | 107.63 | 3.92 |
|  | Time history analysis (scaled to EN1998-1) (most unfavorable time step) |  |  |  |
|  | Kocaeli | 371.73 | 727.89 | 18.12 |
|  | Northridge | 382.23 | 635.52 | 17.54 |
|  | Loma Prieta | 398.56 | 684.64 | 17.93 |

Decree on the Seismic Code for Building Structures, 1959). However, historical structures do not meet seismic demands specified in modern codes, especially in regions with high seismic activity.

3. The expected damage indicated by the present analyses seems to be in agreement with damage recorded during the visit to the site, thus validating the proposed finite element model and numerical analyses.

4. The introduction of rigid diaphragms led to the compliance of the structural performance with the old codes, which require lower safety levels than the modern codes. The key aspects of this method are that it is relatively cost-effective, reversible, and minimally alters the appearance of the building. If Eurocodes are applied, further retrofits and interventions are required.

5. In the absence of rigid diaphragms, stresses were mainly concentrated in the corners of openings for walls parallel to the seismic action and approximately at the middle of the walls perpendicular to the seismic action. However, once rigid diaphragms had been included in the analysis, the stresses were uniformly distributed on every wall irrespective of the direction of the seismic forces.

6. Not only did the maximal displacements reduce as a result of the effect of the diaphragm, but the difference in terms of maximal displacement between the orthogonal directions also decreased.

7. The base shear forces applied to the resisting elements were more uniformly distributed. Moreover, the diaphragms restricted the spread of stresses to within the height of each floor, while in the case where there was no diaphragm, the

stresses spread freely from the foundation to the top of the building.

8. The above observations indicate that the introduction of rigid diaphragms led to a global improvement of structural response, which was characterized by the uniform behavior of the structural elements and better utilization of the material.

9. The presence of rigid diaphragms at the floor levels led to a decrease in the structure's fundamental period. Therefore, this retrofitting method can also have a beneficial effect in cases where the structure is founded on soft soils characterized by a long period by preventing dynamic amplifications generated by the resonance between the underlying soil layers and the superstructure. Conversely, this strengthening method should be selected carefully in cases where the structure is founded on firm soils, because a further decrease in the structure's fundamental period can lead to the tuning of the soil–structure system, with detrimental effects on its seismic performance.

## DATA AVAILABILITY STATEMENT

All data generated or analyzed during this study are available by the author.

## AUTHOR CONTRIBUTIONS

The author confirms being the sole contributor of this work and has approved it for publication.

## REFERENCES

Abrahamson, N. A. (1992). Non-stationary spectral matching. *Seismol. Res. Lett.* 63:30.

Apostolopoulou, M., Aggelakopoulou, E., Siouta, L., Bakolas, A., Douvika, M., Asteris, P. G., et al. (2017). A methodological approach for the selection of compatible and performable restoration mortars in seismic hazard areas. *Constr. Build. Mater.* 155, 1–14. doi: 10.1016/j.conbuildmat.2017.07.210

Asteris, P. G., Chronopoulos, M. P., Chrysostomou, C. Z., Varum, H., Plevris, V., Kyriakides, N., et al. (2014). Seismic vulnerability assessment of historical masonry structural systems. *Eng. Struct.* 62–63, 118–134. doi: 10.1016/j.engstruct.2014.01.031

Asteris, P. G., Douvika, M. G., Apostolopoulou, M., and Moropoulou, A. (2017). Seismic and restoration assessment of monumental masonry structures. *Materials* 10:895. doi: 10.3390/ma10080895

Asteris, P. G., and Giannopoulos, I. P. (2012). Vulnerability and restoration assessment of masonry structural systems. *Electronic J. Struct. Eng.* 12, 82–93.

Asteris, P. G., Moropoulou, A., Skentou, A. D., Apostolopoulou, M., Mohebkhah, A., Cavaleri, L., et al. (2019). Stochastic vulnerability assessment of masonry structures: concepts, modeling and restoration aspects. *Appl. Sci.* 9:243. doi: 10.3390/app9020243

Asteris, P. G., Tzamtzis, A. D., Vouthouni, P. P., and Sophianopoulos, D. S. (2005). Earthquake resistant design and rehabilitation of masonry historical structures. *Pract. Period. Struct. Design Constr.* 10, 49–55. doi: 10.1061/(ASCE)1084-0680(2005)10:1(49)

Autodesk Robot Structural Analysis Professional v.29.0 (2016). Available online at: https://www.autodesk.com/products/robot-structural-analysis/overview (accessed September 13, 2019).

BBC website (2017). Available online at: https://www.bbc.com/news/world-europe-40251100 (accessed September 13, 2019).

Boscato, G., Dal Cin, A., Riva, G., Russo, S., and Sciarretta, F. (2014). Knowledge of the construction technique of the multiple leaf masonry façades of Palazzo Ducale in Venice with ND and MD tests. *Adv. Mater. Res.* 919–921, 318–324. doi: 10.4028/www.scientific.net/AMR.919-921.318

Boscato, G., Di Tomasso, A., Guerra, F., Lazzarini, L., Mazzucato, A., Pizzolato, M., et al. (2010). "Approach and methodology in understanding the structural behaviour of historic arch bridges through dynamic monitoring: the case of Rialto Bridge in Venice," in *Proceedings of 34th IABSE Symposium* (Venice).

Caddemi, S, Caliò, I, Cannizzaro, F, and Pantò B. (2017). New frontiers on seismic modeling of masonry structures. *Front. Built Environ.* 3:39. doi: 10.3389/fbuil.2017.00039

Casamassima, V. M., and D'Amato, M. (2019). Fatigue assessment and deterioration effects on masonry elements: a review of numerical models and their application to a case study. *Front. Built Environ.* 5:65. doi: 10.3389/fbuil.2019.00065

Chronopoulos, P. M., Zigouris, N., and Asteris, P. G. (2012). "Investigation/documentation and aspects of seismic assesment and redesign of traditional masonry buildings in Greece," in *5th European Conference on Structural Control (EACS 2012)* (Genoa).

Dutu, A., Gomes- Ferreira, J., Goncalves, A. M., and Covaleov, A. (2012). Components interaction in timber framed masonry structures subjected to lateral forces. *J. Civil Eng. Res.* 13, 62–67.

Dutu, A., Sakata, H., and Yamazaki, Y. (2017). "Comparison between different types of connections and their influence on timber frames with masonry infill structures' seismic behavior," in *16th Conference on Earthquake Engineering* (Santiago).

EN 1996-1-1 (2005). *Eurocode 6–Design of Masonry Structures–Part 1-1: General Rules for Reinforced and Unreinforced Masonry Structures.* Brussels: CEN.

EN 1998-1-1 (2003). *Eurocode 8–Design of Structures for Earthquake Resistance–Part 1: General Rules, Seismic Actions and Rules for Buildings.* Brussels: CEN.

Fardis, M. N. (2009). *Seismic Design, Assessment and Retrofitting of Concrete Buildings (Based on EN-Eurocode 8).* Dordrecht: Springer Science + Business Media BV.

Gabellieri, R., Diotallevi, P. P., and Landi, L. (2012). "E"fect of diaphragm flexibility on the dynamic behaviour of unreinforced masonry walls in out-of-plane bending," in *15th World Conference on Earthquake Engineering (15WCEE)* (Lisbon).

Greek Loading Code (1945). *Code of Loads for the Design of Structures*, Royal decree 10/1945

Hancock, J., Watson-Lamprey, J., Abrahamson, N. A., Bommer, J. J., Markatis, A., McCoy, E., et al. (2006). An improved method of matching response spectra of recorded earthquake ground motion using wavelets. *J. Earthquake Eng.* 10, 67–89 doi: 10.1080/13632460609350629

Kyriakides, N., Illampas, R., Lysandrou, V., Agapiou, A., Masini, N., Sileo, M., et al. (2018). "Study of ancient monuments' seismic performance based on Passive and Remote Techniques," in *16th European Conference on Earthquake Engineering* (Thessaloniki).

Kyriakides, N., Lysandrou, V., Agapiou, A., Illampas, R., and Charalambous, E. (2016). Correlating damage condition with historical seismic activity in underground sepulchral monuments of Cyprus. *J. Archaeol. Sci. Rep.* 14, 734–741 doi: 10.1016/j.jasrep.2016.07.007

Langroudi, J., Ranjbar, M., Hashemi, S., and Moghadam, A. (2011). "Evaluation of roof diaphragm effect on seismic behavior of masonry buildings," in *Proceedings of 8th International Conference on Structural Dynamics* (Leuven).

Lekkas, E., Voulgaris, N., Karydis, P., Tselentis, G. A, Skourtsos, E., Antoniou, B., et al. (2017). *The Earthquake in Lesbos, Mw 6.3, 12th of June 2017* (in Greek). Athens: Newsletter.

Lysandrou, V., Agapiou, A., Kyriakides, N., and Hadjimitsis, D. G. (2017). F"rom space to ground. Digital techniques for the investigation of monuments and sites," in *10th International Symposium on the Conservation of Monuments in the Mediterranean Basin* (Athens). doi: 10.1007/978-3-319-78093-1_65

Maraveas, C., Miamis, K., Tasiouli, K., and Fasoulakis, Z. (2014). "Structural analysis and retrofitting of "Tzotza" building in Kastoria, Greece," in *9th International Conference on Structural Analysis of Historical Construction* (Mexico City).

Maraveas, C., and Tasiouli, K. (2015). Assessment and restoration of the first Greek power plant - registered monument of industrial heritage. *Case Stud. Struct. Eng.* 2, 1–10. doi: 10.1016/j.csse.2014.12.001

Maraveas, C., Tasiouli, K., and Fasoulakis, Z. (2015). "Assessment of the new Faliron steam–electric station in Greece," in *14th International Conference on Studies, Repairs and Maintenance of Heritage Architecture* (A Coruña), 247–259.

Oyarzo-Vera, C., and Chouw, N. (2008). "Comparison of record scaling methods proposed by standards currently applied in different countries," in *14th World Conference on Earthquake Engineering* (Beijing).

Pantazopoulou, S. J. (2013). *State of the Art Report for the Analysis Methods for Unreinforced Masonry Heritage Structures and Monuments*. European Centre on Prevention and Forecasting of Earthquakes (ECPFE).

Papanicolaou, C. G., Triantafillou, T. C., Karlos, K., and Papathanasiou, M. (2007). Textile-reinforced mortar (TRM) versus FRP as strengthening material of URM walls: in-plane cyclic loading. *Mater. Struct.* 40:1081. doi: 10.1617/s11527-006-9207-8

Royal Decree on the Seismic Code for Building Structures (1959). *Government's Gazette, Issue A, No. 36, February, 1959, Greece* (in Greek).

Sciarretta, F., Antonelli, F., Peron, F., and Caniglia, S. (2018). Final outcomes on the multi-disciplinary long-term monitoring and preservation state investigation on the medieval external Façades of Palazzo Ducale in Venice, Italy. *J. Civil Struct. Health Monit.* 8, 111–133. doi: 10.1007/s13349-017-0263-2

SeismoMatch v.2.1.0 (2018). *Seismosoft*. Available online at: www.seismosoft.com (accessed September 13, 2019).

Simsir, C., Aschheim, M., and Abrams, D. (2001). "Influence of diaphragm flexibility on the out-of-plane response of unreinforced masonry walls," in *Proc. 9th Canadian Masonry Symposium* (Fredericton, NB).

Syrmakezis, C. A., Antonopoulos, A. K., and Mavrouli, O. A. (2005). "Historical structures' vulnerability evaluation using fragility curves," in *Proceedings of 10th International Conference on Civil, Structural and Environmental Engineering Computing* (Rome).

Syrmakezis, C. A., Chronopoulos, M. P., Sophocleous, A. A., and Asteris, P.G. (1995). "Structural analysis methodology for historical buildings," in *Proceedings, Fourth International Conference on Structural Studies of Historical Buildings, STREMA 95, Vol. 1* (Crete), 373–382.

Tetta, Z. C., Koutas, L. N., and Bournas, D. A. (2015). Textile-reinforced mortar (TRM) versus fiber-reinforced polymers (FRP) in shear strengthening of concrete beams. *Compos. B Eng.* 77, 338–348. doi: 10.1016/j.compositesb.2015.03.055

Tomaževič, M. (1999). *Earthquake-Resistant Design of Masonry Buildings*. Imperial College Press.

Triantafillou, T. (2016). Strengthening of existing masonry structures: concepts and structural behavior. *Text. Fibre Composites Civil Eng.* 361–374. doi: 10.1016/B978-1-78242-446-8.00016-1

Vintzileou, E., Zagkotsis, A., Repapis, C., and Zeris, C. (2007). Seismic behaviour of the historical structural system of the island of Lefkada, Greece. *Constr. Build. Mater.* 21, 225–236. doi: 10.1016/j.conbuildmat.2005.04.002

## NOMENCLATURE

| | |
|---|---|
| $f_b$ | Normalized mean compressive strength of masonry units |
| $f_m$ | Compressive strength of mortar |
| $f_k$ | Characteristic compressive strength of masonry |
| $f_k$ | Design compressive strength of masonry |
| $f_{vk0}$ | Characteristic shear strength of masonry under zero compression |
| $\gamma_M$ | Partial safety factor of material |
| $t$ | Thickness of wall |
| $b$ | Length of wall |
| $\sigma_0$ | Compressive strength on masonry |
| $l_c$ | Length of compressed part of wall |
| $\Phi$ | Capacity reduction factor allowing for effects of slenderness |
| $N_{Rd}$ | Axial resistance of design |
| $V_{Rd1}$ | Shear resistance against sliding in design |
| $V_{Rd2}$ | Shear resistance against diagonal cracking in design |
| $M_{Rd}$ | Bending moment resistance in design. |

Check for
updates

# Comparative Seismic Assessment Methods for Masonry Building Aggregates: A Case Study

*Nicola Chieffo[1]* and Antonio Formisano[2]*

[1] Faculty of Architecture and Urbanism, Politehnica University of Timisoara, Timisoara, Romania, [2] Department of Structures for Engineering and Architecture, School of Polytechnic and Basic Sciences, Naples, Italy

Recent seismic events produced considerable socio-economic losses. An important step for the reduction and mitigation of seismic risk in urban areas with a high population density is the assessment of global vulnerability of clustered buildings. The proposed work aims at appraising the seismic vulnerability of building aggregates within the historical center of Arsita, damaged by the L'Aquila earthquake (2009 April 6th), through a multi-level approach deriving from the application of different estimation procedures. In particular, the seismic vulnerability quantification has been done by comparing three distinct methods, namely the macroseismic approach according to the EMS-98 scale, the Vulnus methodology, developed by the University of Padua, and the mechanical approach derived from using the 3Muri software. The expected damage has been estimated in terms of fragility curves, respectively, for the entire buildings compound and the individual structural units located in the corner and intermediate positions, in order to evaluate the beneficial or detrimental aggregate effect on the seismic behavior of individual constructions examined.

Keywords: masonry aggregates, vulnerability assessment, macroseismic method, Vulnus method, mechanical method, non-linear analysis, fragility curves

## INTRODUCTION

The evaluation of the seismic safety of existing masonry buildings is one of the most important aspects to be contextualized in the last decades, where the occurrence frequency of seismic events is very high. The characterization of historical buildings is a very demanding task, because many factors influence their global seismic response. In particular, an important cause of disasters is the poor seismic performance of such constructions. In fact, several masonry buildings were built without taking any consideration about seismic actions. This inadequacy generates a drastic increase of the global vulnerability and, therefore, of the seismic risk of entire urbanized sectors, such as historical centers (Pujades et al., 2012). The seismic vulnerability, for definition, is assumed as the propensity of buildings to suffer a certain damage under a given seismic event. The vulnerability assessment methods suggested by current codes are often based on a series of prerequisites, such as strong connections among structural components, presence of rigid floors, etc., which are difficult to be detected in old urban centers (Valluzzi et al., 2004).

The existing masonry buildings in the historic centers are often grouped in aggregates, so that they, in general, can mutually interact under seismic actions.

This type of buildings are often erected according to a traditional code of practice with typologies (multi-materials masonry, multi-leaf walls) and construction details (poor connections among intersecting walls, among walls and floors, and even between layers in the thickness), which in many

cases show behavioral deficiencies in terms of stability and safety against seismic actions (Borzi et al., 2008; Formisano, 2017a). Nevertheless, several factors exist conditioning their performance, mainly depending on the interactions among the single structural units (SUs). Generally, the presence of effective connections among SUs prevents the occurrence of local collapse mechanisms in several cases. However, the presence of construction irregularities (e.g., walls not well-connected to each other) and/or geometric ones (e.g., buildings with different heights) are the main causes of the activation of out-of-plane collapse mechanisms (Barbieri et al., 2013).

The interactions between adjacent buildings must be properly considered when studying the vulnerability of the whole aggregate, since the dynamic response of a building is often strongly influenced by the presence of adjacent structural units. Generally, the capacity of the single SUs can differ significantly from the capacity of the whole aggregate, especially in case of flexible floors. In fact, this type of construction can show complex non-linear responses, which vary greatly from the degree of connection between adjacent buildings.

There are many vulnerability factors that must be taken into consideration to study the seismic capacity of buildings in aggregate configuration. These vulnerabilities significantly affect the dynamic response of the structure. In particular, it is worth highlighting the in-plan-distribution of the resistant elements (walls), the presence of staggered floors and the structural heterogeneity between adjacent buildings. Mechanical models were developed in different works (Formisano et al., 2011, AGGIUNGERE ALTRI LAVORI DI ALTRI AUTORI), where the uncertainties related to the vulnerability factors were taken into account in order to quantify the seismic response of the entire aggregate. From a computational point of view, the structural model must be akin to what is found in reality. In this case, the influence of adjacent structural units is an intrinsic condition of the mechanical model itself.

Due to the structural continuity, the seismic behavior of single buildings is strongly affected by the interactions between their structural parts, connected to each other. In most cases, it is quite difficult to uniquely identify a structural unit (SU).

Anyway, the investigation of the seismic global behavior of the single building as part of the aggregate is desirable in order to obtain a better evaluation of its seismic performance, which is a fundamental phase to set up efficient retrofitting techniques (Formisano et al., 2011).

However, Formisano and Massimilla (2018) proposed simplified theoretical and refined non-linear analyses of the seismic response of structural units in aggregate condition. In particular, the authors proposed a procedure calibrated on the results of a numerical model, used to investigate a basic building compound representative of the constructive techniques developed in the Southern Italy. To this purpose, two basic models were considered for mechanical analysis. The first one was related to the whole aggregate, while the second one was the structural model of the single structural unit modeled as an isolated structure. Thus, the isolated structure was equipped with proper boundary elements under form of elasto-plastic links, whose non-linear behavior was calibrated on the results

of the structural analysis performed on the model of the whole aggregate, in order to represent the real seismic behavior of the structural unit placed either in the intermediate position or in the head one. Basically, the reconstruction of the pushover curves of the single SU when the whole aggregate is modeled allows for estimating the influence of other SUs on the seismic behavior of the SU under study in aggregate configuration. In fact, once the capacity curve of the whole aggregate is known, for each step of the non-linear analysis, it is possible to evaluate shear forces and nodal displacements of the different SUs. Therefore, in each analysis direction, the total base shear of the aggregate SU is given by the contribution of both its walls and those of adjacent SUs, whereas, the top-displacements are estimated as those of the building centroid at the last level, whose entity results to be increased or reduced with respect to that of the isolated SU centroid, depending on the position, the latter occupies in the building compound. In particular, the top floor centroid displacements are amplified for the heading building, where the in-plane torsion effects of the aggregate are significantly large, while they are reduced for the intermediate SU, where the two structures next to those considered reduce its deformability (Formisano et al., 2016).

As an example, the 2009 L'Aquila Earthquake showed the high vulnerability of old city centers, whose ancient masonry buildings were seriously damaged by disastrous effects resulting from the combination of horizontal and vertical accelerations (D'Ayala and Paganoni, 2011; Lagomarsino, 2012).

Therefore, the seismic vulnerability evaluation of historical buildings, with particular attention to the clustered ones, represents a key issue in the field of Seismic Engineering. It can be performed by means of two main approaches of hybrid (Kappos et al., 2006) and mechanical (Lourenço and Roque, 2006; Penna et al., 2014; Formisano, 2017b) type.

The first approach allows for the estimation of the global vulnerability through quick analyses principally based on vulnerability forms widely used all over Europe (Ferreira et al., 2013; Brando et al., 2017; Formisano et al., 2017; Tiberti and Milani, 2017; Chieffo et al., 2018). This methodology allows to univocally correlate the building seismic vulnerability index, $I_v$, deriving from filling specific survey forms, with the possible expected damage (Lagomarsino and Giovinazzi, 2006), which is expressed through the mean damage grade, $\mu_D$, following the European Macroseismic Scale, EMS-98 (Grünthal, 1998). The peculiarity of this procedure, therefore, is to have a direct correlation between the cause (expected damage) and the effect (seismic event). Another congenial methodology, developed by the University of Padua, is the Vulnus method, which allows to estimate the seismic vulnerability of building aggregates by means of statistical-parametric analysis based on their probable collapse mechanisms (Munari et al., 2010).

On the other hand, the mechanical approach, which is based on refined non-linear FEM analyses, is not very adaptable to the seismic vulnerability study of urban centers constructions, due to it being highly time consuming to obtain information on all the clustered buildings interacting under earthquakes. Nevertheless, some simplified assumptions were developed to study only single SUs, neglecting the modeling of adjacent constructions,

by taking into account, at the same time, their inclusion in the building compound (Formisano and Massimilla, 2018). Normally, in the framework of this approach, the knowledge of the building typology, as well as its mechanical characteristics, are the essential starting points for the calibration of the structural model (Calvi et al., 2006).

Therefore, an accurate investigation plan and an adequate analysis methodology (non-linear static or dynamic) allows for calibration of the structural model based on fundamental issues, such as preliminary historical researches, interpretation of the constructive development during the time and evaluation of general structural characteristics of the construction. In addition, it is advisable, as proposed by Ramos and Lourenço (2004), to make a complete diagnosis of the building by means of *in-situ* investigations or non-destructive tests on materials, in order to set up a reliable numerical model for performing careful seismic assessments and for implementing appropriate retrofitting interventions aimed at satisfying security and reversibility requirements. Therefore, based on these considerations, this paper proposes the seismic vulnerability evaluation of a building aggregate located in Arsita (district of Teramo, Italy) affected by the 2009 L'Aquila seismic sequence. The study performed focuses attention on the vulnerability analysis of the case study by means of three distinct procedures, in order to compare the expected seismic behavior in terms of fragility curves for the whole aggregate and for individual structural units placed in the corner and intermediate positions.

# THE HISTORICAL CENTER OF ARTISTA

## Historical Background

Arsita is an Italian town with 889 inhabitants in the province of Teramo in Abruzzo. Located below the Camicia Mountain group (eastern side of the Gran Sasso of Italy massif), it is placed in the upper valley of the Fino river and is part of the mountain community of Vomano, Fino, and Piomba (**Figure 1**).

Localized about 30 km south of Teramo, its origins date back to the pre-Roman period, as evidenced by some archaeological findings, such as tombs, grave goods and various jewels, discovered in 1985. In addition, cinerary urns, tear vessels, oil lamps, floors, Roman coins of the city of Cerbolongo, mentioned by Tito Livio and destroyed in the lower empire, were found (Morisi, 1998). Its current urban configuration can be traced back to the late Middle Ages, at the beginning of the Renaissance period. In the 18th century, Arsita was transformed into a noble residence, keeping the aspect that still retains today, where some parts are in a serious state of abandonment.

## The L'Aquila Seismic Sequence

The Aterno valley is an area affected by devastating earthquakes in the last few centuries. The seismic history of this region recalls,
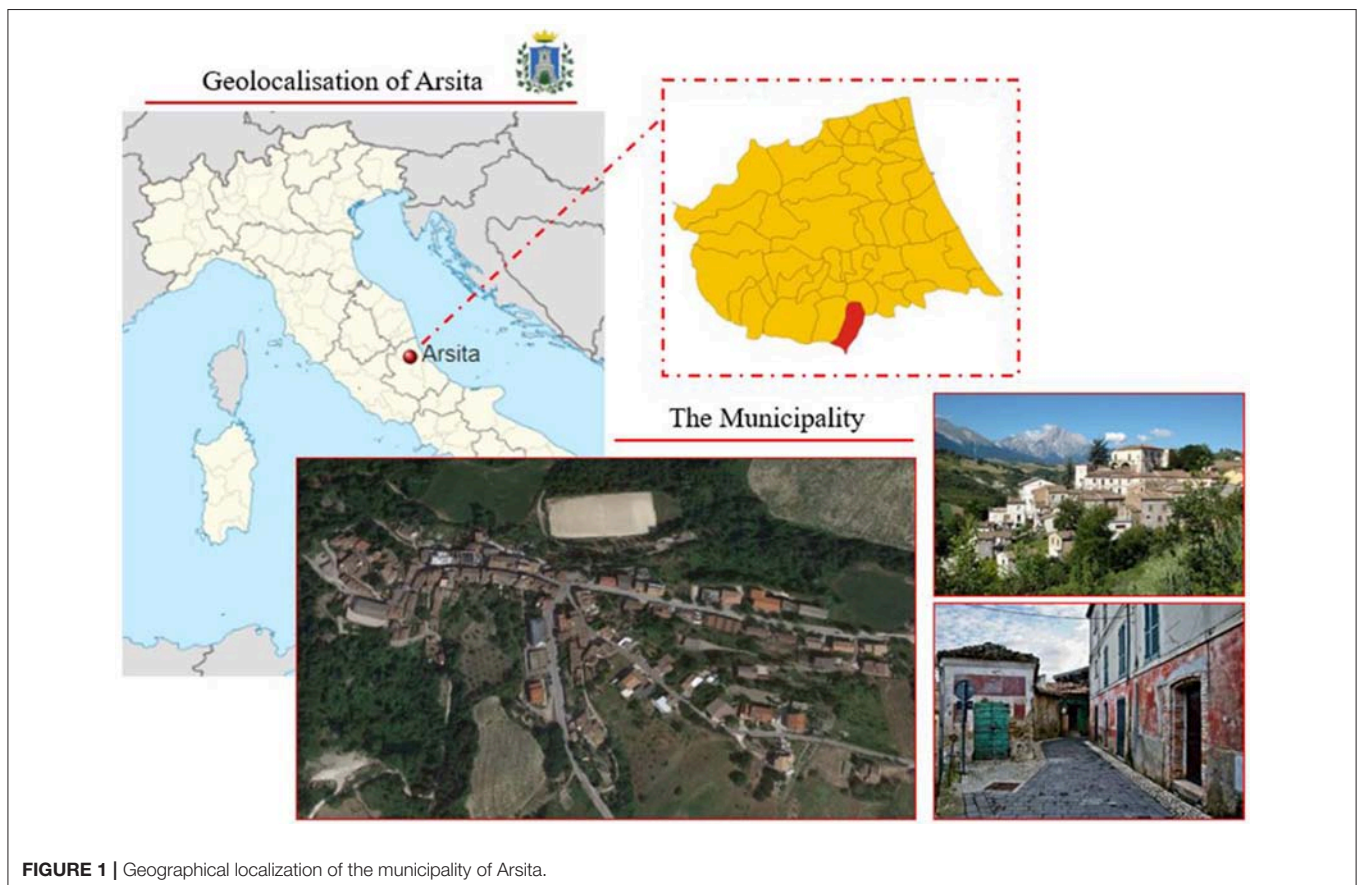


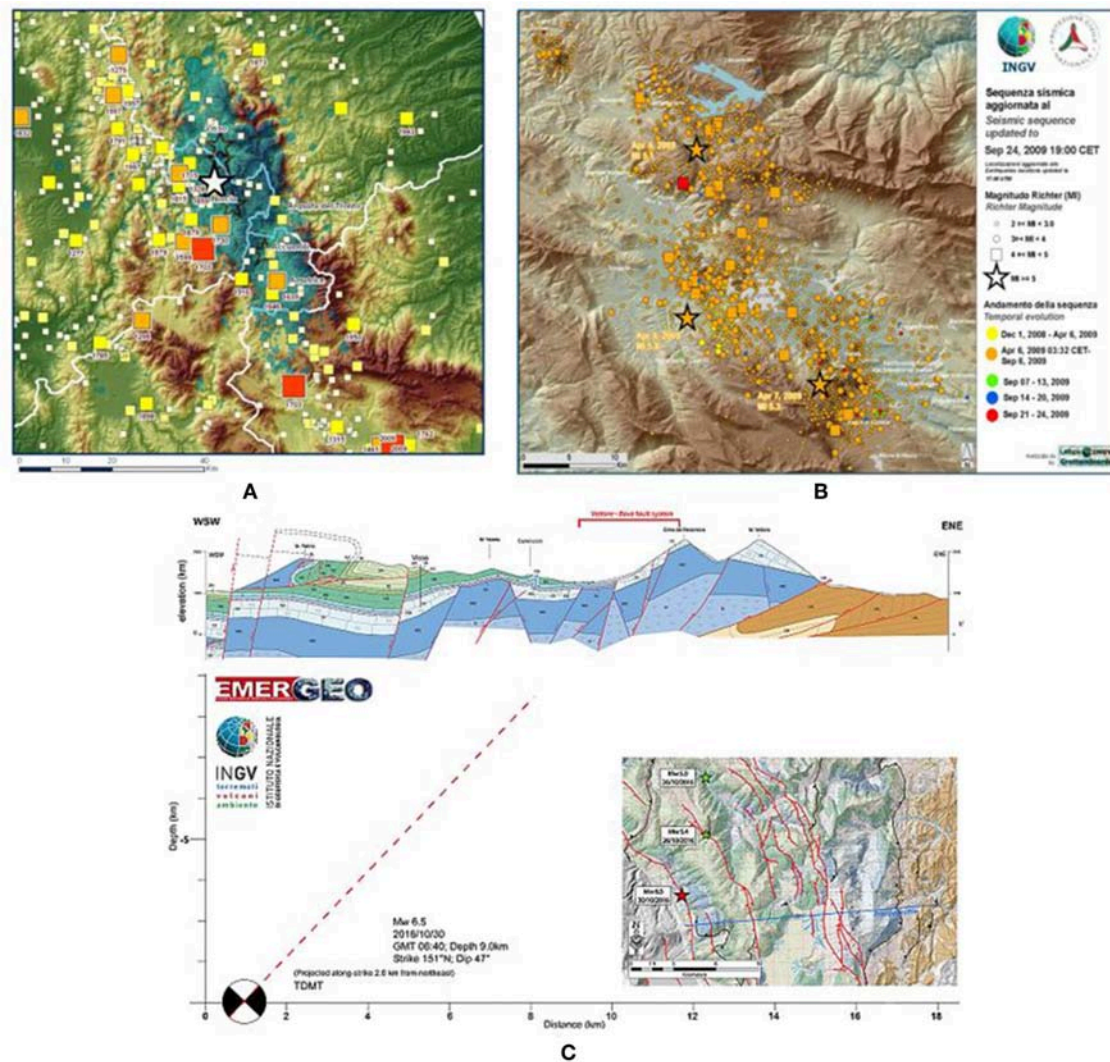**FIGURE 1 |** Geographical localization of the municipality of Arsita.

**FIGURE 2 | (A)** Historical seismic events, **(B)** distribution of epicenters recorded during the Central Italy earthquake, and **(C)** distribution of seismogenic source (National Institute of Geophysics Vulcanology, 2009).

of course, that of the city of L'Aquila. In fact, since its foundation in the late 13th century, this city underwent six destructive earthquakes, with maximum intensity in the Mercalli-Cancani-Sieberg scale, $I_{MCS}$, equal to IX recorded on 1349 September 9th, 1461 November 27th, and 1703 February 2nd. The 1349 earthquake had several epicenter areas, with the most important occurring in Venafro (Boncio et al., 2012).

However, the most severe seismic event affecting the Umbria-Abruzzo Apennines was that which occurred in 1,703 with magnitude moment $M_w = 6.7$. It hit several places (e.g., Poggio Picenze, San Gregorio, Sant'Eusanio Forconese, Paganica, Bazzano, Onna, Santa Rufina, and Tempera), including Castelnuovo, which reached an intensity equal to X (**Figure 2A**).

On April 6th 2009 at 3:33 a.m., the area of L'Aquila was hit by a strong earthquake, whose main shock had a Richter magnitude ($M_l$) of 5.8 and moment magnitude $M_w$ of 6.3 (Ameri et al., 2009).

After the main shock, a seismic sequence started with many replicas involving the epicenter area and the surrounding municipalities, as reported in **Figure 2B** (National Institute of Geophysics Vulcanology, 2009).

The distribution of replicas highlighted the area affected by the seismic sequence very well, which extends for over 30 km in the direction North-West—South-East, parallel to the axis of the Apennine chain. The strongest replica, recorded at 7:47 p.m. on April 7th, affected the southernmost sector of the area, near the centers of San Martino d'Ocre, Fossa, and San Felice d'Ocre, where small shocks were also detected in the same day. The event of April 9th having $M_l = 5.1$ is instead north located, along a structure of more limited extension, always parallel to the Apennine chain.

The extensional processes characterizing the deformation of the Apennine crust dominate the seismo-tectonic context of
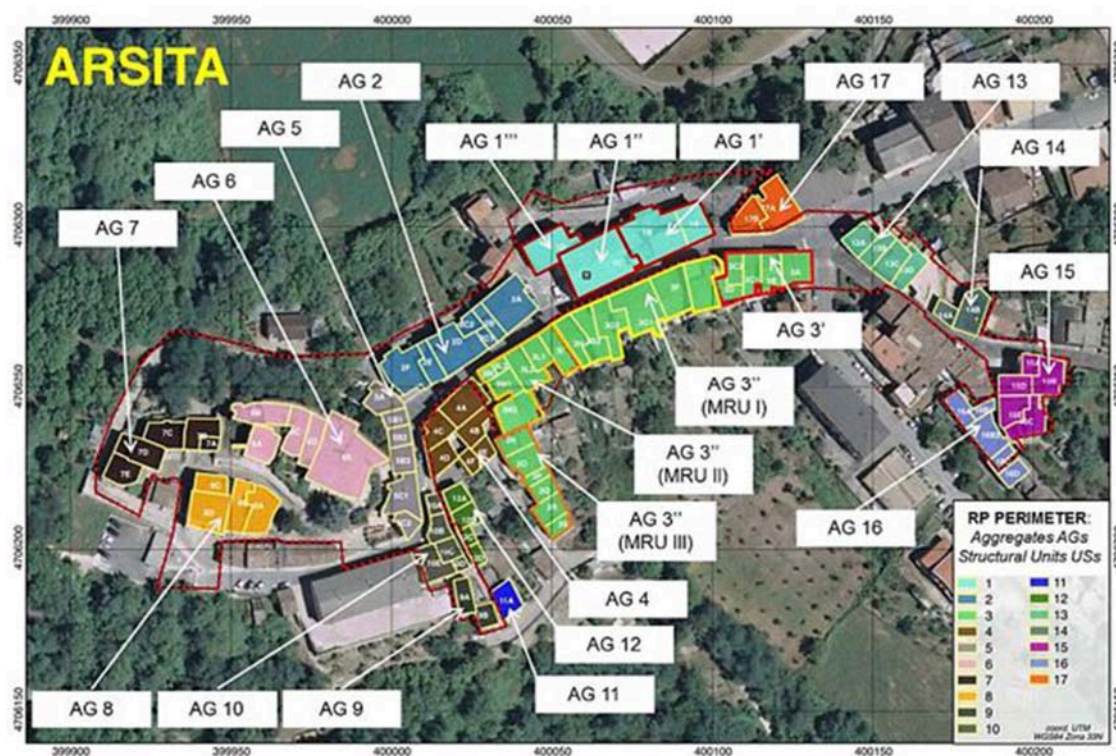
**FIGURE 3 |** Structural identification of masonry AGs and SUs (Indirli et al., 2014).

the L'Aquila area and, in particular, related to the North-East—South-West extension of this mountain chain.

This extension, estimated by GPS measurements as about 3 mm per year (D'Agostino et al., 2011), is accommodated by normal faults in the North-West—South-East direction, which all the major seismicity of the central Apennines should be ascribed to. The distribution of the effects induced by the 2009 April event was characterized by both the geometry and orientation of the activated fault and the rupture propagation depicted in **Figure 2C** (Galli and Naso, 2009). The latter figure shows a geological section (shown in the map with a blue line) between Norcia and Monte Vettore, with a 9 km depth hypocentre causing an earthquake of magnitude 6.5. The extension of the surface fault plane, according to the inclination ($dip \approx 47°$) of the focal mechanism, is reasonably indicated as the system responsible for this last seismic sequence. The damage in the epicenter area is determined not only by the earthquake magnitude, but also by the propagation direction and by the land geology. In particular, the greatest damage is observed in the direction where faulting spreads (directivity effect of the source) are amplified due to the presence of "soft" sediments, such as alluvial deposits and land to be returned, etc. In the case of the L'Aquila earthquake, the soil rupture spreads from the bottom upwards (then toward the city of L'Aquila) and from the North-West to the South-East, toward the Valle dell'Aterno.

## Typological and Structural Characterization of the Study Area

Considering the reconstruction plan of the Municipality of Arsita setup by the collaboration among National Agency for New Technologies, Energy and Sustainable Economic Development (ENEA—Bologna), University of Naples "Federico II," University of Chieti "Gabriele D'Annunzio" and University of Ferrara, 20 aggregates (AGs) consisting of 91 structural units (SUs), most of which are inside the perimeter area (RP perimeter), have been identified, as reported in **Figure 3** (Indirli et al., 2014).

In the study area, there are very different types of buildings. Together with historical buildings, usually made of not-squared stones (often alluvial pebbles) sustaining timber floors, there are groups of constructions completely abandoned and partially ruined, and have been so for several decades (Indirli et al., 2012). The spatial distribution of these typologies of buildings came from the simple centrifugal expansion of the old town. The identification of the mechanical characteristics of the masonry types have been done according to the National Code (M.D. 2 February 2009, 2009) through on-site data acquisitions (**Figure 4A**). In general, masonry walls have a thickness of about 0.65 m. Buildings develop in elevation from 2 to 3 stories.

The inter-story height is about 3.00 to 4.00 m for the first level and 3.00 to 3.50 m for the upper floors. Horizontal structures are generally made of timber elements, as reported in **Figure 4B**. The foundations consist of a shallow wall footing, which, in practice,
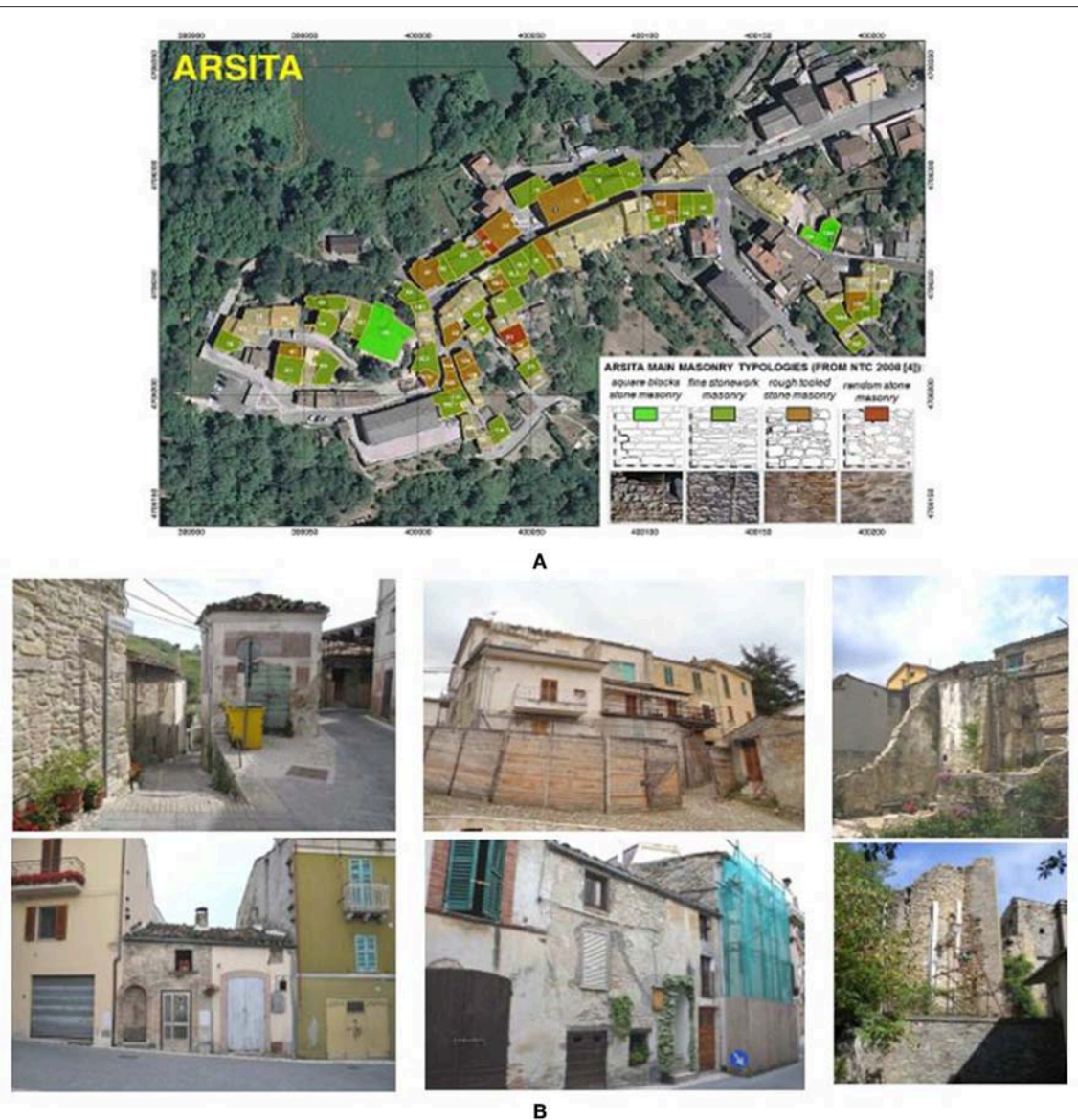
**FIGURE 4 |** Main masonry typology **(A,B)** street view of SUs within the historical center (Indirli et al., 2014).

is realized by arranging the masonry walls directly on the ground at a depth of about 1.50 m.

As a consequence of the seismic event that occurred, most of serious damages were found in stone structures, especially in the higher parts of the buildings (roofs, cornices, corners, etc.). Also, the lack of connections among perimeter walls orthogonal to each other (corners), which did not guarantee a structure global behavior, was the cause of numerous partial collapses.

## SEISMIC VULNERABILITY ASSESSMENT

### The Case Study

The case study herein examined is a masonry aggregate identified with the number 8 (AG.8), consisting of 4 structural units (SUs),

denominated 8A, 8B, 8C, 8D, having different seismic behavior deriving from diverse in-plane positions they have (**Figure 5**).

The case study aggregate, erected earlier than 1919, has both residential and productive destinations of use. The constitutive materials are masonry stones typical of the Abruzzo region. Horizontal structures are made of steel beams and hollow tiles. Timber beams, which sustain overlying timber plank and tiles, are the load-bearing members of roofing.

Regarding the morphology, the aggregate is rather regular in plan, while the major discontinuities are detected in elevation, with the presence of staggered floors and floors at different heights due to the soil slope.

In the present study, the seismic vulnerability of inspected clustered buildings has been appraised by means of three different
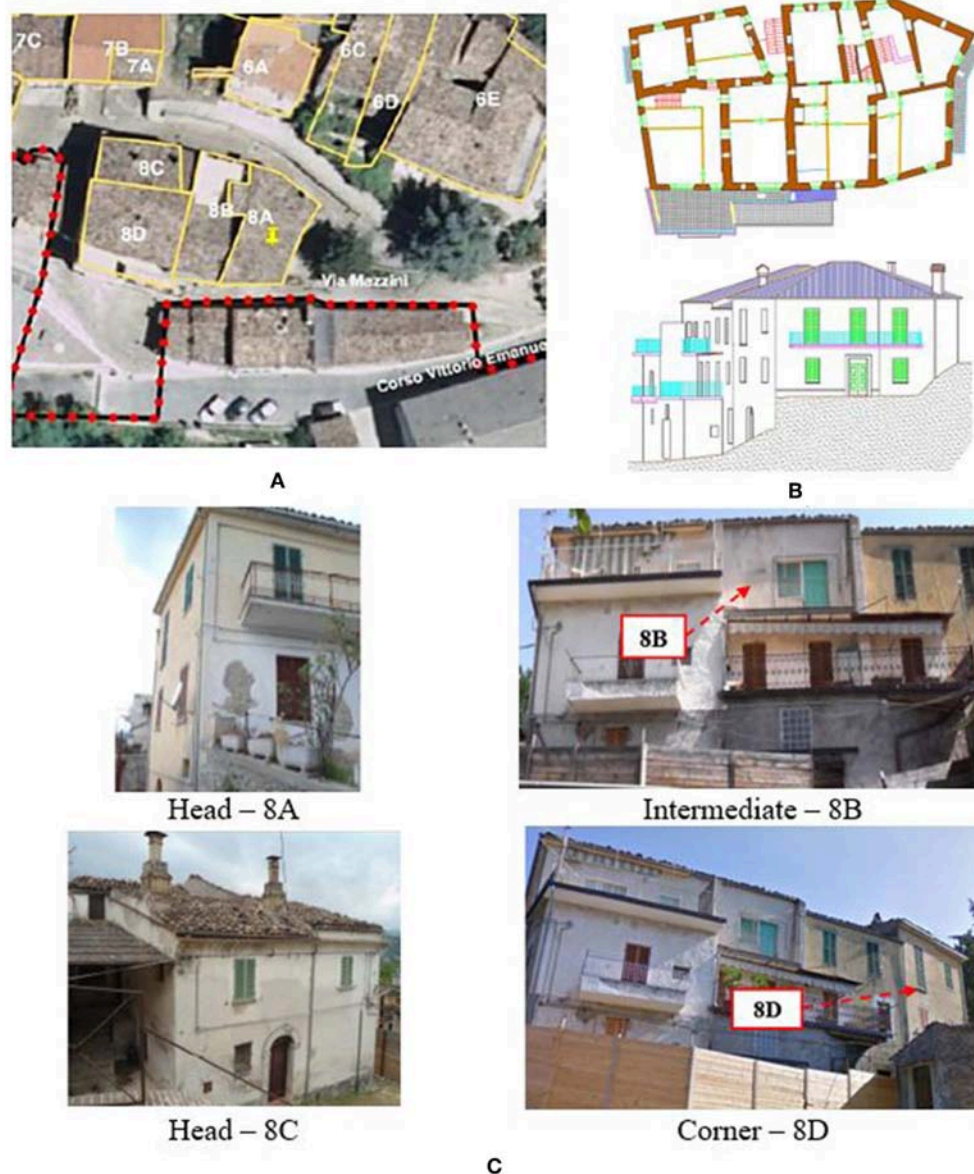
**FIGURE 5 |** Structural configuration of the case study masonry buildings aggregate: **(A)** plan layout of the intermediate floor, **(B)** South-West view, and **(C)** positions of SUs in the compound of buildings.

methods (macroseismic, Vulnus, and mechanical), in order to have both a general overview of the seismic health state of the building compound and a careful comparison among examined analysis approaches.

## Macroseismic Approach

The macroseismic approach is a reliable method for large-scale seismic assessment of historical centers buildings, which is widely adopted at international level (Ferreira et al., 2012; Azizi-Bondarabadi et al., 2016; Cavaleri et al., 2017; Azap et al., 2018; Formisano and Chieffo, 2018a). It allows to determine the expected damage of constructions, defined according

to the EMS-98 scale (Grünthal, 1998), starting from their vulnerability index.

A quick seismic evaluation procedure for masonry aggregates based on a dedicate survey form has herein been used for determination of the vulnerability index (Formisano et al., 2011, 2015; Chieffo and Formisano, 2019; Chieffo et al., 2019).

This new form is based on the Benedetti and Petrini's vulnerability index method (Benedetti and Petrini, 1984), widely used in the past as a rapid technique for a detailed screening of the main features of individual buildings to investigate their seismic vulnerability. This method is based on a vulnerability form, consisting of 10 parameters that take into account the

constructive and structural characteristics of isolated buildings. Such a form was subsequently modified with minor adjustments by the Italian Defense National Group against Earthquakes (GNDT) for seismic vulnerability assessment of masonry and RC buildings located in historical centers.

The new form for masonry building aggregates is obtained by adding five supplementary parameters to the 10 basic parameters of the original form. The introduction of these new parameters takes into account the structural or typological heterogeneity, the interaction effects and the different opening areas among adjacent SUs when they are subjected to seismic actions. Methodologically, this kind of approach is based on the calculation, for each SU, of a vulnerability index, $I_v$, as the weighted sum of 15 parameters. These parameters are distributed into 4 classes (A, B, C, and D) with scores, $S_i$, of growing intensity. Each parameter is characterized by a weight $W_i$, representing the more or less importance for vulnerability estimation, that can range from a minimum value of 0.25 to a maximum one of 1.50. The vulnerability index, $I_v$, can be calculated as the sum of the class score individuated for each parameter multiplied by the respective weight, as shown in the following equation:

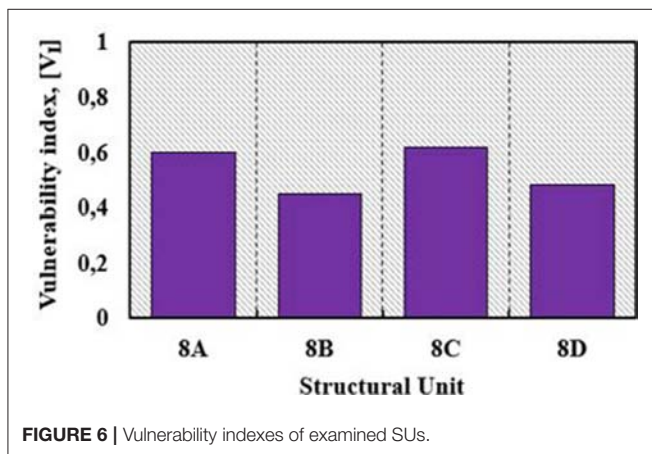$$I_V = \sum_{i=1}^{15} S_i \times W_i \qquad (1)$$



FIGURE 6 | Vulnerability indexes of examined SUs.

Subsequently, $I_v$ is normalized in the range [0 ÷ 1], adopting the notation $V_I$, by means of the following relationship:

$$V_I = \left[ \frac{I_V - (\sum_{i=1}^{15} S_{min} \times W_i)}{\left| \sum_{i=1}^{15} [(S_{max} \times W_i) - (S_{min} \times W_i)] \right|} \right] \qquad (2)$$

The application of this procedure to the selected clustered buildings has allowed to obtain the seismic vulnerability index of the four SUs (**Figure 6**).

In the previous figure, it is seen that the intermediate SU (8B) has the less vulnerability index, while the highest index has been achieved by the corner SU (8C). In particular, the unit 8B shows a vulnerability decrease of about 30% with respect to unit 8C. However, in order to take into account, the vulnerability of the whole aggregate, a global average vulnerability, $V_{IM}$, intended as the average of the vulnerability indexes of individual SUs, has been estimated as equal to 0.53 with a standard deviation ($\sigma_i$) of 0.085.

Subsequently, vulnerability curves have been derived to estimate the propensity at damage of the analyzed SUs for different seismic intensities (Lagomarsino and Giovinazzi, 2006). More in detail, these curves can be properly defined as the probability P[SL|I] that a building class reaches a certain damage threshold "DS" at a given macroseismic intensity "$I_M$," defined according to the European Macroseismic Scale (EMS-98) (Grünthal, 1998).

In particular, as mathematically expressed by Equation (3), vulnerability curves depend on three variables: the vulnerability index ($V_I$), the hazard, expressed in terms of macroseismic intensity ($I$), and a ductility factor $Q$, ranging from 1 to 4, which describes the ductility of typological classes of buildings and has been assumed as equal to 2.3 (Lagomarsino, 2006).

$$\mu_D = 2.5 \left[ 1 + tanh \left( \frac{I + 6.25 \times V_I - 13.1}{Q} \right) \right] \qquad (3)$$

Finally, it is also been possible to derive vulnerability curves for the single SUs and for the whole aggregate, the latter using the
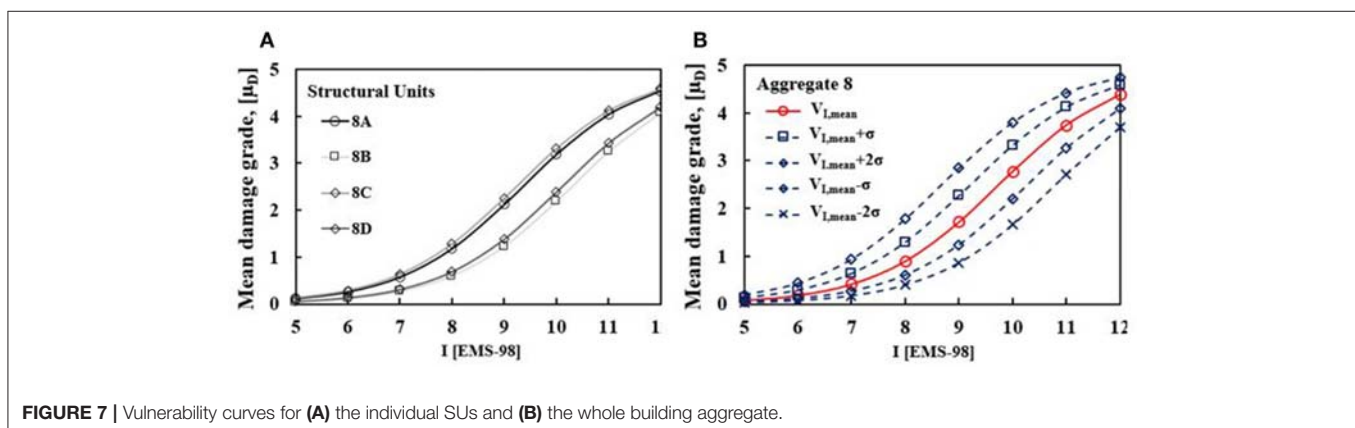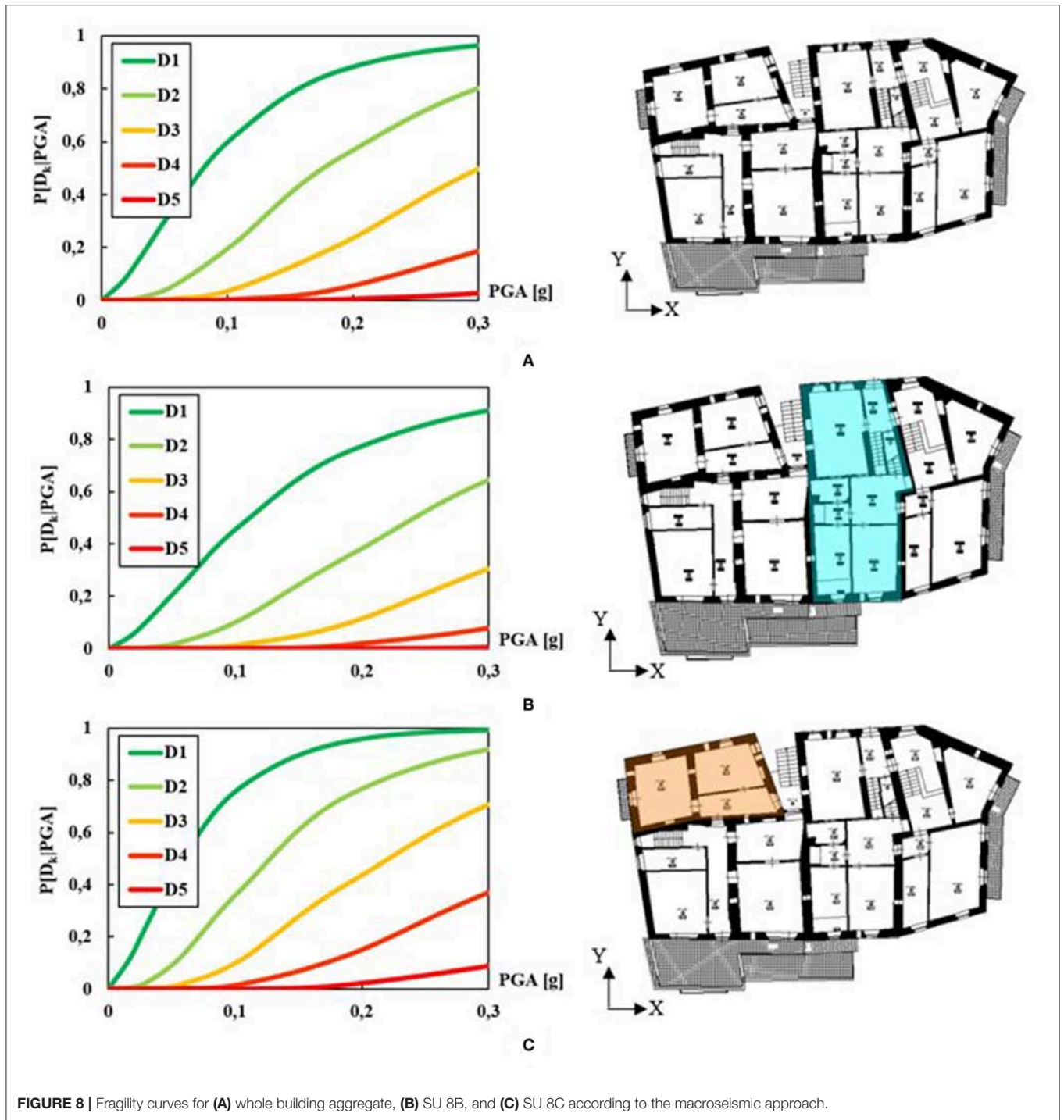


FIGURE 7 | Vulnerability curves for (A) the individual SUs and (B) the whole building aggregate.

**FIGURE 8 |** Fragility curves for **(A)** whole building aggregate, **(B)** SU 8B, and **(C)** SU 8C according to the macroseismic approach.

mean value of the vulnerability index, $V_{I,mean}$, and the upper and lower bound ranges of the vulnerability index distribution for different scenarios ($V_{I,mean} - \sigma$; $V_{I,mean} + \sigma$; $V_{I,mean} - 2\sigma$; $V_{I,mean} + 2\sigma$). The obtained results have been plotted in **Figure 7**.

Moreover, in order to have an estimation of the expected damage in terms of PGA, it has been possible to derive the fragility curves (**Figure 8**) by a direct correlation between

macroseismic intensity, $I_{EMS-98}$, and ground motion $a_{max}$ according to the law proposed by Guagenti and Petrini (1989):

$$\log a_{max} = C_1 \bullet I_{EMS-98} - C_2 \ [g] \tag{4}$$

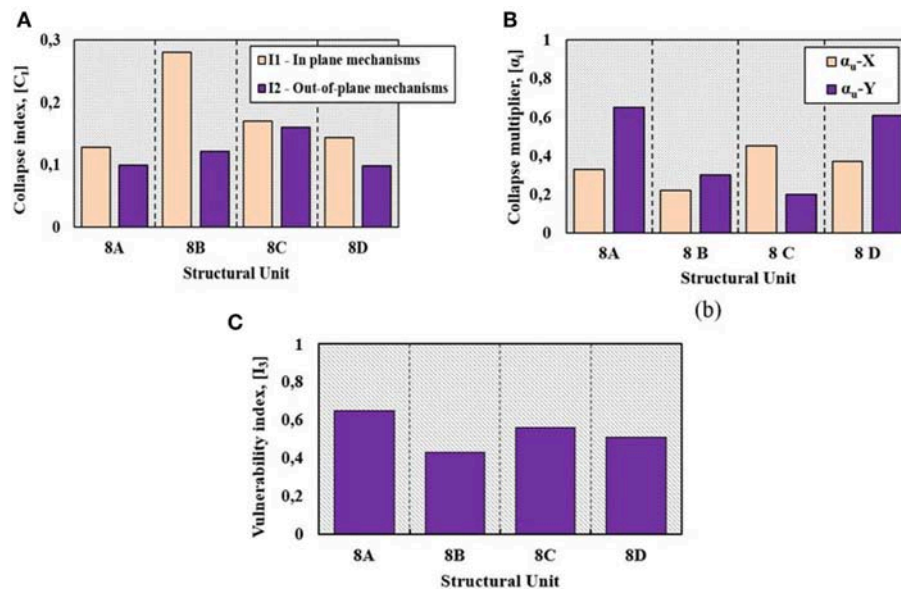where the correlation coefficients $C_1$ and $C_2$ are 0.602 and 7.073, respectively.

According to the national seismic classification (OPCM, 2003), the Municipality of Arsita belongs to the Zone 2, that is affected by strong earthquakes with an expected maximum PGA of 0.25 g, which has a 10% probability of being exceeded in 50 years. The result obtained shows that the aggregate position strongly affects the global vulnerability and, therefore, the expected damage. In particular, it is possible to see how the expected damage for SU 8C is more marked than those which should be attained in the other examined cases.

## Vulnus Method

The Vulnus Method (Da Porto et al., 2013), developed by the University of Padua, is a seismic vulnerability assessment approach mainly based on statistical analysis of possible collapse mechanisms that could be activated into masonry buildings. It is a procedure to identify the collapse multiplier, $\alpha_i$, calculated by means of kinematic analysis, to ascertain whether a mechanism occurs or not and, in positive case, to establish what is the corresponding probable damage.

This methodology, mainly used for unreinforced masonry (URM) buildings, is based on the fuzzy set theory for estimation of collapse multipliers (Bernardini et al., 1990) and definition of fragility curves (Fava et al., 2016). Operatively, the vulnerability is studied by means of three indexes: $I_1$ and $I_2$, which take into account the probable in-plane and out-of-plane mechanisms, respectively, and $I_3$, which considers the vulnerability parameters of the GNDT method and is assigned depending on the relative importance of the factors affecting the building vulnerability.

More in detail, for in-plane behavior, $I_1$ is defined as the ratio between the in-plane shear strength of walls in the weakest building direction and the total building weight ($W$), whereas for the out-of-plane behavior, $I_2$ is the ratio between the average

acceleration related to out-of-plane mechanisms of perimeter walls and the gravity acceleration.

Finally, the method allows to estimate the probability of reaching a specific damage threshold due to the occurrence of collapse mechanisms, according to the indexes previously described (Da Porto et al., 2018).

Referring to the examined building, the geometric characteristics of the entire building aggregate have been appropriately defined using the form provided by the Vulnus method. In accordance with the prescriptions of NTC18 (M.D. 17 January 2018, 2018), the masonry material has been classified as stone masonry. Therefore, adopting a knowledge level LC1 with a confidence factor (FC) equal to 1.35, the mean values of the resistances and the average of the elastic modules have been adopted. In particular, it has been assumed that the compressive strength, $f_m$, is equal to 1.0 MPa, the characteristic tensile strength, $f_t$, is equal to 0.1 MPa and the shear strength, $\tau_0$, is equal to 0.018 MPa. In addition, the elastic modules, $E$ and $G$, are equal to 870 MPa and 290 MPa, respectively.

Subsequently, the $I_1$, $I_2$, and $I_3$ factors have been calculated for estimating the collapse indexes, $C_i$, the collapse multipliers, $\alpha_i$, and the vulnerability indexes of different SUs (**Figure 9**).

As it is seen in **Figure 9A**, the greatest propensity at in-plane damages is for SU 8B, while the SU that should suffer the highest out-of-plane damage is the 8C one. This circumstance denotes how the intermediate structural units are more influenced by in-plane mechanisms than out-of-plane ones.

On the contrary, SUs in head position are more susceptible to undergo out-of-plane collapse mechanisms, as they do not take profit of the confinement action induced by adjacent buildings. These results are confirmed by the ranking of collapse multipliers achieved in **Figure 9B**. In fact, it is worth noting that the minimum collapse multiplier of the SU 8B corresponds to the X
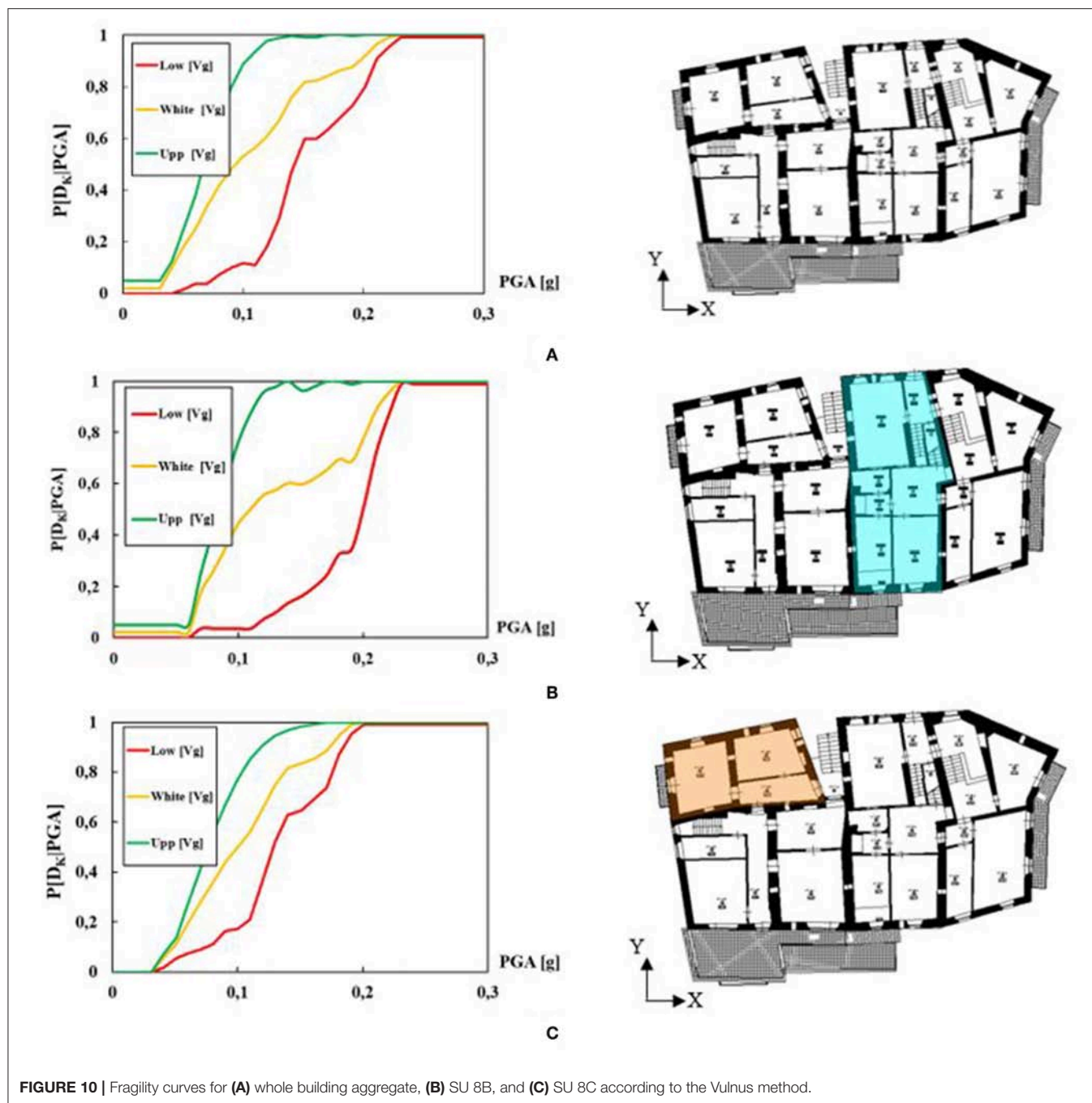
**FIGURE 10 |** Fragility curves for **(A)** whole building aggregate, **(B)** SU 8B, and **(C)** SU 8C according to the Vulnus method.

direction ($\alpha_u - {}_X = 0.22$), while for the SU 8C, this multiplier is equal to 0.2 in the Y direction. Moreover, referring to the index $I_3$ (**Figure 9C**), the vulnerability indexes, calculated according to the GNDT method, are comparable with those deduced through the macroseismic method.

Finally, fragility curves (**Figure 10**) have been defined as cumulative probability distributions of the damage. They have been represented by the upper (Upp [$V_g$]) and lower (Low [$V_g$]) bounds of the fragility domain and by a mean distribution curve (White [$V_g$]), which represents the most probable expected damage values for different seismic accelerations.

As it is noticed in **Figure 10**, the expected damage frequency for SU, 8C is greater than that detected for both the SU 8B and the whole building compound.

## Mechanical Method

The mechanical method has been applied by means of non-linear analysis performed using the 3Muri software (S.T.A.data srl, 2017). This software is based on the equivalent frame model, assuming that the response of masonry walls with openings can be considered to be equivalent to that of a set of single-dimensional macro-elements (columns, beams, and
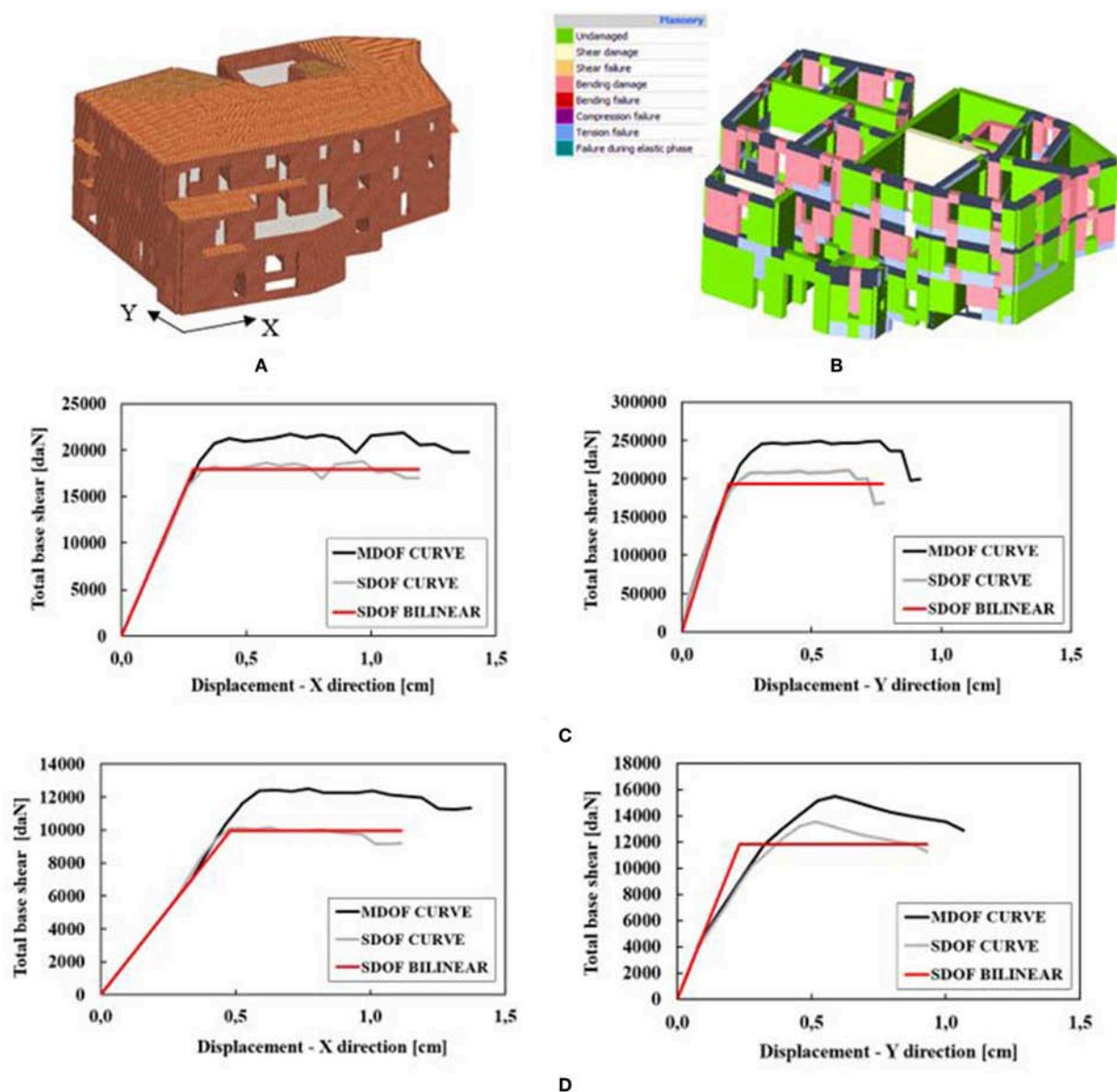
**FIGURE 11 |** Numerical analysis on the building aggregate under study: **(A)** 3D macroelement model, **(B)** failure mechanisms in direction X, and **(C,D)** pushover curves of SUs 8B and 8C.

**TABLE 1 |** Damage levels for mechanical fragility curves.

| Damage Level | | |
|---|---|---|
| D1 | $0{,}7 \cdot \Delta_y$ | No damage |
| D2 | $1{,}1 \cdot \Delta_y$ | Moderate |
| D3 | $0{,}5 \cdot (\Delta_y + \Delta_u)$ | Intensive |
| D4 | $\Delta_u$ | Collapse |

nodes). The damage is concentrated into deformable columns and beams, while rigid nodes consist of undamaged masonry parts confined between the two previously mentioned elements. The strength criteria of deformable elements have been given

on the basis of EN 1998-3 (Eurocode 8, 2005) provisions, which are established as allowable maximum drifts for shear and flexural collapse mechanisms the values of 0.4% and 0.8% of the ultimate displacement ($d_u$). The analyses have been performed according to the two main directions, X and Y. For each direction, the accidental eccentricity (positive and negative) has been considered. The aforementioned analyses have been interrupted at 20% decay of the maximum shear resistance, as suggested in Formisano et al. (2013) and Formisano and Chieffo (2018b). The mechanical characteristics of used materials have been taken as indicated in Section Vulnus Method. The 3D macroelement model of the case study building aggregate and failure mechanisms in the X direction are presented in
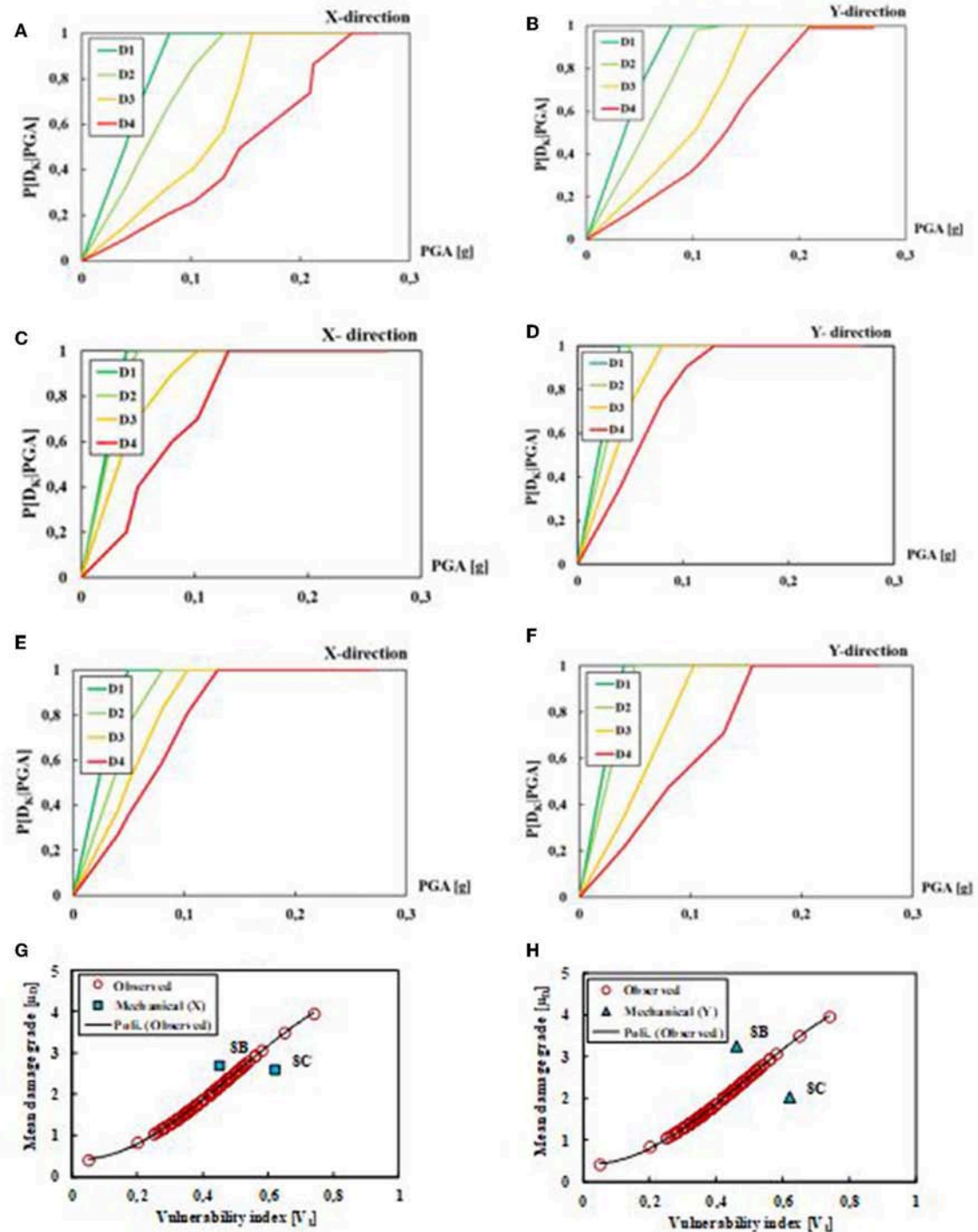
FIGURE 12 | Discretised mechanical fragility curves in the main analysis directions for (A,B) building aggregate, (C,D) SU 8B, (E,F) SU 8C and correlation among numerical results and observed damages for SUs 8B and 8C in directions X (G), and Y (H).

**Figures 11A,B**, respectively. Furthermore, in order to consider the effect of the mutual interaction among single SUs in the aggregate, the pushover curves of intermediate and head buildings in the two main directions, X and Y, have been derived through an appropriate procedure (Formisano et al., 2016) (**Figures 11C,D**).

This procedure allows extraction of the seismic response of single SUs from that of the whole building compound.

Later on, discretised mechanical fragility curves have been defined on the basis of both damage thresholds ($D_K$, with $K = 1$, 2, 3, and 4) recalled in **Table 1** (Lagomarsino and Cattari, 2014) and different punctual seismic acceleration intensities.

In the mechanical approach, the damage threshold, is estimated as the ratio between the seismic demand displacement ($D$) and the seismic capacity one ($C$).

Thus, referring to the SDoF system, the fragility curves of the whole aggregate, as well as of SUs 8B and 8C, in X and Y directions have been derived (**Figure 12**).

From the obtained fragility curves, it is apparent that, for the whole building aggregate, the occurrence probability of predetermined damage states are lesser than ones underwent by single SUs. As an example, for the expected PGA of 0.25 g and for the D4 limit state (collapse), the damage probabilities are equal to 60% (X direction) and 80% (Y direction) for the whole building aggregate.

On the other hand, under the same conditions of PGA and limit state, the considered SUs exhibit an occurrence probability of 100% in both analysis directions.

Finally, in **Figures 12G,H**, the comparison among numerical analysis results achieved on the aggregated SUs and observed damages occurred in the study area has been presented. Comparing the 3Muri results in both analysis directions with damages detected in the historical center of Arsita under the occurred seismic intensity, $I_{EMS-98} = VI$ (Indirli et al., 2012), it has been observed that the formers are close to the observational damage curve in direction X only. Moreover, if compared to the real damages detected from the *in-situ* survey, the numerical damages achieved from 3Muri analysis are on the safe side for SU 8B only. Therefore, the 3Muri program is able to foresee the seismic damages expected by intermediate SUs in compound in satisfactory way.

## COMPARISON OF RESULTS

In the current section, the comparison of results obtained through the applied analysis methodologies for the whole building aggregate and single SUs has been performed. About the clustered buildings, the results in terms of vulnerability index have been compared to each other, in order to have a direct assessment of the use effectiveness of simplest methodologies.

Therefore, the vulnerability indexes deriving from the macroseismic (EMS-98) analysis and the Vulnus method have been considered as the average values deriving from the indexes of single SUs in order to be compared appropriately to the results obtained from the mechanical (3Muri) methodology (**Figure 13**).

The obtained comparison provides similar results between the macroseismic method and the Vulnus one. This means that the two methods have the same reliability level in predicting the building compound seismic vulnerability. However, the results obtained with these methods are not on the safe side if compared to those deriving from the 3Muri method. In fact, the mechanical analysis provides vulnerability indexes higher than the average values of the two methodologies of 16 and 36% in X and Y directions, respectively.
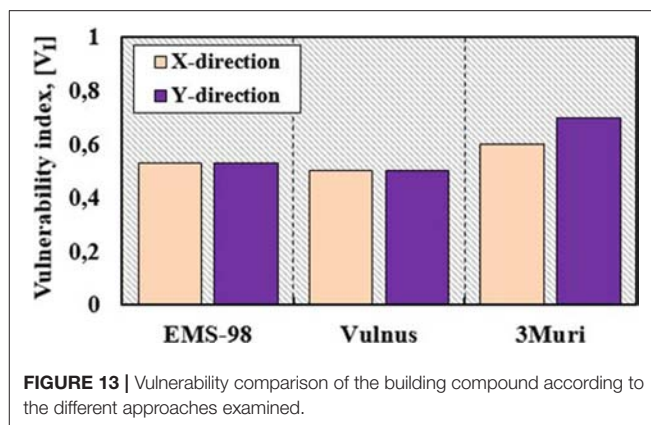


**FIGURE 13 |** Vulnerability comparison of the building compound according to the different approaches examined.

Subsequently, the comparison has been also carried out in terms of expected damage through the fragility curves reported in **Figure 14**.

From comparison results, it is noticed that, in the case of aggregate condition, the mechanical procedure and the Vulnus method provide very similar results, while the macroseismic method underestimates the expected damage. In fact, for the sake of example, in X direction (**Figure 14A**) and similarly in Y one (**Figure 14B**), for an expected PGA of 0.25 g, referring to the damage threshold D4–D5 (collapse), the mechanical procedure and Vulnus give rise to a probability of occurrence equal to 60 and 65%, respectively, whereas the macroseismic method provides an almost zero probability.

On the contrary, for single SUs, a clear distinction among the curves of analyzed methodologies is noticed.

In fact, the most conservative approach is the mechanical one, which provides in X and Y directions much more restrictive values of the occurrence probability than those related to the other two methodologies. Particular attention must be paid to the SU 8C, since the occurrence probability values related to low damages derived from the Vulnus and the macroseismic procedures are very similar in the two directions (**Figures 14E,F**). On the contrary, for medium-high damage levels, the Vulnus procedure is on the safe side in predicting the occurrence probability values. Moreover, it is possible to note how the SU 8C is the most vulnerable at damage, since the initial slopes of the fragility functions are higher than the ones characterizing the curves obtained from the other methods.

Finally, the Vulnus fragility curves are placed in a middle range between the upper limit curves (mechanical method) and the lower limit ones (macroseismic approach) of the fragility domain.

## CONCLUDING REMARKS

The present study has allowed to compare the seismic vulnerability of a building aggregate located in the municipality of Arsita, hit by the 2009 L'Aquila earthquake, through three distinct procedures, namely the macroseismic approach, the
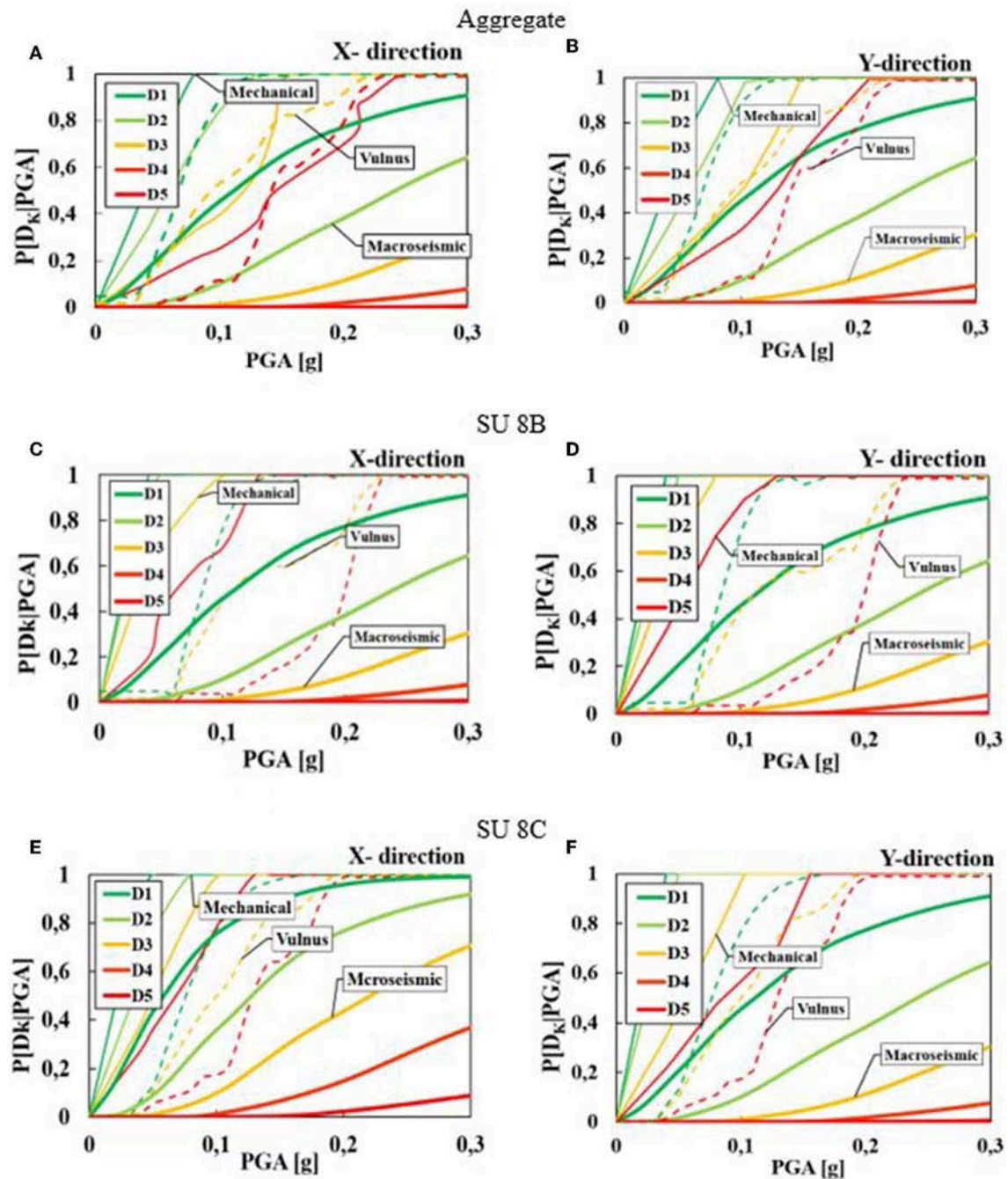
**FIGURE 14** | Comparison among examined vulnerability analysis methods in terms of fragility curves for Aggregate **(A,B)**, SU 8B **(C,D)**, SU 8C **(E–F)**.

Vulnus method and the mechanical non-linear macroelement analysis with the 3Muri software.

The first comparison has been made in terms of vulnerability index of the whole building compound achieved by the three proposed procedures. The vulnerability indexes of both the macroseismic analysis and the Vulnus method have been considered as the average values deriving from the single SUs indexes, in order to be compared with the

results obtained from the mechanical methodology. The obtained comparison has provided similar results between the macroseismic method and the Vulnus one, but both of them have not been on the safe side if compared to those deriving from the 3Muri method. In fact, these latter values have been 16% and 36% higher than the average values of the two methodologies in X and Y directions, respectively.

Subsequently, the analysis of results has been also made in terms of fragility curves. In particular, fragility curves of the whole aggregate derived from analysis with 3Muri have been compared to those of single structural units. From achieved results, it is apparent that, for the whole building aggregate, the occurrence probability of predetermined damage states has been lesser than that of single SUs. Also, it has been noticed that the intermediate SU (8B) behaves better that the corner one (8C).

On the other hand, with reference to the comparison among the inspected methodologies in terms of expected damage, it has been obtained that, in case of aggregate condition, the mechanical procedure and the Vulnus method provide very similar results, while the macroseismic method underestimates the seismic damage. On the contrary, for single SUs, a clear distinction among the curves of analyzed methodologies is noticed. In fact, the most conservative approach is the mechanical one, which provides in X and Y directions much more restrictive values of the occurrence probability than those related to the other two methodologies. With reference to the SU 8C, it has been noticed that the damage occurrence probability related to the serviceability limit state derived from the Vulnus and the macroseismic procedures are very similar in the two analysis directions. On the contrary, for life safety and collapse limit states, the Vulnus procedure is on the safe side in predicting the occurrence probability values.

Moreover, the SU 8C has resulted to be the construction most vulnerable at damage, since the initial slopes of the fragility functions have been higher than those characterizing the curves obtained from the other methods. Finally, the 3Muri numerical results have been compared with the empirical fragility curve deriving from observed damages in the study area. From the comparison, it has been noticed that the 3Muri software is able to predict quite well the occurred damages in the longitudinal (X) direction only. Moreover, the numerical damages predicted for SU 8B are on the safe side if compared to those detected under

observational way. Therefore, the achieved results have shown the difficulties in predicting safely from numerical point of view the seismic vulnerability of corner buildings.

In conclusion, from the results obtained using the proposed methods, it is clear that the mechanical approach gives more refined results in terms of expected damage than the other methods examined (empirical nature), of both clustered buildings and single SUs. On the other hand, the macroseismic method is a useful tool for large-scale vulnerability analysis of SUs of masonry aggregates, while it is not able to predict the damages suffered by historical center constructions under seismic actions. Intermediate results between those achieved with the aforementioned analysis approaches are obtained with the Vulnus method, which provides, if compared to the mechanical method fragility curves, an estimation of the expected damage for clustered buildings better than that achievable for single SUs.

## DATA AVAILABILITY STATEMENT

The raw data supporting the conclusions of this manuscript will be made available by the authors, without undue reservation, to any qualified researcher.

## AUTHOR CONTRIBUTIONS

## ACKNOWLEDGMENTS

## REFERENCES

Ameri, G., Massa, M., Bindi, D., D'Alema, E., Gorini, A., Luzi, L., et al. (2009). The 6 April 2009 Mw 6.3 L'Aquila (Central Italy) earthquake: strong-motion observations. *Seismol. Res. Lett.* 80, 951–966. doi: 10.1785/gssrl.80.6.951

Azap, B., Apostol, I., Mosoarca, M., Chieffo, N., and Formisano, A. (2018). "Seismic vulnerability scenarios for historical areas of Timisoara," in *Proceedings of the 8th International Conference on Engineering Failure Analysis* (Budapest: Elsevier), 4–9.

Azizi-Bondarabadi, H., Mendes, N., Lourenço, P. B., and Sadeghi, N. H. (2016). Empirical seismic vulnerability analysis for masonry buildings based on school buildings survey in Iran. *Bull. Earthq. Eng.* 14, 3195–3229. doi: 10.1007/s10518-016-9944-1

Barbieri, G., Biolzi, L., Bocciarelli, M., Fregonese, L., and Frigeri, A. (2013). Assessing the seismic vulnerability of a historical building. *Eng. Struct.* 57, 523–535. doi: 10.1016/j.engstruct.2013.09.045

Benedetti, D., and Petrini, V. (1984). Sulla vulnerabilità si sismica di edifici in muratura: un metodo di valutazione. *L'Industria delle Costr.* 149, 66–74.

Bernardini, A., Gori, R., and Modena, C. (1990). "Application of coupled analytical models and experiential knowledge to seismic vulnerability analyses of masonry buildings," in *Earthquake Damage Evaluation and Vulnerability Analysis of Buildings Structures*, ed A. Koridze (Oxon: INEEC, Omega Scientific), 161–180.

Boncio, P., Galli, P., Naso, G., and Pizzi, A. (2012). Zoning surface rupture hazard along normal faults: Insight from the 2009 Mw 6.3 L'Aquila, central Italy,

earthquake and other global earthquakes. *Bull. Seismol. Soc. Am.* 102, 918–935. doi: 10.1785/0120100301

Borzi, B., Crowley, H., and Pinho, R. (2008). Simplified pushover-based earthquake loss assessment (SP-BELA) method for masonry buildings. *Int. J. Archit. Herit.* 2, 353–376. doi: 10.1080/15583050701828178

Brando, G., De Matteis, G., and Spacone, E. (2017). Predictive model for the seismic vulnerability assessment of small historic centres: application to the inner Abruzzi Region in Italy. *Eng. Struct.* 153, 81–96. doi: 10.1016/j.engstruct.2017.10.013

Calvi, G. M., Pinho, R., Magenes, G., Bommer, J. J., and Crowley, H. (2006). Development of seismic vulnerability assessment methodologies over the past 30 years. *J. of Earthquake Tecn.* 43, 75–104.

Cavaleri, L., Di Trapani, F., and Ferrotto, M. F. (2017). A new ibrid procedure for the definition of seismic vulnerability in Mediterranean cross-border urban areas. *Nat. Hazards* 86, 517–541. doi: 10.1007/s11069-016-2646-9

Chieffo, N., and Formisano, A. (2019). The influence of geo-hazard effects on the physical vulnerability assessment of built heritage: an application in a district of Naples. *Buildings* 9, 1–21. doi: 10.3390/buildings9010026

Chieffo, N., Formisano, A., and Ferreira, T. M. (2019). Damage scenario-based approach and retrofitting strategies for seismic risk mitigation: an application to the historical Centre of Sant'Antimo (Italy). *Euro. J. Environ. Civil Eng.* doi: 10.1080/19648189.2019.1596164

Chieffo, N., Mosoarca, M., Formisano, A., and Apostol, I. (2018). "Seismic vulnerability assessment and loss estimation of an urban district of Timisoara,"

in *Proceeding of 3rd World Multidisciplinary Civil Engineering, Architecture, Urban Planning Symposium* (Prague: WMCAUS), 1–10.

Da Porto, F., Munari, M., Prota, A., and Modena, C. (2013). Analysis and repair of clustered buildings: case study of a block in the historic city centre of L'Aquila (Central Italy). *Constr. Build. Mater.* 38, 1221–1237. doi: 10.1016/j.conbuildmat.2012.09.108

Da Porto, F., Valluzzi, M. R., Munari, M., Modena, C., Arede, A., and Costa, A. A. (2018). "Strengthening of brick and stone masonry buildings," in *Strengthening and Retrofitting of Existing Structures*, Vol. 9, eds A. Costa, A. Arede, and H. Varum (Singapore: Springer Nature), 59–84.

D'Agostino, N., Mantenuto, S., D'Anastasio, E., Giuliani, R., Mattone, M., Calcaterra, S., et al. (2011). Evidence for localized active extension in the central Apennines (Italy) from global positioning system observations. *Geology* 39, 291–294. doi: 10.1130/G31796.1

D'Ayala, D. F., and Paganoni, S. (2011). Assessment and analysis of damage in L'Aquila historic city centre after 6th April 2009. *Bull. Earthq. Eng.* 9, 81–104. doi: 10.1007/s10518-010-9224-4

Eurocode 8 (2005). *European Standard EN 1998-3:2005: Design of structures for earthquake resistance - Part 3: Assessment and retrofitting of buildings.* Brussels: Com. Eur. Norm.

Fava, M., Munari, M., Da Porto, F., and Modena, C. (2016). "Seismic vulnerability assessment of existing masonry buildings by nonlinear static analyses and fragility curves," in *Brick and Block Masonry: Trends, Innovations and Challenges: Proceedings of the 16th International Brick and Block Masonry Conference* (Padua: IBMAC), 2409–2416. doi: 10.1201/b21889-315

Ferreira, T. M., Vicente, R., Mendes da Silva, J. A. R., Varum, H., and Costa, A. (2013). Seismic vulnerability assessment of historical urban centres: case study of the old city centre in Seixal, Portugal. *Bull. Earthq. Eng.* 11, 1735–1773. doi: 10.1007/s10518-013-9447-2

Ferreira, T. M., Vicente, R., and Varum, H. (2012). "Vulnerability assessment of building aggregates: a macroseimic approach," in *Proceedings of the 15th World Conference on Earthquake Engineering* (Lisbon: WCEE), 2–9.

Formisano, A. (2017a). Local- and global-scale seismic analyses of historical masonry compounds in San Pio delle Camere (L'Aquila, Italy). *Nat. Hazards* 86, 465–487. doi: 10.1007/s11069-016-2694-1

Formisano, A. (2017b). Theoretical and numerical seismic analysis of masonry building aggregates: case studies in San Pio Delle Camere (L'Aquila, Italy). *J. Earthq. Eng.* 21, 227–245. doi: 10.1080/13632469.2016.1172376

Formisano, A., Castaldo, C., and Mazzolani, F. M. (2013). "Non-linear analysis of masonry building compounds: a comparison of numerical and theoretical results," *Civil-Comp Proceedings* (Stirlingshire). doi: 10.4203/ccp.102.66

Formisano, A., and Chieffo, N. (2018a). Expected seismic risk in a district of the Sant'Antimo's historical centre. *Trends Civ. Eng. its Archit.* 2, 1–15. doi: 10.32474/TCEIA.2018.02.000130

Formisano, A., and Chieffo, N. (2018b). Non-linear static analyses on an Italian masonry housing building through different calculation software packages. *Int. J. Energy Environ.* 12, 30–40.

Formisano, A., Chieffo, N., Monaco, D., and Fabbrocino, F. (2016). On the influence of the aggregate condition on the vibration period of masonry buildings: a case study in the district of Naples. *AIP Conf. Proc.* 1790:130005. doi: 10.1063/1.4968723

Formisano, A., Chieffo, N., and Mosoarca, M. (2017). Seismic vulnerability and damage speedy estimation of an urban sector within the mucipality of San Potito Sannitico (Caserta, Italy). *Open Civ. Eng. J.* 11, 1106–1121. doi: 10.2174/1874149501711011106

Formisano, A., Florio, G., Landolfo, R., and Mazzolani, F. M. (2011). "Numerical calibration of a simplified procedure for the seismic behaviour assessment of masonry building aggregates," *Proceedings of 13th International Conference on Civil, Structure and Environmental Engineering Computating* (Stirlingshire).

Formisano, A., Florio, G., Landolfo, R., and Mazzolani, F. M. (2015). Numerical calibration of an easy method for seismic behaviour assessment on large scale of masonry building aggregates. *Adv. Eng. Softw.* 80, 116–138. doi: 10.1016/j.advengsoft.2014.09.013

Formisano, A., and Massimilla, A. (2018). A novel procedure for simplified nonlinear numerical modeling of structural units in masonry aggregates. *Int. J. Archit. Herit.* 12, 1162–1170. doi: 10.1080/15583058.2018.1503365

Galli, P. A. C., and Naso, J. A. (2009). Unmasking the 1349 earthquake source (southern Italy): paleoseismological and archaeoseismological indications from the Aquae Iuliae fault. *J. Struct. Geol.* 31, 128–149. doi: 10.1016/j.jsg.2008.09.007

Grünthal, G (Ed.). (1998). *Chaiers du Centre Européen de Géodynamique et de Séismologie*, Vol. 15. Luxembourg: European Center for Geodynamics and Seismology.

Guagenti, E., and Petrini, V. (1989). "The case of old buildings: towards a new law - intensity damage," in *Proceedings of the 12th Italian conference on earthquake engineering—ANIDIS* (Pisa: Italian National Association of Earthquake Engineering).

Indirli, M., Bruni, S., Candigliota, E., Geremei, F., Immordino, F., and Moretti, L. (2012). "Assessment of historic centres through a multidisciplinary approach based on the simultaneous application of Remote Sensing, GIS and quick procedures for survey and vulnerability evaluation : the Arsita case," in *Proceeding of the Conference EACH 2011, 5th International Congress on "Science Technology for the Safeguard of Culture Heritage in the Mediterranean Basin"* (Istanbul), 1–13.

Indirli, M., Bruni, S., Geremei, F., Marghella, G., Marzo, A., Moretti, L., et al. (2014). "The reconstruction plan of the town of Arsita after the 2009 Abruzzo (Italy) seismic event," in *Proceedings of the 9th International Conference on Structural Analysis of Historical Constructions - SAHC2014* (Mexico City).

Kappos, A. J., Panagopoulos, G., Panagiotopoulos, C., and Penelis, G. (2006). A hybrid method for the vulnerability assessment of R/C and URM buildings. *Bull. Earthq. Eng.* 4, 391–413. doi: 10.1007/s10518-006-9023-0

Lagomarsino, S. (2006). On the vulnerability assessment of monumental buildings. *Bull. Earthq. Eng.* 4, 445–463. doi: 10.1007/s10518-006-9025-y

Lagomarsino, S. (2012). Damage assessment of churches after L'Aquila earthquake (2009). *Bull. Earthq. Eng.* 10, 73–92. doi: 10.1007/s10518-011-9307-x

Lagomarsino, S., and Cattari, S. (2014). Fragility Functions of Masonry Buildings. *Geotech. Geol. Earthq. Eng.* 27, 111–156. doi: 10.1007/978-94-007-7872-6_5

Lagomarsino, S., and Giovinazzi, S. (2006). Macroseismic and mechanical models for the vulnerability and damage assessment of current buildings. *Bull. Earthq. Eng.* 4, 415–443. doi: 10.1007/s10518-006-9024-z

Lourenço, P. B., and Roque, J. A. (2006). Simplified indexes for the seismic vulnerability of ancient masonry buildings. *Constr. Build. Mater.* 4, 200–208. doi: 10.1016/j.conbuildmat.2005.08.027

M.D. 17 January 2018 (2018). *Updating of Technical Codes for Constructions*, Official Gazette n. 42 of 20/02/18, Ordinary Supplement n. 8.

M.D. 2 February 2009 (2009). *Instructions for the application of the ≪New technical standards for buildings≫ referred to in the Ministerial Decree of 14 January 2008*, Official Gazette n.47 of 26/02/2009, Ordinary Supplement n. 27.

Morisi, C. (1998). *Arsita, ambiente, cultura, tradizione*, ed C. Esperidi.

Munari, M., Valluzzi, M. R., Cardani, G., Anzani, A., Binda, L., and Modena, C. (2010). "Seismic vulnerability analyses of masonry aggregate buildings in the historical centre of Sulmona (Italy)," in *Proceeding 13th International Conference on Structural Faults and Repair* (Edinburgh), 1–10.

National Institute of Geophysics and Vulcanology (2009). *La Sequenza Sismica de L'Aquilano - Aprile 2009*. Available online at: http://terremoti.ingv.it/en/component/content/article/13-eventi/approfondimenti/710-la-sequenza-sismica-de-laquilano-aprile-2009.html

OPCM, 3274/2003 (2003). *Primi Elementi in Materia di Criteri Generali per la Classificazione Sismica del Territorio Nazionale e di Normative Tecniche per le Costruzioni in Zona Sismica.* Rome.

Penna, A., Morandi, P., Rota, M., Manzini, C. F., da Porto, F., and Magenes, G. (2014). Performance of masonry buildings during the Emilia 2012 earthquake. *Bull. Earthq. Eng.* 12, 2255–2273. doi: 10.1007/s10518-013-9496-6

Pujades, L. G., Barbat, A. H., González-Drigo, R., Avila, J., and Lagomarsino, S. (2012). Seismic performance of a block of buildings representative of the typical construction in the Eixample district in Barcelona (Spain). *Bull. Earthq. Eng.* 10, 331–349. doi: 10.1007/s10518-010-9207-5

Ramos, L. F., and Lourenço, P. B. (2004). Modeling and vulnerability of historical city centers in seismic areas: A case study in Lisbon. *Eng. Struct.* 26, 1295–1310. doi: 10.1016/j.engstruct.2004.04.008

S.T.A.data srl (2017). *3Muri 10.9.0 - User's Manual.*

Tiberti, S., and Milani, G. (2017). Historic city centers after destructive seismic events, the case of finale Emilia during the 2012 Emilia-Romagna earthquake: Advanced numerical modelling on four case studies. *Open Civ. Eng. J.* 11, 1059–1078. doi: 10.2174/18741495017110 11059

Valluzzi, M. R., Cardani, G., Binda, L., and Modena, C. (2004). "Seismic vulnerability methods for masonry buildings in historical centres: validation and application for prediction analyses and intervention proposals," in *Proceeding of 13th World Conference on Earthquake Engineering* (Vancouver, BC: WCEE), 2–12.

# Advantages of publishing in Frontiers

**OPEN ACCESS**
Articles are free to read
for greatest visibility
and readership

**FAST PUBLICATION**
Around 90 days
from submission
to decision

**HIGH QUALITY PEER-REVIEW**
Rigorous, collaborative,
and constructive
peer-review

**TRANSPARENT PEER-REVIEW**
Editors and reviewers
acknowledged by name
on published articles

**REPRODUCIBILITY OF RESEARCH**
Support open data
and methods to enhance
research reproducibility

**DIGITAL PUBLISHING**
Articles designed
for optimal readership
across devices

**FOLLOW US**
@frontiersin

**IMPACT METRICS**
Advanced article metrics
track visibility across
digital media

**EXTENSIVE PROMOTION**
Marketing
and promotion
of impactful research

**LOOP RESEARCH NETWORK**
Our network
increases your
article's readership